Acta Biologica Hungarica

VOLUME 51, NUMBER 1, 2000

Akadémiai Kiadó, Budapest

ACTA BIOL. HUNG. ABAHAU 51 (1) 1–107 (2000) HU ISSN 0236-5383

ACTA BIOLOGICA HUNGARICA

A QUARTERLY OF THE HUNGARIAN ACADEMY OF SCIENCES

Acta Biologica Hungarica publishes original papers on experimental biology.

Acta Biologica Hungarica is published in yearly volumes of four issues by

AKADÉMIAI KIADÓ
H-1117 Budapest, Prielle Kornélia u. 4, Hungary
http: //www.akkrt.hu

Manuscripts and editorial correspondence should be addressed to

Acta Biologica Hungarica
H-8237 Tihany, Hungary

Phone: (36-87) 448-244
Fax: (36-87) 448-006
E-mail: salanki@tres.blki.hu; elekes@tres.blki.hu

Subscription information

Orders should be addressed to

AKADÉMIAI KIADÓ
H-1519 Budapest, P.O. Box 245, Hungary
Fax: (36-1) 464-8221
E-mail: kiss.s@akkrt.hu

Subscription price for Volume 51 (2000) in 4 issues US$ 180.00, including normal postage, airmail delivery US$ 20.00.

"This periodical is included in the document delivery program THE GENUINE ARTICLE of the Institute of Scientific Information, Philadelphia. The articles published in the periodical are available through *The Genuine Article* at the Institute for Scientific Information, 3501 Market Street, Philadelphia PA 19104."

Acta Biologica Hungarica is abstracted/indexed in Biological Abstracts, Chemical Abstracts, Current Contents–Agriculture, Biology and Environmental Sciences, database (EMBASE), Elsevier BIOBASE, Index Medicus, International Abstracts of Biological Sciences

---

CONTENTS

Acta Biologica Hungarica 51 (1), pp. 1–29 (2000)

PEPTIDES AND ANTITUMOR ACTIVITY*

DEVELOPMENT AND INVESTIGATION OF SOME PEPTIDES WITH ANTITUMOR ACTIVITY

I. TEPLÁN

Department of Medical Chemistry, Semmelweis University of Medicine,
Puskin u. 9, H-1088 Budapest, Hungary

(Received: January 12, 1999; accepted: February 12, 1999)

We developed a group of synthetic analogs of GnRH and Somatostatin to inhibit the tumor growth of different kind. The GnRH analogs decreasing the gonadotrop and steroid hormone levels act on the hormone dependent tumors and influence their growth. One of the most effective antitumor analog was patented under the name FOLLIGEN which inhibited the breast cancer caused by DMBA in rats without any side-effects. Other inhibitory analogs of GnRH with long-lasting effect were effective in the treatment of breast, ovary and prostate tumors. Another analog [α-Asp(DEA)]^{6},Gln^{8}-hGnRH showed a very low endocrine but high antitumor effect in both *in vitro* and *in vivo* experiments. Its tritium labeled derivative exhibited specific binding sites on human tumor cell lines. We synthesized the analogs of GnRH-III with effective selective antitumor activity which does not alter the ovarian cycle of rats but inhibits the colony-formation of human breast cancer cell lines and has a significant antiproliferative effect. We also synthesized conjugates of potent GnRH analogs with a branched chain polylysine backbone which induce a 33–35% decrease of cell numbers of MCF-7 and MDA-MB-231 human breast cancer cell lines and 45–50% inhibition of cell proliferation. Another conjugate decreased the tumor growth of MDA-MB-231 xenografts by 80% in a treatment of 9 weeks and even tumor free animals could be found among the ones treated. Using these radiolabeled peptide hormone analogs we found that human tumor cell lines and xenografts specifically bind the GnRH conjugates. We also synthesized a series of Somatostatin analogs which inhibit tyrosine kinases and the growth of several breast, prostate and colon tumor cell lines. One of our best analogs was a heptapeptide, TT-232, which strongly inhibited the tyrosine kinase activity and the cell-proliferation in different colon tumor cells. However, it did not inhibit the growth hormone release either *in vitro* or *in vivo* from rat pituitary cells. The TT-232 was found to be effective on 60 human tumor cell lines, it significantly inhibited the tumor growth on different animal tumor models, and induced apoptosis, as a result of which some animals became tumor free. The TT-232 inhibited the tumor growth of PC3 prostate xenografts with 60% and caused a 100% survival of mice 60 days after the transplantation. It is being preclinically tested at present.

We have shown that the new GnRH analogs acting without any hormonal effect and the Somatostatin analogs with strong antitumor and tyrosine kinase inhibitory activity but no hormonal effect may represent a breakthrough in the research of the antitumor peptides, having direct effect on tumor cells.

Keywords: GnRH agonist analog – antagonist analog – antitumor activity – inhibition of tyrosine kinase – polymer conjugates – radiolabeling – Somatostatin analog – multidrug resistance

*Prof. István Teplán's inaugural lecture for the membership of the Hungarian Academy of Sciences, held on 17th March, 1998.

0236-5383/2000/$ 5.00

ANTITUMOR ACTIVITY OF GnRH ANALOGS AND THEIR CONJUGATES

The discovery and isolation of hypothalamic releasing hormones initiated a research of very wide spectrum. The most important among these releasing hormones is the Gonadotropin Releasing Hormone, a decapeptide stimulating the release of the Luteinizing Hormone and the Folliculus Stimulating Hormone [1–4] (Fig. 1).

1 2 3 4 5 6 7 8 9 10

Glp-His-Trp-Ser-Tyr-Gly-Leu-Arg-Pro-Gly-NH_2

Fig. 1. The amino acid sequence of human GnRH

On the basis of the endocrinological effect of GnRH some biological problems of reproduction were expected to be treated during the application of both the GnRH agonist and antagonist analogs.

Initiated by these expectations, efforts were started in many laboratories all over the world (in our laboratory, too) to synthesize and investigate super active agonist and antagonist analogs.

Our earlier results in the field of GnRH agonists have been published [5]. These super active GnRH analogs were developed and synthesized to solve the problems of infertility among cattle. However, before the clinical and veterinary application it was necessary to study the mechanism of action of GnRH analogs.

In the course of these studies our first observation led to the discovery of the desensitization and down-regulation of the LHRH receptors of the pituitary gland [6] (Fig. 2).

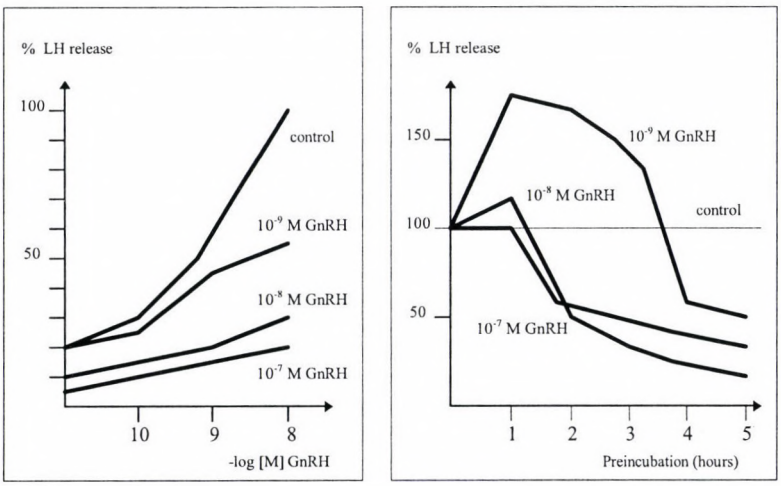

Mol. Cell. Endocrinol. *30* 109-120 (1983)

Fig. 2. Desensitization of LH release on GnRH treatment

Both *in vitro* and *in vivo* experiments showed a paradox phenomenon, namely if the GnRH dose is higher it releases fewer LH hormones than in lower concentration. This observation is in accordance with the earlier finding according to which GnRH is not released continuously but in a pulsative manner from the hypothalamus. The GnRH released this way controls the reproductive processes – among others the gonadal steroidogenesis and gametogenesis – by way of gonadotrop hormones released from the hypophysis.

We developed a series of antagonist derivatives of GnRH analogs to inhibit the ovulation. These antagonistic analogs act in a way completely different from the agonists: they do not increase but significantly decrease the release of the LH and FSH hormones of the hypophysis. Table 1 shows the structure and antiovulatory effect of some antagonistic analogs.

Table 1
Structure and antiovulatory effect of GnRH inhibitors

1	2	3	4	5	6	7	8	9	10	Inhibition of ovulation (μM)	Code
Glp-	DPhe-	Phe-	Ser-	Tyr-	DPhe-	Leu-	Arg-	Pro-	Gly-NH_2	1000	
	DPhe-	DTrp-			DPhe-					1000	
DGlp-	DCpa-	DTrp-			DPhe-					120	
AcDCpa-	DCpa-	DTrp-			DPhe-					50	
AcDCpa-	DCpa-	DTrp-			DPhe-				DAla-NH_2	10	
AcDCpa-	DCpa-	DTrp-			DLys-				DAla-NH_2	8	
AcDNaI-	DCpa-	DTrp-			DArg-				DAla-NH_2	1	
AcDTrp-	DCpa-	DTrp-			DLys-				DAla-NH_2	2	MI-1544
AcDNaI-	DCpa-	DTrp-			DCit-				DAla-NH_2	3	SB-30*
AcDNaI-	DCpa-	DPaI-			DCit-				DAla-NH_2	–	SB-75**

BBRC *100,* 915 (1981), Peptides *3,* 969 (1982), Endorcrinology *110,* 1445 (1982), Peptides *4,* 149 (1983),* BBRC *118,* 351 (1984), **PNAS *85,* 1637b (1988)

The inhibitory mechanism of the GnRH agonists and antagonists developed so far is the following: the presence of GnRH decreases the number of GnRH receptors desensitizing them, as a consequence the release of the gonadotropins decreases. However, the antagonist analogs have a strong bond to the hypophyseal receptors and competitively inhibit the binding of the GnRH of endogen origin. And this way they inhibit the secretion of LH and FSH as well. It follows that it is possible to achieve the inhibition of the ovulation both by superactive and antagonistic analogs since the result of both mechanisms leads to the decrease of the steroid level which blocks the ovulation.

These observations resulted in forming a new concept which was proved later by our experiments, namely the significant decrease of steroid level might affect the hormone dependent tumors and influence their growth.

The application of GnRH analogs makes it possible to avoid most of the undesirable side-effects of other treatments which cause irreversible castration since the steroid level can be restored after the GnRH analog treatment.

In the eighties several pharmaceutical companies developed superactive GnRH analogs of long-lasting effect, which were effective in the treatment of breast, ovary and prostate tumors [7–9]. Since we also had both GnRH agonist and antagonist analogs it seemed obvious for us to study the antitumor activity of our analogs as well. One of them the OVURELIN, D-Phe^6-hGnRH[1–9]-EA which is in use for veterinary application, was tested by us for its antitumor activity (Fig. 3).

OVURELIN®

Glp-His-Trp-Ser-Tyr-D-Phe-Leu-Arg-Pro-NH-Et

Hung Pat. No.: 185 535
US Pat. No. 4 552 864

Fig. 3. The amino acid sequence of OVURELIN®

We studied the binding of tritium labeled OVURELIN in a radioreceptor assay, and we found that OVURELIN receptors are present both in MCF-7 (Estrogen-positive) and MDA-MB-231 (Estrogen-negative) human mammary tumor cell-lines. From our results it became obvious that the D-Phe^6-hGnRH[1–9]-ethylamide ought to be investigated *in vitro* antitumor assays [10–11] as *in vivo* studies had demonstrated that the labeled hormone was significantly enriched in tumor cells (Table 2).

Table 2
Specific binding of (^{3}H)OVURELIN in tumor cell suspension and membrane

	Dissociation constant ($K_d \times 10^{-9}$ M)	(^{3}H)OVURELIN binding capacity (pmol/mg protein)
MCF-7 cell suspension	36.48	3.95
MDA-MB-231	37.12	4.62
MCF-7 xenograft membrane fraction	30.22	3.56
MDA-MB-231 xenograft membrane fraction	30.12	4.23

J. Steroid Biochem. Molec. Biol. *38,* 119 (1996)

At the same time, *in vivo* experiments also showed that the Zoladex and Decapeptyl [12] dramatically decreased the weight of tumors of xenografted mice in depo formulation after a short period of stimulation of tumor growth, while Ovurelin and some other superagonists in non-depo formulation did not exhibit antitumor activity even if administered twice a day. These results called our attention to the necessity of finding a suitable device to enhance the long-lasting high concentration of the GnRH analog in the organs.

Besides the OVURELIN another interesting GnRH analog with antitumor activity was developed from the chicken GnRH derivative. Proceeding this development in the middle of the eighties we produced a lot of GnRH analogs using the best combinations of chicken, salmon and mammal GnRH analogs.

The most effective antitumor analog was patented under the name FOLLIGEN. Its structure and synthesis is shown in Fig. 4.

BOC-His(Dnp)OH + H-Trp-OMe
BOC-His(Dnp)-Trp-OMe — Z-Pro-ONp + NHEt
Glp-OH + H-His(Dnp)-Trp-OMe — Z-Pro-NH-Et
Glp-His(Dnp)-Trp-OMe — BOC-Ser-OH + H-Tyr-OMe — BOC-Gln-ONp + H-Pro-NH-Et
Glp-His-Trp-OMe — BOC-Ser-Tyr-OMe — Z-Leu-OPcp + H-Gln-Pro-NH-Et
Glp-His-Trp-N_3 + H-Ser-Tyr-OMe — Z-Leu-Gln-Pro-NH-Et
Glp-His-Trp-Ser-Tyr-OMe — BOC-DPhe-OPcp +H-Leu-Gln-Pro-NH-Et
Glp-His-Trp-Ser-Tyr-N_2H_3 — BOC-DPhe-Leu-Gln-Pro-NH-Et
Glp-His-Trp-Ser-Tyr-N_3 + — H-DPhe-Leu-Gln-Pro-NH-Et

Glp - His - Trp - Ser - Tyr - **DPhe** - Leu - **Gln** - Pro - **NHEt**

1 2 3 4 5 6 7 8 9

Fig. 4. The structure and chemical synthesis of FOLLIGEN

Figure 5 presents the inhibitory effect on *in vivo* tumor volume of the FOLLIGEN and two other superactive analogs [13].

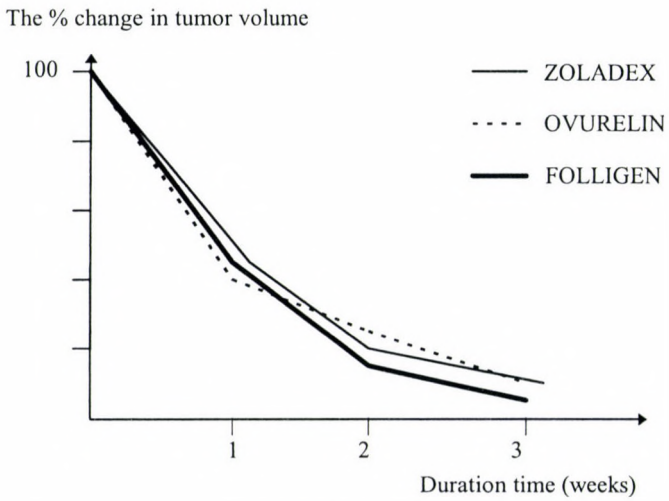

Tumor Biology *13*, 44 (1992) Us Pat. No. 2218335 (1991)

Fig. 5. The effect of FOLLIGEN on the volume of breast tumors induced by DMBA

Furthermore, we have found that the FOLLIGEN inhibited the breast cancers caused by dimethyl benzantracene (DMBA) in rats to the same extent as the ZOLADEX {D-Ser(tBu)^6,AzaGly^{10}-GnRH}, a product of ICI, which is in clinical use. However, while the latter caused hormone castration and complete inhibition of ovarian function the FOLLIGEN treatment never had these side-effects. This is due to the different action mechanisms based on their different structures.

Parallel to tumor inhibition we also started to examine the molecular mechanism of tyrosine kinase enzyme playing a decisive role in oncogen transformation and also started to plan and synthesize different peptide substrate inhibitors and antigen determinants.

The importance of this field is supported by the fact that the tyrosine kinase type enzymes play a crucial role in the regulation of cell proliferation and this is why they are important target molecules of pharmacological research. When testing the action mechanism of our antitumor peptides we discovered that many breast, prostate and colony tumor cell lines have a significant tyrosine kinase activity which can be beneficially influenced by peptide hormones. Thus for example, both FOLLIGEN and another GnRH agonist the OVURELIN inhibit the tyrosine kinase activity of MDA-MB231 breast tumor cell line [14] (Fig. 6).

However, we found that this tyrosine kinase inhibitory effect does not correlate necessarily with the proliferation inhibition of tumor cells, since the FOLLIGEN decreased the tyrosine kinase activity to a lesser extent than BUSERELIN {D-Ser(tBu)^6-GnRH-(1-9)-EA}, whereas the FOLLIGEN inhibited the cell proliferation more effectively than the BUSERELIN.

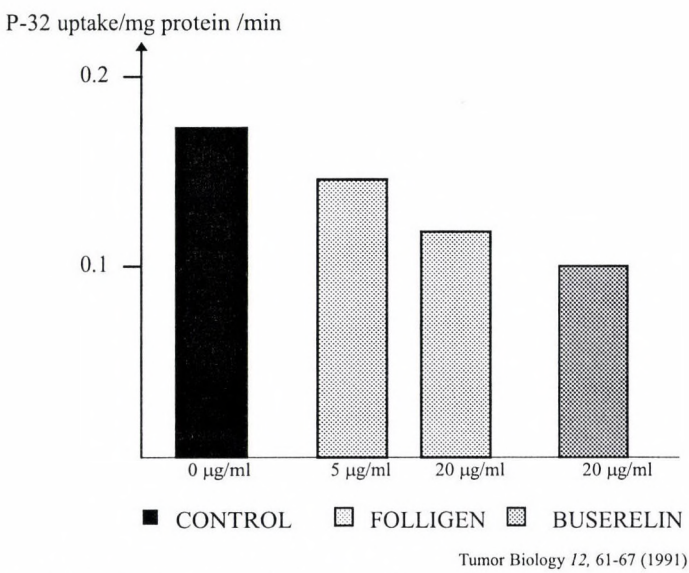

Fig. 6. Effect of FOLLIGEN on the tyrosine kinase enzim activity in MDA-MB-231 human breast tumor cell line

Besides all these we also proved that both the FOLLIGEN and BUSERELIN have an influence on the activity of protein kinase C. Although these hormones do not alter the total enzyme activity, they both, but especially the FOLLIGEN, decrease the enzyme activity in the cytosol and on the other hand, increase it in the cell membrane to a significant extent (Fig. 7.).

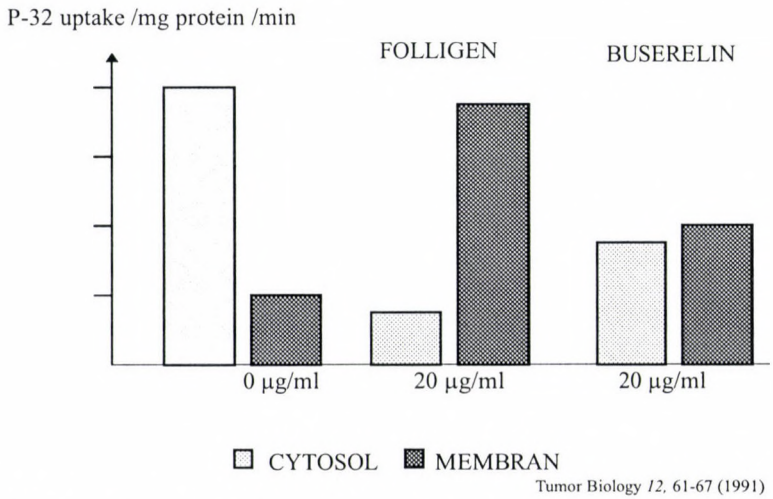

Fig. 7. Effect of FOLLIGEN and BUSERELIN on the protein kinase C enzyme in MDA-MB 231 cells

Our results undoubtedly seem to prove the fact that the antitumor mechanism of the FOLLIGEN is significantly different not only *in vitro* but also *in vivo* from that of the well-known superactive GnRH analogs in use.

We have also found in our earlier studies that the D-amino acids in the sequence of superactive GnRH analogs can be replaced by a β-aspartyl moiety having different substituents on its α-carboxyl group. This type of β-aspartyl residue may lead to a very similar conformation to that of the D-amino acids e.g. the D-Ser(^{t}Bu) in the structure of the BUSERELIN (Fig. 8).

On the basis of this it was to be expected that a biologically active conformation containing a β-turn might be stabilized by this structural feature. That is why we decided to combine the advantages of the low LH-release and the significant antiproliferative effect originating from the special structure of the FOLLIGEN with those of the β-aspartyl substitution in order to obtain analogs of low endocrine, but with high antiproliferative effect.

This analog proved to be the [β-Asp(DEA)]^6,Gln^8-hGnRH (TH-332) showing a very low endocrine effect in both *in vitro* tests and *in vivo* experiments without altering the ovarian cycle of rats [15] (Fig. 9).

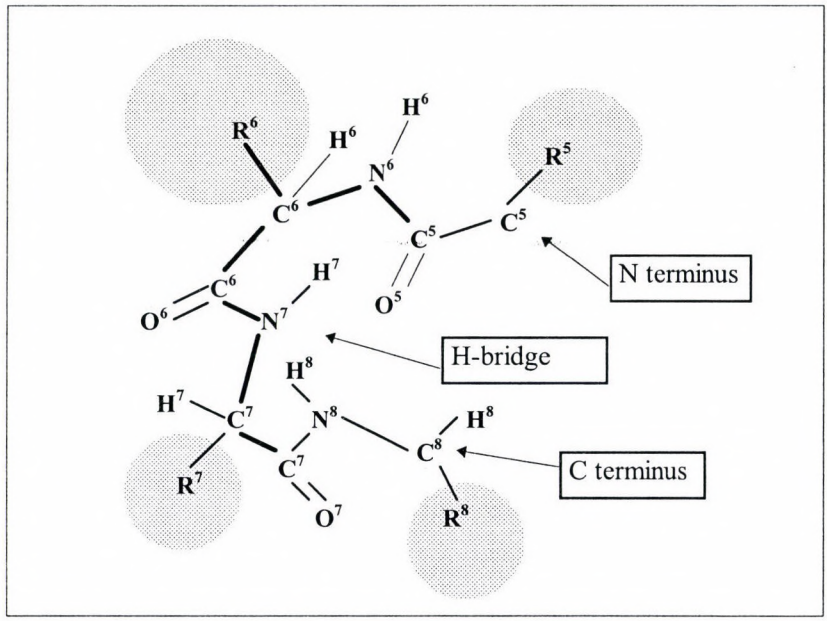

Fig. 8a. The β-turn around the 6th amino acid

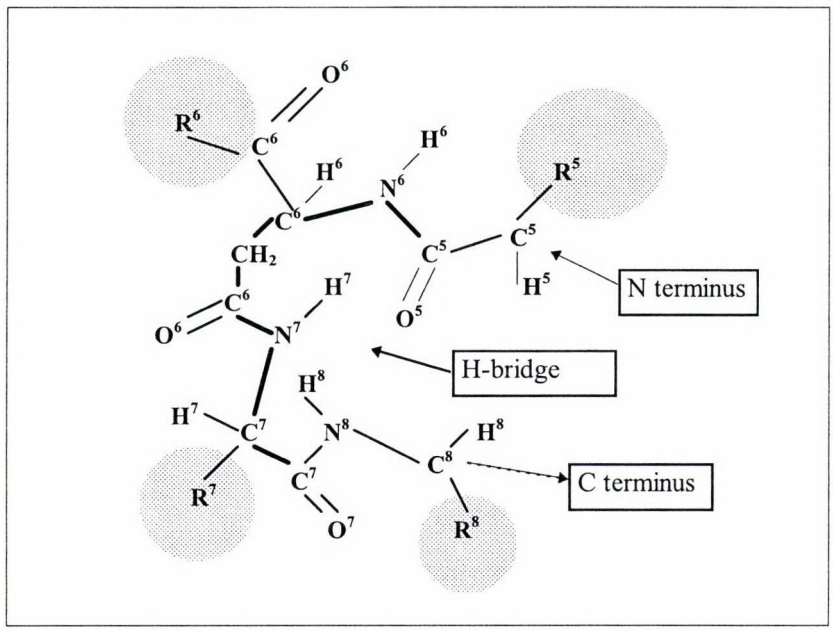

Biomed. Pept. Prot. *2*, 33-40 (1996)

Fig. 8b. The β-turn around the β-aspartyl residue

MAMMAL GnRH:
Glp-His-Trp-Ser-Tyr-Gly-Leu-Arg-Pro-Gly-NH_2

CHICKEN-I GnRH:
Glp-His-Trp-Ser-Tyr-Gly-Leu-*Gln*-Pro-Gly-NH_2

TT-232:
Glp-His-Trp-Ser-Tyr-β*Asp(DEA)*-Leu-*Gln*-Pro-Gly-NH_2

Fig. 9. The structure of GnRH analogs

The tritium labeled [^{3}H-Tyr]^5,[β-Asp(DEA)]^6,Gln^8-hGnRH specifically bound on human tumor cell lines. In *in vitro* experiments the analog TH-332 inhibited the proliferation of prostate tumor cell lines causing a significant apoptosis [16].

In addition to agonist analogs we extended our studies to antagonist GnRH analogs, too. In the frame of these efforts we studied the binding properties of our antagonist analog, the MI-1544, and found that both our agonist analog, the OVURELIN and the MI-1544 antagonist analog bind to the MCF-7 and MDA-MB-231 cell lines and presumably to the same receptors.

On the basis of our good results with the TH-332 agonist and MI-1544 antagonist analogs, we incorporated the L-β-aspartyl-α-diethylamide and Gln moieties into the antagonist sequence in the positions 6 and 8, respectively. Since in the meantime we recognized the increased antitumor activity of the GnRH analog and its polymer conjugates we planned and synthesized a GnRH analog suitable for conjugation. So 5-Tyr was replaced by Lys in the above-mentioned peptide sequence, resulting the Ac-D-Trp^{1,3}, D-Cpa^2, Lys^5, [β-Asp(α-DEA)]^6, Gln^8, D-Ala^{10}-NH_2 (MI-1892) (Fig. 10).

MI-1544:
Ac-*DTrp-DCpa-DTrp*-Ser-Tyr-**DLys**-Leu-Arg-Pro-**DAla**-NH_2

MI-1892:
Ac-*DTrp-DCpa-DTrp*-Ser-**Lys**-*L*-β-*Asp(DEA)*-Leu-*Gln*-Pro-*DAla*-NH_2

Biomed. Pept. Prot. *2*, 33-40 (1996)

Fig. 10. The structure of some inhibitory analogs of GnRH

In an extremely high dose this analog inhibits the release of LH induced by hGnRH when used in *in vitro* superfusion assays, but in *in vivo* experiments it does not influence the ovarian cycle of rats even at 20-fold higher doses than the effective dose of the best antagonists. On the other hand, this weak antagonist exhibits significant antiproliferative and clonogenic effect [15] (Table 3).

Table 3
The antitumor effect of MI-1892 analog

	Dose		
	1 μM	30 μM	50 μM
MCF-7 colony formation	8.0	34.0	38.2
MDA-MB-231 colony formation	30.0	40.5	36.0
MCF-7 antiproliferation	21.7	26.8	35.0
MDA-MB-231 antiproliferation	18.0	20.5	35.0

Biomed. Pept. Prot. *2*, 33-40 (1996)

In our *in vivo* experiments the MI-1892 caused about 30% inhibition of tumor growth of the MDA-MB-231, the steroid independent human breast cancer xenografts when mice were treated with 2×25 μg MI-1982 i.c. in every 12 h [17].

In the early '90s an interesting GnRH analog was isolated and synthesized from the sea-lamprey [18]. After this, we started to investigate the biological effects of this Lamprey-GnRH-III with the collaboration of the scientists of the Creighton University (Omaha).

The GnRH-III has an interesting structure which is significantly different from that of the mammalian GnRH (Fig. 11).

HUMAN GnRH:
Glp-His-Trp-Ser-Tyr-Gly-Leu-Arg-Pro-Gly-NH_2

LAMPREY GnRH-III:
Glp-His-Trp-Ser-*His-Asp-Trp-Lys*-Pro-Gly-NH_2

Fig. 11. The structure of GnRH-III

The GnRH-III does not alter the ovarian cycle of rats even in the case of large dose administration, but on the other hand, it inhibits the colony-formation of human breast cancer cell lines and has a significant antiproliferative effect which is comparable with the antitumor activity of some well-known antagonist GnRH analogs (Fig. 12).

From these results we have concluded that GnRH-III is an effective, naturally occurring peptide hormone with a selective antitumor activity [19–20]. We consider this antitumor activity of GnRH-III very remarkable, because GnRH-III contains only the natural L-amino acids in contrast with the antagonists including 4–5 very hydrophobic D-amino acids. Usually the metabolism of these D-amino acids is not known well enough.

As it was shown in Fig. 11 the structure of GnRH-III is different from that of the human-(mammalian)GnRH in the 5–8 amino acid sequence. Therefore it was obvi-

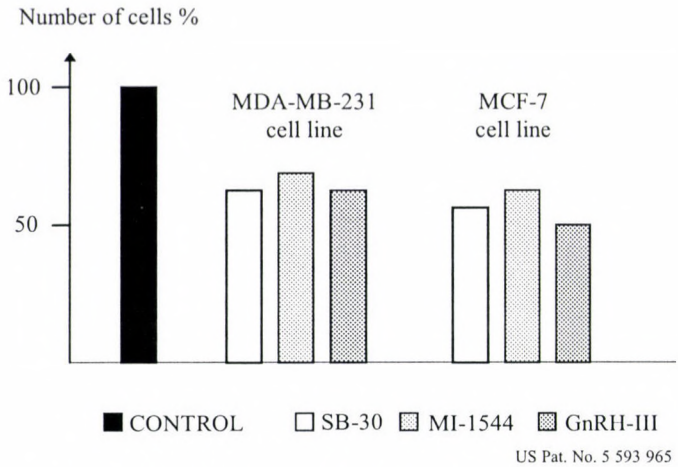

Fig. 12. Antiproliferative effects of GnRH analogs in 50 μM dose

ous to suppose that the antitumor activity of GnRH-III may be connected with this special structural feature. To prove it, a structure-biological activity study was initiated to elucidate the roles of amino acids of this sequence [21]. As a result, it was found that

i) Asp^6 and Lys^8 amino acids an "ionic interaction" is existing stabilizing a biologically active conformation. This special conformation and the sequence of GnRH-III may cause the significant antitumor activity of the analog;

ii) the replacement of Trp^7 with Phe causes a dramatic decrease in antitumor activity, suggesting the involvement of the indole ring in the interaction of the peptide with the receptor;

iii) the displacement of the side chain carboxyl group from a β to a γ position in residue 6 (Asp → Glu) does not alter the bioactive conformation of GnRH-III (Table 4).

Since the metabolism of GnRH analogs presumably took place rather quickly in the living organism, we synthesized more stable analogs against the enzymatic hydrolyses. The C-terminal replacement of Gly-NH_2 with ethyl amide resulted in slight loss of antitumor activity, whereas the $D\text{-}Ala^{10}$ replacement and N-terminal pGlu with Ac-D-Trp caused a higher loss of activity.

The GnRH analogs exhibited antitumor activity only in the case of continuous and high hormone level in the circulation. That is why different efforts have been made to provide this possibility e.g. formulation in microcapsules and/or conjugation to macromolecular carrier.

The MI-1544, GnRH antagonist analog, (Ac-$D\text{-}Trp^{1,3}$,$D\text{-}Cpa^2$,$D\text{-}Lys^6$,$D\text{-}Ala^{10}$-GnRH) covalently bound to poly[Lys-(Ac-$Glu_{0.96}$-DL-$Ala_{3.1}$)], (AcEAK), resulted in the MI-1544-AcEAK conjugate with a branched chain polylysine backbone (Fig. 13).

Table 4
Effect of GnRH analogs on the colony formation of tumor cells

Analogs	Cell lines				
	MCF-7	MDA-MB-231	Ishikawa	PC3	LNCaP
1. Lys^5-*l*GnRH-III	0	0	0	0	0
2. [Lys(N$^\varepsilon$-Fmoc)]^5-*l*GnRH-III	–	–	–	–	–
3. Lys^5,cyclo[Asp^6,Lys^8]-*l*GnRH-III	+++	++	+	+	–
4. cyclo[Asp^6,Lys^8]-*l*GnRH-III	+++	++	+	+	–
5. Lys^4,[Lys(N$^\varepsilon$-Fmoc)]^8-*l*GnRH-III	+++	+++	++	+	–
6. Lys^4-*l*GnRH-III					
7. [Lys(N$^\varepsilon$-Ac)]^4-*l*GnRH-III	+++	+++	+	+	–
8. Glu^6-*l*GnRH-III	+++	++	0	+	–
9. Phe^7-*l*GnRH-III	++	++	–	–	–
10. [Trp(For)]^{3,7}, ΔPro^9-*l*GnRH-III	+++	+++	++	+	–
11. *l*GnRH-III-(1-9)-EA	++	++	+	++	–
12. D-Ala^{10}-*l*GnRH-III	0	+	0	0	–
13. Ac-D-Trp^1, D-Ala^{10}-*l*GnRH-III	+	0	+	–	+
14. [Trp(For)]^{3,7},[^{3}H-Pro]^9-*l*GnRH-III	–	–	–	–	–
15. Asu^6-*l*GnRH-III [30]	+	–	–	–	++
16. ΔPro^9-*l*GnRH-III	+++	+++	++	+	+++
*l*GnRH-III	+++	+++	+	++	+++
Decapeptyl	++	++	+	+	–

0: ineffective (0–10%), +: weak (11–20%), ++: medium (21–30%), +++: strong (>30%)

J. Med. Chem. *40,* 3353 (1997)

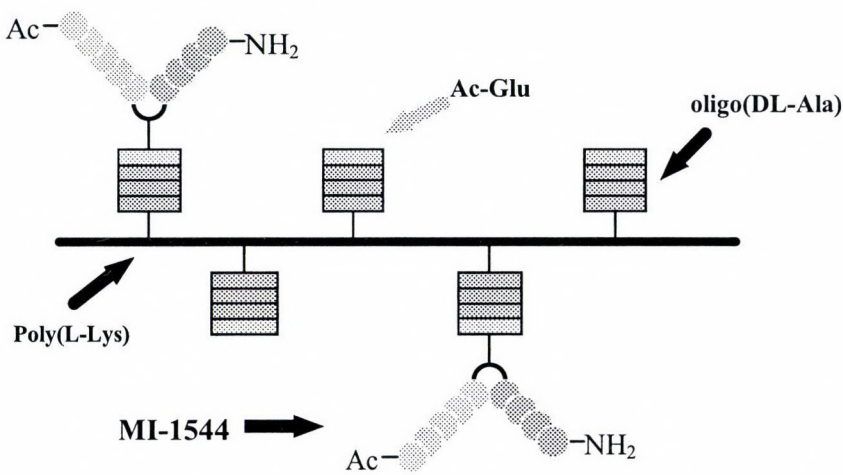

J. Cancer Res. Clin. Oncol *120,* 578 (1994)

Fig. 13. The shematic diagram of the branched chain AcEAK-peptide conjugate

According to our *in vitro* experiments the MI-1544 induces a 33–35% decrease of cell numbers of MCF-7 and MDA-MB-231 human breast cancer cell lines at a dose of 30 μM. The biodegradable polymeric carrier AcEAK alone inhibited cell proliferation by only 13–15%, while the MI-1544-AcEAK conjugate, applied in the same dose, was capable of producing 45–50% inhibition of cell proliferation. Our *in vivo* experiments using immune suppressed mice showed that MI-1544 applied twice daily s.c., inhibited the growth of xenografts by 30%. This effect was potentiated (70%) by the presence of the polymeric carrier in the conjugate, while the carrier by itself did not cause any tumor growth inhibition [22]. Thus, the polymeric polypeptide carrier may be supposed to increase the stability of the GnRH antagonist and to prevent the rapid excretion of the covalently bound peptide molecule. While the tumorous animals died after 3–4 months of tumor implantation, 25–30% of the conjugate treated animals became tumor-free and their lifetime was equal to the tumor-non-treated animals (Fig. 14).

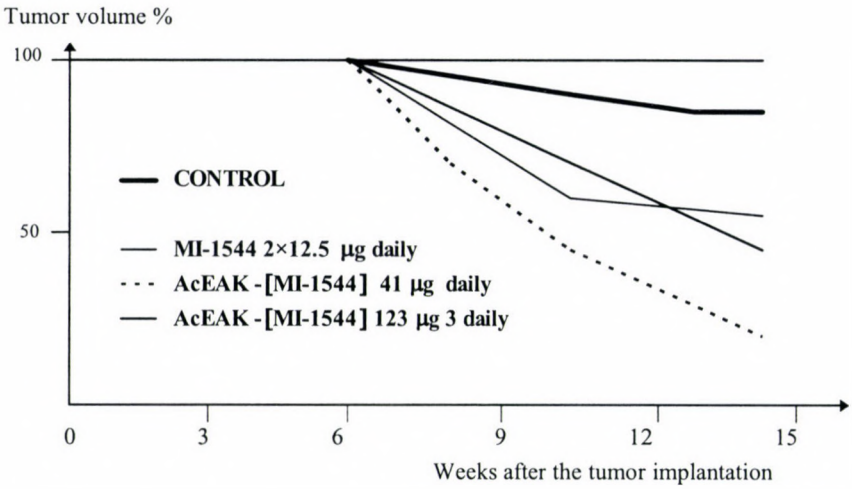

J. Cancer. Res. Clin. Oncol. *120,* 578 (1994)

Fig. 14. The antitumor effects of GnRH analogs on MDA-MB-231 human breast tumor xenografts

The blood survival and the biodistribution of [^{125}I]-MI-1544 and its conjugate ([^{125}I]-MI-1544-AcEAK) was also studied and it was found that the conjugate showed longer blood survival and there was also a different pattern of biodistribution. The higher levels in organs and the greater blood survival resulted in an increased whole body retention of ^{125}I, at about 60%. AcEAK was labeled with ^{111}In, too. [^{121}In]-AcEAK-MI-1544 conjugate had a greater whole body retention of about 80%. From our studies it may be concluded that the tissue biodistribution results with the ^{111}In-labeled and ^{125}I-labeled MI-1544-AcEAK are unlikely to be identical [23] (Fig. 15).

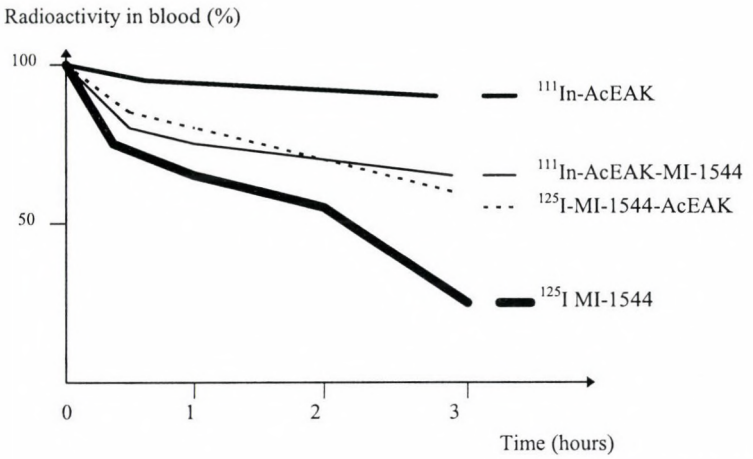

Fig. 15. The clearence of GnRH analogs labeled with ^{125}I and ^{111}In isotopes

On the basis of these favorable results we decided to develop a more water soluble, in large-scale economically producible macromolecular carrier. We found that poly(N-vinyl-pyrrolidone-co-maleic acid) polymer (NVP-MA) could fulfill this criterion. Our analogs were also coupled to the carrier by a tetrapeptide spacer (GFLG) (Fig. 16).

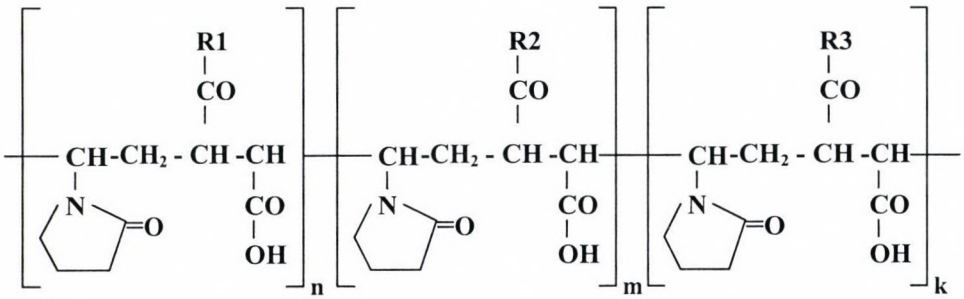

R1: OH, NH_2 or $NH(CH_2)_XCH_3$, X:0-7

R2: GFLG-OH

R3: GFLG-GnRH antagonist MI-1544 or MI-1892

Hung. Pat. No. 212662

Fig. 16. The structure of NVP-MA-GnRH analog conjugates

The glycin residue of the R2 spacer moiety acylated the ε-amino group of Lysine residue of the peptide hormone molecules. The spacer could keep a distance between the backbone of the carrier and the hormone, so the conjugate could bind to the receptor mediated by the hormone residue. On the other hand, the spacer might undergo an enzymatic cleavage causing the peptide hormone to act as a free peptide, too.

The effect of antagonist peptide hormones and their conjugates was tested on the colony-forming ability of four human malignant cell lines [24] (Fig. 17). While the hormone analogs reduced cell survival but only slightly and the copolymer (carrier-spacer) showed also a small effect on the cloning efficiency, the survival of all cell lines was dramatically reduced by the conjugates: the colony formation of cells decreased to practically 0%. The effect of the compounds on proliferation of different human cancer cell lines was studied, as well. In our *in vitro* experiments the conjugates decreased the cell proliferation at a higher rate than did the free peptide hormones themselves.

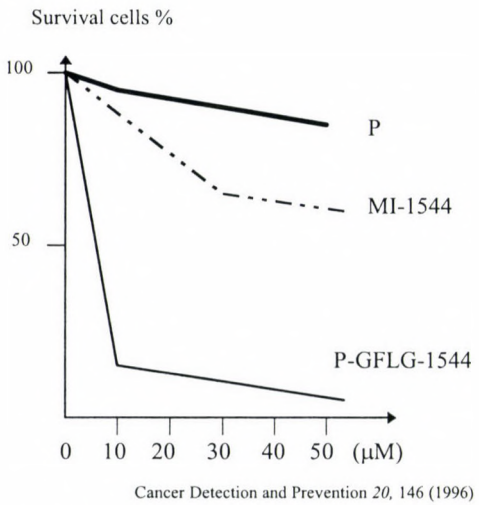

Fig. 17. Inhibition of colony formation by GnRH analogs and conjugates on MDA-MB-231 cell lines

On the other hand, in *in vivo* experiments the MI-1544-NVP-MA and MI-1892-NVP-MA conjugates decreased the tumor growth of steroid dependent and independent breast cancer xenografts by 40–50% [17] (Fig. 18).

The GnRH-III-NVP-MA (P-X-GnRH-III) conjugate showed in *in vivo* experiments outstandingly good results. It decreased the tumor growth of MDA-MB-231 xenografts by 80% in a treatment of 9 weeks and even tumor free animals could be found. In case of MCF-7 xenografts c/a. 70% decrease of tumor growth was found in a 6 week experiment [25] (Fig. 19).

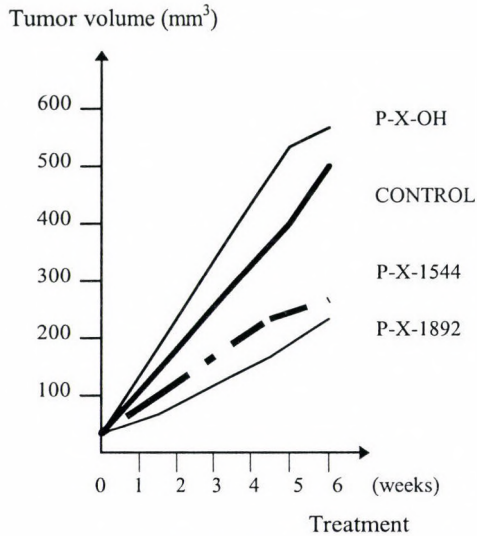

Fig. 18. The effect of GnRH conjugates on MDA-MB-231 xenografts

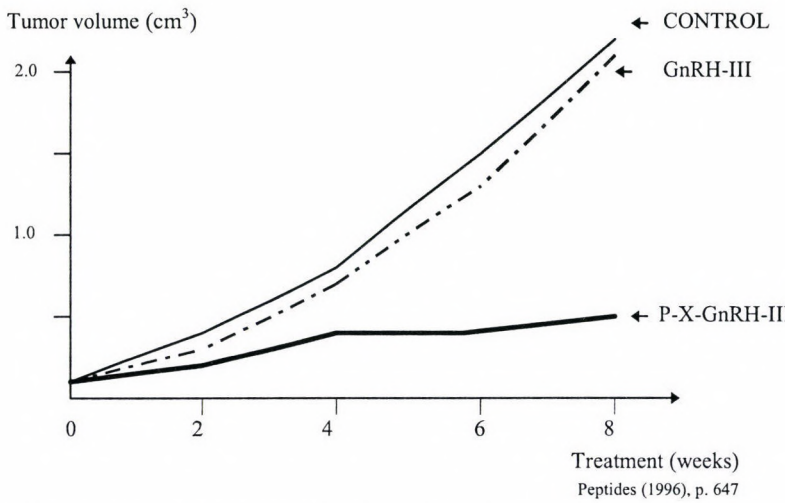

Fig. 19. The effect of GnRH-III and P-X-GnRH-III conjugate on MDA-MB-231 xenografts

It is important to note that the conjugate did not diminish at all the number of binding sites of tumor cells, neither did the inhibition of tumor growth alter during the long-lasting treatment. It was in good agreement with our other results when we stud-

ied the kinetic parameters of the binding and cell-distribution of peptides and their conjugates in our further experiments. For these studies tritium labeled peptides and ^{125}I labeled hormone analogs were used (Fig. 20).

LAMPREY GnRH-III:
Glp-His-Trp-Ser-His-Asp-Trp-Lys-*Pro*-Gly-NH_2 *LG3

HUMAN GnRH ANTAGONIST:
Ac-DTrp-DCpa-DTrp-Ser-*Tyr*-DLys-Leu-Arg-Pro-DAla-NH_2 *HGA

SPACER:
-Gly-Phe-Leu-Gly- X

POLIMER CARRIER:
POLY(N-VINYL PYRROLIDON-CO-MALEIC ACID) *P
|
Tyr-NH_2

LABELED CONJUGATES:

P-X-*LG3 *P-X-LG3
P-X-*HGA *P-X-HGA

15th Amer. Pept. Symp. Abstr. 2-143 (1997)

Fig. 20. Labelling of conjugates in different positions

The tritium labeled peptides were synthesized according to our method called precursor amino acid method [26].

Using these radiolabeled peptide hormone analogs we found that GnRH conjugates specifically bind to human tumor cell lines and xenografts. But we could not find any binding effect with the radiolabeled carrier. Comparing the kinetics of the binding of free peptide hormones and their conjugates, we found that the conjugation increases the stability of the receptor-conjugate complex, and the binding is determined by the GnRH molecule in the conjugate.

Other experiments with tumor free animals showed that the conjugation increased the biological half-life of hormone analogs in different organs. These results are in harmony with the phenomenon that the concentration of conjugates 5-times surpasses that of the free hormones in the tumor cells. Forty-eight hours after the treatment the highest radioactivity was found in tumors and in the kidney verifying the retard effect of conjugates which create the constant, high hormone concentration required for tumor inhibition [27] (Fig. 21).

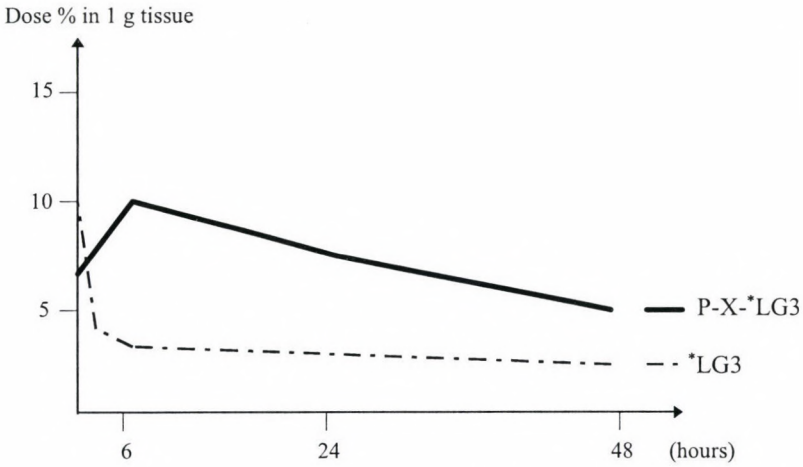

Proc. Am. Assoc. Cancer Res. *38*, 433 (1997)

Fig. 21. Doses of radioactivity in 5 organs of CBA/CA female mice after s.c. treatment

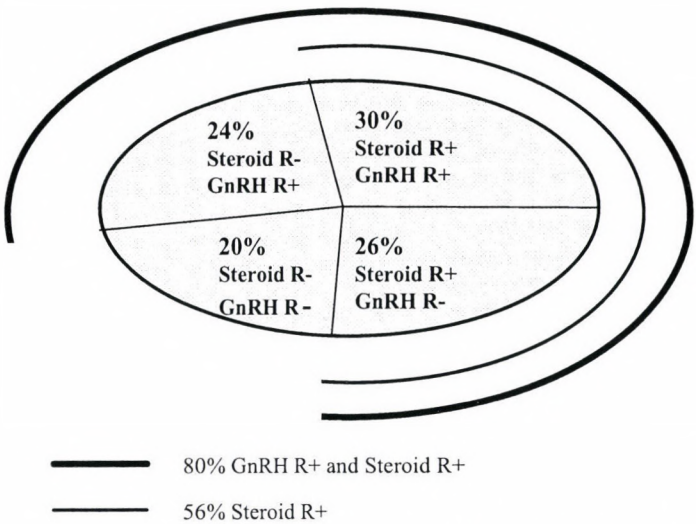

Fig. 22. The distribution of receptor status of human breast cancers

The fundamental condition of selective antitumor effect of GnRH analogs is the presence of GnRH receptors in the tumors. In the National Institute of Oncology (Budapest) GnRH receptor estimations were carried out on primer breast cancer patients parallel with steroid receptor estimations. Fifty-four per cent of breast cancer samples proved to be GnRH receptor positive. Fifty-six per cent of tumors were

steroid receptor positive, while 24 per cent of them were steroid receptor negative, but GnRH receptor positive [28] (Fig. 22).

Thus the GnRH conjugates with direct antitumor effect may be suitable for the treatment of steroid independent breast cancer patients.

Antitumor effect of peptides derived from Somatostatin analogs

As it is known, the native Somatostatin is a general antisecretory hormone which inhibits the secretion of growth hormone and the release of some other hormones as glucagon, insulin and gastrin controlling some cell functions, too.

The inhibitory effect of the Somatostatin analogs against tumor cells have been observed in the past few years, but their clinical application as antitumor drugs was inhibited by their nondesirable side-effects. Although some antisecretory hormones are in use for the treatment of tumors, an intensive research is still in progress for the development of Somatostatin analogs with more selective antitumor effect (Fig. 23).

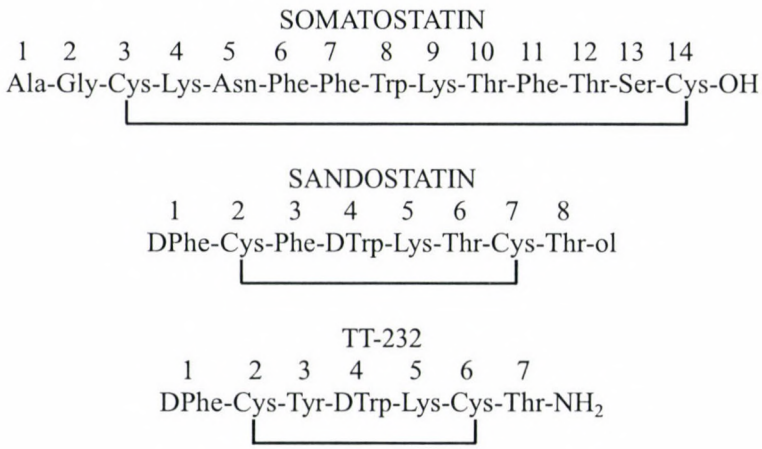

Fig. 23. The structure of Somatostatin analogs

We have also produced a large number of small peptide derivatives of Somatostatin in order to increase their biological action, selectivity and duration time. We selected the cyclic octapeptide of somatostatin as a leadcompound systematically substituting this molecule. The best of these analogs can be seen in [29] (Fig. 24).

From a large number of compounds we selected the most active analogs on the basis of their tyrosine kinase inhibitory and antiproliferative effects. One of our best analogs was a heptapeptide, TT-232 containing a 5 member ring of amino acids which strongly inhibited the tyrosine kinase activity in different colon tumor cells,

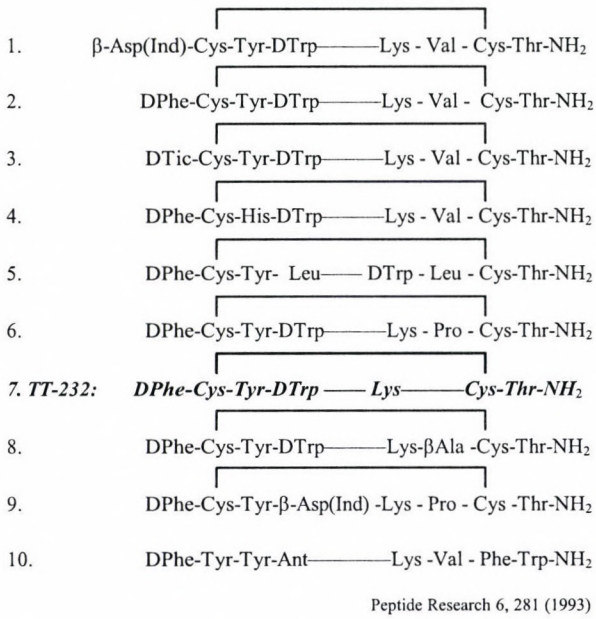

Fig. 24. Structure of small peptide derivatives of Somatostatin

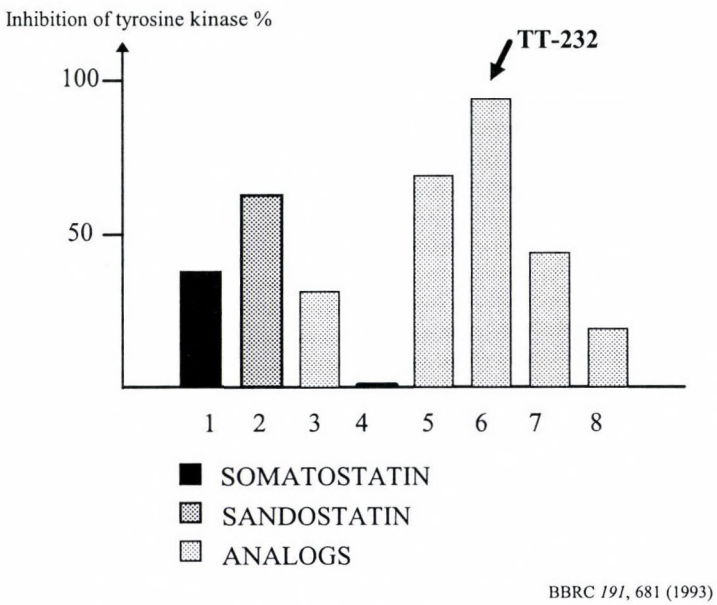

Fig. 25. Tyrosine kinase activity of somatostatin analogs on HT-29 colon tumor cells

which well correlated with the cell-proliferative inhibitory effect. However, at the same time it did not inhibit the growth hormone release either *in vitro* or *in vivo* from rat pituitary cells [30] (Fig. 25).

We have shown that the TT-232 is not bound in the hypothalamus, the hypophysis or in the cortex, but it is significantly bound to the tumor cells, supporting our earlier investigations. We have also shown that this tumorselective peptide significantly inhibits the tumor growth on different animal tumor models (S 180 sarcoma, Colon 26) *in vivo* inducing apoptosis, as a result of which some animals became tumor free (Fig. 26).

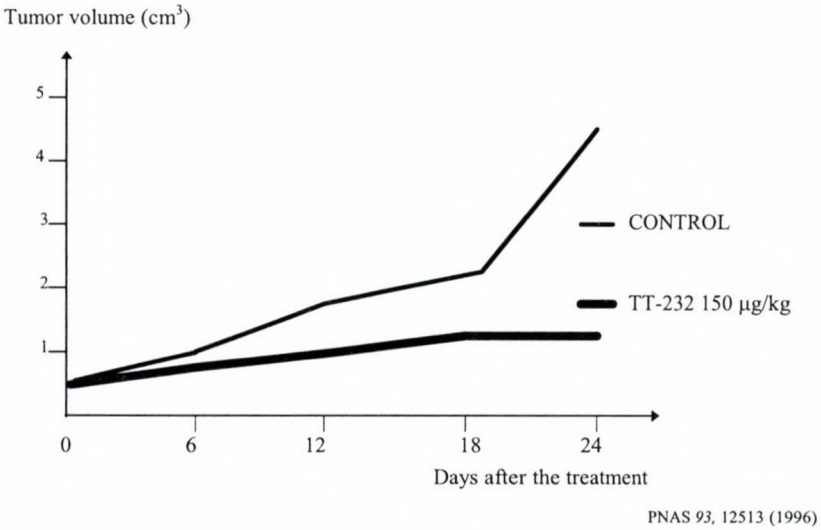

Fig. 26. The effect of TT-232 on the growth of Colon 26 tumors in mice

The TT-232 Somatostatin analog selected for drug developing purposes also showed antiproliferative effect on many other tumor cell lines (MCF-7 human breast, PC3 human prostate, SW 620 and HT 29 human colon tumor cells) in *in vitro* experiments. This analog proved to be effective on more than 60 human tumor cell lines by the measurements of the National Cancer Research Institute of the USA [31].

Figure 27 illustrates the antitumor effect of TT-232 on human breast xenograft (MDA-MB-231) model [31].

As it can be seen, tumor-free animals could be found after the 30 day treatment, but the response of some mice to the TT-232 treatment showed big differences. In case of mice more sensitive against the Somatostatin analog the decrease of tumor volume and the high inhibition of tumor growth was also observed after finishing the treatment. The antitumor effect of the compound was significant relatively to the

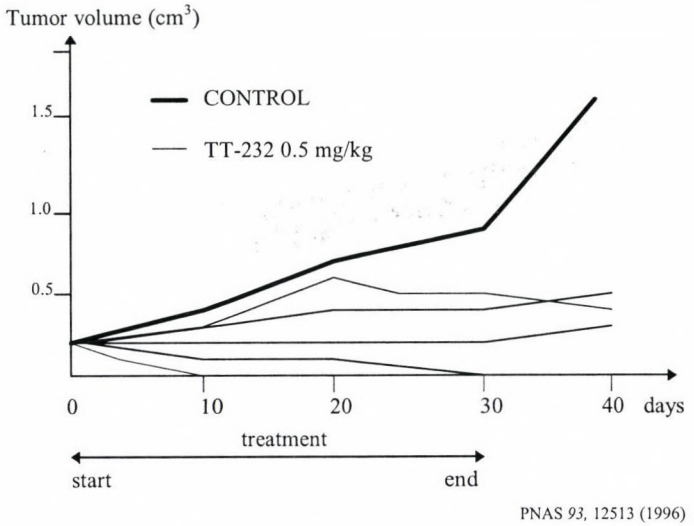

Fig. 27. The effect of TT-232 on the MDA-MB-231 xenografted mice

control group. Besides this, the TT-232 inhibited the tumor in 60% in a 3-week treatment on PC3 prostate tumor (Fig. 28).

The TT-232 treatment at 20 mg/kg caused 100% survival of mice 60 days after the transplantation contrary to the control group which showed only 20% survival.

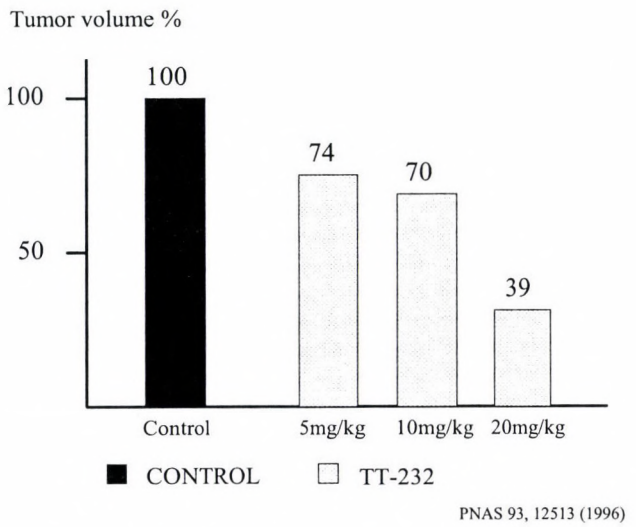

Fig. 28. The effect of TT-232 on PC3 xenografted prostate tumors

This Somatostatin analog also inhibited the formation of tumor in spleen-liver metastasis models of Lewis' lung-tumor cells in mice (Fig. 29).

Investigating the mechanism of action of this compound we have shown that its wide range, dose-dependent and strong antiproliferative effects are in connection with the induction of the apoptosis, and the inhibition of the tyrosine kinases which play an important role in apoptosis (Fig. 30).

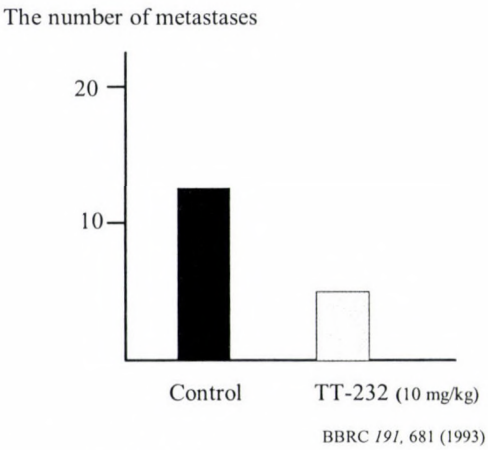

Fig. 29. The effect of TT-232 in the Lewis'-lung tumor metastasis model

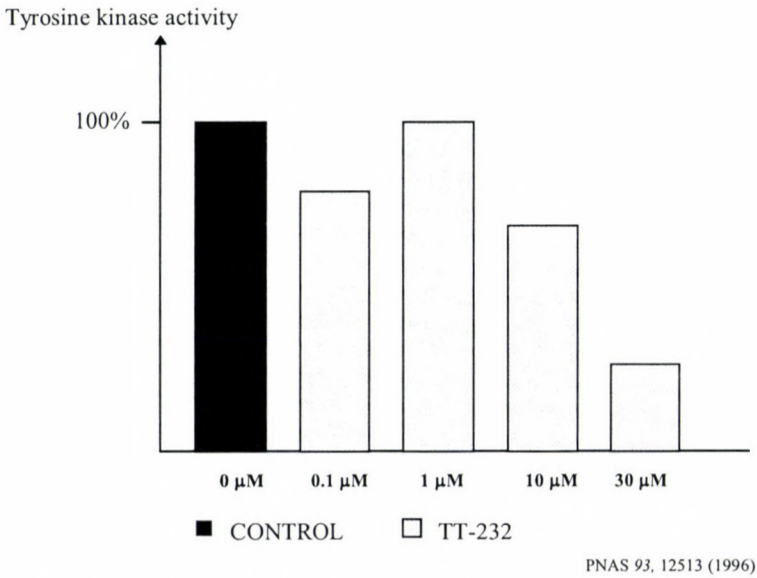

Fig. 30. The effect of TT-232 on the dose-dependence of tyrosine kinase activity

It has also come to light that the TT-232 activates tyrosine phosphatases in HT-29 human colon tumor cells for a short period of time [32] (Fig. 31).

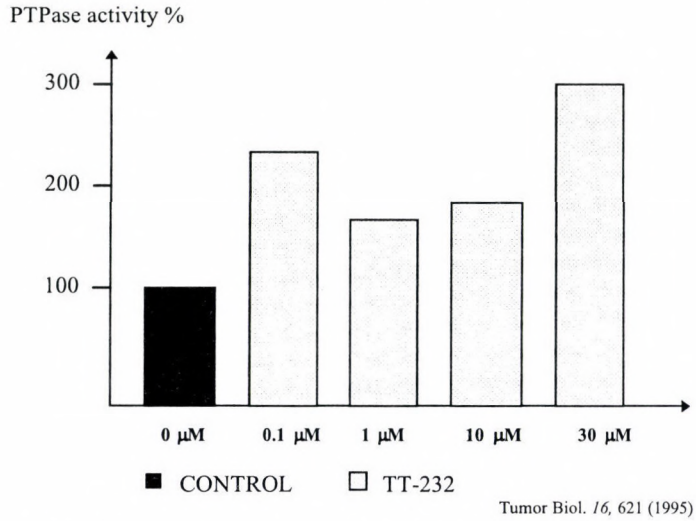

Fig. 31. The dose-dependence of the PTPase activity induced by TT-232

The TT-232 inhibits the tyrosine kinases in the long run, leading finally to apoptosis. Figure 32 shows the time dependence of apoptosis [33].

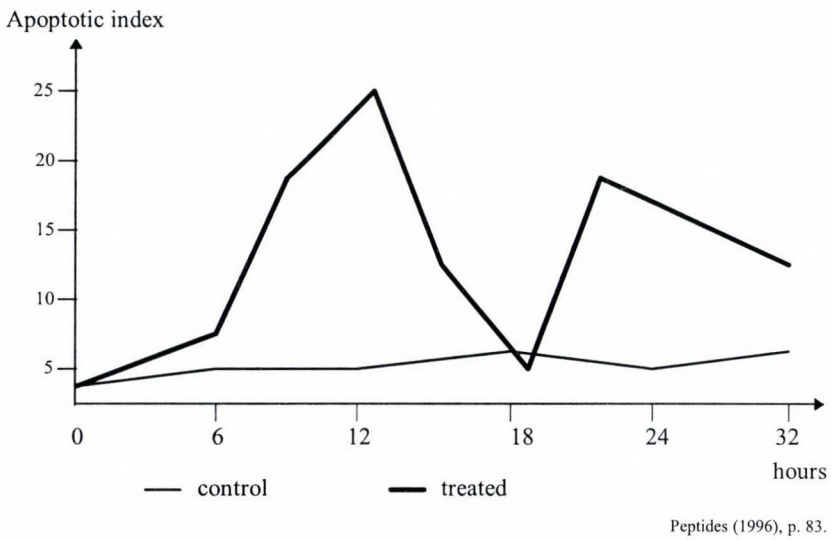

Fig. 32. Time dependence of the apoptotic effect of TT-232 on HT-29 human colon tumor cells

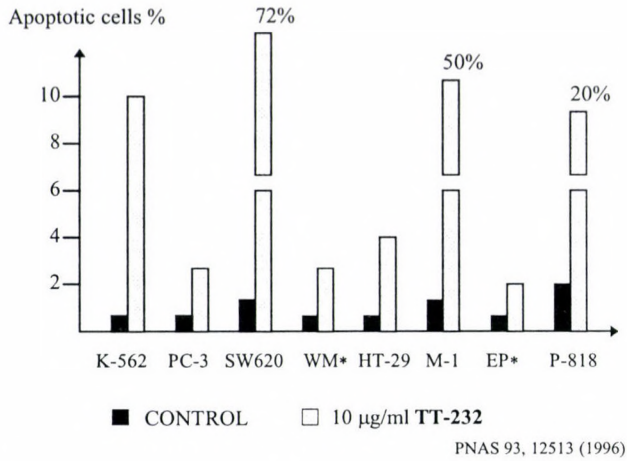

Fig. 33. The apoptotic inducing effect of TT-232 in different cell lines

We have shown the strong apoptosis-inductive effect of TT-232 in many of human cell lines [31] (Fig. 33), and it is being preclinically tested at present.

Summarizing the significance of this research we can say that while the antitumor effect of peptide hormones was formerly regarded as a nonspecific side-effect, as a consequence of the natural hormonal effect, we have shown that the new GnRH analogs acting without any hormonal effect and Somatostatin analogs with strong antitumor and tyrosine kinase inhibitory activity but no hormonal effect may be regarded as a real breakthrough in the research of the antitumor peptides. We have shown that these new peptide derivatives exert their *in vivo* antitumor activity not by their endocrine effects.

These peptides selectively inhibit not only the proliferation of some breast, prostate an colon tumor cells, but they also change their signal transduction mechanisms and induce apoptosis.

HYDROPHOBIC PEPTIDE DERIVATIVES AGAINST THE DRUG-RESISTANT TUMORS

To complete the review of our work searching for new and effective drug candidates against tumors the significance of the peptide derivatives against the multidrug resistance (MDR) developed in our laboratory has to be pointed out.

It is known that the majority of the tumor cells become resistant against the most effective antitumor agents. The reason for this drug resistance is the function of a transmembrane protein so-called P-glycoprotein or MDR1. This protein actively inhibits the cellular uptake of antitumor drugs, which are generally hydrophobic in

nature. We observed and proved in *in vitro* test systems that small peptides containing many hydrophobic groups but no polar groups at all are able to inhibit the resistance of P-glycoprotein, which plays an active role in drug transport. Structure, activity and retention times of some peptides are shown in [34–35] (Table 5).

Table 5
Some effective small peptide substrates of MDR1

Structure	K_m (nM)	T_{ret} (min)
1. [BOC-Pro-Glu(OH)]$_2$-Lys-OMe	>50000	1.1
2. (Z-Pro)^2-Lys-OMe	1650	1.6
3. [BOC-Pro-Pro-Glu(OBzl)]$_2$-Lys-OMe	100	2.8
4. [BOC-Pro-Glu(OBzl)]$_2$-Lys-OMe	40–50	3.4
5. (Boc-Glu(OBzl))$_2$-DAB-OMe	30–40	3.6
6. (Boc-Glu(OBzl))$_2$-Lys-OMe	20–30	3.9
7. Boc-Asp(OBzl)-Lys(Z)-OtBu	50	5.3
8. [BOC-Asp(OBzl)-Glu(OBzl)]$_2$-Lys-OMe	20–60	11.1
9. FMOC-Glu[Lys(Z)OtBu)]$_2$	10–20	12.5

Peptides (1996), p. 801.

On the one hand, a close correlation can be seen between the retention time measured by HPLC method and the activation constants of the ATPase enzyme attached to the P-glycoprotein of different peptides. On the other hand, it was successfully proved that these strongly hydrophobic peptides effectively inhibit the drug transport

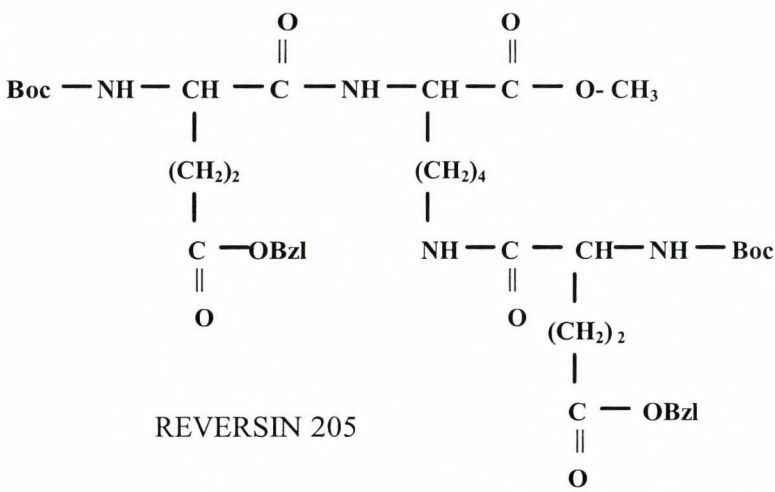

Hung. Pat. Appl. No. P 96032123 (1996)

Fig. 34. The structure of our best MDR1 substrate and inhibitor

out of the cells and doing so, they can stop the resistance of tumor cells in *in vitro* systems. These peptide derivatives inhibit the function of P-glycoprotein and this way the tumor cells which are resistant against vincristin can also uptake the antitumor drugs e.g. vincristin.

The mechanisms of action of two peptides were investigated in detail by *in vitro* methods. The most active compound the Reversin 205 (Fig. 34) was 1–2 magnitude higher active than the Cyclosporin analog which was developed by American scientists and which is being tested clinically against drug resistance at the moment. According to the preliminary tests these peptides showed no toxicity and at the same time they increased the survival of mice having resistant tumor.

REFERENCES

1. Matsuo, H., Baba, Y., Nair, R. M., Arimura, A., Schally, A. V. (1971) Structure of the porcin LH- and FSH-releasing hormone. I. The proposed amino acid sequence. *Biochem. Biophys. Res. Commun. 43,* 1334.
2. Burgus, R., Burcher, M., Amoss, M., Ling, N., Monahan, M. W., Rivier, J., Fellows, R., Blackwell, R., Vale, W., Guillemin, R. (1972) Primary structure of the ovine hypothalamic luteinizing hormone-releasing factor (LRF). *Proc. Natl. Acad. Sci. USA 69,* 278.
3. Érchegyi, J., Coy, D. H., Nekola, M. V., Coy, E. J., Schally, A. V., Mező, I., Teplán, I. (1981) Luteinizing hormone-releasing hormone analogs with increased antiovulatory activity. *Biochem. Biophys. Res. Commun. 100,* 915.
4. Karten, M. J., Rivier, J. E. (1986) Gonadotropin-releasing hormone analog design. Structure-function studies forward the development of agonist and antagonists: rationale and perspective. *Endocrine Reviews 7,* 44–66.
5. Teplán, I. (1989) Role, mechanism of action and application of gonadoliberins in reproductive processes. *Acta Biologica Hungarica 40,* 3–36.
6. Kéri, Gy., Nikolics, K., Teplán, I., Molnár, J. (1983) Desenzitization of luteinizing hormone release in cultured pituitary cells by gonadotropin-releasing hormone. *Mol. Cell. Endocrinol. 30,* 109–120.
7. Nicholson, R. J., Maynard, P. V. (1979) Anti-tumour activity of ICI 118630, a new potent luteinizing hormone-releasing hormone agonist. *Br. J. Cancer 39,* 268–273.
8. Klijn, J. G. M., deJong, F. H. (1982) Treatment with a luteinizing hormone-releasing hormone analogue (buserelin) in premenopausal patients with metastatic breast cancer. *Lancet 1,* 1213–1216.
9. Schally, A. V., Redding, T. W., Comaru-Schally, A. M. (1983) Inhibition of prostate tumors by agonistic and antagonistic analogs of LH–RH. *Prostate 4,* 545–552.
10. Vincze, B., Pályi, I., Kremmer, T., Számel, I., Sugár, J., Mező, I., Seprődi, J., Teplán, I. (1990) Effect of LHRH agonist on estradiol sensitive and insensitive human breast cancer cells. *J. Cancer Res. Clin. Oncol. 116,* Suppl. I. 427.
11. Vincze, B., Pályi, I., Daubner, D., Kremmer, T., Bodrogi, I., Számel, I., Sugár, J., Seprődi, J., Mező, I., Teplán, I., Eckhart, S. (1991) Influence of luteinizing hormone releasing hormone agonist on human mammary carcinoma cell lines and their xenografts. *J. Steroid Biochem. Molec. Biol. 38,* 119–126.
12. Vincze, B., Pályi, I., Daubner, D., Kremmer, T., Bodrogi, J., Számel, I., Sugár, J., Mező, I., Seprődi, J., Teplán, I. (1990) Influence of LHRH agonist treatment on the steroid receptor synthesis in the MCF-7 cell line and in xenograft-bearing mice. In: Görög, S. (ed.) *Proc. 4th Symp. Analysis of Steroids.* Akadémiai Kiadó, Budapest, pp. 61–68.
13. Nicholson, R. I., Kéri, Gy. (1992) Antitumor activity of Folligen a novel gonadotropin analogue against DMBA-induced tumours in the rat. *Tumor Biology, 13,* 44–50.

14. Kéri, Gy., Balogh, Á., Szőke, B., Teplán, I., Csuka, O. (1991) Gonadotropin-releasing hormone analogues inhibit cell proliferation and activate signal tranduction pathways in MDA-MD-231 human breast cancer cell line. *Tumor Biology 12,* 61–67.
15. Mező, I., Seprődi, J., Vincze, B., Pályi, I., Kéri, Gy., Vadász, Zs., Tóth, G., Kovács, M., Koppán, M., Horváth, E. J., Kálnay, A., Teplán, I. (1996) Synthesis of GnRH analogs having direct antitumor and low LH-releasing activity. *Biomed. Pept., Prot., Nucleic Acid 2,* 33–40.
16. Szende, B., Takács, J., Mező, I., Szegedi, Zs., Kéri, Gy. (1994) Binding of a radiolabelled tumorselective GnRH analog to PC-3 human prostate cancer cells and the induction of apoptosis. *Endocrine 2,* 645–649.
17. Vincze, B., Pályi, I., Gaál, D., Pató, J., Móra, M., Mező, I., Teplán, I., Seprődi, J. (1996) *In vivo* studies of the new gonadotropin-releasing hormone antagonist-copolimer conjugates having antitumor activity. *Cancer Detect., Prev. 20,* 153–159.
18. Sower, S. A., Chiang, Y.-C., Lovas, S., Conlon, J. M. (1993) Primary structure and biological activity of a third gonadotropin-releasing hormone from lamprey brain. *Endocrinology 132,* 1125–1131.
19. Lovas, S., Conlon, J. M., Vincze, B., Pályi, I., Gaál, D., Seprődi, J., Kálnay, A., Mező, I., Teplán, I., Tóth, G., Kovács, M. (1997) Anti-tumor effect of GnRH-III. US. Pat. No.: 5,593,965
20. Lovas, S., Pályi, I., Vincze, B., Mező, I., Teplán, I., Tóth, G., Kovács, M., Murphy, R. F. (1998) Antitumor activity of lamprey-GnRH-III. *Peptides Res. J. Peptide Res. 52,* 389–398.
21. Mező, I., Lovas, S., Pályi, I., Vincze, B., Kálnay, A., Turi, G., Vadász, Zs., Seprődi, J., Idei, M., Tóth, G., Gulyás, É., Ötvös, F., Mák, M., Horváth, E. J., Teplán, I., Murphy, R. F. (1998) Synthesis of gonadotropin-releasing hormone III. analogs, structure-antitumor activity relationships. *J. Med. Chem. 40,* 3353–3358.
22. Vincze, B., Pályi, I., Daubner, D., Kálnay, A., Mező, I., Hudecz, F., Szekerke, M., Teplán, I., Mező, I. (1994) Antitumor effect of a gonadotropin-releasing hormone antagonist (MI-1544) and its conjugate on human breast cancer cells and their xenografts. *J. Cancer Res. Clin. Oncol. 120,* 578–584.
23. Mező, G., Mező, I., Pimm, V. M., Kajtár, M., Seprődi, J., Teplán, I., Kovács, M., Vincze, B., Pályi, I., Idei, M., Szekerke, M., Hudecz, F. (1996) Synthesis conformation, biodistribution and hormon-related *in vitro* antitumor activity of a gonadotropin-releasing hormone antagonist-branched polypeptide conjugate. *Bioconjugate Chem. 7,* 642–650.
24. Pályi, I., Vincze, B., Kálnay, A., Turi, G., Mező, I., Teplán, I., Seprődi, J., Pató, J., Móra, M. (1996) Effect of gonadotropin-releasing hormone analogs and their conjugates on gonadotropin-releasing hormone receptor-positive human cancer cell lines. *Cancer Det. Prev. 20,* 146–152.
25. Mező, I., Seprődi, J., Vadász, Zs., Teplán, I., Vincze, B., Pályi, I., Kálnay, A., Turi, G., Móra, M., Pató, J., Tóth, G., Lovas, S., Murphy, R. F. (1996) Antitumor activity of GnRH analogs and their conjugates with poly(N-vinylpyrrolidone-co-maleic acid). In: Kaumaya, P. T. P., Hodges, R. S. (eds), *Peptides: Chemistry, Structure and Biology.* Mayflower Scientific Ltd. Kingswinford, pp. 239–240.
26. Mező, I., Teplán, I., Seprődi, J., Morgat, J. L., Fromageot, P., Tóth, G., Sirokmán, F. (1978) Synthesis of (Tyr-^{3}H)4-Angiotensin II. and (Phe-^{3}H)^{8}-Angiotensin II. via halogen-derivatives of Angiotensin II. *J. Lab. Comp. Radiopharm. 14,* 557
27. Vincze, B., Pató, J., Mező, I., Tóth, G., Pályi, I., Gaál, D., Kálnay, A., Stefik, I., Lovas, S., Teplán, I., Murphy, R. F. (1997) GnRH analogue conjugates with selective antitumor activity: pharmacological studies. *Proc. Am. Assoc. Cancer Res. 38,* 433.
28. Mező, I., Vincze, B., Pató, J., Pályi, I., Tóth, G., Gulyás, É., Kálnay, A., Teplán, I., Lovas, S., Murphy, R. F. (1998) Studies on antitumor activity of GnRH analog conjugates. In: Bajusz, S., Hudecz, F. (ed.) *Peptides,* Akadémiai Kiadó, Budapest, p. 436.
29. Kéri, Gy., Mező, I., Vadász, Zs., Horváth, A., Idei, M., Vántus, T., Balogh, Á., Bökönyi, Gy., Bajor, T., Teplán, I., Tamás, J., Mák, M., Horváth, J., Csuka, O. (1993) Structure-activity relationship studies of novel somatostatin analogs with antitumor activity. *Peptide Research 6,* 281–288.
30. Kéri, Gy., Mező, I., Horváth, A., Vadász, Zs., Balogh, Á., Idei, M., Vántus, T., Teplán, I., Mák, M., Horváth, J., Pál, K., Csuka, O. (1993) Novel somatostatin analogs with tyrosine kinase inhibitory and antitumor activity. *Biochem. Biophys. Res. Commun. 191,* 681–687.

31. Kéri, Gy., Érchegyi, J., Horváth, A., Mező, I., Idei, M., Vántus, T., Balogh, Á., Vadász, Zs., Bökönyi, Gy., Seprődi, J., Teplán, I., Csuka, O., Tejeda, M., Gaál, D., Szegedi, Zs., Szende, B., Roze, C., Kalthoff, H., Ullrich, A. (1996) A tumor-selective somatostatin analog (TT-232) with strong *in vitro* and *in vivo* antitumor activity. *Proc. Natl. Acad. Sci. USA 93,* 12513–12518.
32. Vántus, T., Csermely, P., Teplán, I., Kéri, Gy. (1995) The tumor-selective somatostatin analog, TT-232 induces a biphasic activation of phospotyrosine phosphatase activity in human colon tumor cell line, SW620. *Tumor Biology 16,* 261–267.
33. Kéri, Gy., Érchegyi, J., Horváth, A., Idei, M., Teplán, I., Csuka, O., Tajeda, M., Gaál, D., Őrfi, L., Szegedi Zs., Szende, B. (1998) Induction of apoptosis and non-apoptotic programmed cell death by antitumor peptides and peptidomimetics. In: Ramage, R., Epton, R. (eds) *Peptides* p. 83.
34. Sarkadi, B., Seprődi, J., Teplán, I., Mező, I., Vadász, Zs., Magócsi, M., Vincze, B., Pályi, I., Csuka, O., Vegyületek drogrezisztencia megszüntetésére, Magyar szabadalom: 215132 (1998), PCT bejelentés: IB 9400144.
35. Seprődi, J., Mező, I., Vadász, Zs., Szabó, K., Sarkadi, B., Teplán, I. (1998) Peptide derivatives against multidrug resistance. In: Ramage, R., Epton, R. (eds) *Peptides* p. 801.

Acta Biologica Hungarica 51 (1), pp. 31–36 (2000)

PHOTOPERIODIC INDUCTION OF OVARIAN GROWTH AND PLASMA ESTRADIOL SECRETION IN A MIGRATORY FINCH, *EMBERIZA MELANOCEPHALA:* INVOLVEMENT OF CIRCADIAN RHYTHM

MANOJ KUMAR MISHRA and P. D. TEWARY*

Reproduction Biology Unit, Department of Zoology, Banaras Hindu University, Varanasi-221 005, India

(Received: May 17, 1998; accepted: October 29, 1998)

To demonstrate the involvement of circadian rhythm in photoperiodic time measurement, photosensitive female blackheaded buntings were kept under different photoperiodic schedules consisting of 6 h of main photophase coupled with scotophases of various durations. Ovarian mass and circulating plasma estradiol concentration were found to be elevated in cycles of 6L:6D, 6L:36D, 6L:54D and in control 15L:9D groups. But cycles of 6L:18D, 6L:42D and 6L:66D did not stimulate ovarian growth or elevate circulating plasma estradiol concentration. These results are consistent with the Bünning hypothesis according to which a photoperiodic response is elicited as a result of the coincidence of light with the photoinducible phase of an endogenous circadian rhythm. The results thus indicate the involvement of a circadian rhythm of photoinducibility in ovarian growth and estradiol secretion.

Keywords: Photoinducible – blackheaded bunting – estradiol – external coincidence model

INTRODUCTION

An endogenous circadian rhythm with a period of 24 h is involved in various photoperiodic responses of birds. To date much evidence has been gathered indicating that photoperiodic induction of gonadal maturation involves an endogenous circadian component [6, 9, 11, 12, 14, 17, 19, 26, 33, 37]. In some avian species a circadian rhythm has also been implicated for photorefractoriness and its dissipation [13, 14, 22, 26, 27, 32]. It has been established that endogeous circadian rhythm are entrained by natural light-dark cycles, their properties and functions have been tested by several workers through artificial manipulation of light-dark schedules, and Nanda and Hamner [23] first introduced resonance light-dark cycles to test the role of endogenous circadian rhythm in the photoperiodic time measurement which involves alternating light and dark schedules so that the amount of light experienced is dissociated from when during the circadian period light is experienced.

* Corresponding author.

0236-5383/2000/$ 5.00

For last three and half decades the resonance experiments have been performed to study the involvement of circadian rhythmicity on several avian species such as house finches *(Carpodacus mexicanus),* Japanese quails *(Coturnix coturnix japonica),* white crowned sparrows *(Zonotrichia leucophrys gambelii),* golden crowned sparrows *(Zonotrichia atricapilla),* European starlings *(Sturnus vulgaris),* black-headed bunting *(Emberiza melanocephala),* rose finches *(Carpodacus erythrinus),* and house sparrows *(Passer domesticus)* [9, 10, 11, 18, 26, 28, 29, 32, 33]. Under the Nanda–Hamner protocol the males of avian species have usually been investigated and very few reports on females are available. The objective of the present study was to determine whether an endogenous circadian rhythm is involved in the photoperiodic time measurement of female blackheaded buntings. As variables, we measured ovarian growth and circulating plasma estradiol levels.

MATERIAL AND METHODS

The blackheaded bunting is a migratory finch that arrives in Varanasi (25°18′N; 83°1′E) in the fall (September/October) and returns to its breeding grounds (West Asia and Eastern Europe) in late spring [1]. Adult female buntings were captured locally in December and placed in an outdoor aviary. They were acclimatized in the laboratory for two week. Birds were exposed to short photoperiods (8L:16D) for two months to ensure photosensitivity. Photosensitive buntings were divided into seven groups (n = 5 birds/group) one control and six experimental, placed in wirenet cages (5 birds/cage) and were kept under different photoperiodic schedules 6L:6D, 6L:18D, 6L:30D, 6L:42D, 6L:54D, and 6L:66D as experimental, and 15L:9D as control.

Food and water were supplied *ad libitum* during light hours. The photoperiodic chambers were illuminated by 20 W fluorescent tubes, and the light intensity was about 400 lux at perch level. All birds were laparotomized before the beginning of the experiments. Ovarian weight was observed *in situ* and compared with the standard sets of known ovarian weight. The error possible by this method is ±20% [30]. Before the beginning of the experiment, four birds were killed and their blood was collected in heparinized tubes and centrifuged at 4 °C. Blood plasma was collected and stored at –20 °C for further assay of estradiol. On day 35, all birds from each group were weighed and killed, and ovaries were dissected out. Blood was collected in heparinized tubes, centrifuged and plasma was stored at –20 °C untill assayed. The dissected ovaries were cleared of extra tissues and weighed on an electronic balance after the luminal fluid was pressed gently on folded filter paper. The circulating plasma estradiol level was measured by using an estradiol direct radioimmunoassay kit. The radioactive was I^{125} and this kit was used without extraction (Biotecx laboratories Inc. 6023, South loop, East Huston, TX 77033). The kit was highly specific for estradiol. The cross reactivity of 17β-estradiol was 100%. Statistical analysis was done using one way analysis of variance (ANOVA) and Student's *t*-test.

RESULTS

Results obtained from present investigation is summarised in Fig. 1. Significant variations in ovarian growth ($F = 194.051$, df 28, 6, $P < 0.001$) and circulating plasma estradiol level ($F = 38.706$, df 14, 6, $P < 0.001$) were observed. With regard to pretreatment, significant increases ($P < 0.001$) in ovarian growth and plasma estradiol level were found in control group, when exposed to long days (15L:9D), indicating that at the time of experimental exposure, birds were completely photosensitive.

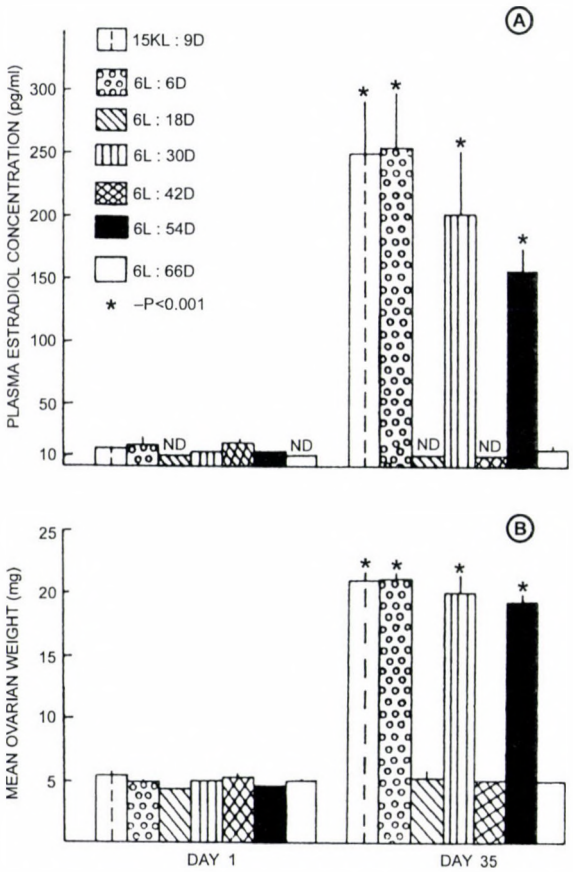

Fig. 1. Plasma estradiol level (A) and ovarian growth (B) of female blackheaded bunting in response to different light-dark cycles, consisting of main photophase of 6 h followed by darkphase of different durations. The ovarian growth and plasma estradiol levels were significantly increased ($P < 0.001$) compared to pretreatment levels in control (15L:9D) as well as 6L:6D, 6L:30D and 6L:54D groups. The photoperiodic groups 6L:18D, 6L:42D and 6L:66D showed no significant variation with pretreatment levels of ovarian growth and plasma estradiol concentration. Vertical lines: ±Standard Error of Mean, n = 5 birds/group. ND = non detectable (<10 pg/ml)

Significant increases ($P < 0.001$) in ovarian mass and plasma estradiol level were also observed in birds under photoperiod of 6L:6D, 6L:30D and 6L:54D groups. No significant effects were observed in 6L:18D, 6L:42D and 6L:66D photoperiodic groups. Further, the average ovarian gowth and plasma estradiol level of 15L:9D and 6L:6D groups were also significantly higher ($P < 0.01$ and $P < 0.05$, respectively) than those of 6L:54D group. The ovarian growth of 15L:9D and 6L:6D groups were also significantly higher ($P < 0.1$) than that of the 6L:30D group but the difference in plasma estradiol level was statistically not varied significantly. The ovarian growth was at its minimum level (about 4–6 mg) and plasma estradiol was at its basal level in 15L:9D, 6L:6D, 6L:30D, 6L:42D and 6L:54D while it was non-detectable in 6L:18D and 6L:66D before photostimulation.

DISCUSSION

The results of the present study show photoperiodic response in the control group 15L:9D and birds under photoperiods of 6L:6D, 6L:30D and 6L:54D. No response was obtained for 6L:18D, 6L:42D and 6L:66D. This clearly suggests that the photoperiodically induced ovarian growth and estradiol production in female blackheaded bunting involves an endogenous circadian component of photosensitivity. This is in agreement with the external coincidence model proposed by Bünning [4] which was further developed by Pittendrigh and Minis [24] and Bünning [5]. Using the framework of the external coincidence model, we interprete our data as follows: In the 15L:9D and 6L:6D light falls daily, and in 6L:30D and 6L:54D groups it falls at alternate cycles in the photosensitive phase resulting in a positive response. On the other hand, in photoperiodic groups of 6L:18D, 6L:42D and 6L:66D light is restricted only to the photoinsensitive or non-photoinducible phase of the circadian rhythm, and thus a response fails to occur [18, 28, 34].

The ovarian response of the female blackheaded bunting is consistent of several avian species with males such as house finches [11]; Japanese quails [9, 14]; white and golden crowned sparrow [33]; male blackheaded buntings [16, 17, 29]; yellow throated sparrows [31], rose finches [18], and those of females such as yellow throated sparrows and rose finches [28]. Wolfson [36] also observed gonadal growth in Juncos *(Junco hyemalis)* under 8L:8D. In contrast, 8L:8D cycles have no gonadal response in white and golden crowned sparrows [33]. It was suggested that the zeitgeber with a period of 16 h is insufficient to entrain the circadian rhythm of photosensitivity in both *Zonotrichia* species. The plasma estradiol response also showed consistency with earlier reports in Japanese quails, white browned sparrows and female buntings [2, 20, 21, 35]. The blackheaded buntings in 6L:30D and 6L:54D showed slower ovarain growth and estradiol secretion than those of 15L:9D and 6L:6D. This difference can be easily interpretable since no cycle constituted long day treatment, except the control (15L:9D) group in usual photoperiodic sense and it has also been reported that the role of gonadal growth decreases as a number of intervening short days [7, 15]. A weak response in 6L:30D and 6L:54D suggests that pho-

toinducible phase in these groups is not act as strong circadian component and is dampened if not turned over each day by a dawn signal. A similar situation has been reported in Japanese quail and Brahminy myna in which photosensitivity behaves like a damped oscillator [8, 16].

While concluding two points become very clear (i) a circadian rhythm is involved in the photoperiodic time measurement during initiation and maintenance of ovarian growth and plasma estradiol secretion and (ii) the buntings are able to recognize the stimulatory and non-stimulatory photoperiodic schedules assessing whether light is in photoinducible phase or photo non-inducible phase supporting the involvement of an endogenous circadian component during day length measurement.

ACKNOWLEDGMENT

Financial support from Council of Scientific and Industrial Research, New Delhi (Grant No. 0808/EMR-II/93) to PDT is gratefully acknowledged.

REFERENCES

1. Ali, S., Ripley, S. D. (1983) *Handbook of Birds of India and Pakistan.* Vol. 10. Oxford University Press, New York.
2. Brain, P. C., Onagbesan, O. M., Peddie, M. J., Taylor, T. G. (1988) Change in plasma concentration in reproductive steroids in female Japanese quail *(Coturnix coturnix japonica)* raised on long or short photoperiods. *Gen. Comp. Endocrinol. 69,* 174–180.
3. Brünning, J. L., Kintz, B. L. (1977) *Computational Handbook of Statistics* (2nd edition), Foresman&Co., Glenview, Illionis.
4. Brünning, E. (1936) Die endogene Tages rhythmik als Grundlage der photoperiodischen Reaktion. *Berichte der Deutschen Bot. Ges. 54,* 590–607.
5. Bünning, E. (1973) *The Physiological Clock* (3rd edition), Springer, Berlin.
6. Farner, D. S. (1965) Circadian systems in the photoperiodic responses of vertebrates. In: Aschoff, J. (ed.) *Circadian Clocks,* North Holland, Amsterdam. pp. 357–369.
7. Follett, B. K., Farner, D. S., Morton, M. L. (1967) The effects of alternating long and short daily photoperiods on gonadal growth and pituitary gonadotropins in the white crowned sparrow, *Zonotrichia leucophrys gambelii. Biol. Bull. 133,* 330–342.
8. Follett, B. K., Kumar, V., Juss, T. S. (1992) Circadian nature of the photoperiodic clock in Japanese quail. *J. Comp. Physiol. A171,* 533–540.
9. Follett, B. K., Sharp, P. J. (1969) Circadian rhythmicity in photoperiodically induced gonadotropin release and gonadal growth in the quail. *Nature 223,* 968–971.
10. Gwinner, E., Eriksson, L. (1977) Circadian Rhythmik und photoperiodische Zeitmessung beim star *(Sturnus vulgaris). J. Ornithology 118,* 60–67.
11. Hamner, W. M. (1963) Diurnal rhythm and photoperiodism in testicular recrudescence of the house finch. *Science 142,* 1294–1295.
12. Hamner, W. M. (1964) Control of photoperiodism in the house finch demonstrated by interrupted night experiments. *Nature 203,* 1400–1401.
13. Hamner, W. M. (1968) The photorefractory period of the house finch. *Ecology 49,* 211–227.
14. King, V. M., Bentley, G. E., Follett, B. K. (1997) A direct comparison of photoperiodic time measurement and the circadian system in European starlings and Japanese quail. *J. Biol. Rhythm 12,* 431–442.

15. Kumar, V. (1986) Carry over effects of long and short photoperiods on fattening and gonadal development of blackheaded bunting, *Emberiza melanocephala. Acta Physiol. Hung. 67,* 193–198.
16. Kumar, B. S., Kumar, V. (1993) Photoperiodic control of annual reproductive cycle in subtropical Brahminy myna, *Sturnus pagodarum. Gen. Comp. Endocrinol. 89,* 149–160.
17. Kumar, V., Kumar, B. S. (1995) Entrainment of circadian system and variable photocycles (T-photocycle) alters the critical daylength for photoperiodic induction in blackheaded buntings. *J. Exp. Zool. 273,* 297–302.
18. Kumar, V., Tewary, P. D. (1982) Photoperiodic regulation of gonadotrophic recrudescence in common Indian Rose finch: dependence of circadian rhythm. *J. Exp. Biol. 223,* 37–40.
19. Menaker, M. L. (1965) Circadian rhythms and photoperiodism in *Passer domesticus.* In: Aschoff, J. (ed.) *Circadian Clocks,* North Holland, Amsterdam, pp. 325–395.
20. Mishra, M. K., Tewary, P. D. (1998) Photoperiodic regulation of reproduction in migratory bunting, *Emberiza melanocephala:* An evidence for external coincidence model. *Curr. Sci. 74,* 246–248.
21. Mishra, M. K., Tewary, P. D. (1998) Involvement of circadian rhythm in response to ultrashort photoperiods in blackheaded bunting, *Emberiza melanocephala. Acta Biol. Hung. 48,* 453–461.
22. Morton, R. K., Lofts, P., Westwood, N. J. (1969) Manipulation of photorefractoriness in house sparrow *(Passer domesticus)* by circadian light regimes. *General and Comparative Endocrinology 14,* 107–113.
23. Nanda, K. R., Hamner, K. C. (1958) Studies on the nature of endogenous rhythm affecting photoperiodic responses of Biloxi soyabean. *Botanical Gazette 120,* 14–25.
24. Pittendrigh, C. S., Minis, D. H. (1964) The entrainment of circadian oscillations by light and their role as photoperiodic clocks. *American Naturalist 94,* 261–294.
25. Ravikumar, G., Senthilkumaran, B., Tewary, P. D., Goel, A. K. (1995) Circadian aspects of photoperiodic time measurement in a female house sparrow, *Passer domesticus. J. Biol. Rhythm 10,* 319–323.
26. Ravikumar, G., Tewary, P. D. (1990) Photorefractoriness and its termination in the subtropical house sparrow, *Passer domesticus:* involvement of circadian rhythm. *Chronobiol. Int. 7,* 187–191.
27. Sansum, E. L., King, J. R. (1975) Photorefractoriness in a sparrow: phase of circadian sensitivity elucidated by skeleton photoperiods. *J. Comp. Physiol. 98,* 183–188.
28. Tewary, P. D., Dixit, A. S., Kumar, V. (1984) Circadian rhythmicity and initiation of reproductive functions of female passerines. *Physiol. Zool. 57,* 563–566.
29. Tewary, P. D., Kumar, V. (1981) Circadian periodicity and the initiation of gonadal growth in male blackheaded buntings *(Emberiza melanocephala). J. Comp. Physiol. 144,* 201–203.
30. Tewary, P. D., Tripathi, B. K., Kumar, V. (1983) Effect of exogenous prolactin on ovarian growth and fattening in the redheaded bunting, *Emberiza bruniceps. Gen. Comp. Endocrinol. 52,* 315–318.
31. Tripathi, P. M., Tewary, P. D. (1988) Participation of circadian periodicity in the photoperiodic response of the male yellow throated sparrow, *Gymnorhis xanthocollis. Arch. Biol.* (Bruxelles) *99,* 1–9.
32. Turek, F. W. (1972) Circadian involvement in termination of the refractory period in two sparrows. *Science 178,* 1172–1173.
33. Turek, F. W. (1974) Circadian rhythmicity and initiation of gonadal growth in sparrows. *J. Comp. Physiol. 92,* 59–64.
34. Turek, F. W. (1978) Diurnal rhythms and seasonal reproductive cycles in birds. In: Assenmacher, I., Farner, D. S. (eds), *Environmental Endocrinology,* Springer, New York, pp. 144–152.
35. Wingfield, J. C., Hegner, R. E., Lewis, D. M. (1991) Circulating levels of luteinizing hormone and steroid hormone in relation to social status in the cooperatively breeding white browned sparrow weaver, Plocepasser maholi. *J. Zool. London 225,* 23–58.
36. Wolfson, A. (1959) The role of light and darkness in the regulation of spring migration and reproductive cycles in birds. In: Withrow, R. B. (ed.) *Photoperiodism and Related Phenomena in Plants and Animals.* American Association for the Advancement of Science, Washington, pp. 676–716.
37. Wolfson, A. (1965) Circadian rhythm and photoperiodic regulation of the annual reproductive cycle in birds. In: Aschoff, J. (ed.) *Circadian Clocks,* North Holland, Amsterdam, pp. 371–378.

Acta Biologica Hungarica 51 (1), pp. 37–44 (2000)

SEASONAL ADIPOSITY AND ANDROSTENEDIONE PRODUCTION AS A POSSIBLE MECHANISM FOR ASYNCHRONOUS REPRODUCTIVE ACTIVITY BETWEEN MALES AND FEMALES OF VESPERTILIONID BAT, *SCOTOPHILUS HEATHI*

A. KRISHNA,* ABHILASHA and K. SINGH

Department of Zoology, Banaras Hindu University, Varanasi-221 005, India

(Received: May 17, 1998; accepted: November 16, 1998)

Relationship between changes in the body weight and circulating androstenedione concentration was examined in order to find out their involvement in asynchronous gametic cycle of male and female *S. heathi.* Body weight of both male and female bats increased from September due to accumulation of white adipose tissue and reached to a peak in November. The body weight declined gradually due to consumption of adipose tissue during December and January reaching basal level in February. A significant correlation between body weight and serum androstenedione concentration was observed. Correlated with maximum body weight, peak androstenedione level was found during November in both male and female bats. Peak androstenedione level during November may be responsible for stimulating spermatogenesis in the male, but may suppress follicular growth and ovulation in the female, thus resulting in asynchronous gametic cycle of male and female *S. heathi.*

Keywords: Body weight – androstenedione – bat – reproduction – adipose tissue

INTRODUCTION

Seasonally reproductive mammalian species generally exhibit elevated circulating gonadal steroids concentrations during the breeding season(s) and there is a corresponding synchronous stimulation of gonadal activity simultaneously in both males and females. On the contrary, in most temperate-zone vespertilionid bats, male and female reproductive activities are not synchronous. In these bat species, final maturation of Graafian follicle and ovulation in female occurs several months after the period of peak spermatogenesis in male and time of copulation [15, 22]. The asynchrony between male and female reproductive activities has led to the several unique reproductive adaptations in these bats such as sperm storage, delayed fertilization and delayed ovulation [5, 24, 28]. One of the proposed reason for the unique reproductive asynchrony in the case of temperate-zone bats is the superimposition of the period of hibernation on the season of reproduction [22, 24]. Studies from our laboratory have shown that *S. heathi,* a tropical-subtropical vespertilionid bat, also

* Corresponding author, E-mail: akrishna@banaras.ernet.in

0236-5383/2000/$ 5.00

exhibits phenomenon of sperm storage and delayed ovulation [1, 17]. Our recent studies have suggested that increase in food intake prior to winter resulted in the increase in body weight as well as in circulating androstenedione concentration in both male and female *S. heathi* [2, 27]. Increase in androstenedione level in male resulted in the increase in testosterone concentration and activation of gonadal activity particularly spermatogenesis whereas increase in androstenedione level in female resulted in the suppression of follicular maturation and ovulation. This may be the reason for asynchrony between male and female reproductive activity in the bat. Therefore, relationship between body weight and androstenedione in both male and female *S. heathi* are reported here and involvement of such relationship in asynchronous reproductive activity between male and female is discussed.

MATERIALS AND METHODS

All bats were trapped alive in the areas adjacent to Banaras Hindu University Campus. Body weight of each bat was recorded. Bats were sacrificed as soon as they arrived in the laboratory. Their blood serum was collected and stored at –20 °C until assayed. Location and amount of adipose tissue deposited in the body of female bats were also recorded.

Steroid Radioimmunoassay (RIA)

Circulating concentration of androstenedione was measured by RIA. Antibodies for androstenedione was obtained from Dr. Resko (Portland, USA). Extracted the serum samples with 2 ml of diethyl ether, decanted the ether extract, evaporated to dryness at 37 °C and resuspended in PBSG (0.01 M) for further analysis as described by Abhilasha and Krishna [1].

Statistical analysis

The data were analyzed by one-way analysis of variance (ANOVA) followed by Duncan's test. Correlation coefficient was used to compare to data. Date are expressed as mean ±SE.

RESULTS

Monthly changes in the body weight of female and male bat are shown in Figs 1, 3. Changes in body weight of male and female bat was marked with weight gain before winter dormancy due to gradual accumulation of adipose tissue reaching maximum level in November. White adipose tissue mainly accumulated subcutaneously in the

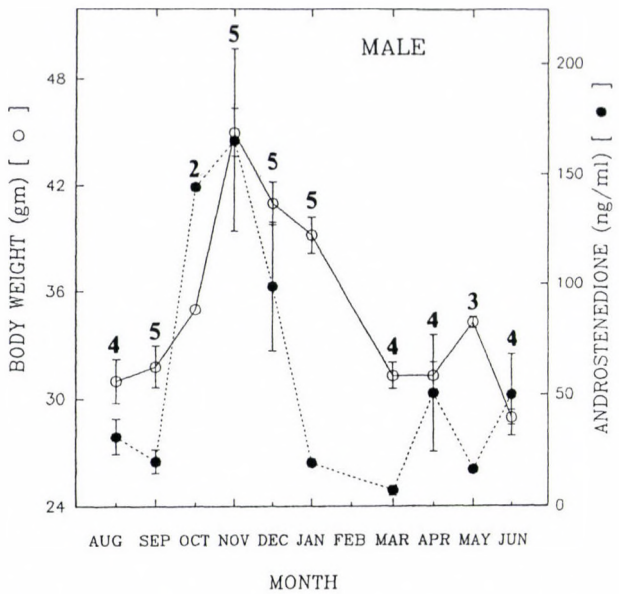

Fig. 1. Mean body weight and circulating androstenedione concentration of male *S. heathi* during different months. Number of bats used during each months are indicated

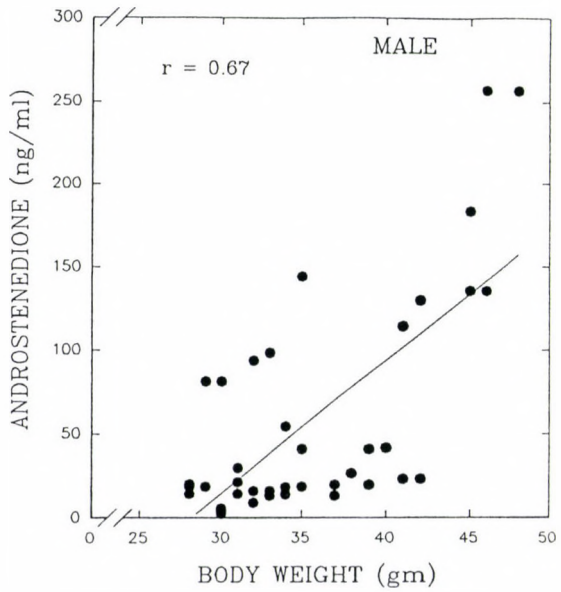

Fig. 2. Correlation between body weight and circulating androstenedione concentration of male *S. heathi*

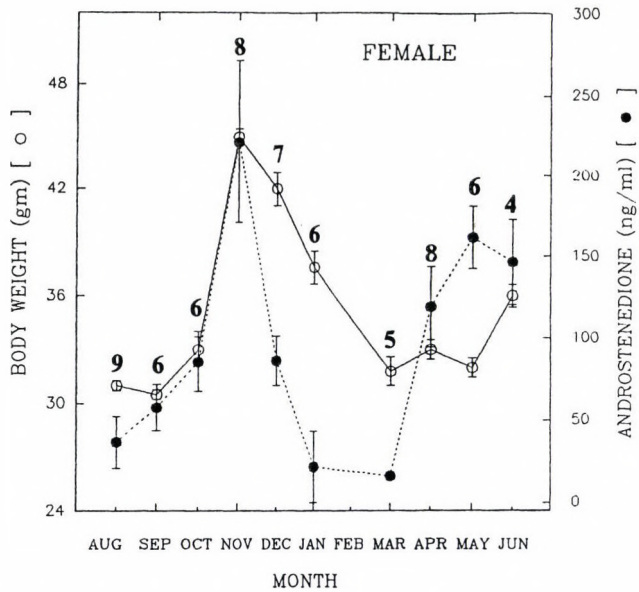

Fig. 3. Mean body weight and circulating androstenedione concentration of female *S. heathi* during different months. Number of bats used during each months are indicated

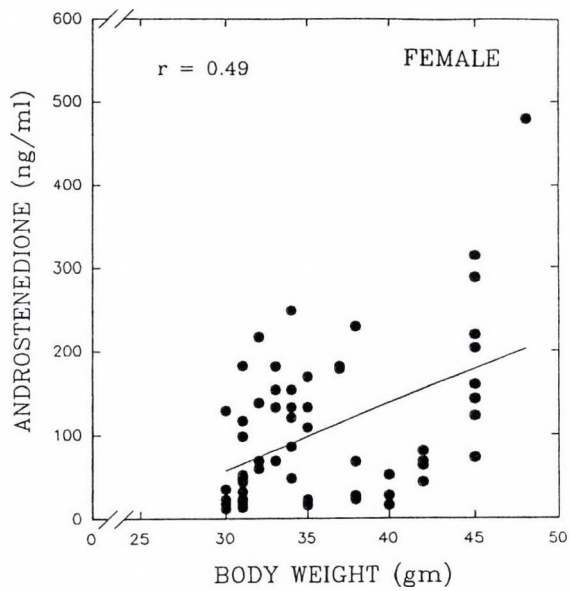

Fig. 4. Correlation between body weight and circulating androstenedione concentration of female *S. heathi*

Table 1
Monthly changes in the body weight, amount of subcutaneous white adipose tissue and weight of uterus with fetus in *S. heathi*

Month	Body weight in male (gm)	Body weight in female (gm)	White Adipose tissue (gm)*	Uterus with fetus (gm)
August	31.0±1.2	31.0±0.3	–	–
September	31.8±1.2	30.5±0.3	0.9±0.1	–
October	35.3±1.1	33.0±0.7	3.9±0.4	–
November	45.0±1.3	45.0±0.5	11.4±0.8	–
December	41.0±1.2	42.0±1.0	4.6±0.2	–
January	39.2±1.0	37.6±0.9	2.6±0.3	–
February	35.3±2.8	31.8±0.8	–	0.02±0.0**
March	31.3±0.7	33.0±0.6	–	0.03±0.0
April	31.3±0.7	32.0±0.5	–	0.06±0.0
May	34.3±0.3	36.0±0.6	–	2.47±0.21
June	29.0±0.4	42.6±1.6	–	3.18±0.48
July	34.0±2.6	34.2±1.2	–	–
ANOVA	<0.05	<0.05	<0.01	<0.01

Values are mean ±SE of six samples.
*Data from male and female bats are pooled.
**Showed the weight of uterus only.
– Showed either only traces of adipose tissue or absence of fetus in the uterus.

neck, back, lateral abdominal and pelvic regions. The adipose tissues were gradually consumed during winter dormancy resulting in weight loss with basal level attained in February. Females also showed an increase in weight during June due to increase in fetal weight (Table 1).

Serum androstenedione concentrations of both male and female bat varied significantly during different calendar months (Figs 1, 3). Highest level of androstenedione in both male and female bats was observed during November when the body weight and accumulation of adipose tissue were also maximum. Changes in the body weight showed significant statistical correlation with serum androstenedione concentrations in both male and female bats (Figs 2, 4). Androstenedione level was also high during the months from April to June in female which coincided with the pregnancy in *S. heathi.* A short peak of androstenedione in male during April was statistically not significant compared with the values during March and May.

DISCUSSION

Annual changes in the body weight are reported in several microchiropterans and these are usually associated with changes in the availability of food resources and hibernation [3, 7, 14, 24]. Present study demonstrates seasonal variation in the body weight of both male and female *S. heathi.* A gradual increase in the body weight was observed in this bat from September to November. This increase in the body weight

was mainly due to the accumulation of white adipose tissue as a result of overfeeding prior to winter dormancy. It has been shown that the fat deposition in this species is preceded with the period of increased insect availability (August–October) and consumption [16]. Since the stored fat is gradually depleted during December–January, it suggests that fat deposition is an adaptation to overcome the scarcity of food during winter dormancy.

It has long been recognized that nutritional status can have profound effects on reproductive function. Body fat plays a role in transmitting information about the nutritional status of the body to the reproductive axis [6]. Periods of chronic or severe under nutrition often result in the suppression of reproductive hormone secretion with an accompanying decrease in fertility [8]. The effect of obesity on reproductive activities are more complex, though only fewer studies, mainly in females, have examined the effects of enhanced nutrition. Overfeeding produces a significant increase in plasma insulin, IGF-I and androgen [10, 13, 21, 26]. All of these hormones have anabolic properties and may facilitate the accumulation of fat in response to energy surfeit. Increase in androgenic activity when combined with a excess of caloric intake could lead to enlargement of abdominal adipocytes and upper body fat predominance. The white adipocytes efficiently synthesize and store triglycerides in periods of nutritional abundance and can hydrolyze and release unesterified fatty acids when they are needed [29].

The present study demonstrates an unusually high circulating androstenedione level in the bats coinciding with period of increased body weight. A significant correlation between androstenedione and body weight was found in both the male and female bats. A low correlation coefficient in the female ($r = 0.49$) as compared to the male ($r = 0.67$) was due to lack of correlation between body weight and androstenedione during the period from March to June, when increase in the body weight was because of fetus but not due to fat accumulation. How does obesity or overfeeding causes increased androgen production is not clearly known, but the mechanism seems to be identical in both the male and female bats. Hyperinsulinemia has long been recognized as a feature of obesity [4, 9]. It is recently suggested that hypersecretion of insulin during obesity is probably caused by enhanced level of glucose metabolism that is induced by increased free fatty acid due to enhance food intake [20]. Thus, greater the degree of obesity, greater may be the pancreatic insulin production. A similar increase in the level of circulating insulin was also observed in *S. heathi* during the period of increasing body weight (September to December) [11]. A number of studies have shown a significant correlation between elevated serum insulin and androgen levels [23, 25].

The increase in androstenedione level may be responsible for a number of effects on the reproductive system. In female, intra-ovarian effects of excess androgen includes inhibition of follicular growth and ovulation and an enhanced rate of follicular atresia [1, 12]. Recent studies on *S. heathi* showed two peaks of circulating estradiol during reproductive cycle. First peak of estradiol during recrudescence phase in November coincided with abnormally high serum androstenedione level and presence of nonovulatory antral follicle in the ovary. Second peak of estradiol during pre-

ovulatory period in February coincided with low serum androstenedione and presence of ovulatory follicle in the ovary. This observation thus suggests that the presence of nonovulatory follicle during recrudescence may be because of the high serum androstenedione level. Whereas in male, high androstenedione level may lead to higher availability of testosterone in the testes which may lead to stimulation of testicular growth and spermatogenesis [19]. The increased testosterone level and active spermatogenesis coinciding with the period of peak androstenedione level has recently been demonstrated in *S. heathi* [18]. This differential effect of high androstenedione on the male and female reproductive system may be responsible for the asynchrony between male and female gametic cycle.

In conclusion, both male and female *S. heathi* showed an increase in the body weight during September to November due to accumulation of adipose tissue to meet food scarcity during winter dormancy. Coinciding with increase in the body weight, circulating androstenedione level also increased in both the sexes. High androstenedione may lead to stimulation of gonadal activity in the male but may suppress follicular development and ovulation in the female. The results thus suggest that obesity may have stimulatory effects on male but inhibitory effects on female reproductive activities. This may be responsible for asynchrony between male and female gametic cycle in *S. heathi.*

ACKNOWLEDGEMENTS

The authors thank Dr. John Resko for providing androstenedione antibodies. This work was supported in part by UGC and CSIR, India and Rockefeller Foundation (PS-9516), New York, USA.

REFERENCES

1. Abhilasha, Krishna, A. (1996) High androgen production by ovarian thecal-interstitial cells: a mechanism for delayed ovulation in a tropical vespertilionid bat, *Scotophilus heathi. J. Reprod. Fertil. 106,* 207–211.
2. Abhilasha, Krishna, A. (1997) Adiposity and androstenedione production in relation to delayed ovulation in the Indian bat, *Scotophilus heathi. Comp. Biochem. Physiol. 116C,* 97–101.
3. Anand Kumar, T. C. (1965) Regulation in the rat-tailed bat, *Rhinopoma kinneari. J. Zool. 147,* 147–155.
4. Barbieri, R. L., Smith, S., Ryan, K. J. (1988) The role of hyperinsulinemia in the pathogenesis of ovarian hyperandrogenism. *Fertil. Steril. 50,* 197–212.
5. Bernard, R. T. F. (1989) The adaptive significance of reproductive delay phenomena in some South African Microchiroptera. *Mammal. Rev. 19,* 27–34.
6. Bronson, F. H. Manning, J. M. (1991) The energetic regulation of ovulation: a realistic role for body fat. *Biol. Reprod. 44,* 945–950.
7. Brosset, A. (1961) L'hibernation chez les' chiripoteres tropicaux. *Mammalia 25,* 413–452.
8. Cameron, J. L. (1996) Regulation of reproductive hormone secretion in primates by short-term changes in nutrition. *Rev. Reprod. 1,* 117–126.
9. Conway, G. S., Jacobs, H. S. Holly, J. M. P., Wass, J. A. H. (1990) Effects of luteinizing hormone, insulin, insulin-like growth factor-1 and insulin-like growth factor binding protein in the polycystic ovary syndrome. *Clin. Endocrinol. 33,* 593–603.

10. Cordido, F., Casanuvea, F. F., Vidal, J. I., Dieguez, C. (1991) Study of insulin like growth factor-1 in human obesity. *Horm. Res. 36,* 187–191.
11. Doval, J., Krishna, A. (1996) Insulin enhances androstenedione production by ovary: a mechanism of delayed ovulation in a vespertilionid bat, *Scotophilus heathi.* Proc. Symp. Emerging Frontier Hormone Research, p. 31. (Abstract).
12. Faimen, C., Reyes, F. I., Dent, D. W., Fuller, G. B., Hobson, W. C., Thilveris, J. A. (1988) Effect of long term testosterone exposure on ovarian function and morphology in the rhesus monkey. *Anat. Rec. 222,* 245–251.
13. Forbes, G. B. (1989) Hormonal response to overfeeding. *Am. J. Clin. Nutr. 49,* 608–611.
14. Gustafson, A. W. (1975) Observations on the hydroxysteroid dehydrogenase and lipid histochemistry and ultrastructure of the Leydig cells in adult *Myotis lucifugus* (Chiroptera: Vespertilionid) during the annual reproductive cycle. *Anat. Rec. 181,* 366–367.
15. Gustafson, A. W. (1987) Changes in Leydig cell actively during the annual testicular cycle of the bat *Myotis lucifugus lucifugus:* histology and lipid histochemistry. *Am. J. Anat. 178,* 312–325.
16. Krishna, A. (1982) Reproduction in Indian bats. *Life Sci. Adv. 1,* 113–119.
17. Krishna, A., Dominic, C. J. (1978) Storage of spermatozoa in the female genital tract of the Indian vespertilionid bat, *Scotophilus heathi. J. Reprod. Fertil. 54,* 319–321.
18. Krishna, A., Singh, K. (1997) The relationship between testicular activity, accessory sex organ and circulating steroid concentration during reproductive cycle of an Indian male vespertilionid bat, *Scotophilus heathi. Can. J. Zool. 75,* 1042–1050.
19. Matsumoto, A. M. (1995) Spermatogenesis. In: Adashi, E. Y., Rock, J. A., Rosenwaks, Z. (eds), *Reproduction, Endocrinology, Surgery and Technology.* Lippincott-Raven Publishers, New York, pp. 359–387.
20. Milburn, J. L. Jr., Hirose, H., Lee, Y. H. et al. (1995) Pancreatic β-cell in obesity: evidence for induction of functional, morphologic and metabolic abnormalities by increased long chain fatty acids. *J. Biol. Chem. 270,* 1295–1299.
21. Morovat, A., Burton, K. A., Dauncey, M. J. (1994) Short-term regulation of plasma IGF-I concentration by food intake in young growing pigs. *Horm. Metab. Res. 26,* 265–269.
22. Oxberry, B. A. (1979) Female reproductive patterns in hibernating bats. *J. Reprod. Fertil. 56,* 359–367.
23. Portesky, I. (1991) On the paradox of insulin-induced hyperandrogenism in insulin-resistant states. *Endocrin. Rev. 12,* 3–13.
24. Racey, P. A. (1982) Ecology of bat reproduction. In: Kunz, T. H. (ed.), *Ecology of Bats,* Plenum Press, New York, pp. 57–164.
25. Rajkhowa, M., Bicknell, J., Jones, M., Clayton, R. N. (1994) Insulin sensitivity in women with polycystic ovary syndrome: relationship to hyperandrogenemia. *Fertil. Steril. 61,* 605–612.
26. Ravussin, E., Schutz, Y., Acheson, K. J., Dusmit, M., Bourquin, L., Jequier, E. (1985) Short term mixed diet overfeeding in man; no evidence for "lux uskonsumption". *Am. J. Physiol. 249,* 470–477.
27. Singh, K., Krishna, A. (1996) Seasonal changes in circulating serum concentration and *in vitro* testicular section of testosterone and androstenedione in the male vespertilionid bat, *Scotophilus heathi. J. Exp. Zool. 276,* 43–52.
28. Singh, U. P., Krishna, A. (1996) A mini review on the female chiropteran reproduction. *J. Endocrinol. Reprod. 1,* 1–19.
29. Spiegelman, B. M., Choy, L., Hotamisligil, G. S., Graves, R. A., Tontonoz, P. (1993) Regulation of adipocyte gene expression in differentiation and syndromes of obesity/diabetes. *J. Biol. Chem. 268,* 6823–6826.

Acta Biologica Hungarica 51 (1), pp. 45–53 (2000)

METHALLIBURE INHIBITION OF TESTICULAR AND SEMINAL VESICLE ACTIVITY IN CATFISH, *CLARIAS BATRACHUS* (LINN.): A STUDY CORRELATING CHANGES IN SERUM SEX STEROID PROFILES

MADHU SHREE SINGH and K. P. JOY*

Department of Zoology, Banaras Hindu University, Varanasi-221 005, India

(Received: September 21, 1998; accepted: November 9, 1998)

The administration of methallibure (2 μg/g BW, daily for 15 days) in *Clarias batrachus* in prespawning phase (May–June) resulted in decreased weights of seminal vesicle (SV) and testis, and reductions in the concentrations of total proteins, fructose, hexosamines, and sialic acid in SV and testis. The inhibitory changes can be attributed to impairment of steroidogenesis, serum levels of testosterone and estradiol –17β decreased significantly. Withdrawal of methallibure treatment for 7 and 15 days resulted in gradual recovery and restoration of all the above parameters except the sialic acid levels in the SV and testis, and fructose level in the SV. The methallibure induced regressive changes in the SV and testis were discussed in the light of its GTH inhibiting property.

Keywords: Seminal vesicle – testis – catfish – total protein – fructose – hexosamine – sialic acid – testosterone – estradiol-17β – methallibure – gonadotropin-II

INTRODUCTION

Seminal vesicle (SV) is a unique feature of the male reproductive system of some teleosts, like catfishes, blennies and gobies [9, 17, 24]. In catfishes, it secretes a protein-carbohydrate-lipid-rich secretory material in which sperm are stored temporarily [16, 19, 24]. It is a steroidogenic organ as well and synthesizes a number of androgens and androgen glucuronides [20]. The androgen glucuronides serve pheromonal functions [23]. Previous studies have shown that the catfish seminal vesicle shows seasonal histological changes that can be correlated with the annual testicular cycle [17, 19]. Seasonal changes have been also demonstrated in the concentrations of total proteins, fructose, sialic acid and hexosamines which are chemical constituents of the SV secretion [19]. These biochemical parameters are good indices of SV secretory function compared to histological, gravimetric or histochemical analyses used by earlier authors. The secretory activity of the SV has been demonstrated to be under the control of pituitary-gonadal-endocrine axis [16, 22]. Surgical hypophysectomy or castration followed by replacement therapy of hormones, such as gonadotropin (GTH) and androgens was the experimental approach adopted by Sundararaj and

* Corresponding author, E-mail: kpjoy@banaras.ernet.in

0236-5383/2000/$ 5.00

coworkers [16, 22] to elucidate the role of GTH and androgens in the control of testicular and SV activities. Methallibure (I.C.I. 33828; N-methylthiocarbamoyl-N'-[(1-methylallyl)thiocarbamoylhydrazine]; a non-steroidal gonadotropin inhibitor) has been used as an antigonadotropic agent to investigate hypophysial-gonadal relationship in a variety of teleosts [5, 7, 11, 14, 15, 18, 21, 28]. Those studies have shown that methallibure inhibits gonadotropin (GTH) secretion and gonadal functions, such as steroidogenesis, vitellogenesis and gestation. In *C. batrachus,* methallibure inhibits gonadotropin-II (GTH-II) secretion in a dose and sex (male 84.63%; female 65.20%) – dependent manner (our unpublished data). In the present study effects of administration of methallibure and its withdrawal on SV and testicular activities of *C. batrachus* were investigated.

MATERIALS AND METHODS

Collection and maintenance

Catfish (55–60 g) were collected in late preparatory phase (April). Males were separated and maintained under natural photoperiod and temperature (12L : 12D; 24 ± 2 °C) for 15 days. They were treated daily for 1 h with benzanthine penicillin (1,000,000 IU/litre) for 3 days to prevent skin infection and were fed daily with goat liver during acclimation and the course of experiment.

Experimental design

The experiment was conducted in May–June (prespawning phase). The acclimatized fish were divided into 7 groups of 60 each. The first group served as initial control. Fish in this group were weighed and blood was collected by caudal puncture. The blood samples were allowed to clot at 4 °C and centrifuged at 4000 rpm to separate serum which was stored at –20 °C for measurement of hormones. The fish were sacrificed by decapitation immediately after blood collection. The testes and seminal vesicles (SV) were removed quickly and weighed. They were stored at –20 °C for biochemical analysis. Groups 2, 3 and 4 were injected with methallibure, a generous gift of Mr. D. E. Riley, Zenenca Pharmaceuticals, U.K. The injections were made intraperitoneally daily for 15 days in a dose of 2 μg/g body weight. Methallibure was dissolved in 2% polyethylene glycol (PEG). Groups 5, 6 and 7 were injected with the same volume of the vehicle and served as control for groups 2, 3 and 4, respectively. The group 2 and 5 fish were killed after 15 days. The treatments were discontinued in groups 3, 4, 6, and 7 for recovery. The fish in groups 3 and 6 were killed on day 21 (7 days after discontinuation of the treatments) and groups 4 and 7 were killed on day 30 (15 days after discontinuation of the treatments). In all cases, serum, testis and SV were collected and stored at –20 °C for various estimations, as described above.

Study parameters

The weight of the seminal vesicle and testis were expressed as percentage of the body weight to calculate seminal vesicle-somatic index (SVSI) and gonado-somatic index (GSI). Levels of total proteins, fructose, hexosamines and sialic acid in the SV and testis were measured spectrophotometrically according to the methods of Lowry et al. [12]; Mann [13]; Elson and Morgan [6], as modified by Davidson [4] and Warren [26], respectively.

Radioimmunoassay (RIA) of serum testosterone and estradiol-17β (E_2)

E_2 and testosterone RIAs were carried out according to the procedure of Abraham [1]. [2,4,6,7-^{3}H(N)] E_2 (sp. act. 87.0 Ci/mMol) and [1,2,6,7-^{3}H(N)] testosterone (sp. act. 92.1 Ci/mMol) were purchased from NEN, Boston, MA, USA and were used for the assays. E_2 antibody was a generous gift of Professor G. D. Niswender and testosterone antibody was a generous gift of Dr. Chandana Das, AIIMS, New Delhi, through the courtesy of the ICMR, New Delhi. The sensitivity of both assays was found to be 10 pg/ml. E_2 antiserum cross-reacted with estrone (4%) and estriol (0.5%). The testosterone antiserum cross-reacted with 5α-dihydrotestosterone (3%), Δ^4-androstenedione (4.3%), 5α-androstanediol (1.9%), progesterone (1.1%), androstane-3α-diol (1.5%), cortisol (0.096%), androstane-3β-diol (2.5%), estradiol-17β (0.061%) and dehydroisoandrosterone sulphate (0.72%). The intra- and interassay coefficients of variation (n = 5, mean ± SD) for E_2 were 2.28% (SD ± 0.011) and 5.3% (SD ± 0.025), respectively and those for testosterone were 1.43% (SD ± 0.014) and 2.40% (SD ± 0.023), respectively.

Statistical analysis

Data were expressed as means ± standard error of means (SEM). The data were analyzed by one-way analysis of variance (ANOVA), followed by Newman–Keuls' test for multiple group comparisons.

RESULTS

Changes in SVSI and GSI

One-way ANOVA showed that the methallibure treatment caused overall significant variations in SVSI ($F = 206.36$; $p < 0.001$), and GSI ($F = 222.39$; $p < 0.001$). The treatment caused a significant reduction of the SVSI and GSI (Newman–Keul's test, $p < 0.05$; Fig. 1). Withdrawal of the treatment elevated the values at both the inter-

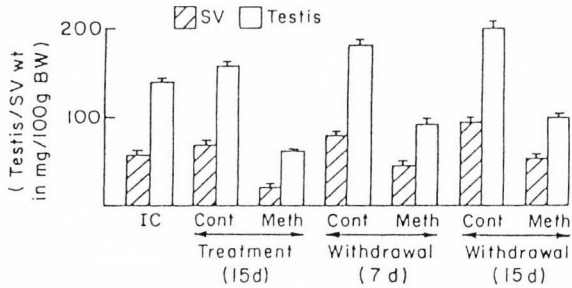

Fig. 1. Effects of injection of methallibure (15 days) and its withdrawal (7 and 15 days) on weights of testis and seminal vesicle (SV) in *C. batrachus* (means ± SE; n = 5). The values are significantly low ($p < 0.05$) in the methallibure-treated and withdrawal groups compared to respective control groups (Newman–Keuls' test). IC – initial control; Cont – control; Meth – methallibure

vals (7 and 15 days) compared to those of the methallibure-treated group, but the values were still significantly low compared to those of the respective control (7 and 15 days) values.

Changes in serum hormone profiles

One-way ANOVA showed that methallibure treatment produced significant variations in testosterone ($F = 23.70$; $p < 0.001$) and E_2 ($F = 1026.96$; $p < 0.001$). The drug treatment decreased significantly the hormone levels (Newman–Keuls' test, $p < 0.05$, Table 1). Withdrawal of the treatment resulted in gradual recovery of the hormone levels but only the testosterone level was fully restored. The significant difference in vehicle control testosterone levels may be due to temporal variations.

Table 1

Effects of injection of methallibure (15 days) and its withdrawal (7 and 15 days) on serum levels of estradiol-17β (E_2) and testosterone in *C. batrachus* (means ± SE; n = 5, * $P < 0.05$; Newman–Keuls' test)

Group	E2 (ng/ml)	Testosterone (ng/ml)
Treatment		
Initial Control	1.75 ± 0.01	3.76 ± 0.47
Vehicle Control	1.92 ± 0.02	3.29 ± 0.24
Methallibure	0.75 ± 0.005*	1.41 ± 0.09*
Withdrawal		
Vehicle Control (7)	2.00 ± 0.025	4.78 ± 0.12
Methallibure (7)	0.9 ± 0.012*	2.18 ± 0.17*
Vehicle Control (15)	2.10 ± 0.027	8.12 ± 1.21
Methallibure (15)	0.95 ± 0.01*	7.32 ± 0.22

Changes in biochemical parameters

Total proteins

One-way ANOVA showed that methallibure treatment produced overall significant changes in protein levels in the SV ($F = 32.22$; $p < 0.001$) and testis ($F = 17.49$; $p < 0.001$). The administration of the drug decreased significantly the protein levels in both SV and testis (Newman–Keuls' test, $p < 0.05$). Withdrawal of the treatment resulted in recovery of protein levels only at day 15 (Fig. 2A).

Fructose

One-way ANOVA showed that the drug treatment resulted in highly significant variations of fructose levels in the SV ($F = 20.48$; $p < 0.001$) and testis ($F = 7.58$; $p < 0.001$). The treatment decreased significantly the sugar level in both SV and testis (Newman-Keuls' test, $p < 0.05$). The sugar level was still low in the SV and testis at day 7 of withdrawal but was restored only in the testis at day 15 of withdrawal compared to that of the respective control (Fig. 2B).

Hexosamines

One-way ANOVA showed that the drug treatment caused significant variations of the hexosamine levels in the SV ($F = 3.78$; $p < 0.01$), and testis ($F = 19.53$, $p < 0.001$). The drug treatment did not significantly alter the amino- sugar level in the SV, but decreased it significantly in the testis (Newman–Keuls' test, $p < 0.05$). On withdrawal of the treatment, the amino-sugar level was restored in the testis at day 15 (Fig. 2C).

Sialic acid

One-way ANOVA showed that the drug treatment produced significant variations of sialic acid levels in the SV ($F = 103.31$; $p < 0.001$) and testis ($F = 72.77$; $p < 0.001$). The administration of the drug decreased the sialic acid content beyond the detection range in the SV and significantly in the testis. Withdrawal of the treatment resulted in the reappearance of the SV sialic acid content in the 7-day group and gradual recovery. However, the values were not restored in comparison to those of the respective control groups at day 7 and 15 of the withdrawal (Fig. 2D).

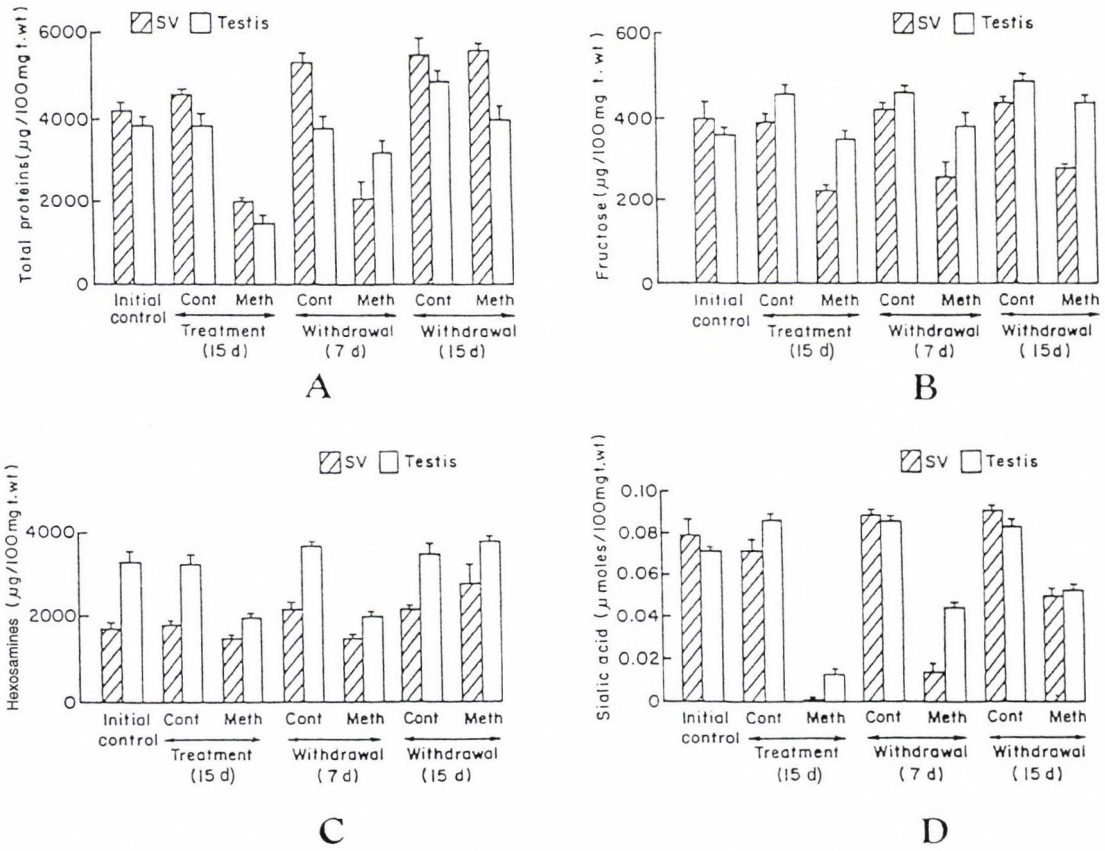

Fig. 2. Effects of methallibure administration (15 days) and its withdrawal (7 and 15 days) on seminal vesicle (SV) and testis concentrations of total proteins (A), fructose (B), hexosamines (C), and sialic acid (D) (means ± SE; n = 5). The values are significantly low ($p < 0.05$) in the methalliburetreated group compared to respective control groups. In the 7-day withdrawal, the values are significantly low for all parameters except testis fructose level. In the 15-day withdrawal group, all the values were restored (not significantly different) except SV fructose and sialic acid values (Newman–Keuls' test). Other details as in Fig. 1

DISCUSSION

The data of the present study show that the administration of methallibure inhibited steroidogenic activity, as evident from low circulating titres of testosterone and E_2. The steroid hormone inhibition can be attributed to the GTH inhibiting property of the drug, since the serum level of GTH-II was significantly lowered by 61.45% in the 2 μg/g BW dose group [19]. The changes were reversible as gradual recovery of hormone levels was noticed upon withdrawal of the treatment; the testosterone level recovered fully at 15 days of the withdrawal. The GTH inhibiting activity of the drug was also reported in goldfish [2] and *Heteropneustes fossilis* [21]. In *H. fossilis* the study has shown that the inhibition of GTH-II secretion was due to differential actions of methallibure on the hypothalamic monoaminergic system; the treatment stimulated dopamine activity which is inhibitory too, and suppressed the activities of serotonin and noradrenaline which are stimulatory to GTH-II secretion. The methallibure-induced inhibition of steroidogenesis was attributed to inhibition of 3β-HSD (the enzyme involved in the conversion of pregnenolone to progesterone) activity in the testes of *Cymatogaster aggregata* [27, 28] and *Poecilia latipinna* [25], and in both gonads of *Cyprinus carpio* [8]. Likewise, methallibure caused a reduction of plasma 11-ketotestosterone in the male Atlantic salmon parr [15]. In the testis of methallibure-treated catfish, spermatogenesis was inhibited at the spermatid-spermatozoa transformation stage, the tubules were small without any lumina and contained spermatids, spermatocytes and large spermatogonial cells like the ones in the mid-preparatory phase [19] resulting in decreased weight of the testis (GSI). Although the inhibitory effect of methallibure on spermatogenic activity of the testis is well documented [10], there are no reports on the effect of methallibure on the chemical constituents of the testis or on the composition of seminal plasma. The present data on methallibure-induced inhibition of proteins, fructose, hexosamine and sialic acid indicate decreased testicular secretory activity of the testis under inhibited production of testosterone. Apparently, this is the first report on the effect of methallibure on biochemical constituents of the testis. The concentrations of these correlates (except sialic acid level) were fully or partially restored after withdrawal of the drug treatment suggesting that the changes were reversible as a result of restoration of testosterone level.

Inhibitory effect of methallibure on the SV activity is reported for the first time in this study. As in the testis, the SV weight and concentrations of proteins, fructose, hexosamines, and sialic acid decreased following the drug treatment as a sequel to the inhibition of testosterone. Histologically, the SV lobules were extensively shrunken, reduced and empty without secretion [19]. As in the testis, almost all the correlates were partially or fully restored after the withdrawal of the drug treatment. However, the concentrations of sialic acid was not restored after the withdrawal, as in the case of the testis. The gradual and slow recovery of sialic acid may suggest that the drug might have interfered with the sialic acid metabolism directly or through other mechanisms. In conclusion, the inhibitory actions of methallibure on the testis and SV are mediated through the inhibition of GTH-II and testosterone production.

ACKNOWLEDGEMENTS

The investigation was supported by a research grant from the Indian Council of Agricultural Research New Delhi to K. P. Joy. We are grateful to Mr. D. E. Riley, Zeneca Pharmaceuticals, Cheshire, England for a generous gift of methallibure and literature on methallibure, Prof. G. D. Niswender, Colorado State University, Colorado, USA for E_2 antiserum, and the Indian Council of Medical Research, New Delhi and Dr. Chandana Das, AIIMS, New Delhi for testosterone antiserum.

REFERENCES

1. Abraham, G. E. (1974) Radioimmunoassay of steroids in biological materials. *Acta Endocrinol. 183* (Suppl. 75), 1–42.
2. Breton, B., Jalabert, B., Billard, R. (1973) Pituitary and plasma gonadotropin levels and spermatogenesis in the goldfish *Carassius auratus* after methallibure treatment. *J. Endocrinol. 59,* 415–420.
3. Chiba, A., Honma, Y., Lanzing, W. J. R. (1978) Effect of methallibure on the hypophysis and gonadal development of the cichlid fish, *Tilapia mossambica. Jap. J. Ichthyol. 25,* 107–114.
4. Davidson, E. A. (1966) Analysis of sugars found in mucopolysaccharides. In: Neufeld, E. F., Ginsburg, V. (eds) *Methods in Enzymology,* Vol. VIII. Academic Press, New York, pp. 52–60.
5. Donaldson, E. M. (1973) Reproductive endocrinology of fishes. *Am. J. Zool. 13,* 909–927.
6. Elson, L. A., Morgan, W. T. J. (1933) A colorimetric method for the determination of glucosamine and galactosamine. *Biochem. J. 27,* 1824–1828.
7. Hoar, W. S., Wiebe, J., Hui, E. V. (1967) Inhibition of the pituitary gonadotropic activity of fishes by a dithiocarbamoylhydrazine derivative (I.C.I. 33,828). *Gen. Comp. Endocrinol. 8,* 101–109.
8. Kapur, K., Toor, H. S. (1978) The effect of methallibure (I.C.I. 33,828) on the steroidogenesis in the ovary and testis of a freshwater teleost *Cyprinus carpio. Experientia 34,* 811–812.
9. Lahnsteiner, F., Richtarski, U., Patzner, R. A. (1990) Functions of the testicular gland in two blenniid fishes, *Salaria* (= *Blennius*) *pavo* and *Lipophrys* (= *Blennius*) *dalmatinus* (Blenniidae, Teleostei) as revealed by electron microscopy and enzyme histochemistry. *J. Fish Biol. 37,* 85–97.
10. Lam, T. J., Pavri, S. C., Ng, K. L. (1985) Effect of methallibure on gestation in the guppy, *Poecilia reticulata. Gen. Comp. Endocrinol. 60,* 315–323.
11. Leatherland, J. F. (1969) Studies on the structure and ultrastructure of the intact and methallibure-treated mesoadenohypophysis of the viviparous teleost *Cymatogaster aggregata* Gibbons. *Z. Zellforsch. 98,* 122–134.
12. Lowry, O. H., Rosebrough, N. J., Farr, A. L., Randall, R. J. (1951) Protein measurement with folin-phenol reagent. *J. Biol. Chem. 193,* 265–275.
13. Mann, T. (1964) *The Biochemistry of Semen and of the Male Reproductive Tract.* Methuen, London.
14. Martin, P., Bromage, N. R. (1970) The effect of methallibure on spermatogenesis in *Poecilia reticulata. J. Fish Biol. 2,* 47–51.
15. Murphy, T. M. (1980) The effect of methallibure and cyproterone acetate on the gonadotrophic cells, plasma androgen levels and testes of precocious 1+ male Atlantic salmon parr *Salmo salar* (L.) *J. Fish Biol. 17,* 673– 680.
16. Nayyar, S. K., Keshavanath, P., Sundararaj, B. I., Donaldson, E. M. (1976) Maintenance of spermatogenesis and seminal vesicles in the hypophysectomized catfish, *Heteropneustes fossilis* (Bloch): Effect of ovine and salmon gonadotropin, and testosterone. *Can. J. Zool. 54,* 285–292.
17. Nayyar, S. K., Sundararaj, B. I. (1970) Seasonal reproductive activity in the testes and seminal vesicles of the catfish, *Heteropneustes fossilis* (Bloch). *J. Morph. 130,* 207–226.
18. Pandey, S. (1970) Effect of methallibure on the testes and secondary sex characters of the adult and juvenile guppy *Poecilia reticulata. Biol. Reprod. 2,* 239–244.
19. Rai, M. S. (1996) *Reproductive Endocrinology of catfish: Aspects of Structure and Physiology of Seminal Vesicle in Clarias batrachus* (L.). Ph. D. Thesis, Banaras Hindu University, Varanasi. India.

20. Schoonen, W. G. E. J., Lambert, J. G. D. (1987) Gas chromatographic-mass spectrometric analysis of steroids and steroid glucuronides in the seminal vesicle fluid of the African catfish, *Clarias gariepinus. Gen. Comp. Endocrinol. 68,* 375–386.
21. Senthilkumaran, B., Joy, K. P. (1998) Methallibure-induced inhibition of hypothalamo-hypophyseal-oranian activity in the catfish *Heteropneustes fossilis* involves changes in hypothalamic monoamine metabolism. *Fish Physiol. Biochem.* 19, 359–364.
22. Sundararaj, B. I., Goswami, S. V. (1965) Seminal vesicle response of intact, castrate, and hypophysectomized catfish, *Heteropneustes fossilis* (Bloch), to testosterone propionate, prolactin, and growth hormone. *Gen. Comp. Endocrinol. 5,* 464–474.
23. Van den Hurk, R., Resink, J. W. (1992) Male reproductive system as sex pheromone producer in teleost fish. *J. Exp. Zool. 261,* 204–213.
24. Van den Hurk, R., Resink, J. W., Peute, J. (1987) The seminal vesicle of the African catfish, *Clarias gariepinus.* A histological, histochemical, enzyme-histochemical, ultrastructural and physiological study. *Cell Tiss. Res. 247,* 573–582.
25. Van den Hurk, R., Testerink, G. J. (1975) The effect of methallibure and methyltestosterone on gonadotropic cells, Leydig cells and the intratesticular efferent duct systems of the adult male black molly *(Mollienisia latipinna). Proc. K. Ned. Akad. Wet. Ser. C 78,* 265–274.
26. Warren, L. (1959) The thiobarbituric acid assay of sialic acids. *J. Biol. Chem. 234,* 1971–1975.
27. Wiebe, J. P. (1968) Inhibition of pituitary gonadotropic activity in the viviparous seaperch *Cymatogaster aggregata* Gibons by dithiocarbamoylhydrazine derivative (I.C.I. 33, 828). *Can. J. Zool. 46,* 751–858.
28. Wiebe, J. P. (1969) Steroid dehydrogenases and steroids in gonads of the seaperch *Cymatogaster aggregata* Gibbons. *Gen. Comp. Endocrinol. 12,* 256–266.

Acta Biologica Hungarica 51 (1), pp. 55–64 (2000)

ANNUAL CYCLIC VARIATIONS IN SOME BIOCHEMICAL CONSTITUENTS OF SEMINAL VESICLE AND TESTIS OF THE CATFISH *HETEROPNEUSTES FOSSILIS* (BLOCH): A STUDY CORRELATING PLASMA TESTOSTERONE LEVEL

I. CHOWDHURY and K. P. JOY*

Department of Zoology, Banaras Hindu University, Varanasi-221 005, India

(Received: January 21, 1999; accepted: July 31, 1999)

In *Heteropneustes fossilis,* significant annual variations were observed in seminal vesicle-somatic index (SVSI), gonadosomatic index (GSI), concentrations of total proteins, hexosamines, fructose and glucose in both SV and testis, and in plasma testosterone with high values in late prespawning–early spawning phases (June–July) and low or undetectable levels in resting phase (December–January) except for glucose. There is an inverse relationship between the annual patterns of fructose and glucose with fructose dominant in the prespawning and early spawning phases (June–July), and glucose in the resting phase (November–January). The increase in the concentrations of SV and testicular protein, hexosamine and fructose can be correlated with the increase in testosterone concentration on one hand and with the increase of SVSI and GSI, on the other. The decrease in glucose level in the recrudescent phase may be due to its increased conversion into fructose, the main seminal sugar in this species.

Keywords: Seminal vesicle – testis – proteins – hexosamines – fructose – glucose – testosterone – catfish – annual variations

INTRODUCTION

Seminal vesicle (SV) is a unique feature of the male reproductive system of teleosts, such as gobies, blennies and catfishes, and has been the subject of several morphological and histological/histochemical investigations [4, 11, 19, 27]. Studies in blennies have shown that it is involved in differentiation and nutrition of spermatids; enhancing seminal fluid viscosity by sialomucin secretion, agglutination of spermatozoa helping chances of fertilization, and in storage of lipids and phospholipids during interspawning period [7, 11]. Previous studies in catfish have shown that annual changes in histological features of SV can be correlated with the testis [19, 20, 27]. The SV consists of an exocrine component (lobules), and a steroidogenic endocrine component (interstitial cells) that produces androgens and glucuronides [20, 22, 27]. The exocrine secretion which peaks during prespawning–spawning phase is a gelatinous, viscous, yellowish fluid in which sperms are stored in an immobile state temporarily and discharged during spawning [19, 20, 27]. Histochemically, the secretion

* Corresponding author.

0236-5383/2000/$ 5.00

contains complex mucopolysaccharides, proteins and lipids [19, 27]. However, quantitative chemical analyses on the SV secretion are scarce although the chemical composition of semen (testicular fluid) has been demonstrated to contain glucose, fructose, lactate, pyruvate, malate, isocitrate, glutamate, lipids, proteins, free amino acids, enzymes, etc., in a few teleosts [5, 6, 10, 13]. However, no data are available on the seasonal patterns of any of these constituents either in the testis or in the SV except for reports from our laboratory [20, 24]. Such information will be useful to understand the functional significance and hormonal control of secretory activity of the organ. Keeping this in view, annual changes in total proteins, fructose, glucose and hexosamines in both the SV and testis of *H. fossilis* were studied and correlated with those of plasma testosterone and organ weights.

MATERIALS AND METHODS

Adult male *H. fossilis* (25–35 g) were collected in the second week of each month in 1994 from local fish markets in Varanasi, India. The fish were weighed and immediately sacrificed by decapitation. The SVs and testes were dissected out carefully, weighed to nearest mg weight, washed in ice-cold 0.6% normal saline and stored at –20 °C for biochemical analysis. Blood samples were collected in heparinized tubes by caudal puncture. Plasma was separated and stored at –70 °C for testosterone assay.

Seminal vesicle-somatic index (SVSI): The weight of the SV was expressed in g % of body weight (BW).

Gonado-somatic index (GSI) was expressed as weight of the testis in g % of BW.

Total proteins

Protein contents of the SV and testis were determined by the method of Lowry et al. [14]. Optical density of the blue colour developed was read in a spectrophotometer (Systronics) at 750 nm against concentrations of bovine serum albumin (Sigma) standard.

Hexosamines

Hexosamine content was estimated by the procedure of Elson and Morgan [3] as modified by Davidson [2]. Optical density of the pink colour developed was measured at 530 nm. The standard curve was prepared from concentrations of a mixture of glucosamine and galactosamine.

Fructose

Fructose content of the SV and testis was measured according to the method of Mann [16]. The optical density of the pink brown colour (end point) was measured at 490 nm.

Glucose

Glucose was measured by a standard glucose test reagent (acetic acid 94% + o-toluidiene 6%). Tissues were homogenised in TDW and centrifuged at 3000 rpm for 10 minutes. To the supernate, 3 ml of the glucose reagent was added and shaken properly. The mixture was incubated in a boiling water bath for 10 minutes. The optical density of the colour was measured at 630 nm.

Testosterone

Plasma testosterone was assayed by an Equate-RIA ^{125}I testosterone diagnostic kit procedure (Binax, Portland, USA). Plasma (0.1 ml) was incubated with 0.2 ml ^{125}I testosterone and 0.2 ml antiserum at 37 °C for 1 h. After incubation, 1.0 ml PEG-second antibody (polyethylene glycol 6% w/v + goat anti-rabbit antibody) was added to all tubes, mixed by vortexing and centrifuged at 1500 × g for 20 minutes at 4 °C. The supernate was decanted and the pellet dried. Radioactivity was taken in a Beckman gamma counter (DP 5000). The minimum sensitivity of the assay was 18 pg per assay.

Statistical Analysis

Seasonal data were analyzed by a one-way analysis of variance (ANOVA), followed by Newman–Keuls' test. Differences were considered significant at $P < 0.001$ for ANOVA and at $P < 0.05$ for Newman–Keuls' test.

RESULTS

SVSI and GSI

The weights of the SV and testis showed significant annual variations (SVSI, $F = 370.76$, $P < 0.001$; GSI, $F = 211.10$, $P < 0.001$; one-way ANOVA) (Fig. 1). The lowest values were recorded during November–March. The values increased steadily during April–June and attained peak levels in early spawning phase (July). Thereafter, it declined during postspawning phase. Newman–Keuls' analysis showed that the July values are significantly higher than all other values.

Testosterone

The plasma testosterone concentrations showed significant annual variations ($F = 52.08$, $P < 0.001$) with the highest value in the prespawning phase (June) (Fig. 2). The levels decreased gradually until November and not detectable in December and January (resting phase). Newman–Keuls' test showed that the June value was significantly higher ($P < 0.05$) than all other values except those of May and July.

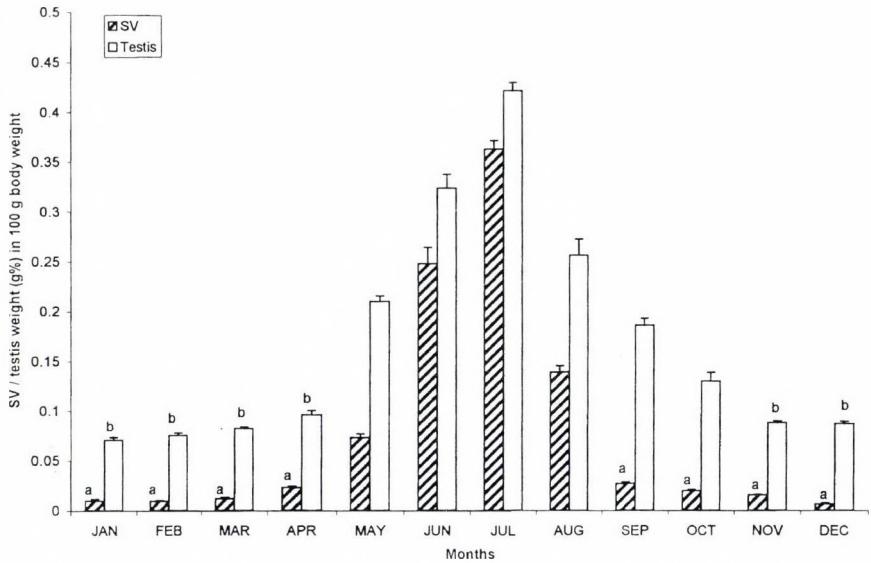

Fig. 1. Significant annual variations in seminal vesicle somatic index (SVSI) and gonadosomatic index (GSI) in *H. fossilis* (Mean ± SEM; n = 5; One-way ANOVA: SVSI, F = 37.76, P < 0.001; GSI, F = 211.10, P < 0.001). a – comparison with SVSI values; b – comparison with GSI values. Bars showing the same alphabetic letter and number are not significantly different (Newman–Keuls' test)

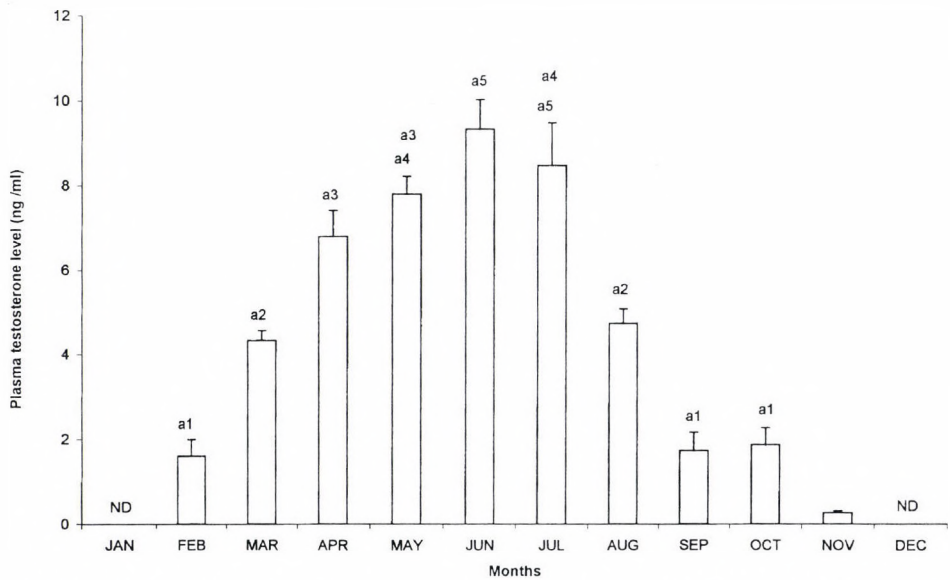

Fig. 2. Significant annual variation in plasma testosterone level in *H. fossilis* (Mean ± SEM; n = 3; One-way ANOVA: F = 52.03, P < 0.001). Bars showing the same number (a1, a2, etc.) are not significantly different (Newman–Keuls' test). ND = no data

Total Proteins

The levels of total proteins showed significant annual changes in the SV ($F = 340.81$, $P < 0.001$) and testis ($F = 176.56$, $P < 0.001$) (Fig. 3). The protein levels were higher in the SV than in testis (April–August). The values increased to a peak in the spawning phase (July), decreased drastically in August and then gradually during the postspawning and resting phases. From Newman–Keul's test analysis, the SV protein level in July is significantly higher ($P < 0.05$) than that of all other months. The testicular protein level in June and July were not significantly different but were higher than all other values.

Hexosamines

Concentrations of hexosamines showed significant annual variations in the SV ($F = 555.44$, $P < 0.001$) and testis ($F = 528.35$, $P < 0.001$) (Fig. 4). The levels were higher in the SV than testis during May–August and were not detected in the SV in the resting phase (December–January). The contents increased steadily during preparatory to prespawning phases reaching high values in June, declined drastically in the spawning phase, and maintained a low level in the testis in resting phase. Newman–Keuls' analysis revealed that the SV hexosamine level in June is significantly higher ($P < 0.05$) than all other values.

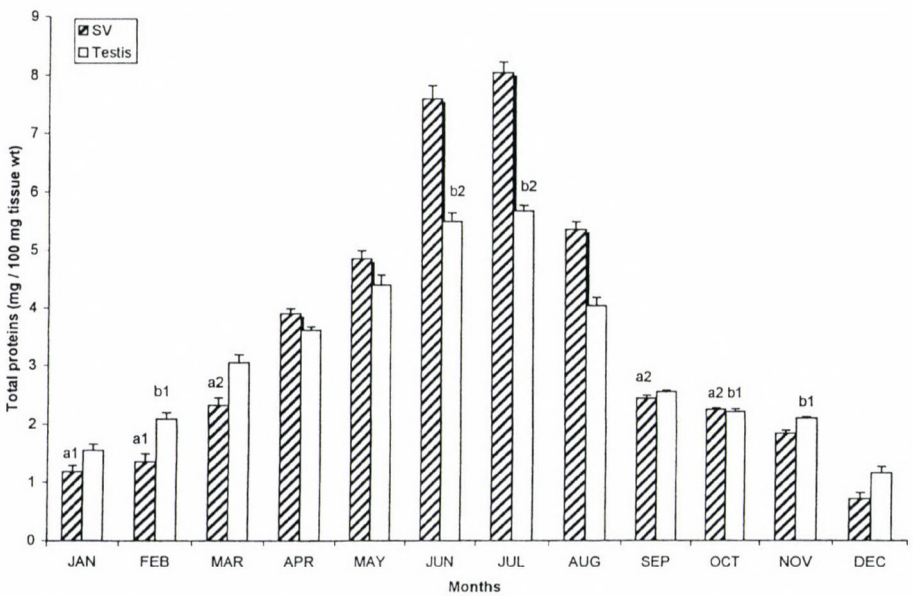

Fig. 3. Significant annual variations in total protein level in seminal vesicle and testis of *H. fossilis* (Mean ± SEM; n = 5; One-way ANOVA: SV, $F = 340.81$, $P < 0.001$; testis, $F = 176.56$; $P < 0.001$). a – comparison with SV values; b – comparison with testis values. Bars showing the same alphabetic letter and number are not significantly different (Newman–Keuls' test)

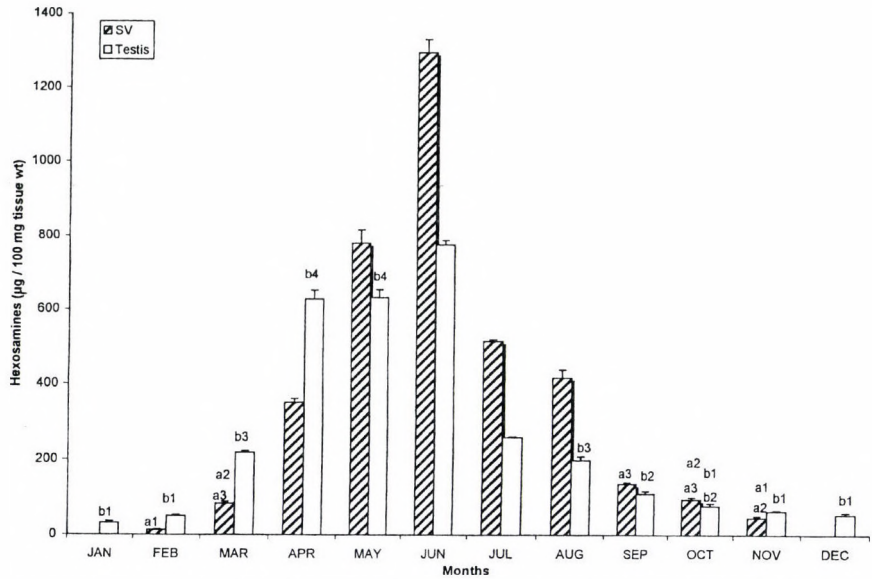

Fig. 4. Significant annual variations in hexosamine level in the seminal vesicle and testis of *H. fossilis* (Mean ± SEM; n = 5; One-way ANOVA: SV, F = 555.44, P < 0.001; testis, F = 528.35, P < 0.001). a – comparison with SV values; b – comparison with testis values. Bars showing the same alphabetic letter and number are not significantly different (Newman–Keuls' test)

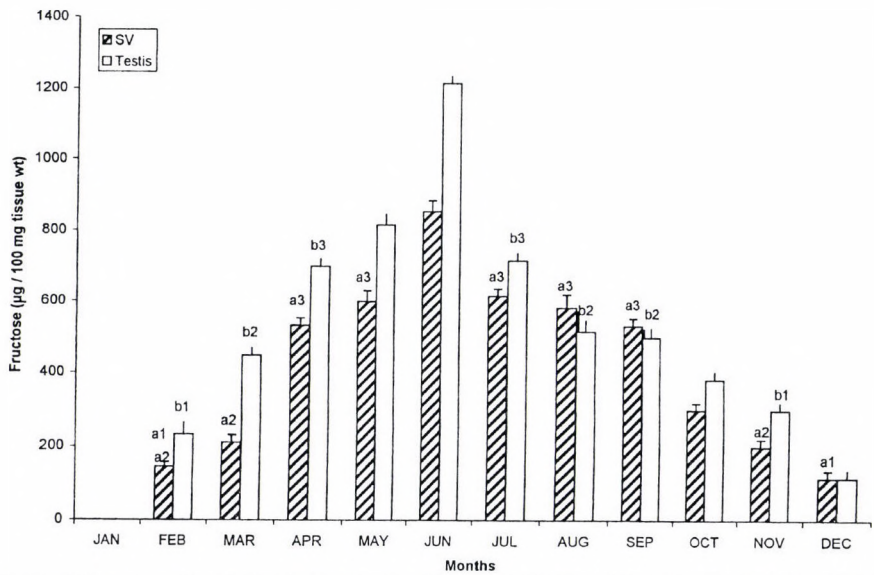

Fig. 5. Significant annual variation in fructose level in the seminal vesicle and testis of *H. fossils* (Mean ± SEM; n = 5; One-way ANOVA: SV, F = 126.44, P < 0.001; testis, F = 204.71, P < 0.001). a – comparison with SV values; b – comparison with testis values. Bars showing the same alphabetic letter and number are not significantly different (Newman–Keuls' test)

Fructose

The concentrations of fructose showed significant annual variations in the SV ($F = 126.44$, $P < 0.001$) and testis ($F = 204.71$, $P < 0.001$) with the highest values in the prespawning phase (June) in either case (Fig. 5). The levels decreased thereafter gradually until December and disappeared altogether in January. The levels were higher in the testis than SV. Newman–Keuls' test showed that the fructose concentrations in the SV and testis in the prespawning phase are significantly higher ($P < 0.05$) than all other values.

Glucose

The concentrations of glucose were detectable throughout the year and showed significant annual variations both in the SV ($F = 377.37$, $P < 0.001$) and testis ($F = 482.25$, $P < 0.001$) with the levels higher in the testis, especially in nonbreeding phase. The level was maximum in resting phase (December–January) and minimum in July–August (spawning phase) (Fig. 6). Newman–Keuls' test showed that the December value was significantly higher than all other values in both the organs.

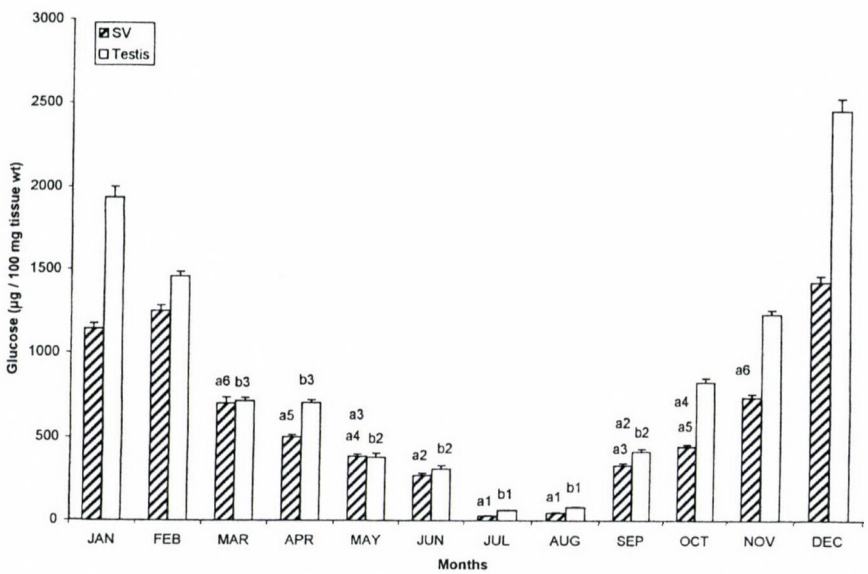

Fig. 6. Significant annual variation in glucose level in the seminal vesicle and testis of *H. fossils* (Mean ± SEM; n = 5; One-way ANOVA: SV, $F = 377.37$, $P < 0.001$; testis, $F = 482.25$, $P < 0.001$). a – comparison with SV values; b – comparison with testis values. Bars showing the same alphabetic letter and number are not significantly different (Newman–Keuls' test)

DISCUSSION

The annual patterns of testosterone, GSI and SVSI reported in this study are similar to those reported earlier [12, 19, 24]. In catfishes, the SV is also steroidogenic like the testis and synthesizes androgens, including testosterone [20, 22, 23]. Testosterone has been shown to promote spermatogenesis and SV secretory activity in both *H. fossilis* [18, 25] and *C. batrachus* [20]. The decline in testosterone production correlates very well with the quiescence of these organs during the reproductive cycle.

Significant annual variations in testicular and SV concentrations of total proteins, hexosamines and fructose were noticed in the present study, as has been reported in *C. batrachus* [20]. The occurrence of these correlates in the semen (seminal fluid + spermatozoa) of some teleosts has been reported earlier [1, 5, 6, 10, 13]. In mammalian epididymis and accessory sex organs, it has been documented that proteins, hexosamines, and fructose, among others are secreted into the lumen under androgenic control [15, 17]. In *C. batrachus,* the concentrations of proteins, hexosamines and fructose in the testis and SV showed dose-dependent increases after testosterone administration and decreased upon cyproterone acetate (an anti-androgen) treatment [20]. The increase in the concentrations of these biochemical constituents can be correlated with the increase in plasma titre of testosterone. This is further supported by the fact that in the absence of testosterone in the resting phase (December and January), hexosamine and fructose levels were not detectable.

Although total protein levels (including both structural and secretory proteins) were measured in this study, the high levels in the prespawning-spawning phases occurred along with peak spermatogenic and secretory activities in the testes and SV, respectively. In the SV of catfish, presence of proteins complexed with carbohydrates and lipids were demonstrated by both histochemical and qualitative biochemical tests [19, 27]. Likewise, the presence of proteins in seminal plasma of several teleosts has been also demonstrated [1, 5, 6]. The specific role of proteins in the semen or SV is not clearly understood, but may have a protective or osmotic function during maintenance/storage of spermatozoa [6, 10]. Hexosamines are six-carbon sugars with an amino group, present in high concentrations in reproductive organs, such as testis, epididymis, and accessory sex organs of mammals, and are important intermediates in the biosynthesis of sialic acid [17, 21]. Sialic acid shows annual variations in the SV and testis of the catfish [24]. The high content of hexosamine may promote sperm survival during maintenance and storage of the sperm and fertilization ability. In blennies, sialomucins make the seminal fluid more viscous and facilitate agglutination of spermatozoa [7, 8]. High levels of hexosamines and sialic acid in both the testis and SV during the prespawning–spawning phase may suggest a similar role in the catfish.

An interesting aspect of the present study was that the testicular and SV fructose and glucose showed significant seasonal variations with inverse relationships. The fructose levels were the highest in the prespawning-spawning phase and the glucose levels the lowest. To our knowledge, such an inverse relationship between the sugar levels was shown for the first time in this study. The nature and concentration of sem-

inal sugars show species and individual variations [1, 5, 6, 10]. In *C. batrachus,* fructose is the dominant sugar in the testis and SV and its level is stimulated by testosterone treatment in a dose-dependent manner and depressed by cyproterone acetate treatment [20] as in most mammals [17]. In the seminal fluid of some cyprinid fishes, both glucose and fructose were found in equal amounts (*Alburnus alburnus* and *Leuciscus cephalus*) or glucose in high amounts (*Vimba vimba*) [9, 10]. In *Cyprinus carpio,* the fructose level was higher than glucose level in early spring [6]. The present data show a positive correlation of testosterone with the fructose level and a negative correlation with the glucose level. This suggests that testosterone promotes fructose synthesis probably from glucose. Synthesis apart, the high level of fructose may be also due to minimal utilization as spermatozoa are present in an immobile state. In the resting phase with regressed testis and SV containing no spermatozoa, the low fructose to high glucose ratio suggests a minimal or lack of synthesis of fructose in the absence of testosterone resulting in high levels of glucose. Thus, during the reproductive cycle of the catfish, distinct pools of glycolysable energy source are maintained, fructose being specifically available for mature sperm during the peak recrudescent phase.

In conclusion, the significant annual increases of total proteins, hexosamines and fructose in both testis and SV which can be correlated with plasma testosterone are associated with secretory and gametogenic activities. As chemical constituents of the seminal fluid, they help in sperm maintenance and survival. Fructose is the main seminal sugar as against glucose for energy requirements of spermatozoa.

ACKNOWLEDGEMENT

I. Chowdhury is thankful to the University Grants Commission of India, New Delhi for a research fellowship.

REFERENCES

1. Billard, R., Cosson, J., Perche, G., Linhart, O. (1995) Biology of sperm and artificial reproduction in carp. *Aquaculture 129,* 95–112.
2. Davidson, E. A. (1966) Analysis of sugars found in mucopolysaccharides. In: Neufeld, E. F., Ginsburg, V. (eds) *Methods in Enzymology.* Vol. VIII. Academic Press, New York. pp. 52–60.
3. Elson, L. A., Morgan, W. T. J. (1933) A colorimetric method for determination of glucosamine and galactosamine. *Biochem. J. 27,* 1824–1828.
4. Fishelson, L., van Vuren, J. H. J., Tyran, A. (1994) Ontogenesis and ultrastructure of seminal vesicles of the catfish, *Clarias gariepinus. J. Morphol. 219,* 59–71.
5. Kara, M. H., Derbal, F., Labed, S. (1996) Composition du liquide seminal de *Sparus aurata* au cours d'une saison de spermiation. *J. Appl. Ichthyol. 12,* 69–70.
6. Kruger, J. C., De, W., Smit, G. L., van Vuren, J. H. J., Ferreira, T. (1984) Some chemical and physical characteristics of the semen of *Cyprinus carpio* L. and *Oreochromis mossambicus* (Peters). *J. Fish Biol. 24,* 263–272.
7. Lahnsteiner F., Patzner, R. A. (1990) The spermatic duct of blenniid fish (Teleostei, Blenniidae): Fine structure, histochemistry and function. *Zoomorph. 110,* 63–73.

8. Lahnsteiner, F., Patzner, R. A. Weismann, T. (1991) Energy metabolism in spermatozoa of the grayling *(Thymallus thymallus).* In: Scott, A. P., Sumpter, J. P., Kime, D. E., Solfe, M. S. (eds) *Reproductive Physiology of Fish* (Fish Symp. 91, Sheffield), pp. 279.
9. Lahnsteiner, F., Patzner, R. A., Weismann, T. (1992) Monosaccharides as energy resources during motility of spermatozoa in *Leuciscus cephalus* (Cyprinidae, Teleostei). *Fish Physiol. Biochem.* 10(4), 283–289.
10. Lahnsteiner, F., Patzner, R. A., Weisman, T. (1994) The testicular main ducts and the spermatic ducts in some cyprinid fishes-II. Composition of the seminal fluid. *J. Fish Biol. 44,* 449–467.
11. Lahnsteiner, F., Richtarski, U., Patzner, R.A. (1990) Functions of the testicular gland in two blennid fish, *Salaria* (= *Blennius) pavo* and *Lipophrys* (= *Blennius) dalmatinus* (Blenniidae, Teleostei) as revealed by electron microscopy and enzyme histochemistry. *J. Fish Biol. 37,* 85–97.
12. Lamba, V. J., Goswami, S. V., Sundararaj, B. I. (1983) Circannual and circadian variations in plasma levels of steroids (cortisol, estradiol-17β, estrone and testosterone) correlated with the annual gonadal cycle in the catfish, *Heteropneustes fossilis* (Bloch). *Gen. Comp. Endocrinol. 50,* 205–225.
13. Linhart, O., Slechta, V., Slavik, T. (1991) Fish sperm composition and biochemistry. *Bull. Inst. Zool. Acad. Sinica Monogr. 16,* 285–311.
14. Lowry, O. H., Rosebrough, N. J., Farr, A. L., Randall, R. J. (1951) Protein measurement with folin-phenol reagent. *J. Biol. Chem. 193,* 265–275.
15. Luke, M. C., Coffey, D. S. (1994) The male sex accessory tissues: structure, androgen action, and physiology. In: Knobil, E., Neill, J. D. (eds) *The Physiology of Reproduction.* Vol. 1, Second edition, Raven Press, New York. pp. 1435–1487.
16. Mann, T. (1964) *The Biochemistry of Semen and of the Male Reproductive Tract. Methuen,* London.
17. Mann, T., Lutwak-Mann, C. (1981) *Male Reproductive Function and Semen: Themes and Trends in Physiology, Biochemistry and Investigative Andrology.* Springer-Verlag, Berlin.
18. Nayyar, S. K., Sundararaj, B. I. (1969) Effects of pituitary hormones, androgens and corticosteroids on the seminal vesicles of the castrate catfish, *Heteropneustes fossilis* (Bloch). *J. Exp. Zool. 172,* 385–398.
19. Nayyar, S. K., Sundararaj, B. I. (1970) Seasonal reproductive activity in the testes and seminal vesicles of the catfish *Heteropneustes fossilis* (Bloch). *J. Morph. 130,* 207–226.
20. Rai, M. (1996) *Reproductive Endocrinology of Catfish: Aspects of Structure and Physiology of Seminal Vesicle in Clarias batrachus* (L.). Ph. D. Thesis, Banaras Hindu University, Varanasi, India.
21. Roseman, S. (1977) Hexosamines and higher amino sugars. In: Williams R. J., Lansford (Jr) E. M. (eds) *The Encyclopedia of Biochemistry.* Robert E. Krieger Publishing Company, New York. pp. 404–405.
22. Schoonen, W. G. E. J., Lambert, J. G. D. (1987) Gas chromatographic-mass spectrometric analysis of steroids and steroid glucuronides in the seminal vesicle fluid of the African catfish *Clarias gariepinus. Gen. Comp. Endocrinol. 68,* 375–386.
23. Schulz, R. W., van den Corput, L., Janssen-Dommerholt, J., Goos, H. J. Th. (1994) Sexual steroids during puberty in male African catfish *(Clarias gariepinus):* serum levels and gonadotropin stimulated testicular secretion *in vitro. J. Comp. Physiol. B164,* 195–205.
24. Senthilkumaran, B., Joy, K. P. (1993) Annual cyclic, and castration and cyproterrone acetate-induced, changes in sialic acid content of the seminal vesicle of the catfish, *Heteropneustes fossilis* (Bloch). *Fish Physiol. Biochem. 10,* 425–430.
25. Sundararaj, B. I., Nayyar, S. K. (1967) Effect of exogenous gonadotrophins and gonadal hormones on the testes and seminal vesicles of hypophysectomized catfish, *Heteropneustes fossilis* (Bloch). *Gen. Comp. Endocrinol. 8,* 403–416.
26. Sundararaj, B. I. (1981) *Reproductive physiology of teleost fishes: A review of present knowledge and needs for future research.* Aquaculture Development and Coordination Programme, FAO Rome, pp. 1–82.
27. van den Hurk, R., Resink, J. W., Peute, J. (1987) The seminal vesicle of the African catfish, *Clarias gariepinus:* A histological, histochemical, enzymehistochemical, ultrastructural and physiological study. *Cell Tissue Res. 247,* 573–582.

Acta Biologica Hungarica 51 (1), pp. 65–71 (2000)

CALMODULIN GENE EXPRESSION IN AN IMMORTALIZED STRIATAL GABAERGIC CELL LINE

A. PÁLFI, MÓNIKA TARCSA, SZILVIA VÁRSZEGI and K. GULYA*

Department of Zoology and Cell Biology, University of Szeged, Egyetem u. 2, H-6722 Szeged, Hungary

(Received: July 28, 1999; accepted: October 6, 1999)

We have demonstrated the presence of the mRNAs transcribed from the three calmodulin (CaM) genes in the GABAergic cell line M26-1F derived from embryonic rat striatal cells and immortalized by oncogene transduction. Similarly as in the rat striatum *in vivo,* these clonal cells express CaM I, CaM II and CaM III mRNAs differently, the CaM I mRNA population being the most abundant, followed in sequence by the CaM II and CaM III mRNA populations. The proportions of these transcripts resemble those in the adult striatum. The possibility of deriving immortalized cell lines from primary neuronal tissue which exhibit characteristics similar to those of the tissue of origin could provide an important tool in many types of *in vitro* studies.

Keywords: Calmodulin mRNAs – gene expression – immortalized cell line – *in situ* hybridization – striatal cell line

INTRODUCTION

Two embryonic cell lines derived from rat striatal tissue were recently generated through use of the A58 temperature-sensitive allele of the SV40 large T antigen [8]. One of these cell lines, M26-1F, is characterized by fibroblast-like, usually bipolar morphology, expresses the SV40 large T antigen and glutamate decarboxylase, both at the permissive (33 °C) and at the nonpermissive temperature (39.3 °C), and microtubule-associated protein-2 (MAP-2) at the nonpermissive temperature. Moreover, M26-1F cells contain GABA, have GABA uptake but are negative for vimentin. These characteristics suggest a neuronal lineage of the M26-1F cells.

The multifunctional intracellular Ca^{2+}-receptor protein calmodulin (CaM) is involved in the regulation of numerous processes [5, 10, 11, 19]. CaM is particularly abundant in the mammalian brain [20], where it plays an important role in the Ca^{2+}-mediated neuronal functions [9]. Apart from the many neuronal functions, CaM is required for various nuclear functions, including cell-cycle progression and mito-

* Corresponding author, E-mail: gulyak@bio.u-szeged.hu

0236-5383/2000/$ 5.00

sis [1]. As several lines of evidence point to the importance of CaM in neuronal and cell-cycle functions, we decided to study the expression pattern of the multiple CaM genes in immortalized striatal M26-1F cells by utilizing specific [^{35}S]cRNA probes complementary to CaM mRNAs, with detection by Northern analysis and high-resolution emulsion autoradiography.

MATERIALS AND METHODS

The M26-1F cell line was generated by Giordano et al. [8]. The cells were plated either on poly-L-lysine-coated (0.1 mg/ml) plastic Petri dishes or glass slides, and incubated in a medium consisting of Dulbecco's Modified Eagle Medium/Nutrient Mix F12 (Life Technologies GmbH, Eggenstein, Germany) complemented with 10% fetal bovine serum, 100 U/ml penicillin and 0.1 mg/ml streptomycin and adjusted to pH 7.4 with 1.125 g/l $NaHCO_3$ in an atmosphere containing 5% CO_2 at 33 °C for 3 days. Cell density on the third day was 100–200 cells/mm^3. The cells grown on slides were used for *in situ* hybridization, while the cells cultured in Petri dishes were treated with 0.5% trypsin for 3 min, collected, centrifuged at 2,000 g for 5 min and frozen and stored at –86 °C for Northern analysis.

[^{35}S]cRNA probes were prepared as previously described by Pálfi et al. [14, 15]. Genomic sequences of the 3'-nonhomolog regions of CaM I, II and III mRNAs [12, 13] were amplified by polymerase chain reactions (PCRs). PCRs were performed by employing EcoR I and BamH I restriction enzyme cleavage site-extended primers. The primer sequences complementary to rat genomic DNA were as follows: for CaM I, 5'-AGACCTACTTTCAACTACT, corresponding to the 30–48 bp sequence, and 5'-TGTAAAACTCATGTAGGGG, corresponding to the 237–255 bp sequence of exon 6; for CaM II, 5'-ATTAGGACTCCATTCCTCC, corresponding to the 1929–1947 bp sequence, and 5'-CACAACTCCACACTTCAACAGC, corresponding to the 2138–2159 bp sequence of exon 5; and for CaM, III 5'-ATGATGACTGC-GAAGTGAAG, corresponding to the 7058–7077 bp sequence, and 5'-CAGGAG-GAAGGAGAAAGAGC, corresponding to the 7228-7247 bp sequence of exon 6. Standard PCRs were run for 35 cycles, and the resulting PCR products were cloned into a pcDNA3 vector (Invitrogen Corp., Carlsbad, CA, USA) and sequenced to confirm their identity. A cDNA fragment corresponding to exon 5 and 6 of the murine β-actin gene cloned into a pGEM vector (Promega, Madison, WI, USA) was used as control. *In vitro* RNA syntheses from the purified and linearized vectors were carried out to prepare antisense and sense [^{35}S]cRNA probes. The complementary probe sequences were 225 bp (CaM I), 231 bp (CaM II), 157 bp (CaM III) and 250 bp (β-actin) long. Labeled probes were purified by size exclusion chromatography on a ProbeQuant G-50 Sephadex micro column (Pharmacia Biotech, Uppsala, Sweden) and the probe-specific activity was determined to be 4.1–6.3 × 10^8 cpm/mg.

Total RNA was prepared by the guanidinium isothiocyanate method, extracted with phenol-chloroform-isoamyl alcohol, precipitated with isopropanol, dissolved in guanidinium isothiocyanate solution, reprecipitated, washed in 70% ethanol and

finally dissolved in RNase-free water. The RNA content and purity were determined by UV spectrophotometry. For electrophoresis, RNA was denatured in a solution containing 15% formaldehyde, 20% formamide and 10 mM MOPS buffer (10 mM MOPS, 4 mM Na-acetate, 0.5 mM EDTA, pH 7.0) at 65 °C for 15 min. Samples (3 μg/lane) were loaded onto 1.2% agarose gel containing 20 mM guanidinium isothiocyanate and 20 mM MOPS buffer and run in the same buffer at 5 V/cm for 100 min at room temperature (RT). RNA was pressure-transferred (PosiBlot Pressure blotter, Stratagene Ltd., La Jolla, CA, USA) in 2 × SSC at 75 mm Hg for 60 min to Duralon-UV nylon membrane (Stratagene) and fixed by UV crosslinking (120,000 μJ/cm^2; Stratalinker, Stratagene). Hybridization was carried out at 60 °C with [^{35}S]cRNA probes (1.5 × 10^6 cpm/lane) in a hybridization buffer (as described for *in situ* hybridization, but complemented with 0.1% SDS and 5 × Denhardt's reagent) for 20 h. Washing was performed under high stringency conditions (2 × SSC, 0.5% SDS at RT for 5 min; 2 × SSC, 0.1% SDS at RT for 20 min; 0.1 × SSC, 0.5% SDS at 37 °C for 20 min; 0.1 × SSC, 0.5% SDS at 65 °C for 40 min; and 0.1 × SSC at RT for 20 min). Finally, the membranes were dried at 37 °C for 30 min and processed for autoradiography.

In situ hybridization with [^{35}S]cRNA probes was carried out according to Pálfi et al. [14, 15]. Briefly, M26-1F cells cultured on poly-L-lysine-coated slides were fixed for 15 min in 0.01 M phosphate-buffered saline containing 4% formaldehyde, washed twice in 2 × SSC (0.3 M NaCl and 0.03 M Na-citrate, pH 7.0) for 1 min, then rinsed in 0.1 M triethanolamine containing 0.25% acetic anhydride for 5 min at RT. The cells were dehydrated, air-dried and hybridized in 50 ml hybridization solution (50% formamide, 5 × SSPE (0.75 M NaCl, 60 mM NaH_2PO_4 and 6 mM EDTA, pH 7.4), 1 × Denhardt's reagent, 10% dextran sulfate, 50 mM DTT, 100 μg/ml salmon sperm DNA and 100 μg/ml yeast tRNA) containing 10^6 cpm cRNA probe/specimen. Hybridization was performed under parafilm coverslips in a humidified chamber at 48 °C for 20 h. The slides were rinsed in 2 × SSC/50% formamide at RT for 5 min, twice in 2 × SSC/50% formamide at 50 °C for 10 min, and in 2 × SSC at RT for 5 min. The cells were incubated in 1 × TE (0.01 M Tris and 0.001 M EDTA, pH 8.0) buffer containing 0.5 M NaCl and 16 μg/ml RNase A for 30 min at 37 °C, rinsed twice in 2 × SSC/50% formamide at 50 °C for 10 min, and in 2 × SSC at 50 °C for 10 min, then dehydrated, air-dried and processed for autoradiography.

Northern blots were apposed to Kodak X-AR autoradiographic film (Eastman Kodak Co., Rochester, NY, USA) for 36 h at 4 °C. Cells cultured on glass slides were dipped into Hypercoat nuclear emulsion (Amersham, Amersham Int., Arlington Heights, IL, USA) and exposed for 10–30 days at 4 °C. Films and emulsion-coated cells were developed in Kodak D19 developer for 3.5 and 5 min, respectively, at 19 °C and fixed in Kodak Fixer for 10 min at 19 °C.

RESULTS

Northern blot analysis of the total RNA revealed 3 transcripts for CaM I (approximately 4.0 kb, 1.7 kb and 0.8 kb), a single transcript for CaM II (approximately 1.4 kb), and one transcript for CaM III (approximately 1.8 kb; Fig. 1). In contrast with the *in vivo* studies, the two minor forms of CaM III (2.3 kb and 0.9 kb) were not detected in these cells. The CaM gene expression detected in the M26-1F cells exhibited similar intensity to that of the mature neurons *in vivo,* however the observed CaM mRNA pattern (CaM I ≈ CaM II >> CaM III) differed from that of the adult rat striatum *in vivo* [15]. Cultured M26-1F cells displayed their characteristic fibroblast-like morphology at 33 °C (Fig. 2A). *In situ* hybridization of [^{35}S]cRNA probes to cultured M26-1F cells established a specific distribution (Fig. 2B-D). The CaM gene-specific riboprobes labeled both the soma of the cells and their processes. Heavy labeling was seen when CaM I- and II-specific [^{35}S]cRNAs were hybridized (Fig. 2B, C), while only a very low hybridization signal was observed with the CaM III-specific antisense probe (Fig. 2D). No autoradiographic signal was observed when the sense probes were hybridized, and pretreatment of sections with RNase A resulted in a complete loss of the measurable signals (data not shown).

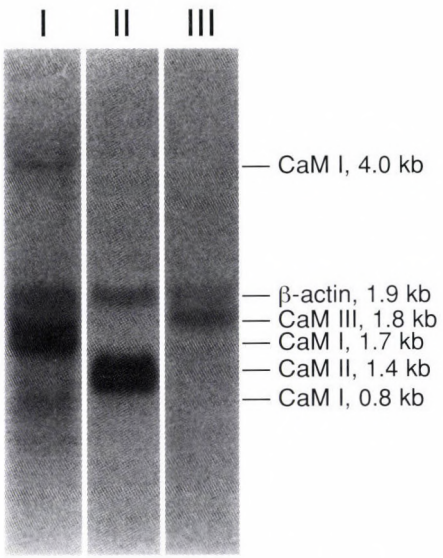

Fig. 1. Northern blot analysis of multiple CaM mRNAs expressed in M26-1F cells cultured at 33 °C for 3 days. Three mg total RNA prepared from the cells was loaded and separated in each lane. Blots were separately probed with antisense [^{35}S]cRNA probes for CaM I (lane I), CaM II (lane II) or CaM III (lane III) and visualized by film autoradiography. All blots were cohybridized with a probe for β-actin which detects a single transcript of 1.9 kb. Three transcripts for CaM I (approximately 4.0 kb, 1.7 kb and 0.8 kb), a single transcript for CaM II (approximately 1.4 kb), and one transcript for CaM III (approximately 1.8 kb) were detected

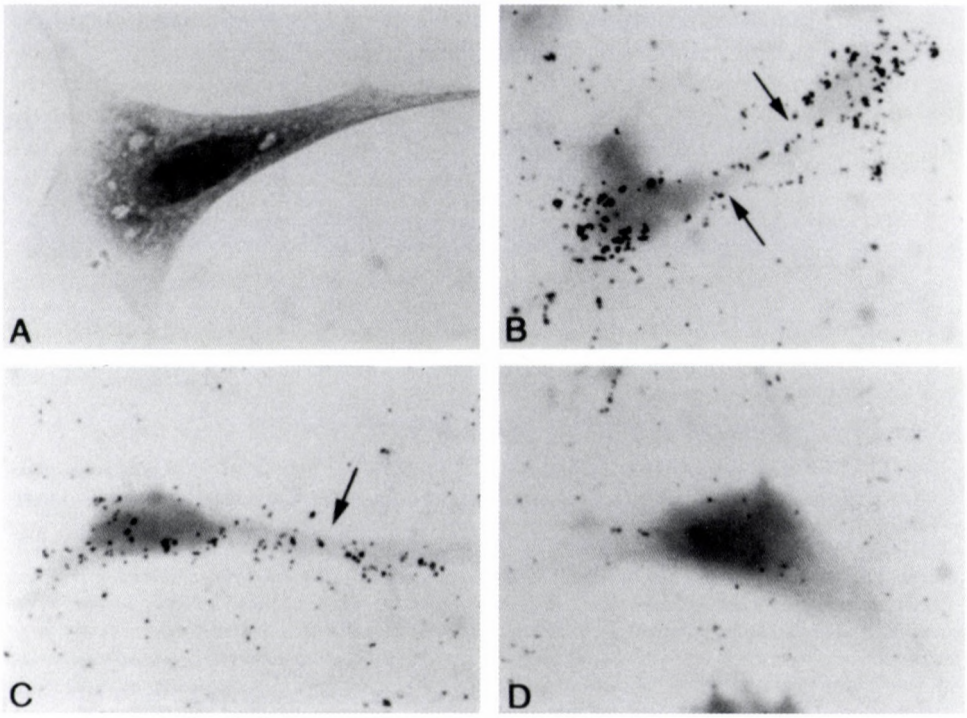

Fig. 2. A) Microphotograph of a safranin-counterstained M26-1F cell cultured at 33 °C for 3 days. B-D) Representative, safranin-counterstained autoradiograms of (B) CaM I-, (C) CaM II- and (D) CaM III-specific mRNA distribution in M26-1F cells cultured at 33 °C for 3 days. *In situ* hybridization signals were detected over the cytoplasm around the nucleus and processes. While heavy labeling was seen with CaM I- and II-specific [^{35}S]cRNAs (B and C, respectively), hybridization with a CaM III-specific probe (C) resulted in only very low labeling. Arrows indicate cell processes. Bar: 25 μm

DISCUSSION

Several cell lines have been generated that express proteins characteristic of primary neurons. These include cell lines from raphe neurons [18], cerebellar [10], hippocampal [4, 6], and striatal cells [8, 17] and the PC12 cell line [19]. However, there are reports on the characterization of multiple CaM gene expression only in PC12 cells [2, 3, 19]. For example, upon nerve growth factor treatment, PC12 cells underwent a 10-fold increase in CaM mRNA content and a 3-fold increase in CaM level [2], while cAMP selectively upregulated CaM I and II in these cells [3]. Our present study is the first that provides an initial characterization of the CaM gene expression in immortalized cells other than those of neuroendocrine origin.

The interest in immortalized cells stems from the possibility that they might deliver a variety of factors endogenously present in these cells into the brain. As an alter-

native to transgene expression that decreases over time, oncogene transduction to immortalize primary cell lines has become feasible [4, 6, 7]. The possibility of deriving immortalized cell lines from primary neuronal tissue which express characteristics similar to those of the tissue of origin will undoubtedly be an important tool in many types of *in vivo* and *in vitro* studies.

ACKNOWLEDGEMENTS

The M26-1F cell line was a kind gift from the late Dr. Ferenc Joó. This work was supported by grants from the National Scientific Research Fund, Hungary (OTKA F22658 and T22822 to A.P. and K.G., respectively) and from the ETT (096/98 to K.G.). The skillful technical assistance of Mrs. Susan Ambrus is appreciated.

REFERENCES

1. Agell, N., Aligué, R., Alemany, V., Castro, A., Jaime, M., Pujol, M. J., Rius, E., Serratosa, J., Taulés, M., Bachs, O. (1998) New nuclear functions for calmodulin. *Cell Calcium 23,* 115–121.
2. Bai, G., Weiss, B. (1991) The increase of calmodulin in PC12 cells induced by NGF is caused by differential expression of multiple mRNAs for calmodulin. *J. Cell Physiol. 149,* 414–421.
3. Bai, G., Nichols, R. A., Weiss, B. (1992) Cyclic AMP selectively up-regulates calmodulin genes I and II in PC12 cells. *Biochim. Biophys. Acta 1130,* 189–196.
4. Berger, F., Gage, F. H., Vijayaraghavan, S. (1998) Nicotinic receptor-induced apoptotic cell death of hippocampal progenitor cells. *J. Neurosci. 18,* 6871–6881.
5. Cheung, W. Y. (1982) Calmodulin: an overview. *Fed. Proc. 41,* 2253–2257.
6. Eves, E. M., Tucker, M. S., Roback, J. D., Downen, M., Rosner, M. R., Wainer, B. H. (1992) Immortal rat hippocampal cell lines exhibit neuronal and glial lineages and neurotropin gene expression. *Proc. Natl. Acad. Sci. USA 89,* 4373–4377.
7. Gage, F. H., Ray, J., Fisher, L. J. (1995) Isolation, characterization, and use of stem cells from the CNS. *Ann. Rev. Neurosci. 18,* 159–192.
8. Giordano, M., Takashima, H., Herranz, A., Poltorak, M., Geller, H. M., Marone, M., Freed, W. J. (1993) Immortalized GABAergic cell lines derived from rat striatum using a temperature-sensitive allele of the SV40 large T antigen. *Exp. Neurol. 124,* 395–400.
9. Kennedy, M. B. (1989) Regulation of neuronal function by calcium. *Trends Neurosci. 12,* 417–420.
10. McManus, J. P., Gillen, M. F., Korczak, B., Nojima, H. (1989) Differential calmodulin gene expression in fetal, adult and neoplastic tissues of rodents. *Biochem. Biophys. Res. Commun. 159,* 278–282.
11. Means, A. R., VanBerkum, M. F. A., Bagchi, I., Lu, K. B., Rasmussen, C. D. (1991) Regulatory functions of calmodulin. *Pharmac. Ther. 50,* 255–270.
12. Nojima, H. (1989) Structural organization of multiple rat calmodulin genes. *J. Mol. Biol. 208,* 269–282.
13. Nojima, H., Sokabe, H. (1987) Structure of a gene for rat calmodulin. *J. Mol. Biol. 193,* 439–445.
14. Pálfi, A., Hatvani, L., Gulya, K. (1998) A new quantitative film autoradiographic method of quantifying mRNA transcripts for in situ hybridization. *J. Histochem. Cytochem. 46,* 1141–1149.
15. Pálfi, A., Vízi, S., Gulya, K. (1999) Differential distribution and intracellular targeting of mRNAs corresponding to the three calmodulin genes in rat brain: a quantitative in situ hybridization study. *J. Histochem. Cytochem. 47,* 583–600.
16. Snyder, E. Y., Deitcher, D. L., Walsh, C., Arnold-Aldea, S., Hartwieg, E. A., Cepko, C. L. (1992) Multipotent neural cell lines can engraft and participate in development of mouse cerebellum. *Cell 68,* 33–51.

17. Wainwright, M. S., Perry, B. D., Won, L. A., O'Malley, K. L., Wang, W. Y., Ehrlich, M. E., Heller, A. (1995) Immortalized murine striatal neuronal cell lines expressing dopamine receptors and cholinergic properties. *J. Neurosci. 15,* 676–688.
18. White, L. A., Eaton, M. J., Castro, M. C., Klose, K. J., Globus, M. Y., Shaw, G., Whittemore, S. R. (1994) Distinct regulatory pathways control neurofilament expression and neurotransmitter synthesis in immortalized serotonergic neurons. *J. Neurosci. 14,* 6744–6753.
19. Zhang, S. P., Natsukari, N., Bai, G., Nichols, R. A., Weiss, B. (1993) Localization of the multiple calmodulin RNAs in differentiated PC12 cells. *Neurosci. 55,* 571–582.
20. Zhou, L. W., Moyer, J. A., Muth, E. A., Clark, B., Palkovits, M., Weiss, B. (1985) Regional distribution of calmodulin activity in rat brain. *J. Neurochem. 44,* 1657–1662.

Acta Biologica Hungarica 51 (1), pp. 73–82 (2000)

SYNTHESIS AND ACCUMULATION OF POLY(3-HYDROXYBUTYRIC ACID) BY *RHIZOBIUM* SP.

A. MANNA, S. PAL and A. K. PAUL*

Microbiology Laboratory, Department of Botany, Calcutta University, 35, Ballygunge Circular Road, Calcutta-700019, India

(Received: January 12, 1999; accepted: September 15, 1999)

Forty-two *Rhizobium* strains obtained from different culture collections were evaluated quantitatively for poly(3-hydroxy-butyric acid) [PHB] production in shake flask culture. The majority of the strains produced the maximum amount of PHB during the late exponential or stationary phase of growth. Synthesis and accumulation of PHB in different species of *Rhizobium* were found to vary between 1–38% of their dry biomass. Growth and PHB production by the *Rhizobium* strain TAL-640 were greatly influenced by the C-source and D-mannitol was fundamental to both processes. The identity and purity of PHB isolated from TAL-640 have also been confirmed by UV-, IR- and ^{1}H-NMR spectroscopic analyses.

Keywords: Rhizobium – poly(3-hydroxybutyric acid)

INTRODUCTION

Petrochemical based thermoplastics that have become part of our daily lives are now causing serious environmental problems, mainly due to their non-biodegradability. Use of biodegradable plastics has been identified as one of the alternatives to reduce environmental pollution caused by plastic waste. Among the candidates for biodegradable plastics, the polymer poly(3-hydroxybutyric acid) [PHB] has attracted the attention due to its characteristic features similar to synthetic plastics and biodegradable narure [2, 3, 6, 12]. PHB, the best-known member of polyhydroxyalkanoic acids [PHAs] is a reserve material that is synthesized and accumulated by a wide variety of bacteria under nutrient-limiting conditions in the presence of excess carbon source [1, 19].

Occurrence of PHB as the reserve compound in rhizobia has been demonstrated by several workers [8, 9, 11, 17, 22, 24] although very little in known about the quantitative evaluation of the accumulated polymer in different species. Synthesis and accumulation of PHB in different species of *Rhizobium* were found to vary between 35–50% of cell dry weight. Moreover, *Rhizobium meliloti* strain 41 was able to synthesize the copolymer poly(3-hydroxybutyrate-co-3 hydroxyvalerate) at concentra-

* Corresponding author.

0236-5383/2000/$ 5.00

tions up to 55% of the biomass dry weight, containing up to 22 mol% 3-hydroxyvalerate [12].

Accumulation of PHB in root nodules of tropical and temperate leguminous plants [11] and *Rhizobium japonicum* bacteroids [13] was reported. The polymer content has been shown to decline during maturation and to increase during senescence of nodules [14]. In nodules of *Vicia faba* and *Lupinus* PHB is reported to be involved in the maintenance of N_2-fixation when the availability of photosynthate to bacteroids is restricted [10, 15, 24]. On the other hand, *Rhizobium etli* was reported to synthesize and accumulate PHB in symbiosis as well as free life [5, 7]. It was proposed that in free life PHB synthesis sequestered reductive power, allowing the tricarboxylic acid cycle to proceed under oxygen limiting conditions [5].

In this report we describe the synthesis and accumulation of PHB by different *Rhizobium* species in shake flask cultures. Production and characterization of the polymer isolated form *Rhizobium* strain TAL-640 are also reported.

MATERIALS AND METHODS

Microorganisms and growth conditions

A total of 42 rhizobial strains obtained from culture collection of NIFTAL Project, University of Hawaii; Bose Institute Culture Collection, Bose Institute, Calcutta and Department of Botany Culture Collection, Calcutta University, Calcutta were used in this study. The bacterial cultures were maintained on Yeast-extract mannitol agar (YMA) medium (pH 6.8) by regular sub-culturing at monthly intervals. Inocula were prepared in Yeast-extract mannitol broth (YMB) by incubating the strains at 30 °C for 48 h in a rotary shaker (120 rpm). Screening of rhizobial strains for PHB production was carried out after growing them in YMB with 2% (w/v) mannitol. The medium (25 ml/250 ml Erlenmeyer flask) was inoculated with 2.5 ml of freshly prepared inoculum and incubated in a rotary shaker (120 rpm) at 30 °C.

Determination of growth

Growth of the rhizobial strains was determined by measuring the optical density of the culture at 540 nm using a Photochem-5 (PEI Pvt. Ltd., India) visible spectrophotometer and also by determining the dry weights of the biomass.

Determination of PHB

The PHB content of the bacterial cell mass was determined following the method of Law and Slepecky [16]. The dried cell mass (2 mg) was suspended in 20 ml of alkaline sodium hypochlorite and incubated at 37 °C for 12–16 h. The resulting suspen-

sion was centrifuged at 12,000 × g and the residue was washed twice with equal amount of distilled water, followed by acetone, ethanol and diethyl ether. PHB was then extracted from the residue with 10 ml of boiling chloroform and filtered through Whatman No. 1 filter paper. The chloroform extract was evaporated to dryness and the residue thus obtained was dissolved in equal volume of concentrated H_2SO_4 keeping in a boiling water bath for 10 min. The absorbance of the sample was measured at 235 nm using Varian-DMS 100S UV spectrophotometer. Authentic PHB obtained from Sigma chemical company, USA was used as the standard.

UV spectrophotometric analysis of the polymer

For UV-spectrophotometric analysis polymer samples were converted to crotonic acid following digestion in concentrated H_2SO_4 for 10 min in a boiling water bath. Absorbance of the crotonic acid was scanned between 200–280 nm by using Varian-DMS 100S UV spectrophotometer.

Infrared spectra of whole cells and PHB

The infrared spectra of whole cells and isolated PHB preparations were recorded with a Perkin-Elmer, Model 297 IR spectrophotometer following the methods of Stockdale et al. [20] and Wakisaka et al. [23] respectively.

NMR spectroscopic analysis of the polymer

^{1}H-NMR spectrum of the purified polymer (in $CDCl_3$) was recorded in a Bruker AM 300 L (300 MHZ).

RESULTS

Accumulation of PHB

The majority of the *Rhizobium* strains tested was able to accumulate PHB towards the end of the exponential phase or during stationary phase of growth when grown in Yeast-extract mannitol broth. Twenty-three out of 42 rhizobial strains were found to accumulate PHB and the PHB content of the rhizobial strains varied from 1 to 38% of their dry biomass with an optimum time requirement of 24–96 h (Table 1). *Rhizobium* strain TAL-640 was identified as the best PHB producer and was selected for some detailed studies.

Table 1
Growth and PHB production by different *Rhizobium* sp.

Organism	Optimum incubation, h	Biomass, mg/100 ml	PHB, % cell dry mass
R. leguminosarum			
TAL-182	60	50.0±2.1	27.8±1.3
TAL-634	72	23.0±1.8	33.5±0.4
TAL-1397	48	18.0±1.0	26.6±1.4
DBCC-151	72	18.1±1.1	13.7±0.6
DBCC-211	72	18.9±1.3	12.6±0.6
DBCC-241	72	23.1±1.9	16.9±0.3
R. meliloti			
TAL-1372	48	13.6±0.5	25.7±0.6
R. loti			
BICC-620	72	43.3±2.0	19.7±1.0
Rhizobium sp.			
TAL-640	60	26.5±1.7	38.6±1.7
TAL-1148	48	26.2±1.8	15.9±0.4
Bradyrhizobium sp.			
TAL-385	48	28.9±1.9	12.0±0.6
DBCC-116	24	27.1±2.0	18..4±1.6
DBCC-117	24	40.0±2.1	25.7±1.1
B. japonicum			
BICC-705	48	64.0±2.5	12.7±1.0

The weak PHB producers (<10% PHB) are not shown in Table. Figures are averages of triplicates ±S.D. TAL, NIFTAL Project, Hawai; BICC, Bose Institute Culture Collection, Calcutta; DBCC, Department of Botany Culture Collection, Calcutta University, Calcutta.

Time course of growth and PHB production

Time course of growth and PHB production by *Rhizobium* strain TAL-640 (Fig. 1) showed that PHB synthesis was slow until the end of the exponential phase, increased rapidly and attained its maximum at the end of the active phase of growth. This was followed by a sharp decline in the later stages of growth. Concomitant with growth and PHB production the pH of the medium gradually decreased to 6.5.

Effect of carbon source on PHB production

Growth and PHB production by *Rhizobium* strain TAL-640 were significantly affected by the carbon source (Table 2). PHB accumulation was maximum (38% dry biomass) with 2% (w/v) mannitol followed by sodium-fumerate and sodium-acetate at

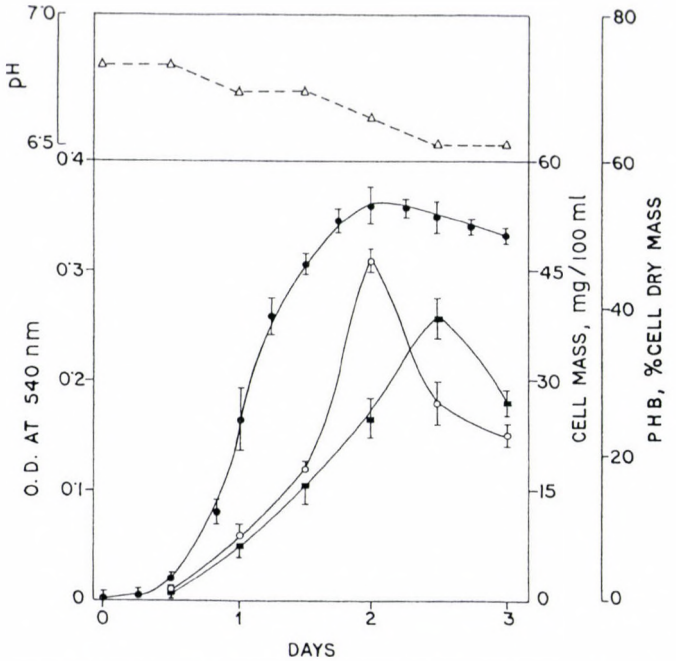

Fig. 1. Time course of growth and PHB production by *Rhizobium* sp. TAL-640. ● Optical density; ○ Cell mass; ■ PHB; △ pH

Table 2
Effect of carbon source on growth and PHB production by *Rhizobium* sp. TAL-640

C source*	Biomass mg/100 ml	PHB, % Cell dry mass	Final pH of the medium
Glucose	10.6 ± 0.4	5.7 ± 0.6	6.4
Fructose	9.6 ± 0.4	5.2 ± 0.2	6.8
Maltose	11.5 ± 0.5	6.0 ± 0.1	6.7
Lactose	2.2 ± 0.2	ND	6.7
Sucrose	12.8 ± 0.6.	14.6 ± 0.6	6.7
Mannitol	27.2 ± 1.3	7.7 ± 1.6	6,7
Na-acetate	19.7 ± 0.8	22.8 ± 1.2	7.0
Na-butyrate	20.2 ± 0.7	4.7 ± 0.1	7.1
Na-fumarate	21.5 ± 1.0	24.6 ± 1.2	7.5
Na-gluconate	19.7 ± 0.8	1.8 ± 0.1	7.0
Na-malonate	23.3 ± 1.1	18.3 ± 1.0	7.0
Na-propionate	8.0 ± 0.2	4.6 ± 0.2	6.0
Na-valerate	8.8 ± 0.2	2.4 ± 0.1	6.2

All values are average of tripicates, ± SD. ND, not detected.

*Glucose, fructose, maltose, lactose, sucrose and mannitol were used at 2% (W/V) level. Sodium-acetate, -butyrate, -fumarate, -gluconate, -malonate, -propionate and -valerate were added at 0.5% (W/V) level.

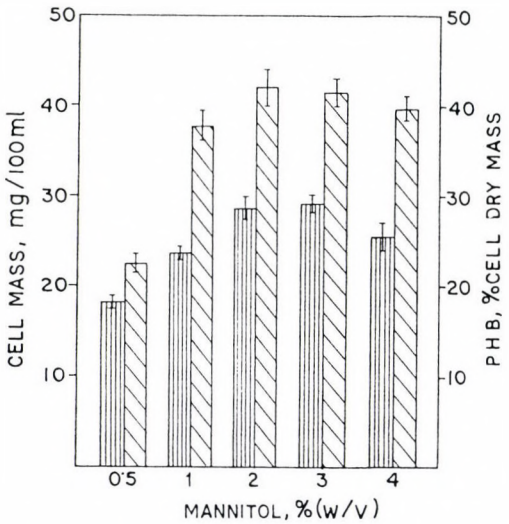

Fig. 2. Growth and PHB production by *Rhizobium* sp. TAL-640 as influenced by mannitol concerations. ▯ Cell mass; ▨ PHB

0.5% (w/v). The strain failed to accumulate PHB with lactose although it allowed feeble growth. The optimum concentrations of mannitol for growth and PHB production were 2 and 3% (w/v), respectively (Fig. 2).

Isolation and characterisation of PHB

Rhizobium sp. TAL-640 was grown in PHB production medium under shake condition (120 rpm) at 30 °C for 60 h. Cell mass was harvested by centrifugation (at 12,000 × g), washed thoroughly with distilled water and dehydrated with acetone. The PHB was extracted with chloroform at room temprature and the process was repeated for three times. The chloroform extracts were pooled, concentrated under reduced pressure and precipitated with double volume of pre-chilled diethyl ether. The pellet was redissolved in chloroform and reprecipitated with diethyl ether. The process was repeated twice and the polymer was obtained as white mass.

The polymer was highly soluble in chloroform, 1N sodium hydroxide, dimethyl formamide and acetic anhydride; moderately soluble in pyridine, dioxane and toluene; but insoluble in water, alkaline hypochlorite, acetone, ethanol, methanol, propanol and diethyl ether.

The purified polymer when digested with concentrated H_2SO_4 in a boiling water bath for 10 min. gave a sharp peak at 235 nm characteristic of crotonic acid (Fig. 3).

The infrared spectra (Fig. 4) of whole cells and isolated PHB showed the presence of a sharp peak at 1734 cm^{-1} characteristic of ester carbonyl stretching (C=0).

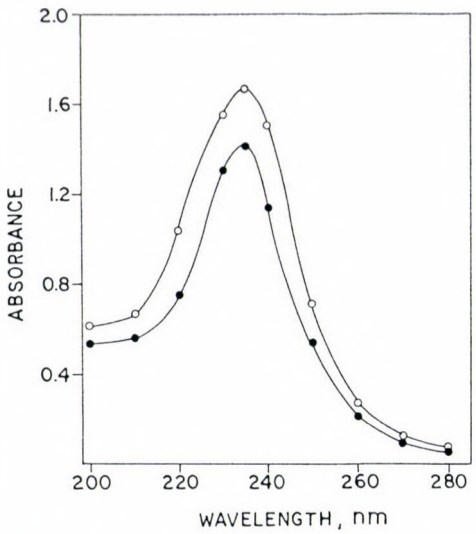

Fig. 3. Comparsion of UV-absorption spectra of polymer (●) isolated from *Rhizobium* sp. TAL-640 with that of authentic PHB (○)

The ^{1}H-NMR spectroscopic study (Fig. 5) revealed that the peak at 1.4 PPM represented the $-CH_3$ group. The doublet at 2.4–2.6 PPM showed the two protons of $-CH_2$ group. The third peak at high s-value (5.2–5.6 PPM) represented the –CH group due to the presence of adjacent etherial oxygen. The last peak was due to an alcoholic –OH group, possibly from the ($-CH_2-CO$) group of the polymer.

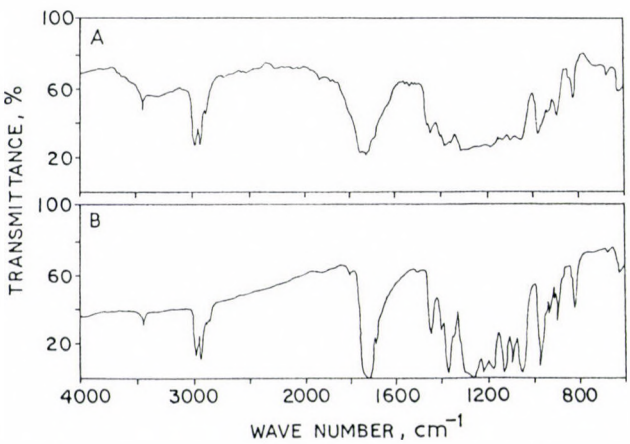

Fig. 4. Infrared absorption spectra of whole cells (A) and PHB (B) of *Rhizobium* sp. TAL-640

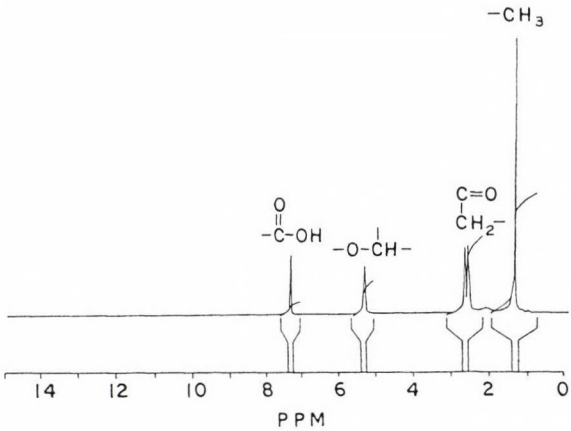

Fig. 5. ^{1}NMR spectra of PHB isolated from *Rhizobium* sp. TAL-640

DISCUSSION

Nearly some 55% of the rhizobial strains so far tested were found to synthesize PHB during nitrogen-limiting and carbon excess conditions. Moreover, strains beloging to the same species were found to accumulate different amounts of PHB, for example strains TAL-1397 and TAL-182 of *R. leguminoserum* (Table 1). Similar results were also obtained by Tombolini and Nuti [21].

Unlike other organisms, the accumulation of PHB by *Rhizobium* TAL-640 after the cessation of growth may be due to the flow of carbon towards cellular metabolism or delayed appearance of enzymes concerned with PHB synthesis in the actively growing cells. These results also support the earlier observations of Patel and Gerson [18] who demonstrated that PHB synthesis in *Rhizobium* NZP 2037 was slow during its active growth phase, but increased during the late exponential phase. The sharp decline of PHB in the later stages of growth indicate possible utilization of polymer as source of carbon and energy.

The utilization of mannitol for better growth and PHB accumulation by the strain TAL-640 is interesting. Casella et al. [4] in their studies with wild type *Rhizobium* 'hedysari' strain HCNT 1 and heat shock mutants also demonstrated that D-mannitol was fundamental to cell growth and PHB production. Carbon source utilization pattern, therefore, indicates that PHB synthesis by a particular strain is not determined by high C:N ratios alone but also requires easily utilizable carbon source.

Results of isolation and characterization of PHB have confirmed and extended our knowledge of the PHB producing potential of the *Rhizobium* strains in the free living state. Further, they also indicate that some selected rhizobial strains could be effectively utilized as a biological source for the production of biodegradable bioplastics.

ACKNOWLEDGEMENTS

The authors are indebted to Prof. A. Chatterjee, CAS on Natural Products, Calcutta University and Mr. R. K. Pal, Jadavpur University for NMR and IR spectral analyses. This work was supported by the Council of Scientific and Industrial Research, New Delhi, India.

REFERENCES

1. Anderson, A. J., Dawes, E. A. (1990) Occurrence, metabolism, metabolic role and industrial uses of bacterial polyhydroxyalkanoates. *Microbiol. Rev. 54,* 450–472.
2. Brandl, H., Gross, R. A., Lenz, R. W., Fuller, R. C. (1990) Plastics from bacteria and for bacteria: poly(beta-hydroxyalkanoates) as natural, biocompatible and biodegradable polyesters. *Adv. Biochem. Eng. Biotechnol. 41,* 77–73.
3. Byrom, D. (1987) Polymer synthesis by microorganisms: technology & economics. *Trends Biotechnol. 5,* 246–250.
4. Casella, S., Leporini, C., Corti, A., Pici, G., Chiellini, E., Casini, E. (1990) Culture substrate effect in the production of poly-β-hydroxybutyrate by *Rhizobium* 'hedysari'. In: *Novel Biodegradable Microbial Polymer.* Kluwer Academic Publishers, Dordrecht, pp. 73–80.
5. Cevallos, M. A., Encarnacion, S., Leija, A., Mora, Y., Mora, J. (1996) Genetic and physiological characterisation of a *Rhizobium etli* mutant strain unable to synthesize poly-β-hydroxybutyrate. *J. Bacteriol. 178,* 1646–1654.
6. Doi, Y. (1990) *Microbial Polyesters.* Verlag Chemie, Weinheim, Germany.
7. Encarnacion, S., Dunn, M., Willms, K., Mora, J. (1995) Fermentation and aerobic metabolism in *Rhizobium etli. J. Bacteriol. 177,* 3058–3066.
8. Forsyth, W. G. C., Hayward, A. C., Roberts, J. B. (1958) The occurrence of poly-β-hydroxybutyric acid in aerobic Gram negative bacteria. *Nature 182,* 800–801.
9. Fottrell, P. F., O'Hara, A. (1969) Multiple forms of D(-) 3-hydroxybutyrate dehydrogenase in *Rhizobium. J. Gen. Microbiol. 57,* 287–292.
10. Gerson, T., Patel, J. J., Wong, M. N. (1978) The effects of age, darkness and nitrate on Poly-β-hydroxybutyrate levels and nitrogen-fixing ability of *Rhizobium* in *Lupinus angustifolius. Physiol. Plant. 42,* 420–424.
11. Hayward, A. C., Forsyth, A. C., Roberts, J. B. (1959) Synthesis and breakdown of poly-β-hydroxybutyric acid by bacteria. *J. Gen. Microbiol. 20,* 510–518.
12. Holmes, P. (1985) Applications of PHB: a microbially produced biodegradable thermoplastics. *Phys. Technol. 16,* 32–36.
13. Karr, D. B., Waters, J. K., Emerich, D. W. (1983) Analysis of poly-β-hydroxybutyrate in *Rhizobium japonicum* bacteroids by ion-exclusion high-pressure liquid chromatography and UV detection. *Appl. Environ. Microbiol. 46,* 1339–1344.
14. Klucas, R. H. (1974) Studies on soybean nodule senescence. *Plant Physiol. 54,* 612–616.
15. Kretovich, W. L., Romanov, V. I., Yushkova, L. A., Shramko, V. I., Fedulova, N. G. (1977) Nitrogen fixation and poly-β-hydroxybutyric acid content in bacteroids of *Rhizobium lupini* and *Rhizobium leguminosarum. Plant and Soil 48,* 291–302.
16. Law, J. H., Slepecky, R. A. (1961) Assay of poly-β-hydroxybutyric acid. *J. Bacteriol. 82,* 33–36.
17. Nuti, M. P., De Bertoldi, M., Lepidi, A. A. (1972) Influence of phenylacetic acid on poly-β-hydroxybutyrate (PHB) polymerization and cell elongation in *Azotobacter chroococcum* Beij. Can *J. Microbiol. 18,* 1257–1261.
18. Patel, J. J., Gerson, T. (1974) Formation and utilisation of carbon reserves by *Rhizobium. Arch. Microbiol. 101,* 211–220.
19. Steinbüchel, A. (1991) Polyhydroxyalkanoic acids. In: Byrom, D. (ed.) *Biomaterials: Novel materials from biological sources.* Macmillan Publishers Ltd. Basingstoke. pp. 123–213.
20. Stockdale, H., Ribbons, D. W., Dawes, E. A. (1968) Occurrence of poly-β-hydroxybutyrate in the Azotobacteriaceae. *J. Bacteriol. 95,* 1798–1803.

21. Tombolini, R., Nuti, M. P. (1989) Poly (β-hydroxyalkanoate) biosynthesis and accumulation by different *Rhizobium* species. *FEMS Microbiol. Lett. 60,* 299–304.
22. Vincent, J. M., Humphrey, B., North, R. (1962) Some features of the fine structure and chemical composition of *Rhizobium trifolii. J. Gen. Microbiol. 29,* 551–555.
23. Wakisaka, Y., Masaki, E., Nishimoto, Y. (1982) Formation of crystalline asporogenous mutants of *Bacillus thuringiensis. Appl. Environ. Microbiol. 43,* 1473–1480.
24. Wong, P. P., Evans, H. J. (1971) Poly-β-hydroxybutyrate utilisation by soybean (*Glycine max* Merr.) nodules and assessment of its role in maintenance of nitrogenase activity. *Plant Physiol. 47,* 750–755.

Acta Biologica Hungarica 51 (1), pp. 83–90 (2000)

EFFECTS OF δ-AMINOLEVULINIC ACID ON PIGMENT FORMATION AND CHLOROPHYLLASE ACTIVITY IN FRENCH BEAN LEAF

H. M. EL-SAHT

Department of Botany, Faculty of Science, Mansoura University, El-Mansoura, Egypt

(Received: October 10, 1998; accepted: March 29, 1999)

Chloroplast development and chlorophyll biosynthesis are co-regulated. Treatment by levulinic acid resulted in a linear relation in both chlorophyll and carotenoid contents, during greening of etiolated French bean leaf discs. Chlorophyll biosynthesis appeared to control that of caroteins. In the prsence of levulinic acid; at different levels, photosystem II (PS II) activity decreased when expressed on a chlorophyll basis. Chlorophyllase activity was increased progressively by increasing levulinic acid concentration. Thus, levulinic acid could be used to arrest the light-induced chloroplast development at a desired phase of greening and acts as determinator of chloroplast development in green tissues.

Keywords: Chlorophyll biosynthesis – carotenoid biosynthesis – levulinic acid – chlorophyllase activity – photosystem II activity – French bean leaf discs

INTRODUCTION

Chloroplast development has been studied using the study of chloroplast biogenesis method during phototransformation of etioplasts to chloroplasts after exposing the etiolated tissues to light [10].

When etiolated tissues are illuminated, only a limited amount of chlorophyll "a" accumulates during a lag phase of a few hours after which time, levels of both chlorophyll "a" and "b" increase rapidly. Newly synthesized chlorophyll "a" is incorporated into apoproteins of P 700-chl. "a"-protein complex (CPI)and chl. "a"-protein complex of photosystem II (CPA) which are used for the formation of the core of photosystems [4, 26]. Some of the chl. "a" is converted to chl. "b", which is incorporated into light harvesting chl. "a"-protein complex of photosystem II (LHCH) apoproteins, together with chl. "a" to form antenna complexes [26].

Chlorophyll plays an important role in plastid development [5, 10, 24].

Chlorophyll and carotenoids synthesized during the greening process bind to apoproteins and form light-harvesting chlorophyll protein complexes that harvest

* Corresponding author.

Abbreviations: ALA, δ-aminolevulinic acid; Chl., chlorophyll; Car., carotenoid; LHCP II, light harvesting chlorophyll-protein complex II.

0236-5383/2000/$ 5.00

solar energy and transfer it to the reaction center. Therefore, inhibition of chlorophyll biosynthesis could lead to the down regulation of chloroplast development.

Levulinic acid (ALA), inhibits the first enzyme in the chlorophyll biosynthetic pathways, ALA dehydratase, which condenses two molecules of ALA to porphobilinogen [13]. Application of levulinic acid to a developed green plant will not have much impact as its photosynthetic apparatus is already well developed. The rate of chlorophyll synthesis in a mature plant is also significantly lower than those of a developing and greening seedling [10].

Treatment with levulinic acid, delays the accumulation of LHC II and the appearance of PS II activity during greening [14]. It was reported that chl. "b" was formed when the size of the poole of chlorophyllide "a" exceeded a threshold value [18]. These observations suggest that the accumulation of chl. "b" and LHC II may be correlated with the rate of synthesis of chl. "a" [26].

In the light of the above-mentioned survey of literature showing close interrelationship between chloroplast development and levulinic acid, this investigation studied pigment formation by exposing etiolated french bean leaf discs to light in the presence of the chlorophyll biosynthesis inhibitor (levulinic acid).

MATERIAL AND METHODS

Time course experiment

French bean (*Phaseolus vulgaris* var. contender) seedlings were grown in plastic dishes in the dark for 11 days at 25 °C and were watered with 1/4-strength Hoagland's solution. Leaf discs (0.5 cm) were excised from the basal part of leaf in the dark from etiolated plants and were incubated in 1/4-strength Hoagland's solution without or with the increasing concentration (0–15 mM) of levulinic acid (ALA) pH adjusted to (5.0) in Petri dishes for 4 hours in the dark to allow sufficient time for diffusion of levulinic acid [10]. The incubation medium was supplemented with 50 μM Kinetin to prevent senescence. Subsequently the leaf discs were transferred to light (3500 Lux) obtained from white fluorescent lamps (Philips 40 W) and incubated for 48 hours at 22 °C.

Analytical methods

Determination of pigments

Photosynthetic pigments (chl. "a", chl. "b" and carotenoids) were determined using the spectrophotometric method as developed by Metzer et al. [16].

A known fresh weight of leaf discs was homogenized in 85% aqueous acetone for 5 min. The homogenate was suction filtered through Whatman No. 1 paper. The filtered extract was made up to volume with 85% acetone. The extract was measured

against a blank of pure 85% aqueous acetone at three wavelengths of 452.5, 644 and 663 nm using a Spekol spectrocolourimeter. Taking into consideration the dilution made, it was possible to determine the concentrations of pigment fractions (chl. a, chl. b and carotenoids) as μg/cm^3 using the following equations:

$$\text{Chl. a} = 10.3\ E_{663} - 0.918\ E_{644} = \quad \mu g/cm^3$$

$$\text{Chl. b} = 19.7\ E_{644} - 3.870\ E_{663} = \quad \mu g/cm^3$$

$$\text{Carotenoids} = 4.2\ E_{452.5} - (0.0264 \text{ chl. a} + 0.426 \text{ chl. b}) = \quad \mu g/cm^3$$

Hill reaction assay (PS II reaction)

As described by Arnon [2], leaf discs were used for preparation of chloroplast pellets that were suspended in 1 mM Tricine-NaOH (pH 7.8), 10 mM NaCl and 10 mM $MgCl_2$ and then kept at 0.4 °C until required.

PS II activity, as indicated by the rate of 2,6-dichlorophenol indophenol (DCPIP) photoreduction was monitored at 606 nm using a Spekol spectrocolourimeter.

Chlorophyllase preparation and assay

As described by Johnson-Flangan and Spencer [11], chloroplast pellets were resuspended in a small volume (0.8–1.0 cm^3) of ice-cold chlorophyllase resuspension buffer (5 mM Na phosphate buffer, pH 7.0, 50 mM KCl and 0.24% Triton-X-100), vortexed briefly and stored on ice. Chlorophyllase activity was measured by HPLC over a 6 minutes assay period using a modification of a previously published method [11]. Chlorophyllase assay buffer 0.5 cm^3 (0.1 M Na-phosphate buffer, pH 7.0, 0.24% Triton-X-100) was equilibrated at 35 °C and the reaction was initiated by the addition of 0.5 cm^3 chloroplasts, adjusted with resuspension buffer to contain 200 μg protein. Each assay was run with a final chl. a concentration of 8 μM, was added to preparations derived from leaf discs without levulinic acid. A 0.4 cm^3 aliquot was removed at time zero mixed with an equal volume of methylene chloride, vortexted and pigments were extracted. Dephylation was allowed to proceed in the remaining assay mix for 6 min. at 35 °C in the dark, after which a second 0.4 cm^3 aliquot was removed. Pigments were partioned into methylene chloride, the extracts were dried under a stream of N_2 and stored at –80 °C or analyzed immediately. Samples were redissolved in 0.05 cm^3 methylene chloride prior to HPLC analysis. Chlorophyllase activities were determined in triplicates. The change in chl. "a" over 6 minutes assay period expressed in ng. min^{-1} · mg protein^{-1}.

RESULTS

Chlorophyll and carotenoid content

Levulinic acid treatment resulted in the reduction of the synthesis of chlorophyll in greening French bean leaf discs. All treatments resulted in a reduction in chlorophyll content (Table 1). The chl. "a/b" ratio of French bean leaf discs increased with increasing concentration of levulinic acid (Table 1).

Although levulinic acid is not a specific inhibitor of carotenoid biosynthesis, carotenoid synthesis was inhibited. Carotenoid content decreased in the presence of levulinic acid (Table 1). Treatment of etiolated French bean leaf discs with increasing concentrations of levulinic acid induced significant decrease in both chl. a, chl. b and car contents as compared with controls (Table 1). The magnitude of decrease was most pronounced with the highest concentration of levulinic acid.

Table 1

Pigment content (Chl – chlorophyll, Car – carotenoid) [mg. 100 g^{-1} (fr. m.)] of etiolated French bean leaf discs exposed to light for 48 hours in the absence or presence of different concentrations of levulinic acid

Concentrations (mM) of levulinic acid	Chl a	Chl b	Chl a + b	Chl a/b	Car
0	59.03	27.66	86.70	2.134	22.63
2.5	54.76**	25.73**	80.50**	2.128*	19.36**
5	47.96**	20.30**	68.26**	2.363**	15.30**
7.5	43.46**	15.50**	58.96**	2.804**	10.46**
10	32.66**	8.80**	41.46**	3.712**	6.40**
12.5	18.83**	4.20**	23.03**	4.483**	4.26**
15	10.86**	2.33*	13.19**	4.661**	1.36**

*p = 0.05, **p = 00.01.

Chl. a + b content of etiolated French bean leaf discs follow a pattern similar to that of chl a and chl b contents (Table 1). On the other hand, chl. a/b ratio of such tissues showed significant increases by increasing levulinic acid concentration i.e. the highest concentration of levulinic acid showed the highest chl. a/b ratio as compared with untreated French bean leaf discs (Table 1).

Photosynthetic activity (PS II)

As the concentration of levulinic acid was increased from 2.5 to 15 mM, the rate of PS II decreased. The magnitude of decrease was more pronounced in the higher than in the lower concentrations of ALA (Table 2).

Thus, the following sequence of treatments (0 > 2.5 mM ALA > 5.0 mM ALA > 7.5 mM ALA > 12.5 mM ALA > 15 mM ALA), was displayed with respect to PS II activity of etiolated French bean leaf discs (Table 2).

Table 2
PS II activity (μM DCPIP reduced mg^{-1} chloroplast) of etiolated French bean leaf discs exposed to light for 48 hours in the absence or presence of different concentrations of levulinic acid

Concentrations (mM) of levulinic acid	Photosynthetic activity (PS II)
0	248.66*
2.5	210.46**
5	173.53**
7.5	145.96**
10	110.23**
12.5	90.56**
15	35.16**

*p = 0.05. **p = 0.01

Chlorophyllase activity

Treatment of French bean leaf discs with increasing concentrations of levulinic acid led to a significant progressive increase in the activity of chlorophyllase (Table 3). Thus, levulinic acid led to a significant increase or to stimulated the activity of chlorophyllase in etiolated French bean leaf discs. The higher levulinic acid concentration, the higher chlorophyllase activity was detected in such tissues.

The following sequence of treatments (15 mM ALA > 12.5 mM ALA > 10.0 mM ALA > 7.5 mM ALA > 5 mM ALA > 2.5 mM ALA > 0), was displayed with respect to chlorophyllase activity in etiolated French bean discs (Table 3).

Table 3
Chlorophyllase activity (ng. min^{-1} · mg $protein^{-1}$) of etiolated French bean leaf discs exposed to light for 48 hours in the absence or presence of different concentrations of levulinic acid

Concentrations (mM) of levulinic acid	Chlorophyllase activity
0	0.72*
2.5	0.79**
5	0.84**
7.5	0.92**
10	1.05**
12.5	1.25**
15	1.74**

*p = 0.05, **p = 0.01

DISCUSSION

Levulinic acid, a competitive inhibitor of the ALA-dehydratase, inhibited chlorophyll biosynthesis and increased the chl. a/b ratio (Table 1). The increased chl. a/b ratio was not due to the preferential inhibition of chl. b over that of chl. a. It has been proposed that, the level of chl. a must accumulate before chl. b synthesis can begin [17]. Therefore, reduced chl. a synthesis due to levulinic acid treatment resulted in a low chl. b synthesis and high chl. a/b ratio.

Although levulinic acid is not an inhibitor of carotenoid biosynthesis, a decrease in carotenoid content was observed in levulinic acid-treated French bean plants (Table 1). This suggests that the amount of carotenoid is proportional to the amount of chlorophyll synthesized. During greening of etiolated tissues, chlorophyll biosynthesis is triggered by light. It has been shown that accumulation of carotenoids is regulated by light [10, 21].

Most of the studies on light induced carotenoid synthesis has been done in chlorophyll-less fungal systems and in barely leaves [8, 10]. In green tissues, carotenoids are synthesized in chloroplasts and are essential for the formation of LHCP II [19]. In higher plants, there are insufficient reports on the photoregulation of enzymes or genes responsible for carotenoid biosynthesis [3].

When expressed on a chlorophyll basis, PS II activity decreased in response to levulinic acid treatment (Table 2). The results suggest that chl.-mediated developmental regulation of PS II is under stricter regulation than that of PS I. PS II is enriched in chl. b, whereas chl. a is more abundant in PS I. Due to application of levulinic acid, the chl. a/b ratio increases i.e. the relative amount of chl. a remains higher than that of chl. b. This could explain the differential regulation of PS II activity in the presence of levulinic acid. The inhibition of photosynthetic activity as a result of levulinic acid application could be attributed to inhibition of PS II activity [6, 9] by the inhibition of electron transport in PS II and the production of ATP and NADPH needed to reduce CO_2 [10, 15] and decrease in rate of photosynthetic flow [7, 10, 22], by acting the protein-plastoqunione level [27].

Chlorophyllase activity increased in response to levulinic acid treatment (Table 3). The results suggest that chlorophyllase plays a central role in the regulation of chloroplasts of French bean leaves. This enzyme was the key enzyme in chlorophyll biosynthesis and degradation. The decrease in chlorophyll content was consistent with the increase in chlorophyllase activity due to the effect of levulinic acid.

Numerous studies of pigment degradation associated with senescence have implicated the involvement of chlorophyllase [1, 12, 20, 25].

Results from the present study show that chlorophyllase activity is higher during treatment with levulinic acid. Johnson-Flanagan Spencer [11] showed that during maturation the green pigment (chl. and related pigments), content of canola seeds decreased linearly. Green pigment degradation was associated with increased chlorophyllase activity in canola [12].

REFERENCES

1. Amir-Shapira, D., Gold, Chmidt, E. E., Altman, A. (1987) Chlorophyll catabolism in senescing plant tissues: *In vivo* breakdown intermediates suggest; different degradative pathway, for citrus fruit and parsley leaves. *Proc. Nat. Acad. Sci. USA. 84,* 1901–1905.
2. Arnon, D. I. (1949) Copper enzyme in isolated chloroplasts. Polyphenol oxidase in *Beta vulgaris. Plant Physiol. 24,* 1–15.
3. Bartley, G. E., Scolink, P. A., Giuliano, G. (1994) Molecular biology of carotenoid biosynthesis in plants. *Ann. Rev., Plant Physiol. Plant Mol. Biol. 45,* 287–301.
4. Bhaya, D., Gastelfranco, P. A. (1985) Chlorophyllase biosynthesis and assembly into chlorophyll-protein complexes in isolated developing chloroplasts. *Proc. Nat. Acad. Sci. W8A. 82,* 5360–5374.
5. Eichacker, L. A., Soll, J., Lauterback, P., Rudiger, W., Klein, P. R., Mullet, J. E. (1990) *In vitro* synthesis of chlorophyll a in the dark triggers accumulation of chlorophyll a apoproteines in barley etioplasts. *J. Biol. Chem. 265,* 13566–13571.
6. El-Maghraby, Y. H. (1997) *Physiological and biochemical studies of some herbicides in French bean plants.* M. Sc. Thesis, Mans. Univ. Mansoura, Egypt.
7. Fedtke, C. (1979) Physiological responses of soybean *(Glycine max)* plants to metabolism. *Weed Sci. 27,* 192–195.
8. Harding, R. W., Shropshike, W. (1980) Photocontrol of carotenoid biosynthesis. *Ann. Rev. Plant Physiol. 31,* 217–238.
9. Hiranpradit, H., Foy, C. L., Shear, G. M., Fletch, C. E., Kirkwood, R. C. (1972) *Herbicides and plant growth regulators.* Vol. 2, 268–273. Granada, London, Toronto and New York.
10. Jilani, A., Kar, S., Bose, S., Tripathy, B. C. (1996) Regulation of the carotenoid content and chloroplast development by levulinic acid. *Physiol. Plant. 96,* 139–145.
11. Johnson-Flanagan, A. M., McLachan, G. (1990) The role of chlorophyllase in degreening canola *(Brassica rapus)* seeds and its activation by sublethal freezing. *Physiol. Plant. 80,* 460–466.
12. Johnson-Flanagan, A. M., Spencer, M. S. (1996) Chlorophyllase and peroxidas activity during degreening of maturing canola *(Brassica rapus)* and mustard *(Brassica juncea). Physiol. Plant. 97,* 353–359.
13. Klein, S., Harel, E., Neman, E., Katz, E., Meller, E. (1975) Accumulation of 5-amino levulinic acid and its relation to chlorophyll synthesis and development of plastid structure in greening leaves. *Plant Physiol. 56,* 486–496.
14. Konis, Y., Klein, S., Ohad, I. (1978) The effect of levulinic acid on the light induced development of photosystem I and II activities in greening maize leaves. *Photochem. Photobiol. 27,* 177–182.
15. Masarovecova, E., Jesko, T., Navara, I., Elias, P., Dedicova, E., Vizarova, A. (1985) CO_2-exchange in sugar beet leaves following the application of the sublethal concentration of the herbicide. *Biol. Plant. 40,* 891–901.
16. Metzner, H., Reu, H., Senger, H. H. (1965) Untersuchungen zur Synchronisierbarkeit einzelner Pigment. Mangel mutantent von *Chlorella. Planta 65,* 186–199.
17. Qelze-Karow, H., Mohr, H. (1978) Control of chlorophyll b biosynthesis by phytochrome. *Photochem. Photobiol. 27,* 189–193.
18. Qelze-Karow, H., Kasemir, H., Mohr, H. (1978) Control of chlorophyll b formation by phytochrome and a threshold level of chlorophyllide a. In: Koyunogbu, A., Argyroudi, G. (eds) *Chloroplast development.* Elsevier/North-Holland Biomedical Press, Amsterdam, pp. 787–792.
19. Paulsen, H., Rumler, V., Rudiger, W. (1990) Reconstitution of pigment-containing complexes from light-harvesting chlorophyll a/b – binding protein overexpressed in *Escherichia coli. Planta 181,* 204–211.
20. Purohit, S. S. (1982) Prevention by kinetin of ethylene-induced chlorophyllase activity in senescing detached leaves of *Helianthus annus. Biochem. Physiol. Pflanz.* 177, 625–627.
21. Reur, W. (1976) Photoregulation carotenoid biosynthesis in plants. *Pure App. Biochem. 47,* 237–243.
22. Richard, E. P., Goss, T. R., Arntzens, C. H., Slife, F. W. (1983) Determination of herbicide inhibition of photosynthetic electron transport by fhrxace. *Weed Sci. 31,* 361–367.

23. Richmond, A. F., Lang, A. (1957) Effect of kinetin on protein content and survival of detached *Xanthium* leaves. *Science 125,* 650–651.
24. Rudiger, W. (1993) The esterification of chlorophyllide and its implication for thylakoid development. In: Sundquist, C., Ryberg, M. (eds). *Pigment-protein complexes in plastids. Synthesis and assembly.* Academic Press, San Diego, pp. 219–240.
25. Shimokava, K., Shimada, S., Yaeo, K. (1978) Ethylene-enhanced chlorophyllase activity during degreening of citrus. *Un Shiu. Marc. Sci. Hortic. 8,* 129–135.
26. Tanaka, Y., Tanaka, A., Tsuji, H. (1993) Effects of δ-aminolevulinic acid on the accumulation of chlorophyll b and apoproteins of the light-harvesting chlorophyll a/b – protein complex of photosystem II. *Plant Cell Physiol. 34,* 465–472.
27. Turesanyi, G. (1984) An altered concept of the model of the binding sites for triazine in *Amaranthus revetoflexes* and *Senico vulgaris. Acta Bot. Hung. 30,* 201–204.

Acta Biologica Hungarica 51 (1), pp. 91–97 (2000)

MORPHOMETRY OF THE FRTL-5 CELLS AFTER IRRADIATION

DRAGA ŠTIBLAR-MARTINČIČ*, ZDENKA PAJER and A. CÖR

Institute of Histology and Embryology, Medical Faculty, University of Ljubljana, Korytkova 2/I, 1000 Ljubljana, Slovenia

(Received: September 8, 1998; accepted: January 12, 1999)

The morphological changes of *in vitro* irradiated FRTL-5 cells and their ability to grow in semi-solid medium were studied morphometrically. FRTL-5 cells were grown in medium with 4 different concentrations of TSH (0, 0.1, 1, 10 mU/ml). After irradiation with 0 Gy, 2 Gy and 4 Gy, the cells were seeded on glass cover-slips and in methocel. Fourteen days after irradiation, the morphometric analysis of FRTL-5 cells and their nuclei was performed. The results showed that irradiation and different doses of TSH have influence on FRTL-5 cell size, more on their nuclei than on the cells as a whole. Growing of FRTL-5 cells in the methocel indicates the possible transformation of these cells after long-culturing in the TSH medium and after irradiation.

Keywords: Astereology – FRTL-5 cells – FRTL-5 cell colonies – irradiation – methocel

INTRODUCTION

Recent technical advances in *in vitro* culturing of epithelial cells have made it possible to study the effects of irradiation at the cellular level. Exposure of cells to ionizing irradiation results in molecular damages which can be expressed at the cellular, metabolic or chromosomal levels [19]. The most important step in cell injury caused by irradiation is thought to be an irreversible DNA alteration [13].

Irradiation energy can affect cytoplasm enzymes, macromolecules or organelles, of which the nucleus is the most vulnerable target. With sufficient exposure, the nucleus appears swollen and the chromatin clumped. After whole-body X-irradiation of mice, the doses of 0.1 to 2 Gy induced a considerable increase of lymphocyte nuclear volume [18]. At high doses, pyknosis and even fragmentation of the nucleus, abnormal mitotic figures and bizarre nuclear morphology may appear. Irradiation inhibits the proliferate activity of cells. Irradiated cells sometimes undergo nuclear division without the formation of daughter cells, thus producing multinucleated giant cells. However, normal individual cells are capable of repairing sublethal irradiation injuries [5].

* Corresponding author, E-mail: Draga.Stiblar@MF.UNI-LJ.SI.

0236-5383/2000/$ 5.00

Transformation of normal cells in tissue cultures to tumour cells can arise from infection with a transforming virus [20], from incorporation of new genomic DNA [7] or following exposure to a chemical carcinogen [11] or also irradiation [12]. The transformed cells acquire altered growth characteristics and can be selected as colonies in a semi-solid medium such as agar or methocel [9]. They also form tumours in animals of origin or in nude athymic mice [8, 12].

Fischer Rat Thyroid cells in low serum or FRTL-5 cells is a cloned cell line that was derived from follicular cells of Fischer rat thyroids. The cells grow as a monolayer culture. *In vitro* they maintain thyroid morphology and function and require the mitogenic thyroid hormone TSH (thyroid stimulating hormone) for growth. In the absence of TSH these cells remain viable, but non-proliferative for an extended period of time [1].

FRTL-5 cells also show a primary-like epithelial cell morphology, the lack of growth in semi-solid media and at least lack of any detectable signs of spontaneous transformation. They should be non-tumourogenic in syngenic animals [2].

However, our experiences with the FRTL-5 cell line showed that continuous culturing of this cell line in a medium with 1 mU/ml of TSH had certain effects. The morphological characteristics were changed, especially the size of their nuclei [17]. Unexpectedly, we also found that FRTL-5 cells grew in the methocel, although the morphometrical data, such as colony areas, perimeters, maximal diameters and form factors, showed that FRTL-5 cells are untransformed [15].

The aim of our study was to evaluate the morphological changes of FRTL-5 cells after irradiation with 2 Gy and 4 Gy and their ability to grow in the semi-solid medium. Besides, the influence of different TSH doses on irradiated FRTL-5 cells was analysed. The basic aim of this research was to detect any morphological identifiable sign of transformation of the irradiated cells using morphometric methods.

MATERIAL AND METHODS

FRTL-5 cells were grown in Coon's modification of Ham's F-12 medium (Sigma) supplemented with 5% calf serum (Gibco), MEM non-essential amino acids (Gibco), L-glutamin, penicillin (100 U/ml), streptomycin (100 μg/ml) and the following 6 hormones: insulin (10 μm/ml), hydrocortisone (10 nM/ml), transferrin (5 μg/ml), glycyl-L-histidyl-L-lysine acetate (10 ng/ml), somatostatin (10 ng/ml) and bovine TSH (thyroid-stimulating hormone, 1 mU/ml) (all Sigma, Deisenhofen, Germany).

The cells were trypsinised with a mixture of 0.25% trypsin (Gibco) and 2.5 mM ethylene-diaminetetraacetic acid (EDTA, Gibco) and counted in a hemocytometer slide at an objective magnification of ×10. 0.5×10^6 of trypsinised FRTL-5 cells were seeded in 4 different concentrations of TSH: 0, 0.1, 1 and 10 mU/ml in 3 parallel culture dishes. After 4 days growth in the corresponding concentrations of TSH, the cells were irradiated with one dose of 0 Gy, 2 Gy and 4 Gy on Röntgen apparatus DARPAC 2000-XE with the radiation dose 2.5 Gy/min.

After irradiation, the cells grew further in 4 different concentrations of TSH for 6 days. After 6 days, the cells were again trypsinised and counted. 0.5×10^6 of FRTL-5 cells were seeded on glass cover-slips for 8 days, fixed in methanol and stained with haematoxylin-eosin. Parallel 1×10^5 of FRTL-5 cells were seeded in a semi-solid medium of 0.6% methocel suspension (methylcellulose, 4000 cps, Sigma) over a layer of 1% agar (Difco Bacto Agar) in 4 different TSH culture media (0, 0.1, 1, 10 mU TSH/ml). They were left to grow in the methocel for 8 days without feeding (14 days after irradiation of the cells) and than photographed.

The astereological morphometrical analysis was first performed on systematically sampled, haematoxylin-eosin stained FRTL-5 cells. A ×10 ocular fitted with B-100 double square lattice test system and a ×100 oil immersion objective were employed [21]. The mean areas of 200 cells, their nuclei and cytoplasm were estimated. The second part of the analysis was carried out with a semi-automatic image analysis system (IBAS-1000, Kontron, Eching, Germany). A ×40 objective was used for estimating the mean nuclear area of 300 FRTL-5 cells.

On the same IBAS-1000 system the astereological analysis of a total 50 photographed colonies of the FRTL-5 cells developed in the methocel after 8 days in culture was carried out. For the randomly selected colonies their mean areas were measured.

The results were statistically evaluated using Student's *t*-test.

RESULTS

Unirradiated cells (Fig. 1a) were small, round shaped with small nuclei containing one or two nucleoli. The cytoplasm was often stretched in various directions. The cells growing in colonies sometimes developed follicular lumina at their center. The cells reached the described morphological characteristics 4 days after trypsinization [16]. After irradiation with 2Gy or 4 Gy, the cells with big, irregular shaped nuclei and abundent cytoplasm containing many vacuoles appeared between morphologically normal cells (Fig. 1b). We found large cells also in unirradiated group with fre-

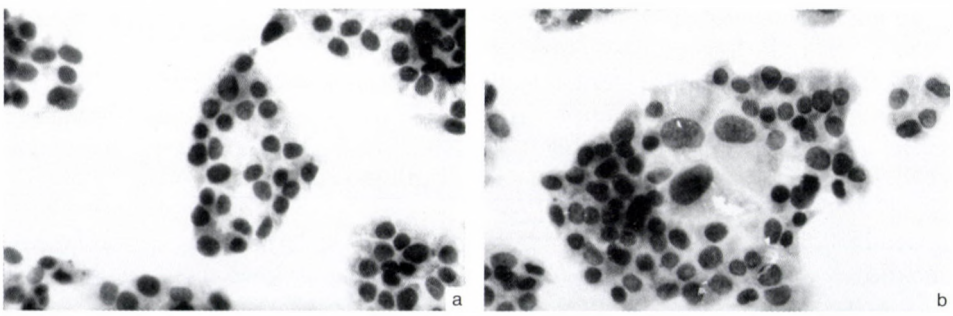

Fig. 1. Morphology of unirradiated (a) and 4 Gy irradiated (b) FRTL-5 cells stained with haematoxylin-eosin 14 days after irradiation (×400)

quency of 4.4%. The frequency of large cells was 6.3–8.9% after irradiation with 2 and 4 Gy, respectively.

Unirradiated FRTL-5 cells as well as cells irradiated with 2 Gy formed colonies or clones in a semi-solid medium of 0.6% methocel over 1% agar base (Fig. 2a) while the cells irradiated with 4 Gy did not grow in the same medium. The colonies of FRTL-5 cells irradiated with 2 Gy were more or less round. The size and number of cells was different in each colony (Fig. 2b).

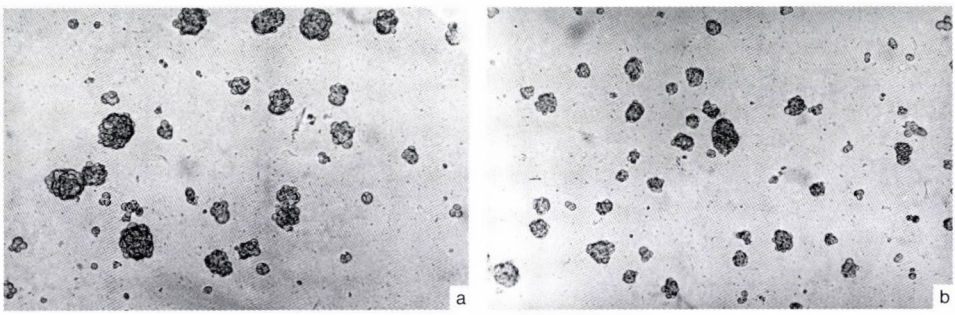

Fig. 2. FRTL-5 cell colonies of unirradiated cells (a) and 14 days after irradiation (b) in a semi-solid medium (×400)

Our morphometric results represent comparison of irradiated FRTL-5 cells with unirradiated ones and evaluation of their growth characterisctics in the semi-solid medium without or with TSH 14 days after irradiation.

The mean areas of the unirradiated FRTL-5 cells increased significantly ($P < 0.01$) with the increased concentrations of TSH. After irradiation with 2 Gy and 4 Gy the mean areas of the unirradiated FRTL-5 cells increased significantly at the concentra-

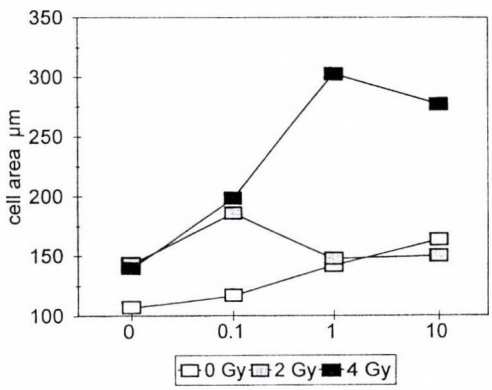

Fig. 3. The mean areas of FRTL-5 cells irradiated with single doses of 0, 2 and 4 Gy 14 after irradiation with different concentration of TSH

tions of 0 and 0.1 mU/ml TSH according to unirradiated cells ($P < 0.001$, $P < 0.01$). While after irradiation with 4 Gy the mean areas of the FRTL-5 cells also increased significantly ($P < 0.01$) at the concentrations of 1 and 10 mU/ml TSH (Fig. 3).

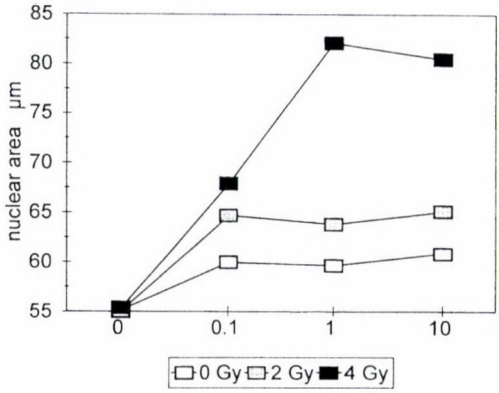

Fig. 4. The mean areas of FRTL-5 cells nuclei irradiated with single doses of 0, 2 and 4 Gy 14 after irradiation with different concentration of TSH

The mean areas of the FRTL-5 cells nuclei increased significantly ($P < 0.001$) after irradiation with 2 Gy and 4 Gy with the increased concentrations of TSH (Fig. 4).

The mean areas of the FRTL-5 cells colonies were significantly ($P < 0.001$) smaller after irradiation with 2 Gy in comparison with 0 Gy, but increased significantly ($P < 0.001$) with the increased concentrations of TSH. After irradiation with 4 Gy, the FRTL-5 cells did not form colonies in the methocel (Fig. 5).

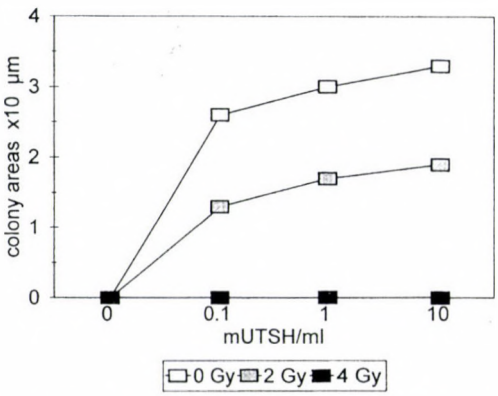

Fig. 5. The mean areas of FRTL-5 cells colonies irradiated with single doses of 0, 2 and 4 Gy 14 after irradiation with different concentration of TSH

DISCUSSION

Little information is available concerning the cellular level-effects of irradiation on FRTL-5 cells *in vitro*. Low and high irradiation doses lead to chromosomal damage and DNA alteration. Under the influence of irradiation, the DNA molecules are changed chemically directly or indirectly through free radicals that arise in the cells and react with the DNA. In both cases, the chemical changes are reflected as noxious biological effects. Loss of reproductive ability occurs in an appreciable fraction of the cells after a moderate dose of a few hundred rads [10].

Our results showed that the areas of the FRTL-5 cells and their nuclei increased in size with increasing concentration of TSH. After irradiation this increase was more obvious after 4 Gy than after 2 Gy in comparison with unirradiated cells. With the increased concentrations of TSH, the size of the cells as well as their nuclei increased after 4 Gy of irradiation. After irradiation with 2 Gy the size of the cell increased only at the concentration of 0.1 mU/ml TSH, while the size of their nuclei after 4 Gy of irradiation increased at the concentrations of 1 and 10 mU/ml TSH as well.

Namba and coworkers [14] found that after low doses of irradiation (0.2 – 2 Gy) the cell cycle of human thyroid cells were arrested because of accumulation at G1. Wild-type p53 expression in primary thyroid cells was increased following irradiation. The relationship between radiation-induced cell survival and DNA damage in primary human fibroblasts of different radiosensitivity is connected with the amount of DNA damage remaining after repair [22]. The study of Brosing et al. [3] indicates that radiation response in FRTL-5 cells is indipendent of proliferative status. Proliferative status of the cells is not a major determinant of radiation response.

According to Ambesi-Impiombato and Villone [2], FRTL-5 cells, as normal follicular thyroid cells, do not grow in semi-solid media. If cells are transformed with different agents, or if they are cancer cells, they form colonies in a semi-solid medium [4]. Different criteria are used to determine the growth characteristics of colonies raised from different kinds of transformed cells in a semi-solid medium. One is the size of the colonies [6].

Since the FRTL-5 cells formed colonies in the semi-solid medium, we used the mean areas of the cell colonies to evaluate their growth characteristics. The colonies of the FRTL-5 cells were smaller after irradiation with 2 Gy in comparison with colonies of unirradiated cells, while after 4 Gy the colonies did not grow at all in the methocel. TSH increased the size of the colonies.

Our results showed that irradiation and different doses of TSH have influence on FRTL-5 cell size, more on their nuclei than on the cells as a whole. Growing of the FRTL-5 cells in the methocel indicates the possible transformation of these cells after long-culturing in the TSH medium and after irradiation. According to Kuettel et al. [12] the transformation of normal cells in tissue culture to tumour cells can arise also from irradiation. Therefore, we assumed that the injection into the animal of Fischer strain could confirm the transformation of irradiated FRTL-5 cells.

REFERENCES

1. Ambesi-Impiombato, F. S., Parks, L. A. M., Coon, H. G. (1980) Culture of hormone-dependent functional epithelial cells from rat thyroids. *Proc. Natl. Acad. Sci. 77,* 3455–3459.
2. Ambesi-Impiombato, F. S., Villone, G. (1987) The FRTL-5 thyroid cell strain as a model for studies on thyroid cell growth. *Acta Endocrinol. (Copenh) Suppl. 281,* 242–246.
3. Brosing, J. W., Giese, W. L., Mulcahy, R. T. (1989) Lack of a differential radiation response for proliferative and non-proliferative rat thyroid cells (FRTL-5) *in vitro.* I. *J. Radiation Oncology, Biology, Physics 16,* 1511–1517.
4. Calaf, G., Russo, J. (1993) Transformation of human breast epithelial cells by chemical carcinogens. *Carcinogenesis 14,* 483–492.
5. Cotran, R. S., Kumar, V., Robbins, S. L. (1994) *Pathologic Basis of Disease.* WB Saunders Company, Philadelphia, London, Toronto, Montreal, Sidney, Tokyo, 402–440.
6. Dai, Z., Takahashi, S. I., van Wyk, J. J., D'Ercole, A. J. (1992) Creation of an autocrine model of insulin-like growth factor-I action in transfected FRTL-5 cells. *Endocrinology 130,* 3175–3183.
7. Derwahl, M., Broecker, M., Aeschimann, S., Schatz, H., Studer, H. (1992) Malignant transformation of rat thyroid cells transfected with the human TSH receptor cDNA. *Biochem. Biophys. Res. Commun. 183,* 220–226.
8. Endo, T., Shimura, H., Saito, T., Onaya, T. (1990) Cloning of malignant transformed rat thyroid (FRTL) cells with thyrotropin receptors and their growth inhibition by 3',5'-cyclic adenosine monophosphate. *Endocrinology 126,* 1492–1497.
9. Freshney, R. I. (1994) Culture of animal cells: A manual of basic technique. 3rd ed. John Wiley & Sons, Inc., New York, Chichester, Brisbane, Toronto, Singapore, 166–169.
10. Hall, E. J. (1994) *Radiobiology for the Radiologist.* JB Lippincott Company, Philadelphia, 46–69.
11. Hashimura, T., Kanamura, H., Yoshida, O. (1987) Soft agar formation of bladder cells during carcinogenesis induced by N-butyl-N-(4-hydroxybutyl)nitrosamine and application to detection of bladder cancer promoters. *Jpn J. Cancer Res. (Gann) 78,* 473–479.
12. Kuettel, M. R., Thraves, P. J., Jung, M., Varghese, S. P., Prasad, S. C., Rhim, J. S., Dritschilo, A. (1996) Radiation-induced neoplastic transformation of human prostate epithelial cells. *Cancer Res. 56,* 5–10.
13. Nakamura, N., Sposto, R. (1989) X-ray-induced mutations in cultured human thyroid cells. *Radiat. Res. 119,* 123–133.
14. Namba, H., Hara, T., Tukazaki, T., Migita, K., Ishikawa, N., Ito, K., Nagataki, S., Yamashita, S. (1995) Radiation-induced G1 arrest is selectively mediated by the p53-WAF1-Cip1 pathway in human thyroid cells. *Cancer Research 55,* 2075–2080.
15. Pajer, Z. (1996) *Growth of FRTL-5 and MCF-7 cells in semi-solid medium.* Proc. 3rd Inter Confer, Life Sciences 1996, Gozd Martuljek, Slovenia, 27– 28.
16. Pajer, Z., Cör, A. (1996) Astereological analysis of FRTL-5 cells up to four days after trypsinisation. *Eur. J. Physiol. 431/Suppl* R209–R210.
17. Pajer, Z., Cör, A., Štiblar-Martinčič, D. (1996) *Long-term effect of thyrotropin on FRTL-5 cells.* Proc 3rd Inter Confer, Life Sciences 1996, Gozd Martuljek, Slovenia, 25–26.
18. Somosy, Z., Pikli, A., Kubasova, T., Köteles, G. J., Bodo, M. (1985) Alteration of nuclear diameter of murine lymphocytes upon the effect of X-irradiation *in vivo. Radiobiol. Radiothem. 26,* 305–310.
19. Tannock, I. F., Hill, R. P. (1987) *The Basic Science of Oncology.* Pergamon Press, England, 106–124.
20. Temin, H. M., Rubin, H. (1958) Characteristics of an assay for Rous sarcoma virus and Rous sarcoma cells in tissue culture. *Virology 6,* 669–688.
21. Weibel, E. R. (1979) *Stereological Methods.* Academic Press, New York, 101–161.
22. Wurm, R., Burnet, N. G., Duggal, N., Yaenold, J. R., Peacock, J. H. (1994) Cellular radiosensitivity and DNA damage in primary human fibroblasts. I *J. Radiation Oncology, Biology, Physics 30,* 625–633.

Acta Biologica Hungarica 51 (1), pp. 99–105 (2000)

AUTOMATED FLUORESCENT DETECTION OF A 10 LOCI MULTIPLEX FOR PATERNITY TESTING

A. LÁSZIK[1], B. BRINKMANN[2], P. SÓTONYI[1] and A. FALUS[3]*

[1]Department of Forensic Medicine, [3]Department of Genetics, Cell and Immunbiology, Semmelweis University, Budapest, P.O. Box 37, H-1445 Hungary;
[2]Department of Forensic Medicine, Westfälische Wilhelms Universität, Münster, Germany

(Received: July 28, 1999; accepted: September 21, 1999)

The discovery of new highly efficient tetra repeat STR loci, development of fluorescence multicolour dye technology and capillary electrophoresis have made it possible to amplify ten loci in a single reaction. This combination provides an extraordinary effectiveness of simultaneous amplification and detection. With this method it became possible to determine individual identity and paternity at an enhanced level of precision and accuracy in 1 to 2 days with a high biostatistical probability. This review demonstrates the role of automated fluorescent multicolour dye genotyping technology in forensic paternity testing.

Keywords: STR systems – paternity testing – automated genotyping – fluorescent detection

INTRODUCTION

In the human genome numerous STR (microsatellite) loci have been discovered, where alleles can be amplified under the same conditions. These STRs are composed of two to seven nucleotide repeat units, widespread throughout the genome and have been evaluated for forensic purposes [2, 6, 13, 19]. The recently developed fluorescent multicolour dye technology and capillary electrophoresis (CE) allows multiple loci, including those with overlapping allel-size ranges, to be amplified and analysed in a single reaction and capillary injection by locus-specific, different colour dye-labelled primers. The aim of this study was to introduce the automated fluorescent multicolour dye genotyping technology into forensic paternity testing.

Short tandem repeat markers (microsatellites) are polymorphic DNA loci that contain a repeated nucleotide sequence and are less than 350 bp long. Tetranucleotide repeat loci are the most widely used STRs in human identity testing because they are less prone to produce PCR stutter bands than tri- or dinucleotide repeats. The number of nucleotides per repeat unit is the same for the majority of repeats within an STR locus. The number of repeat units at an STR locus may differ, so alleles of many different lengths are possible. Polymorphic STR loci are therefore very useful for

* Corresponding author.

0236-5383/2000/$ 5.00

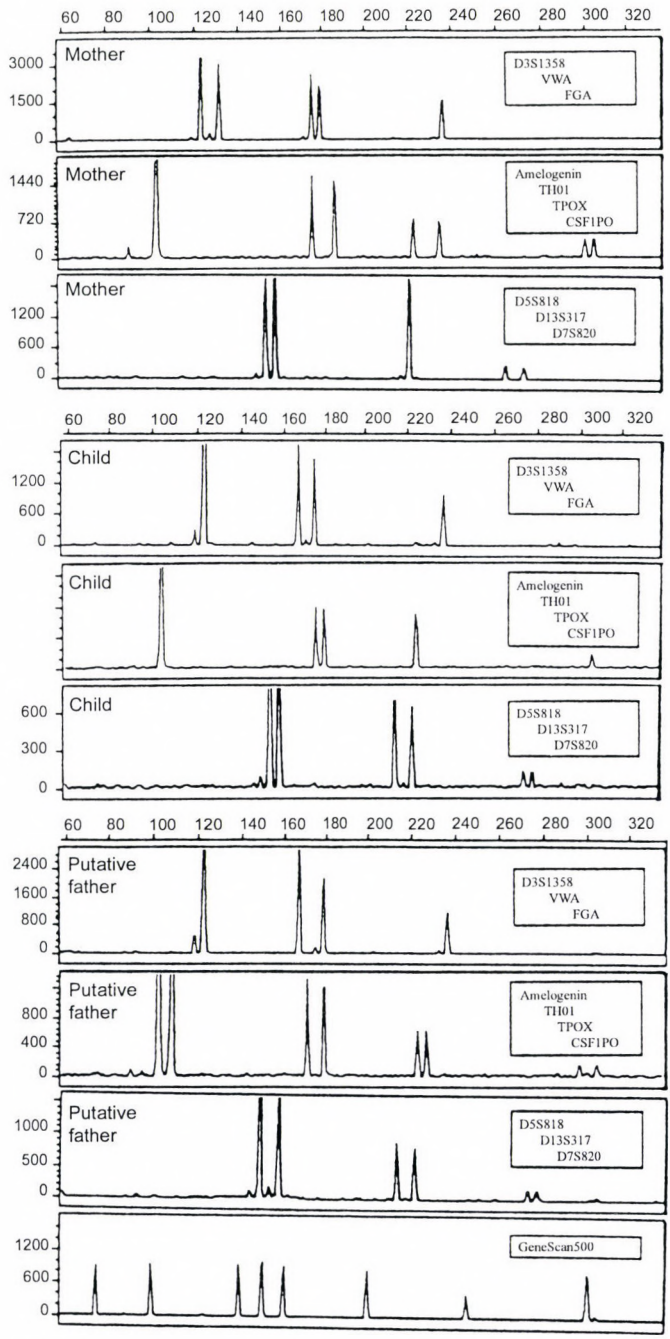

Fig. 1. The electropherogram of 10 loci of the examined persons on the ABI Prism 310 Genetic Analyser (mother, child and the putative father from top to bottom). In the final row of the father's results, the internal standard GeneScan 500(ROX) is shown

human identification purposes [5, 6, 18]. PCR based STR analysis has more advantages over conventional methods of DNA analysis such as Restriction Fragment Length Polymorphism (RFLP), which offers a high degree of discrimination, but it also presents some limitations. Thus, relatively high amounts (~500 ng) of undegraded DNA are required for profiling and several days are necessary to detect the allelic patterns [14]. The small size of STR loci improves the chance of obtaining a result, particularly for samples containing very small amounts of DNA or degraded DNA and makes them ideal candidates for co-amplification while keeping all amplified alleles smaller than 350 base pairs. Many STR loci can therefore be typed from a single PCR. The amplified STR alleles have discrete sizes, allowing relatively simple interpretation of the results. PCR-based tests are rapid, giving results in 24 hours or less and they are easy to standardise and automate, ensuring reproducible results [5, 8] (Fig. 1).

To separate amplified STR fragments capillary electrophoresis (CE) represents a powerful technique. A CE instrument consists of an injection system, a separation capillary tube, a high voltage source, electrodes and detector (Fig. 2). In the ABI Prism 310 Genetic Analyser capillary electrophoresis system the electrokinetic injection technique and low viscosity polymers are used [4, 24].

With capillary electrophoresis and laser-induced fluorescence multicomponent analysis it is possible to separate and detect with multiple primers – each labelled with a distinct fluorescent dye – 10 loci amplified in a single test tube, including loci that have alleles with overlapping size ranges. The three fluorescent dyes used in the AmpFLSTR Profiler PCR Amplification Kit are the NHS-ester dyes: 5-FAM, JOE and NED. The fourth dye, ROX, is used for the GeneScan 500 internal size standard. Each of these fluorescent dyes emits its maximum fluorescence at a different wavelength (525–605 nm). During data collection the wavelengths are separated by a diffraction grating onto a CCD camera in a predictably spaced pattern. 5-FAM emits at the shortest wavelength and is detected as blue, followed by JOE(green), NED (yellow), and ROX (red), listed in order of increasing wavelength. Automatic allele sizing and quantitation are made possible by running an internal lane standard (GeneScan500) that is recognised by computer to generate a calibration curve. Thus, electrophoretic mobility variations (from injection to injection) that can lead to inconsistent allelic sizing are automatically normalized [8]. The precision of the ABI Prism 310 Genetic Analyser capillary electrophoresis system, with a software developed for automated genotyping of alleles, allows the accurate genotyping of STR loci. Sizing precision of ≤0.16 nucleotide standard deviation can obtained with this system, allowing on accurate genotyping even of length variants that differ in length by a single nucleotide [3, 15]. Employing capillary electrophoresis rather than gel electrophoresis reduces the manual work load and therefore dependence on varying manual skills of different analysts. With CE manual gel pouring, sample loading and sample injection can be automated or eliminated. Electrophoretic separations are possible at higher field strengths due to the higher surface area-to-volume ratio. This results in faster separation times and better resolution. CE performs detection simultaneously, and results are stored in the computer. This simplifies data analyses [3].

The combined power of discrimination of the AmpFLSTR Profiler systems exceeds 1 in 3.58×10^9, while the combined paternity exclusion (P_E value) is 0.9994 in Caucasoid populations (PE/ABI User manual).

CASE REPORT

At the Institute of Forensic Medicine at the University of Münster, Germany, paternity is investigated in hundreds of cases by automated fluorescence analysis of STRs. In the following, we present one of them to illustrate the efficiency of these techniques. DNA was extracted from saliva swabs of one family with the Chelex method as described previously [25]. Special precautions and care had been taken during DNA extraction and PCR setup to prevent transfer of DNA from one sample to another. The following loci were co-amplified in a single PCR reaction and separated by capillary electrophoresis: D3S1358 [16], vWA [12], FGA [17], TH01 [6, 21], TPOX [1], CFS1PO [10], D5S818 [11], D13S317 [11], D7S820 [9, 11] and the sex test amelogenin [23] (Table 1).

Approximately 1 ng of DNA was amplified in a final volume of 25 µl. Each of the individuals was typed for 10 systems which were co-amplified in the same tube, according to the AmpFLSTR Profiler PCR Amplification Kit manufacturer's recommendations. The use of Amplitaq Gold (Perkin Elmer) polymerase was crucial for successful multiplex analysis.

The *cycling conditions* were 95 °C – 11 min, followed by 28 cycles for 94 °C – 1 min, 59 – 1 min, 72 °C – 1 min; 60 °C and a 30 min hold at 10 °C in Thermalcycler 9600 Perkin Elmer.

Table 1
The examined STR loci and their characteristics

Locus	Chromosome location	Sequence motif	Size range (bp)*	Dye label
D3S1358	3p	TCTA $(TCTG)_{1-3}(TCTA)_n$	114–142	5-FAM (blue)
vWA	12p12-pter	TCTA $(TCTG)_{3-4}(TCTA)_n$	157–197	5-FAM (blue)
FGA	4q28	$(TTTC)_3TTTT$ TTCT $(CTTT)_nCTCC(TTCC)_2$	219–267	5-FAM (blue)
Amelogenin	X:p22.1-22.3	–	107	JOE (green)
	Y:p11.2	–	113	
TH01	11p15.5	$(AATG)_n$	169–189	JOE (green)
TPOX	2p23-2per	$(AATG)_n$	218–242	JOE (green)
CSF1PO	5q33.3-34	$(AGAT)_n$	281–317	JOE (green)
D5S818	5q21-31	$(AGAT)_n$	135–171	NED (yellow)
D13S317	13q22-31	$(GATA)_n$	206–234	NED (yellow)
D7S820	7q	$(GATA)_n$	258–294	NED (yellow)

*The size range is the actual base pair size of sequenced alleles contained in the AmpFLSTR Allelic Ladders. The sizes in table include the 3' A nucleotide addition.

Electrophoresis conditions

Amplified DNA samples (1 µl) or 1 µl from each of three differently labelled allelic ladders was added to 12 µl of deionised formamide (Sigma), 0.5 µl internal standard GeneScan 500(ROX) and denatured for 3 min on 94 °C. At least three ladders were included in each run (in the beginning, the middle and the end of run).

The samples were electrophoresed in an ABI PRISM 310 Genetic Analyzer (Applied Biosystems/Perkin Elmer) in an uncoated 47 cm/50 µm capillary, using performance optimised polymer 4 (POP 4 Applied Biosystems). The injection time was 5 s at 15 kV and the run time was 24 min at 60 °C. The argon laser power was 9.9 mW. Evaluation of results was done with the software, GeneScan 2.1 and Genotyper 2.0 using the local Southern algorithm [22].

RESULT AND DISCUSSION

The nine autosomal STR loci and one gender locus (amelogenin) were typed in the three persons (mother, child and putative father) with the laser induced multicomponent fluorescence method and capillary electrophoresis (Fig. 2). In all studied systems the alleles of the child matched those of the putative father. These matches are marked in bold in Table 2. Analysis of the amelogenin system revealed the expected gender in all cases. Using the nine common allele frequencies after the method of Essen-Möller [7], a paternity likelihood of 99.98% was calculated. No mutations were detected. PCR based DNA typing with fluorescently labelled primers and automated analysis of a single test tube containing 10 amplified loci offers a reliable, sen-

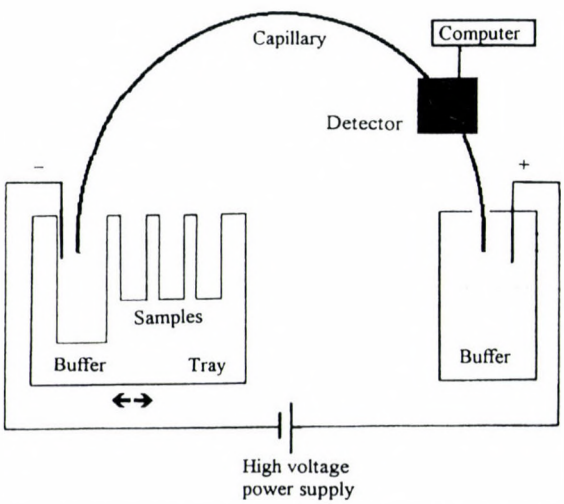

Fig. 2. Scheme of the capillary electrophoresis instrumentation

Table 2
The detected alleles of the three persons in the examined STR systems

System	D3S1358		vWA		FGA	
	fragm. (bp)	allele	fragm. (bp)	allele	fragm. (bp)	allele
Mother	123.34	15	175.21	16		
	131.47	17	179.19	17	236.79	**23**
Child			167.32	**14**		
	123.34	**15**	175.15	16	236.83	**23**
Putative			167.4	**14**		
Father	123.46	**15**	179.25	17	236.81	23
	TH01		TPOX		CSF1PO	
Mother	175.09	7.0	223.11	8	300.13	11
	186.07	9.3	235.13	11	304.18	12
Child	175.04	7				
	179.04	**8**	223.05	**8**	304.23	**12**
Putative	171.07	6	223.12	**8**	296.26	10
Father	179.14	**8**	227.12	9	304.19	**12**
	D5S818		D13S317		D7S820	
Mother	152.73	12			264.48	8
	157.18	13	221.36	12	272.50	10
Child	152.74	12	213.28	**10**	272.49	10
	157.06	**13**	221.28	12	276.56	**11**
Putative	148.25	11	213.31	**10**	272.57	10
Father	157.18	**13**	221.48	12	276.61	**11**

sitive and accurate method for forensic paternity testing. Furthermore this approach enables routine processing of large numbers of DNA samples, facilitates and enables investigators to perform the simultaneous screening of several different loci from single individuals.

ACKNOWLEDGEMENTS

This study-work was made in the Institute of Forensic Medicine, Westfälische Wilhelms Universität, Münster, and assisted by Roman Herzog Fellowship of the Alexander von Humboldt Foundation.

REFERENCES

1. Anker, R., Steinbreuck, T., Donnis-Keller, H. (1992) Tetranuleotide repeat polymorphism at the human thyroid peroxidase (HTPO) locus. *Hum. Mol. Genet. 1,* 137.
2. Beckmann, J. S., Weber, J. L. (1992) Survey of human and rat microsatellites. *Genomics 12,* 627–631.

3. Budowle, B., Isenberg, A. R. (1998) Capillary electrophoresis for forensic DNA Typing analyses. In: B. Olaisen, B. Brinkmann, P. J. Lincoln (eds) *Progress in Forensic Genetics 7,* Elsevier Science Amsterdam Lausanne New York Oxford, pp. 61–67.
4. Deyl, Z., Mikšík, I., Tagliaro, F. (1998) Advances in capillary electrophoresis. *Forensic Sci. Int. 92,* 89–124.
5. Edwards, A., Civitello, A., Hammond, H. A., Caskey, C. T. (1991) DNA typing and genetic mapping with trimeric and tetrameric tandem repeats. *Am. J. Hum. Genet. 49,* 746–756.
6. Edwards, A., Hammond, H. A., Lin, J., Caskey, C. T., Chakraborty, R. (1992) Genetic variation at five trimeric and tetrameric tandem repeat loci in four human population groups. *Genomics 12,* 241–253.
7. Essen-Möller, E., Quensel, C. E. (1939) Zur Theorie des Vaterschaftsnachweis aufgrund von Ähnlichkeitsbefunden. *Dtsch. Z. Gerichtl. Med. 31,* 70–96.
8. Frégeau, C. J., Fourney, R. M. (1993) DNA typing with fluorescently tagged short tandem repeats: a sensitive and accurate approach to human identification. *Biotechniques 15,* 100–119.
9. Green, E. D. (1991) Systematic generation of sequence-tagged sites for physical mapping of human chromosomes: application to the mapping of human chromosome 7 using yeast artificial chromosomes. *Genomics 11,* 548–564.
10. Hammond, H. A., Jin, L., Zhong, Y., Caskey, C. T., Chakraborty, R. (1994) Evaluation of thirteen STR Loci for use in personal identification applications. *Am. J. Hum. Genet. 55,* 175–189.
11. Jin, L., Underhill, P. A., Buonchriastiani, M., Robertson, J. M. (1997) Defining microsatellite alleles by genotyping global indigenous human populations and non-human primates. *J. Forensic Sci. 42,* 496–499.
12. Kimpton, C. P., Walton, A., Gill, P. (1992) A further tetranucleotide polymorphism at the vWA gene. *Hum. Mol. Genet. 1,* 287.
13. Kimpton, C., Gill, P., Walton, A., Urquhardt, A., Millican, E. S., Adams, M. (1993) Automated DNA profiling employing multiplex amplification of short tandem repeat loci. *PCR Methods Appl. 3,* 13–22.
14. Lászik, A., Pöche, H., Mauer, V., Schneider, V. (1995) Apaságmegállapítás a DNS technológia (RFLP) alkalmazásának segítségével. *Orv. Hetilap 136 (39),* 2117–2119. (In Hungarian)
15. Lazaruk, K., Walsh, P. S., Oaks, F., Gilbert, D., Rosenblum, B. B., Menchen, S., Scheibler, D., Wenz, H. M., Holt, C., Wallin, J. (1998) Genotyping of forensic short tandem repeat (STR) systems based on sizing precision in a capillary electrophoresis instrument. *Electrophoresis 19(1),* 86–93.
16. Li, H., Schmidt, L., Wie, M. H., Hustad, T., Lerman, M. I., Zbar, B., Tory, K. (1993) Three tetranucleotide polymorphisms for loci: D3S1352; D3S1358; D3S1359. *Hum. Mol. Genet. 2,* 1327.
17. Mills, K. A., Even, D., Murray, J. C. (1992) Tetranucleotide repeat polymorphism at the human alpha fibrinogen locus (FGA). *Hum. Mol. Genet. 1,* 779.
18. Möller, A., Meyer, E., Brinkmann, B. (1994) Different types of structural variation in STRs: HumFES/FPS, Hum vWA and HumD21S11 Int. *J. Legal. Med. 106,* 319–323.
19. Urquhart, A., Oldroyd, N. J., Kimpton, C. P., Gill, P. (1995) Highly discriminating heptaplex short tandem repeat PCR system for forensic identification. *Biotechniques 18,* 116–121.
20. PE Applied Biosystem AmpFlSTR Profiler PCR Amplification Kit (1997) User's manual
21. Polymeropoulos, M. H., Hiao, H., Rath, D. S., Merril, C. R. (1991) Tetranucleotide repeat polymorphism at the human thyrosine hydrolase gene (TH). *Nucleic Acids Res. 19,* 3753.
23. Southern, E. M. (1979) Measurement of DNA length by gel electrophoresis. *Anal. Biochem. 100,* 319–323.
24. Sullivan, K. M., Mannucci, A., Kimpton, C. P., Gill, P. (1993) A rapid and quantitative DNA sex test: fluorescence-based PCR analysis of X–Y homologous gene amelogenin. *Biotechniques 15,* 636–641.
25. Tagliaro, F., Manetto, G., Crivellente, F., Smith, F. P. (1998) A brief introduction to capillary electrophoresis. *Forensic Sci. Int. 92,* 75–88.
26. Walsh, P. S., Metzgar, D. A., Higuchi, R. (1991) Chelex 100 as a medium for the simple extraction of DNA for PCR based typing from forensic material. *Biotechniques 1,* 91–98.

BOOK REVIEW

Biochemistry
by
J. Stenesh
Plenum Press, New York and London, 1998., pp. 526.
ISBN 0-306-45732-6 (Hardbound) 95 US$
ISBN 0-306-45733-4 (Paperback) 55 US$

Is is not an easy task to write a book of biochemistry neither for trained biologists working at various specialised fields nor for undergraduates who should receive a comprehensive, logic and, as far as possible, comprised text to get acquainted with chemical structures, processes and interactions bounding to living systems and life processes. The present book aimed to meet the requirements of students in obtaining basic knowledge in this subject and also of teachers, who should transmit general principles and all important particular information in a comparatively short time scale.

The more than five hundred pages text is divided into four main Parts, containing altogether 19 well defined, specific Chapters. The setting up and the logic of the book differ from the usual biochemical textbooks, namely, in having an introductory part: Foundation of Biochemistry, dealing with origin of life, with cell types and their general structures, with water as solvent of life and with noncovalent interactions. The two main parts are on Biomolecules and on Metabolism. Part Biomolecules includes chapters on amino acids and peptides, proteins, enzymes, carbohydrates, lipids and membranes as well as nucleic acids. Part Metabolism deals with general principles of synthesis and degradation of biomolecules, with bioenergetics, with the citric acid cycle, with electron transport and oxidative phosphorilation, with the photosynthesis, further on with major pathways of carbohydrate, lipid, amino acid and nucleotide metabolism. The fourth part called Transfer of Genetic Information describes basic concepts of molecular biology and particularly molecular genetics, including the synthesis of DNA, RNA and proteins.

Each Chapter includes a great number of tables, illustrations, diagrams and figures, important in understanding difficult and complicated mechanisms and processes. Selected reading list, review questions and solution manual supplements the basic text, and a detailed, 20 pages long index help the handling of the book for readers who wish to have rapid information on one or another biochemical expression or process.

The book is excellent in its style, well understandable if the reader has the necessary knowledge in inorganic and organic chemistry. It can be recommended first of all for department staffs teaching biochemistry and for students, but also for biologists in general, who wish to refresh or complete their knowledge by consulting a contemporary overview on present state in biological chemistry.

J. SALÁNKI (Tihany)

Akadémiai Kiadó, Budapest

PRINTED IN HUNGARY

Akadémiai Nyomda, Martonvásár

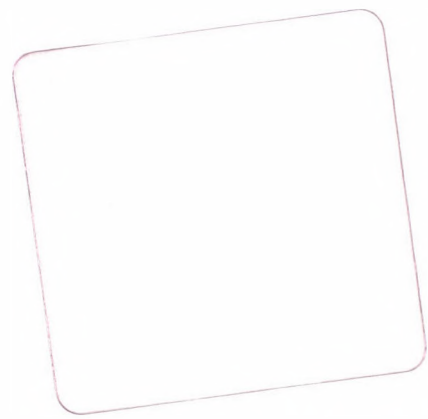

DIRECTIONS TO CONTRIBUTORS

ACTA BIOLOGICA HUNGARICA publishes original works in the field of experimental biology.

Manuscripts should be addressed to Dr. János Salánki, Editor-in-Chief or Dr. Károly Elekes, Editor, *Acta Biologica Hungarica,* H-8237 Tihany, Hungary.

Only original papers will be published and a copy of the Publishing Agreement will be sent to the authors of papers accepted for publication. Manuscripts will be processed only after receiving the signed copy of the agreement.

The manuscripts should not exceed 16 typed pages in general. The manuscripts should be typed double-spaced, on one side of the paper. In order to assure rapid publication, contributors are requested to submit two copies of the manuscript including an abstract (max. 200 words), tables and figures. An electronic version of the manuscript (including the figures) should also be submitted on a 3.5" diskette, using Word for Windows 7.0, 6.0 or 2.0 wordprocessor package in Microsoft Windows '95 or Windows 3.1 system. Each table should be typed on a separate sheet, numbered and provided with a title. All figures, either photographs or drawings or graphs, should be numbered consecutively. Figure legends should be typed in sequence on a separate sheet. Color plates (micrographs and drawings) will be charged to the authors.

Papers should be headed with the title of the paper, the names of the authors (male authors use initials, female authors use one given name in full), department, institute and town where the work was performed. A running title, not to exceed 50 letter spaces, should be included on a separate sheet and immediately following the summary 5 keywords must be supplied.

The *full paper* should be divided into the following parts in the order indicated:

1. *Abstracts*
2. *Introduction*
3. *Materials and Methods*
4. *Results*
5. *Discussion*
6. *References.* Papers – the essential ones only – cited in the manuscript should be listed on a separate sheet in alphabetical order according to the first author's surname. The references should be numbered so that each may be referred to in the text by its number only.

Examples:

1. Boas, N. F. (1953) Method for determination of hexosamine in tissue. *J. Biol. Chem. 204,* 553–563.
2. De Duve, C. (1959) Lysosomes, a new group of cytoplasmic particles. In: Hayashi T. (ed.) *Subcellular Particles.* Ronald Press, New York, pp. 1–72.
3. Umbreit, W. E., Burris, R. H., Stauffer, I. F. (1957) *Manometric Techniques.* Burgess Publishing Co., Minneapolis.

Short communication. Manuscripts, in English, should not exceed 1000 words (4 types pages) including references. The text of manuscripts containing tables and/or figures must be correspondingly shorter. Accepted short communications will be published within six months after submission of manuscripts. In order to speed up publication, no proof will be sent to authors.

Authors will be furnished, free of charge, with 25 reprints. Additional reprints may be obtained at cost.

Acta Biologica Hungarica

VOLUME 51, NUMBERS 2–4, 2000

Akadémiai Kiadó, Budapest

ACTA BIOL. HUNG. ABAHAU 51 (2–4) 109–445 (2000) HU ISSN 0236-5383

ACTA BIOLOGICA HUNGARICA

A QUARTERLY OF THE HUNGARIAN ACADEMY OF SCIENCES

Acta Biologica Hungarica publishes original papers on experimental biology.

Acta Biologica Hungarica is published in yearly volumes of four issues by

AKADÉMIAI KIADÓ
H-1117 Budapest, Prielle Kornélia utca 4, Hungary
http: //www.akkrt.hu

Manuscripts and editorial correspondence should be addressed to

Acta Biologica Hungarica
H-8237 Tihany, Hungary

Phone: (36-87) 448-244
Fax: (36-87) 448-006
E-mail: salanki@tres.blki.hu; elekes@tres.blki.hu

Subscription information

Orders should be addressed to

AKADÉMIAI KIADÓ
H-1519 Budapest, P.O. Box 245, Hungary
Fax: (36-1) 464-8221
E-mail: kiss.s@akkrt.hu

Subscription price for Volume 51 (2000) in 4 issues US$ 180.00, including normal postage, airmail delivery US$ 20.00.

"This periodical is included in the document delivery program THE GENUINE ARTICLE of the Institute of Scientific Information, Philadelphia. The articles published in the periodical are available through *The Genuine Article* at the Institute for Scientific Information, 3501 Market Street, Philadelphia PA 19104."

Acta Biologica Hungarica is abstracted/indexed in Biological Abstracts, Chemical Abstracts, Current Contents–Agriculture, Biology and Environmental Sciences, database (EMBASE), Elsevier BIOBASE, Index Medicus, International Abstracts of Biological Sciences

---

ABiol 51 (2000) 2–4

PRINTED IN HUNGARY

Akadémiai Nyomda, Martonvásár

ACTA BIOLOGICA HUNGARICA

Volume 51, 2000

INDEX

Number 1

Numbers 2–4

CONTENTS

Acta Biologica Hungarica 51 (2–4), p. 109 (2000)

PREFACE

The present three issues of Acta Biologica Hungarica are devoted to publication of research papers presented at the 9th Symposium of the International Society for Invertebrate Neurobiology held between 1–5 July, 1999 at Lake Balaton, Tihany, Hungary. The Balaton Limnological Research Institute of the Hungarian Academy of Sciences is the traditional place of these symposia since 1967.

Invertebrate animals, characterized by simpler nervous systems as compared to vertebrates, are not only useful models in understanding the structure and function of the human brain, but – as definite entities on the line of the evolution – they possess own distictions, typical to the given species. In explaining the behavior characteristic to the animal not only the morphological construction, the form and way of adaptation to the outside circumstances, etc. are important, but also, beside common properties, the specific features of the neural regulation may play a role. For example, the significance of the existence of giant neurons in gastropods is not yet understood, nevertheless, it is clear, that the large soma offers a greater surface to extrasynaptic receptors and a larger reactive area for signal molecules occurring in the intercellular space, than in small neurons. It has certainly consequences in the neural communication and integration mechanisms in these animals. Another example is the regulation of muscle activity. Although the muscle concentration is based on the same molecular principles (actin-myosin interaction) in the whole animal kingdom, the neurotransmitters resulting in excitation or inhibition of muscle fibres can be different in different phyla: glutamate in insects, 5HT in molluscs, Ach in some other invertebrates and in vertebrates. The type of the transmitter substance can make distinction among species also at other levels of the neural regulation.

The papers presented at the recent ISIN Symposium give an emphasis to these "invertebrate" specificities. Studies conducted on worms, molluscs and arthropods deal in most cases with mechanisms characteristic to the given species, like chromatophore regulation, feeding in molluscs, molluscan peptides, the function of octopamin. Many of the results presented, however, concern basic problems of neurobiology, common to all animals, emphasizing the overall unity of the neuroregulatory processes and mechanisms.

The articles collected in this volume represent latest results and reflect recent ideas of research groups working since long time at this area of experimental biology.

JÁNOS SALÁNKI
Editor-in-Chief

Akadémiai Kiadó, Budapest

Acta Biologica Hungarica 51 (2–4), pp. 111–132 (2000)

COMPARATIVE ASPECTS OF INVERTEBRATE NEUROPEPTIDES+

Y. MUNEOKA[1]*, F. MORISHITA[2], Y. FURUKAWA[2], O. MATSUSHIMA[2], M. KOBAYASHI[1], M. OHTANI[1], T. TAKAHASHI[1], E. IWAKOSHI[3], YUKO FUJISAWA[3] and H. MINAKATA[3]

[1] Faculty of Integrated Arts and Sciences, Hiroshima University, Higashi-Hiroshima 739-8521,
[2] Faculty of Science, Hiroshima University, Higashi-Hiroshima 739-8526, and
[3] Suntory Institute for Bioorganic Research, Osaka 618-8503, Japan

(Received: August 31, 1999; accepted: November 30, 1999)

1. We searched for bioactive peptides, most of which were considered to be neuropeptides, in various animals of several phyla. These peptides were compared with each other and with peptides identified by many other investigators. Consequently, we found that structures of neuropeptides are generally conserved in each phylum.
2. We also found some exceptional interesting aspects. First, there are a number of peptide groups whose members are distributed among several phyla. Second, there are many structural similarities between molluscan and annelidan peptides as if molluscs and annelids were the animals in a phylum. Third, certain toxic peptides of invertebrates are closely related to vertebrate neuropeptides.
3. In addition to the above phylogenetic aspects, we found some other interesting aspects. A wide structural variety of members of a peptide group is generally found in invertebrate species. Invertebrate muscles seem to be generally regulated not only by some or several classical non-peptidic neuromediators but also by various peptidic neuromediators. Peptides containing a D-amino acid residue are not rare.

Keywords: Neuropeptide – Cnidaria – Mollusca – Annelida – Echinodermata.

INTRODUCTION

Neuromediators can be divided into two large groups, non-peptidic and peptidic groups. As to the non-peptidic neuromediators, such as biogenic amines and amino acids, the number of the known substances including candidates does not exceed 20, and they seem to be utilized commonly in the nervous systems of almost all animals. As to the peptidic neuromediators, in contrast, hundreds of substances are supposed to be present in an animal species, and phylogenetic distribution of each of the peptides is suspected to be generally restricted within a certain small group of animals. That is, peptidic neuromediators are considered to have changed with phylogenetic evolution, while non-peptidic ones have been conserved. For systematization of the

+ Presented at the 9th ISIN Symposium on "Neurobiology of Invertebrates", July 1–5, 1999, Tihany, Hungary.

*Corresponding author, present address: Shiwahori 3524-2, Shiwacho, Higashi-Hiroshima 739-0269, Japan.

0236-5383/2000/$ 5.00

neuropeptide world, therefore, it seems to be important to search for neuropeptides in various animals and to compare structure and action of each peptide with those of others. During the last 15 years, we have searched for bioactive peptides, especially neuropeptides, in various animals from cnidarians to chordates. To the present, more than 500 species of peptides have been isolated and sequenced in collaboration with other laboratories. These peptides have been compared with each other and with peptides identified by many other investigators. Consequently, we found several interesting comparative aspects of structure and action of the bioactive peptides.

Peptides in the anterior byssus retractor muscle of Mytilus

The anterior byssus retractor muscle (ABRM) of the sea mussel *Mytilus edulis* is known to be a catch muscle which has been studied intensively for many years [for a review, see 71]. As to the neural control of contraction and relaxation in the ABRM, there is evidence that acetylcholine is the principal excitatory neurotransmitter which brings about a contraction followed by catch while serotonin is the principal relaxing neurotransmitter which relaxes catch tension [97; for a review, see 71]. Serotonin, however, does not inhibit active contraction but potentiates it [97]. There is another line of evidence suggesting that several other monoamines, such as dopamine, octopamine, noradrenaline and adrenaline, are also involved in the regulation of the ABRM as catch-relaxing and/or contraction-potentiating neuromediators [65, 87, 97, 98; for a review, see 63].

It was shown that the foregoing biogenic amines are all present in the ABRM [66]. It was also shown that contraction followed by catch, relaxation of catch and potentiation of contraction can be induced by appropriate neural stimulations, respectively [for a review, see 64]. That is, the ABRM was speculated to be innervated by aminergic contractile, catch relaxing and contraction-potentiating neurons. In addition to these kinds of neurons, inhibitory neurons were suspected to innervate into the ABRM [64]. However, none of the known non-peptidic transmitter substances have been shown to have inhibitory effect on the ABRM. Therefore, it was considered that some neuropeptides might be involved in the regulation of the ABRM as inhibitory neuromediators.

In 1977, Price and Greenberg [85] isolated a cardioexcitatory peptide designated FMRFamide from the ganglia of the clam *Macrocallista nimbosa.* This is the first finding of molluscan neuropeptide. Soon after the finding, FMRFamide was shown to have excitatory effect not only on the heart of *M. nimbosa* but also on various other molluscan muscles including the ABRM of *M. edulis* [25]. Muneoka and Matsuura [68), therefore, precisely examined the action of FMRFamide on the ABRM and found that it has three kind effects. That is, at 10^{-9} M or higher, FMRFamide potentiates contraction, at around 10^{-7} M the peptide relaxes catch tension, and at 10^{-6} M or higher it elicits a contraction of the muscle. Muneoka and Saitoh [69] studied structure-activity relations of FMRFamide for the contraction and the relaxation in the ABRM, and found that the relations for the contraction are similar to those found

in other molluscan muscles [49, 82], while the relations for the relaxation are different from those for the contraction. Accordingly, it was supposed that *M. edulis* might have relaxing peptides which are more or less related to FMRFamide and that FMRFamide might relax catch tension acting on the receptors of the endogenous relaxing peptides as an agonist. Based on the foregoing speculation that the ABRM might be regulated not only by biogenic amines but also by some or several neuropeptides, Hirata and Muneoka started to isolate bioactive peptides from the *Mytilus* pedal ganglion which has been shown to be the main origin of the nerves innervating the ABRM. With the helps of several other investigators, they soon isolated one relaxing and two inhibitory peptides [31, 32]. The former peptide (AMPMLRLamide) was termed catch-relaxing peptide (CARP) and the latter two (GSPMFVamide and GAPMFVamide) were termed *Mytilus* inhibitory peptides (MIPs). CARP was found to be an analog of myomodulin which was isolated from *Aplysia* [8].

CARP powerfully relaxes catch tension and, further, inhibits contraction of the ABRM [29, 32]. MIPs powerfully inhibit contraction but do not affect catch tension of the muscle [30, 31]. These facts suggest that the peptides are involved in the physiological regulation of the ABRM. If this is the case, the peptides are present in the ABRM and, therefore, they can be isolated from the muscle. In collaboration with other investigators, Fujisawa and Muneoka attempted to isolate bioactive peptides from the ABRM and identified a number of peptides including the three peptides found in the pedal ganglion [19–23]. In addition to the peptides, several biogenic amines were found in the ABRM [66] as already mentioned. The peptides and biogenic amines found in the ABRM and their effects on the muscle are shown in Table 1. Localizations of FMRFamide, CARP, SCP (unpublished) and MIP [17] immunoreactive substances in the ABRM were also examined. Further, the MIP immunoreactive substances were demonstrated to be released in the surrounding medium of the muscle in response to neural stimulation. The release was shown to be Ca^{2+} dependent [17].

Although we don not know whether all of the bioactive substances shown in Table 1 are involved in the regulation of the ABRM, the muscle seems to be controlled by a number of biogenic amines and peptides. As in the case of this *Mytilus* muscle, invertebrate muscles, as well as vertebrate visceral muscles, seem to be generally regulated by a number of peptidic neuromediators in addition to some or several non-peptidic neuromediators. We do not have any answer to the questions why such many mediators are required to regulate a muscle and how they are utilized in the physiological regulation mechanism. It seems to be very important to answer these questions.

A wide structural variety of members of MIP family

Members of MIP family have been found in various molluscs. Most of them are hexapeptides having PXFVamide at their C-terminal portion. Figure 2 shows the MIP family members isolated from several molluscs [18, 20, 23, 34, 36, 37, 53, 79]. The

Table 1
Bioactive substances in the ABRM of *Mytilus edulis* and their effects on the muscle [20, 21, 22, 23, 66]

Substance		Effect			
		Contraction	Potentiation of contraction	Relaxation of catch	Inhibition of contraction
Biogenic amines					
Acetylcholine		+++	–	–	–
Serotonin		–	+++	+++	–
Dopamine		–	+++	+++	–
Noradrenaline		±	+++	++	–
Adrenaline		±	+++	+	–
Octopamine		–	+++	++	–
Peptides					
MIPs	GS PMFVamide	–	–	–	+++
	GAPMFVamide	–	–	–	+++
	DSPLFVamide	–	–	–	+++
	YAPRFVamide	–	–	–	+++
	RSPMFVamide	–	–	–	+++
	RAPLFIamide	–	–	–	+++
	ASHIPRFVamide	–	–	–	+++
MIP-RP	MRYFVamide	–	–	–	++
CARP	AMPMLRLamide	–	±*	+++	+++
SCP-RPs	APNFLAYPRLamide	–	+++	+	–
	LAYPRLamide	–	+++	+	–
Fa	FMRFamide	+	+++	+**	–
Fa-RP	AdLAGDHFFRFamide	+	+++	–	–
GPFGs	GPFGLNKHGamide	++	–	–	–
	GPFGTHIKamide	++	–	–	–

+++: potent. ++: moderate. +: weak. ±: slight. –: no. dL: D-Leucine. *: at around 10^{-9} M. **: at around 10^{-7} M. Fa: FMRFamide. RP: related peptide. SCP: small cardioactive peptide.

members have been shown to have potent inhibitory effect not only on muscles but also on central neurons in molluscs [46, 47, 48, 83, 84, 104]. They are considered to constitute a representative inhibitory peptide group in molluscs. Most of the MIP family members shown in Table 2 were purified by applying biologically active fractions to HPLC systems. Therefore, it is suspected that many other members have been missed during the purification. In fact, based on the sequence of the MIP analogues purified from *Aplysia kurodai* (Table 2), Fujisawa et al. [18] cloned a cDNA

Table 2
MIP family members isolated from several molluscs

Mytilus edulis [20, 23]	*Helix pomatia* [34, 36]
GSPMFVamide	GAPAFVamide
GAPMFVamide	GAPRFVamide
DSPLFVamide	AAPRFVamide
YAPRFVamide	GAPKFVamide
ASHIPRFVamide	AAPKFVamide
RAPLFlamide	GPPRFVamide
RSPMFVamide	GAPMFVamide
	GAPRFlamide
Meretrix lusolia [79]	DPPYFVamide
YTPKFlamide	GSPYFVamide
YRPMFVamide	GAPYFVamide
GSNRPFFVamide	RAPYFVamide
YVPRFlamide	GPPMFVamide
YTPYFVamide	AAPFFVamide
YVPSFVamide	GYPYFVamide
YTPRFVamide	RAPFFVamide
YTPKFVamide	GAPLFVamide
YRPRFVamide	SVPI FVamide
	VAPKFVGRRDPPYFVamide
Anodonta cygnea (unpublished)	*Lymnaea stagnalis* [53]
RVPNFVamide	GAPRFVamide
Achatina fulica [37]	*Aplysia kurodai* [18]
AAPKFVamide	GAPRFVamide
GAPKFVamide	GPPRFlamide
GAPVFVamide	GSPHFlamide
GAPYFVamide	GSPRFFamide
AAPYFVamide	GAPRFIamide
GPPMFVamide	
GAPFFVamide	
DAPKFVGRRDPPYFVamide	
AAPKFVGRRGSPYFVamide	
AAPKFVGRRGAPYFVamide	

encoding the precursor protein from *Aplysia californica* and found 14 different MIP family members including the members isolated from *A. kurodai.* They were designated *Aplysia* MIP-related peptides (AMRPs). The expression of the 14 AMRPs was confirmed by matrix-assisted laser desorption/ionization time-of-flight mass spectrometry (MALDI-TOF MS). Further, two peptides modified N-terminally to pyroglutamate were found by the MS. MIP family members, all of which have a Pro at the fourth position from their C-terminus, seem to be distributed only in molluscs. However, peptides related structurally to MIPs but having another amino acid than Pro at the fourth position from the C-terminus are distributed not only in molluscs

[23, 24, 36, 103] but also in annelid [101] and echiuroid [35] worms. The MIP-related peptides can be divided into three groups, pentapeptide [23, 35, 36, 101], enterin [24, 36] and fulicin gene-related peptide (FGRP) [36, 103] groups. Members of the pentapeptide group have a basic amino acid at the fourth position from the C-terminus, and they seem to be distributed in molluscs, annelids and echiuroids. Members of the enterin group have been found in *Aplysia* and *Helix*. In *Aplysia californica* 20 species of enterins were shown to be present by the analysis of the encoding gene [24]. Most of them have HSFVamide sequence at their C-terminal portion. Members of the FGRP group were found in *Achatina* and *Helix*. In *Achatina fulica* 10 species of FGRPs were found [103]. Most of them have a Tyr at the fourth position and an acidic amino acid at the third position from their C-terminus.

As in the case of MIPs and MIP-related peptides, a wide structural variety of members of a peptide family or superfamily is generally found in invertebrate species. Thus, some questions arise. How have they been evolved? Are they functionally redundant or not? Is there any member which is functionally neutral, lacking biological activity? It seems to be also very important to answer these questions.

Peptides containing a D-amino acid residue

In 1989, a neuropeptide termed achatin-1 was isolated from the ganglia of the land snail *Achatina fulica* and its structure was determined to be GdFAD [44]. Before achatin-1, several D-amino-acid-containing bioactive peptides, such as dermorphins and dertorphins, had been found in the frog skin [for a review, see 51]. However, it is not clear whether they function as neuropeptides or not. It seems that achatin-1 is the first D-amino-acid-containing neuropeptide to be found. Soon after the finding, achatin-1 was shown to be present also in the atrium of the snail [14]. However, the peptide does not have any prominent effect on the atrium, while it has potent excitatory effect on the ventricle of the animal [50]. One of the roles of achatin-1 seems to act on the ventricle as a cardioexcitatory local hormone which is released from the terminals of the nerves innervating the atrium.

After the finding of achatin-1, a number of D-amino-acid-containing peptides have been isolated from various invertebrates. In molluscs, eight species of D-amino-acid-containing neuropeptides have been found to the present. These peptides are shown in Table 3. All of the neuropeptides have a D-amino acid residue at position 2. Most of D-amino-acid-containing peptides found in non-molluscan animals also have a D-type residue at position 2.

The D-amino-acid-containing peptides shown in Table 3 can be divided into three groups according to the activities of the neuropeptides and their stereoisomers. (i) Both D-type and L-type peptides show potent activity (*Mytilus* FFRFamide). (ii) D-type peptide shows no or slight activity while L-type stereoisomer shows potent activity (*Octopus* achatin-RP-II and *Helix* CCAP-RP-III). (iii) D-type peptide shows potent activity while L-type stereoisomer shows no or slight activity (the other five peptides). D-amino-acid-containing inactive peptides cannot be purified by bioassay

Table 3
Molluscan neuropeptides containing a D-amino acid residue

Peptide	Structure	Mollusc
Achatin-I	GdFAD	*Achatina* [44]
Octopus achatin-RP-I	GdFGD	*Octopus* [39]
Octopus achatin-RP-II	GdSWD*	*Octopus* [39]
Fulicin	FdNEFVamide	*Achatina* [74]
Fulyal	YdAEFL amide	*Achatina* [102]
Mytilus FFRFamide	AdLAGDHFFRFamide**	*Mytilus* [19]
Helix CCAP-RP-III	LdFCNGYGGCGNLamide*	*Helix* [58]
NdWFamide	NdWFamide	*Aplysia* [60]

*: These peptides have no or slight effect, although the L-type stereorsomers have potent effect. **: The L-type stereoisomer is almost equipotent to this peptide. RP: related peptide. CCAP: crustacian cardioactive peptide.

method. Therefore, it is suspected that there are many such peptides remained unidentified.

It is believed that, in precursor gene of D-amino-acid-containing peptide, the position of D-amino acid is encoded by corresponding normal codon for L-amino acid and that isomerization is caused after the precursor protein has been produced by ribosomal pathway [58]. However, it is not yet clear whether the isomerization occurs during the processing or after the processing of the L-type peptide.

Many important questions arise concerning D-amino-acid-containing peptides. How have they been evolved? What is the role of D-amino acid residue? What is the physiological meaning of the presence of inactive peptides? Are they functionally neutral or are they precursors of their active stereoisomers? How and when does the isomerization take place? Why does the isomerization occur at position 2 in most of the D-amino-acid-containing peptides?

Activities of crude peptide extract

The procedures for extraction and purification of the peptides, which we have isolated, are shown in Fig. 1. The supernatant obtained from fresh animal or tissue was forced through disposable C-18 cartridges, and the retained material was eluted with 5–10% methanol at first and then with 60% methanol. Because most of the retained peptides were considered to be eluted in 60%-methanol eluate, we used it as the crude peptide extract. Before purification of the peptides in the crude extract, its biological activities were examined on several kinds of muscles from animals of different phyla. After this examination, the crude extract was subjected to HPLC purification. In most of the cases, fractions obtained at each HPLC step were subjected to

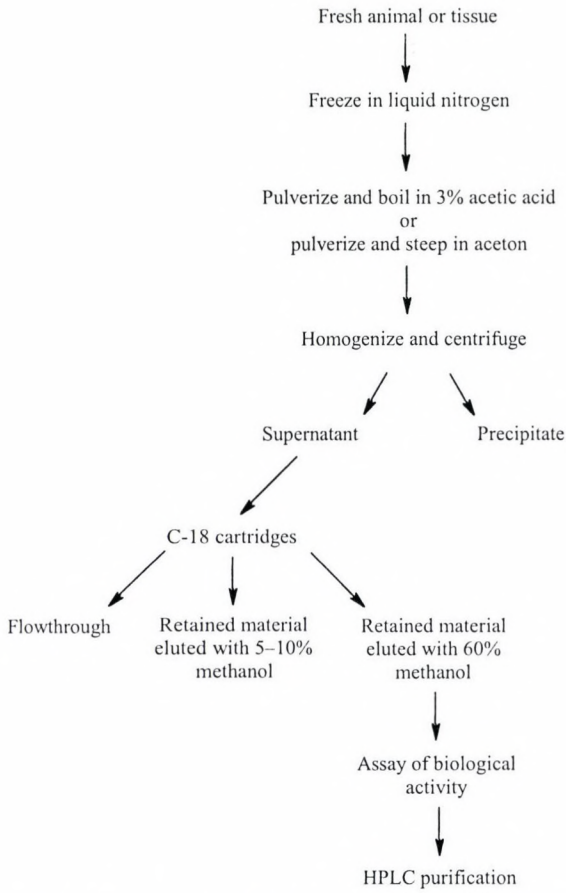

Fig. 1. Procedures for extraction and purification of peptides

bioassay using appropriate muscles, but in some other cases, they were subjected to ELISA.

Figure 2 shows the biological activities of the crude peptide extract from the body wall of the echinoderm sea cucumber *Stichopus japonicus.* The extract had little effect on twitch contraction of the body-wall muscle of the echiuroid worm *Urechis unicinctus,* tetanic contraction of the ABRM of the bivalve *Mytilus edulis* and spontaneous contractions of the crop of the insect *Gryllus bimaculatus,* and the extract had weak excitatory effect on the rectum of the bird *Coturnix japonica.* On the contrary, the extract had potent excitatory effect on the radial longitudinal muscle and the intestine of the sea cucumber *S. japonicus.* The extract was also found to have potent excitatory effect on the intestines of some starfishes. That is, the extract showed marked activity on the muscles of the echinodens, but it showed little activity on the muscles of the non-echinoderm animals, though there was an exception.

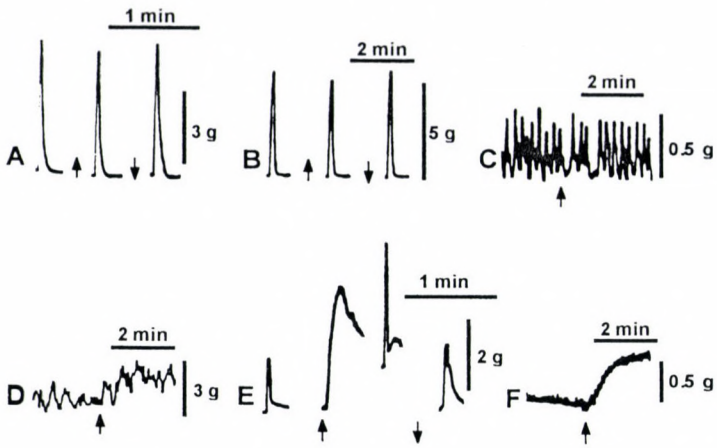

Fig. 2. Effects of the crude peptide extract of the body wall of the sea cucumber, *Stichopus japonicus,* on several kinds of muscles from animals of different phyla. (A) twitch contraction of the longitudinal body-wall muscle of *Urechis unicinctus* (Echiuridea). (B) tetanic contraction of the ABRM of *Mytilus edulis* (Mollusca). (C) spontaneous contractions of the crop of *Gryllus bimaculatus* (Arthropoda). (D) spontaneous contractions of the rectum of *Coturnix japonica* (Chordata). (E) twitch contraction of the radial longitudinal muscle of *Stichopus japonicus* (Echinodermata). (F) spontaneous contractions of the intestine of *S. japonicus*. The extract was applied at the upward arrows and washed out at the downward arrows. In A, B and E, the extract was applied 8 min prior to the electrical stimulations

As in the case of the sea cucumber, an extract from an animal of a phylum usually shows marked activity also on muscles from other animals in the same phylum and does not generally show marked activity on muscles from animals in the other phyla, though there are a number of exceptions. From these facts, it is supposed that structures of neuropeptides are generally conserved in each phylum.

Table 4 shows the peptides isolated from the body-wall extract of the sea cucumber, *S. japonicus,* and their actions on the radial longitudinal muscle and the intestine of the animal [77]. None of the peptides appears to be member of any of the peptide families or superfamily identified previously in non-echinoderm animals. Holokinins are significantly related to vertebrate bradykinin, although the peptides cannot be regarded as members of bradykinin family. Further, holokinins have bradykinin-like effect on vertebrate intestines [40]. This was probably the reason why the crude peptide extract from the sea cucumber showed weak excitatory activity on the rectum of the bird *C. japonica.*

Myoactive and neuroactive peptides of echinoderms have been poorly studied. Therefore, except for sticho-MFamides, the peptides in Table 4 or peptides related to them are not yet clear whether they are distributed in other echinoderms. Sticho-MFamides are closely related to the SALMFamides found in some starfishes [10, 11] and a sea cucumber [9]. Sticho-MFamides are regarded as the members of SALMF-amide family or superfamily. Members of this peptide group seem to be distributed

Table 4
Structures of the peptides isolated from the sea cucumber, *Stichopus japonicus*, and their effects on the radial longitudinal muscle (RLM) and the intestine [77, 40]

Name	Structure	Effect	
		RLM	Intestine
SWYG-1	SWYGSLG	Inhi or Poten	No
SWYG-2	SWYGTLG	Inhi or Poten	No
SWYG-3	SWYGSLA	Inhi	No
Holokinin-1	PLGYMFR	Inhi	Cont
Holokinin-2	PLGYM(O)FR	Inhi	Cont
Holokinin-3	PLGY(Br)M(O)FR	Inhi	Cont
Holokinin-1(3-7)	GYMFR	Inhi	Cont
NGIWYamide	NGIWYamide	Cont	Cont
Stichopin	DRQGWPACYDSKGNYKC	Inhi	No
Sticho-MFamide-1	GYSPFMFamide	No	Relax
Sticho-MFamide-2	FKSPFMFamide	No	Relax
KFamide-9	KHKTAYTGIamide	Inhi	Cont
GLRFA	GLRFA	Poten	Cont
GN-19	GGRLPNYAGPPRMPWLHIN	No	Cont or Relax

Inhi: Inhibition of twich contraction. Poten: potentiation of twitch contraction. Cont: contraction. Relax: relaxation. No: no effect. M(O): oxidized Met. Y(Br): (*o*-Br)-Tyr.

widely in echinoderms. In the nervous system of a brittle star, SALMFamide-like immunoreactivity has been observed [5].

It has been shown that some connective tissues of echinoderms change their mechanical properties in response to chemical messengers [61, 62]. Recently, it was shown that holokinins softened the body-wall connective tissue in a sea cucumber whereas NGlWYamide stiffened it [3, 38]. However, it is not yet clear whether those peptides or peptides closely related to them are widely distributed throughout echinoderms or not.

Peptide structures in some animals of different phyla

To the present, we isolated and sequenced more than 500 of peptides from various animals of several phyla. The results of this study supported our speculation that structures of peptides are generally conserved in each phylum. Table 5 shows myoactive peptides isolated from the clam *Meretrix lusoria* [79]. Except for the peptide

ELRRPFIL, which is related to the vertebrate peptide neurotensin, all of the peptides seem to be members of the previously identified molluscan neuropeptide groups such as MIPs and S-Iamides. ALPMLRMamide, which is closely related to the members of the myomodulin family, has a Met-NH_2 at its C-terminus, though the other myomodulin family members found in molluscs have a Leu-NH_2 at their C-terminus [6, 70]. Takahashi et al. [91] found a myomodulin-related peptide, AMGMLRM-amide, in a polychaete annelid *Perinereis vancaurica.* The peptide also has a Met-NH_2 at its C-terminus. Actions of the peptides with Met-NH_2 on the ABRM of *Mytilus* were found to be almost identical with those of the myomodulin family members which have Leu-NH_2 [92]. The peptides with Met-NH_2 are considered to be also members of the myomodulin group. It seems to be interesting to search for myomodulin-related peptides in lower molluscs such as chitons and in annelids.

The peptide pQVPLPRYamide is a member of the new family PLPRYamide [76]. In other molluscs, a member of this family has been found. It is pQPPLPRYamide isolated from the ganglia of *Helix pomatia* [57] and *H. aspersa* [78]. Therefore, it is supposed that members of this family are widely distributed in molluscs. Ikeda et al. [35] isolated a peptide which is closely related to the PLPRYamides, from the echiuroid worm *Urechis unicinctus.* The structure of this peptide is AAPLPRLamide. Furthermore, peptides having PRXamide at their C-terminus are known to be widely distributed in invertebrates [70].

The neurotensin-related peptide ELRRPFIL was designated clamtensin. We could not observe any activity of the peptide on molluscan muscles, and it is not yet clear

Table 5
Peptides isolated from the clam *Meretrix lusoria* [79]

Peptide	Family
YTPKFIamide	MIP
YRPMFVamide	
YVPRFIamide	
YTPYFVamide	
YVPSFVamide	
YTPRFVamide	
YTPKFVamide	
YRPRFVamide	
GSNRPFFVamide	
GLSSFIRIamide	S-Iamide
ELRRPFIL	Neurotensin
ALPMLRMamide	Myomodulin
FLRFamide	FMRFamide
pQVPLPRYamide	PLPRYamide

Table 6
Peptides isolated from the hydra, *Hydra magnipapillata* [93]

Function	Peptide	Structure	
Morphogenesis	Hym-323	KWVQGKPTGEVKQIKF	
	Hym-346	AFEDVSHLEEKEKALANHS	
	Hym-53	NPYPGLWamide	GL Wamides
	Hym-54	GPMTGLWamide	
	Hym-248	EPLPIGLWamide	
	Hym-249	KPIPGLWamide	
	Hym-331	GPPPGLWamide	
	Hym-338	GPPhPGLWamide	
	Hym-370	KPNAYKGKLPIGLWamide	
	Hym-301	KPPRRCYLNGYCSPamide	
Cell diffentiation	Hym-33H	AALPW	PWs
	Hym-35	EPSAAIPW	
	Hym-37	SPGLPW	
	Hym-310	DPSALPW	
	Hym-355	FPQSFLPRGamide	
Muscle contraction	Hym-176	APFIFPGPKVamide	
	GLWamides		

hP: hydroxy proline.

Table 7
Bioactive peptides isolated from the Japanese newt, *Gynops pyrrhogaster* [95, 96, unpublished]

Peptides	Origin	Structures
Newt Neurotensin	Body, Head	VKKPRRPYIL
6–13 Neurotensin	Body	KPRRPYIL
Newt CNP	Body	SNSKPKPKKGQSSGCFGLKLDRIGSMSGLGC
Newt Substance P	Head	KPRPDQFYGLMamide
Newt Neuromedin N	Body	KTPYIL
Newt VIP-1	Body	HSDAVFTDNYSRLLGKTALKNYLDGALKKE
Newt VIP-2	Body	HSDAVFTDNYSRLLAKTALKNYLDGALKKE
Newt VIP-3	Body	HSDAVFTDNYSRLLGKIALKNYLDEALKKE
Newt VIP-4	Body	HSDAVFTDNYSRLLGKTALKNYLDSALKKE
Newt Eye Peptide	Eyeball	GIAGLSPFRSVAL

whether the peptide is a biologically active substance in the clam or not. It is possible that the peptide is a fragment of a protein. However, the peptide has potent neurotensin-like excitatory effect on the intestines of vertebrates [unpublished, see also 79]. Kinjo et al. [45] isolated a neurotensin-like peptide, TSKGKRKPYF, from a planarian *Dugesia japonica,* and designated it planatensin. Planatensin as well as clamtensin has potent neurotensin-like effect on the intestines of vertebrates. Therefore, another possibility is considered. That is, neurotensin-related peptides having unknown functions are widely distributed in invertebrates.

Bioactive peptides have also been isolated from cnidarians and members of the cnidarian peptide families have been shown to be widely distributed among animals of this phylum [for a review, see 26]. For example, members of the antho-RFamide (pQGRFamide) family have been found in hydromedusae, sea anemones and sea pansies [27, 59]. However, any peptide which is considered to be a member of the cnidarian peptide family or superfamily has not been found in non-cnidarian animals, except for that the peptide termed head activator (pQPPGGSKVILF) has been shown to be conserved from hydra to human [4, 88].

Table 6 shows bioactive peptides isolated from the hydra, *Hydra magnipapillata,* by Takahashi et al. [93]. None of the hydra peptides appears to be member of any of the peptide families identified in non-cnidarian animals. Among cnidarians, however, peptides related closely to these hydra peptides are supposed to be distributed. In fact, metamorphosin A (pQQPGLWamide) which was previously found in a sea anemone [52] appears to be a member of the GLWamide family shown in Table 6.

We have also isolated a number of bioactive peptides from several vertebrates. Most of the isolated peptides were found to be of new sequences. Except some of the peptides, however, they were regarded as members of the previously identified vertebrate peptide families. Table 7 shows bioactive peptides isolated from the Japanese newt *Cynops pyrrhogaster* [95, 96; unpublished]. The newts were cut into four tissue groups, eyeballs, heads without the eye balls, visceral organs and bodies without the visceral organs, and those tissue groups were used for peptide isolation experiments, respectively. Except the newt eye peptide, each of the peptides appears to be a member of any of the previously identified vertebrate peptide families. The newt eye peptide is a bradykinin-related peptide, though it cannot be regarded as a member of bradykinin family. The peptide was found to have potent bradykinin-like effect on the intestine of the newt.

Among the peptides isolated from the vertebrates, only one peptide obtained from the brain of the Japanese crucian carp *Carassius auratus* and designated *Carassius* RFamide (C-RFa, SPEIDPFWYVGRGVRPIGRFamide) was found to be significantly related to a previously isolated invertebrate peptide [16]. The invertebrate peptide is ACEP-1 (SGQSWRPQGRFamide) which was obtained from the African giant snail *Achatina fulica* as a cardioexcitatory peptide [15]. Recently, two peptides related closely to ACEP-1 were found in the molluscs *Lymnaea stagnalis* [94] and *Aplysia californica* [1], respectively. They are regarded as members of ACEP-1 group. Soon after the finding of the C-RFa, sequences of prolactin-releasing peptides (PrRPs) found in some mammals including human were reported [28]. The

sequences of the PrRPs were found to be quite homologous to that of the C-RFa, suggesting that it is a fish prolactin-releasing peptide. In fact, the peptide was found to have potent and specific prolactin-releasing effect on fishes (personal communication from M. Fujimoto). Comparison of the cDNAs encoding the PrRPs with that encoding the C-RFa supported that the peptide is a fish prolactin-releasing peptide [86].

Similarity between annelidan and molluscan peptides

As we have mentioned, it seems that structures of neuropeptides are generally conserved in each phylum, although there are some exceptional aspects. One of the exceptional aspects is that most of the annelidan peptides, which we have isolated so far, are closely related to molluscan peptides, as if annelids and molluscs were the animals in the same phylum [100]. Table 8 shows myoactive peptides isolated from annelids. Except for GGNGs and pev-myotropins, the annelidan peptides appear to be members of the previously identified molluscan peptide families, such as FMRFamide, S-Iamide, myomodulin and MATP families. Any GGNG-related peptide is not yet found in molluscs. However, the amidated GGNG family-member isolated from a leech was found to have potent excitatory effect on some molluscan muscles, while the non-amidated members isolated from earthworms had no effect on the muscles [67]. Therefore, amidated GGNG-like peptides are probably present in molluscs. Pev-myotropins were isolated from a polychaete annelid. The peptides also show myotropic activity on visceral muscles of an earthworm. However, they do not have any effect on molluscan muscles [90].

It should be noted here that there are a number of molluscan peptides whose structures are more or less related to arthropodan peptides [70]. Recently, Iwakoshi et al. [42] isolated a cadioexcitatory peptide, PKYMDT, from the brain of the Japanese octopus, *Octopus minor*. This peptide is significantly related to the well-known arthropodan cadioexcitatory peptide proctolin. Furthermore, this peptide is somewhat related to ATWLDT which is one of the pev-myotropins.

Interphyletically distributed peptide-group members

The second exceptional aspect is that there are a number of peptide groups whose members are widely distributed among several phyla [for a review, see 33]. The most well-known such group is the oxytocin-vasopressin superfamily. The members of this group are shown to be distributed among the Chordata, Mollusca, Arthropoda and Annelida [33, 80]. Another well-known group is tachykinin-related peptides. The members of this group are shown to be distributed among the Chordata, Mollusca, Arthropoda and Echiuridea [for a review, see 73]. The tachykinin-related peptides can be divided into two main types, vertebrate and invertebrate types. The vertebrate-type peptides have FXGLMamide at their C-terminal portion, while most of the

Table 8
Myoactive peptides isolated form annelids

Peptide	Structure	References
FMRFamide-related peptides	FMRFamide	[43]
	FLRFamide	[13]
	YMRFamide	[2]
	GGKYMRFamide	[2]
S-Iamide-related peptides	VSSFVRIamide	[55]
	AKSGFVRIamide	[55]
Myomodulin-related peptides	AMGMLRMamide	[91]
Conopressin-related peptides	CFVRNCPTGamide	[80]
MRYFVamide-related peptides	SRLFVamide	[101]
	SHLFVamide	[101]
	VHLFVamide	[101]
MATP-related peptides	GFKDGAADRISHGFamide	[99]
	GFRDGSADRISHGFamide	[99]
GGNGs	APKCSGRWAIHSCGGGNG	[81]
	GKCAGQWAIHACAGGNG	[81]
	RPKCAGRWAIHSCGGGNG	[81]
	AKCEGEWAIHACLGGNamide	[56]
Pev-myotropins	ATWLDT	[90]
	FYEGDVPY	[90]

invertebrate-type peptides have FX_1GX_2Ramide. The amino acid sequences of the vertebrate-type peptides are not highly homologous with those of the invertebrate-type peptides. However, as pointed out by Nässel [73], there are some other similarities between the two types, and hence they seem to have an ancestral relationship [see also 89].

It is well known that the tachykinin-related peptide eledoisin isolated from the salivary gland of the octopus, *Eledone mochata,* as a toxic peptide has FIGLMamide at its C-terminal portion [12]. That is, the peptide is of vertebrate type. Recently, two

other vertebrate-type tachykinin-related peptides with FXGLMamide were found in an invertebrate. They are sialokinin I and II isolated from the salivary gland of the yellow fever mosquito, *Ades aegypi* [7]. More recently, Iwakoshi et al. [41] isolated two novel tachykinin-related peptides having FXGLMamide from the salivary gland of the octopus, *Octopus vulgaris*. All of the vertebrate-type invertebrate tachykinin-related peptides have been isolated from the salivary glands. The peptides seem to be utilized by the invertebrates as toxic substances against target animals such as fishes and mammals.

As in case of vertebrate-type invertebrate tachykinin-related peptides, certain toxic peptides of invertebrates are closely related to vertebrate peptides. These toxic peptides may have evolved from non-toxic related peptides to be able to act on target animals under a selection pressure. We have shown that bradykinin-related peptides are also present in a sea cucumber. It is well known that insect wasps have a number of peptides, which are closely related to bradykinin, in their venoms [72]. Bradykinin-related peptides may be widely distributed also in invertebrates, and the toxic bradykinin-like peptides of the wasps may have changed from some non-toxic ancestral bradykinin-related peptides.

Development of antagonists of invertebrate neuropeptides

A large number of invertebrate neuropeptides have been isolated and their primary structures have been determined. However, physiological roles of most of the peptides are not yet clear. To clarify the roles, it seems to be very important to develop specific antagonists of the peptides and to use them for investigation of the functions of the peptides. Therefore, development of antagonists of some invertebrate neuropeptides was attempted by using a combinatorial chemistry method.

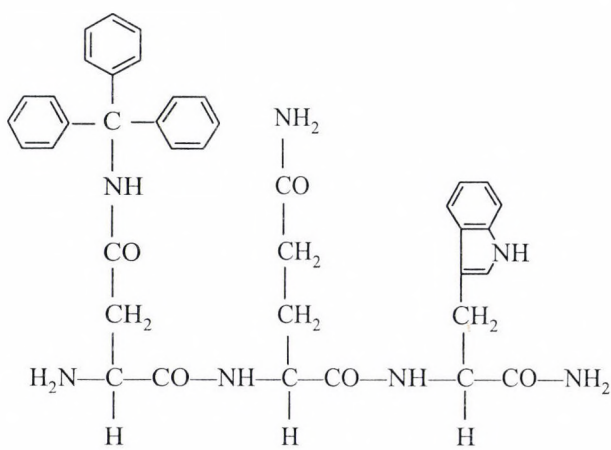

Fig. 3. Structure of Asn (trt)-Gln-Trp-NH_2 [54]

At the outset, development of antagonists of the molluscan neuropeptide APGWamide was tried, and several antagonists were obtained. Among the antagonists, APGWGNamide was found to be most potent. At 10^{-4} M APGWGNamide almost completely blocked the inhibitory actions of 10^{-6} M APGWamide on tetanic contraction of the ABRM of *Mytilus edulis* and on spontaneous contractions of the crop of the Japanese land snail *Euhadra congenita* [75].

In the course of the combinatorial chemistry experiments, a new analgesic tripeptide was obtained by Maeda et al. [54]. The structure of the analgesic peptide is shown in Fig. 3. The peptide was found to be more potent than morphine.

It seems not to be difficult to develop antagonists and agonists of neuropeptides by using combinatorial chemistry method. In future, various specific antagonists will be developed and they will be used to clarify functions of invertebrate neuropeptides, and thus systematization of invertebrate neuropeptide world will be progressed more.

REFERENCES

1. Aloyz, R. S., DesGroseillers, L. (1995) Processing of the L5-67 precursor peptide and characterization of LUQIN in the LUQ neurons of *Aplysia californica. Peptides 16,* 331–338.
2. Baratte, B., Gras-Masse, H., Ricart, G., Bulet, P., Dhainaut-Courtois, N. (1991) Isolation and characterization of authentic Phe-Met-Arg-Phe-NH_2 and the novel Phe-Thr-Arg-Phe-NH_2 peptide from *Nereis diversicolor. Eur. J. Biochem. 198,* 627–633.
3. Birenheide, R., Tamori, M., Motokawa, T., Ohtani, M., Iwakoshi, E., Muneoka, Y., Fujita, T., Minakata, H., Nomoto, K. (1998) Peptides controlling stiffness of connective tissue in sea cucumbers. *Biol. Bull. 194,* 253–259.
4. Bodenmuller, H., Schaller, H. C. (1981) Conserved amino acid sequence of a neuropeptide, the head activator, from coelenterates to humans. *Nature 293,* 579–580.
5. Bremaeker, N. D., Deheyn, D., Thorndyke, M. C., Baguet, F., Mallefet, J. (1997) Localization of S1- and S2-like immunoreactivity in the nervous system of the brittle star *Amphiphelis squamata* (Delle Chiaje 1828). *Proc. R. Soc. Lond. B 264,* 667–674.
6. Brezina, V., Bank, B., Cropper, E. C., Rosen, S., Vilim, F. S., Kupfermann, I., Weiss, K. R. (1995) Nine members of the myomodulin family of peptide cotransmitters at the B16-ARC neuromuscular junction of *Aplysia. J. Neurophysiol. 74,* 54–72.
7. Champagne, D. E., Ribeiro, J. M. C. (1994) Sialokinin I and II: vasodilatory tachykinins from the yellow fever mosquito *Aedes aegypt. Proc. Natl. Acad. Sci. USA 91,* 138–142.
8. Cropper, E. C., Tenenbaum, B., Kolks, M. A. G., Kupfermann, I., Weiss, K. R. (1987) Myomodulin: a bioactive neuropeptide present in an identified cholinergic buccal motor neuron of *Aplysia. Proc. Natl. Acad. Sci. USA 84,* 5483–5486.
9. Díaz-Miranda, L., Price, D. A., Greenberg, M. J., Lee, T. D., Doble, K. E., Garcia-Arraras, J. E. (1992) Characterization of two novel neuropeptides from the sea cucumber *Holothuria glaberrima. Biol. Bull. 182,* 241–247.
10. Elphick, M. R., Price, D. A., Lee, T. D., Thorndyke, M. C. (1991) The SALMFamides: a new family of neuropeptides isolated from an echinoderm. *Proc. R. Soc. Lond. B 243,* 121–127.
11. Elphick, M. R., Reeve, J. R., Burke, R. D., Thorndyke, M. C. (1991) Isolation of the neuropeptide SALMFamide-1 from starfish using a new antiserum. *Peptides 12,* 455–459.
12. Erspamer, V., Anastasi, A. (1962) Structure and pharmacological actions of eledoisin, the active endecapeptide of the posterior salivary glands of *Eledone. Experientia 18,* 58–61.
13. Evans, B. D., Pohl, J., Kartsonis, N. A., Calabrese, R. L. (1991) Identification of RFamide neuropeptides in the medicinal leech. *Peptides 12,* 897–908.

14. Fujimoto, K., Kubota, I., Yasuda-Kamatani, Y., Minakata, H., Nomoto, K., Yoshida, M., Harada, A., Muneoka, Y., Kobayashi, M. (1991) Purification of achatin-1 from the atria of the African giant snail, *Achatina fulica,* and its possible function. *Biochem. Biophys. Res. Commun. 177,* 847–853.
15. Fujimoto, K., Ohta, N., Yoshida, M., Kubota, I., Muneoka, Y., Kobayashi, M. (1990) A novel cardioexcitatory peptide isolated from the atria of the African giant snail, *Achatina fulica. Biochem. Biophys. Res. Commun. 167,* 777–783.
16. Fujimoto, M., Takeshita, K., Wang, X., Takabatake, I., Fujisawa, Y., Teranishi, H., Ohtani, M., Muneoka, Y., Ohta, S. (1998) Isolation and characterization of a novel bioactive peptide, *Carassius* RFamide (C-RFa), from the brain of the Japanese crucian carp. *Biochem. Biophys. Res. Commun. 242,* 436–440.
17. Fujisawa, Y. (1996) Immunohistochemical localization and Ca^{2+}-dependent release of *Mytilus* inhibitory peptides in the ABRM of *Mytilus edulis. Zool. Sci. 13,* 795–801.
18. Fujisawa, Y., Furukawa, Y., Ohta, S., Elis, T. A., Dembrow, N. C., Li, L., Eloyd, P. D., Sweedler, J. V., Minakata, H., Nakamaru, K., Morishita, F., Matsushima, O., Weiss, K. R., Vilim, F. S. (1999) The *Aplysia Mytilus* inhibitory peptide-related peptides (AMRPs): identification, cloning, processing, distribution, and action. *J. Neurosci.* 19, 9618–9634.
19. Fujisawa, Y., Ikeda, T., Nomoto, K., Yasuda-Kamatani, Y., Minakata, H., Kenny, P. T. M., Kubota, I., Muneoka, Y. (1992) The FMRFamide-related decapeptide of *Mytilus* contains a D-amino acid residue. *Comp. Biochem. Physiol. 102C,* 91–95.
20. Fujisawa, Y., Kubota, I., Ikeda, T., Minakata, H., Muneoka, Y. (1991) A variety of *Mytilus* inhibitory peptides in the ABRM of *Mytilus edulis:* isolation and characterization. *Comp. Biochem. Physiol. 100C,* 525–531.
21. Fujisawa, Y., Kubota, I., Kanda, T., Kuroki, Y., Muneoka, Y. (1992) Neuropeptides isolated from *Mytilus edulis* (Bivalvia) and *Fusinus ferrugineus* (Prosobranchia). In: Florey, E., Stefano, G. B. (eds) *Comparative Aspects of Neuropeptide Function.* Pergamon Press, Oxford, pp. 97–114.
22. Fujisawa, Y., Kubota, I., Nomoto, K., Minakata, H., Yasuda-Kamatani, Y., Ikeda, T., Muneoka, Y. (1993) A *Mytilus* peptide related to the small cardioactive peptides (SCPs): structure determination and pharmacological characterization. *Comp. Biochem. Physiol. 104C,* 469–475.
23. Fujisawa, Y., Takahashi, T., Ikeda, T., Muneoka, Y., Kubota, I., Minakata, H., Nomoto, K., Nose, T., Miki, W. (1993) Further identification of bioactive peptides in the anterior byssus retractor muscle of *Mytilus:* two contractile and three inhibitory peptides. *Comp. Biochem. Physiol. 106C,* 261–267.
24. Furukawa, Y., Fujisawa, Y., Minakata, H., Nakamaru, K., Wakayama, H., Nakabayashi, K., Morishita, F., Matsushima, O., Ellis, T. A., Dembrow, N. C., Weiss, K. R., Vilim, F. S. (1999) The enterins: a novel family of neuropeptides isolated from the enteric and central nervous system of *Aplysia. Comp. Biochem. Physiol. 124A,* S-14.
25. Greenberg, M. J., Price, D. A. (1979) FMRFamide, a cardioexcitatory neuropeptide of molluscs: an agent in search of a mission. *Amer. Zool. 19,* 163–174.
26. Grimmelikhuijzen, C. J. P., Carstensen, K., Darmer, D. D., Moosler, A., Nothacker, H.-P., Reinscheid, R. K., Schmutzler, C., Vollert, H. (1992) Coelenterate neuropeptides: structure, action and biosynthesis. *Amer. Zool. 32,* 1–12.
27. Grimmelikhuijzen, C. J. P., Graff, D. (1986) Isolation of <Glu-Gly-Arg-Phe-NH_2 (antho-RF-amide), a neuropeptide from sea anemones. *Proc. Natl. Acad. Sci. USA 83,* 9817–9821.
28. Hinuma, S., Habata, Y., Fujii, R., Kawamata, Y., Hosoya, M., Fukusumi, S., Kitada, C., Masuo, Y., Asano, T., Matsumoto, H., Sekiguchi, M., Kurokawa, T., Nishimura, O., Onda, H., Fujino, M. (1998) A prolactin-releasing peptide in the brain. *Nature 393,* 272–276.
29. Hirata, T., Kubota, I., Imada, M., Muneoka, Y., Kobayashi, M. (1989) Effects of the catch-relaxing peptide on molluscan muscles. *Comp. Biochem. Physiol. 92C,* 283–288.
30. Hirata, T., Kubota, I., Iwasawa, N., Fujisawa, Y., Muneoka, Y., Kobayashi, M. (1989) Effects of *Mytilus* inhibitory peptides on mechanical responses of various molluscan muscles. *Comp. Biochem. Physiol. 93C,* 381–388.
31. Hirata, T., Kubota, I., Iwasawa, N., Takabatake, I., Ikeda, T., Muneoka, Y. (1988) Structures and actions of *Mytilus* inhibitory peptides. *Biochem. Biophys. Res. Commun. 152,* 1376–1382.

32. Hirata, T., Kubota, I., Takabatake, I., Kawahara, A., Shimamoto, N., Muneoka, Y. (1987) Catch-relaxing peptide isolated from *Mytilus* pedal ganglia. *Brain Res. 422,* 374–376.
33. Hoyle, H. V. (1998) Neuropeptide families: evolutionary perspectives. *Regulatory Peptides 73,* 1–33.
34. Ikeda, T., Kiss, T., Hiripi, L., Fujisawa, Y., Kubota, I., Muneoka, Y. (1991) MIP (*Mytilus* inhibitory peptide) analogues isolated from the ganglia of the pulmonate mollusc *Helix pomatia.* In: Shimonishi, Y. (ed.) *Peptide Chemistry 1990.* Protein Research Foundation, Osaka, pp. 357–362.
35. Ikeda, T., Kubota, I., Miki, W., Nose, T., Takao, T., Shimonishi, Y., Muneoka, Y. (1993) Structures and actions of 20 novel neuropeptides isolated from the ventral nerve cords of an echiuroid worm, *Urechis unicinctus.* In: Yanaihara, N. (ed.) *Peptide Chemistry 1992.* ESCOM, Leiden, pp. 583–585.
36. Ikeda, T., Minakata, H., Fujita, T., Muneoka, Y., Kiss, T., Hiripi, L., Nomoto, K. (1993) Neuropeptides isolated from *Helix pomatia.* Part I. Peptides related to MIP, buccalin, myomodulin-CARP and SCP. In: Yanaihara, N. (ed.) *Peptide Chemistry 1992.* ESCOM, Leiden, pp. 576–578.
37. Ikeda, T., Yasuda-Kamatani, Y., Minakata, H., Kenny, P. T. M., Nomoto, K., Muneoka, Y. (1992) *Mytilus*-inhibitory peptide analogues isolated from the ganglia of a pulmonate mollusc, *Achatina fulica. Comp. Biochem. Physiol. 101C,* 245–249.
38. Inoue, M. Birenheide, R., Koizumi, O., Kobayakawa, Y., Muneoka, Y., Motokawa, T. (1999) Localization of neuropeptide NGIWYamide in the holothurian nervous system and its effects on muscular contraction. *Proc. R. Soc. Lond. B 266,* 993–1000.
39. Iwakoshi, E., Minakata, H. (1999) Cardioactive peptides isolated from the brain of a Japanese octopus, *Octopus minor. Comp. Biochem. Physiol. 124A,* S-84.
40. Iwakoshi, E., Ohtani, M., Takahashi, T., Muneoka, Y., Ikeda, T., Fujita, T., Minakata, H., Nomoto, K. (1995) Comparative aspects of structure and action of bioactive peptides isolated from the sea cucumber *Stichopus japonicus.* In: Ohno, M. (ed.) *Peptide Chemistry 1994.* Protein Research Foundation, Osaka, pp. 261–264.
41. Iwakoshi, E., Takuwa, K., Hisada, M., Fujisawa, Y., Minakata, H. (1999) Isolation of two novel tachykinins from the posterior salivary gland of *Octopus vulgaris. Zool. Sci. 16,* Suppl., 103.
42. Iwakoshi, E., Takuwa, K., Minakata, H. (2000) Structures and functions of molluscan neuropeptides cardioactive peptides isolated from the cephalopod, *Octopus minor.* In: Fujii, N. (ed.) *Peptide Chemistry 1999.* Protein Research Foundation, Osaka (in press).
43. Kajniak, K., Price, D. A. (1990) Authentic FMRFamide is present in the polychaete *Nereis virens. Peptides 11,* 75–77.
44. Kamatani, Y., Minakata, H., Kenny, P. T. M., Iwashita, T., Watanabe, K., Funase, K., Sun, X. P., Yongsiri, A., Kim, K. H., Novales-Li, P., Novales, E. T., Kanapi, C. G., Takeuchi, H., Nomoto, K. (1989) Achatin-1, an endogenous neuroexcitatory tetrapeptide from *Achatina fulica* Férussac containing a D-amino acid residue. *Biochem. Biophys. Res. Commun. 160,* 1015–1020.
45. Kinjo, S., Takahashi, T., Ohtani, M., Muneoka, Y., Watanabe, K., Umezono, Y., Takao, T., Shimonishi, Y. (1994) Planatensin: a neurotensin-like peptide isolated from the planarian, *Dugesia japonica. Zool. Sci. 11,* 103.
46. Kiss, T. (1990) Effects of *Mytilus* inhibitory peptide on identified molluscan neurones. *Comp. Biochem. Physiol. 95C,* 207–212.
47. Kiss, T., Elekes, K., Fujisawa, Y., Muneoka, Y. (1999) Ionic mechanism mediating *Mytilus* inhibitory peptides elicited membrane currents in identified *Helix* neurons. *Brain Res. 830,* 258–267.
48. Kiss, T., Osipenko, O. N. (1991) Opposite effects of molluscan neuropeptides CARP and MIP on LVA Ca-currents in *Helix pomatia* L. neurones. *Comp. Biochem. Physiol. 99C,* 91–97.
49. Kobayashi, M., Muneoka, Y. (1986) Structure requirements for FMRFamide-like activity on the heart of the prosobranch *Rapana thomasiana. Comp. Biochem. Physiol. 84C,* 349–352.
50. Kobayashi, M., Muneoka, Y., Fujimoto, K., Ohta, N., Yoshida, M., Kubota, I., Nomoto, K., Minakata, H., Yasuda-Kamatani, Y. (1992) Structure and function of neuropeptides containing a D-amino acid residue isolated from the African giant snail *Achatina fulica.* In: Suzuki, A. (ed.) *Peptide Chemistry 1991.* Protein Research Foundation, Osaka, pp. 321–326.
51. Kreil, G. (1994) Peptides containing a D-amino acid from frogs and molluscs. *J. Biol. Chem. 269,* 10967–10970.

52. Leitz, T., Morand, K., Mann, M. (1994) Metamorphosin A: a novel peptide controlling development of the lower metazoan *Hydractinia echinata* (Coelenterata, Hydrozoa). *Dev. Biol. 163,* 440–446.
53. Li, K. W., Van Minnen, J. W., Van Veelen, P. A., Van der Greef, T., Geraerts, W. P. M. (1996) Structure, localization and action of a novel inhibitory neuropeptide involved in the feeding of *Lymnaea. Molecular Brain Research 37,* 267–272.
54. Maeda, I., Kanemoto, N., Ogino, K., Kuwahara, M., Goto, Y., Adachi, M., Taki, T., Ohtani, M., Muneoka, Y., Kawakami, T., Aimoto, S. (1999) Identification of a novel analgesic peptide including an unnatural amino acid from peptide libraries synthesized with a multipeptide synthesizer. In: Shimonishi, Y. (ed.) *Peptide Science – Present and Future.* Kluwer Academic Publishers, Dordrecht, pp. 139–140.
55. Matsushima, O., Takahashi, T., Morishita, F., Fujimoto, M., Ikeda, T., Kubota, I., Nose, T., Miki, W. (1993) Two S-Iamide peptides, AKSGFVRIamide and VSSFVRIamide, isolated from an annelid, *Perinereis vancaurica. Biol. Bull. 184,* 216–222.
56. Minakata, H., Fujita, T., Kawano, T., Nagahama, T., Oumi, T., Ukena, K., Matsushima, O., Muneoka, Y., Nomoto, K. (1997) The leech excitatory peptide, a member of the GGNG peptide family: isolation and comparison with the earthworm GGNG peptides. FEBS Lett. 410, 437–442.
57. Minakata, H., Ikeda, T., Fujita, T., Kiss, T., Hiripi, L., Muneoka, Y., Nomoto, K. (1993) Neuropeptides isolated from *Helix pomatia.* Part 2. FMRFamide-related peptides, S-Iamide peptides, FR peptides and others. In: Yanaihara, N. (ed.) *Peptide Chemistry 1992.* ESCOM, Leiden, pp. 579–582.
58. Minakata, H., Ikeda, T., Mumeoka, Y., Nomoto, K. (1996) A new peptide containing a D-amino acid from the snail, *Helix pomatiae* – roles of D-amino acid residue –. In: Nishi, N. (ed.) *Peptide Chemistry 1995.* Protein Research Foundation, Osaka, pp. 169–172.
59. Moosler, A., Rinehart, K. L., Grimmelikhuijzen, C. J. P. (1996) Isolation of four novel neuropeptides, the hydra-RFamides I–IV, from *Hydra magnipapillata. Biochem. Biophys. Res. Commun. 229,* 596–602.
60. Morishita, F., Nakanishi, Y., Kaku, S., Furukawa, Y., Ohta, S., Hirata, Y., Ohtani, M., Fujisawa, Y., Muneoka, Y., Matsushima, O. (1997) A novel D-amino-acid-containing peptide isolated from *Aplysia* heart. *Biochem. Biophys. Res. Commun. 240,* 354–358.
61. Motokawa, T. (1981) The stiffness change of the holothurian dermis caused by chemical and electrical stimulation. *Comp. Biochem. Physiol. 70C,* 41–48.
62. Motokawa, T. (1982) Rapid change in mechanical properties of echinoderm connective tissues caused by coelomic fluid. *Comp. Biochem. Physiol. 73C,* 223–229.
63. Muneoka, Y., Fujisawa, Y., Fujimoto, N., Ikeda, T. (1990) The regulation and pharmacology of muscles in *Mytilus.* In: Stefano, G. B. (ed.) *Neurobiology of Mytilus edulis.* Manchester University Press, Manchester, pp. 209–245.
64. Muneoka, Y., Fujisawa, Y., Matsuura, M., Ikeda, T. (1991) Neurotransmitters and neuromodulators controlling the anterior byssus retractor muscle of *Mytilus edulis. Comp. Biochem. Physiol. 98C,* 105–114.
65. Muneoka, Y., Kamura, M. (1982) The multiplicity of neurotransmitters and neurohormones controlling *Mytilus* muscle. *Comp. Biochem. Physiol. 73C,* 149–156.
66. Muneoka, Y., Kobayashi, M. (1992) Comparative aspects of structure and action of molluscan neuropeptides. *Experientia 48,* 148–156.
67. Muneoka, Y., Matsushima, O., Morishita, F. (1998) Phylogenetic aspects of structure and aetion of neuropeptides. In: Kunz, H. (ed.) *Proceedings of the 7th Akabori Conference.* Universität Mainz, Mainz, pp. 103–108.
68. Muneoka, Y., Matsuura, M. (1985) Effects of a molluscan neuropeptide FMRFamide and the related opioid peptide YGGFMRFamide on *Mytilus* muscle. *Comp. Biochem. Physiol. 81C,* 61–70.
69. Muneoka, Y., Saitoh, H. (1986) Pharmacology of FMRFamide in *Mytilus* catch muscle. *Comp. Biochem. Physiol. 85C,* 207–214.
70. Muneoka, Y., Takahashi, T., Kobayashi, M., Ikeda, T., Minakata, H., Nomoto, K. (1994) Phylogenetic aspects of structure and action of molluscan neuropeptides. In: Davey, K. G., Peter, R. E., Tobe, S. S.

(eds) *Perspective in Comparative Endocrinology.* National Research Council of Canada, Tront, pp. 109–118.
71. Muneoka, Y., Twarog, B. M. (1983) Neuromuscular transmission and excitation-contraction coupling in molluscan muscle. In: Saleuddin, A. S. M., Wilbur, K. M. (eds) *The Mollusca Vol. 4.* Academic Press, New York, pp. 35–76.
72. Nakajima, T. (1988) Active peptides of non-mammalian origin. In Nakajima, T., Yanaihara, N., Miyazawa, T. (eds) *Physiologically Active Peptides.* Kodansha, Tokyo, pp, 1–26.
73. Nässel, D. R. (1999) Tachykinin-related peptides in invertebrates: a review. *Peptides 20,* 141–158.
74. Ohta, N., Kubota, I., Takao, T., Shimonishi, Y., Yasuda-Kamatani, Y., Minakata, H., Nomoto. K., Muneoka, Y., Kobayashi, M. (1991) Fulicin, a novel neuropeptide containing a D-amino acid residue isolated from the ganglia of *Achatina fulica. Biochem. Biophys. Res. Comm. 178,* 486–493.
75. Ohtani, M., Aimoto, S., Muneoka, Y. (2000) Development of an antagonist of molluscan neuropeptide APGWamide using a peptide library. In: *Comp. Biochem. Physiol. 124A,* 585.
76. Ohtani, M., Fujisawa, Y., Muneoka, Y., Takao, T., Shimonishi, Y. (1997) pQVPLPRYamide isolated from the clam *Meretrix lusoria:* a member of a novel molluscan neuropeptide family. In: Kitada, C. (ed.) *Peptide Chemistry 1996.* Protein Research Foundation, Osaka, pp. 117–120.
77. Ohtani, M., Iwakoshi, E., Muneoka, Y., Minakata, H., Nomoto, K. (1999) Isolation and characterization of bioactive peptides from the sea cucumber, *Stichopus japonicus.* In: Shimonishi, Y. (ed.) *Peptide Science – Present and Future.* Kluwer Academic Publishers, Dordrecht, pp. 419–420.
78. Ohtani, M., Muneoka, Y., Matsushima, O., Takao, T., Shimonishi, Y., White, A. R., Pedder, S., Sharma, R., Lennon, M. A., Katugmpda, S., Walker, R. J. (1997) Isolation of bioactive compounds from *Helix aspersa* nerve tissue and effect of pQPPLPRYamide on heart, esophagus and central neurons of *H. aspersa* and rectum of *Anodonta woodiana. Gen. Pharmacol. 29,* 103–111.
79. Ohtani, M., Muneoka, Y., Takahashi, T., Teranishi, H. (1995) Bioactive peptides isolated from the clam *Meretrix lusoria. Acta Biol. Hung. 46,* 449–452.
80. Oumi, T., Ukena, K., Matsushima, O., Ikeda, T., Fujita, T., Minakata, H., Nomoto, K. (1994) Annetocin: an oxytocin-related peptide isolated from the earthworm, *Eisenia foetida. Biochem. Biophys. Res. Commun. 198,* 393–399.
81. Oumi, T., Ukena, K., Matsushima, O., Ikeda, T., Fujita, T., Minakata, H., Nomoto, K. (1995) The GGNG peptides: novel myoactive peptides isolated from the gut and the whole body of the earthworms. *Biochem. Biophys. Res. Commun. 216,* 1072–1078.
82. Painter, S. D., Morley, J. S., Price, D. A. (1982) Structure-activity relations of the molluscan neuropeptide FMRFamide on some molluscan muscles. *Life Sci. 31,* 2471–2478.
83. Pedder, S. M., Chen, M. L., Muneoka, Y., Walker, R. J. (1998) Structural requirements and ionic mechanism of the *Mytilus* inhibitory peptides (MIPs) on *Helix* central neurones. *Gen. Pharmacol. 30,* 213–220.
84. Pedder, S. M., Muneoka, Y., Walker, R. J. (1998) Evidence for the involvement of nitric oxide in the inhibitory effect of GSPYFVamide on *Helix aspersa* central neurones. *Regulatory Peptides, 74,* 121–127.
85. Price, D. A., Greenberg, M. J. (1977) Structure of a molluscan cardioexcitatory neuropeptide. *Science 197,* 670–671.
86. Satake, H., Minakata, H., Wang, X., Fujimoto, M. (1999) Characterization of a cDNA encording a precursor of *Carassius* RFamide, structurally related to a mammalian prolactin-releasing peptide. *FEBS Lett. 446,* 247–250.
87. Satchell, D. G., Twarog, B. M. (1979) Identification of dopamine released from the anterior byssus retractor muscle of *Mytilus californianus* in response to nerve stimulation. *Comp. Biochem. Physiol. 64C,* 231–235.
88. Schaller, H. C., Bodenmliller, H. (1981) Isolation and amino acid sequence of a morphogenetic peptide from hydra. *Proc. Natl. Acad. Sci. USA 78,* 7000–7004.
89. Schoofs, L., Holman, G. M., Hayes, T. K., Nachman, R. J., De Loof, A. (1990) Locustatachykinin I and II, two novel insect neuropeptides with homology to peptides of the vertebrate tachykainin family. *FEBS Lett. 261,* 397–401.

90. Takahashi, T., Furukawa, Y., Muneoka, Y., Matsushima, O., Ikeda, T., Fujita, T., Minakata, H., Nomoto, K. (1995) Isolation and characterization of four novel bioactive peptides from a polychaete annelid, *Perinereis vancaurica. Comp. Biochem. Physiol. 110C,* 297–304.
91. Takahashi, T., Matsushima, O., Morishita, F., Fujimoto, M., Ikeda, T., Minakata, H., Nomoto, K. (1994) A myomodulin-CARP-related peptide isolated from a polychaete annelid, *Perinereis vancaurica. Zool. Sci. 11,* 33–38.
92. Takahashi, T., Minakata, H., Morishita, F., Matsushima, O., Ikeda, T., Fujita, T., Muneoka, Y., Nomoto, K. (1995) Effects of myomodulin-CARP-family peptides and analogues on the anterior byssus retractor muscle of *Mytilus edulis.* In: Ohno, M. (ed.) *Peptide Chemistry 1994.* Protein Research Foundation, Osaka, pp. 289–292.
93. Takahashi, T., Mumeoka, Y., Lohmann, J., deHaro, M., Solleder, G., Bosch, T. C. G., David, C. N., Bode, H. R. Koizumi, O., Shimizu, H., Hatta, M., Fujisawa, T., Sugiyama, T. (1997) Systematic isolation of peptide signal molecules regulating development in hydra: LWamide and PW families. *Proc. Natl. Acad. Sci. USA 94,* 1241–1246.
94. Tensen, C. P., Cox, K. J. A., Smit, A. B., van der Schors, R. C., Meyerhof, W., Richter, D., Planta, R. J., Hermann, P. M., van Minnen, J., Geraerts, W. P. M., Knol, J. C., Barke, J. F., Vreugdenhil, E., van Heerikhuizen, H. (1998) The *Lymnaea* cardioexcitatory peptide (LyCEP) receptor: a G-protein-coupled receptor for a novel member of the RFamide neuropeptide family. *J. Neurosci. 18,* 9812–9821.
95. Teranishi, H., Muneoka, Y., Uesaka, T., Ando, M., Chiba, C., Saito, T., Takao, T., Shimonishi, Y., Minakata, H., Nomoto, K. (1996) Structure and action of bioactive peptides isolated from the newt, *Cynops pyrrhogaster* – I. a C-type natriuretic peptide (CNP). In: Nishi, N. (ed.) *Peptide Chemistry 1995.* Protein Research Foundation, Osaka, pp. 173–176.
96. Teranishi, H., Takahashi, T., Ohtani, M., Ando, M., Muneoka, Y., Chiba, C., Saito, T., Takao, T., Shimonishi, Y. (1996) Structure and action of bioactive peptides isolated from the newt, *Cynops pyrrhogaster* – II. four VIP-related peptides and two neurotensin-related peptides. In: Nishi, N. (ed.) *Peptide Chemistry 1995.* Protein Research Foundation, Osaka, pp. 177–180.
97. Twarog, B. M. (1954) Responses of a molluscan smooth muscle to acetylcholine and 5-hydroxytryptamine. *J. Cell. Comp. Physiol. 44,* 141–163.
98. Twarog, B. M. (1959) The pharmacology of a molluscan smooth muscle. *Br. J. Pharmacol. 14,* 404–407.
99. Ukena, K., Oumi, T., Matsushima, O., Ikeda, T., Fujita, T., Minakata, H., Nomoto, K. (1995) A novel gut tetradecapeptide isolated from the earthworm, *Eisenia foetida. Peptides 16,* 995–999.
100. Ukena, K., Oumi, T., Matsushima O., Morishita, F., Fujita, T., Minakata, H., Nomoto, K. (1995) Bioactive peptides of annelids are closely related to those of molluscs. *Acta Biol. Hung. 46,* 453–456.
101. Ukena, K., Oumi, T., Matsushima, O., Takahashi, T., Mumeoka, Y., Fujita, T., Minakata, H., Nomoto, K. (1996) Inhibitory pentapeptide isolated from the gut of the earthworm, *Eisenia foetida. Comp. Biochem. Physiol. 114A,* 245–249.
102. Yasuda-Kamatani, Y., Kobayashi, M., Yasuda, A., Fujita, T., Minakata, H., Nomoto, K., Nakamura, M., Sakiyama, F. (1997) A novel D-amino acid-containing peptide, fulyal, coexists with fulicin gene-related peptides in *Achatina* atria. *Peptides, 18,* 347–354.
103. Yasuda-Kamatani, Y., Nakamura, M., Minakata, H., Nomoto, K., Sakiyama, F. (1995) A novel cDNA sequence encoding the precursor of the D-amino acid-containing neuropeptide fulicin and multiple alpha-amidated neuropeptides from *Achatina fulica. J. Neurochem. 64,* 2248–2255.
104. Yongsiri, A., Takeuchi, H., Kubota, I., Muneoka, Y. (1989) Effects of *Mytilus* inhibitory peptides on a giant neurone of *Achatina fulica* Férussac., *Eur. J. Pharmacol. 171,* 159–165.

Acta Biologica Hungarica 51 (2–4), pp. 133–145 (2000)

MYTILUS INHIBITORY PEPTIDE (MIP) INDUCES A Na^+-ACTIVATED K^+-CURRENT IN SNAIL NEURONS+

T. KISS[1]*, Y. FUJISAWA[2], ZITA LÁSZLÓ[1] and Y. MUNEOKA[2]

[1]Department of Experimental Zoology, Balaton Limnological Research Institute of the Hungarian Academy of Sciences, P. O. Box 35, H-8237 Tihany, Hungary, and
[2]Faculty of Integrated Arts and Sciences, Hiroshima University, Hiroshima 730, Japan

(Received: August 31, 1999; accepted: November 30, 1999)

Two microelectrode voltage-clamp and single-channel recordings were performed on D-cluster neurons of snail right parietal ganglion in order to study the properties of MIP-activated potassium current. It was found that the octapeptide member of the MIP-family, ASHIPRFVa elicits an outward current, which possesses all the properties characteristic for the hexapeptide(s) inward membrane response. The main component of the peptide elicited response is highly $[K^+]_o$ dependent, however the response was attenuated in Na-free extracellular saline. The peptide elicited response was mimicked by raising the $[Na^+]_i$ by pressure injection of Na^+ into the cell. Single channel recordings indicated that MIP-induced outward K-current is Na-dependent. The probability to find a channel in open state increases with increasing intracellular Na^+-concentration. Excised inside-out patches obtained from D-neurons contained $I_{K(Na)}$ channels could be activated by exposure of the cytoplasmic face of the patch membrane to 40 mM Na^+, and 40 mM Li^+, as well. The single channel current amplitude at –60 mV is 15 pA and the single channel conductance is 212 pS between –80 and 0 mV. It was concluded that MIP's activate a novel type of K^+-current in the snail neurons. This current is the Na-activated K^+-current. The single channel properties of the MIP activated channel is in concert with $I_{K(Na)}$ data obtained on different vertebrate and invertebrate preparations.

Keywords: Invertebrates – snail – neuron – neuropeptide – cation-activated potassium channels.

INTRODUCTION

K^+-channels are a major target of inhibitory synaptic transmitters and of variety of neuropeptides. The slow K^+-current responses to neurotransmitters, including dopamine, histamine, acetylcholine and serotonin, all appear to share properties of the FMRFa and APWGa-induced current [1, 3, 11, 13, 28, 31].

Earlier it was shown that members of the *Mytilus* inhibitory peptide (MIP)-family elicit a slow K^+-current in *Helix* neurones. The response is composed from two inde-

+Presented at the 9th ISIN Symposium on "Neurobiology of Invertebrates", July 1–5, 1999, Tihany, Hungary.

*Corresponding author, E-mail: kisst@tres.blki.hu

0236-5383/2000/$ 5.00

pendent responses at least, each of them was associated with different voltage and concentration dependences, and with different ionic mechanisms (K^+ and Cl^-) [19, 25]. We have, however suspected that the potassium component of the peptide-activated response was not identical to that activated by the above-mentioned transmitters and neuropeptides. The main difference is that MIP-elicited current was blocked or substantially decreased by Na-free extracellular solution. MIP-family peptides are widely distributed in invertebrates [24] and all of them have a potent inhibitory effect on various molluscan muscles [10, 13, 22]. It was also found that these peptides may alter the activity of neurones in the central nervous system, as well. MIPs inhibit the spontaneous firing of the molluscan neurons by inducing a hyperpolarization, increasing the potassium conductance of the membrane [20, 23, 25, 32].

Recently, we have analysed in detail the properties of the potassium component of the MIP-activated response in the D-cluster neurones of *Helix pomatia,* applying the two microelectrode voltage-clamps and a patch-clamp approach. D-cluster neurons forms a homogenous group of cells in right parietal ganglion [27] and were not labelled by an antibody raised against neuropeptide RAPYFVa (a member of MIP family) [8]. Here we have analyzed the properties of the ASHIPRFVa peptide-(an octapeptide member of the MIP-family) elicited membrane response and compared with that obtained by the application of hexapeptide members.

Furthermore we report that MIP's activate a potassium current, which is probably triggered by the increase of intracellular cation (sodium) concentration.

MATERIALS AND METHODS

Adult specimens of *Helix pomatia* L. collected locally in autumn, were used. They were stored at 4 °C from October until the end of March. A week before of the use snails were placed under wet conditions at the room temperature (20 °C) and supplied with food. Experiments were carried out on D-cluster neurons [27]. Prior to intracellular recording, the thick connective tissue was removed and the innermost layer enveloping the ganglia was softened by protease treatment (1% V/V XIV protease, Sigma for 10 min at room temperature). Thereafter, cells were exposed and placed in a 0.5 ml volume perfusing chamber and the experiments were performed at a constant perfusion rate of 1–2 ml/min. Replacement of the chamber volume required ~2 min at 1 ml/min. The physiological solution had the following composition (mM): 80 NaCl, 4 KCl, 10 $CaCl_2$, 5 $MgCl_2$, 10 Tris-HCl, with the pH adjusted to 7.4 with HCl. In elevated K^+-saline, the appropriate amount of NaCl was replaced by KCl. In Na^+-free solution, Na^+ was replaced with equimolar amounts of LiCl, CsCl, TrisHCl (tris(hydroxymethyl)-aminometane hydrochloride), sucrose or NMG-Cl (N-methyl-D-glucamine chloride). In Cl^- free saline Cl^- ions were replaced with equimolar amount of acetate or propionate. The standard pipette solution for the patch-clamp contained (mM): 120 KCl, 1 EGTA, 5 HEPES, 1 $MgCl_2$, pH 7.4. Peptides were prepared in an appropriate physiological solution from a stock solution of 1 mM MIP dissolved in distilled water and stored until the use at –18 °C.

Before the experiments peptides were diluted 10–100 times and pressure applied onto the cell surface. Na-ions (100 mM) were pressure ejected or iontophoretized intracellularly.

Electrophysiological recordings

Conventional recordings

Conventional single and two electrode techniques were employed to obtain current- or voltage-clamp recordings using an Axoclamp 2B amplifier. The membrane potential was recorded differentially between voltage sensing microelectrode and a saline-agar bridge placed in the bath. Glass micropipettes of resistance 1–2 MΩ (were used and filled with 2.5 M KCl or 2.0 M potassium acetate). Single electrode voltage-clamp was performed in a discontinous SEVC mode.

Patch clamp recording

Single channel currents were obtained using standard patch-clamp techniques [15]. The current of the Na^+ activated K^+ channel was recorded in the inside/out recording configuration with a patch-clamp amplifier (EPC-7, List-Electronic). Patch pipettes were pulled from borosilicate glass and fire polished to a tip diameter <1 μm resulting 6–10 MΩ pipette resistance. After forming a gigaseal the patch was excised into a divalent cation free physiological solution and moved into a compartment containing intracellular saline of the following composition (mM): 80 KCl, 40 NaCl, 1 EGTA, 5 HEPES 1 $MgCl_2$, pH 7.4 adjusted with KOH. In some experiments NaCl was substituted with LiCl or NMG-Cl in equimolar amount.

The data were directly filtered at 1 kHz and stored in a computer using pCLAMP (Axon Instrument) software.

Drugs

Thapsygargin was obtained from Alomone Labs (Jerusalem, Israel) and all other substances were Sigma products.

RESULTS

Recently, we have studied the properties of K-channels activated by octapeptide ASHIPRFVa (AS, a member of the MIP-family). The AS elicited response possesses all of the properties characteristic for the hexapeptide-induced currents [19]. The current-voltage relationship show outward rectification, increase in membrane con-

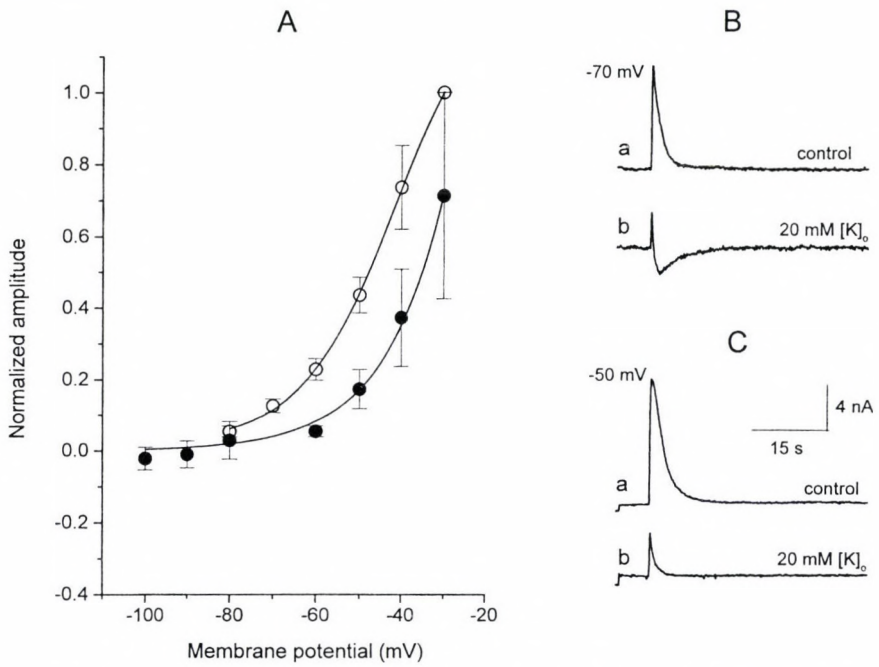

Fig. 1. Effect of extracellular potassium concentration on ASHIPRFVa elicited currents. A – Current-voltage relation of AS induced outward currents in the presence of 4 mM $[K]_o$ and 20 mM $[K]_o$. Normalized data points are averages obtained from 8–12 neurons. Vertical bars are S.D. of the mean. B–C – Representative current traces recorded at two different holding potentials (B = –70 mV and C = –50 mV) and at two different $[K]_o$ (a = 4 mM and b = 20 mM)

ductance and the reversal potential is at –85 mV in extracellular solution containing 4 mM K^+. Increasing the concentration of $[K^+]_o$ shifts the reversal potential right along voltage axis according to the potassium electrode (Fig. 1). This means that the peptide elicited response is highly potassium dependent. The peptide elicited response was biphasic at 20 mM $[K_o]$, suggesting the response is composed of two or three components (Fig. 1Bb). At –50 mV membrane potential the response is already monophasic with attenuated amplitude as is expected at increased $[K_o]$ (Fig. 1Cb). The current is blocked by Cs^+ and 4AP and partly blocked by Ba (5 mM), TEA (10 mM), apamin (10^{-6} M) and the response is highly sensitive to the changing of the extracellular Na-concentration [19]. Superfusion of Na-free TrisHCL, NMGCl or sucrose containing solution over neurones, while having no effect on the reversal potential, reversibly decreased the peptide induced response up to 20% (by 80%) of the control (Fig. 2A). In Na-substituted Cs^+, or sucrose containing extracellular solution, the amplitude of the peptide-elicited outward current was almost completely ceased or blocked (Fig. 2B, C). The recovery following the removal of Cs^+ or sucrose solutions was successful. In order to exclude the involvement of the Na^+/K^+ pump-

ing mechanism in the peptide induced response, the effect of MIP was examined in Li^+-saline and in the presence of ouabain (strophantidine). In Na^+-substituted Li^+-saline the MIP elicited response was only slightly attenuated, but not blocked (Fig. 3A, B). Na^+-free sucrose containing solution the peptide induced response was almost completely abolished. Ouabain (10^{-4} M), a cardiac glycoside, which blocks electrogenic Na^+/K^+ pump had no or little influence on the MIP-induced potassium current (Fig. 3C, D). Although apamin (2.5×10^{-6} M) decreased the amplitude of MIP elicited response, changing of the Ca-concentration in the extracellular solution had no visible effect (Fig. 4A). Removal of Ca^{2+} from the extracellular saline had no dramatic effect on the MIP-induced currents. Neither thapsigargin, a releaser of Ca^{2+} from intracellular depot, caused a remarkable effect at 10 μM concentrations (Fig. 4B) on the current.

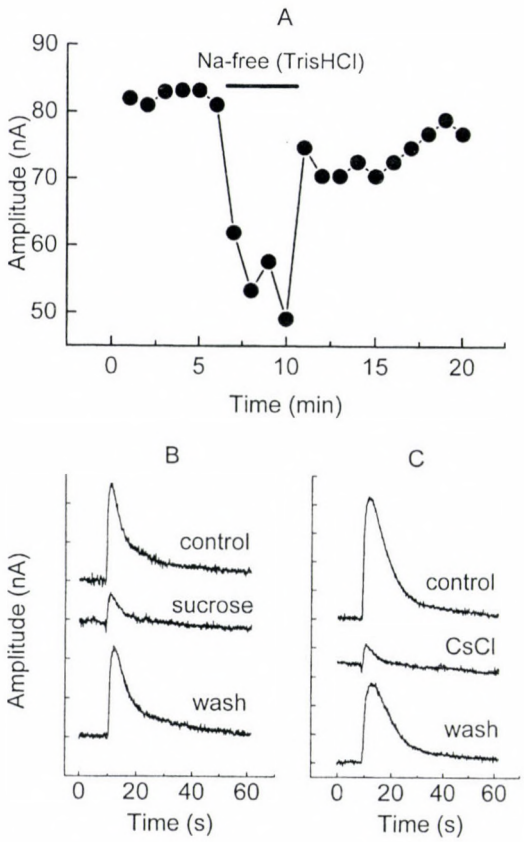

Fig. 2. Removal of Na^+-ions from the extracellular solution ceases or blocks amplitude of the octapeptide induced currents. A – Response elicited by pressure application of the peptide at holding potential of –40 mV in every 2.5 min. The duration of the Na-free solution application is marked by horizontal bar. B and C – representative current records in sucrose and CsCl substituted Na^+-free extracellular salines. Ticks on the vertical axis denote 10 nA

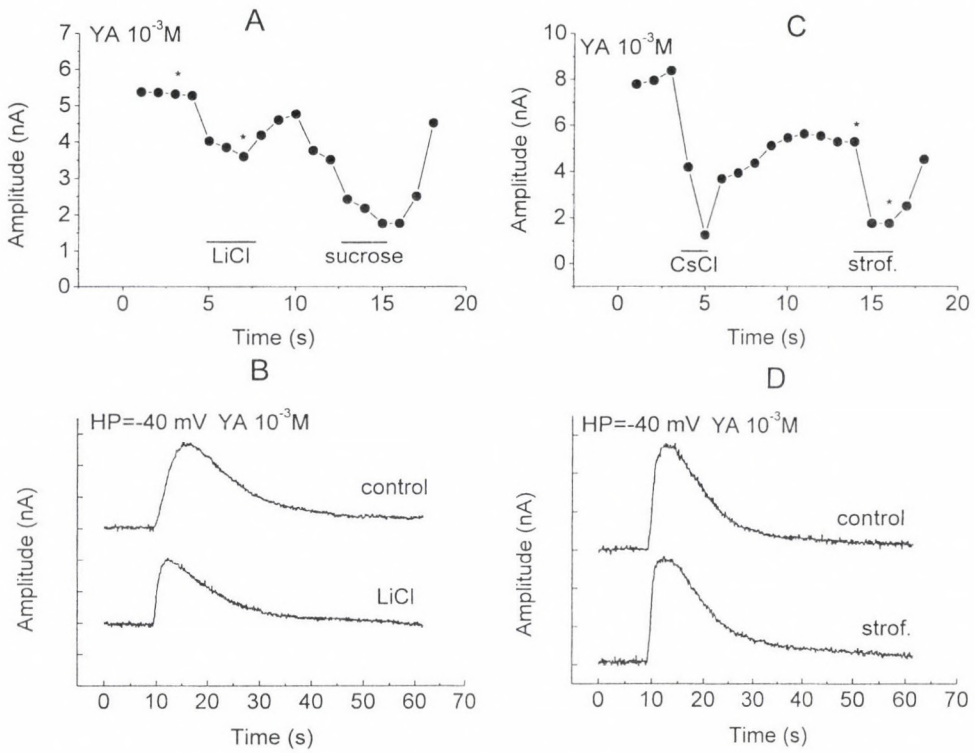

Fig. 3. Effect of Li^+ and ouabain on the MIP-elicited current amplitude. Calibration 2nA/tick. A, B – in Li^+ substituted Na-free solution the amplitude decreased not significantly. C, D – Ouabain (strophantin 10^{-5} M) had little or no effect both on the amplitude and shape of the peptide elicited currents

We have proposed therefore that the decreasing effect of the Na-free extracellular solution of peptide-induced response was due to the inhibition of the Na-activated K-current. In order to prove this hypothesis we have injected Na-ions iontophoretically, as well as by pressure, and an outward current was obtained, which mimicked the time course of MIP elicited current (Fig. 5A, B). The significant difference between the amplitudes of currents evoked by iontophoretic and pressure application of Na^+-ions was due to the different amount of the injected Na^+ ions. Pressure application is more powerful, because the intracellular concentration of the injected ions reaches a much higher value during a shorter time. It is possible however, that the MIP elicited outward current and the response induced by intracellular Na-injection have basically different mechanisms. In order to test this possibility additivity experiments were made. Immediately after iontophoretic Na-injection a puff of MIP was ejected onto the surface of the neurone to initiate current. It was seen that following Na-injection the amplitude of the peptide elicited response was attenuated, suggesting that in both case the same channels were activated (Fig. 5C). Loading the cell with

Na^+ the peptide was not able to induce further increase of the intracellular Na-concentration resulting a smaller response compared to the control.

Direct evidences on the presence of Na-activated K-channels induced by MIP application are provided by patch-clamp experiments, because single-channel measurements eliminate the possibility of macroscopic voltage-clamp artifacts [4]. Single channels were investigated in cell-attached and inside-out recording configuration of the patch-clamp technique. The patch of the membrane was held at a potentials between –80 and +60 mV (pipette potential), and different solutions were applied to the intracellular site of the membrane. In cell-attached patch single-channel activity was already observed probably due to the high K^+ contained (120 mM) of the pipette solution. In inside-out patches in Na-free solution no channel activity was observed or the channel activity decreased substantially (Fig. 6A, upper line).

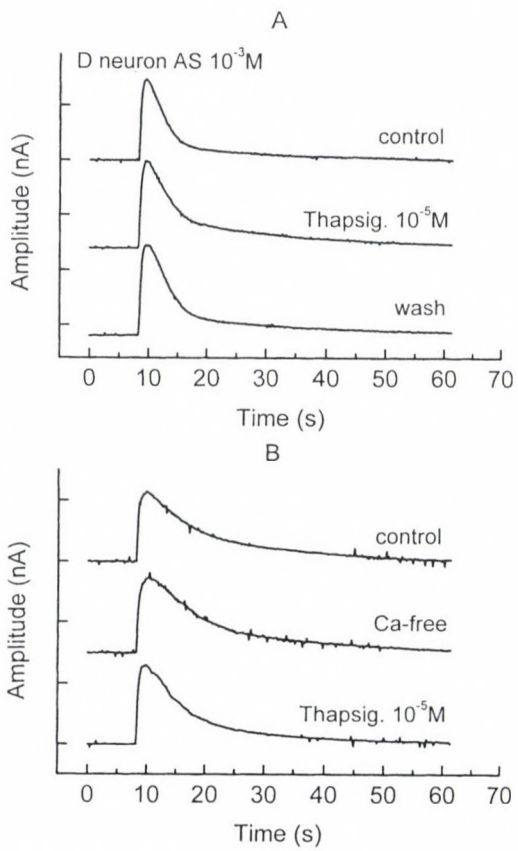

Fig. 4. The peptide induced response is not sensitive against extra- and intracellular Ca^{2+}. Amplitude calibration is 10 nA/tick. A – Thapsigargin at 10^{-5} M did not influence neither the amplitude nor the time course of the AS-elicited outward current. B – Ca-free extracellular solution and the same saline plus 10^{-5} M thapsigargin added had no effect

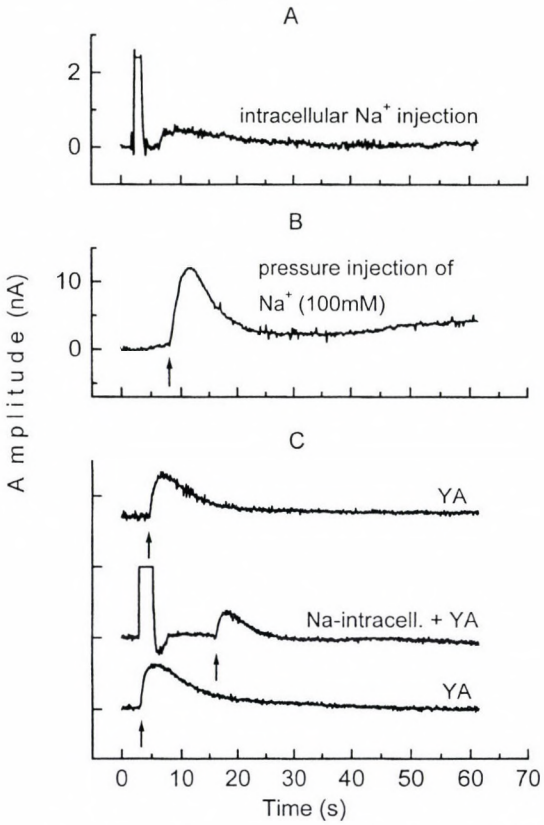

Fig. 5. Effect of intracellular Na-injection on the peptide activated current. A – Iontophoretic Na^+-injection. The pipette contained 100 mM NaCl. The injection artifact is seen at the beginning of the trace. B – Pressure ejection of Na^+ was more effective. The arrow shows the moment of injection (100 ms). C – Upper trace – the control curve; middle trace – the peptide application was preceeded by intracellular Na^+ iontophoresis lower trace – peptide application alone. Calibration 10 nA

Superfusion of intracellular saline containing 40 mM Na^+ a bursts of openings were observed (Fig. 6A bottom line). Two channels became active and this activity persisted during several minutes exposure to sodium. No run-down of the channel activity was observed up to 15 min. Mostly the channel openings occurred in bursts with a rapid flickering between open and closed states. Li^+ was capable of substituting the sodium ions, inducing single channel activity (Fig. 6B).

Figure 7A illustrates, on a faster time scale, examples of the elementary current with several substates, some of which are indicated by asterisks. Subconductance states were usually preceeded and followed by the main conducting state and were ocasionally seen in isolation. Current-voltage relationship for the main conducting

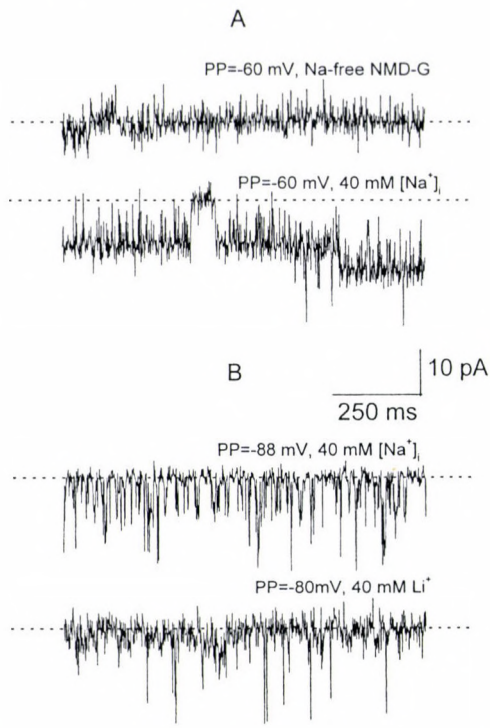

Fig. 6. Single channel currents from inside-out patches (120 mM $[K]_o$/80 mM $[K]_i$) from the soma of D-neuron, showing the Na^+-activated channel at different membrane potentials and different solutions. A – upper record Na-free, glucamin containing intracellular saline, lower record-activity in the presence by 40 mM NaCl added intracellulary. B – single channel activity in control (upper record) and Li^+ substituted Na-free solution (lower record)

state of $I_{K(Na)}$ channels in 80 mM $[K]_i$/120 mM $[K]_o$ solutions is shown in Fig. 7B. The fitting of the data with linear regression revealed single channel conductance of 212 pS between –80 and 0 mV. The reversal of currents through the Na-activated channels in solutions containing 80 mM $[K]_i$ and 120 mM $[K]_o$ was arround +12 mV.

The average open and closed times were determined from the open- and closed-time distributions of the main conductance state (Fig. 8A, B). The open-time distribution was fitted with one exponential giving 1.5 ms mean open time. The closed-state histogram was best fitted with two exponentials ($\tau_1 = 1.65$ ms, $\tau_2 = 16.2$ ms).

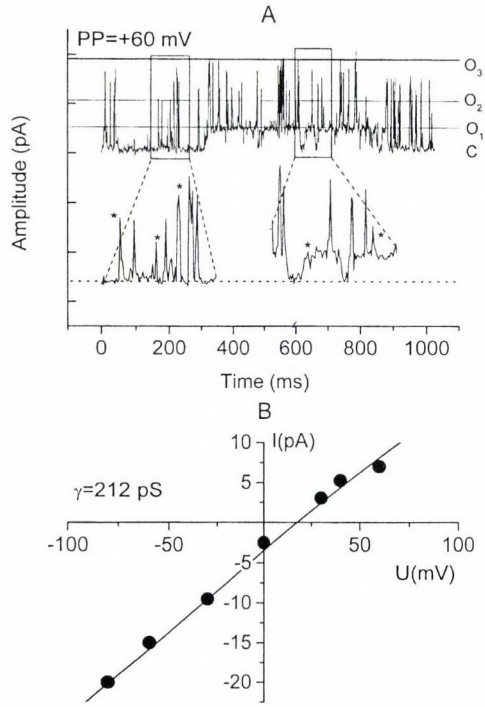

Fig. 7. A – Subconductance states (asterisks) of Na-dependent K channel in inside-out patch activated by 40 mM NaCl from the cytoplasmic side of the membrane. C – resting level, O_1– O_3 are subconductance levels. Lower record was made at expanded time scale. Amplitude calibration is 5 pA. B – Current-voltage (i–v) relationship for the main conducting state of $I_{K(Na)}$ channels in 120 mM $[K]_o$ 80 mM $[K]_i$ (equilibrium potential, EK = 10.2 mV) solution. Single channel conductance is 212 pS

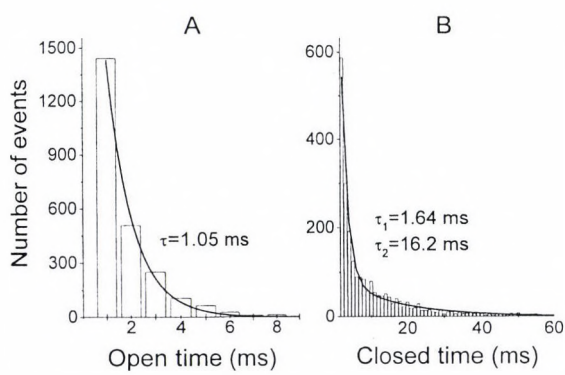

Fig. 8. PP = –88 mV, inside-out patch, 40 mM NaCl inside. The open-time (B) and closed-time (C) distributions from the same patch

DISCUSSION

The octapeptide ASHYPRFVa elicit an outward current above –80 mV membrane potential in snail D-cluster neurons and possessed all properties characteristic for the hexapeptide members of the MIP-family [19]. At increased extracellular [K^+] (20 mM) a second component was observed, which proved to be a Cl^--dependent current. The main outward current component reversed at –80 mV and decreased or ceased in Na-free saline without changing the reversal potential of the current. Because of the ineffectiveness of ouabain, and Li^+ to abolish the MIP effect on the outward current it seems unlikely, that this current component is generated by an electrogenic Na-pump. In snail neurons, intracellular Na injection but not the injection of similar quantities of K^+ or Li^+, stimulated the electrogenic Na pump [30]. Taken into account all the above-mentioned facts suggest that MIP elicited response does not involve Na^+/K^+ pump.

On the other hand, the sensitivity of the MIP-induced response to potassium channel blockers indicates that the peptide enhances a potassium current. The physiological and pharmacological properties of this ligand gated K^+-current distinguish it from other receptor coupled K^+ currents such as the S-current and G-protein dependent inward rectifiers.

The dependence of the MIPs elicited response upon the Na^+ ion in the extracellular solution indirectly suggests that the peptide activated current is a Na-dependent K-current. In order to prove this hypothesis we have injected Na^+ intracellularly and the response obtained was identical to that induced by peptide application. Additivity test supported the hypothesis, that the peptide-elicited response is carried by a current through Na-activated K-channels.

More direct evidences have been obtained from single channel experiments. Rising the Na^+ ion concentration (40 mM) at the cytoplasmic phase of the membrane, channels were activated with a main amplitude of 12–15 pA at –60 mV membrane potential.

It appears that the channel may enter at least two open states in addition to the main conducting state, like in quail trigeminal ganglion neurons [14]. The slope conductance was around 200 pS, which is in the range obtained in different vertebrate and invertebrate preparations [6].

Originally, Na enters through voltage dependent TTX-sensitive channels in different vertebrate neurons. Our investigated neurons do not have voltage-activated Na-channels. Therefore, one of the possible explanations might be that the rise of $[Na]_i$ is mainly due to the influx of Na^+ through the Ca-channels. More plausible explanation would be, however, that Na enters via leakage channels into the cell from the extracellular space. Li^+ could substitute Na^+ in activating K^+-channels meanwhile Cs^+ was unable to activate these channels. Therefore we conclude that the MIP peptides induced channel are Na-activated channels ($I_{K(Na)}$).

Sodium-activated K^+ channels ($I_{K(Na)}$) are a class of large conductance ion channels expressed in several population vertebrate neurons, mammalian cardiac muscle cells and *Xenopus* oocytes [2, 4, 5, 7, 14, 17, 26, 33]. According to Dreyer [6]

Kameyama et al. [17] reported first that K^+ channels can be activated by increasing the Na^+ concentration on the cytoplasmatic side of inside-out patches from guinea-pig myocytes. These channels are not affected by Ca^{2+} or ATP. The probability of finding channels in the open state is a function of the Na^+ concentration, with half maximal activation occurring at 30–60 nM and a Hill-coefficient of 3. The presence of $I_{K(Na)}$ channels was also reported in invertebrate neurons [12, 16] and in peptidergic nerve terminals in crustacean neurosecretory system [29].

In snail neurons the hyperpolarizing effect of intracellular Na^+-injection was described by Kerkut and Thomas [18] and Thomas [30]. They have concluded that the effect was due to the stimulation of an electrogenic Na-pump. Kononenko et al. [21] have shown however, that this current is potential dependent, which was difficult to explain solely by the presence of the electrogenic Na-pump. They concluded therefore, that Na^+-induced membrane current is a result of a "specific increase in the membrane conductance", that is coupled with high activity of the Na-pump. This special type of ion channel could be identical with the Na-activated K-channel.

Consequently, the presence of the Na^+-activated K channels in the snail neurons is not unique. Although in mammalian cortical neurones there is some evidence that $I_{K(Na)}$ is modulated by neurotransmitter norepinephrine [9] this is the first demonstration of the involvement of $I_{K(Na)}$ in peptide action. Hence, it is proposed that MIP-family peptides elicit a novel type of K-channels in *Helix* neurones gated by a transient increase of intracellular Na concentrations.

ACKNOWLEDGEMENT

This work was supported by a Hungarian Scientific Research Fund (OTKA) grant, No. 29559.

REFERENCES

1. Ascher, P. (1972) Inhibitory and excitatory effects of dopamine on *Aplysia* neurones. *J. Physiol. 225,* 173–209.
2. Bischoff, U., Vogel, W., Safronov, B. V. (1998) Na^+-activated K^+ channels in small dorsal root ganglion neurones of rat. *J. Physiol. 510,* 743–754.
3. Bolshakov, V. Y., Gapon, S. A., Katchman, A. N., Magazanik, L. G. (1993) Activation of a common potassium channel in molluscan neurones by glutamate, dopamine and muscarinic agonist. *J. Physiol. 468,* 11–33.
4. Dreyer, S. E. (1991) Na^+-activated K^+ channels and voltage-evoked ionic currents in brain stem and parasympathetic neurones of the chick. *J. Physiol. 435,* 513–532.
5. Dreyer, S. E. (1989) Na^+-activated K^+ currents in cultured brain stem neurones from chicks. *J. Physiol. 410,* 283–296.
6. Dreyer, S. E. (1994) Na^+-activated K^+ channels: a new family of large-conductance ion channels. *TINS 17,* 155–160.
7. Egan, T. M., Dagan, D., Kupper, J., Levitan, I. B. (1992) Na^+-activated K^+ channels are widely distributed in rat CNS and in *Xenopus oocytes. Brain Res. 584,* 319–321.
8. Elekes, K., Fujisawa, Y., Hernádi, L., Kiss, T., Muneoka, Y. (1999) Immunocytochemical localization of *Mytilus* inhibitory peptides (MIP) in the central and peripheral nervous system of snails, *Lymnaea stagnalis* and *Helix pomatia. Cell Tissue Res.* (submitted).
9. Foehring, R. C., Schwindt, P. C., Crill, W. E. (1989) Norepinephrine selectively reduces slow Ca^{2+}- and Na^+-mediated K^+ currents in cat neocortical neurons. *J. Neurophysiol. 61,* 245–256.

10. Fujisawa, Y., Takahashi, T., Ikeda, T., Muneoka, Y., Kubota, I., Minakata, H., Nomoto, K., Nose, T., Miki, W. (1993) Further identification of bioactive peptides in the anterior byssus retractor muscle of *Mytilus:* two contractile and three inhibitory peptides. *Comp. Biochem. Physiol. 106C,* 261–267.
11. Gerschenfeld, H. M., Paupardin-Tritsch, D. (1974) Ionic mechanisms and receptor properties underlying the responses of molluscan neurones to 5-hydroxitryptamine. *J. Physiol. 243,* 427–456.
12. Grolleau, F., Lapied, B. (1994) Transient Na^+-activated K^+ current in beating pacemaker-isolated adult insect neurosecretory cells (DUM neurones). *Neurosci. Lett. 167,* 46–50.
13. Gruol, D. L., Weinreich, D. (1979) Two pharmacologically distinct histamine receptors mediating membrane hyperpolariation on identified neurons of *Aplysia* californica. *Brain Res. 162,* 281–301.
14. Haimann, C., Bernheim, L., Bertrand, D., Bader, C. R. (1990) Potassium current activated intracellular sodium in quail trigeminal ganglion neurons. *J. Gen. Physiol. 95,* 961–979.
15. Hamill, O. P., Marty, A., Neher, E., Sakmann, B., Sigworth, F. J. (1981) Improved patch-clamp techniques for high-resolution current recordings from the cells and cell-free membrane patches. *Pflügers Archiv 391,* 85–100.
16. Hartung, K. (1985) Potentiation of a transient outward current by Na^+ influx in crayfish neurones. *Pflügers Archiv 404,* 41–44.
17. Kameyama, M., Kakei, M., Sato, R., Shibasaki, T., Matsuda, H., Irisawa, H. (1984) Intracellular Na^+ activates a K^+ channel in mammalian cardiac cells. *Nature 309,* 354–356.
18. Kerkut, G. A., Thomas, R. C. (1965) An electrogenic sodium pump in snail nerve cells. *Comp. Biochem. Physiol. 14,* 167–183.
19. Kiss, T., Elekes, K., Fujisawa, Y., Muneoka, Y. (1999) Ionic mechanism *Mytilus* inhibitory peptides elicited membrane currents in identified *Helix* neurons. *Brain Res. 830,* 258–267.
20. Kiss, T. (1990) Effect of *Mytilus* inhibitory peptide on identified molluscan neurones. *Comp. Biochem. Physiol. 95C,* 207–212.
21. Kononenko, N. I., Kostyuk, P. G. (1976) Further studies of the potential-dependence of the sodium-induced membrane current in snail neurones. *J. Physiol. 256,* 601–615.
22. Li, K. W., Van Minnen, J. W., Van Veelen, P. A., Van der Greef, J., Geraerts, W. P. M. (1996) Structure, localization and action of a novel inhibitory neuropeptide involved in the feeding of *Lymnaea.* Mol. *Brain Res. 37,* 267–272.
23. Liu, G. J., Santos, E. D., Takeuchi, H. (1991) Mapping study of *Achatina* giant neurons sensitive to molluscan peptides. *Comp. Biochem. Physiol. 100C,* 553–558.
24. Muneoka, Y., Matsushima, O., Minakata, H. (2000) Comparative aspects of invertebrate neuropeptides. *Acta Biol. Hung. 51,* 111–132.
25. Pedder, S. M., Chen, M. L., Muneoka, Y., Walker, R. J. (1998) Structural requirements and ionic mechanism of the *Mytilus* inhibitory peptides (MIPs) on *Helix* central neurons. *Gen. Pharmac.* 30, 213–220.
26. Safronov, B. V., Bischoff, U., Vogel, W. (1996) Single voltage-gated K^+ channels and their functions in small dorsal root ganglion neurones of rat. *J. Physiol. 493,* 393–408.
27. Sakharov, D. A., Salánki, J. (1969) Physiological and pharmacological identification of neurons in the central nervous system of *Helix pomatia. Acta Physiol. Acad. Sci. Hung. 35,* 19–30.
28. Sasaki, K., Sato, M. (1987) A single GTP-binding protein regulates K^+-channels coupled with dopamine, histamine and acetylcholine receptors. *Nature 325,* 259–533.
29. Stuenkel, E. L., Ruben, P., Cooke, I. M., Lemos, J. R. (1990) Sodium-activated cation channnels in peptidergic nerve terminals. *Brain Res. 517,* 35–43.
30. Thomas, R. C. (1969) Membrane current and intracellular sodium changes in a snail neurone during extrusion of injected sodium. *J. Physiol. 201,* 495–514.
31. Tol-Steye, H., van Lodder J. C., Planta, R. J., van Heerikhuizen, H., Kits, K. S. (1997) Convergence of multiple G-protein-coupled receptors onto a single type of potassium channel. *Brain Res. 777,* 119–130.
32. Yongsiri, A., Takeuchi, H., Kubota, I., Muneoka, Y. (1989) Effects of *Mytilus* inhibitory peptides on a giant neurone of *Achatina fulica* Férussac. *J. Pharmacol. 171,* 159–165.
33. Wang, Z., Kimitsuki, T., Noma, A. (1991) A conductance properties of the Na^+-activated K^+ channel in guinea-pig ventricular cells. *J. Physiol. 433,* 241–257.

Acta Biologica Hungarica 51 (2–4), pp. 147–152 (2000)

THE PRESENCE AND SPECIFICITY OF CRUSTACEAN CARDIOACTIVE PEPTIDE (CCAP)-IMMUNOREACTIVITY IN GASTROPOD NEURONS

L. HERNÁDI[1]* and H. J. AGRICOLA[2]

[1]Department of Experimental Zoology, Balaton Limnological Research Institute of the Hungarian Academy of Sciences, P. O. Box 35, H-8237 Tihany, Hungary
[2]Institute of General Zoology, Friedrich Schiller University, Jena, Germany

(Received: August 31, 1999; accepted: November 30, 1999)

CCAP-like immunoreactivity was detected in central neurons with small and medium diameters in both *Helix* and *Lymnaea* CNS. The intensity of immunoreactivity showed seasonal changes with a maximum intensity during spring. The overwhelming majority of nerve cell bodies exhibiting CCAP immunoreactivity is located in the cerebral and parietal ganglia of both *Helix* and *Lymnaea*. The neurons of pleural and buccal ganglia were devoid of CCAP-immunoreactivity. Following preabsorbtion of CCAP antibody in 1:15000 dilution with 10^{-3} M CCAP or CCAP-related peptide (*Helix* –CCAP), immunoreactivity could not be observed in neurons, demonstrating the specificity of the antibody to CCAP-related molecules in both *Helix* and *Lymnaea*.

Keywords: CCAP – CCAP-related peptides – immunocytochemistry – *Helix* – *Lymnaea*.

INTRODUCTION

The crustacean cardioactive peptide (CCAP) was originally identified from the pericardial organs of the shore crab, *Carcinus maeans*, as a potent cardioexcitatory substance [16]. CCAP evokes inotropic effects on the *Locusta* heart at 10^{-9} M threshold concentration [5]. Cardioexcitatory effects of CCAP was also demonstrated in the larvae of the blowfly [8] and hawkmoth [2]. CCAP affects not only the heart muscles in different arthropods acting as neurohormone, but noncardiac muscles as the hindgut [18] and neurons in the stomatogastric ganglion of crustaceans [11, 20] are also targets for CCAP.

A CCAP-related new peptide family, the members of which have a very similar amino acid sequence to that of the CCAP, have been isolated and characterized from *Helix pomatia* [10, 12]. Significant differences can be seen only at the amidated end of the molecule as it is demonstrated with a member of the family (H24).

[+] Presented at the 9th ISIN Symposium on "Neurobiology of Invertebrates", July 1–5, 1999, Tihany, Hungary.

*Corresponding author, E-mail: hernadi @tres.blki.hu

0236-5383/2000/$ 5.00

Pro-Phe-**Cys**-Asn-Ala-Phe-Thr-Gly-**Cys**-NH_2 (CCAP)
Pro-Phe-**Cys**-Asn-Ser-Tyr-Gly-**Cys**-Tyr-Asn-Ser-NH_2 (*Helix*-CCAP)

CCAP-related peptides were shown to be effective on different invertebrate muscles by potentiating their contractions [12]. CCAP affected heart muscle contraction and *Helix*-CCAP affected the behavior of *Helix pomatia* (Hernádi and Agricola in preparation). Although CCAP-related peptides have been isolated and characterized in molluscan species but neurons showing CCAP-like immunoreactivity have not been described. The aim of the present study was to perform immunocytochemistry on the CNS of two different gastropod species *Helix pomatia* and *Lymnaea stagnalis,* to see if the antibody raised against CCAP labels neurons of the gastropod CNS which does not contain CCAP but CCAP-related peptide molecules.

MATERIAL AND METHODS

Adult specimens of the snail *Helix pomatia L.* and *Lymnaea stagnalis* were used in different seasons. The CNS was dissected and immersed into fixative containing 4% paraformaldehyde buffered with 0.1 M phosphate buffer (pH 7.4) for 6 h at 4 °C. After fixation the samples were washed in phosphate buffered saline (PBS) overnight at 4 °C.

Immunocytochemistry was carried out on both whole-mounts and on 25 μm thick serial cryostat sections cut from the CNS of both *Helix* and *Lymnaea*. Samples were incubated with CCAP antibody [1, 6] diluted 1:5000, 1:10000, 1:15000 in PBS-TX-BSA for 2 days at room temperature. To visualize the CCAP-immunoreaction the peroxidase-antiperoxidase (PAP) three-steps method [19] was applied. The immunoreaction was developed in TRIS-HCl buffer containing 0.05% diaminobenzidine (DAB) and 0.01% H_2O_2. Samples were dehydrated and embedded into Canada balsam.

For specificity tests of the immunoreaction polyclonal CCAP antibody [1] diluted 1:5000 or 1:15000 in PBS-TX-BSA was preabsorbed with 10^{-3} M CCAP (875, Peninsula Laboratories, San Carlos, CA) or 10^{-3} M *Helix*-CCAP (H24), see Minakata et al. [10] for 12–48 h at 4 °C. The preabsorbed antibody was used as method control on cryostat sections.

In control experiments, when the CCAP antibody was replaced by normal goat serum in PBS-TX-BSA, no immunoreaction could be observed. After preabsorbtion with 10^{-3} M CCAP or *Helix*-CCAP molecules the antibody in 1:15000 dilution did not give immunoreactivity in neurons of both *Helix* and *Lymnaea*. In case of *Helix*-CCAP, the preabsorbtion time affected the activity of the antibody; 48 h long preabsorbtion time at 4 °C was needed for the total abolishment of the immunoreaction.

RESULTS AND DISCUSSION

CCAP-immunoreactivity obtained in the different seasons of the year was different in the CNS of both *Helix* and *Lymnaea*. The staining intensity was found to be the highest in spring whereas it was the lowest in autumn and winter. Therefore, we used CCAP antibody in 1:15000 dilution in spring and 1:5000 in autumn and winter.

CCAP-ir cell bodies could be observed in all ganglia of the CNS of both *Helix* and *Lymnaea* except the pleural and buccal ganglia (Fig. 5). However, CCAP-ir fibers were present in each ganglia. The CCAP-ir cell bodies appeared regularly in the same positions in the different preparation and they showed cluster-like arrangements in the different ganglia (Figs 1, 4). The majority of CCAP-ir cell bodies is concentrated in the cerebral and parietal ganglia in both *Helix* (Fig. 1) and *Lymnaea* (Figs 3, 4). CCAP immunoreactivities could be detected mainly in small (10–12 μm) neuronal cell bodies (Figs 1, 4), however larger (55–60 μm) CCAP-ir cell bodies were also seen in the cerebral (Figs 1, 2, 3) and parietal ganglia. The majority of CCAP-ir neurons were unipolar and their processes exhibited extensive varicose arborizations (Fig. 2).

Authentic CCAP has been identified and isolated not only from the shore crab *Carcinus* [16] but from the nervous system of insects such as *Locusta migratoria* [18] and *Manduca secta* [7, 9]. These observations indicate that the primary structure of CCAP is highly conserved since it could be detected in phylogenetically divergent arthropod groups. Immunocytochemistry demonstrated CCAP-ir neurons in different arthropod species like the crab [4], the horseshoe crab *Limulus* [3] and the grasshopper *Locusta* [5]. Although authentic CCAP has not been demonstrated, CCAP-ir neurons could be found also in other phyla as the annelid leech located in both the brain and ventral nerve cord [3].

Authentic CCAP could not be found in gastropods only CCAP-related peptides were isolated with a very similar amino acid sequence to CCAP [10, 12], CCAP antibody stained neurons in the different ganglia of *Helix* and *Lymnaea*. Although significant differences could be seen at the amidated end of CCAP and CCAP-related peptide molecules, the cistein bridge makes the conformation of CCAP related peptide molecules very similar to that of the CCAP [12]. Since no cross-reacting substance with CCAP antibody has yet been found with any other known peptides [4, 18], our confidence that the antibody recognised CCAP-related peptides was based upon the complete abolishment of immunostaining by preabsorbtion with CCAP or CCAP-related molecules. Therefore, we suggest that the antibody raised against CCAP can recognize CCAP-related molecules specifically and we may consider the obtained immunoreactivity in the neurons of both *Helix* and *Lymnaea* specific to CCAP-related molecules.

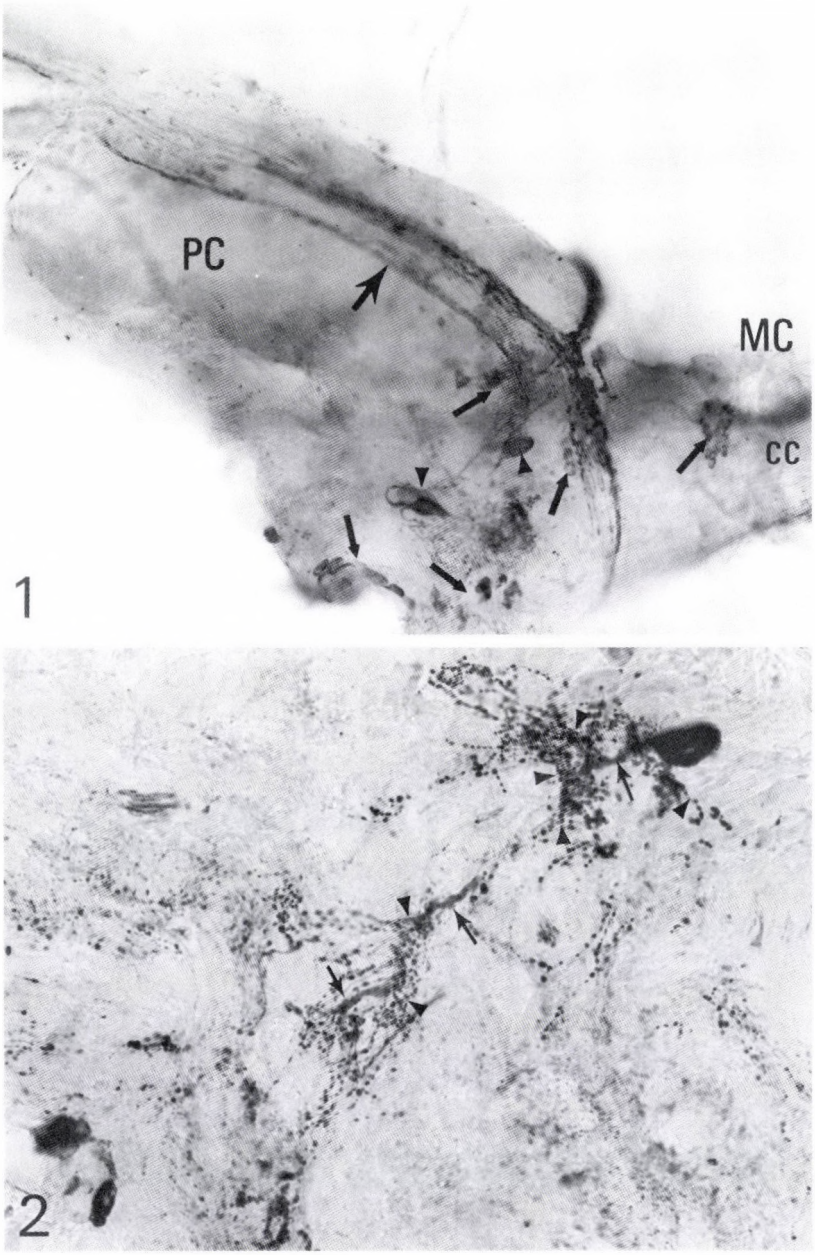

Fig. 1. The whole-mount preparation shows the distribution of CCAP-ir neurons on the dorsal surface of *Helix* cerebral ganglion. Arrows show the characteristic groups of small CCAP-ir neurons. Arrowheads show solitary CCAP-Ir. neurons. Large arrow shows the main CCAP-ir pathway running to the olfactory and tentacular nerves. cc. Cerebral commissure, MC. mesocerebrum, PC. Procerebrum ×125. *Fig. 2.* The cryostat section shows a medium diameter unipolar CCAP-ir neuron in the dorsal surface of *Helix* cerebral ganglion. The main process (arrows) runs towards the ventral surface and gives off fine varicose sidebranches (arrowheads). ×250

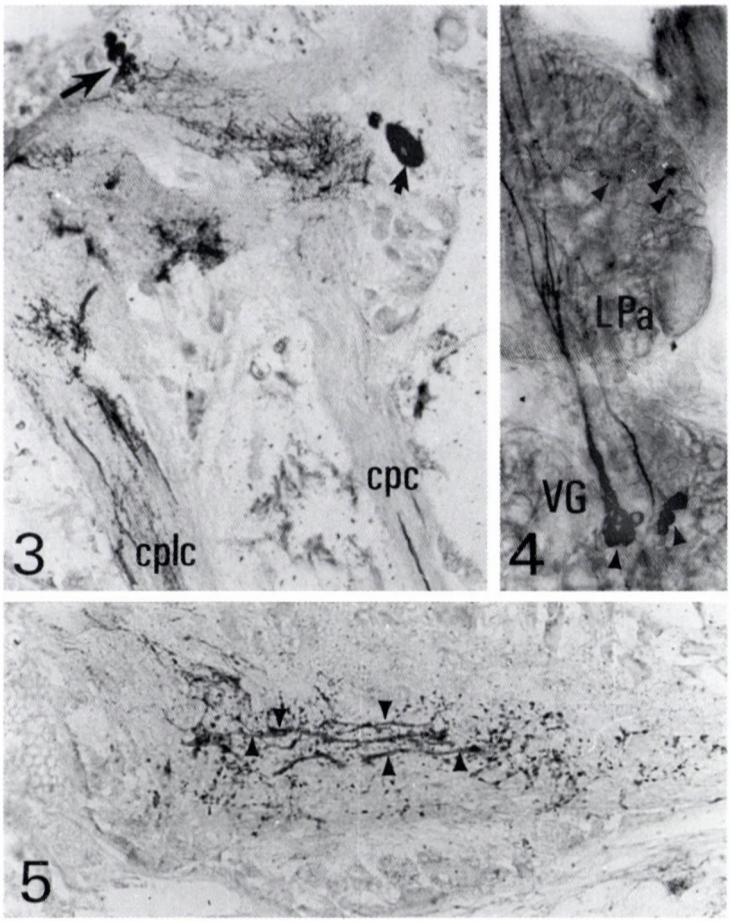

Fig. 3. Horizontal cryostat section of *Lymnaea* cerebral ganglion shows the characteristic group of small CCAP-ir neurons (arrow) close to the lip nerves. Arrowhead shows a medium diameter CCAP-ir neuron. cpc. cerebro-pedal connective, cplc. cerebro-pleural connective ×125. *Fig. 4.* The whole-mount preparation of *Lymnaea* CNS shows the small CCAP-ir neurons (arrowheads) in the visceral (VG) and left parietal (LPa) ganglia. ×125. *Fig. 5.* The cryostat section of *Lymnaea* buccal ganglion exhibits no CCAP-ir cell bodies only thick CCAP-ir fibers (arrowheads) making fine varicose arborization in the neuropil of the ganglion. ×250

ACKNOWLEDGEMENT

This work was supported by DAAD, and OTKA grants No. 16015 and 29559.

REFERENCES

1. Agricola, H.-J., Bräunig, P., Meisser, R., Nauman, W., Wollweber, L., Davis, N. (1995) Colocalization of allostatin-like immunoreactivity with other neuromodulators in the CNS of *Periplaneta americana.* In: Elsner, N., Menzel, R. (eds) *Learning and Memory.* Thieme Verlag, Stuttgart, p. 616.

2. Davis, N. T., Homberg, U., Dircksen, H., Levine, R. B., Hildebrand, J. G. (1993) Crustacean cardioactive peptide-immunoreactive neurons in the hawkmoth *Manduca secta* and changes in their immunoreactivity during postembrionic development. *J. Comp. Neurol. 338,* 612–627.
3. Dircksen, H. (1994) Distribution and physiology of crustacean cardioactive peptide in arthropods. In: Davey, K. G., Peter, R. E., Tobe, S. S. (eds) *Perspectives in Comparative Endocrinology.* National Research Council of Canada, Ottawa, pp. 139–148.
4. Dircksen, H., Keller, R. (1988) Immunocytochemical localization of CCAP a novel crustacean cardioactive peptide, in the nervous system of the shore crab, *Carcinus maeans L. Cell Tissue Res. 254,* 347–360.
5. Dircksen, H., Müller, A., Keller, R. (1991) Crustacean cardioactive peptide in the nervous system of the locust, *Locusta migratoria:* an immunocytochemical study on the ventral nerve cord and peripheral innervation. *Cell Tissue Res. 263,* 439–457.
6. Ewer, J., Truman, J. W. (1996) Increases in cyclic 3,5,-guanosine monophosphate (cGMP) occur at ecdysis in an evolutionarily conserved crustacean cardioactive peptide-immunoreactive insect neuronal network. *J. Comp. Neurol. 370,* 330–341.
7. Hildebrand, J. G., Lehman, H. K., Miller, T. A., Davis, N. T. (1990) A peptide related to crustacean cardioactive peptide in *Manduca secta:* characterization and distribution. *Soc. Neurosci. Abstr. 16,* 856.
8. Jahn, G., Käuser, G., Koolman, J. (1991) Localization of crustacean cardioactive peptide (CCAP) in the central nervous system of larvae of the blowfly, *Calliphora vicina. Gen. Comp. Endocrinol. 82,* 287.
9. Lehman, H. K., Murgiuc, C. M., Miller, T. A., Lee, T. D., Hildebrand, J. G. (1993) Crustacean cardioactive peptide in the sphinx moth, *Manduca sexta. Peptides 14,* 735–741.
10. Minakata, H., Ikeda, T., Fujita, T., Kiss, T., Hiripi, L., Muneoka, Y., Nomoto, K. (1993) Neuropeptides isolated from *Helix pomatia.* Part 2. FMRFamide-related peptides, S-Iamide peptides, FR peptides and others. In: Yanaihara, N. (ed.) *Peptide chemistry 1992.* ESCOM Science Publishers B.V., Leiden, The Netherlands. pp. 579–582.
11. Mulloney, B., Namba, H., Agricola, H.-J., Hall, W. M. (1997) Modulation of force during locomotion: Differential action of crustacean cardioactive peptide on power-stroke and return-stroke motor neurons. *J. Neuroscience 17,* 6872–6883.
12. Muneoka, Y., Takahashi, T., Kobayashi, M., Ikeda, T., Minakata, H., Nomoto, K. (1994) Phylogenetic aspects of structure and action of molluscan neuropeptides. In: Davey, K. G., Peter, R. E., Tobe, S. S. (eds) *Perspectives in Comparative Endocrinology.* National Research Council of Canada, Ottawa, pp. 109–118.
13. Schwiemann, K. (1991) Vorkommen, Verteilung und biochemische Charakterisierung von CCAP (Crustacean cardioactive peptide) beim Hummer. Diploma Thesis, University of Bonn, Bonn, Germany.
14. Stangier, J. (1991) Biological effects of crustacean cardioactive peptide (CCAP), a putative neurohormone/neurotransmitter from crustacean pericardial organs. In: Stefano, G. B., Florey, E. (eds) *Comparative Aspects of Neuropeptide Function.* Manchester University Press, Manchester, pp. 201–210.
15. Stangier, J., Dircksen, H., Keller, R. (1986) Identification and immunocytochemical localization of proctolin in the pericardial organs of the shore crab, *Carcinus maeans. Peptides 7,* 67–72.
16. Stangier, J., Hilbich, C., Beyreuther, K., Keller, R. (1987) Unusual cardioactive peptide (CCAP) from pericardial organs of the shore crab *Carcinus maeans. Proc. Natl. Acad. Sci. USA 84,* 575–79.
17. Stangier, J., Hilbich, C., Dircksen, H., Keller, R. (1988) Distribution of a novel cardioactive neuropeptide (CCAP) in the nervous system of the shore crab *Carcinus maeans. Peptides 9,* 795–800.
18. Stangier, J., Hilbich, C., Keller, R. (1989) Occurrence of crustacean cardioactive peptide (CCAP) in the nervous sytem of an insect, *Locusta migratoria. J. Comp. Physiol. B. 159,* 5–11.
19. Sternberger, R. A. (1979) *Immunocytochemistry.* John Wiley, Chichester.
20. Weimann, J. M., Skiebe, P., Heinzel, H.-G., Soto, C., Kopell, N., Jorge-Rivera, J. C., Marder, E. (1997) Modulation of oscillator interactions in the crab stomatogastric ganglion by crustacean cardioactive peptide. *J. Neurosci. 17,* 1748–1760.

Acta Biologica Hungarica 51 (2–4), pp. 153–163 (2000)

COMPARATIVE PHARMACOLOGY OF FEEDING IN MOLLUSCS[+]

C. J. H. ELLIOTT* and ÁGNES VEHOVSZKY

Department of Biology, University of York, P. O. Box 373, York, YO10 5YW, UK

(Received: August 31, 1999; accepted: November 30, 1999)

1. This paper reviews the role of transmitters in identified neurons of gastropod molluscs in generating and modulating fictive feeding.
2. In *Lymnaea* and *Helisoma* the 3 phase rhythm is generated by sets of interneurons which use acetylcholine for the N1 (protraction) phase, glutamate for the N2 (rasp) phase interneurons. The N3 interneurons are likely to use several different transmitters, of which one is octopamine.
3. In all the species examined, serotonin (5-HT) is released from giant cerebral cells. Other amines, including dopamine and octopamine, are present in the buccal ganglia and all these amines activate or enhance feeding.
4. Nitric oxide (NO), mostly originating from sensory processes, can also activate fictive feeding, but (at least in *Lymnaea*) may also be released centrally from buccal (B2) and cerebral neurons (CGC).
5. The central pattern generator for feeding is also modulated by peptides including APGWamide, SCP_B and FMRFamide.
6. There is increasing evidence that most of these transmitters/modulators act on feeding neurons through second messenger systems – allowing them to act as longer-lasting neuromodulators of the feeding network.
7. Many of the transmitters are used in similar ways by each of the gastropods examined so far, so that their function in the CNS seems to have been conserved through evolution.

Keywords: Monoamines – neuropeptides – nitric oxide – feeding – gastropods.

INTRODUCTION

In the search to understand neural organisation, work with gastropod molluscs has been particularly fruitful. Analysis of their feeding systems has provided many insights into how rhythmic patterns are generated, modulated by sensory inputs and changed due to experience. Although the feeding network initially appeared simple, it is complex and adaptable, as the behaviour can be configured for ingestion, egestion and for egg laying. At a physiological level, a variety of different, identifiable

[+] Presented at the 9th ISIN Symposium on "Neurobiology of Invertebrates", July 1–5, 1999, Tihany, Hungary.

*Corresponding author, E-mail: cje2@york.ac.uk

0236-5383/2000/$ 5.00

neurons is required to construct each phase of the rhythmic pattern. The behavioural and physiological complexity is reflected in the use of a wide range of neurotransmitters – both classical, peptidergic and gaseous in the network.

This review seeks to summarise the role of neurotransmitters in generating and modulating the rhythmic pattern for fictive feeding. Our understanding of the closely related basommatophoran snails *Lymnaea* and *Helisoma,* where the central pattern

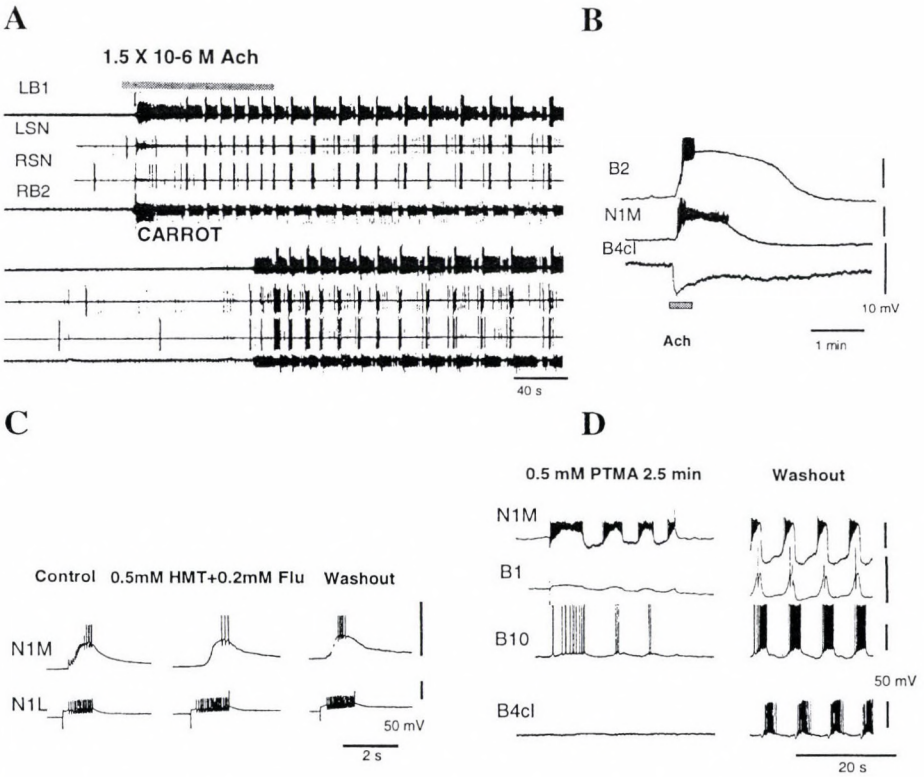

Fig. 1. Role of acetylcholine in feeding. A. Application of acetylcholine to the cerebral ganglia of *Limax* activates fictive feeding in a manner similar to carrot juice applied to the lips (Reproduced with permission from Ref. 22). B. In *Lymnaea,* application of acetylcholine to buccal neurons (B2 and 4CL motoneurons and N1M interneuron in a saline with no calcium produces direct effects (Reproduced with permission from Ref. 14). C. In *Lymnaea,* application of the cholinergic antagonist hexamethonium blocks the fast EPSPs produced by the protraction phase interneuron N1L. This is combine with the dopaminergic antagonist fluphenazine, but neither antagonist blocks the slower component (Reproduced with permission from Ref. 48). D. In *Lymnaea,* the partial cholinergic antagonist PTMA dissolved in normal saline blocks the fictive feeding rhythm evoked by stimulating the N1M interneuron; rhythmic activity is just confined to the N1 neuron and its follower (B10). The lack of activity in the B4cl motoneuron indicates that the N2 and N3 interneurons which control the rasping and swallowing are not takint part in the PTMA rhythm. In the washout, the full feeding pattern is recovered (Reproduced with permission from Ref. 11)

generator is well known, is compared with the stylommatophorans (*Helix* & *Limax*) and with the more distantly related opisthobranchs (*Aplysia, Clione*, and *Pleurobranchaea*).

ACETYLCHOLINE

Acetylcholine, long-established a molluscan neurotransmitter, plays an important role in the feeding system. In *Limax* and *Aplysia,* application of acetylcholine or cholinergic agonists to the cerebral (but not buccal) ganglia evokes a rhythmic pattern, comparable to that for ingestion [22, 43] (Fig. 1A). This is due to the direct activation of several cerebro-buccal interneurons, including the serotonergic giant cell. However, high concentrations of acetylcholine block feeding [24] probably due to the direct agonist effect on all the buccal neurons to dominating over synaptic inputs. Acetylcholine, and other cholinergic agonists, excite the protraction phase inter- and motoneurons and inhibit the retraction phase neurons [14] (Fig. 1B).

In *Lymnaea* acetylcholine is present in all 3 of the protraction phase premotor interneurons (SO, N1L, N1M) so far analysed. Application of antagonists – either general, like curare, or specific, like methylxylocholine and hexamethonium block the fast PSPs produced by these neurons, but do not reduce the second, slower component, which suggests these neurons also release a cotransmitter (Fig. 1C) [12, 48, 53]. One example is the peptide myomodulin, which is present in the SO [40].

Application of cholinergic antagonists also prevents the full rhythmic pattern from occurring; instead, activity is confined to the protraction phase neurons [11]. The rhythmic activation of the N2 (rasping) phase neurons does not occur because of the disruption of the N1 → N2 connections (Fig. 1D).

GLUTAMATE

There is strong evidence that glutamate is used as a transmitter by retraction phase interneurons in *Helisoma* and *Lymnaea*. Immunocytochemistry shows that the retraction phase interneuron B2 of *Helisoma* contains elevated levels of glutamate [35]. Many of the feeding motoneurons respond to bath or iontophoretic application of glutamate in the same way (excitation or inhibition) that they do to the retraction phase synaptic inputs. In *Lymnaea* the B3 motoneuron is excited by glutamate and rasp phase inputs, while the 7 cell motoneuron and SO interneuron are inhibited [6]. Both these effects are mimicked by the agonists quisqualate and AMPA (Fig. 2A). In *Helisoma,* the inhibitory effects of glutamate were mimicked by quisqualate, and the excitatory ones by kainate (Fig. 2B). Some *Helisoma* cells (e.g. B19, homologous to the B4 motoneuron of *Lymnaea*) were inhibited by glutamate but excited by kainate [35, 36]. Moreover, CNQX blocks the excitatory responses selectively. The excitatory responses of the *Lymnaea* B3 motoneuron to stimulation of the retraction phase

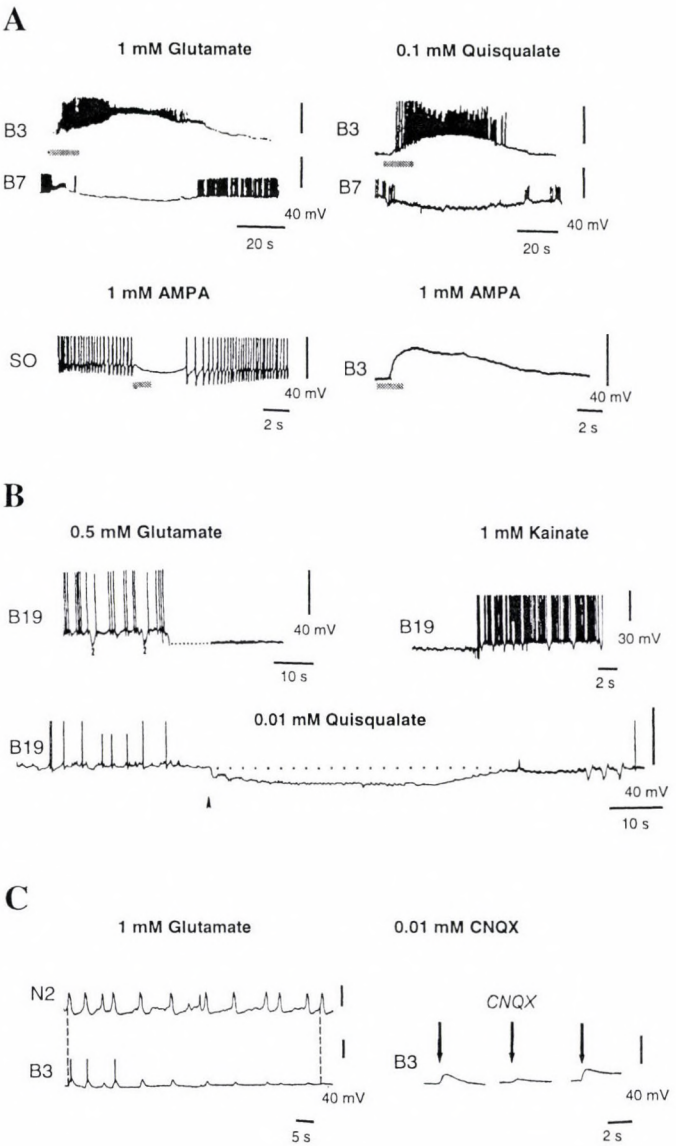

Fig. 2. Pharmacology of glutamate in *Helisoma* and *Lymnaea* feeding system: A. *Lymnaea* the agonists quisqualate and AMPA both have similar effects to glutamate (Reproduced with permission from Ref. 6). B. In *Helisoma* glutamate and quisqualate inhibit the B19 motoneuron, but this cell is excited by kainate. The B19 motoneuron is the homolog of B4 in *Lymnaea* (Reproduced with permission from Ref. 36). C. The excitatory response to N2 bursts and to glutamate are both blocked by CNQX. (Reproduced with permission from Ref. 6)

interneurons, and the depolarising S2 (rasp) phase inputs in *Helisoma* were reduced by CNQX [6, 36] (Fig. 2C).

Thus, there are multiple types of glutamate receptor present in the feeding system, and despite the lack of pharmacological detail obtained so far, it is clear that none of these receptors match the vertebrate classification of NMDA and non/NMDA glutamate receptors.

The sequence for one of these receptors, mediating excitation, has been obtained and is expressed in the B4 motoneuron of *Lymnaea* [42].

Finally, the presence of glutamate in the retraction phase interneurons and acetylcholine in the protraction phase interneurons means that the feeding central pattern generator has pharmacological similarities to the swimming central pattern generator of *Clione* [4] where the up- and down-stroke neurons use acetylcholine and glutamate [31].

SEROTONIN

Serotonin modulates the feeding system in all levels: at the neuromuscular junction, and at the sensory input, as well in the CNS modulating feeding interneurons and motoneurons as well. Serotonin-containing giant cerebral cells have been located in all species examined (including the pulmonates *Lymnaea*, *Helisoma*, *Helix*, and the opisthobranchs *Aplysia* and *Pleurobranchaea*). Application of serotonin to buccal ganglia of *Lymnaea* shows that all the cells respond to serotonin in the same way as to CGC stimulation (see Fig 3A, Hitchcock, Elliot and Vehovszky, unpubl. and ref. [1]).

Buccal cells show both ionotropic responses to serotonin and also metabotropic responses linked through a wide range of pathways. In *Helisoma* the B5 neuron was inhibited by serotonin though a pathway, which involve arachidonic acid and activated K^+ influx [1]. The excitatory responses of B19 however, are cAMP dependent with an increased Na^+ influx [1]. In *Helix,* the three buccal neurons A, M & P respond with differently, either due to activation of a ligand-gated channel or to metabotropic receptor or to a mixture of the two [7, 19]. A similar complexity of response exists in the buccal motoneurons of *Aplysia* [44].

Serotonin also affects the central pattern generator: the response is normally to activate fictive feeding (though, at least in *Lymnaea*), but strong fictive feeding may be disrupted by an excess of serotonin [47]. In weakly feeding preparations, stimulation of the CGC increases the intensity and feeding rate but may also alter the pattern, reducing the duration of the N3 phase selectively [5]. The effects on feeding rate and pattern long outlast the burst of CGC spikes, as the prolonged effects of CGC modulation were shown by laser ablation of the CGC axon, while fictive feeding was evoked by SO stimulation [52] (Fig. 3).

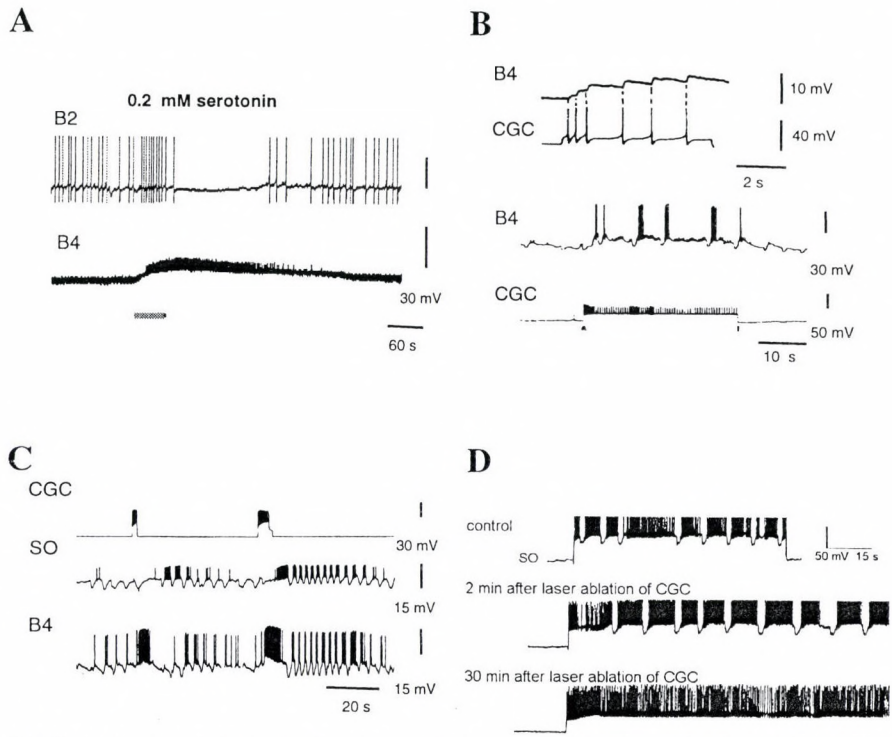

Fig. 3. Effects of serotonin in the feeding system of *Lymnaea* A. The effects of bath application of serotonin to the buccal motoneurons mimics the effects of CGC stimulation: excitation then inhibition of the B2 motoneuron and excitation of the B4 motoneuron (Hitchcock and Elliott, unpubl.). B. Rapid EPSPs from the serotonergic CGC to the B4 motoneuron follow 1:1. Prolonged stimulation of the CGC depolarises the B4 motoneuron and it now fires in the rhythmic pattern. (Reproduced with permission from Ref. 5). C. Brief stimulation of the CGC excites the B4 motoneuron, but also enhances the fictive feeding rhythm caused by steady depolarisation of the SO. Note that the CGC excites the B4 motoneuron much quicker than its effect on the feeding rate (Reproduced with permission from Ref. 5). D. Laser ablation of the CGC reduces the ability of the SO to drive the feeding rhythm. After 2 minutes, the SO still drives the network (note the rhythmic strong N2 inhibitory inputs); after 30 minutes no patters is seen in response to SO stimulation (Yeoman, Kemenes, Benjamin and Elliott, unpubl.)

OCTOPAMINE

Octopamine was among the first neurotransmitters to be identified in molluscs [16]. The paired buccal ganglia of *Aplysia, Lymnaea* and *Helix* contain high concentrations of octopamine suggesting that it plays an important role in feeding behaviour [10, 20, 25]. In *Lymnaea* the buccal octopamine is confined to three homologous swallowing phase interneurons (OC cells) which can activate and/or modulate fictive feeding [49, 50]. Interneurons with similar anatomy and physiology have been reported in

Helisoma [37]. Two sequences for molluscan octopamine receptors have been published: both of these are G-protein linked, suggesting that these receptors (like those found in insects) act through activation of second messengers [17, 18].

DOPAMINE

Dopamine has been located in buccal cells of *Aplysia*, *Helisoma, Lymnaea* and *Limax* has been suggested to modulate the pattern in these species [22, 24, 45, 46]. Dopamine acts to increase the intensity and/or the frequency of fictive feeding. In *Aplysia*, the dopaminergic neuron, B20, can activate a rhythmic pattern [45], while B65 can switch the pattern from a rejection to ingestion like rhythm [21]. Finally, the *Aplysia* buccal ganglia receive dopaminergic innervation from the cerebral ganglia [38] and *Lymnaea* from the oesophageal nerves [8].

In *Lymnaea* and *Helisoma,* there is a group of laterally located neurons in the buccal ganglia, which are dopamine immunoreactive [9]. These cells in *Helisoma* may be part of the S1 (= N1) protraction phase network [34]. In *Lymnaea,* N1L interneurons have similar electrophysiology and morphology [54]. However, the synapses formed by the N1L neurones are highly likely to be cholinergic, as cholinergic antagonists blocked their synaptic outputs, while neither their fast EPSPs nor slower smooth depolarising output was reduced by well-known dopamine antagonists [48] Thus, it is possible that neurons with similar physiological connections could use different transmitters.

GASES

At least part of the chemosensory input comes from neurons in the lips, which have peripheral cell bodies that stain for NO [27]. NO applied to the isolated CNS activates the feeding pattern in *Lymnaea* [15] and in *Pleurobranchaea* [28]. Moreover, injection of NO scavengers into intact *Lymnaea* can block the activation of the feeding rhythm by sucrose [15]. Two *Lymnaea* feeding neurons are known to release NO. The B2 motoneuron has an excitatory effect on the B7 motoneuron [32], but its significance in the feeding pattern is not known since the B2 cell fires arrhythmically. The other nitrergic cell may be the serotonergic CGC as this cell contains the NO-synthase, but it has not yet been shown to release NO [23].

PEPTIDES

Three peptides (FMRFamide, APGWamide and SCP_B) have so far been shown to modulate the central pattern generator of the molluscan feeding system.

FMRFamide slows rhythmic activity in *Helisoma* [30]. One possible source is a cell in the pleural ganglion, which might provide a possible locus for interactions

between withdrawal and feeding systems [29]. It has not been shown if the native peptide in this pleural cell is FMRFamide or a related RFamide. This pathway is conserved in many species, including *Helix* and *Lymnaea* and the carnivorous predator *Clione* (where FMRFamide also inhibits feeding) [2, 3]. In *Lymnaea,* most of the pleural cells expressing the FMRFamide like peptides express a tetrapeptide transcript as do just 2 unidentified buccal neurons with axons in the latero-buccal nerve [39].

APGWamide is contained in a single pair of cerebro-buccal interneurons [26]. Bath application of APGWamide mimics the effect of stimulating these cells, with activation of fictive feeding in slowly active preparations, and disruption of actively cycling preparations [26]. SCP_B has also been reported to activate and enhance the feeding rate in *Helisoma, Aplysia* and *Tritonia* [30, 41, 51]. However, in *Limax* and *Lymnaea* SCP_B could not initiate or accelerate fictive feeding [13, 33], even though SCP_B seems to be present in several *Lymnaea* feeding neurons, including the N2 interneurons [40]. In the intact snail, SCP_B in fact decreases feeding behaviour [13].

Many of the peptides have been located in feeding interneurons (including myomodulins in the SO, see above) and motoneurons, but most of their physiological analysis has been on their peripheral, rather than central actions.

CONCLUSIONS

The variety of transmitters found so far in this "simple system" is substantially greater than that expected 25 years ago.

One simple explanation for this observation is Dale's principle, that a neuron may only respond to a transmitter in one way, so that at least two transmitters are needed to alternate excitation and inhibition. The need to use pharmacologically different transmitters can explain the presence of acetylcholine and glutamate in the protraction and retraction phase interneurons.

Similar arguments may be applied to the presence of multiple transmitters in the N3 (swallowing) phase. Differential changes to the three kinds of N3 interneuron using separate transmitters would allow the network to be reconfigured to produce different patterns of what motor activity, e.g. switching between feeding, egestion and egg laying behaviours.

Modulators are important in allowing the response of the system to change dynamically, so that the responses of the behaving animal can adapt to changes in the environment. However, there is a gradual recognition that neurotransmitter/ neuromodulator function cannot be clearly separated, and similarly defining the modulatory function for an interneuron is difficult. Furthermore, we have recognised that many peptides and even gaseous substances (as NO) may act as transmitters/modulators. The signalling across the synapse may also be important, not just for behavioural control, but also for bi-directional signalling to establish and maintain synaptic structure and function.

The membrane receptors sensitive to the same transmitter/neuromodulator substance also display a great diversity, particularly, when second messenger pathways are involved (e.g. in response to serotonin, octopamine, dopamine and probably to peptides). These pathways provide an opportunity for longer-lasting synaptic effects (for example, to reducing the firing threshold when presynaptic stimuli are repeated).

Lastly, much of the evidence suggests that molluscs use similar transmitters in their feeding system, and use them in similar ways, despite the evolutionary changes in the pharmacology of the receptors.

ACKNOWLEDGEMENT

We would like to thank the BBSRC for their support.

REFERENCES

1. Achee, N. L., Zoran, M. J. (1997) Serotonin-induced modulation of excitability in an identified *Helisoma trivolvis* neuron. *J. Exp. Biol. 200,* 1537–1548.
2. Alania, M. (1995) Pleuro-buccal projections in pulmonate molluscs. *Acta Biol. Hung. 46,* 267–270.
3. Alania, M., Sakharov, D. A. (1998) The cellular basis of movement coordination is conservative in gastropods differing in feeding strategies. *Zh. Obsh. Biol. 59,* 400–408. (In Russian)
4. Arshavsky, Y. I., Deliagina, T. G., Orlovsky, G. N., Panchin, Y. V., Popova, L. B., Sadreyev, R. I. (1998) Analysis of the central pattern generator for swimming in the mollusk. *Clione. Ann. New York Acad. Sci. 860,* 51–69.
5. Benjamin, P. R., Elliott, C. J. H. (1989) Snail feeding oscillator: the central pattern generator and its control by modulatory interneurons. In: Jacklet, J. W. (ed.) *Neuronal and Cellular Oscillators.* Marcel Dekker, New York, Basel, 173–214.
6. Brierley, M. J., Yeoman, M. S., Benjamin, P. R. (1997) Glutamate is the transmitter for N2v retraction phase interneurons of the *Lymnaea* feeding system. *J. Neurophysiol. 78,* 3408–3414.
7. Cottrell, G. A. (1988) Slow synaptic responses mediated by the *Helix* giant serotonin-neurones on identified follower neurons. *Comp. Biochem. Physiol. 91C,* 165–169.
8. Croll, R. P., Voronezhskaya, E. E., Hiripi, L., Elekes, K. (1999) Development of catecholaminergic neurons in the pond snail, *Lymnaea stagnalis:* II. Postembryonic development of central and peripheral cells. *J. Comp. Neurol. 404,* 297–309.
9. Elekes, K., Kemenes, G., Hiripi, L., Geffard, M., Benjamin, P. R. (1991) Dopamine-immunoreactive neurons in the central-nervous-system of the pond snail *Lymnaea stagnalis. J. Comp. Neurol. 307,* 214–224.
10. Elekes, K., Voronezhskaya, E., Hiripi, L., Eckert, M., Rapus, J. (1996) Octopamine in the developing nervous system of the snail, *Lymnaea stagnalis. Acta Biol. Hung. 47,* 73–87.
11. Elliott, C. J. H. (1992) Cholinergic interneurons in the feeding system of the pond snail *Lymnaea stagnalis*. 3. Pharmacological dissection of the feeding rhythm. *Phil. Trans. Soc. London 336,* 181–189.
12. Elliott, C. J. H., Kemenes, G. (1992) Cholinergic interneurons in the feeding system of the pond snail *Lymnaea stagnalis.* 2. N1 interneurons make cholinergic synapses with feeding motoneurons. *Phil. Trans. Roy. Soc. London B336,* 167–180.
13. Elliott, C. J. H., Kemenes, G., Waddington, S. (1991) The modulatory peptide SCP_B inhibits feeding in the mollusk, *Lymnaea stagnalis. Comp. Biochem. Physiol. 100C,* 615–618.
14. Elliott, C. J. H., Stow, R. A., Hastwell, C. (1992) Cholinergic interneurons in the feeding system of the pond snail *Lymnaea stagnalis.* 1. Cholinergic receptors on feeding neurons. *Phil. Trans. Roy. Soc. London B336,* 157–166.

15. Elphick, M. R., Kemenes, G., Staras, K., Oshea, M. (1995) Behavioral role for nitric-oxide in chemosensory activation of feeding in a mollusk. *J. Neurosci. 15,* 7653–7664.
16. Erspamer, V., Boretti, G. (1951) Identification and characterization by paper chromatography of enteramine, octopamine, tyramine, histamine, and allied substances in extracts of posterior salivary glands of *Octopoda* and in other tissue extracts of vertebrates and invertebrates. *Arch. Int. Pharmacodyn. Ther. 88,* 296–332.
17. Gerhardt, C. C., Bakker, R. A., Piek, G. J. et al. (1997) Molecular cloning and pharmacological characterization of a molluscan octopamine receptor. *Mol. Pharmacol. 51,* 293–300.
18. Gerhardt, C. C., Lodder, H. C., Vincent, M. et al. (1997) Cloning and expression of a complementary DNA encoding a molluscan octopamine receptor that couples to chloride channels in HEK293 cells. *J. Biol. Chem. 272,* 6201–6207.
19. Hillvenning, C., Cottrell, G. A. (1992) Modulation of voltage-dependent calcium current in *Helix aspersa* buccal neurons by serotonin and protein-kinase-c activators. *Exp. Physiol. 77,* 891–901.
20. Hiripi, L., Vehovszky, A., Juhos, S., Elekes, K. (1998) An octopaminergic system in the CNS of the snails, *Lymnaea stagnalis* and *Helix pomatia. Phil. Trans. Roy. Soc. London B353,* 1621–1629.
21. Kabotyanski, E. A., Baxter, D. A., Byrne, J. H. (1998) Identification and characterization of catecholaminergic neuron B65, which initiates and modifies patterned activity in the buccal ganglia of *Aplysia. J. Neurophysiol. 79,* 605–621.
22. King, M. S., Delaney, K., Gelperin, A. (1987) Acetylcholine activates cerebral interneurons and feeding motor program in *Limax maximus. J. Neurobiol. 18,* 509–530.
23. Korneev, S. A., Piper, M. R., Picot, J., Phillips, R., Korneeva, E. I., Oshea, M. (1998) Molecular characterization of NOS in a mollusc: Expression in a giant modulatory neuron. *J. Neurobiol. 35,* 65–76.
24. Kyriakides, M. A., McCrohan, C. R. (1989) Effect of putative neuromodulators on rhythmic buccal motor output in *Lymnaea stagnalis. J. Neurobiol. 20,* 635–650.
25. McCaman, M. W., McCaman, R. E. (1978) Octopamine and phenylethanolamine in *Aplysia* ganglia and in individual neurons. *Brain Res. 141,* 347–352.
26. McCrohan, C. R., Croll, R. P. (1992) Modulation of feeding motor output by the neuropeptide, APGWamide, in the isolated central-nervous-system of *Lymnaea stagnalis. J. Physiol. 452,* 147.
27. Moroz, L. L., Bulloch, A. M., Lukowiak, K., Syed, N. I. (1994) Putative no-synthesizing neurons of *Lymnaea* in vivo and in vitro. *Neth. J. Zool. 44,* 535–549.
28. Moroz, L. L., Gillette, R. (1996) NADPH-diaphorase localization in the CNS and peripheral-tissues of the predatory sea-slug *Pleurobranchaea-californica. J. Comp. Neurol. 367,* 607–622.
29. Murphy, A. D. (1990) An identified pleural ganglion interneuron inhibits patterned motor- activity in the buccal ganglia of the snail, *Helisoma. Brain Res. 525,* 300–303.
30. Murphy, A. D., Lukowiak, K., Stell, W. K. (1985) Peptidergic modulation of patterned motor-activity in identified neurons of *Helisoma. Proc. Natl. Acad. Sci. USA 82,* 7140–7144.
31. Panchin, Y. V., Sadreyev, R. I. (1997) Effects of acetylcholine and glutamate on isolated neurons of locomotory network of *Clione. Neuro Report 8,* 2897–2901.
32. Perry, S. J., Dobbins, A. C., Schofield, M. G., Piper, M. R., Benjamin, P. R. (1999) Small cardioactive peptide gene: structure, expression and mass spectrometric analysis reveals a complex pattern of co-transmitters in a snail feeding neuron. *Eur. J. Neurosci. 11,* 655–662.
33. Prior, D. J., Watson, W. H. (1988) The molluscan neuropeptide, SCP_B, increases the responsiveness of the feeding motor program of *Limax maximus. J. Neurobiol. 19,* 87–105.
34. Quinlan, E. M., Arnett, B. C., Murphy, A. D. (1997) Feeding stimulants activate an identified dopaminergic interneuron that induces the feeding motor program in *Helisoma. J. Neurophysiol. 78,* 812–824.
35. Quinlan, E. M., Gregory, K., Murphy, A. D. (1995) An identified glutamatergic interneuron patterns feeding motor-activity via both excitation and inhibition. *J. Neurophysiol. 73,* 945–956.
36. Quinlan, E. M., Murphy, A. D. (1991) Glutamate as a putative neurotransmitter in the buccal central pattern generator of *Helisoma trivolvis. J. Neurophysiol. 66,* 1264–1271.

37. Quinlan, E. M., Murphy, A. D. (1996) Plasticity in the multifunctional buccal central pattern generator of *Helisoma* illuminated by the identification of phase 3 interneurons. *J. Neurophysiol. 75,* 561–574.
38. Rosen, S. C., Teyke, T., Miller, M. W., Weiss, K. R., Kupfermann, I. (1991) Identification and characterization of cerebral-to-buccal interneurons implicated in the control of motor programs associated with feeding in *Aplysia. J. Neurosci. 11,* 3630–3655.
39. Santama, N., Brierley, M., Burke, J. F., Benjamin, P. R. (1994) Neural-network controlling feeding in *Lymnaea stagnalis* – immunocytochemical localization of myomodulin, small cardioactive peptide, buccalin, and FMRFamide-related peptides. *J. Comp. Neurol. 342,* 352–365.
40. Santama, N., Wheeler, C. H., Burke, J. F., Benjamin, P. R. (1994) Neuropeptides myomodulin, small cardioactive peptide, and buccalin in the central-nervous-system of *Lymnaea stagnalis* – purification, immunoreactivity, and artifacts. *J. Comp. Neurol. 342,* 335–351.
41. Sossin, W. S., Kirk, M. D., Scheller, R. H. (1987) Peptidergic modulation of neuronal circuitry controlling feeding in *Aplysia. J. Neurosci. 7,* 671–681.
42. Stuhmer, T., Amar, M., Harvey, R. J., Bermudez, I., VanMinnen, J., Darlison, M. G. (1996) Structure and pharmacological properties of a molluscan glutamate-gated cation channel and its likely role in feeding behavior. *J. Neurosci. 16,* 2869–2880.
43. Susswein, A. J., Rosen, S. C., Gapon, S., Kupfermann, I. (1996) Characterization of buccal motor programs elicited by a cholinergic agonist applied to the cerebral ganglion of *Aplysia californica. J. Comp. Physiol. 179A,* 509–524.
44. Taussig, R., Sweetcordero, A., Scheller, R. H. (1989) Modulation of ionic currents in *Aplysia* motor neuron-b15 by serotonin, neuropeptides, and 2nd messengers. *J. Neurosci. 9,* 3218–3229.
45. Teyke, T., Rosen, S. C., Weiss, K. R., Kupfermann, I. (1993) Dopaminergic neuron-b20 generates rhythmic neuronal-activity in the feeding motor circuitry of *Aplysia. Brain Res. 630,* 226–237.
46. Trimble, D. L., Barker, D. L. (1984) Activation by dopamine of patterned motor output from the buccal ganglia of *Helisoma trivolvis. J. Neurobiol. 15,* 37–48.
47. Tuersley, M. D., McCrohan, C. R. (1988) Serotonergic modulation of patterned motor output in *Lymnaea stagnalis. J. Exp. Biol. 135,* 473–486.
48. Vehovszky, Á., Elliott, C. J. (1995) The hybrid modulatory/pattern generating N1L interneuron in the buccal feeding system of *Lymnaea* is cholinergic. *Inv. Neurosci. 1,* 67–74.
49. Vehovszky, Á., Elliott, C. J. H. (2000) The octopamine-containing buccal neurons. Octopamine: A new feeding modulator in *Lymnaea. Acta Biol. Hung. 51,* 165–176.
50. Vehovszky, Á., Elliott, C. J. H., Voronezhskaya, E. E., Hiripi, L., Elekes, K. (1998) Octopamine: A new feeding modulator in *Lymnaea. Phil. Trans. Roy. Soc. London B353,* 1631–1643.
51. Willows, A. D., Lloyd, P. E., Masinovsky, B. P. (1988) Multiple transmitter neurons in *Tritonia.* 3. Modulation of central pattern generator controlling feeding. *J. Neurobiol. 19,* 69–86.
52. Yeoman, M. S., Kemenes, G., Benjamin, P. R., Elliott, C. J. H. (1994) Modulatory role for the serotonergic cerebral giant-cells in the feeding system of the snail, *Lymnaea.* 2. Photoinactivation. *J. Neurophysiol. 72,* 1372–1382.
53. Yeoman, M. S., Parish, D. C., Benjamin, P. R. (1993) A cholinergic modulatory interneuron in the feeding system of the snail, *Lymnaea. J. Neurophysiol.* 70, 37–50.
54. Yeoman, M. S., Vehovszky, A., Kemenes, G., Elliott, C. J. H., Benjamin, P. R. (1995) Novel interneuron having hybrid modulatory-central pattern generator properties in the feeding system of the snail, *Lymnaea stagnalis. J. Neurophysiol. 73,* 112–124.

Acta Biologica Hungarica 51 (2–4), pp. 165–176 (2000)

THE OCTOPAMINE-CONTAINING BUCCAL NEURONS ARE A NEW GROUP OF FEEDING INTERNEURONS IN THE POND SNAIL *LYMNAEA STAGNALIS*+

ÁGNES VEHOVSZKY* and C. J. H. ELLIOTT

Department of Biology, University of York, Heslington, York, P.O. Box 373, YO10, 5YW, UK

(Received: August 31, 1999; accepted: November 30, 1999)

In the pond snail, *Lymnaea stagnalis,* the paired buccal ganglia contain 3 octopamine-immunoreactive neurons, which have previously been shown to be part of the feeding network. All 3 OC cells are electrically coupled together and interact with all the known buccal feeding motoneurons, as well as with all the modulatory and central pattern generating interneurons in the buccal ganglia.

N1 (protraction) phase neurons: Motoneurons firing in this phase of the feeding cycle receive either single excitatory (depolarising) synaptic inputs (B1, B6 neurons) or a biphasic response (hyperpolarisation followed by depolarisation) (B5, B7 motoneurons). Protraction phase feeding interneurons (SO, N1L, N1M) also receive this biphasic synaptic input after OC stimulation. All of protraction phase interneurons inhibit the OC neurons.

N2 (retraction) phase neurons: These motoneurons (B2, B3, B9, B10) and N2 interneurons are hyperpolarised by OC stimulation. N2 interneurons have a variable (probably polysynaptic) effect on the activity of the OC neurons.

N3 (swallowing) phase: OC neurons are strongly electrically coupled to both N3 phase (B4, B4cluster, B8) motoneurons and to the N3p interneurons. In case of the interneuronal connection (OC↔N3) the electrical synapse is supplemented by reciprocal chemical inhibition. However, the synaptic connections formed by the OC neurons or N3p interneurons to the other members of the feeding network are not identical.

CGC: The cerebral, serotonergic CGC neurons excite the OC cells, but the OC neurons have no effect on the CGC activity.

In addition to direct synaptic effects, the OC neurons also evoke long-lasting changes in the activity of feeding neurons. In a silent preparation, OC stimulation may start the feeding pattern, but when fictive feeding is already occurring, OC stimulation decreases the rate of the fictive feeding.

Our results suggest that the octopaminergic OC neurons form a sub-population of N3 phase feeding interneurons, different from the previously identified N3p and N3t interneurons. The long-lasting effects of OC neurons suggest that they straddle the boundary between central pattern generator and modulatory neurons.

Keywords: Lymnaea stagnalis – mollusc – feeding – octopamine – neuromodulation.

+ Presented at the 9th ISIN Symposium on "Neurobiology of Invertebrates", July 1–5, 1999, Tihany, Hungary.

*Corresponding author, E-mail: av13@york.ac.uk

0236-5383/2000/$ 5.00

INTRODUCTION

Octopamine is best known as a neurohormone/neuromodulator in arthropods, being mostly involved in behaviours which require rhythmic pattern of muscular activity e.g. flight [1], swimming [19], walking [9] or feeding [2, 13, 15].

Because of the anatomical features of their central nervous system (CNS), molluscs can provide a more easily accessible model for neuronal studies of central organisation of behaviour, especially feeding. In fact, feeding is one of the best known neuronal networks in molluscan neurobiology [3, 11].

In the pond snail, *Lymnaea stagnalis*, the consummatory phase of the feeding is characterised by sequences of co-ordinated movements carried out by the feeding muscles of the buccal mass. Three phases of the feeding activity can be clearly separated: first the animal opens its mouth and protracts its radula (N1 phase, protraction), then it rasps across the food with its toothed radula (N2 phase, radula retraction), and finally it transfers food into the oesophagus (N3 phase, swallowing). For simplicity, the motoneurons involved may be classified as protraction (N1), retraction (N2) and swallowing (N3) phase motoneurons, depending on the phase of the feeding cycle in which they fire fastest. The activity of feeding motoneurons is controlled and co-ordinated by members of the central pattern generator (CPG) network located in the buccal ganglia, which form three main neuronal groups (N1, N2, N3), each firing in the corresponding phase of the feeding cycle [3]. Moreover, the higher order modulatory interneurons of the buccal ganglia (SO), or the cerebral ganglia (CGCs, CV neurons) are able to initiate or modify the activity of the feeding network [14, 21]. When the feeding system is activated, members of the feeding network display a highly co-ordinated cyclic pattern of firing activity (fictive feeding), which can be recorded in isolated CNS.

Although octopamine was suggested to be a modulator of the feeding muscles in the mollusc *Rapana* 15 years ago [12], direct evidence for the role of octopamine in the CNS was only established recently [10, 18]. After injection of the octopaminergic antagonists (phentolamine, NC-7 and DCDM) into intact animals, the feeding response evoked by sucrose was either blocked or reduced, while extracellular application of octopamine evokes fictive feeding from members of the buccal neuronal network [18].

Immunocytochemical studies showed three octopamine-containing neurons in the buccal ganglia [5, 6] while electrophysiological experiments suggested that these new cells (OC neurons) were members of the feeding network [18].

To establish the role of the OC neurons in the feeding network we have thoroughly studied the individual synaptic connections between OC neurons and the previously identified members (both motoneurons and higher order interneurons) of the feeding system. These studies provide us with a more detailed insight into the cellular basis of the octopaminergic modulation of feeding.

MATERIALS AND METHODS

Recordings were made from an OC interneuron and up to 3 other neurons in the isolated CNS of *Lymnaea stagnalis* as described previously Fig. 1A [17, 18].

The experimental chamber was continuously perfused first by standard snail saline [8] then by a Hi-Di solution [17] with raised concentration of both Mg^{2+} and Ca^{2+} which reduced the polysynaptic connections evoked by intracellular stimulation of the neurons [4].

RESULTS

In spontaneously active preparations OC neurons fire in the swallowing (N3) phase of the feeding cycle. Their activity pattern and synaptic inputs follow those of the B4 motoneurons very closely: they show IPSPs in the N2 phase and small EPSPs in the N3 phase. The regular and accurate synchronisation suggests these neurons share a common source of synaptic inputs from the feeding network (Fig. 1B).

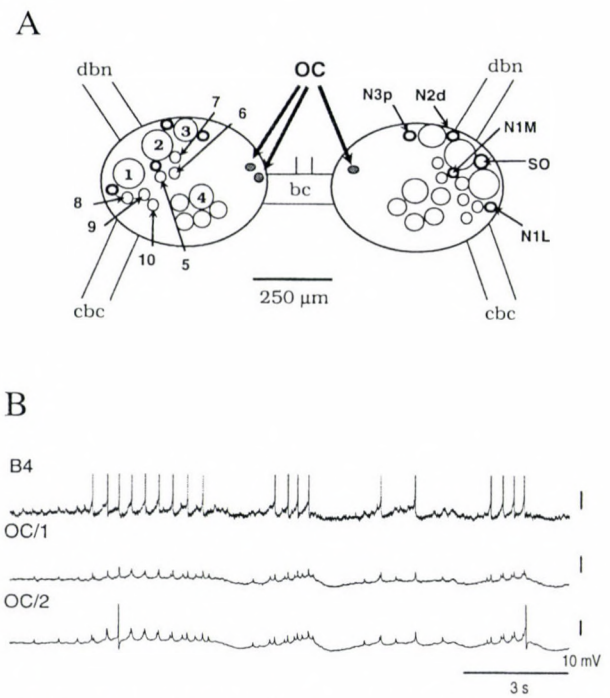

Fig. 1. OC interneurons in the buccal ganglia of *Lymnaea stagnalis*. A. Schematic representation of the dorsal surface of the paired buccal ganglia indicating the position of the three OC interneurons, feeding motoneurons (B1, B2, B... on the left) and the interneurons (SO, N1L, N1M, N2d, N3p on the right). bc: buccal commissure, dbn: dorsobuccal nerve, cbc: cerebrobuccal commissure. B. Simultaneous intracellular recording from a B4 motoneuron and two of the OC interneurons (OC/1, OC/2) displaying highly synchronous activity pattern

1. Synaptic connections of OC neurons with protraction phase feeding neurons

Motoneurons active in the N1 phase of the feeding cycle receive excitatory synaptic inputs from OC neurons. Intracellular stimulation of OC neurons increases firing activity on both B1 and B6 motoneurons (Fig. 2A, B). Other protraction phase motoneurons (B5, B7) respond biphasically: an initial hyperpolarisation is followed by depolarisation of the membrane (Fig. 2C). Single EPSPs were never recorded after stimulation of the OC neuron. The persistence of the response in Hi-Di saline suggested that both the single excitatory (OC→B1, and OC→B6) and the biphasic (OC→B5, OC→B7) synaptic responses are monosynaptic.

All the three protraction phase interneurons studied (SO, N1L and N1M) receive similar biphasic inputs from OC neurons: a slight hyperpolarisation followed by

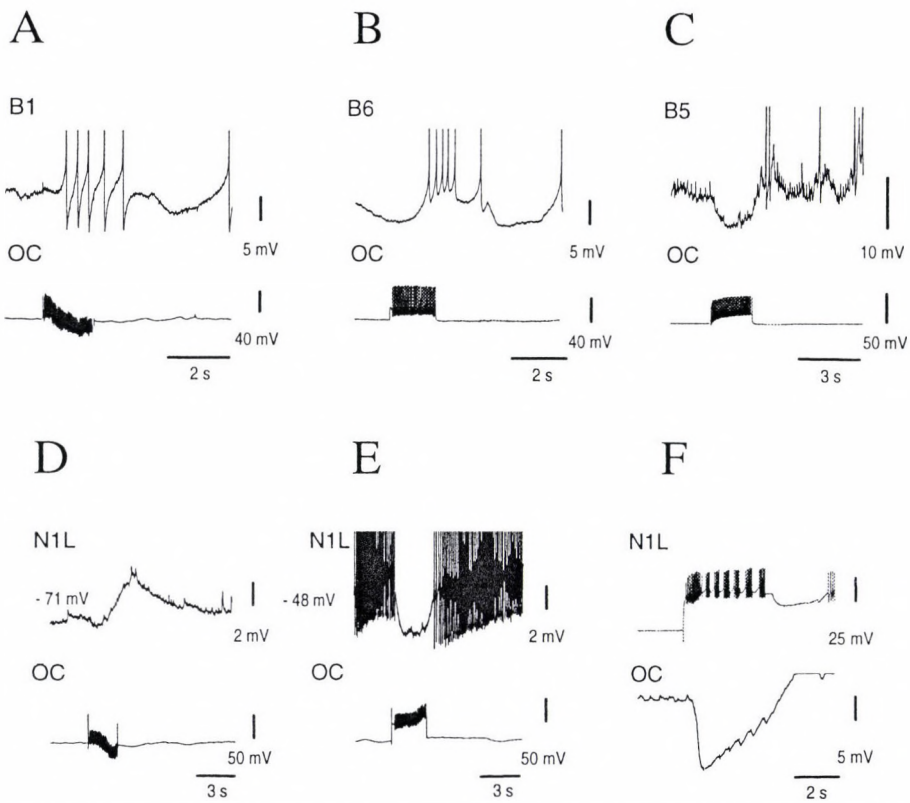

Fig. 2. Synaptic connections between OC interneurons and the protraction phase feeding neurons. B1 (A) and B6 (B) motoneurons receive excitatory inputs, while B5 motoneuron (C) displays a short hyperpolarisation followed by depolarisation after OC stimulation. The N1L feeding interneuron responds with biphasic synaptic inputs when it is silent (D), but when N1L is firing, it is inhibited by OC. D. N1L stimulation evokes strong hyperpolarisation on OC neuron

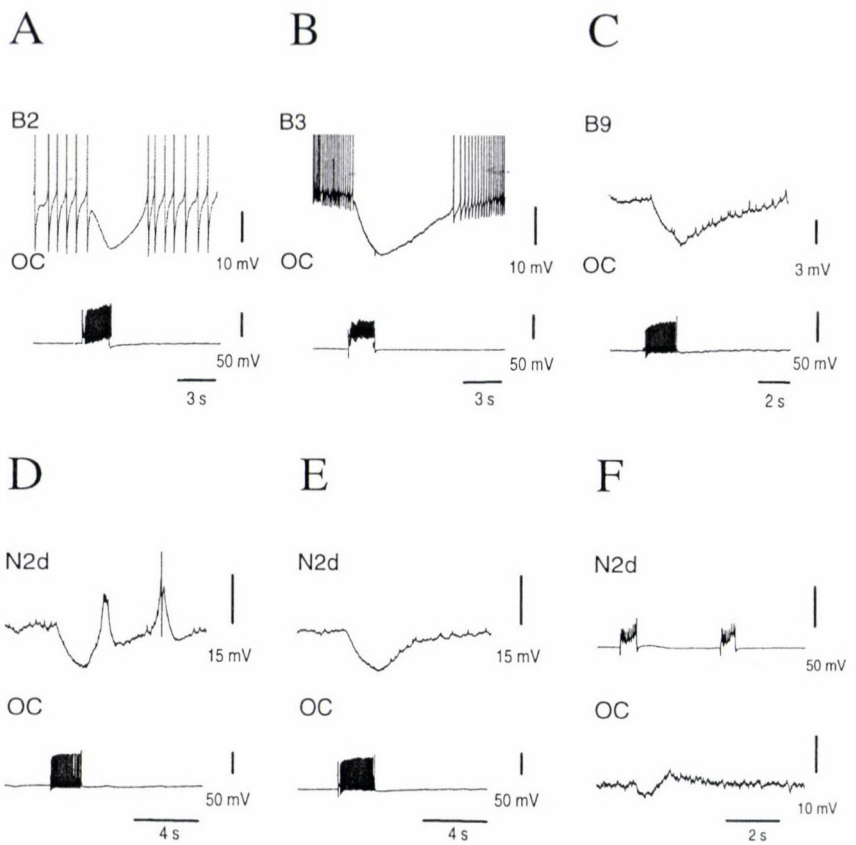

Fig. 3. Synaptic connections between OC interneurons and the retraction phase feeding neurons. OC interneuron stimulation evokes hyperpolarising synaptic responses on B2, (A), B3 (B), and B9 (C) motoneurons. D: In normal saline OC neuron evokes hyperpolarisation on N2d interneuron followed by short depolarisation (D), while in Hi-Di only the inhibitory response is visible (E). N2d stimulation did not always evoke synaptic response from N2d (F)

depolarisation (Fig. 2D). When the postsynaptic neurons are firing, however, OC stimulation evokes hyperpolarisation and inhibits the activity of the protraction phase interneurons (Fig. 2E). Experiments in Hi-Di saline suggest the monosynaptic origin of both components of the postsynaptic responses.

All the three protraction phase (SO, N1L, N1M) interneurons, inhibit the activity of the OC neurons (Fig. 2F). The synaptic connections of either the N1L or the SO interneurons are likely to be monosynaptic, as single IPSPs are occasionally seen in the OC trace; but the connections formed by N1M→OC neurons seem to be polysynaptic.

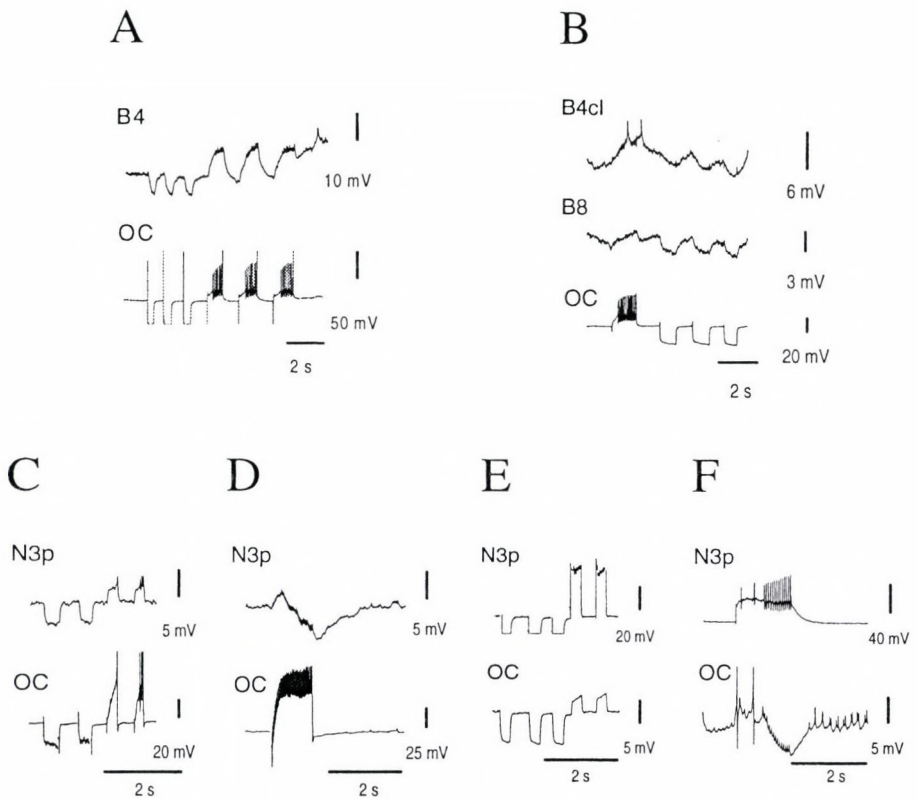

Fig. 4. Synaptic connections between OC interneurons and the swallowing phase feeding neurons. A. The B4 motoneuron and the OC neuron are electrically coupled together. B. OC neuron has electrical connection with both B4 cluster neuron and the B8 motoneuron (which is electrically coupled to the B4 cell). N3p interneurons and OC neurons have symmetrical connections, a mixture of electrical coupling (C, E) and inhibition (D, F)

2. Synaptic connections with retraction phase feeding neurons

Motoneurons active in the N2 phase of feeding cycle are inhibited by the OC neurons (Fig. 3). Both B2 and B3 motoneurons receive large (up to 15mV) hyperpolarisations after OC stimulation (Fig. 3A, B), while B9 and B10 motoneurons respond with a similar, but smaller (up to 8 mV) hyperpolarisation (Fig. 3C). Similarly to the excitatory connections mentioned earlier, single inhibitory postsynaptic potentials (IPSPs) were never recorded even after 50 min Hi-Di perfusion of the experimental chamber.

The retraction phase N2d feeding interneurons receive only inhibitory synaptic inputs from OC neurons, as the excitatory component seen occasionally (Fig. 3D), disappears in Hi-Di saline (Fig. 3E). Although spontaneously active OC neurons

receive clear N2 inputs from the CPG system (Fig. 1B), the postsynaptic responses on the OC neurons are rather variable after stimulation of the N2d interneurons (Fig. 3F) and in Hi-Di solution the postsynaptic response of OC neurons often disappears.

3. Synaptic connections with swallowing phase feeding neurons

OC neurons are electrically connected to all of the neurons firing in the swallowing (N3) phase of the feeding cycle (Fig. 4). The strongest (about 0.2) coupling ratio is with B4 motoneurons (Fig. 4A), which display highly synchronous activity pattern and synaptic inputs with the OC neurons (Fig. 1B). B4 cluster cells and B8 motoneurons also have electrical connections with the OC neurons but these are weaker (Fig.

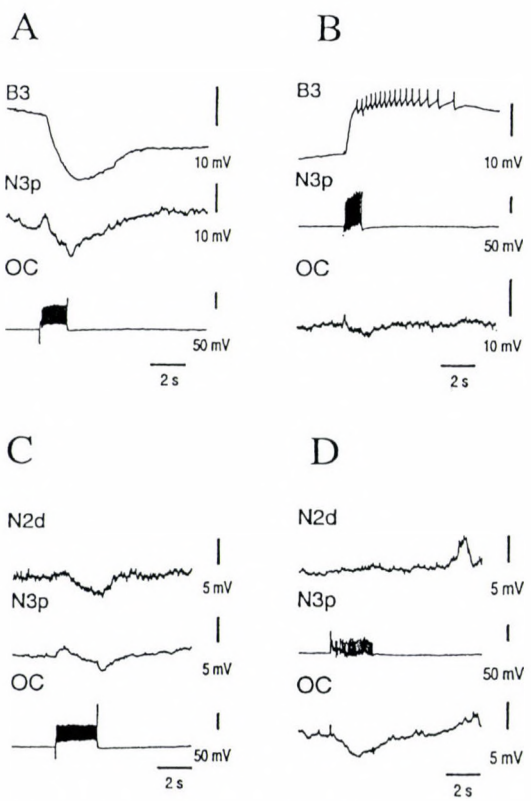

Fig. 5. OC interneurons and N3p interneurons form different synaptic connections with the same followers. Simultaneous recording from an OC neuron and a N3p interneuron together with one of the followers (B3 motoneuron on A,B, N2d interneuron on C,D). OC stimulation is followed by hyperpolarisation on B3 motoneuron (A), while a burst on the N3p interneuron is followed by strongly excitatory response on the same B3 follower (B). C: OC evokes hyperpolarisation on N2d neuron (and a mixed synaptic response on N3p neuron), but stimulating N3p only affects the OC neuron and not the N2 interneuron (D)

4B). Intracellular current injections into one of these neurons is followed by the corresponding potential changes in the other cells (Fig. 4B).

As with the B4 motoneurons, OC neurons have synchronised activity and electrical coupling to the N3p interneurons (Fig. 4C, E). Additionally, OC and N3p neurons form complex, symmetrical synaptic connections with each other. After stimulation of either an OC or N3p neuron, an electrically transmitted potential change is recorded first, which is followed by a hyperpolarising (chemical) response on the follower neurons (Fig. 4D, F). Despite the similarities between the OC and N3p neurons in activity and synaptic inputs, OC neurons and N3p interneurons form different synaptic connections to identified feeding neurons. OC stimulation evokes large hyperpolarisation on B3 neurons (Fig. 5A), while the same neuron is strongly excited by N3p stimulation (Fig. 5B). N2d interneurons display inhibitory synaptic responses after OC stimulation (Fig. 5C), but do not receive any synaptic inputs from the N3p interneurons (Fig. 5D).

4. Synaptic connections with the cerebral serotonergic cells (CGCs)

OC neurons receive excitatory (depolarising) synaptic inputs from the serotonin-containing modulatory CGC neurons (Fig. 6A), which are the only excitatory synaptic effect received by the OC neurons so far. In Hi-Di single EPSPs were often seen in the activity of the CGC neurons suggesting monosynaptic connections from the CGC to the OC neurons (Fig. 6B). OC stimulation, however, has no influence on the activity pattern or membrane potential level of the CGC neurons (Fig. 6C).

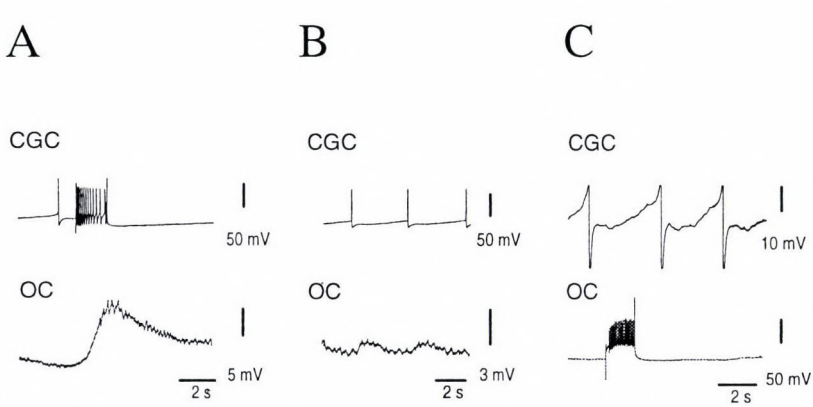

Fig. 6. Synaptic connections between OC neurons and the serotonergic cerebral giant neuron (CGC). A. Stimulating the CGC strongly excites the OC neurons. B. Individual action potentials of the CGC neuron are followed by single postsynaptic responses (EPSPs) on OC neuron. C. Firing of the OC neuron has no effect on the spontaneous activity of the CGC neuron

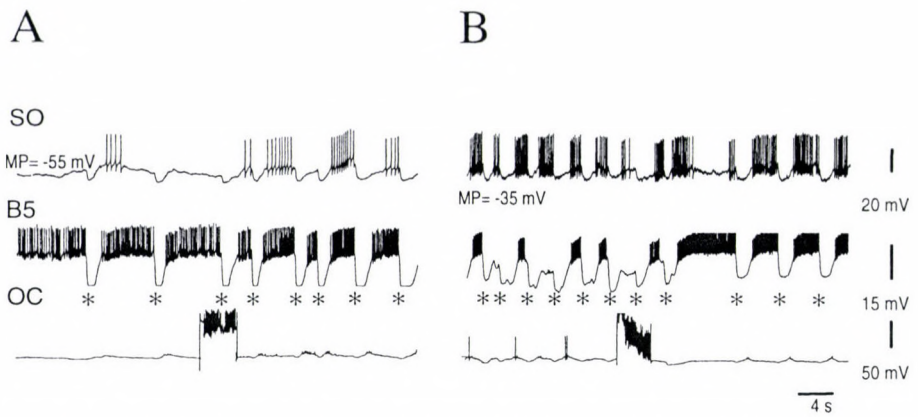

Fig. 7. Activity-dependent effect of the OC neuron on members of the feeding network. A. OC stimulation increase the bursting activity of both SO and B5 neurons and increase the rate of the fictive feeding as seen on the N2 inputs (asterisk) on both SO and B5 neurons as well as the patterned synaptic inputs on the OC record. B. When the fictive feeding is running fast (SO is firing in bursts, and all three neurons receive frequent N2 inputs), stimulation of OC first inhibits the activity of SO then decreases the rate of the fictive feeding

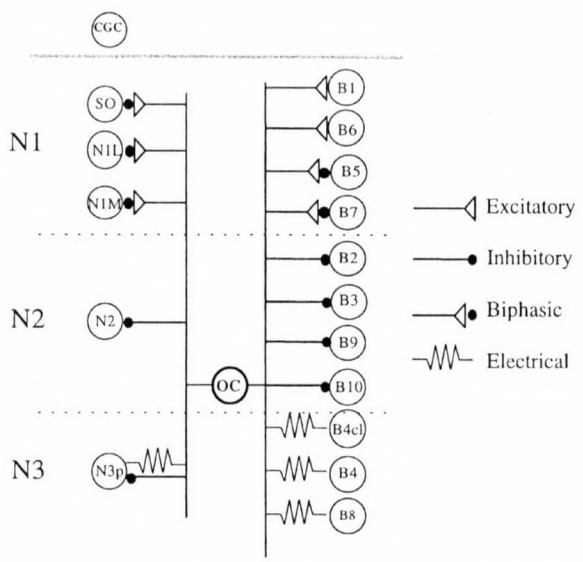

Fig. 8. Summary of the synaptic connections between OC interneurons and the other members of the feeding network. Protraction (N1) phase interneurons (SO, N1L, N1M) and some motoneurons (B5, B7) receive biphasic (inhibitory/excitatory) synaptic inputs, others (B1, B6) only excitatory effect from the OC neurons. All retraction (N2) phase motoneurons and interneurons studied receive inhibitory connections from the OC neurons. All of the motoneurons and interneurons of the swallowing (N3) phase of feeding are electrically coupled to the OC neurons. N3p interneurons have an additional (inhibitory) chemical connection as well

5. Longer-lasting synaptic effects of OC stimulation

The effect of the OC neuron stimulation depends on the activity of the whole feeding network. Intracellular stimulation of OC neurons triggers the feeding rhythm in silent preparation or increases the frequency of spontaneously feeding cycles (Fig. 7A). When the fictive feeding is running fast (either spontaneously or due to stimulation of pattern-generating interneurons, e.g. SO or N1L), stimulation of OC neurons first inhibits the protraction phase interneurons then decreases the frequency of the feeding rhythm (Fig. 7B).

DISCUSSION

OC neurons form synaptic connections with all the buccal feeding motoneurons and interneurons studied so far, but do not influence the activity of the cerebral CGC modulatory neurons (Fig. 8). These electrophysiological results confirm the previous suggestion based on morphological studies [6, 18], that the octopamine-containing neurons are local interneurons with their axons confined to the buccal ganglia.

OC neurons not only fire and receive synchronous synaptic inputs with the N3 phase motoneurons as described earlier [18], they also form tight electrical connections with both N3 phase motoneurons and the N3p interneurons. Electrical coupling between neurons firing in the same phase of the feeding cycle has been suggested to be a general feature of the buccal feeding network of *Lymnaea*, providing phase locking between feeding motoneurons and the corresponding CPG interneurons as well as allowing some contribution of the motoneurons to be involved in the mechanism of central pattern generation [16]. Here we note that the OC $\leftrightarrow$ B4 connection provides for such co-ordination, but the N3p $\leftrightarrow$ B4 electrical connection is supplemented by a N3 $\rightarrow$ B4 inhibitory connection.

The other main feature of many of the synaptic connections formed by the OC neurons is that they are biphasic: this enhances their highly-potential-dependent nature. OC neurons depolarise both modulatory (SO, N1L) and pattern-generating (N1M) interneurons when the cells are silent (in quiescent preparation), therefore shifting their membrane potential levels towards the firing threshold, and so the OC neurons facilitate triggering of the feeding pattern. However, when fictive feeding is on, OC neurons hyperpolarise these cells, and decrease the activity of the feeding network. The synaptic interactions between the OC neurons and N3p interneurons are also regulated by a similar potential-dependent way. The final output of their complex synaptic connections strongly depends on the membrane potential of these cells; if the membrane potential is well negative, then the excitatory effect (depolarisation due to the electrical coupling) is dominant, but if their membrane potential is less negative, the inhibitory (chemical) synaptic connection is more influential.

Although both OC and N3p interneurons receive synchronous synaptic inputs from the feeding system and they fire in the same (swallowing) phase of feeding, their synaptic outputs are not identical. The OC cells also produce different synaptic

outputs from the N3t interneuron [7] The differences between the postsynaptic responses evoked either by the OC neurons (recorded during our studies) or N3p interneurons (already described 3) suggest that OC neurons are a new subpopulation of swallowing phase (N3) interneurons.

OC neurons have both relatively fast synaptic effects as well as longer-lasting modulatory influences on the activity of the feeding system. The OC neurons probably represent a new group of hybrid/modulatory interneurons, similar to the N1L interneurons (which have both CPG and modulatory properties) which are "intermediate" between the modulatory SO and CPG N1M interneurons [20].

The complex and potential-dependent synaptic effects of the OC neurons may explain some of their activity-dependent, longer-lasting effects as well. However, we cannot exclude the involvement of some additional mechanisms of modulation of the feeding network (e.g. modulatory substances released extra-synaptically by OC neurons, and/or through electrically coupled, so far unidentified unknown feeding cells).

ACKNOWLEDGEMENT

We would like to thank the BBSRC for their support.

REFERENCES

1. Adamo, S. A., Linn, C. E., Hoy, R. R. (1995) The role of neurohormonal octopamine during fight or flight behavior in the field cricket *Gryllus bimaculatus. J. exp. Biol. 198,* 1691–1700.
2. Angioy, A. M., Barbarossa, I. T., Crnjar, R., Liscia, A. (1989) Effects of octopaminergic substances on the labellar lobe spreading response in the blowfly *Protophormia terraenovae. Neurosci. Lett. 103,* 103–1077.
3. Benjamin, P. R., Elliott, C. J. H. (1989) Snail feeding oscillator: the central pattern generator and its control by modulatory interneurons. In: J. W. Jacklet (ed.) *Neural and Cellular Oscillators.* New York and Basel: Marcel Dekker, pp. 173–214.
4. Berry, M. S., Pentreath, V. W. (1976) Criteria for distinguishing between monosynaptic and polysynaptic transmission. *Brain Res. 105,* 1–20.
5. Elekes, K., Eckert, M., Rapus, J. (1993) Small sets of putative interneurons are octopamine-immunoreactive in the central nervous system of the pond snail, *Lymnaea stagnalis. Brain Res. 608,* 191–197.
6. Elekes, K., Voronezhskaya, E. E., Hiripi, L., Eckert, M., Rapus, J. (1996) Octopamine in the developing nervous system of the pond snail, *Lymnaea stagnalis L. Acta Biol. Hung. 47,* 73–87.
7. Elliott, C. J. H., Benjamin, P. R. (1985) Interactions of pattern-generating interneurons controlling feeding in *Lymnaea stagnalis J. Neurophysiol. 54,* 1396–1411.
8. Elliott, C. J. H., Stow, R. A., Hastwell, C. (1992) Cholinergic interneurons in the feeding system of the pond snail *Lymnaea stagnalis.* I. Cholinergic receptors on feeding neurons. *Phil. Trans. Roy. Soc. Lond. B 336,* 157–166.
9. Gill, M. D., Skorupski, P. (1996) Modulation of spontaneous and reflex activity of crayfish leg motor neurons by octopamine and serotonin *J. Neurophysiol. 76,* 3535–3549.
10. Hiripi, L., Vehovszky, Á., Juhos, S. Elekes, K. (1998) An octopaminergic system in the CNS of the *Lymnaea stagnalis* and *Helix pomatia. Phil. Trans. Roy. Soc. Lond. B 353,* 1621–1630.
11. Kemenes, G. (1994) Processing of mechano- and chemosensory information in the lip nerve and cerebral ganglia of the snail *Helix pomatia* L. *Neurosci. Behav. Physiol. 24,* 77–87.

12. Kobayashi, M., Hasimoto, T. (1982) Antagonistic responses of the radular protractor and retractor to the same putative neurotransmitters. *Comp. Biochem. Physiol. 72,* 343–348.
13. Long, T. F., Edgecomb, R. S., Murdock, L. L. (1986) Effects of substituted phenylethylamines on blowfly feeding behavior. *Comp. Biochem. Physiol. C. 83,* 201–209.
14. McCrohan, C. (1984) Initiation of feeding motor ouput by an identified interneuron in the snail *Lymnaea stagnalis J. Exp. Biol. 113,* 351–366.
15. Pribbenov, B., Erber, J. (1996) Modulation of antennal scanning in the honeybee by sucrose stimuli, serotonin and octopamine: behavior and electrophysiology. *Neurobiol. Lern. Mem. 66,* 109–120.
16. Staras, K., Kemenes, G., Benjamin, P. (1998) Pattern-generating role for motoneurons in a rhythmically active neuronal network. *J. Neurosci. 18,* 3669–3688.
17. Vehovszky, Á., Elliott, C. J. H. (1995) The hybrid modulatory/pattern generating N1L interneuron in the buccal feeding system of *Lymnaea* is cholinergic. *Invertebrate Neuroscience 1,* 67–74.
18. Vehovszky, Á., Elliott, C. J. H., Voronezhskaya, E. E., Hiripi, L., Elekes, K. (1998) Octopamine: a new feeding modulator in *Lymnaea. Phil. Trans. Roy. Soc. Lond. B 353,* 1631–1643.
19. Wood, D. E., Gleeson, R. A., Derby, C. D. (1995) Modulation of behavior by biogenic amines and peptides in the blue crab, *Callinectes sapidus J. Comp. Physiol. A 177,* 321–333.
20. Yeoman, M. S., Vehovszky, Á., Kemenes, G., Elliott, C. J. H., Benjamin, P. R. (1995) Novel interneuron having hybrid modulatory central pattern generator properties in the feeding system of the snail, *Lymnaea stagnalis J. Neurophysiol. 73,* 112–124.
21. Yeoman, M. S., Brierley, M. J., Benjamin, P. R. (1996) Central pattern generator interneurons are targets for the modulatory serotonergic cerebral giant cells in the feeding system of *Lymnaea. J. Neurophysiol. 75,* 11–25.

Acta Biologica Hungarica 51 (2–4), pp. 177–187 (2000)

THE POSSIBLE ROLES OF THE MONOAMINERGIC SYSTEM IN THE FEEDING OF THE SNAIL *HELIX POMATIA*+

L. HERNÁDI[1*], L. ERDÉLYI[2], L. HIRIPI[1] and K. ELEKES[1]

[1]Balaton Limnological Research Institute of the Hungarian Academy of Sciences, P. O. Box 35, H-8237 Tihany, Hungary
[2]Department of Comparative Animal Physiology, József Attila University, Szeged, Hungary

(Received: August 31, 1999; accepted: November 30, 1999)

The possible role of serotonin and dopamine in the feeding of *Helix pomatia* was studied applying immunocytochemical, biochemical, and behavioral techniques as well as bioassay experiments. Immunocytochemistry showed that dopamine-containing (thyrosin-hydroxylase-immunoreactive) neuronal elements of the crop and the gizzard belong to the intrinsic part, whereas serotonin-containing (serotonin-immunoreactive) neuronal elements belong to the extrinsic part of the gastrointestinal nervous system. Bioassay studies on the spontaneous contractions of the crop and the gizzard showed that dopamine affected only the longitudinal muscle contractions by increasing both the tonus and contractility, whereas serotonin was effective on both the longitudinal and circular muscle contractions. Serotonin increased the tonus and contractility of longitudinal muscles in the crop but decreased them in the gizzard. Serotonin decreased the tonus and contractility of the circular muscles in the crop but increased them in the gizzard. Serotonin effects on the circular muscle of the gizzard were concentration dependent between a range of 10^{-5} M–3×10^{-5} M. HPLC measurements of monoamines in starved and satiated animals showed that the concentration of both dopamine and serotonin significantly decreased in both the CNS and different parts of the gastrointestinal tract of satiated animals, suggesting a significant monoamine liberation during feeding. The injection of monoamines (10^{-3} and 10^{-2} M) into the body cavity of starved animals showed that only dopamine was able to induce feeding whereas serotonin increased the general activity of the animals suggesting that the initiation of feeding is rather dopamine than serotonin dependent.

Keywords: Serotonin – dopamine – feeding – gastrointestinal system – immunocytochemistry, *Helix*.

INTRODUCTION

Both serotonin (5HT) and dopamine (DA) have been shown to exert significant effects on the feeding behavior of invertebrates. 5HT is involved in the feeding arousal and the modulation of feeding behavior in molluscs as *Aplysia* [9, 17], *Helix* [7], *Lymnaea* [19, 20] in the leech *Hirudo* [5, 6]. In semi-intact preparations, DA was capable of initiating or modulating feeding motor program by affecting the central

+ Presented at the 9th ISIN Symposium on "Neurobiology of Invertebrates", July 1–5, 1999, Tihany, Hungary.

*Corresponding author, E-mail: hernadi @tres.blki.hu

0236-5383/2000/$ 5.00

pattern generator neuronal network in *Aplysia* [9, 15] *Lymnaea* [3], *Limax* [18] and *Helisoma* [16].

Stimuli arriving from distended stomach appear to be involved in controlling feeding and ingestion in different invertebrate species. Non-nutritive bulk in the gut reduces the amount of algae required to satiate the herbivorus gastropod *Aplysia* [12] indicating that the actual state of intestine plays a role in the termination of feeding. In *Aplysia,* the ongoing activity of the central pattern generator can be terminated and modulated by significant sensory inputs originated from the gastrointestinal tract in satiated states [2, 13, 14].

During food consumption the crop and the gizzard are the first to be filled with food, therefore their distension significantly increased. In the present study the distribution of 5HT- and DA- immunoreactive neuronal elements in the crop and gizzard was investigated, as well as the effects of 5HT and DA on the spontaneous contraction of the crop and gizzard was tested at different concentrations.

We measured the monoamine content by HPLC in the crop and the salivary gland as well as in the CNS in starved and satiated animals, and also investigated the effects of increased monoamine levels on the feeding induction by the injecting DA and 5HT into the body cavity.

MATERIALS AND METHODS

Adult specimens of the snail *Helix pomatia* L. were used in different seasons.

Immunocytochemistry

The crop and the gizzard were dissected and were used as stretch preparations [1]. The samples were fixed for six hours at 4 °C in 4% paraformaldehyde buffered with 0.1 M phosphate buffer (PB) (pH 7.4).

To demonstrate 5HT-containing neuronal elements, polyclonal anti-5HT antiserum (Immunonuclear, Stillwater, USA) diluted 1:5000 was used. To demonstrate DA containing neuronal elements, a monoclonal anti-tyrosine-hydroxylase antiserum (Immunonuclear) diluted 1:1000 was used. Each antiserum was diluted in PBS-TX containing 0.25% bovine serum albumine (PBS-TX-BSA). The samples were incubated with the antisera for 48 hours at room temperature. The immunoreaction was visualised by a rhodamine conjugated secondary antibody (DAKO, Denmark) or according to the peroxidase anti-peroxidase three steps method [11].

HPLC assay of monoamines in starved and satiated animals

The monoamines were assayed by a Waters high performance liquid chromatograph equipped with an electrochemical detector. The CNS, the crop, the gizzard and the

salivary gland were dissected and homogenized in 0.1 M perchloric acid and centrifuged. Aliquots of the clear supernatant were injected into a reverse phase C18 Nucleosil column [1].

Recording of isotonical muscle contraction

To measure the contractions of circular muscle, rings were cut from the crop and the gizzard whereas for longitudinal muscle contraction measurements the whole crop and gizzard were used. The samples were fixed at their two ends to a myograph transducer. The chemical compounds (serotonin, dopamine) were added to the preparation chamber from stock solutions by injection (100 µl).

Injection of monoamines

5HT or DA was injected into the body cavity of the snail. Starved animals were injected with 25 µl of 10^{-3}, 10^{-2} M 5HT or DA. The effects on feeding induction were tested immediately after the injection. Control and injected animals were placed on a thin paper tissue soaked up with 3% sugar solution. We measured the time from the injection to the beginning of food consumption. Animals were considered to be consuming if they exhibited typical head and tentacle position to the food [8]. The consumption was controlled on the basis of the traces of rasping on the thin paper tissue. The injection of monoamines and the feeding test were made in the early afternoon.

RESULTS

The distribution of TH- and 5HT-immunoreactive neuronal elements in the crop and the gizzard

TH-ir neuronal elements could be observed exclusively in the submucosal layer of the crop and the gizzard. TH-ir neuronal cell bodies were found only in the crop whereas only fibers could be observed in the gizzard. Cell bodies were seen along the nerve trunks located in the longitudinal muscle trabeculae (Figs 1, 2). The cell bodies and fibers showed frequently different intensity of immunoreaction (Fig. 2). Their processes leave the thick nerve trunk and run towards the longitudinal and circular muscle fibers (Fig. 1). They show a varicose appearance over the muscle fibers (Fig. 1).

5HT-ir cell bodies could not be observed, but 5HT-ir fibers occurred in both the mucosal and submucosal layer of the crop and the gizzard (Fig. 3). The density of 5HT-ir fibres was the highest in the submucosal layer (Fig. 3). From the CNS, thick nerve fibers reached the outer submucosa (Fig. 4) and entered the main nerve trunks (Fig. 3). They gave off fine varicose side branches to the longitudinal and circular muscles (Fig. 3).

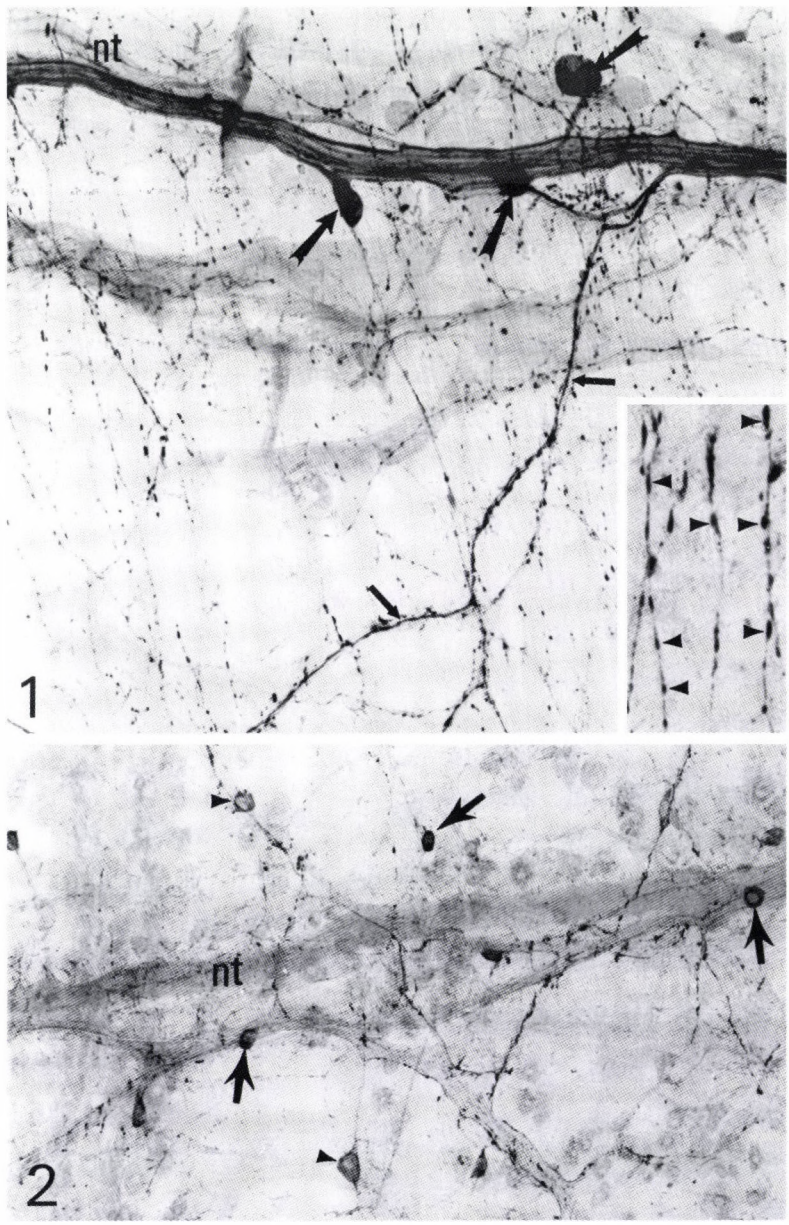

Fig. 1. TH-ir cell bodies (large arrows) and fibers can be seen along the main nerve trunk (nt) among longitudinal muscle trabeculi of the crop. TH-ir fibers leave the nerve trunk (small arrows) and they arborize with varicose sidebranches over muscle fibers. ×140. *Insert:* Varicose TH-ir fibers (arrowheads)over muscle fibers. ×350. *Fig. 2.* The intensity of TH-immunoreactivity in neurons and fibers significantly changes in the different samples. Cell bodies exhibit immunoreactivity with high (arrows) and low (arrowheads) intensity along the main nerve trunk (nt). ×100

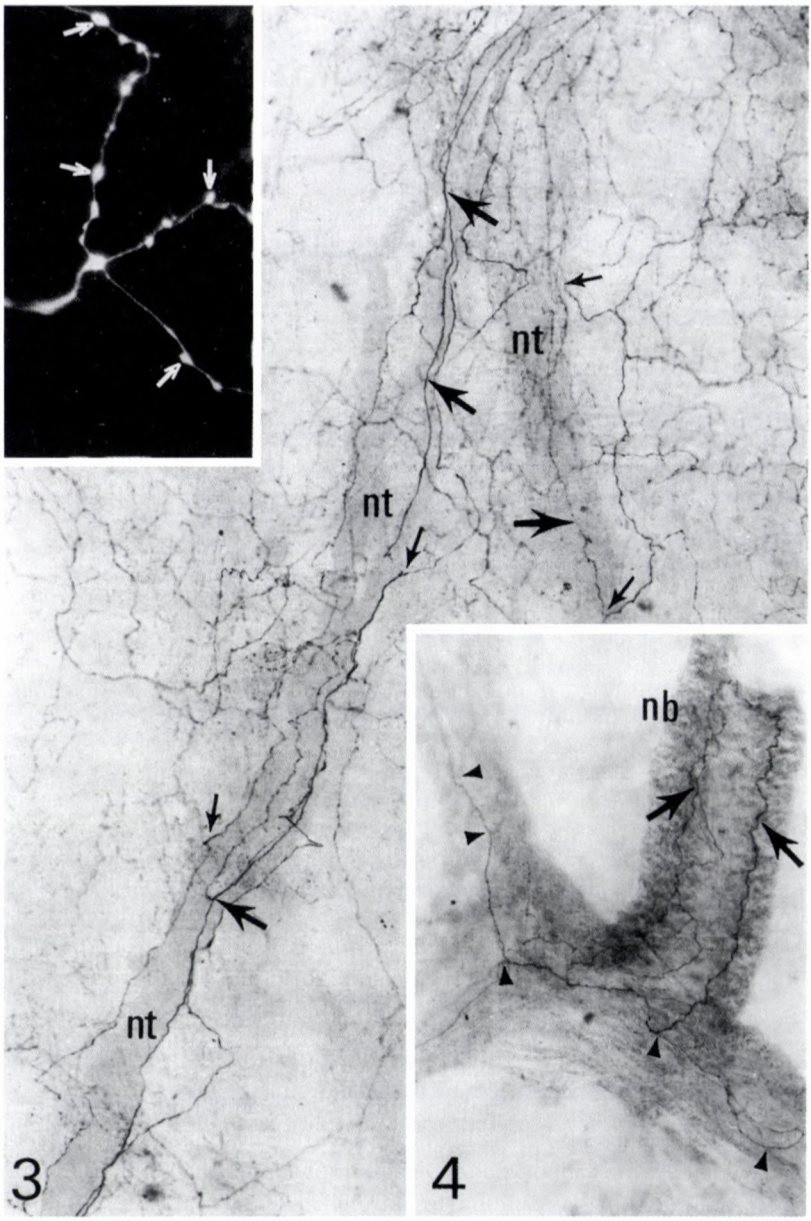

Fig. 3. 5HT-ir fibers (large arrows) are running in the main nerve trunk (nt) of the submucosa. They leave the nerve trunk (thin arrows) and give off varicose fibers over muscle fibers. ×150 *Insert:* Varicose 5HT-ir fibers (arrowheads) over muscle fibers. ×500. *Fig. 4.* Thick 5HT-ir fibers (arrows) reach the submucosa of the crop through fine branches of CNS nerve (nb) and they branch (arrowhead) on the surface of the outer submucosa. ×100

Effects of monoamines on the spontaneous contractions of the crop and the gizzard

The longitudinal muscle preparations of the crop and the gizzard showed low amplitude spontaneous contractions, whereas the circular muscle preparations were rhythmically active only in the crop placed in physiological solution. DA and 5HT modified differently the activity pattern of the two muscle preparations.

Dopamine (10^{-5} M) increased significantly the tone but only mildly the contractility of the longitudinal muscles in the crop and the gizzard, but was ineffective on circular muscles. The effects of DA on the longitudinal muscle contraction of the crop were not concentration dependent between 10^{-5} M and 3×10^{-5} M concentrations (Fig. 5B).

Serotonin influenced the activity of both the longitudinal and circular muscle preparations by increasing the tone and contractility of the longitudinal muscle of the crop. However, it was ineffective in the gizzard. 5HT significantly decreased the contractility of circular muscles in the crop but increased it in the gizzard. The effects of 5HT on the contractility of circular muscle in the gizzard was concentration dependent at 10^{-5} M and 3×10^{-5} M concentrations (Fig. 5A).

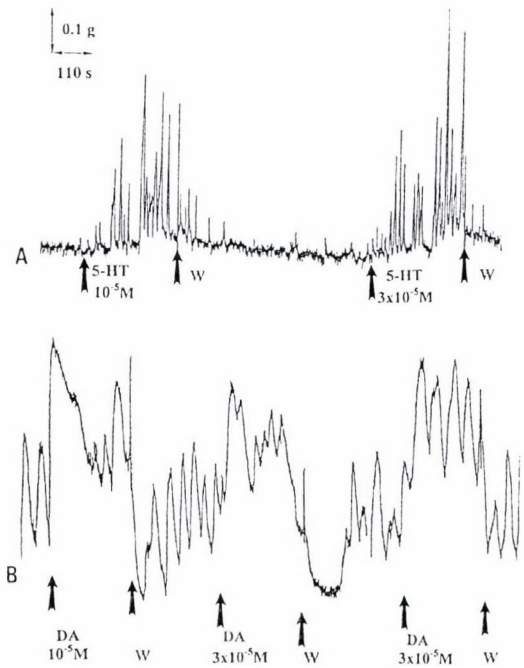

Fig. 5. Serotonin (A) increases the amplitude of contraction of the longitudinal muscles in the gizzard. The increasing effect is concentration dependent at 10^{-5} and 3×10^{-5} M concentrations. Dopamine (B) increases the tone of longitudinal muscles of the crop which effect is not concentration dependent at 10^{-5} and 3×10^{-5} M concentrations. W – washing

HPLC assay of 5HT and DA content in starved and satiated animals

After termination of feeding of satiated animals both DA and 5HT concentrations significantly decreased in the CNS as compared to starved animals (Table 1). However, in the crop and the salivary gland only DA showed significant decrease, but 5HT concentrations were nearly the same as in the control animals (Table 1). The DA/5HT ratios in satiated animals showed a significant decrease especially in the crop and the salivary gland, showing the increased dominance of 5HT in satiated animals (Table 1).

Table 1
DA and 5HT concentrations (pmol/mg wet tissue) in the different tissues in starved and satiated animals

		CNS	Crop	Salivary gland
Starved	DA	56.72 ± 3.23	1.7 ± 0.77	9.57 ± 3.9
	5HT	69 ± 4.51	3.96 ± 2.8	19.18 ± 3.1
	DA/5HT	0.82	0.42	0.49
Satiated	DA	38.16 ± 6.05	0.27 ± 0.27	0.44 ± 0.4
	5HT	53 ± 3.3	2.01 ± 1.2	18.5 ± 4.8
	DA/5HT	0.72	0.13	0.02

Effects of monoamine injections on the induction of feeding

Injection of 25 µl of 10^{-2} or 10^{-3} M DA or 5HT into the body cavity of starved animals changed the behavior of animals, compared to the control non-injected starved animals. Control animals placed on paper tissue soaked up with 3% sugar solution started to feed the paper tissue in 5–10 min. The injection of 10^{-3} M (Fig. 6A) or 10^{-2} M (Fig. 6B) 5HT increased the general activity of the animal by inducing active tentacle and head movements. The animals remained active for about 15 min but they did not feed.

After the injection of 10^{-3} M DA the animals stopped moving in 1–2 min, their tentacles were bent to the paper tissue and started to feed (Fig. 7A). Injection of 25 µl 10^{-2} M DA paralyzed the animals with withdrawn tentacles and oral area (Fig. 7B).

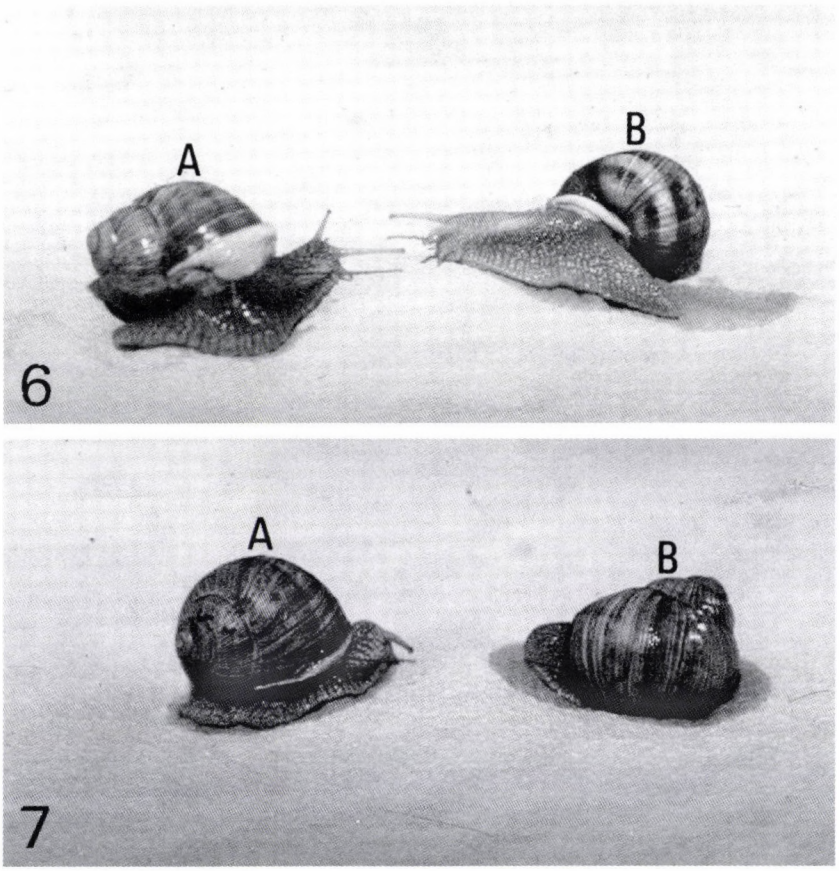

Fig. 6. The injection of 25 µl of 10^{-3} M 5HT (A) or 10^{-2} M 5HT (B) increases the general activity of the animals but does not initiate feeding. *Fig. 7.* After the injection of 25 µl of 10^{-3} M DA, the tentacles and the mouth were bent to the surface and the animals started to feed (A). The injection of 25 µl of 10^{-2} M DA paralyzed the animals and prevented feeding (B)

DISCUSSION

In the present study, it was demonstrated that both the crop and the gizzard is richly innervated by 5HT-ir neuronal elements, whereas they receive a relative poor innervation by TH-ir neuronal elements. TH-ir cell bodies can be detected only in the crop but TH-ir fibers could be seen in both the crop and the gizzard, suggesting that TH-ir fibers originate from TH-ir cell bodies of the crop. 5HT-ir cell bodies could not be found either in the crop or the gizzard. Therefore, the TH-ir DA-containing neurons can be considered as intrinsic elements, whereas 5HT-ir fiber system can be considered as the extrinsic elements of the gastrointestinal nervous system. The 5HT-ir ele-

ments originate from the central ganglia. This suggestion is supported by the present observation that thick 5HT-ir fibers can be seen in the innervating nerves which give off a numerous thin branches in the submucosal layers.

The innervation patterns of the 5HT-ir and TH-ir neuronal elements are different. In the submucosa, both the circular and longitudinal muscle layers are richly innervated by 5HT-ir fibers, whereas TH-ir fibers innervate dominantly the longitudinal muscles, suggesting that 5HT plays a very important role in the regulation of both longitudinal and circular muscle contraction whereas DA play a role in the regulation of the longitudinal muscles [see also 1]. The present observations obtained by bioassay experiments are in good accordance with the morphological observations. 5HT application was effective on both the longitudinal and circular muscles, whereas DA application was effective only on the longitudinal muscles. The spontaneous contractions of circular muscles in the crop could be blocked by very low concentrations of 5HT [1], whereas 5HT increased the contractility of circular muscle in the gizzard. This excitatory effect was concentration dependent between 10^{-5} M and 3×10^{-5} M concentrations. The application of 5HT receptor blocker Deseril prevents the 5HT effects in the crop, suggesting that 5HT exerts its effects on 5HT receptors at postsynaptic sites [1].

In the crop, 5HT and DA may affect the longitudinal muscle contraction in synergism with increasing the tonus and contractility. 5HT relax the wall of the filled and distended crop during ingestion, by blocking the contraction of circular muscle but increasing the contraction of the circular muscle in the gizzard. These opposite effects of 5HT on the two segments of the gastrointestinal tract may contribute to the regulation of the periodical transport of nutrient from the crop to the gizzard.

According to the HPLC assay of monoamine, both 5HT and DA concentrations significantly decreased in the CNS but only DA concentration in the different parts of the gastrointestinal tract (crop, salivary gland) following the termination of feeding in animals of satiated state. Since 5HT-ergic elements (5HT-ir) of the gastrointestinal nervous system originate from the CNS, therefore the significant decrease of 5HT content in the CNS but not in the intestine, suggests that 5HT is continuously transported from the CNS to the intestine during ingestion and digestion. 5HT was shown to be significantly decreased during ingestion also in leech ganglia [4]. These findings suggest that one of the functions of the liberated 5HT is the regulation of the contractility of the gastrointestinal tract during ingestion and digestion. Contrary to the changes of 5HT concentrations, DA concentration decreased in both the CNS and the different parts of the gastrointestinal tract. Considering that DAergic (TH-ir) elements belong to the intrinsic part of the gastrointestinal nervous system, the significant decrease of DA contents in the crop and the salivary gland suggest that DA is continuously liberated during both ingestion and digestion, or it was liberated only during ingestion. In this context, the function of the liberated DA in the intestine is probable to increase the size of stretch receptor evoked contractions of the longitudinal muscle during ingestion which helps the transport of nutrients. In *Aplysia* gill muscle the amplitude of the evoked contraction reflex was significantly increased in the presence of DA [10].

According to the monoamine injections 5HT increased only the general activity of starved animals but only the DA injection (25 µl 10^{-3}M DA) was capable of initiating feeding. These observations suggests that DA is necessary to the initiation of feeding. However, 25 µl of 10^{-2} M DA injection prevented feeding by paralyzing the animals which shows that the increase of DA concentration is not enough to the initiation of feeding but it has to be close to a critical DA concentration.

ACKNOWLEDGEMENT

This work was supported by OTKA grants No. 16015 and 29559.

REFERENCES

1. Hernádi, L., Erdélyi, L., Hiripi, L., Elekes, K. (1998) The organization of serotonin, dopamine and FMRFamide containing neuronal elements and their possible role in the regulation of spontaneous contraction of the gastrointestinal tract in the snail *Helix pomatia*. *J. Neurocytology 27*, 761–775.
2. Kuslansky, B., Weiss, K. R., Kupfermann, I. (1987) Mechanism underlying satiation of feeding behavior of the mollusc *Aplysia*. *Behav. Neural. Biol. 48*, 278–303.
3. Kyriakides, M. A., McCrohan, C. R. (1989) Effect of putative neuromodulators on rhytmic buccal motor output in *Lymnaea stagnalis*. *J. Neurobiol. 20*, 635–650.
4. Lent, C. M. (1985) Ingestive behavior decreases the serotonin in the leech CNS. *Soc. Neurosci. Abstr. 11*: 481.
5. Lent, C. M., Dickinson, M. H. (1984) Serotonin integrates the feeding behaviour of the medicinal leech. *J. Comp. Physiol. 154*, 457–471.
6. Lent, C. M., Dickinson, M. H. (1987) On the termination of ingestive behavior by the medicinal leech. *J. exp. Biol. 131*, 1–15.
7. Pentreath, V. W., Berry, M. S., Osborne, N. N. (1982) The serotonergic cerebral cells in gastropods. In: Osborne, N. N. (ed.), *Biology of Serotonergic Transmission.* Wiley, New York, pp. 457–513.
8. Peschel, M., Straub, V., Teyke, T. (1996) Consequences of food-attraction conditioning in *Helix*: a behavioral and electrophysiological study. *J. Comp. Physiol. A. 178*, 317–327.
9. Rosen, S. C., Weiss, K. R., Goldstein, R. S., Kupfermann, I. (1989) The role of a modulatory neuron in feeding and satiation in *Aplysia:* effects of lesioning of the serotonergic metacerebral cells. *J. Neurosci. 9,* 1562–1578.
10. Ruben, P., Lukowiak, K. (1983) Modulation of the *Aplysia* gill withdrawal reflex by dopamine. *J. Neurobiol. 14*, 271–284.
11. Sternberger, L. A. (1979) *Immunocytochemistry.* John Wiley, Chichester.
12. Susswein, A. J., Kupfermann, I. (1975) Bulk as a stimulus for satiation in *Aplysia*. *Behav. Biol. 13*, 203–209.
13. Susswein, A. J., Kupfermann, I., Weiss, K. R. (1976) The stimulus control of biting in *Aplysia*. *J. Comp. Physiol. 108,* 75–96.
14. Susswein, A. J., Weiss, K. R., Kupfermann, I. (1984) Internal stimuli enhance feeding behavior in the mollusc *Aplysia*. *Behav. Neural. Biol. 41*, 90–95.
15. Teyke, T., Rosen, S. C., Weiss, K. R., Kupfermann, I. (1993) Dopaminergic neuron B20 generates rhythmic neuronal activity in the feeding motor circuitry of *Aplysia*. *Brain Res. 630*, 226–237.
16. Trimble, D. L., Barker, D. L. (1984) Activation by dopamine of patterned motor output from the buccal ganglia of *Helisoma trivolis*. *J. Neurobiol. 15*, 37–48.
17. Weiss, K. R., Koch, U. T., Koester, J., Mandelbaum, D. E., Kupfermann, I. (1980) Neural and molecular mehanisms of food induced arousal in *Aplysia californica*. In: Salánki, J. (ed.) *Advances in Physiological Sciences, Neurobiology of Invertebrates.* Pergamon, Oxford. Vol. 23, pp. 305–344.

18. Wieland, S. J., Gelperin, A. (1983) Dopamine elicits feeding motor program in *Limax maximus*. *J. Neurosci. 3*, 1735–1745.
19. Yeoman, M. S., Pieneman, A. W., Ferguson, G. P., Maat, A. T., Benjamin, P. R. (1994a) Modulatory role for serotonergic cerebral cells in the feeding system of the snail, *Lymnaea*. I. Fine wire recording in the intact animal and pharmacology. *J. Neurophysiol. 72*, 1357–1371.
20. Yeoman, M. S., Kemenes, G., Elliott, C. J. H., Benjamin, P. R. (1994b) Modulatory role for serotonergic cerebral cells in the feeding system of the snail, *Lymnaea*. II. Photoinactivation. *J. Neurophysiol. 72*, 1372–1382.

Acta Biologica Hungarica 51 (2–4), pp. 189–195 (2000)

LOCOMOTOR RHYTHMS IN THE POND SNAIL *LYMNAEA STAGNALIS:* SITE OF ORIGIN AND NEUROTRANSMITTER REQUIREMENTS[+]

V. V. TSYGANOV and D. A. SAKHAROV*

Laboratory of Comparative Physiology, Institute of Developmental Biology, Russian Academy of Sciences, ul. Vavilova 26, 117808 Moscow, Russia

(Received: August 31, 1999; accepted: November 30, 1999)

1. We have found that, in preparations of isolated CNS of the pond snail *Lymnaea stagnalis,* both serotonin (5HT) and dopamine (DA), as well as their respective precursors, 5HTP and DOPA, are effective in producing fictive intense (muscular) locomotion.
2. Phase-coupled to each of the above pedal rhythms are numerous identifiable pedal neurons including the respiratory interneuron RPeD1, thus suggesting interaction between networks responsible for locomotion and air breathing.
3. The novel DA/DOPA-dependent motor rhythm resembles the 5HT/5HTP-dependent one in terms of activity of identifiable pedal neurons, being however considerably slower than the latter.
4. The results of transection experiments suggest that each of the rhythms is generated by a paired CPG lying entirely within the pedal ganglia.

Keywords: Aminergic regulation – central pattern generator – motor rhythms – gastropods – *Lymnaea stagnalis.*

INTRODUCTION

Forward progression of freshwater pulmonate molluscs in generally caused by the activity of pedal cilia. However, in hard situations, the cilia are unable to provide sufficient propulsive force, and snails readily change ciliary locomotion to one of muscular patterns. In the pond snail *Lymnaea stagnalis,* these were described as cyclical, coordinated movements of the foot, body wall and shell [10]. The shell rhythm was found driven by a central pattern generator (CPG) of unknown location [1], but further details of the mechanisms underlying intense locomotion remained lacking.

Our group and others have demonstrated that the metabolic precursor of serotonin (5HT), L-5-hydroxytryptophan (5HTP), induces activity of the CPG for rhythmic shell movements [4] and, the reverse, forced shell movements result in increased 5HT levels [2]. These findings suggested that, in *Lymnaea,* intense locomotion

[+] Presented at the 9th ISIN Symposium on "Neurobiology of Invertebrates", July 1–5, 1999, Tihany, Hungary.

*Corresponding author, E-mail: compar@cityline.ru

0236-5383/2000/$ 5.00

requires higher levels of 5HT, as it does in other molluscs examined so far [3, 7]. Recently, it has been shown that, in fact, there are two varieties of monoamine induced intense locomotion distinguishable in terms of motor behavior, one of which requires 5HT or 5 HTP, whereas the other dopamine (DA) or its precursor, L-DOPA (V. Tsyganov, in preparation). Here we extend these behavioral findings to neurophysiology.

MATERIALS AND METHODS

Experiments on preparations of the isolated CNS of adult specimens of *Lymnaea stagnalis* were performed at the Kropotovo biological station, Moscow Region. The technique involved conventional intracellular and extracellular recordings from identifiable neurons, and nerves, respectively. Animals, equipment, electrodes, Ringer solution, drug treatment were described by Nezlin and Voronezhskaya [6]. Chemicals were from Sigma.

RESULTS

Bath application of either 5HT or DA their respective precursors to isolated CNS preparations initiated fictive intense locomotion manifested as patterned bursting activity in pedal and columellar nerves. The following concentrations of examined substances were found appropriate to induce and maintain the locomotor rhythm: 5HT 0.05 mM, 5HTP 0.4 mM, DA 0.05 mM, and DOPA 0.4 mM.

Bursts in the columellar nerve were used to great advantages in the study of neuronal correlates of intense locomotion. The bursts occur at the shell movement phase of the locomotor cycle thus permitting convenient reference point to monitor the locomotor rhythm.

Following drug treatment, numerous pedal neurons started to exhibit cyclical bursting activity. The bursts (like those in cell RPeD1, Fig. 1) evidently displayed fictive locomotion as they were coupled to a certain phase of the bursting activity in the columellar nerve. For any of the four substances, the onset latency of fictive locomotion was 1–3 min longer than the period of time needed for full development of polarizing effects on neural membrane, thus indicating that an additional, time-consuming mechanism is involved in motor program producing and release.

The following identifiable pedal neurons exhibited the monoamine induced locomotor rhythm (cell nomenclature according to [8]): PeD1, PeD2, PeD3, PeD4, PeD8, PeD9 and PeD10. In the latter, the bursts were exceptionally strong.

None of the above listed pedal neurons caused a change in frequency of the locomotor rhythm following application of either hyperpolarizing or depolarizing current, thus indicating that they are not members of the rhythm generating network, and that their patterned activity was synaptically driven. Powerful excitatory inputs underlying the rhythm were indeed well seen in hyperpolarized neurons.

Within a pair of bilateral neurons, the left and right cells behaved similarly being active at the same phase of the locomotor cycle. The only deviation from this rule was demonstrated by the largest paired pedal neurons, RPeD1 and LPeD1, which exhibited alternating firing coupled to different phases of the cycle. Each burst in LPeD1 was synchronous with that in the columellar nerve, whereas bursts in RPeD1 corresponded to the interburst period in the nerve.

The most remarkable difference between the rhythm, on the one hand, and that induced by drugs, on the other, concerns frequency. With 5HT or 5HTP the cycle duration was 12.8 ± 3.78 s (n = 37), with DA or DOPA it was 1.5–2 times longer. Otherwise, the neural correlates of the 5HT/5HTP- and DA/DOPA-induced rhythms observed so far looked similar. Minor differences in activity phasing (e.g. in that of RPeD1) could only be detected.

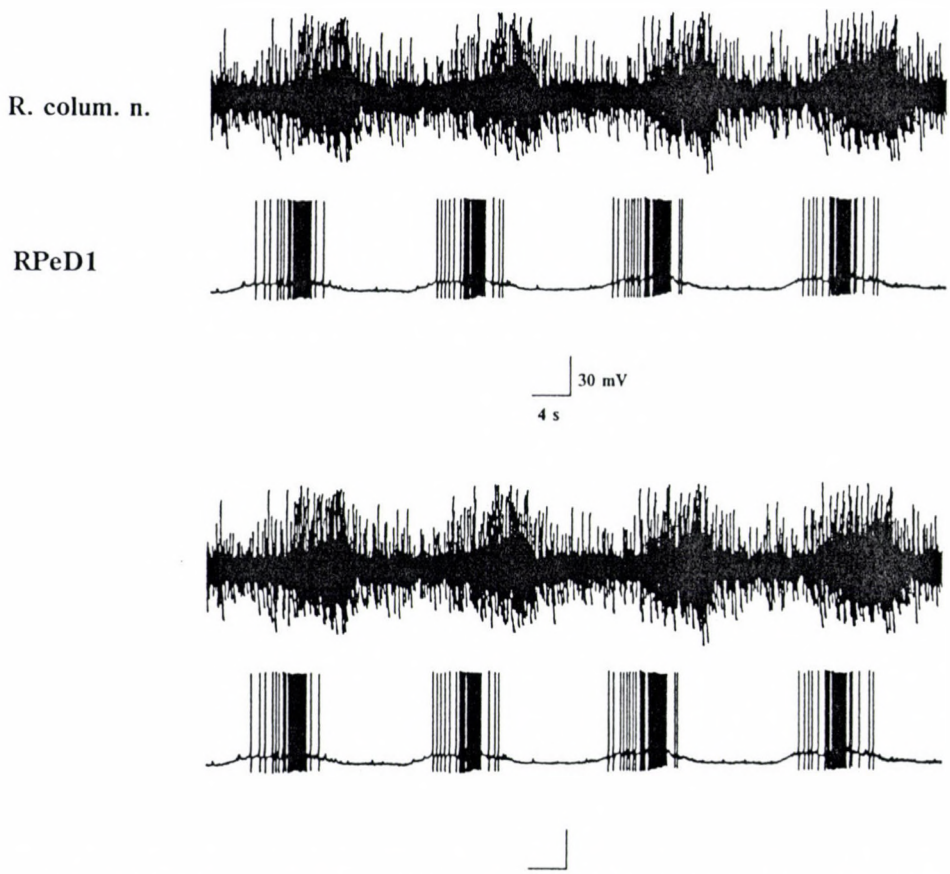

Fig. 1. Dopamine-induced alternating bursts in the right columellar nerve (upper trace) and cell RPeD1 (lower trace)

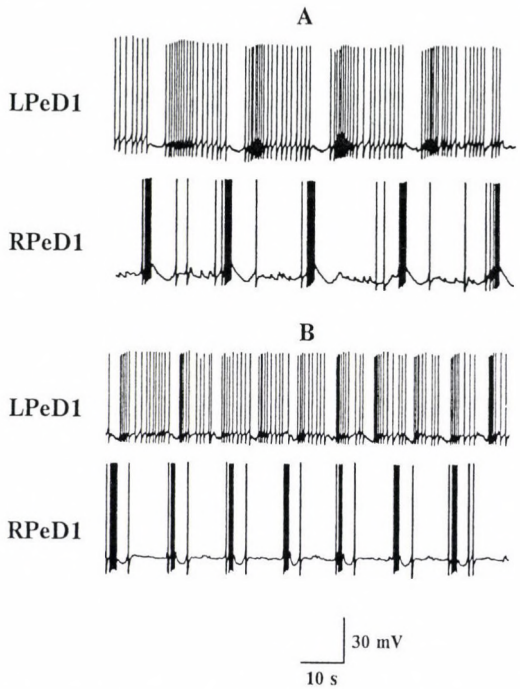

Fig. 2. Retaining of the serotonin-induced rhythm by a left (LPeD1, upper trace) and a right (RPeD1, lower trace) pedal neurons following consecutive transection of the pedal connectives (A) and commissures (B). (A) The isolated paired pedal ganglia. (B) The same preparation, the ganglia being separated from each other. Note that the characteristic pattern of rhythmic activity is mostly retained by both LPeD1 and RPeD1. Although rhythm synchrony is lost

To locate the CPG for intense locomotion, pedal connectives and commissures were consecutively transected in drug-treated preparations with well-developed locomotor rhythm. In this series, cells LPeD1 and RPeD1 were used to monitor the rhythm. As it can be seen in Fig. 2, alternating firing of the two cells was not impaired after complete isolation of the paired pedal ganglia, thus indicating that the rhythm is generated and coordinated within the pedal part of the CNS. Separation of the left pedal ganglion from the right one resulted in loss of synchrony. The characteristic pattern of the rhythmic activity was, however, retained by each of two PeD1 cells.

DISCUSSION

It is generally believed that, in molluscs, cyclical locomotor movements are governed by the pedal ganglia. We have now extended this opinion to intense locomotion of a popular model animal, the pond snail *Lymnaea stagnalis*. The reported here

effects of 5HT and 5HTP are consistent with previous observations of 5HTP requirement for generation of cyclical shell movements in *Lymnaea* [2, 4]. Similarly, in the pteropod *Clione,* locomotion could be intensified by both 5HT and 5HTP [3], whereas 5HTP only was able to induce sustained intense locomotion, swimming, in another marine mollusc, *Aplysia fasciata* [7]. Three original findings are briefly discussed below.

The DA/DOPA-induced rhythm

Our experiments demonstrate for the first time a case of DAergic induction of a central program for locomotion in gastropods. In previous studies, inhibitory action of DA and DOPA on locomotion was observed thus providing a basis for speculation on functional antagonism between 5HTergic and DAergic systems in the locomotion control (e.g., [3]). This is not ruled out by the present results. It may be that, in *Lymnaea* too, the 5HT-induced locomotor rhythm is inhibited by DA. A simple hypothesis to account for the occurrence of DA-dependent locomotion is to postulate that this locomotor variety is a part of a DA-dependent behavior. In the pond snail such is air breathing [5].

Observations by one of us (V. Tsyganov, in preparation) on intact specimens of the pond snail have shown that the 5HT/5HTP-motor rhythm and the novel DA/DOPA-dependent one represent two different modes of coordinated contractions of the locomotory muscles. Actually, only 5HTP produced real, long-lasting locomotion in these behavioral experiments. Injection of either 5-HT, or DA, or DOPA induced cyclical, locomotor-like movements of the foot, body wall and shell, however, no propulsion was observed supposedly due to loss of adhesion of the foot to substratum, and some other impairments.

Coordination of giant dopamine and serotonin neurons

There was no evidence so far, that the largest pedal neurons, cells LPeD1 and RPeD1, are involved in any common activity. In the present experiments well-coordinated rhytmic excitation of the two cells was observed. Unlike other bilateral pairs, these neurons demonstrated alternating (reciprocal, anti-phase) firing. In this connection, it is noteworthy that LPeD1 and RPeD1 express different neurotransmitter phenotypes, the left cell (L) being 5HTergic whereas the right one (R) DAergic. Otherwise, they seem to be bilateral, their perikarya occupying nearly similar positions, and axons branching symmetrically within the visceral loop ganglia to extend to the mantle wall.

In our unpublished experiments, episodes of reciprocal firing were also occasionally observed in spontaneous activity of the two neurons and, furthermore, L and R cells responded in an alternate manner to sensory signals evoked by crossing the water-air border by the mantle pneumostome area of the body. It appears that, under

certain conditions, patterned activities of the two cells are centrally coordinated in a fixed, opposite manner, thus implying that DA and 5HT may function here as phase transmitters.

Control of CPG for respiration by CPG for locomotion

Of particular interest is the phase coupling of the giant pedal dopamine cell RPeD1 to intense locomotion. In our experiments, each of the drug-induced locomotor rhythms was invariably accompanied with powerful bursts in RPeD1. This neuron of *L. stagnalis,* as well as its homologs in related freshwater pulmonates, has been described as a member of a CPG controlling aeral respiratory behavior. Three identifiable, pattern generating interneurons were found both necessary and sufficient to produce rhythmicity, two controlling inspiration and respiration, respectively, and RPeD1 initiating the respiratory cycle (when depolarized to produce action potentials) [8]. In these experiments, RPeD1 could be substituted with phasic (but not tonic) application of DA, suggesting that rhythmic excitation of RPeD1 is essential. The source of rhythmic excitatory input that drives RPeD1 remained, however, obscure. Our experiments have now shown that, at least in certain instances, the RPeD1 rhythmicity is driven by the pedal CPG for intense locomotion. Accordingly, we observed rhythmic closure/opening movements of the pneumostome coupled to the monoamine-induced locomotor rhythm in both intact specimens and semi-intact preparations of *L. stagnalis.*

To conclude, our results suggest that, in the pond snail, a sharp increase of 5HT or DA levels in the pedal portion of the CNS is required to develop neural events underlying intense locomotion and associated pneumostome rhythmicity. Theoretically, such an increase might result from increased release only. Up-regularion of 5HT synthesis was, however, demonstrated in the CNS of *Lymnaea* specimens forced to crawl with additional load [2]. Little is known on how is transmitter synthesis regulated by sensory inputs. Further studies in *Lymnaea* and related gastropod molluscs may help to elucidate the problem of a general interest.

ACKNOWLEDGEMENT

The work was supported by grant #99-04-48411 from RFBI.

REFERENCES

1. Haydon, P. G., Winlow, W. (1986) Shell movements associated with locomotion of *Lymnaea* are driven by a central pattern generator. *Comp. Biochem. Physiol. 83A,* 23–25.
2. Kabotyanski, E. A., Park, J.-H., Bauce, L., Sakharov, D. A., Winlow, W., Lukowiak, K. (1994) Up-regulation of serotonin production is required for generation of a central program for motor behavior in *Lymnaea.* In: Gerearts, W. P. M., Kits, K. S., ter Maat, A. (eds) *Molluscan Neurobiology.* University Press, Vrije Universiteit, Amsterdam, p. 31.

3. Kabotyanski, E. A., Sakharov, D. A. (1988) Monoamine-dependent behavioural states in the pteropod mollusc *Clione limacina.* In: Salánki, J., S.-Rózsa, K. (eds) *Symp. Biol. Hung. 36, Neurobiology of Invertebrates,* Akadémiai Kiadó, Budapest, pp. 463–476.
4. Kabotyanski, E. A., Winlow, W., Sakharov, D. A., Bauce, L., Lukowiak, K. (1992) 5-hydroxytryptophan elicits sustained CPG activity for rhythmic shell movements in *Lymnaea stagnalis. Soc. Neurosci. Abstr. 18,* p. 531.
5. Moroz, L. L. (1991) Monoaminergic control of the respiratory behaviour in freshwater pulmonate snail, *Lymnaea stagnalis* (L.). In: Winlow, W., Vinogradova, O. V., Sakharov, D. A. (eds) *Signal Molecules and Behaviour.* Manchester University Press, Manchester, pp. 101–123.
6. Nezlin, L., Voronezhskaya, E. (1997) GABA-immonoreactive neurones and interactions of GABA with serotonin and FMRFamide in a peripheral sensory ganglion of the pond snail *Lymnaea stagnalis. Brain Res. 772,* 217–225.
7. Sakharov, D. A., Milosevic, I., Salimova, N. (1989) Drug-induced locomotor stereotypies in *Aplysia. Comp. Biochem. Physiol. 93C,* 161–166.
8. Slade, S. T., Mills, J., Winlow, W. (1981) The neuronal organisation of the paired pedal ganglia of *Lymnaea stagnalis. Comp. Biochem. Physiol. 69A,* 789–803.
9. Syed, N. I., Bulloch, A. G. M., Lukowiak, K. (1990) *In vitro* reconstruction of the respiratory central pattern generator of the mollusk *Lymnaea. Science 250,* 282–285.
10. Winlow, W., Haydon, P. G. (1986) A behavioral and neuronal analysis of the locomotory system of *Lymnaea stagnalis. Comp. Biochem. Physiol. 83A,* 13–21.

Acta Biologica Hungarica 51 (2–4), pp. 197–203 (2000)

MORPHOLOGY AND PHYSIOLOGY OF PLEURAL-TO-BUCCAL NEURONS COORDINATING DEFENSIVE RETRACTION WITH FEEDING ARREST IN THE POND SNAIL *LYMNAEA STAGNALIS*[+]

MAGDA ALANIA* and D. A. SAKHAROV

Laboratory of Comparative Physiology, RAS Institute of Developmental Biology,
26 Vavilov str., Moscow, 117808 Russia

(Received: August 31, 1999; accepted: November 30, 1999)

1. We have studied morphology, physiology and chemistry of a bilateral pair of pleural-to-buccal projecting neurons (PlB cells) of the pond snail *Lymnaea stagnalis*. Intracellular dye fills revealed axon arborization within neuropiles of ipsilateral pedal and cerebral ganglia, as well as in both buccal ganglia. Terminal axons of the left and right PlBs showed close proximity within the buccal commissure.
2. The left and right PlB neurons have been found electrotonically coupled and, sometimes, generating synchronous spikes.
3. The results show that two PlB cells operate as a single unit, and that paired buccal networks responsible for feeding rhythm are treated by the PlBs as a single target.

Keywords: Coordinating neurons – electrical coupling – FMRFamide – gastropods – *Lymnaea stagnalis*.

INTRODUCTION

Coordination between different motor centers is important for the orderly production of behavioral output. However, little work has been done on individual coordinating neurons.

Of particular interest in this connection was the identification of a pair of pleural-to-buccal projecting neurons inhibiting activity of feeding neurons in a freshwater pulmonate mollusc *Helisoma*. The neurons are placed so that they link the feeding network to distant parts of the CNS. It has been therefore suggested that they might coordinate a defensive withdrawal with feeding arrest using FMRFamide as a signal molecule [9]. Although homologous neurons were later found in other pulmonates [1], the suggested function of pleural-buccal neurons (named PlB cells, PlBs) remained without firm experimental justification.

[+] Presented at the 9th ISIN Symposium on "Neurobiology of Invertebrates", July 1–5, 1999, Tihany, Hungary.

*Corresponding author, Institute of Developmental Biology, RAS, E-mail: compar@glasnet.ru

0236-5383/2000/$ 5.00

With this goal in mind, we have been investigating PlB neurons of the pond snail *Lymnaea stagnalis*. Of all model pulmonates, this one is the best characterized in terms of individual neurons and neuronal networks. It provides therefore a good opportunity to study the neuronal basis of coordination (e.g. [6, 8, 12]).

We have proved FMRFamide-like immunoreactivity of the *Lymnaea* PlBs by combining a biocytin axon filling technique with FMRFamide immunostaining in the same CNS preparation [3]. Use of additional antibodies has allowed us to suggest that exon II of the FMRFamide gene is expressed in PlB neurons of *Lymnaea* [4]. Here we present the morphological and neurophysiological evidence that terminal axons of the left and right PlB neurons operate as a single unit.

MATERIALS AND METHODS

Snails (*Lymnaea stagnalis)* were cultured in our laboratory or collected in wild at the Kropotovo biological station, Moscow region. Animals were anaesthetized by 0.1 M $MgCl_2$ and the CNS with paired buccal ganglia was dissected. To permit visually controlled implement of the PlB neurons the commissures between the pedal ganglia were cut and the CNS was pinned ventral surface uppermost.

Prior to the start of the experiments, each preparation was treated with 1 mg/ml Pronase E (Sigma), desheathed, and kept in a standard *Lymnaea* saline for several hours at 5 °C. A conventional set-up [10] was used to intracellularly record and display activity of two neurons. Glass microelectrodes used in neurophysiological experiments were filled with lucifer yellow (LY). At the final stage of each experiment, LY was electrophoretically injected into the PlB cell(s). The dye was then allowed to spread within the neuron for 14–16 h at 4 °C. Afterwards the preparation was fixed and processed for fluorescence microscopy. LY was from Sigma, the procedure was according to the protocol of Stewart [11] using a Jenaval microscope.

RESULTS

Microelectrode implement into a PlB cell was greatly facilitated by the results of our previous study which showed, using a retrograde staining technique, that in *Lymnaea* both PlB cells are symmetrically situated within the ventral portion of the pleural ganglion close to the root of the pleuro-pedal connective [1]. The PlB has soma diameter of 25–30 μm. As starting-point of each experiments, it was evidenced that discharge of a candidate PlB cell was producing hyperpolarization in the feeding motoneuron B1. After the experiment, LY was electrophoretically injected into the neuron, and appearance of a stained neurite in the ipsilateral pleuro-pedal and cerebro-buccal connectives (CBC) was taken as verification of exact implement.

Altogether, there were 5 successful bilateral implements into both left and right PlB cells, and more than 40 impalements into one of two neurons. Usually, in isolated CNS preparations, PlB cells had fairly regular firing at 1–5 Hz.

Morphology

In agreement with previous results [1], injection of LY has revealed that axon of the PlB cell enters the ipsilateral pedal ganglion via the pleuro-pedal connective, then turns to the cerebro-pedal connective, traverses the ipsilateral cerebral ganglion and enters the CBC (Fig. 1). It has now turned out that the ipsilateral buccal ganglion is not the ultimate place of PlB destination. The axon ramifies in its neuropile and enters the buccal commissure to ramify again in the contralateral buccal ganglion. The furthest branches project towards, and slightly penetrate to, the contralateral CBC.

Simultaneous injection of the dye into both left and right PlB showed close proximity of terminal axons of the left and right PlBs within the buccal commissure (not shown).

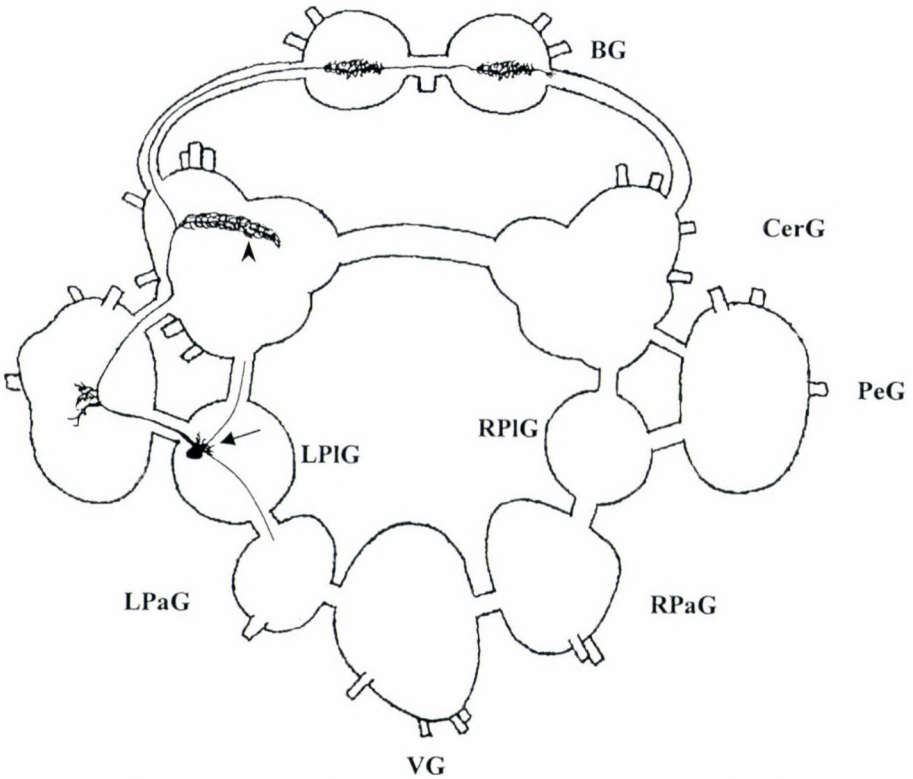

Fig. 1. Diagram of the PlB cell based on the results of the LY (lucifer yellow) intracellular injection. The PlB neuron has multiple somatic processes that arborise within the pleural ganglion. There is a short branch in the parietal ganglion, a small neuritic arbor in the pedal ganglion, a large arbor in the cerebral ganglion (arrowhead) and small arbors in both buccal ganglia. Soma of PlB neuron is indicated by arrow. BG – buccal ganglia, CerG – cerebral ganglia, PeG – pedal ganglia, RPlG – right pleural ganglion, LPlG – left pleural ganglion, RPaG – right parietal ganglion, LPaG – left parietal ganglion, VG – visceral ganglia. Pedal commissures are cut. Dorsal view

Other details of the PlB axon revealed by LY injection include abundant arborization in a well-delineated area of the neuropile of metacerebrum, and branching in the neuropile of the pedal ganglion (Fig. 1). Within the pleural ganglion, a novel PlB process running towards the cerebro-pleural connective was revealed. No dye coupling between left and right cells was observed.

Physiology

The left and right PlB cells were sometimes seen generating synchronous spikes. Injection of a de- (Fig. 2 B, D) or hyperpolarizing (Fig. 2 A, C) current into one cell resulted in corresponding polarization of the other member of the pair. It seems

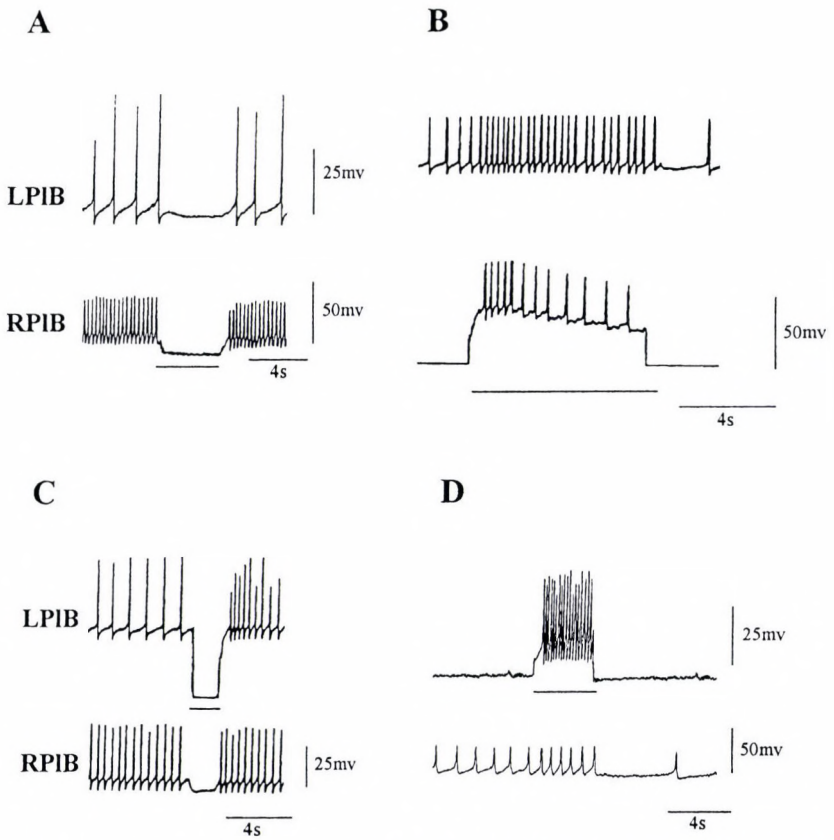

Fig. 2. Demonstration of electrotonic coupling of the left and right PlB neurons. Injection of hyperpolarizing (A, C) or depolarizing (B, D) current into either PlB neuron causes corresponding polarization of the contralateral one

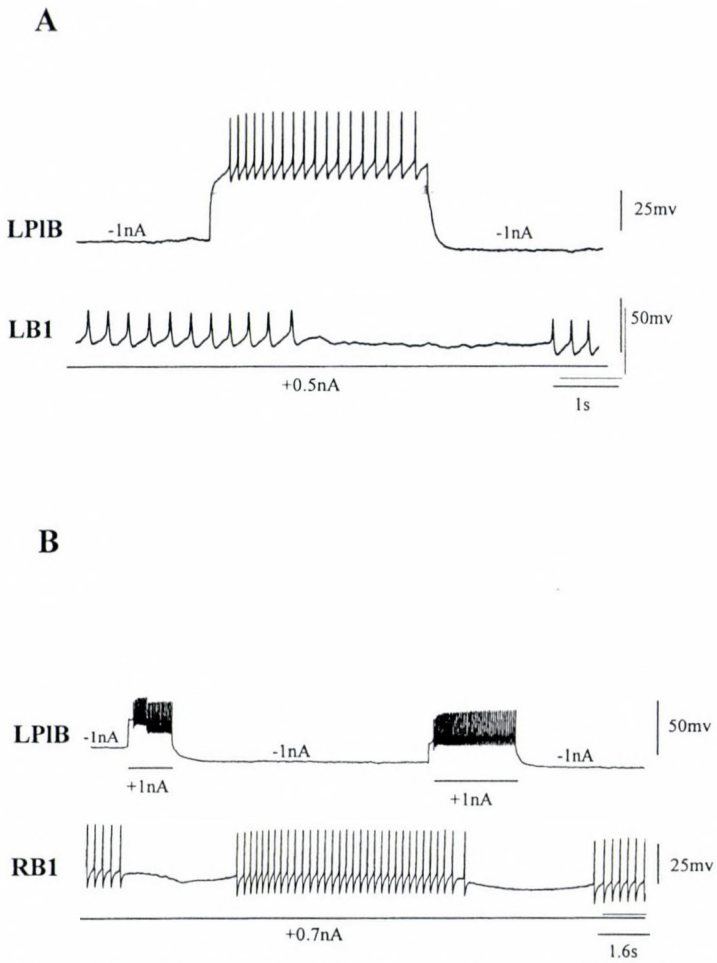

Fig. 3. Inhibitory action of the PlB neuron on salivary gland motoneuron (B1). Ipsilateral (A) and contralateral B1 (B) are activated by depolarizing current injection

obvious that each PlB neuron is electrotonically coupled to its contralateral homologue.

In addition to being electrically coupled to each other, the PlB cells were also found making chemical connections with a variety of follower neurons. In both buccal ganglia, earlier identified protraction phase feeding neuron B1was hyperpolarized by PlB stimulation (Fig. 3). Similarly, the giant cerebral serotonergic cell C1 demonstrated inhibitory response to discharge in a PlB (Fig. 4).

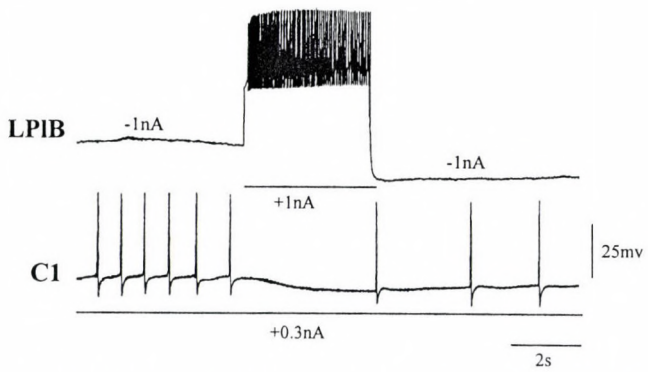

Fig. 4. Inhibitory action of the PlB neuron on serotonergic higher-order modulatory interneuron (C1). Depolarizing current injection to PlB suppresses activity of ipsilateral C1. C1 is activated by depolarizing current injection

DISCUSSION

Abrupt stopping of rhythmical feeding movements is usually observed in herbivorous pulmonates when specimens are disturbed. In experiments on *L. stagnalis* to be reported in full elsewhere, we have found that PlB cells demonstrate excitatory responses to tactile and photic stimuli that evoke defensive retraction. In turn, a discharge of PlB produces suppression of the central pattern generator for feeding. There seems little doubt that it is the function of PlB neurons to mediate interaction and coordination between networks controlling feeding and withdrawal.

The paired PlB neurons and their coordinating function seem to have been well conserved in gastropod evolution. Symmetrical FMRFamide-immunoreactive pleural-buccal projecting neurons were also found in a marine carnivorous pteropod *Clione limacina* [2], the only opisthobranch mollusc investigated so far. Like PlBs of *Lymnaea,* they are electrotonically coupled to each other, contact in the buccal ganglia, and inhibit buccal feeding neurons.

The results of the present work show that, in *L. stagnalis*, this simple, paired coordinating system is provided with two independent mechanisms ensuring effective suppression of the entire feeding machinery. First, each of the PlB cells has been found sending its axon terminals to neuropiles of both left and right buccal ganglia. Electrotonic coupling between left and right PlBs is the second mechanism. The latter finding suggests that the neurotransmitter release occurs simultaneously from secretory terminals of the two PlBs, no matter which one is activated by a sensory signal. Thus, two PlB cells operate as a single unit, and two buccal ganglia are treated by the PlBs as a single target. Interestingly, powerful cerebral projections to the buccal ganglia, represented by a pair of giant serotonin neurons, were described as organized in a similar way in *L. stagnalis* [7] (but not in some other pulmonates, e.g. in *Helisoma* [5]).

We have found that the buccal commissure is the only site of direct contact between left and right PlBs. The advantage of such location of electrical contacts for control of transmitter release is obvious. *A. priori*, however, it cannot be ruled out that the left and right PlB cells are electrotonically coupled via intermediate neuron(s), like in case of another coordinating network of *Lymnaea* [12].

ACKNOWLEDGEMENT

The work was supported by grants 96-04-49181 and 99-04-48411 from RFBI.

REFERENCES

1. Alania, M. A. (1995) Pleuro-buccal projections in diverse pulmonate molluscs. *Acta Biol. Hung. 46,* 267–270.
2. Alania, M., Panchin, Y. V., Sakharov, D. A. (1999) Pleural-buccal interneurons in the pteropod mollusc *Clione limacina. J. Comp. Physiol.* (in press).
3. Alania, M., Sakharov, D. A. (1996) FMRF-amidergic nature of pleuro-buccal projecting neurons common to diverse pulmonate molluscs. *Soc. Neurosci. Abstr. 22* (Part 2), 1405.
4. Alania, M. A., Sakharov, D. A. (1998) Cellular basis of motor coordination is conserved in gastropods differing in feeding strategy. *J. Gen. Biol. 59,* 400–408 (in Russian).
5. Granzow, B., Kater, S. B. (1977) Identified higher-order neurons controlling the feeding motor program of *Helisoma. Neuroscience 2,* 1049–1063.
6. Kyriakides, M. A., McCrochan, C. R. (1988) Central coordination of buccal and pedal neuronal activity in the pond snail *Lymnaea stagnalis. J. Exp. Biol. 136,* 103–123.
7. McCrochan, C. R., Benjamin, P. R. (1980) Patterns of activity and axonal projections of the cerebral giant cells of the snail *Lymnaea stagnalis. J. Exp. Biol. 85,* 149–168.
8. McCrochan, C. R., Croll, R. P. (1992) Inhibition of feeding motor output by identified interneuron in the isolated central nervous system of *Lymnaea stagnalis. J. Physiol. 446:* 317.
9. Murphy, A. D. (1990) An identified pleural ganglion interneuron inhibits patterned motor activity in the buccal ganglia of the snail, *Helisoma. Brain Res. 525,* 300–303.
10. Nezlin, L., Voronezhskaya, E. (1997) GABA-immunoreactive neurones and interactions of GABA with serotonin and FMRFamide in a peripheral sensory ganglion of the pond snail *Lymnaea stagnalis. Brain Res. 772,* 217–225.
11. Stewart, W. W. (1978) Functional connections between cells as revealed by dye-coupling with a highly fluorescent naphtalmide tracer. *Cell 14,* 741–759.
12. Syed, N. I., Winlow, W. (1991) Coordination of locomotor and cardiorespiratory networks of *Lymnaea stagnalis* by a pair of identified interneurones. *J. Exp. Biol. 158,* 37–62.

Acta Biologica Hungarica 51 (2–4), pp. 205–210 (2000)

SEASONAL PLASTICITY OF SYNAPTIC CONNECTIONS BETWEEN IDENTIFIED NEURONES IN *LYMNAEA*+

J. COPPING[1], N. I. SYED[2] and W. WINLOW[1]*

[1]Department of Biological Sciences, University of Central Lancashire, Preston, PR1 2HE, England, U.K.
[2]Department of Anatomy, Faculty of Medicine, the University of Calgary, 3330 Hospital Drive NW, Calgary, Alberta, Canada, T2N 4N1

(Received: August 31, 1999; accepted: November 30, 1999)

Here we investigate the synaptic connectivity of the giant dopamine containing neurone (RPeD1) of *Lymnaea stagnalis* during the winter months, in wild and laboratory bred animals. RPeD1 is one of the three neurones forming the respiratory central pattern generator (CPG) in *Lymnaea* and initiates ventilation under normal circumstances. Many of the follower cells of RPeD1 are ventilatory motor neurones. The connections of RPeD1 to its follower cells were investigated using standard intracellular recording techniques and dopamine was applied to the follower cells using a puffer pipette. During February and early March, RPeD1 was functionally disconnected from its follower cells, but connections reappeared towards the end of March. Most functionally disconnected cells failed to respond to applied dopamine, consistent with the hypothesis that there is down regulation of dopamine receptors in the follower cells of RPeD1 in the winter months. Behaviourally, *Lymnaea* that survive the winter, are not active at this time and do not indulge in lung ventilation, but stay quiescent. Thus functional disconnection of neurones from the CPG may be either a cause or a consequence of this change in behaviour.

Keywords: Seasonality – giant dopamine containing neurone – synaptic disconnection – dopamine – *Lymnaea.*

INTRODUCTION

The giant dopamine-containing neurone, RPeD1, plays a key role in generating the respiratory rhythm in the pond snail *Lymnaea stagnalis* (L.) and is one of the three cells known to make up the central pattern generator (CPG) [6]. At scientific meetings their has been some confusion over the synaptic connections of RPeD1 and it is quite clear that they are somewhat variable [5]. Furthermore some authors have had difficulty in culturing these connections successfully [4] and this could be due to seasonal factors. During the winter months (December to March), it is always difficult to initiate the respiratory rhythm by stimulation of RPeD1 and we have suspected for some years that it is functionally disconnected from its follower cells, many of which

+ Presented at the 9th ISIN Symposium on "Neurobiology of Invertebrates", July 1–5, 1999, Tihany, Hungary.

*Corresponding author, E-mail: winlow@uclan.ac.uk

0236-5383/2000/$ 5.00

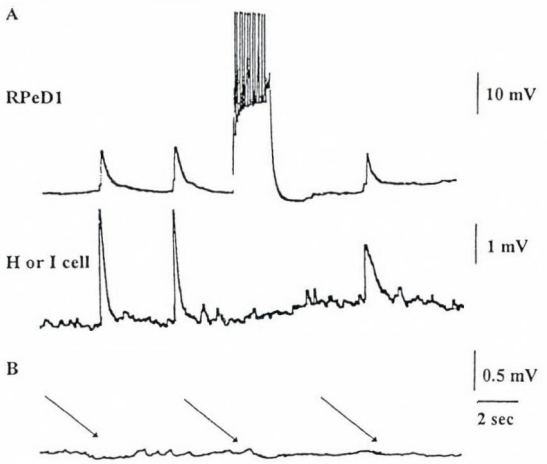

Fig. 1. Functional disconnection of RPeD1 from an H or I cell in winter 1997. (A) In six preparations, depolarisation of the dopamine-containing neurone, RPeD1, had no effects on its usual follower cells in the HIJK cluster. (B) Furthermore, exogenously applied dopamine (10^{-3} M, arrows) had no actions on these cells

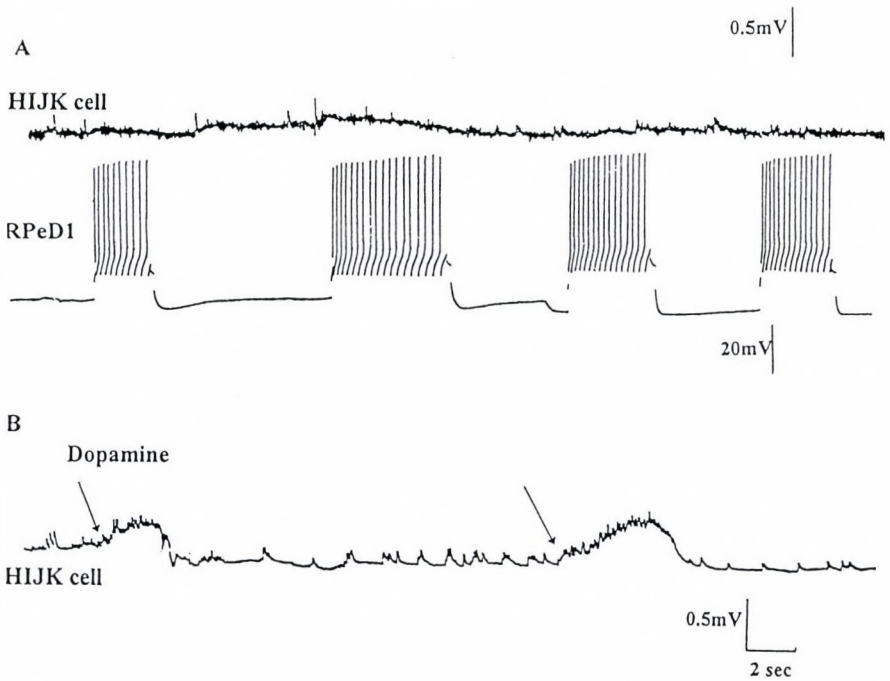

Fig. 2. An example of a functionally disconnected cell responding weakly to extracellular dopamine. (A) In seven HIJK cells, no connections to RPeD1 were seen, but in the case shown here direct application of dopamine (B) caused depolarisation of the neurone

are ventilatory motor neurones, during wintertime. This prompted us to carry out a further study on the connections of RPeD1 and here we report on the absence of functional synaptic connections between RPeD1 and its follower cells [11] during February and March 1997 and compare them with some earlier findings from 1990.

MATERIALS AND METHODS

The isolated brains of wild or laboratory bred specimens of *Lymnaea* were prepared according to the methods of Benjamin and Winlow [2] and recordings were made from RPeD1 and its follower cells using conventional intracellular recording techniques. In a number of experiments, dopamine was pressure ejected onto follower cells in the intact brain via a puffer pipette. The preparation was maintained in a stream of aerated saline flowing at 2–3 ml/min, and the final dopamine concentration was between 10^{-4} and 10^{-5} M.

RESULTS

Unlike the situation at other times of the year, when synaptic connections between RPeD1 and its follower cells are reliably found in all preparations, connections between RPeD1 and the neurones VD2/3 and the HIJK cells from laboratory bred animals were found in only 1 out of 11 preparations and this occurred in late March. Furthermore, in 7 of the 9 preparations in which no functional connections were found, these neurones did not respond to applied dopamine (Figs 1, 3). In one preparation (Fig. 2), dopamine induced weak depolarisations, but no functional connections from RPeD1 were observed. Finally in the one case where connections were found in late March, the postsynaptic cells responded to the exogenous application of dopamine. In Fig. 4A and B, previously unpublished preliminary data from animals taken from the wild in mid and late March 1990 is shown and compared with data from Benjamin and Winlow [2] (Fig. 4C) in which pure epsps and ipsps were recorded on K and J cells respectively. The data from mid-March (Fig. 4A) show that both cell types respond to RPeD1 stimulation with bpsps (i-e on J cells and e-i on K cells), but that the responses are approaching normality by the end of March. The normal, "summer" connections of RPeD1 are summarised in Fig. 4D.

DISCUSSION

The preliminary findings presented here are consistent with the hypothesis that there is down regulation of postsynaptic dopamine receptors in the winter months, leading to functional disconnection of RPeD1 from its follower cells, many of which are respiratory motor neurones [8]. However, there may also be a reduction in transmitter release from RPeD1. Earlier findings [13] indicate that the half width of soma action

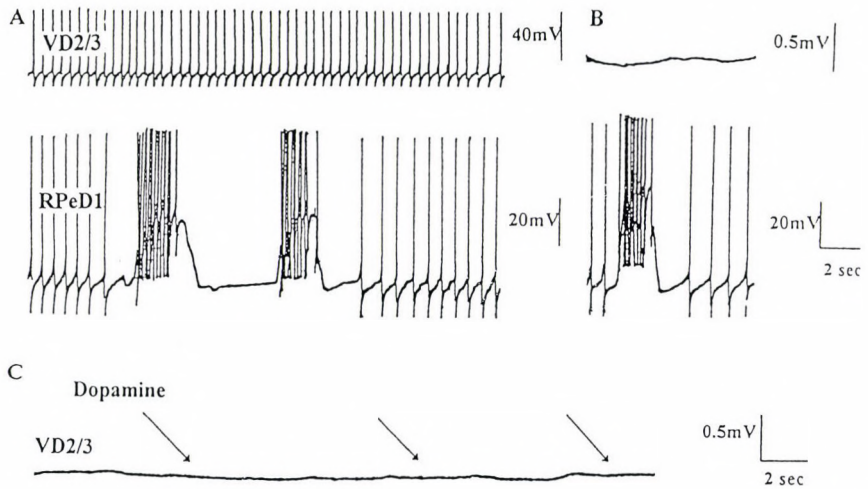

Fig. 3. Functional disconnection of RPeD1 from the giant neurones VD2/3. (A) In three out of four preparations no connections could be found between RPeD1 and VD2/3, even when the follower cell was hyperpolarised and observed at high gain as in (B). In (C), application of dopamine by a puffer pipette (arrows) also failed to elicit any response in VD2/3 following depolarisation

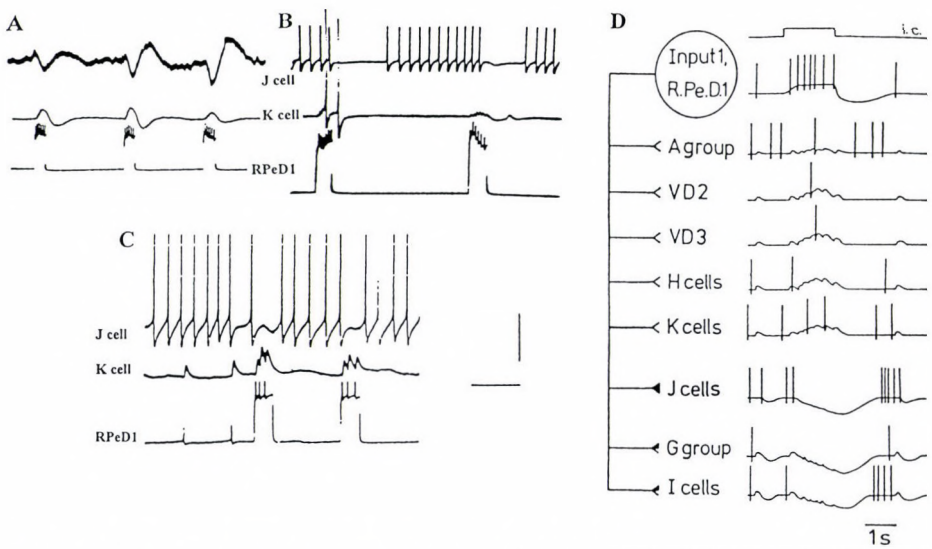

Fig. 4. Preliminary data comparing postsynaptic potentials induced in J and K cells by RPeD1, in mid-March (A, 15/3) and late March (B, 27/3) with those recorded during the summer months (C). In (D) the normal connections of RPeD1 with its follower cells are summarised diagrammatically: i.c. – current pulse injected into RPeD1 via recording electrode. C and D modified from Winlow and Benjamin [11]. Scale bars: *Time,* A and B, 1 sec; C, 2 sec; *Amplitude,* A, upper 10 mV, middle 10 mV, lower 100 mV; B, upper 50 mV, middle 10 mV, lower 100 mV; C, upper 20 mV, middle 10 mV, lower 100 mV

potentials of RPeD1 recorded in February is significantly reduced when compared with those recorded in July [1], suggesting that the presynaptic mechanisms governing transmitter release may also be altered. Measurement of the half width is a reliable way to assess the duration of the plateau phase of an action potential, which is known to be a calcium dependent process in many species. Thus if the calcium currents of the nerve terminals are reduced in a similar way to those of the soma, it is conceivable that synaptic output from RPeD1 is reduced in the winter months, although the intracellular dopamine concentration may rise during that period since whole brain dopamine concentration is high in March/April and falls during the summer [3]. In winter the animal hibernates in the mud at the bottom of its pond and does not come to the surface to respire. Thus the disconnection of a neurone of the respiratory CPG from its follower cells may be either a cause or a consequence of this behaviour.

Another consequence of these alterations in connectivity is that it may become difficult to culture neuronal connections *in vitro* in wintertime and this may explain the data presented by Magoski and Bulloch [4], where they found that normal connections would not form. Authors working on these preparations need to clearly state when the experiments were carried out so that apparent anomalies can be explained.

The concentrations of the biogenic amines dopamine and serotonin appear to exhibit seasonal variability in the brain of *Lymnaea* [3]. Dopamine levels fall progressively from March/April to June/July, whilst serotonin concentrations rise during the same period. It is not yet clear how or if these concentration changes relate to the connectivity of RPeD1, but it is possible that serotonin may modulate the synthesis of new calcium channel proteins in RPeD1 during the spring and summer months.

Whether the effects we observe are presynaptic, postsynaptic or a mixture of the two needs to be determined, but it is probable that maintenance of transmitter release or postsynaptic receptors make significant energy demands on the animal that are best reduced during hibernation. This suggests that other major changes in the physiology of the nervous system should be expected during this period and some of them are described here. For example Wood [12] recently observed that the peak TTX insensitive sodium current in cultured pedal A cluster neurones varied during the year. The current was at its lowest levels in the early part of the year (1–3nA) and rose to maximum levels (4–6 nA) from August to November. The pedal A cluster neurones are ciliomotoneurones [7] driving the pedal cilia of *Lymnaea*. Thus in the colder months when the animal is inactive, there is less need for activity in these cells. As with the disconnection of motor neurones from the respiratory CPG, it is not yet known whether these changes are a cause or a consequence of hibernation. Finally, Winlow [9, 10] demonstrated that the growth hormone-secreting light green cells(LGCs) of *Lymnaea* are more easily activated in June than they are in March. Over 44% of the cells were unable to be activated in March, but all cells could be activated in June. In addition 62% of cells were spontaneously active in June as compared with only 24% in March. The triggers for these changes in activity are as yet unknown, but perhaps growth hormone release is coupled to the peak summer growth period, when food supplies are plentiful.

From the examples cited above it is clear that seasonal changes are of great importance in studying the activity levels of neurones in the brain of *Lymnaea*. The current study was carried out on laboratory bred animals under controlled light (12 h on/12 h off) and constant temperature (16 °C) and compared with previously unpublished data from animals taken from the wild (Fig. 4A, B) and maintained for a few days under laboratory conditions. Thus, neither changes in environmental temperature nor day length are likely to be the environmental cues that trigger the alterations in connectivity pattern of RPeD1. While carefully controlled experiments need to be carried out with respect to illumination and temperature, it is clear that more subtle changes, perhaps in food supply or water supply need to be considered, if we are to understand the extrinsic signals triggering seasonal changes in the nervous system of *Lymnaea*.

REFERENCES

1. Ahmed, I. A., Hopkins, P. M., Winlow, W. (1993) Caffeine and ryanodine differentially modify a calcium-dependent component of soma action potentials in identified molluscan neurones *in situ*. *Comp. Biochem. Physiol. 105C,* 363–372.
2. Benjamin, P. R., Winlow, W. (1981) The distribution of three wide-acting synaptic inputs to identified neurones in the isolated brain of *Lymnaea stagnalis* (L). *Comp. Biochem. Physiol. 70A,* 293–307.
3. Hetherington, M. S., McKenzie, J. D., Dean, H. G., Winlow, W. (1994) A quantitative analysis of the biogenic amines in the central ganglia of the pond snail *Lymnaea stagnalis* (L.). *Comp. Biochem. Physiol. 107C,* 83–93.
4. Magoski, N. S., Bulloch, A. G. M. (1998) Trophic and contact conditions modulate synapse formation between identified neurons. *J. Neurophysiol. 78,* 3279–3283.
5. Park, J.-H., Winlow, W. (1993) Variant synaptic connections in the respiratory central pattern generator in semi-intact preparations of *Lymnaea*. *J. Physiol. 473,* 198P.
6. Syed, N. I., Bulloch, A. G. M., Lukowiak, K. (1990) The respiratory central pattern generator (CPG) of the mollusk *Lymnaea*. *Science 250,* 282–285.
7. Syed, N. I., Harrison, D., Winlow, W. (1988) Locomotion in *Lymnaea* – role of serotonergic motoneurones controlling the pedal cilia. In: Salánki, J., K. S.-Rózsa (eds), *Neurobiology of Invertebrates.* Symp. Biol. Hung. 36, Akadémiai Kiadó, Budapest, pp. 387–402.
8. Syed, N. I., Harrison, D., Winlow, W. (1991) Respiratory behaviour in the pond snail *Lymnaea stagnalis*. I. Behavioural analysis and identification of motor neurones. *J. Comp. Physiol. 169A,* 541–555.
9. Winlow, W. (1987) Action potential plasticity. In: Winlow, W., McCrohan, C. R. (eds) *Growth and Plasticity of Neural Connections.* Manchester University Press, Manchester, pp. 127–144.
10. Winlow, W. (1989) The plastic nature of action potentials. In: Bulloch A. G. M. (ed.), *Cellular Basis of Neuronal Plasticity.* Manchester University Press, Manchester, pp. 3–27.
11. Winlow, W., Haydon, P. G., Benjamin, P. R. (1981) Multiple postsynaptic actions of the giant dopamine-containing neurone R.Pe.D.1 of *Lymnaea stagnalis* (L). *J. Exp. Biol. 94,* 137–148.
12. Wood, G. (1999) Effects of general anaesthetics and ethanol on voltage-activated sodium currents in cultured, identified neurones of *Lymnaea stagnalis*. Ph. D. Thesis, University of Leeds.
13. Wood, G., Winlow, W. (1996) Seasonal variation of spike width in identified neurones of *Lymnaea stagnalis*. *J. Physiol. 495,* 38P.

Acta Biologica Hungarica 51 (2–4), pp. 211–230 (2000)

MODULATION IN FIRING PATTERN AND OSCILLATION IN NERVE CELLS OF *LYMNAEA* DURING NETWORK RECONSTRUCTION+

KATALIN S.-RÓZSA*

Balaton Limnological Research Institute of the Hungarian Academy of Sciences, P. O. Box 35, H-8237 Tihany, Hungary

(Received: August 31, 1999; accepted: November 30, 1999)

The modulation and reconstruction of the cardio-respiratory neural circuit of *Lymnaea stagnalis* L. was compared to that of *Helix pomatia* L. where the input variation and signal molecules were found to have primary importance in network reorganization. From the cardio-respiratory circuit only neurons connected by afferent or efferent pathways to the peripheral chemosensory organ, the osphradium, were used.

It was shown that,

– the general principles of the network reorganization is similar in the two species. The firing pattern of the neurons altered in *Lymnaea* depending on the input activation or presence of signal molecules in the vicinity of the neurons.

– the responses of the neurons to the same sensory information, originating from osphradium varied depending on their firing patterns.

– on central neurones the generation of phasic pattern and/or oscillation was an indicator of network disintegration leading to insensibility to the osphradial sensory inputs

– co-application of signal molecules (5HT, DA, GABA with opioid peptides) to the neurons caused a phasic firing pattern and/or oscillation leading to disintegration of one network and activation of another one.

– the effect of μ-opioid peptides on GABA-induced and voltage activated ion currents were shown to be the cellular target in reconstruction of neural networks in *Lymnaea.*

– the neural network reconstruction in vertebrate brain evoked by signal molecules can be compared to that observed in the identified network of *Lymnaea stagnalis* making this latter a useful model in further studies, too.

Keywords: Neural networks – circuit reconstruction – firing pattern – osphradium – 5HT – DA – GABA – opioid peptides – *Lymnaea stagnalis* L.

INTRODUCTION

Over the past decade it became evident that an identified neural network can undergo permanent and dynamic alterations with a variety of firing patterns indicating the temporary state each of its functioning units. The firing patterns and oscillations were

+ Presented at the 9th ISIN Symposium on "Neurobiology of Invertebrates", July 1–5, 1999, Tihany, Hungary.

*E-mail: srozsa@tres.blki.hu

0236-5383/2000/$ 5.00

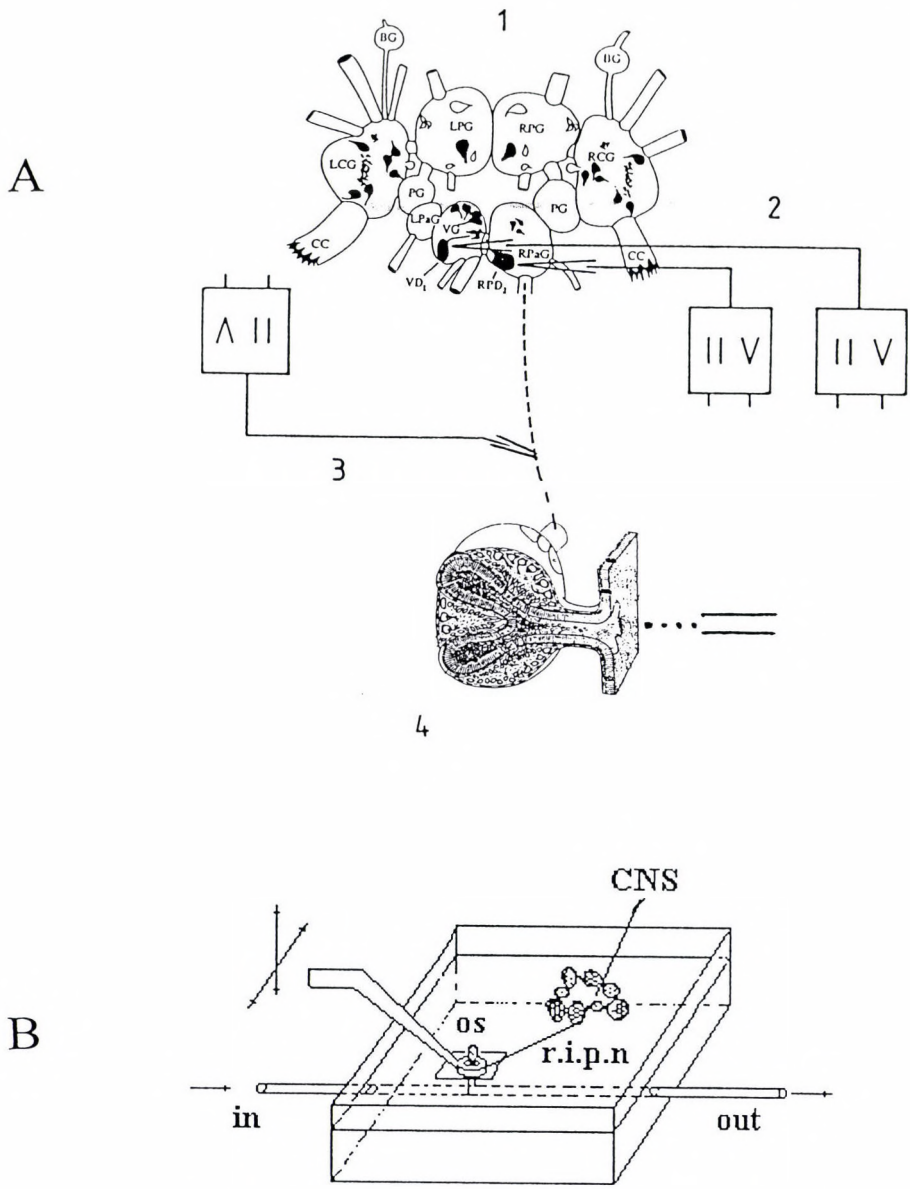

Fig. 1. Semi-intact preparation including central nervous system (CNS), osphradium and the nerve connecting them (A). 1 – CNS – central nervous system (suboesophageal ganglionic ring). 2 – microelectrodes for intracellular recording of nerve cell activity. 3 – extracellular electrode for recording of the activity of osphradial nerve. 4 – osphradium. (B) Chamber used in the experiments with permanent perfusion. CNS – central nervous system r.i.p.n. – right inner parietal nerve. os – osphradium

shown to be modulated either by input variations or a number of signal molecules including neurotransmitters and modulators alike [5, 10, 18, 23].

In the identified neural network of *Helix pomatia* the oscillation and phasic pattern of firing were found to be indicators of network reorganization accompanied by the interrupted reception of peripheral information [24, 25).

The aim of our present studies was to clarify whether a reorganization of neural network comparable to that of described for the cardio-regulatory network of *Helix pomatia* can be demonstrated in *Lymnaea stagnalis*. The cardio-respiratory network of *Lymnaea* was used comprising morphologically and functionally characterized neurons [3, 33, 38].

MATERIAL AND METHODS

The experiments were performed on the adult specimens of the pond snail *Lymnaea stagnalis* L. (Pulmonata, Basommatophora) collected from their natural habitat (Balaton-Minor) during the months May–October, and kept in aquarium at temperature 22 ± 5 °C. The animals were fed with fresh lettuce.

The semi-intact preparation including the central nervous system (CNS) and the osphradium with the right inner parietal nerve (r.i.p.n.) connecting them was isolated. The semi-intact preparation was fixed to the bottom of the Sylgard-lined dish (Fig. 1). The connective tissue of the ganglia was removed by mechanical and enzymatic treatments. The experimental chamber was permanently perfused with snail physiological saline or with the test solutions applied directly either to the surface of the osphradial canal or the central ganglia. Standard physiological solution (SPS) contained (in mM): NaCl 44, KCl 1.7, $CaCl_2$ 4, $MgCl_2$ 1.5, HEPES 10 (pH = 7.3 was adjusted with NaOH). For stimulation of the osphradium L-glutamate and NaCl were used.

Recording of nerve and neuron activities

The extracellular activity of the osphradial branch of the right internal parietal nerve (r.i.p.n.) was recorded using bipolar electrodes. The activity of the identified central neurons was recorded simultaneously with nerve activity using conventional microelectrophysiological methods, sampled by A/D converter.

Substances

5-hydroxytryptamine (5HT), 3-hydroxy-tyramine-HCl (DA), gamma-aminobutyric acid (GABA), methionine enkephalin (met-Enk), [D-Ala, N-Me-Phe, Gly-ol]-enkephalin (DAGO), L-glutamate from Sigma were used.

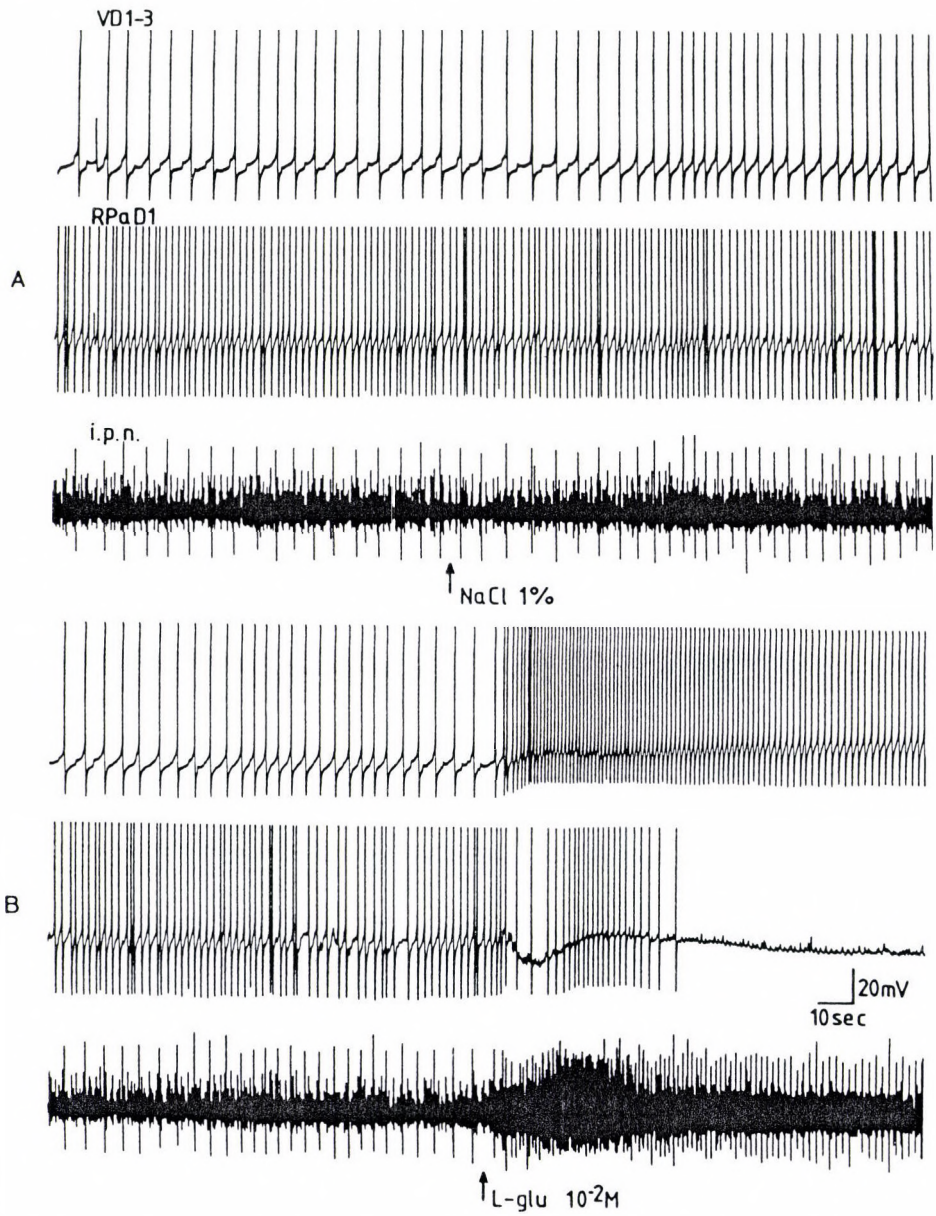

Fig. 2. Responses of the neurons VD1-3 and RPaD1 to the application of NaCl (1%) and L-glutamate (10^{-2} M) to the surface of the osphradium (A and B). The afferent impulsation running from osphradium to central neurons during osphradial stimulation can be seen in the activity of the osphradial nerve (i.p.n.)

RESULTS

1. Central representation of osphradial inputs in CNS and efferent signals running to the osphradium

In the identified neural network of *Lymnaea* involved into the regulation of visceral functions the neurons display a wide variety of pattern alterations [3, 33, 38]. In this neural assembly the inputs originating from the regulated organs were shown to disperse to more than 500 central neurons [20, 33]. As most of the physiologically relevant synapses in this circuit has been detected, it can be used adequately for studying network function and reorganization. Further on, as this circuit can be regarded as an analogous network to that of regulating visceral functions in *Helix pomatia*, it can be used to clarify whether the same principles of network reconstruction exist in the two species [24, 25].

The cardio-respiratory network of *Lymnaea* used in our experiments included the neurons forming respiratory central pattern generators [RPeD1, VD4 and input-3, IP3), some of their followers from A, J, K, I clusters and the neuron RPaD1 [3, 33]. The inputs running from peripheral organs (heart, pneumostoma, mantle, skin-surface, etc.) to these cells and their outputs have been described earlier [3, 33]. In the present studies we introduced a new input originating from the osphradium, transferring information to central neurons from the external environment. The osphradium is a chemosensory organ sensing directly the environmental changes and trasferring information to CNS leading to modulation of various forms of behaviour including respiration, feeding, escape from predators, etc. [30]. Some of the overlapping central representations of the inputs originating from the osphradium and various visceral organs have been described earlier [12, 30].

The aim of our present studies was to demonstrate the variation in the representation of osphradial sensory information running from the environment to the CNS and to show, whether the responses of the central neurons to osphradial stimulation can be altered depending on their firing pattern, input variations they receive and presence of signal molecules in their vicinity.

Although in semi-intact preparation of *Lymnaea* the firing pattern of the neurons varied considerably the responses to osphradial stimulation were successfully traced. The results showed that chemical stimulation of the osphradium caused characteristic changes in the firing pattern of the central neurons (RPaD1, RPeD1, VD1-4, IP3 and A, I, J, K clusters) and in the activity of the osphradial branch of the r.i.p.n. The analysis of the osphradial sensory inputs revealed that both specific and variable responses can be demonstrated on the same central neuron as an answer to the stimulation of the osphradium (Figs 2, 3 and 4).

The responses of the neurons were found to be different depending on the chemical stimuli applied to the osphradium. The responses of the neurons VD1-3 and RPaD1 were weak following application of NaCl to the osphradium (Fig. 2A) while L-glutamate elicited robust increase in firing frequency of the neurons VD1-3 with simultaneous hyperpolarization and blockade of the firing on the cells RPaD1 (Fig.

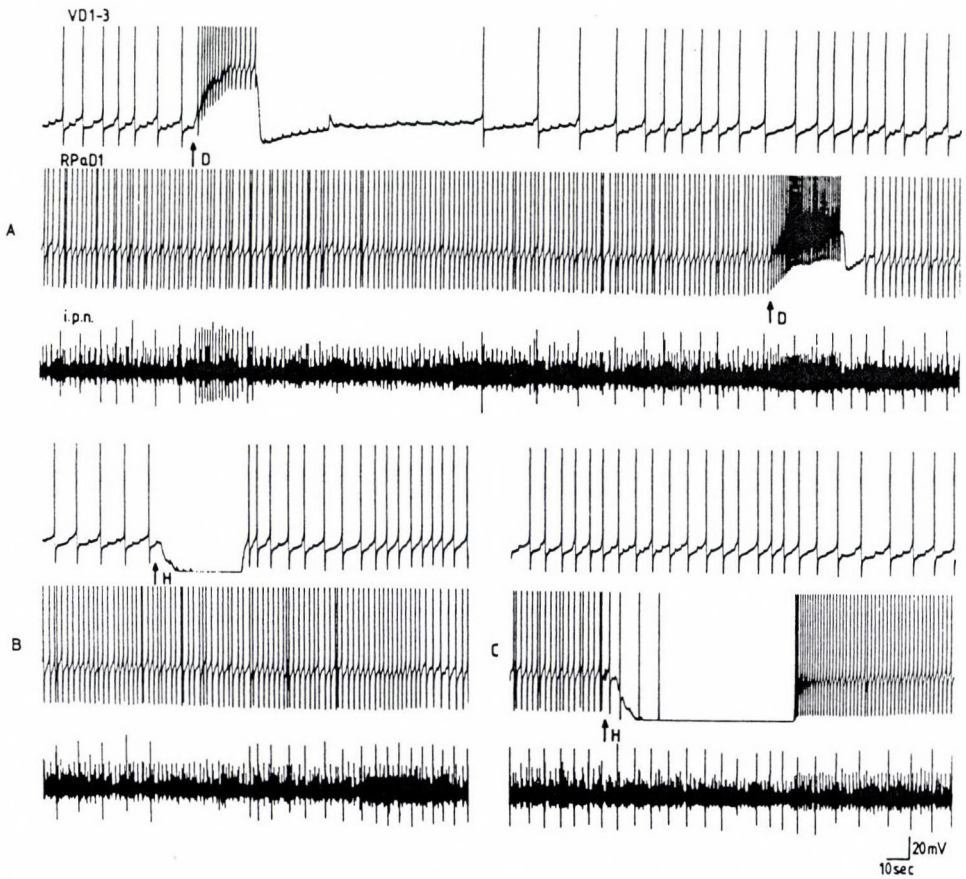

Fig. 3. Efferent impulsation running from central neurons VD1-3 and RPaD1 to the osphradium revealed by de- or hyperpolarization of the soma membrane of the neurons. In the activity pattern of the osphradial nerve the firing pattern of both cells can be clearly recognized as an efferent sign. The largest in amplitude efferent signes originate from the cell VD3. i.p.n. – activity of the osphradial nerve

2B). During application of L-glutamate to the osphradium the intensity and frequency of the extracellular activity of the osphradial nerve was considerably increased (Fig. 2B).

Additionally to the afferent impulsation of the osphradial nerve the efferent signalization running from central neurons to the osphradium was also traced (Fig. 3). Both de- or hyperpolarization of the soma membrane of the neurons VD1-3 altered the largest in the amplitude component of the nerve activity (Fig. 3). Depolarization of the neurones VD1-3 led to the increase in firing frequency of the largest component in the compound activity of the nerve (Fig. 3A), while its hyperpolarization eliminated the above component in the nerve activity (Fig. 3B). At the same time,

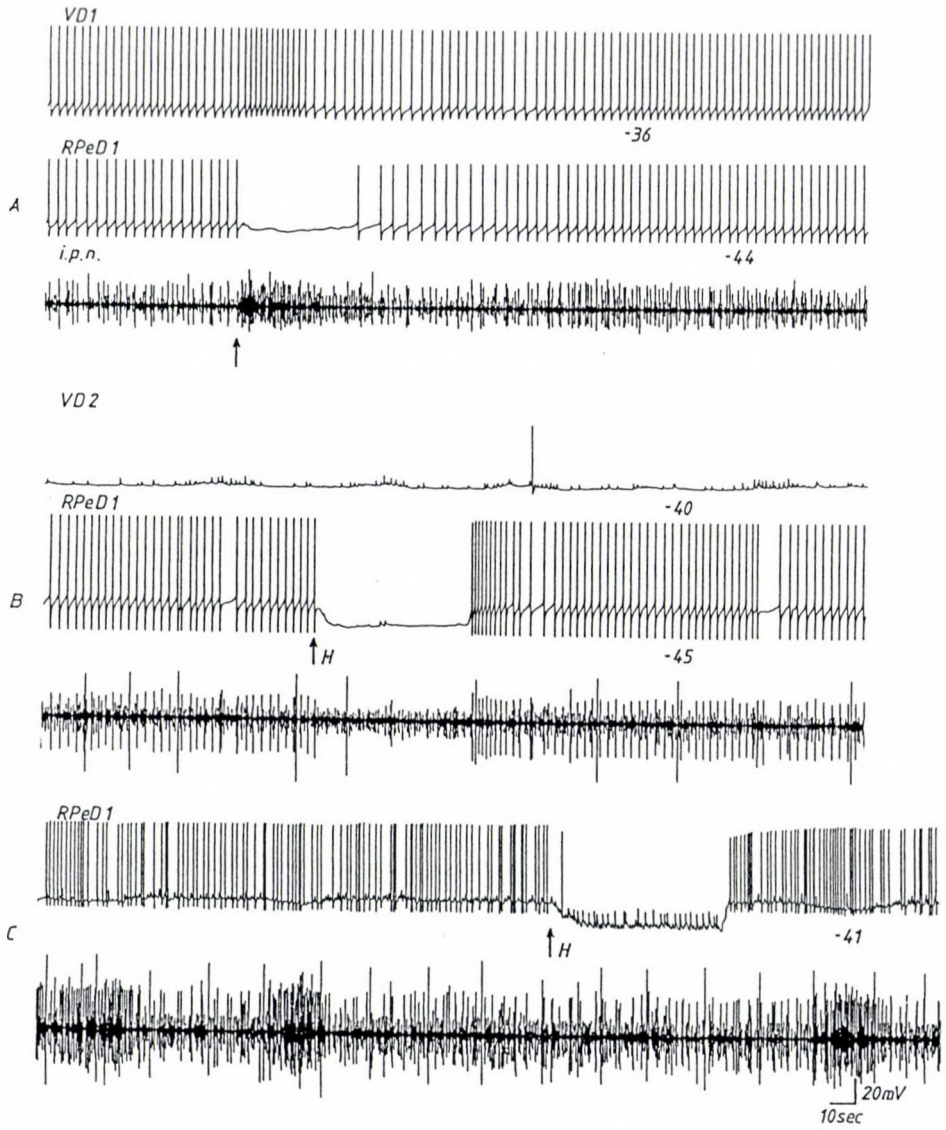

Fig. 4. Spontaneous variations in firing pattern and osphradial input on the neurons VD1, VD2 and RPeD1. A – osphradial input (arrow) to the neurons firing in tonic mode. B – Effect of activation of IP3 can be identified on the neurons VD2 and RPeD1 leading to the changes of firing pattern when the efferent pathways remained unaltered tested by hyperpolarization of the neuron RPeD1 (arrow, H). C – the phasic pattern of the neurones became prevailing and the efferent pathway of the neuron RPeD1 (arrow, H) was no more identifiable but in the nerve activity the activation of a number of new neurons can be traced including respiratory rhythm generator

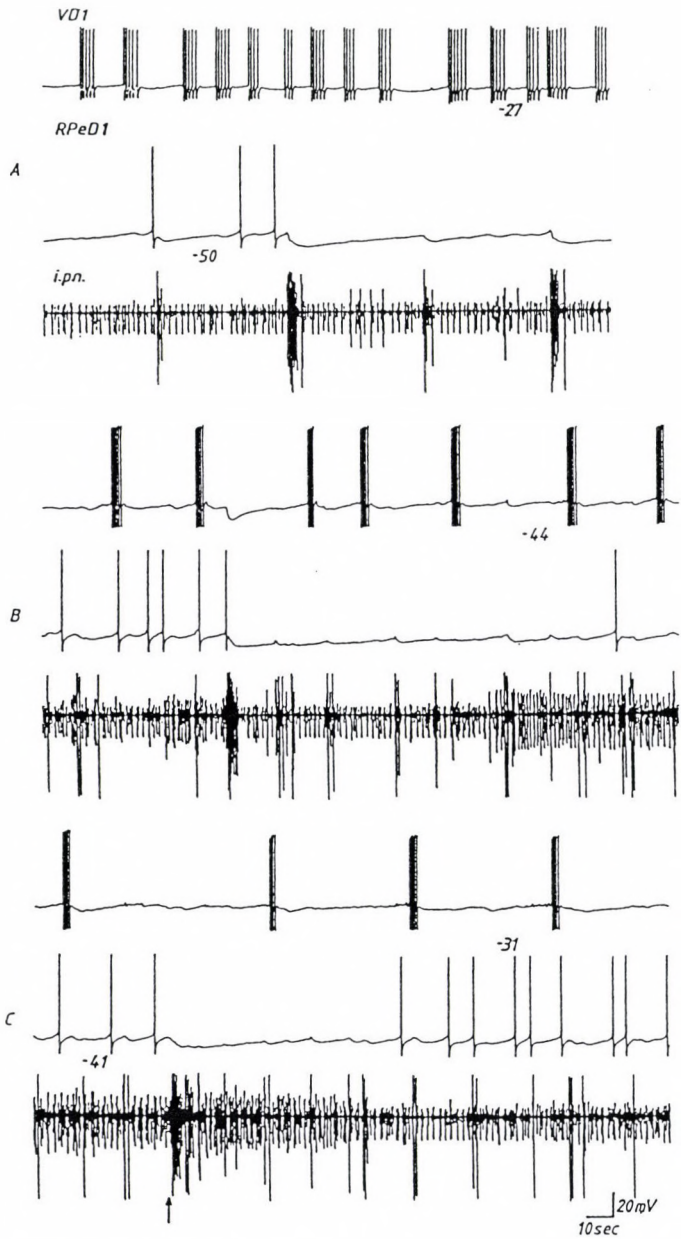

Fig. 5. Input variations on the neurones VD1, VD2 and RPeD1. During bursting activity the neuron VD1 became insensitive to the inputs originating from the osphradium (A, B, C). For comparison see Fig. 4A. The neuron RPeD1 displayed sporadic discharges and received IPSPs and EPSPs from other members of the networks (A and B) but its firing was blocked during osphradial stimulation (C). i.p.n. – osphradial nerve activity

de- or hyperpolarization of the neuron RPaD1 left the largest component of nerve activity unchanged (Figs 3A and 3B) altering another, lower-amplitude component of the nerve activity (Figs 3A and 3B). Similarly, most of the components in nerve activity showed correlation with the firing pattern of one or an other identified neuron, functioning either as an afferent or efferent unit in the regulation of the osphradium (Figs 3A and 3B). However, some of the central neurons studied proved to be multifunctional, involved both in afferent and efferent signalization. One of such a cell was the well-known neuron RPeD1.

In extracellularly recorded nerve activity the pattern of five-seven neurons can be recognised additionally to the neuron activity recorded intracellularly. This contributes to evaluation of alterations taking place during network reconstruction on larger scale without recording from more than two cells.

Using this "trace-following" it can be seen that certain members of the network regularly discharge in bursting mode as an independent unit. However, in other cases the same neuron can produce a regular, tonic firing (Figs 3 and 4).

The results proved that in the regulating networks both the somatic and dendritic spikes are present and their functional importance can be demonstrated during circuit reconstruction when the same neuron can turn its firing pattern according the afferent or efferent impulses they are transferring.

Studying central representation of the osphradium it became evident that responses of the same neurons to the same stimulation of the osphradium can highly vary or it can be absent (Fig. 4) depending on the simultaneous activation of a variety of inputs. It can be seen on the activity patterns of the neurons VD1-RPeD1 that osphradial stimulation can activate the interneuron IP3 leading to the activation of central pattern generator appearing both in the activity of the neuron RPeD1 and osphradial nerve (Figs 4B and 4C). The burst-type of firing of central neurons prevents receiving of sensory inputs from osphradium: such an example is demonstrated in Fig. 5. When the neuron VD1 displayed burst-firing, the input originating from osphradium was omitted from the firing pattern of the cell, while it was seen in the activity pattern of the neuron RPeD1 recorded simultaneously (Figs 5B and 5C). However, during burst-type firing some irregular oscillations appeared on the cell VD1 as an answer to osphradial stimulation (Figs 5B and 5C).

The high variability both in firing pattern and input activation of the neurons studied was suggested to be a result of the modulatory environment, e.g. the signal molecules that are present in the synaptic area or in the vicinity of the neuron modulating permanently the sensitivity of the neurons. The present results proved that osphradial information is represented in a large population of neurons and its distribution overlap with central representation of the heart and pneumostoma.

Various types of oscillations were recorded also from the osphradial cells [12]. In osphradium two types of cells were demonstrated, being either ganglionic or sensory ones [30]. The sensory cells of osphradium were characterized with slow oscillations and slow periodic waves in their activity intensifying during their chemical stimulations [12].

The results emphasise the importance of oscillations from sensory perception to output formation throughout the information processing in nerve centres. As oscillatory and burst discharge is a key element of membrane processing from the level of receptors to output of the central neurons in most sensory system it emphasises the advantage of the osphradial system in studies of network reorganization.

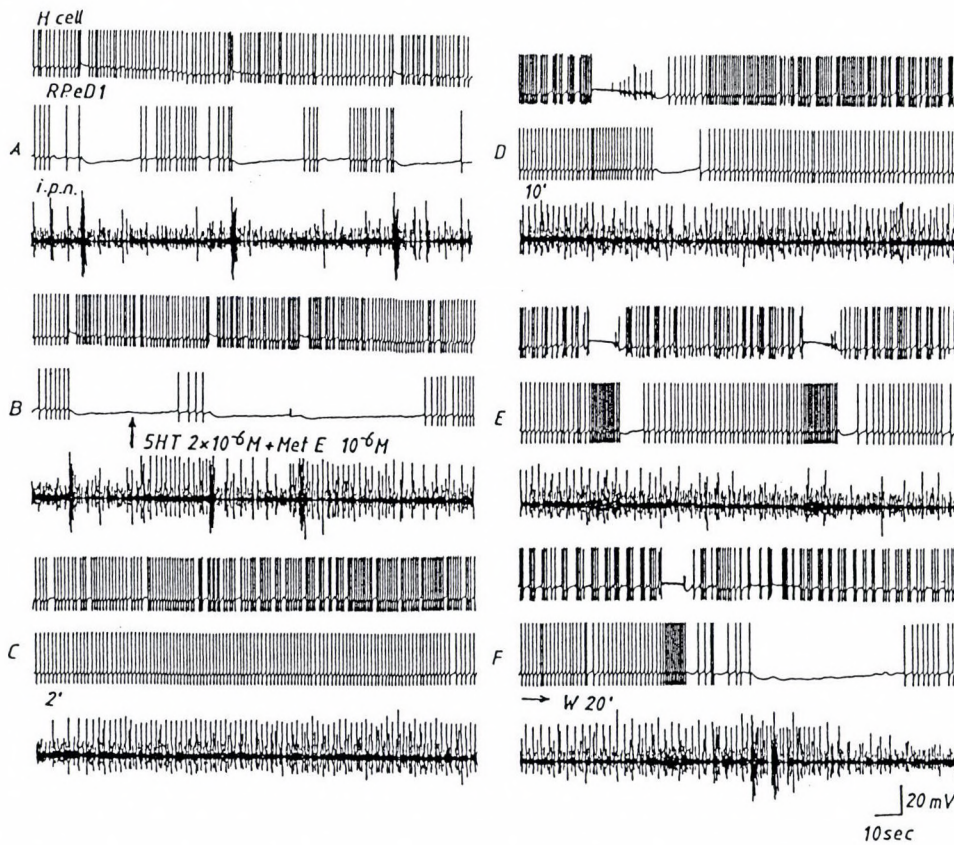

Fig. 6. Modulation of firing pattern and input activation of the neurons from H-cluster and RPeD1 following co-application of 5HT and met-enkephalin. The activation of IP3 can be identified in the firing pattern both of the neurons (A). Following co-application of 5HT and met-enkephalin the IP3 was inactivated (C) and other, newly activated inputs appeared (C and D) in firing pattern of these neurones and osphradial nerve maintained after wash out the signal molecules and following restoration of osphradial input on the neurone RPeD1 (F). i.p.n. – osphradial nerve activity

2. Effect of signal molecules on pattern formation in central neurons

In the model used in our studies both in periphery and CNS the signal molecules were found to initiate oscillations or changes in firing pattern. The neural networks are constantly modified with numerous factors being present in their environment. The homeostatic field surrounding the nerve cells or brain area represents a mixture of unknown number of signal molecules causing either analogues or opposing to each other changes in ion-currents, pattern-formation, synaptic connections and circuit reorganization. The action directed to the same or opposite directions caused by simultaneously acted signal molecules can amplify or weaken the connections between the network units. All the inputs might be modified simultaneously both in number and strength and the neuron must integrate them to cross the firing threshold. Predominance of one or another chemical factor can switch the network from one functional stage to another. Such a situation can be simulated by external application of signal molecules existing in the neurons of network in normal conditions, too.

In the *Lymnaea* neurons involved into our studies 5HT, DA, GABA, FMRFamide and enkephalins were found to be present [6, 7, 13–15, 29, 36]. In *Helix pomatia* we demonstrated earlier the principal role of monoamines, GABA and opioid peptides in reorganizing the neural network regulating visceral functions [23–25].

In our experiments in the *Lymnaea* the mixture of active substances being present in the same neurons or receiving synaptic inputs employing the same transmitters [14, 15] was applied.

Here the effects of simultaneous applications of fast transmitters (5HT and DA) and opioid peptides (met-Enk and DAGO) are summarized:

Following co-application of 5HT (2×10^{-6} M) and met-Enk (10^{-6} M) the inputs appearing on H-cell as an excitation and as an inhibition on RPeD1 neuron became ineffective (Fig. 6B). In two to ten minutes of application the pattern of the inputs recorded from the nerve changed basically. At the same time, it could be seen that immediately after application of the paired signal molecules (e.g. 5HT and met-Enk) the new members of the network started to be activated (Figs 6B and 6C) and the original burst pattern (CPG) disappeared. On H-cells the characteristic IP3 input activation could be seen (Figs 6D and 6E). The changes in firing pattern could be seen on both of the neurons, but it means that the H-cells firing in tonic mode with synaptic interruptions before treatment became of the bursting type, while the RPeD1 having originally irregular phasic-type firing started to work in a tonic mode (Fig. 6C). After washing out of the paired signal molecules the original input pattern started to be restored but the firing pattern and the additionally activated inputs remained active for a long period of time (Figs 6E and 6C). The same was demonstrated for the neurons VD1 and RPaD1 after the application of 5HT and met-Enk combinations, where the disconnection of the input-activated pattern and reorganization of the network could be traced represented by activation of a set of neurons being silent before using these co-acting signal molecules.

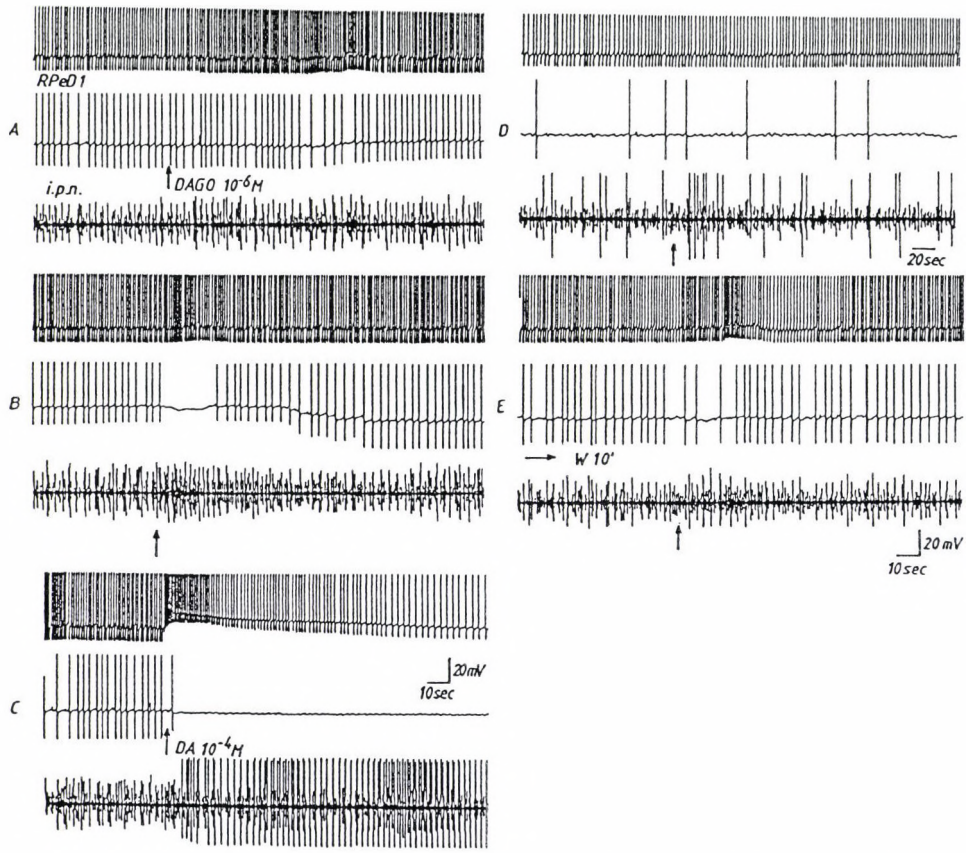

Fig. 7. Effect of dopamine and DAGO on the firing pattern and input activation on the H- and RPeD1 neurons. The stimulation of the osphradium caused an increase on the H-neurone and decrease on the RPeD1 firing frequency (B). DA caused the same but more intensive changes on these neurones (C) while DAGO failed to alter their firing pattern (A). Co-application of these two signal molecules eliminated the inputs originating from the osphradium (D) but it was restored following wash out (E). i.p.n. – osphradial nerve activity

The effect of dopamine was either inhibitory or excitatory on various member of the network studied (Fig. 7).

The bath applied DA (10^{-4}–10^{-6} M) hyperpolarized the neuron and eliminated the firing of the cell RPeD1 with simultaneous increase in firing frequency of H-cells (Fig. 7C). Comparing the same changes of these two cells to the osphradial inputs it can be seen, that DA caused the same type of responses and activated a large number of central neurons monitored on nerve activity (Figs 7C and 7C). In the continuous presence of DA the excitation of cell H and the inhibition of RPeD1 remained long-lasting and effect of the stimulation of the osphradium was very weak on their

soma, although the inputs on the nerve was nearly of the same intensity as before DA-treatment (Fig. 7D).

Long-lasting pretreatment of the ganglia with DAGO (the stable μ-opioid analogue) and DA weaken the effect of osphradial inputs leading to the inhibition of firing frequency and membrane oscillations with bursting (Figs 8C and 8D). Activation of large number of units of circuit can be identified in nerve activity. Long-lasting wash-out restored the efficacy of osphradial inputs (Fig. 8E) on H-, and RPeD1 cells.

Summarizing the results it can be concluded that the network effect of the mixtures of signal molecules in the surrounding of neurons is a main factor leading to disintegration of the functioning neural network and to activation of a new set of neurons.

Recently, to understand dynamic effects of co-applied signal molecules or input variations in circuit organization and their rearrangement, mathematical methods were introduced [4, 34, 35]. Application of non-linear dynamic methods opens a way

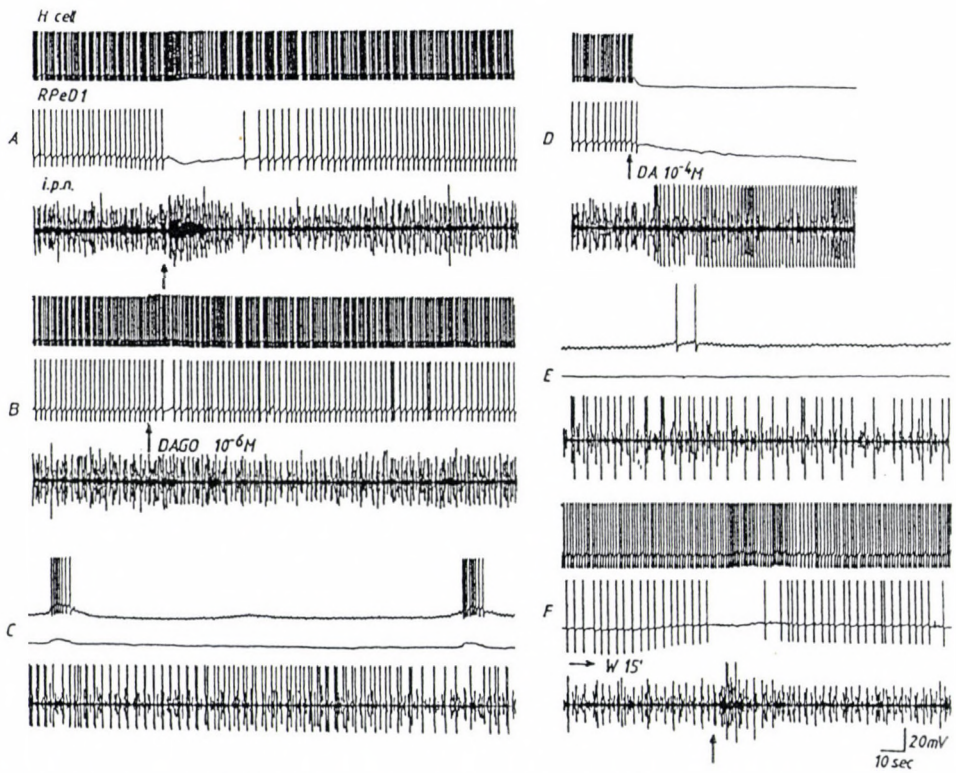

Fig. 8. Effect of co-application of DA and DAGO to CNS on firing pattern and osphradial inputs on the neurons H-and RPeD1. A – osphradial inputs to the neurons. B – effect of DAGO applied alone to CNS. D – effect of DA added alone to CNS. C and E – membrane oscillation and burst firing evoked by long-lasting co-application of DAGO and DA on H-neuron and inhibition of the neuron RPeD1. F – wash out of DA and DAGO restored the osphradial inputs on the neurons. i.p.n. – osphradial nerve activity

for detecting slight changes in the neuronal firing due to synaptic influences or effects of neuromodulatory substances. Using this method it can be predicted how sensitive is the given process, or how stationary or chaotic the process studied in the long-term scale and in this way reorganization of synaptic inputs can be demonstrated [see: Molnár et al., this volume, 19]. This method revealed that both the alteration in firing pattern and the oscillations are closely related to the changes of the homeostasis as they could be simulated by a variations of signal molecules, further on they can contribute to understanding of alterations at systemic levels or to discovering some hidden correlations in the altering firing pattern.

3. The cellular targets for network reorganization

It is generally proved that membrane effect of signal molecules depend on the level of its polarisation being a result of the opposing effects of more than one transmitters on the membrane surface. We demonstrated the interaction of signal molecules on ion currents on the same *Lymnaea* neurons which were used for studying the network reorganization.

On isolated internally perfused *Lymnaea* neurons the GABA-induced ion currents and their modulation by opioid peptides and 5HT have been described [22, 26].

On the majority of *Lymnaea* neurons, GABA depolarized the membrane underlying with slow or fast GABA-induced inward current. However, outward component of GABA induced current was as well-demonstrated either as a part of biphasic current or as a clear K-dependent outward one. The GABA-induced inward current was characterized on the neurons RPeD1, RPaD1, LPaV2, VD1-4 and A-cells [22, 26]. The GABA-induced inward current was biphasic and Cl-dependent on the neuron RPeD1.

Both types of inward-currents induced by GABA were reduced or blocked by met-enkephalin or morphiceptin (μ-opioid) in a dose-dependent manner. Opioid caused reduction of GABA-activated slow inward current which was reversible, whereas that of on the fast current was not. The decrease produced by met-Enk or morphiceptin on the slow GABA-induced inward current was naloxon sensitive, but their effect on fast GABA-current was not eliminated by naloxone (Table 1). No complete blockade in the effect of opioid peptides on GABA-induced inward current was traced.

In the same neurons (RPaD1 and RPeD1) serotonin which causes a circuit reconstruction caused a bimodal effect and apart from opioid peptides potentiates the GABA induced inward current. However, on A-cells 5HT similarly to opioid peptides suppressed the GABA-induced inward current (Table 1). It is known from literature [2] that DA on the neuron VD4 decreased the Ca-dependent inward current and increased the voltage-dependent K-current. DA causes hyperpolarization the neurons used in our experiments (Figs 7 and 8).

The identified, isolated neurons of *Lymnaea* provide a useful model for studying postsynaptic interaction between the signal molecules and to interpret it in regard to

Table 1
Modulation of ion currents by signal molecules on the *Lymnaea* neurons

Neuron	Ligand gated current	Voltage activated current	Modulation
RPeD1	I_{GABA} slow inward		reduced by μ-opioids
	I_{GABA} fast inward		reduced by μ-opioids
	I_{GABA} net inward		potentiated by 5HT
		I_{Ca} inward HVA	reduced by GABA
		$I_{K(A)}$ outward	reduced by GABA
		$I_{K(Ca)}$ outward	potentiated by GABA
RPaD1	I_{GABA} inward		reduced by μ-opioids
	I_{GABA} inward		potentiated by 5HT
A-cells	I_{GABA} inward		reduced by μ-opioids
	I_{GABA} inward		reduced by 5HT
VD1-3	I_{GABA} inward		reduced by μ-opioids
VD4		I_{Ca} inward	potentiated by DA
		$I_{K(V)}$ outward	reduced by DA
LPaV2	I_{GABA} inward		reduced by μ-opioids

Note: μ-opioids used were met-Enk and morphiceptin [26]. See: 3, 15, 22, 26.

their effects in causing a firing pattern alterations in the identified circuits. The results proved that ion-channels of the membrane are the targets for modulation of neuron sensitivity by signal molecules.

DISCUSSION

Comparing the analogous neuronal circuits in *Helix pomatia* L. and *Lymnaea stagnalis* L., their main characteristics were found to be similar. The results indicated that the networks can be dynamically rewired by simultaneously activated inputs and/or mixture of signal molecules in the vicinity of the synapses. Reorganization of the identified neuronal network in *Lymnaea* similarly to that of *Helix* [24, 25] was accompanied by alterations in firing pattern of the neurons and while the neuron generated membrane oscillations and burst firing it remained unresponsive to sensory information. In *Helix pomatia* among signal molecules the combination of 5HT and

DA with opioid peptides and FMRFamide was most effective in causing membrane oscillations and burst firing resulting reorganization of a functioning circuits [23–25]. The present data confirm the same background in network reorganization of the above two species.

5HT was found to have a primary role in network reorganization of crustaceans, where it was shown to regulate a wide variety of rhythm-generating circuits [8]. It was demonstrated that 5HT was able to alter the motor program to be transferred from one dedicated for swimming to one required for burrowing [8, 9].

Our data indicate as well that the network reconstruction involve both pre- and postsynaptic sites of action. In vertebrates most of the authors emphasises the presynaptic interactions of signal molecules directed to modulation of transmitter liberation. In mammals opioid-peptides were shown to decrease the GABA-ergic transmission on hippocampal neurons either through the hyperpolarization of the somatic membrane or through the effects of IPSPs on inhibitory presynaptic terminal leading to disinhibition [21, 31]. Recently, in vertebrates serotonin, operating through a $5HT_2$ receptor was found to activate GABA-ergic interneurons in the prefrontal cortex [1].

In *Lymnaea* the opioid peptides modulate receptor-coupled processes postsynaptically altering the GABA-induced inward current [22, 26]. The interaction of low molecular weight neurotransmitters (5HT, Ach, DA, GABA) with FMRFamide and opioid peptides have been reported earlier on cardio-regulatory circuit of *Helix pomatia* L. [23, 25–27, 32]. In *Lymnaea* the interneuron VD4 was hyperpolarized by DA with membrane oscillations and DA converted the firing pattern from tonic to phasic one [3].The burst of APs in neuron VD4 was suggested to arise as a results of the action of two transmitters, e.g. DA from RPeD1 and the unidentified one from IP3 [3]. Our data indicate that the second factor in the integrated action of two signal molecules can be the opioid peptides, generating with co-acting monoamines phasic pattern accompanied with network reconstruction [23–25].

The co-existence of 5HT, DA and GABA with opioid peptides was demonstrated in nerve cells of both vertebrates and invertebrates including *Lymnaea stagnalis*. In the pedal ganglia of *Lymnaea* met-enkephalin immunoreactive neurons have been localised in an area of 5HT-containing A-cells and in *Achatina* co-localization of 5HT and met-enkephalin was described [36]. In the neuron RPeD1 co-existence of DA with peptides was demonstrated [14, 15]. Met-enkephalin and/or FMRFamide are present in the neurones VD1, RPaD1 and A-cells and they were shown to release into the connective tissue sheath of the ganglia or the blood stream [14]. This is a reason why the semi-intact preparation of *Lymnaea* is useful model for connecting the cellular and network effects of signal molecules at systemic level.

In network analysis it was found that adaptation of neurons to a changing environment (homeostasis) requires that they were able to discriminate between incoming stimuli, and than relevant messages were transmitted inside the cell to elicit a range of co-ordinated modifications according to functional needs of regulation. The multiplicity of receptor subtypes for a given amino- (or peptide) transmitters and the diversity of their coupling to intracellular effectors provide one set of elements underlying their wide functional variety.

However, the variable responses and interactions of signal molecules cannot be interpreted merely by the presence of different receptors since more then 200 GABA and/or 5HT or DA containing neuron were found in CNS of *Lymnaea* [36, 37]. Moreover, it is known that some of the signal molecules can use each other's receptors with varying efficacy. This can be one way how simultaneous activation of various receptors can modify the effects of the neurotransmitter in question. Nearly all the neurotransmitters (5HT, Arch, DA, GABA, etc.) can act either fast, via ion channels or more slowly, via second messengers, causing both short- or long-term effects in target cells.

However, even the widespread distribution of 5HT receptors cannot explain how 5HT modulates the multiple neuronal circuits, which underlie complex behaviour, all the more that 5HT (and other signal molecules) liberates presynaptically and into the hemolymph alike leading to two different effects at systemic level, although both ways can lead to modulation of the firing patterns of a restricted or more distributed populations of neurons.

In *Lymnaea,* oxygen sensitive receptors were demonstrated in the lung cavity [11, 30] and since the neuron RPeD1 was found to ramify to blood vessels supplying the lung area it was suggested that this neuron can be activated by a decrease in oxygen content in the blood, thus switching on the respiratory cycle [38]. Our results indicate that the neurons including RPeD1 can directly react to the alterations of the environment using osphradial receptors sensing alterations in water contamination and oxygen tension, adapting in this way the regulation of the cardio-respiratory system to a momentary need of the organism. The permanent changes in firing pattern of the cardio-respiratory neurons according to the changes in the signal molecules that are present in their vicinity can reflect this type of regulation. This means that the respiratory cycle of *Lymnaea* can be initiated by RPeD1 as an answer to environmental changes transferred from osphradium to CNS [12]. The present results proved that in CNS of *Lymnaea*, similarly to the same network of *Helix pomatia* the input variation and combination of signal molecules play leading role in circuit reconstruction.

As a result of technical achievements more and more data appeared to characterize of network organization and its cellular mechanism. This lead to the acceptance of the idea of network reconstruction in vertebrates, too [17]. A decade ago, the list of animal models used for studying circuit reconstruction was rather brief and included first of all the crustaceans (with their well-known stomato-gastric ganglion) and some of the molluscs (*Helix* and *Aplysia*). At present, the idea of the neural circuit reorganization can be regarded generally accepted.

Recently, using network analysis unexpected similarities were discovered in circuit organization or rebuilding in invertebrate and vertebrate nervous systems. It was shown that somatic and dendritic depolarisation can elicit quite different firing patterns in the same pyramidal neurons and soma spike increased while dendritic AP decreased in bath applied 5HT due to direct modulation of Ca-channels [28]. It can be compared to that in *Lymnaea* when the cerebral giant cells spontaneously changed the direction of spike conduction (orthodromic or antidromic) and the two types of

action-potential generation can be a physiologically relevant mechanism during the action of signal molecules in circuit reorganization, too [11].

The interaction of opioid peptides with 5HT and GABA was demonstrated in vertebrates, too. In the rat dorsal raphe nucleus, bath-applied met-Enk suppressed GABA-ergic inhibitory postsynaptic currents and it resulted in the inhibition of their projections to the serotonergic cells [39]. The GABA-induced inward current was also depressed by enkephalins in the bullfrog dorsal root ganglia [39] like in *Lymnaea* [26]. At presynaptic site met-Enk blocked 5HT-induced excitatory postsynaptic currents in pyramidal cells [16] proving that the main target of these interactions are the ion channels of the neuronal membrane both in vertebrates and invertebrates.

Our results and the above cited data emphasised the deep similarity between the network organization and behaviour of the network elements to alterations of homeostatic factors (e.g. peptides and neurotransmitters). The modulation of network and functional rewiring of the circuits seem to be similar as well. The interactions between opioid peptides and low molecular weight neurotransmitters were found to be similar, too.

Although the restricted forms and repertoire of behaviour of molluscs, including *Lymnaea*, cannot be compared to that of vertebrates, the neural networks are organized and functioning in a very similar way. It means that the elementary events such as ion channels and neural circuits are built up and function according to a common law. This is the reason why the models developed from molluscs can be successfully used for describing organization and modulatory principles using the same mathematical tools and signal molecules.

REFERENCES

1. Abi-Saab, W. M., Bubser, M., Roth, R. H., Deutch, A. Y. (1999) 5-HT_2 receptor regulation of extracellular GABA levels in the prefrontal cortex. *Neuro-psychopharmacology 20,* 92–96.
2. Barnes, S., Syed, N. I., Bulloch, A. G., Lukowiak, K. (1994) Modulation of ionic currents by dopamine in an interneurone of the respiratory central pattern generator of *Lymnaea stagnalis. J. Exp. Biol. 189,* 37–54.
3. Benjamin, P. R., Winlow, W. (1981) The distribution of three wide-acting synaptic inputs to identified neurons in the isolated brain of *Lymnaea stagnalis* (L.). *Comp. Biochem. Physiol. 70A,* 293–307.
4. Canavier, C. C., Baxter, D. A., Clark, J. W., Byrne, J. H. (1993) Nonlinear dynamics in a model neuron provide a novel mechanism for transient synaptic inputs to produce long-term alterations of postsynaptic activity. *J. Neurophysiol. 69,* 2252–2257.
5. Dickinson, P. S., Mecsas, C., Marder, E. (1990) Neuropeptide fusion of two motorpattern generator circuits. *Nature* (Lond), *344,* 155–158.
6. Elekes, K., Stefano, G. B., Carpenter, D. O. (1993) Enkephalin-like immunoreactive neurons in the central nervous system of gastropods (*Helix pomatia, Lymnaea stagnalis, Aplysia californica*): A comparative immunocytochemical study. *Cell Tissue Res. 272,* 329–341.
7. Ewadinger, N. M., Ridgway, R. L., Syed, N. I., Lukowiak, K., Bulloch, A. G. (1996) Identification and localization of a (Met)-enkephalin-like peptide in the mollusc, *Lymnaea stagnalis.* Brain Res. *737,* 1–15.

8. Harris-Warrick, R. M. (1988) Chemical modulation of central pattern generator. In: Cohen, A. H., Rossignol, S., Grillner, S. (eds) *Neural Control of Rhythmic Movements.* Wiley, New York, pp. 285–331.
9. Harris-Warrick, R. M., Marder, E. (1991) Modulation of neural networks for behaviour. *Ann. Rev. Neurosci. 14,* 39–57.
10. Hopper, S. L., Moulins, M. (1990) Cellular and synaptic mechanism responsible for a long-lasting restructuring of the lobster pyloric network. *J. Neurophysiol. 64,* 1574–1589.
11. Jansen, R. F., Pieneman, A. W., ter Maat, A. (1996) Spontaneous switching between ortho- and antidromic spiking as the normal mode of firing in the cerebral giant neurons of freely behaving *Lymnaea stagnalis. J. Neurophysiol. 76,* 4206–4209.
12. Kamardin, N. N., Szűcs, A., S.-Rózsa, K. (1999) Influence of $HgCl_2$ on the osphradial multisensory system of *Lymnaea stagnalis L. Acta Biol. Hung. 50,* 99–116.
13. Leung, M. K., Boer, H. H., Van Minner, J., Lundy, J., Stefano, G. B. (1990) Evidence for an enkephalinergic system in the nervous system of the pond snail, *Lymnaea stagnalis. Brain Res. 531,* 123–130.
14. Magoski, N. S., Bauce, L. G., Syed, N. I., Bulloch, A. G. (1995) Dopaminergic transmission between identified neurons from the mollusk, *Lymnaea stagnalis. J. Neurophysiol. 74,* 1287–1300.
15. Magoski, N. S., Bulloch, A. G. (1997) Localization, physiology, and modulation of a molluskan dopaminergic synapse. *J. Neurobiol. 33,* 247–264.
16. Marek, G. J., Aghajanian, G. K. (1998) 5-hydroxytryptamine-induced excitatory postsynaptic currents in neocortical layer V pyramidal cells: suppression by mu-opiate receptor activation. *Neuroscience 86,* 485–497.
17. Matsugu, M., Duffin, J., Poon, C. S. (1998) Entrainment, instability, quasi-periodicity, and chaos in a compound neural oscillator. *J. Comput. Neurosci. 5,* 35–51.
18. Meyrand, P., Simmers, J., Moulins, M. (1991) Construction of a pattern-generating circuit with neurons of different networks. *Nature* (Lond.) *351,* 60–63.
19. Molnár, G., Szűcs, A., S-Rózsa, K. (1999) Analysis and modulation of spike trains and oscillations in identified neural network of *Lymnaea stagnalis* L. *Acta Biol. Hung. 51,* 231–235.
20. Moroz, L. L. (1991) Monoaminergic control of respiratory behaviour in the freshwater pulmonate snail, *Lymnaea stagnalis* (L). In: Winlow, W., Vinogradova, O. S., Sakharow, D. A. (eds) *Signal molecules and behaviour.* Manchester Univ. Press, Manchester–New York, pp. 101–123.
21. Rekling, J. C. (1993) Effects of met-enkephalin on GABA-ergic spontaneous miniature IPSPs in organotypic slice cultures of the rat hippocampus. *J. Neurosci. 13,* 1954–1964.
22. Rubakhin, S. S., Szűcs, A., S.-Rózsa, K. (1996) Characterization of GABA response on identified dialysed *Lymnaea neurons. Gen. Pharmacol. 27,* 731–739.
23. S.-Rózsa, K. (1988) Modulation of membrane plasticity by low molecular weight neurotransmitters and opiate peptides in the *Helix* neurons. *Symp. Biol. Hung. 36,* 433–450.
24. S.-Rózsa, K. (1992) Reconstruction of neural networks is organized by co-existence of various signal molecules or input activation in *Helix pomatia L. Acta Biol. Hung. 43,* 127–136.
25. S.-Rózsa, K. (1995) Two types of reorganization in multifunctional neural networks of *Helix pomatia* L. *Acta Biol. Hung. 46,* 247–262.
26. S.-Rózsa, K., Rubakhin, S. S., Szűcs, A., Stefano, B. G. (1996) Met-enkephalin and morphiceptin modulate a GABA-induced inward current in the CNS of *Lymnaea stagnalis* L. *Gen. Pharmac. 27,* 1337–1345.
27. Salánki, J., S.-Rózsa, K. (1986) Interaction of opioid peptides and low-molecular-weight neurotransmitters in *Helix* neurons. In: Stefano, G. B. (ed.) *CRC Handbook of Comparative Opioid and Related Neuropeptide Mechanisms,* Vol. 2. CRC Press, Boca Raton, Florida, pp. 103–113.
28. Sandler, M. V., Ross, N. W. (1999) Serotonin modulates spike backpropagation and associated $(Ca^{2+})_i$ changes in the apical dendrites of hippocampal CA1 pyramidal neurons. *J. Neurophysiol. 81,* 216–224.
29. Smith, F. G., Parish, D. C., Benjamin, P. R. (1996) Met-enkephalin Arg-Phe-immunoreactive neurons in the central nervous system of the pond snail *Lymnaea stagnalis. Cell Tissue Res. 283,* 479–491.

30. Sokolov, V. A., Kamardin, N. N., Zaitseva, O. V., Tsirulis, T. P. (1980) Osphradial sensory system of gastropod mollusks. In: Sokolov, V. A. (ed.) *Sensory Systems.* Nauka, Leningrad, pp. 159–176. (in Russian).
31. Stanford, M. I., Cooper, J. A. (1999) Presynaptic μ and δ opioid receptor modulation of $GABA_A$ IPSPs in the rat globus pallidus in vitro. *J. Neurosci. 19,* 4796–4803.
32. Stefano, G. B. (1982) Comparative aspects of opioid-dopamine interaction. *Cell. Molec. Neurobiol. 2,* 167–178.
33. Syed, N. I., Winlow, W. (1991) Respiratory behaviour of the pond snail *Lymnaea stagnalis.* II. neural elements of the central pattern generator (CPG). *J. Comp. Physiol. 169A,* 557–568.
34. Szűcs, A., Molnár, G., S.-Rózsa, K. (1999) Periodic and oscillatory firing patterns in identified nerve cells of *Lymnaea stagnalis* L. *Acta Biol. Hung. 50,* 269–278.
35. Szűcs, A., S.-Rózsa, K., Salánki, J. (1998) Presynaptic modulation of *Lymnaea* neurons evoked by computer generated spike trains. *Neuro Report 9,* 2737–2742.
36. Takayanagi, H., Takeda, N. (1988) Coexistence of FMRFamide, met-enkephalin and serotonin in molluscan neurons. *Comp. Biochem. Physiol. 91A,* 613–620.
37. Werkman, T. R., van Minnen, J., Voorn, P., Steinbusch, H. W., Westerink, B. H., De Vlieger, T. A., Stoof, J. C. (1991) Localization of dopamine and its relation to the growth hormone producing cells in the central nervous system of the snail *Lymnaea stagnalis. Exp. Brain Res. 85,* 1–9.
38. Winlow, W., Syed, N. I. (1992) The respiratory central pattern generator of *Lymnaea. Acta Biol. Hung. 43,* 399–408.
39. Xi, Z. X., Akasu, T. (1997) Opioid peptides modulate GABA(A) receptor responses in neurons of bullfrog dorsal root ganglia. *Brain Res. 758,* 163–168.

Acta Biologica Hungarica 51 (2–4), pp. 231–235 (2000)

ANALYSIS AND MODULATION OF SPIKE TRAINS AND OSCILLATIONS IN IDENTIFIED NEURAL NETWORK OF *LYMNAEA STAGNALIS* L.[+]

G. MOLNÁR*, A. SZŰCS and KATALIN S.-RÓZSA

Balaton Limnological Research Institute of the Hungarian Academy of Sciences,
P. O. Box 35, H-8237 Tihany, Hungary

(Received: August 31, 1999; accepted: November 30, 1999)

Identified neurons and members of functionally characterized clusters of the central nervous system of *Lymnaea stagnalis* L. were studied. Long-term spike trains (10–100 min) were collected using current clamp method. Firing patterns were analyzed by several mathematical tools e.g.: spike density function (SDF), interspike interval (ISI), Fourier-transform. Both the spike trains and oscillation of firing were modulated by 5HT (2×10^{-5} M) and μ-opioid peptides (10^{-5} M). Co-application of 5HT (2×10^{-5} M) and DAGO (10^{-5} M) turned the firing of the neurons (RPeD1 and A cells) opposite to the running pattern and eliminated the 0.3 Hz oscillation causing a new slow periodicity (0.1–0.05 Hz).

Keywords: Lymnaea neurons – spike trains – network modulation – 5HT – opioid peptides.

INTRODUCTION

Neurons form the cardinal units of information processing within the central nervous system, and the action potentials they fire represent the major signal of information exchange. However, no single action potentials but neuronal spike trains are accepted as information carriers between the nerve cells and for neuronal coding. Although the spike trains of a single neuron more often belong to a chaotic type of firing without relevant functional consequences they can be characterized with formal mathematical tools revealing both hidden regularities and temporary modulations [2].

The spike density function (SDF) reflecting dynamic variable of the neuronal activity has been shown most appropriate for characterization of firing patterns for detecting slight changes in the neural firing due to synaptic influences or effects of neuromodulatory substances. Using this method the sensitivity of the given process and the stationary or chaotic character of the process studied in the long-term scale has been shown. This way, reorganization of synaptic inputs can be traced even if the MP remains unchanged within a short period of time. Further on, the interspike intervals (ISI) can be measured according to the time of arrival spike [8].

[+] Presented at the 9th ISIN Symposium on "Neurobiology of Invertebrates", July 1–5, 1999, Tihany, Hungary.

*Corresponding author, E-mail: molnarg@tres.blki.hu

0236-5383/2000/$ 5.00

In understanding information processing one should address the question, what is the message the spontaneous firing transfers and how the neurons can be forced to produce programmable pattern, or how it can be modulated by feeding altered parameters to the system.

We achieved the modulation of spike trains using chemical signals originating either from input variations or from their external application. For applying this method the well-characterized neural network of *Lymnaea* was used comprising central neurons involved into the regulation of several visceral functions where most of the physiologically relevant synaptic connections among moto- and interneurons are identified [3, 4, 5] and both rhythmic and oscillatory activities are generated [7, 8].

MATERIALS AND METHODS

The identified neurons and members of known clusters (RPeD1, J-, H-, A- and K-cells) from the isolated suboesophageal ganglionic ring of the adult pond snail *Lymnaea stagnalis* L. were used [1]. Long-term (10–100 min) spike trains were recorded using standard intracellular microelectrode technique with two-channel current-clamp amplifiers (Axoclamp-2A and home-built intracellular amplifiers). The experiments were carried out at room temperature (22–24 °C).

The method of spike train recording and data analysis have been described earlier [6]. Firing patterns were characterized by various mathematical tools including spike density function (SDF), interspike-interval (ISI) histograms, Fourier-transform and correlation analysis. Spike density functions were calculated by convolving the spike train with a smooth and continuous kernel function, Gaussian-type in most cases. Periodicities and oscillations of the firing rate were detected by Fourier-transform of the SDF. Cumulative interspike interval histograms also called ISI-autocorrelograms were used to detect periodicities in the spike trains and/or signs of precise spike timing. Detected periodic and oscillatory firing patterns in *Lymnaea stagnalis* L. were characterized in a previous paper [8].

In modulation of oscillatory firing pattern the following substances were used: 5-hydroxytryptamine creatinine sulphate (5HT), methionine enkephalin (MetEnk) and [D-Ala, N-Me-Phe, Gly-ol]-enkephalin (DAGO) (SIGMA). After a 10–15 minutes control measurement the neurotransmitters were applied by perfusion either alone or in combination to the surface of ganglia where the final concentrations were 2×10^{-5}–10^{-5} M.

RESULTS AND DISCUSSION

It has been shown that the spike density function (SDF) of A-cells and RPeD1 neuron can reveal correlations between their activity with two peaks ($f = 0.03$ Hz and 0.26 Hz positions) during synaptic activation of interneuron IP3. Additionally, a slow oscillation (0.1–0.3 Hz) can be demonstrated on a large number of visceral and pari-

etal neurons as well as on RPeD1 cell being more detectable if IP3 events are paused [8].

Our present experiments showed that both the alteration in firing patterns and the oscillations are closely related to the changes of the homeostasis of the neurons as they can be modulated by signal-molecules.

The fast synaptic transmitter (5HT) and the μ-opioid peptides (Met-enkephalin and DAGO) were found to cause characteristic changes both in firing pattern and oscillatory activity of the neurons in the identified neural network.

On the neuron RPeD1 the μ-opioid receptor agonist DAGO (10^{-5} M) caused a slight depolarization and the regular spiking became irregular (Fig. 1). During DAGO application the excitatory inputs running from interneuron IP3 to RPeD1 were decreased with a slightly modulated or unaltered oscillation (Fig. 1). In some cases additionally to 0.3 Hz oscillation a slow periodicity (150–250 s) appeared in SDF in the control and as a result of long-term DAGO treatment it disappeared and the firing pattern became irregular (Fig. 1, upper). The interspike interval histogram showed also different distributions in control and in the presence of DAGO (Fig. 1, bottom left). However, the 0.3 Hz oscillation seen on the Fourier spectra remained unaltered on the neuron RPeD1 treated by DAGO (Fig. 1, bottom right).

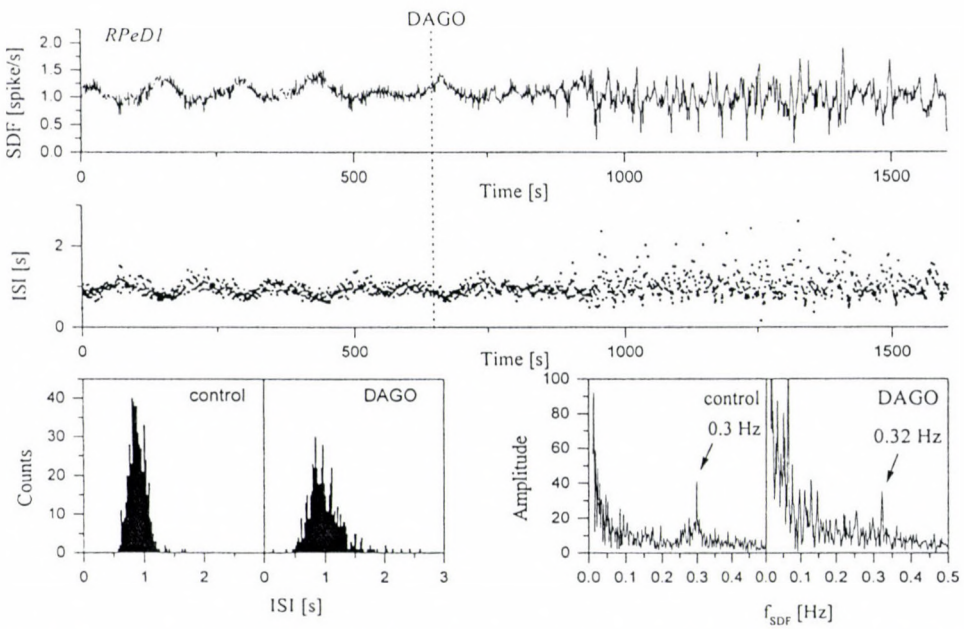

Fig. 1. The effect of DAGO on the oscillatory firing pattern of the neuron RPeD1. Additionally to the 0.3 Hz oscillation a slower periodicity can be seen on the SDF (top). The regular oscillation turned to an irregular type of firing observed only in long-term recording. The distribution of interspike interval histograms (bottom) was different. In contrary to the above changes the 0.3 Hz oscillation remained unaltered (shown with arrows in the Fourier spectra)

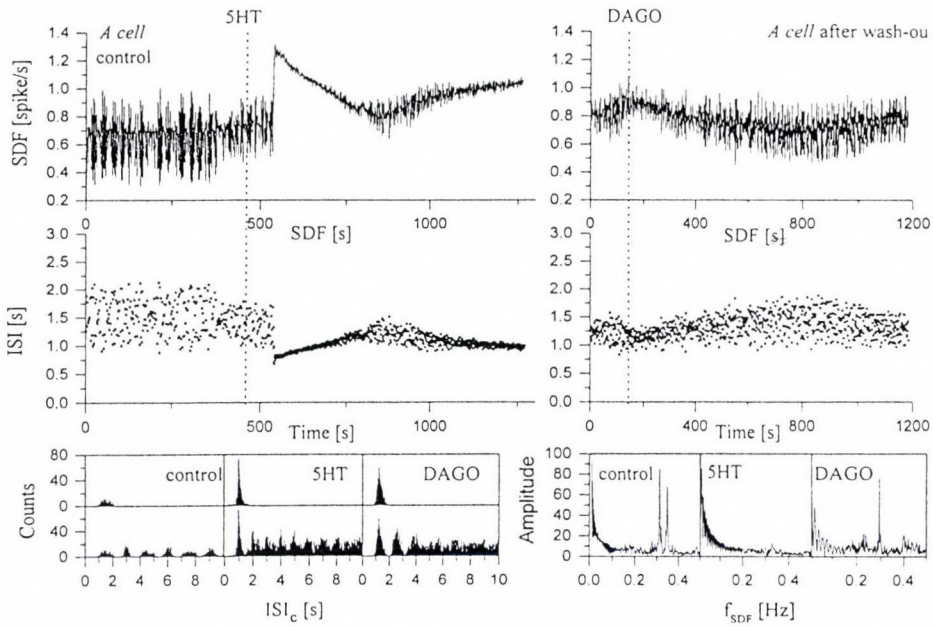

Fig. 2. Modulation of oscillatory firing pattern of an A cell by 5HT and DAGO. In control firing pattern of A cell two peaks of oscillation were found using Fourier diagram. In the top the spike density function (SDF) and in the middle the interspike interval plot (ISI) diagram can be seen. The difference between the control firing and after the application of the substances can be distinguished either in the plots or in the cumulative interspike interval histograms (ISI_c) (bottom). The cumulative ISI histograms demonstrate the changing in the spike timing of the firing. The Fourier spectra (f_{SDF}) show the frequency components of the spike density functions (SDF). In control in the firing patterns of RPeD1 a rare oscillation can be revealed with two components of frequency (0.3 Hz and 0.35 Hz). After application of 5HT depolarizing the cell both components of the oscillation were diminished. The washout did not, but the application of DAGO recovered one of the component of oscillation (0.3 Hz)

The effect of application of 5HT (2×10^{-5} M) and DAGO (10^{-5} M) was demonstrated on the A cell. In control firing pattern of A-cell, two peaks of oscillation can be seen using Fourier diagram corresponding to two frequency components (Fig. 2, control). Following 5HT treatment the membrane was depolarized and the firing pattern became more regular while both types of oscillations diminished. The washout did not but the application of DAGO partially recovered one of the component (0.3 Hz) of oscillations (Fig. 2, upper). The changes in the spike timing of firing was demonstrated by the cumulative ISI histograms (Fig. 2, lower).

Combined application of 5HT (2×10^{-5} M) with DAGO (10^{-5} M) to the neuron RPeD1 caused a hyperpolarization and turned the regular firing to irregular, the 0.3 Hz oscillation was intensified and a slow periodic oscillation (10–20 s) appeared. However, if before the combined treatment the neuron RPeD1 displayed an irregular firing, it became regular and the 0.3 Hz oscillation was eliminated but the slow periodic oscillation (10–20 s) appeared in this case, too. The changes caused by pairing

of 5HT and DAGO could be demonstrated on the neurons A, H, J and I as well. The simultaneous application of 5HT and Met-enkephalin to the neurons was less effective in modulation of firing pattern and oscillation, although it effected slightly the 0.3 Hz oscillation.

CONCLUSIONS

The methods developed for analysis of spike trains proved to be useful tools for detecting synchronization of firing in various neurons and for revealing the phasic, correlating events in the firing patterns. The spike density function (SDF) reflects both the activity of the neurons and the synaptic inputs modifying their firing patterns and reveals slow oscillations in neuronal spike trains.

The technique used in our present experiments provides meaningful information on the contribution of synaptic and neurochemical factors in modulating the neural activity. The results showed that 5HT and DAGO on the neuron RPeD1 modulated the firing pattern without influencing the 0.3 Hz oscillation, while on the A-cell additionally to firing pattern modulation the preexisting two oscillations (0.3 and 0.35 Hz) were as well eliminated. At the same time, the two above substances activated on both neurons a new slow periodic oscillation (10–20 s). Simultaneous application of 5HT and DAGO to the ganglia turned the running firing pattern to the opposite one (e.g. regular one to irregular, or vice versa) and the 0.3 Hz oscillation was either eliminated or restored. The activation of a slow periodic oscillation (10–20 s) was observed in co-application of the 5HT and DAGO.

The changes obtained in the identified network under the influence of neuromodulators might reflect reorganization of *Lymnaea* respiratory circuit, but their exact mathematical characterization remains to be formulated.

REFERENCES

1. Benjamin, P. R., Winlow, W. (1981) The distribution of three wide-acting synaptic inputs to identified neurons in the isolated brain of *Lymnaea stagnalis* (L.). *Comp. Biochem. Physiol. 70A,* 293–307.
2. Rieke, F., Warland, R., de Ruyter van Steveninck, R., Bialek, W. (1997) Spikes. Exploring the neural code. In: A Bradford Book. The MIT Press, Cambridge, Massachusetts, London, England, pp. 1–395.
3. Syed, N. I., Bulloch, A. G. M., Lukowiak, K. (1990) In vitro reconstruction of the respiratory central pattern generator of the mollusk *Lymnaea. Science 250,* 282–285.
4. Syed, N. I., Harrison, D., Winlow, W. (1991a) Respiratory behavior in the pond snail *Lymnaea stagnalis.* I. Behavioral analysis and the identification of motor neurons. *J. Comp. Physiol. 169A,* 541–555.
5. Syed, N. I., Winlow, W. (1991b) Respiratory behavior in the pond snail *Lymnaea stagnalis.* II. Neural elements of the central pattern generator (CPG). *J. Comp. Phys. 169 A* 557–568.
6. Szűcs, A. (1998) Application of the spike density function in analysis of neuronal firing patterns. *J. Neurosci. Meth. 81,* 159–167.
7. Szűcs, A., S.-Rózsa, K., Salánki, J. (1998) Presynaptic modulation of *Lymnaea* neurons evoked by computer generated spike trains. *Neuroreport 9,* 2737–2742.
8. Szűcs, A., Molnár, G., S.-Rózsa, K. (1999) Periodic and oscillatory firing patterns in identified nerve cells of *Lymnaea stagnalis L. Acta Biol. Hung. 50,* 269–278.

Acta Biologica Hungarica 51 (2–4), pp. 237–242 (2000)

NONLINEAR ACTIVITY OF IDENTIFIED *LYMNAEA* NEURONS+

M. Barbi[1]*, S. Chillemi[1], A. Di Garbo[1], G. Molnár[2] and A. Szűcs[2,3]

[1]Istituto di Biofisica del C.N.R., Pisa, Italy
[2]Balaton Limnological Research Institute, Hungarian Academy of Sciences, Tihany, Hungary
[3]INLS, University of California at San Diego, USA

(Received: August 31, 1999; accepted: November 30, 1999)

Two long-lasting discharges of action potentials were recorded from a buccal cell of the pond snail, respectively, before and after superfusing the preparation with low-calcium solution. The corresponding sequences of interspike intervals were then analysed by the nonlinear prediction methods. The results yield evidence of a small but clear nonlinearity only in the second of analysed tachograms. This finding is evaluated and discussed.

Keywords: Buccal neuron – interspike intervals – nonlinear prediction – surrogate data – S-maps.

INTRODUCTION

Most biological signals exhibit the irregular wandering behaviour typical of noise. With the diffusion by the mid-seventies of the *deterministic chaos* paradigm, the possibility of an alternative interpretation of this irregularity has been intensively investigated and some efficient and reliable methods for detecting nonlinearity – a necessary condition for chaos – became available; among them, the methods of *nonlinear prediction* simply implement the rationale that any level of determinism which is present in a system should manifest itself as some predictability in its evolution [3, 7].

In this paper, these methods are applied to the sequences of interspike intervals (or ISIs) recorded, either in normal conditions or after a treatment that lowers synaptic coupling, from a central neuron of the pond snail *Lymnaea stagnalis*. The comparative evaluation of the results should help us to identify the best conditions for detecting nonlinearity in this type of experimental data.

+ Presented at the 9th ISIN Symposium on "Neurobiology of Invertebrates", July 1–5, 1999, Tihany, Hungary.

*Corresponding author, E-mail: barbi@ib.pi.cnr.it

0236-5383/2000/$ 5.00

MATERIALS AND METHODS

Experimental data

Spontaneously firing (central) neurons of the brain of *L. stagnalis* were recorded intracellularly with standard techniques [8]. However, most recordings were unsuitable for the type of analysis to be performed on them, as either they were too short – less than a thousand spikes – or clearly nonstationary, or also exhibiting periodically modulated or bursting activity. So eventually the analysis was restricted to two long-lasting recordings from the same buccal neuron. But while the first was performed in normal saline, the second one was made in low-calcium solution, apt to depress the synaptic input to the cell. The action potentials were detected and the ISIs were measured and saved by computer [8]. The nonlinear prediction methods were then directly applied to two sequences of 2048 intervals, selected from the two recordings and called *tach1* and *tach2*, respectively. Now, it is worth noting that these ones are intrinsically different from the time series obtained by uniformly sampling a physical quantity. However, these methods can still be applied to such data and the features of the driving signal recovered from the ISIs [2, 3, 4]. In fact, they have also been applied to the analogous sequences of RR intervals measured on human ECG [1].

Nonlinear prediction method [3, 7]

Let $x_1, x_2, \ldots, x_N$, be the ISI sequence to be analysed. For every index point x_i, $i = 1 + (m-1)\,\tau, \ldots, N$, the m-dimensional *delay vector* $\boldsymbol{x}_i = (x_{i-(m-1)\tau}, \ldots, x_{i-\tau}, x_i)$ is considered, where m is the *embedding dimension* and t is the *embedding lag*. By running over the time series, the (N/100) vectors having the least Euclidean distance from x_i are found and the weighted average of their h steps ahead evolutions is adopted as the corresponding prediction $\hat{x}_{i+h}$ (noteworthy, a *local* prediction). This calculation is repeated for all index points and the root mean square error

$$\varepsilon(h) = \sqrt{\frac{1}{n}\sum_i \left(\hat{x}_{i+h} - x_{i+h}\right)^2}$$

is computed. Eventually, $\varepsilon(h)$ is divided by the series standard deviation σ, namely the average error incurred by always predicting the average, and so the Normalised Prediction Error (NPE) is obtained. NPE values close to zero imply strong nonlinear *predictability*, while values near 1 correspond to small predictability. As for the embedding parameters τ and m, their choice is important to correctly reproduce the system's space. Herein, the following criteria will be used: τ is set at the first minimum of the signal autocorrelation function, so trying to avoid oversampling. As for m, a quite small value of 4 is usually adopted, but then a check is made that higher m values do not modify the results significantly.

Surrogate data

Unfortunately, although for chaotic time series NPE rises to unity with prediction time in a typical way [11], autocorrelated random series can mimic this behaviour [1, 9]. So, to discriminate the nonlinear predictability, a deeper analysis is needed. This consists in generating a collection of artificial or *surrogate* data sets, which preserve some prescribed linear features of the raw data but are otherwise random. In this work, the so-called IAAFT surrogate time series [5] will be used, which maintain exactly the amplitude distribution and almost exactly the spectrum, of the original data. NPE is then calculated – as a function of prediction time – on all the surrogate series, and the value obtained on the original sequence is checked against the distribution of those of the surrogates. Taking just 19 IAAFT surrogates will entitle us, when the original data set's NPE is smaller than all of the surrogates, to *reject* the corresponding *null hypothesis* that the data are linear at the 5% level for 1-tailed test [9, 10].

S-maps method

This approach [6] is independent of the former one and much more direct. Here too, for every index point, a map is fitted to the system's flow in the phase space and the prediction – at one step in the future – is calculated. But now the map depends on a θ parameter, becoming ever more local (hence nonlinear) as θ is increased, therefore a clear decrease of

$$\frac{\varepsilon(1)}{\sigma}$$

with increasing θ implies nonlinearity.

RESULTS AND DISCUSSION

Figure 1a and b shows the two ISI sequences analysed. The long intervals are more pronounced for the first sequence (*tach1,* Fig. 1a) because of the greater strength of inhibitory synaptic inputs. In Fig. 2 a, b, the NPEs of both the original sequence and the surrogate ones are plotted against the prediction time h for *tach1* and *tach2*, respectively. Note that the higher value adopted for parameter d in the second case is due to the stronger autocorrelation of the *tach2* sequence; and the little linear predictability exhibited from the surrogate series derived from it corresponds to this feature. More importantly, Fig. 2 shows that a clear rejection of the linear hypothesis is only possible for *tach2*. In fact, in this case for all prediction times except one, the raw data's NPE is smaller than all the corresponding NPEs for the surrogate data; what doesn't occur for *tach2*. To further check this result we applied the S-maps method to the two sequences. Their NPEs are plotted against θ in Fig. 3. For tach1

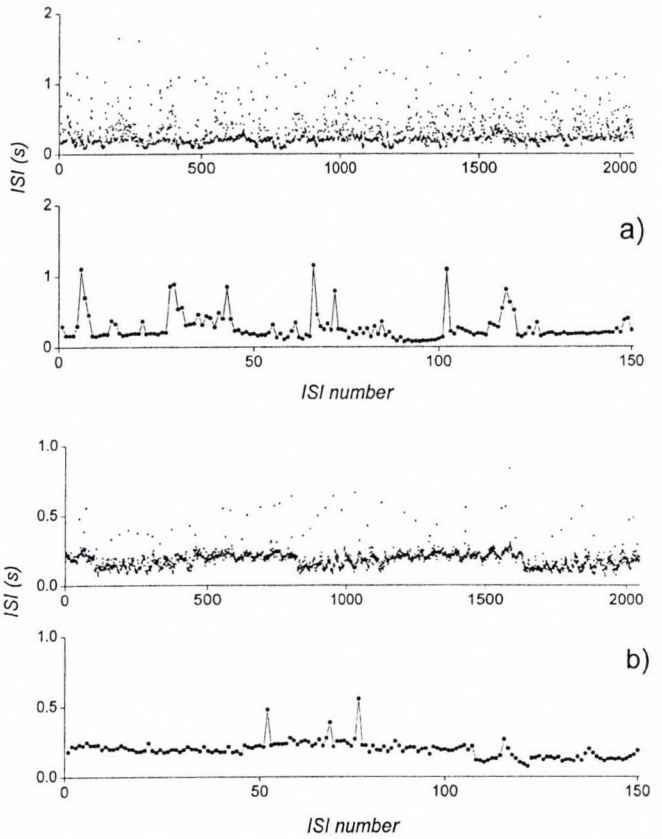

Fig. 1. Tachograms of the two segments analysed: (a) from the first recording (normal conditions), (b) from the second one (in low-calcium solution). Both figures show the complete ISI sequence (above) and a short segment with higher resolution (below)

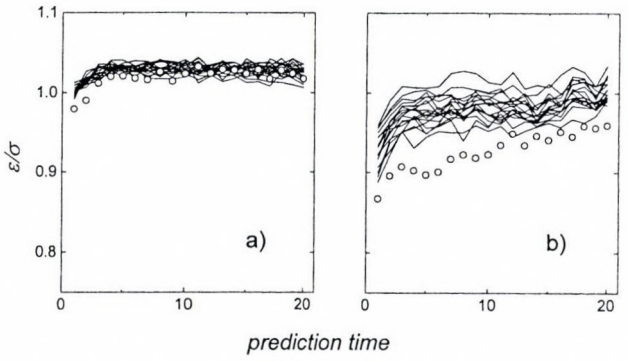

Fig. 2. Prediction curves for: (a) *tach1;* (b) *tach2.* Values of the analysis parameters: (a) $d = 4$, $m = 4$; (b) $d = 24$, $m = 4$

NPE only just decreases, whereas for *tach2* there is a clear initial decrease, implying nonlinearity. What confirms the former result that, for this particular neuron, its partial release from synaptic input makes nonlinearity of firing activity clearly detectable. In some way, the treatment should unmask the underlying nonlinear activity of the bare system. This interpretation suggests that neurons which do not receive strong synaptic inputs – as for instance neural pacemakers or central pattern generators – should also be the best candidates to exhibit nonlinear behaviour. This general conclusion must of course be checked by confirming our results on the firing patterns recorded from different types of neurons. In case of a successful result, nonlinearity could be used as a parameter either apt to identify the investigated cell or to evaluate the strength of its synaptic input.

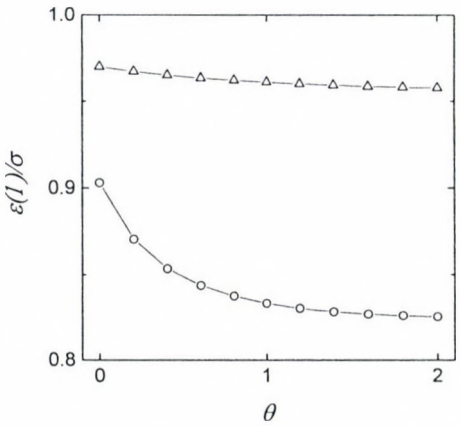

Fig. 3. S-map method. NPE is plotted against θ for *tach1* (triangles) and *tach2* (circles). The same values as in Fig. 2 are used for parameters d and m

REFERENCES

1. Barbi, M., Chillemi, S., Di Garbo, A., Balocchi, R., Carpeggiani, C., Emdin, M., Michelassi, C., Santarcangelo, E. (1998) Predictability and nonlinearity of the heart rhythm. *Chaos Solitons & Fractals 9,* 507–516.
2. S. Chillemi, S., Barbi, M., Di Garbo, A. (1997) Dynamics of the neural discharge in snail neurons. *BioSystems 40,* 21–28.
3. Longtin, A. (1993) Nonlinear forecasting of spike trains from sensory neurons. *Int. J. Bif. and Chaos 3,* 651–661.
4. Sauer, T. (1994) Reconstruction of dynamical systems from interspike intervals. *Phys. Rev. Lett. 72,* 3811–3814.
5. Schreiber, T., Schmitz, A. (1996) Improved surrogate data for nonlinearity tests. *Phys. Rev. Lett. 77,* 635–638.
6. Sugihara, G. (1994) Nonlinear forecasting for the classification of natural time series. *Phil. Trans. R. Soc. A 348,* 477–495.

7. Sugihara, G., May, R. (1990) Nonlinear forecasting as a way of distinguishing chaos from measurement error in a data series. *Nature 344,* 734–741.
8. Szücs, A. (1998) Applications of the spike firing density function in analysis of neuronal firing patterns. *J. Neurosc. Methods 81,* 159–167.
9. Theiler, J., Eubank, S., Longtin, A., Galdrikian, B., Farmer, J. D. (1992) Testing for nonlinearity in time series: the method of surrogate data. *Physica D 58,* 77–94.
10. Theiler, J., Prichard, D. (1996) Constrained-realization Monte-Carlo method for hypothesis testing. *Physica D 94,* 221–235.
11. Tsonis, A. A., Elsner, J. B. (1992) Nonlinear prediction as a way of distinguishing chaos from random fractal sequences. *Nature 358,* 217–220.

Acta Biologica Hungarica 51 (2–4), pp. 243–253 (2000)

MEMBRANE TRANSDUCTION PATHWAY IN THE NEURONAL CONTROL OF PROTEIN SECRETION BY THE ALBUMEN GLAND IN *HELISOMA* (MOLLUSCA)[+]

A. S. M. SALEUDDIN,* S. T. MUKAI, K. ALMEIDA and G. HATIRAS

Department of Biology, York University, Toronto, Ontario, M3J 1P3 Canada

(Received: August 31, 1999; accepted: November 30, 1999)

The albumen gland in *Helisoma* secretes a perivitelline fluid which surrounds each egg and is made up of several 66 kDa protein subunits and polysaccharide complexes. Forskolin, an adenylate cyclase activator, stimulated the secretion and release of the perivitelline fluid. An acidic extract of the central nervous system increased the intracellular concentration of cAMP in the albumen gland and this results in the release of the 66 kDa molecule and other proteins. Digestion of the brain extract with proteases abolished this activity, suggesting that the factor is a peptide. Cyclic AMP analogues and IBMX also stimulated the protein secretion in dose-dependent manner. Forskolin when added with the brain factor had an additive response. SQ22536, a non-competitive inhibitor of adenylate cyclase, inhibited brain extract dependent adenylate cyclase activity whereas aluminum fluoride, a G protein activator, was found to stimulate adenylate cyclase. Dopamine also stimulates protein secretion by the albumen gland and through the application of various agonists and antagonists of dopamine, it was established that the neurotransmitter acts via D_1-like receptors by stimulating adenylate cyclase.

Keywords: Mollusc – albumen gland – cAMP – adenylate cyclase – dopamine.

INTRODUCTION

Helisoma duryi is a freshwater hermaphroditic pulmonate mollusc which reproduces preferably by cross fertilization [20]. The albumen gland (AG), an exocrine female accessory organ, secretes perivitelline fluid (PVF) into the carrefour, the site of fertilization where each egg is coated with PVF following fertilization. The fertilized eggs are then transported via the female duct and are oviposited. The PVF is used for the nutrition of the developing embryos [9]. In *Helisoma,* the PVF is composed of several 66 kDa proteins and polysaccharide complexes [14].

The secretion of PVF in the carrefour must be synchronized with the arrival of eggs from the ovotestis via the hermaphroditic duct and this requires a precise control mechanism either directly by neurons, or indirectly by neurohormone(s). In AG

[+] Presented at the 9th ISIN Symposium on "Neurobiology of Invertebrates", July 1–5, 1999, Tihany, Hungary.

*Corresponding author, E-mail: saber@yorku.ca

0236-5383/2000/$ 5.00

of several pulmonates neuronal plexuses are found in the connective tissue that surrounds the gland [6, 8, 17] and thus the neuronal control of PVF secretion has been suggested [16]. Morishita et al. [14] on the other hand, showed that an acidic extract of the central nervous system (brain) stimulates protein secretion in the AG of *H. duryi*.

Information on the mode of action of neuronal factors, either peptides or neurotransmitters, on the reproductive tissues in pulmonate molluscs through the generation of second messengers is scanty. *In vitro* synthesis of galactogen by the AG of *Helix pomatia* was increased by cAMP analogues but the factor responsible for this increase is not known. In *Lymnaea stagnalis,* a crude extract of the cerebral commissure containing caudodorsal cell hormone (CDCH) stimulated *in vitro* polysaccharide synthesis in AG explants and the neuropeptide calfluxin stimulated intracellular calcium accumulation in the AG. Morishita et al. [14] showed that the secretion of PVF in the AG in *H. duryi* is controlled by a brain factor and that this is mediated by the cAMP transduction pathway. In this paper we offer a partial characterization of the AG adenylate cyclase (AC) activity and report that dopamine which also causes release of PVF, acts on the AG via D_1-like receptors.

MATERIALS AND METHODS

A laboratory population of *H. duryi* was maintained in 40 l glass aquaria under a 18L:6D photoperiod and fed boiled lettuce. Only adult snails measuring about 10 mm in shell diameter were used.

Brain extract preparation

The central nervous systems (CNS) minus the buccal ganglia, hereafter termed brains, were dissected out from reproducing snails and immediately frozen in liquid nitrogen. These brains were boiled in 1% acetic acid and peptides extracted according to Morishita et al. [14].

Membrane preparation

Albumen glands were dissected free of the connective tissue in HEPES-buffered saline (pH 7.4 and at 120 mOsmol kg H_2O), immediately frozen in liquid nitrogen and stored at –80 °C until used. Typically, 50–100 albumen glands were homogenized in a 24 ml glass-on-glass homogenizer (Kontes Glass Co., USA) in a buffer containing 50 mM Tris-HCl, 5 mM $MgCl_2$, 1 mM DTT (dithiothreitol), 1 mM EGTA, 1 mM PMSF (phenylmethylsulphonyl fluoride) at pH 7.5. The homogenate was centrifuged at 2000×*g* for 10 minutes. The supernatant was further centrifuged at 38 000×*g* for 30 minutes. The pellet was resuspended in buffer (see below) and the

protein concentration of the resuspended pellet was determined using the Bio-Rad (USA) protein assay kit. Each control sample consisted of the following: 25 µl of reaction mixture (50 mMTris-HCl, 5 mM $MgCl_2$, 1 mM DTT, 1 mM ATP, 1 mM theophylline, 1 mM EDTA, 5 mM creatine phosphate, 0.1 mg/ml creatine phosphokinase), 25 µl of resuspension buffer and 50 µl containing the equivalent of 10 µg of membrane protein. For test samples, the 25 µl of resuspension buffer contained the test substance: brain extract, forskolin, SQ 22536, $AlFl_4^-$ or GTP γS. For time course assays, triplicates of each time point (0, 5, 10 and 20 minutes) were made with the reaction initiated by the addition of membrane protein. The reaction was terminated by placing the samples in boiling water for 3 minutes. They were then frozen in dry ice and stored at –80 °C until needed for cAMP assay.

Protein secretion assay

Five albumen glands were dissected out, each cut in half and placed in HEPES-buffered saline. The *in vitro* protein secretion of the albumen gland explants was measured according to Morishita et al. [14]. The explants were placed individually in the wells of a culture plate each containing 100 µl of saline. After 60 minutes, the saline surrounding the AG was replaced with 100 µl fresh saline every 20 minutes, 100 µl of test agent (i.e., forskolin, $AlFl_4^-$, dopamine, dopamine agonists and antagonists) in saline was added, and the protein concentration in the well was measured using a modification of the Bio-Rad Protein assay [16]. When testing dopamine agonists and antagonists, positive controls were established by adding either dopamine or forskolin at the end of the experiment. After the last time point, each explant was blotted and weighed to the nearest milligram in order to normalize data.

RESULTS

Effect of the brain extract and other test agents

Preliminary experiments suggested that the membrane protein concentration of 10 µg/100 µl was sufficient to register a significant increase in cAMP concentration in response to 100 µM of forskolin and that this increase was linear during the first 10 minutes of the enzyme reaction. Thus the AC activity was measured in 10 µg of AG membrane protein after 10 minutes. Application of 1 be to AG membrane preparations elicited a significant increase in AC activity ($p = 0.008$) but 2 be produced no further increase (Fig. 1). Forskolin at three concentrations, 1 µM, 10 µM, 100 µM, significantly stimulated AC activity but the levels of increase at 10 µM and 100 µM were almost the same. Even 1 µM of forskolin caused a 2-fold increase in cAMP (Fig. 2). When 1 µM forskolin and 1 be are applied together, there is a synergistic effect compared to either brain extract or forskolin alone (Fig. 3). The AC inhibitor, SQ22536, significantly decreased AC activity ($p = 0.0329$) at 1 mM concentration

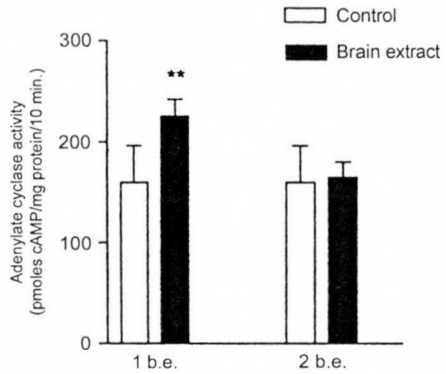

Fig. 1. Effect of brain extract on AC activity in AG membranes. One brain equivalent (be) elicited a significant response ($p = 0.008$), whereas 2 be did not

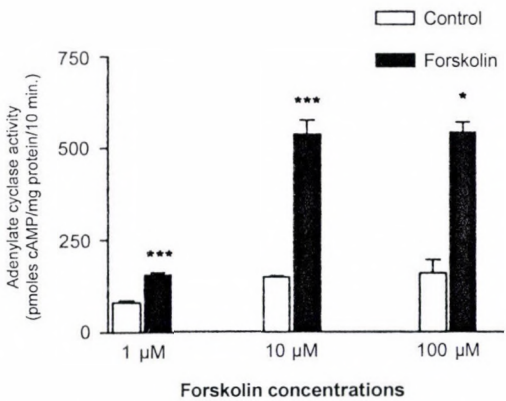

Fig. 2. Effect of forskolin on AC activity in AG membranes. Both 1 μM and 10 μM of forskolin caused significant increases ($p = 0.0006$) whereas 100 μM had lesser effect ($p = 0.0153$)

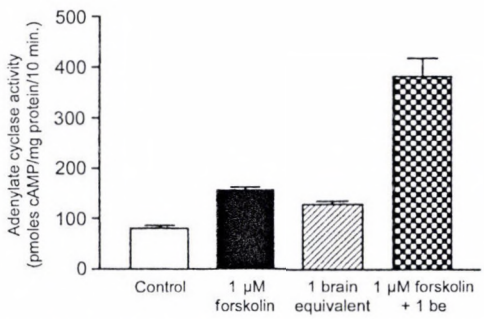

Fig. 3. Brain extract (1 be) plus forskolin potentiates AC activity compared forskolin or brain extract tested alone

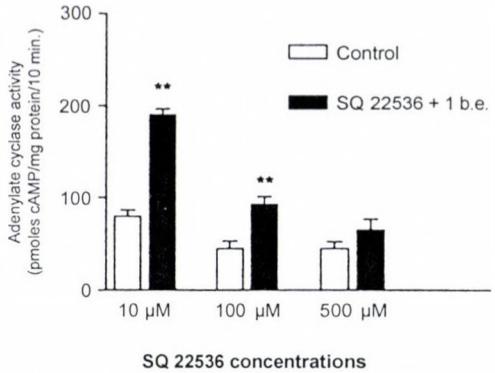

Fig. 4. Effect of SQ 22536 on AC activity. 500 μM significantly inhibited (p = 0.0329) AC activity whereas the inhibition was marginally significant at 100 μM (p = 0.0687)

but not at lower concentrations (Fig. 4). Interestingly, when various concentrations of SQ22536 and 1 be were applied together, a significant increase in AC activity was recorded at lower (10 μM and 100 μM) but not at a high inhibitor (500 μM) concentrations. A mixture of SQ22536 and forskolin caused a significant increase in AC activity compared to forskolin alone (Fig. 5). Aluminum fluoride (500), elicited a significant increase in AC activity but not at two lower concentrations (10–100 μM) (Fig. 6). GTPγS at all three concentrations (10, 100, 500 μM) significantly increased the AC activity in AG membrane preparations but the largest increase, 4-fold, was recorded at 100 μM (Fig. 7).

The effect of forskolin and $AlFl_4^-$ *on protein secretion*

Basal protein secretion *in vitro* was monitored for 60 minutes and then different concentrations of $AlFl_4^-$ were added for 20 minutes AG $AlFl_4^-$ increased AG protein secretion but the effect was highest at 1 mM (Fig. 8).

Effect of dopamine on protein secretion

In order to determine the effect of dopamine on AG protein secretion *in vitro,* various concentrations of dopamine (0.1, 1, 5, 10, 100 μM) were used. Of the concentrations tried, only 10 and 100 μM caused a very significant increase (p = 0.00095) whereas the other concentrations elicited a marginally significant increase (p = = ~0.07). When 100 μM dopamine is added to the AG explants after 60 minutes in culture, the protein secretion increased significantly but returned to the basal level by 120 minutes. Addition of 100 μM of forskolin at this point caused even more significant increase than dopamine (Fig. 9).

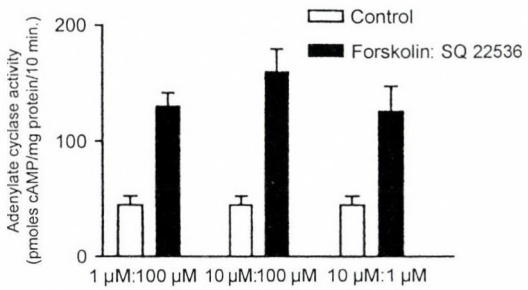

Fig. 5. Effect of forskolin plus SQ 22536 on AC activity. AC levels were slightly lower than the effect of forskolin alone. AC levels between experimental and control levels were significantly different at all concentrations used ($p < 0.0008$) but not different between experimental groups

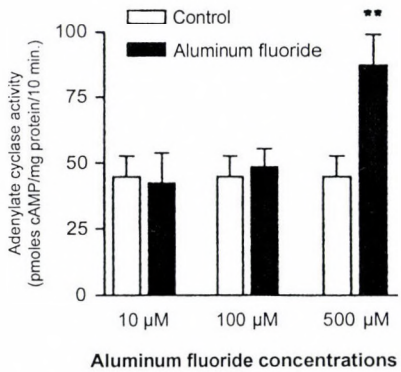

Fig. 6. Effect of $AlFl_4^-$ on AC activity. A significant increase was recorded at a concentration of 500 μM

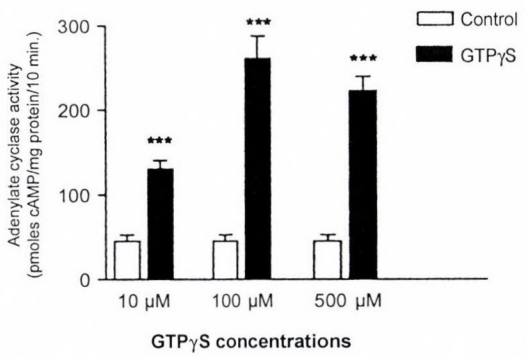

Fig. 7. Effect of GTPγS on AC activity. All three concentrations (10, 100, 500 mM) significantly increased AC activity ($p < 0.001$)

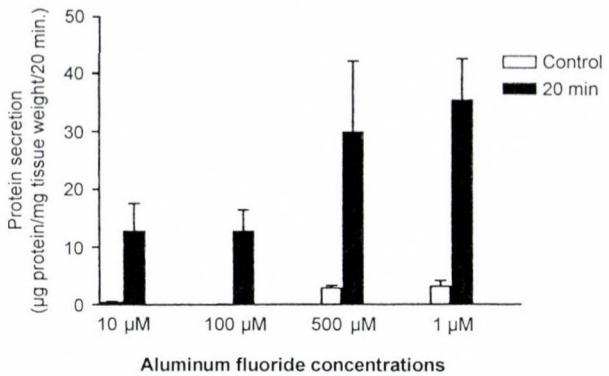

Fig. 8. Effect of $AlFl_4^-$ on protein secretion in AG explants. At 100 µM and 1 mM the protein secretion was significantly increased ($p < 0.0862$)

Effect of dopamine agonists and antagonists on protein secretion

Of the three agonists tried, only 2-amino-6,7-dihydroxy-1,2,3,4-tetrahydronapthalene caused a significant increase in protein secretion in AG *in vitro* whereas bromocriptine, a general DA agonist, and benzazepine (SKF-38393), a D_1 receptor specific agonist, did not (Fig. 10). In general, antagonists to D_2-like receptors (spiperone, eticlopride haloperidol) did not block DA-induced protein secretion whereas a D_1 receptor antagonist (benzazepine, SCH-23390) and a general antagonist (butaclamol) caused a significant decrease in protein secretion (Fig. 11).

DISCUSSION

There is evidence to suggest that membrane transduction via AC/cAMP plays an important role in the function of various molluscan tissues [1, 7, 10, 18]. A 280 kDa glycoprotein has been characterized from the AG of *H. duryi* which is composed of several 66 kDa subunits and polysaccharide complexes. *In vitro* secretion of this glycoprotein can be stimulated by forskolin, cAMP and brain extract [14]. These authors identified immunoreactive G protein α subunits in AG membrane preparations. However, what is less clear is the signal transduction pathway from receptor ligand binding to the production of cAMP. We raise the following questions: Are the receptors for the brain factor(s) G protein linked? Which G proteins are involved in mediating AC production? In this paper we will discuss the above questions in the context of our results obtained by the use of two naturally present ligands and their agonists and antagonists, and activators and inhibitors of AC.

The AC activator forskolin was found to increase AC activity and increase AG protein secretion. Similar results were found by Morishita et al. [14]. Mukai [16] reported that forskolin increased cAMP levels in the AG. Forskolin and brain extract

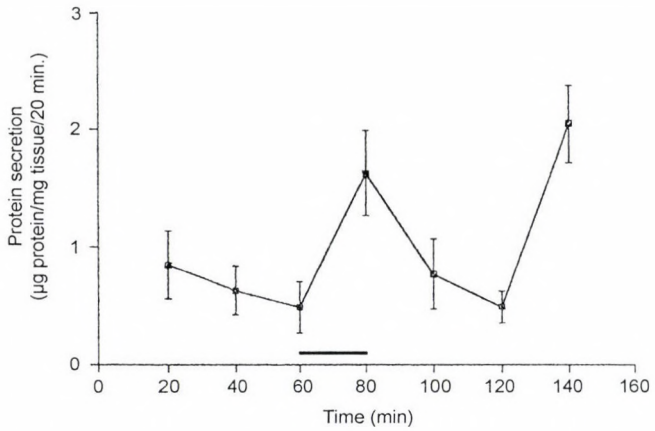

Fig. 9. Effect of 100 µM dopamine on protein synthesis in AG explants. Basal protein secretion was measured for 60 minutes at which point dopamine was added and this caused a 2-fold increase in protein secretion. Addition of forskolin at 120 minutes resulted in a larger (4-fold) increase

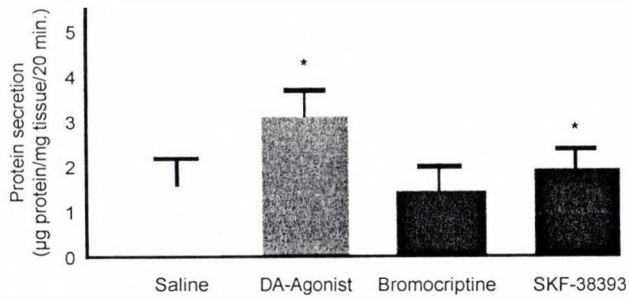

Fig. 10. Effect of dopamine receptor agonists on protein secretion. Only "DA-agonist" (2-amino-6,7-dihydroxy-1,2,3,4-tetrahydronapthalene) elicited a significant increase ($p < 0.0473$)

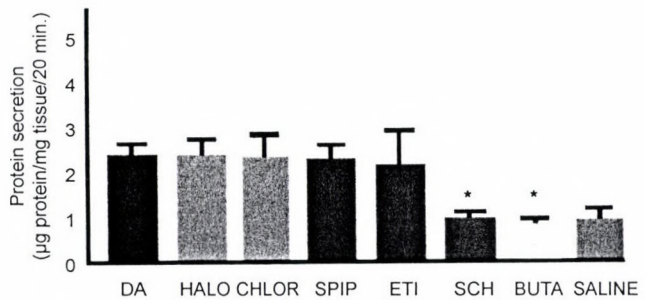

Fig. 11. Effect of some dopamine receptor antagonists on protein secretion. Only butaclamol ($p = 0.0095$) and SCH 23390 ($p = 0.0824$) inhibited protein secretion. DA – dopamine; HA – haloperidol; SPIP – spiperone; ETI – eticlopromide; SCH – SCH-23390; BUTA – butaclamol

when applied together to AG membrane preparations synergistically activated AC activation. Although forskolin binds directly to the cytoplasmic loop of AC, and does not act directly on G proteins, forskolin and brain extract input via G_s to AC are not independent of each other. In many systems, forskolin increases not only the apparent potency of the receptor agonist but also the maximum response elicited by the agonist [21]. This line of evidence suggests that forskolin interacts directly to AC causing an increase in cAMP, which in turn stimulates protein secretion in the AG.

The compound SQ22536 was found to inhibit AC activity at a concentration of 500 μM. Haslam et al. [12] and Goldsmith and Abrams [11] reported similar inhibition while working on human platelets and *Aplysia* sensory neurons, respectively. Adenylate cyclase is also inhibited by adenosine, 3'-AMP and other related analogues. It is thought that SQ22536 interacts with the C_1 and C_2 cytoplasmic domains of AC and that adenosine analogues and SQ22536 do not compete with the substrate [23]. For example, the application of forskolin and SQ22536 together to AG membrane preparations did not inhibit AC activity (this study), and Sunahara et al. [22] reported AC inhibition by SQ22536 is independent of the presence of forskolin in the medium. Thus, forskolin was able to bind to its sites which may be near or at, those for SQ22536 without competition.

The application of SQ22536 plus the brain extract to AG membrane preparations increased AC activity. If the SQ22536 binds directly to AC sites, whereas the brain extract does not, why then there is no inhibition? We provide two possible explanations: first, we showed in this study that at low SQ22536 concentrations, the brain extract augmented high AC activity but at a high concentration (500 μM) it did not. Thus at a higher concentration of SQ22536, most of the P-sites are occupied causing the inhibition. Secondly, there may be different AC isoforms in the AG membrane some of which are activated by the brain extract and others which are inhibited via by SQ22536 via on P-sites.

The ability of GTPγS, a potent G protein activator, to increase AC activity in the AG membrane provides further evidence of the presence of a $G_{s\alpha}$. GTPγS activates $G_{s\alpha}$ and the subunit exchanges GDP for GTPγS for its activation and as AC-$G_{s\alpha}$-GTPγS is stable, the rise in cAMP will be prolonged [4]. Thus GTPγS has proved to be useful in prolonging AC activity and in determining the presence of the α_s subunit of G protein.

Aluminum fluoride activates AC in the membranes of various mammalian tissues [5, 13]. Aluminum fluoride not only activates AC in membrane preparations of AG at 500 μM but it is also able to increase protein secretion in AG explants even at 10 μM. The ability of $AlFl_4^-$ to bind with the γ-phosphate of GTP which activates G protein is primarily the cause of increased protein secretion in AG and this effect of $AlFl_4^-$ is concentration dependent again suggesting the presence of GTP activated Gα subunit in the membrane of AG.

Dopamine is a common biogenic amine found in the CNS of molluscs which has been implicated in various physiological functions such as feeding, respiration, gill movement, and egg laying behaviour [15, 19, 24, 25]. Although the AG is directly innervated by the CNS, dopamine containing neurons have not been identified.

Neuron endings containing neurosecretory granules are commonly found in the basal regions of the AG cells (Saleuddin, unpublished results). Mukai [16] reported that dopamine stimulates the secretion of a 66 kDa protein in the AG of *H. duryi.* Biochemical, pharmacological and neurophysiological evidence suggest that mammalian and molluscan dopamine receptors show some similarities in their membrane transduction pathways. The present study confirms that physiological doses of dopamine increases protein secretion significantly.

Dopamine receptors occur in two broad categories, D_1-like (D_1 and D_5) and D_2-like (D_2, D_3, D_4). In this study various agonists and antagonists of dopamine have been tried in order to identify, the nature of dopamine receptor involved in the release of protein in the AG. Of the three agonists tried, only DA-agonist caused a significant protein release. The D_2 antagonists such as, benzamide eticlopride, butyrophenones spiperone, haloperidol and chlorpromazine, did not effect dopamine mediated release of protein and this suggests that protein secretion is mediated by D_1-like rather than D_2-like receptors. Based on pharmacological and neurophysiological studies, Ali and Orchard [2] reported that dopamine stimulation of cAMP in the salivary gland of the locust, *Locusta migratoria* is mediated by D_1-like receptors. Like the results of the present study, they also found that dopamine agonists were generally ineffective. Furthermore, it has been shown that vertebrate dopamine receptor agonists are not effective in several other insect studies [3] suggesting the agonist binding sites in invertebrates are different from those in vertebrates.

One distinctive feature between D_1- and D_2-like receptors is the mode of receptor mediated signal transduction. The D_1 family receptors mediate biological activity through the activation of AC/cAMP whereas the D_2 family receptors generally inhibit this pathway. Morishita et al. [14] demonstrated that the AC activator forskolin and a cAMP analogue, 8-bromo cAMP stimulated protein secretion in the AG of *H. duryi.* In this study, forskolin was also found to have a stimulatory effect on protein secretion which combined with the fact that dopamine was able to stimulate the AC activity causing AG protein release suggest that D_1-like receptors are involved.

ACKNOWLEDGEMENTS

This work was supported by the National Science and Engineering Council of Canada. We thank Dr. B. G. Loughton and Tania Di Renna for help in the preparation of the manuscript.

REFERENCES

1. Abraham, I., Khan, H. R., Saleuddin, A. S. M. (1991) The elevation of cAMP levels by a putative diuretic hormone in the osmoregulatory organs of the freshwater snail *Helisoma duryi. Can. J. Zool. 69,* 2800–2804.
2. Ali, D., Orchard, I. (1994) Characterization of dopamine and serotonin receptors on the salivary glands of the locust, *Locusta migratoria. Biogenic Amines 10,* 195–212.
3. Baines, R. A., Downer, R. G. H. (1991) Pharmacological characterization of a 5-hydroxytryptamine sensitive receptor/adenylate cyclase complex in the mandibular closer muscles of the cricket, *Gryllus domestica. Arch. Insect Biochem. Physiol. 16,* 153–163.

4. Barritt, G. J., Gregory, R. B. (1997) An evaluation of strategies available for the identification of GTP-binding proteins required in intracellular signaling pathways. *Cell. Signal. 9,* 207–218.
5. Bigay, J., Deterre, P., Pfister, C., Chabre, M. (1987) Fluoride complexes of aluminum or beryllium act on G-proteins as reversibly bound analogues of the γ phosphate of GTP. *The EMBO Journal 6,* 2907–2913.
6. Brisson, P. (1982) Aminergic structures in the genital tract of pulmonate gastropods and their possible role in the reproductive system. In: Lever, J., Boer H. H. (eds) *Molluscan Neuroendocrinology.* North-Holland Publishing Co., Amsterdam, pp. 120–125.
7. deJong-Brink, M., Bergamin-Sassen, M. J. M., Kuyt, J. R. M., Tewari-Kanhai, A. L. (1986) Enzyme cytochemical evidence for the activation of adenylate cyclase in the follicle cells of vitellogenic oocytes by the dorsal body hormone in the snail *Lymnaea stagnalis. Gen. Comp. Endocrinol. 63,* 212–219.
8. deJong-Brink, M., Goldschmeding, J. T. (1983) Endocrine and nervous regulation of female reproductive activity in the gonad and albumen gland of *Lymnaea stagnalis.* In: Lever, J., Boer, H. H. (eds) *Molluscan Neuroendocrinology.* North-Holland Publishing Co., Amsterdam, pp. 126–131.
9. Duncan, C. J. (1975) Reproduction. In: Fretter, V., Peake, J. (eds) *Pulmonates, Vol. 1.* Academic Press, New York, pp. 309–365.
10. Ferretti, M. E., Sonetti, D., Pareschi, M. C., Biondi, C. D. (1993) Effects of the small cardioactive peptide B (SCP_B) on adenylate cyclase of the central nervous system and peripheral organs of the freshwater snail *Planorbarius corneus. Neurochem. Int. 22,* 479–486.
11. Goldsmith, B. A., Abrams, T. W. (1991) Reversal of synaptic depression by serotonin at Aplysia sensory neuron synapses involves activation of adenylyl cyclase. *Proc. Natl. Acad. Sci. USA. 88,* 9021–9025.
12. Haslam, R. J., Davidson, M. M. L., Desjardins, J. V. (1978) Inhibition of adenylate cyclase by adenosine analogues in preparations of broken and intact human platelets. *Biochem. J. 176,* 83–95.
13. Jamali, A. E., Rachdaoui, N., Jacquemin, C., Correze, C., (1996) Long-term effect of forskolin on the activation of adenylyl cyclase in astrocytes. *J. Neurochem. 67,* 2532–2539.
14. Morishita, F., Mukai, S. T., Saleuddin, A. S. M. (1998) Release of proteins and polysaccharides from the albumen gland of the freshwater snail *Helisoma duryi:* Effect of cAMP and brain extracts. *J. Comp. Physiol. A182,* 817–825.
15. Moroz, L. L., Winlow, W. (1992) Respiratory behaviour in *Lynmaea stagnalis:* pharmacological and cellular analyses. *Acta Biol. Hung. 3,* 88.
16. Mukai, S. T. (1998) Involvement of the endocrine dorsal bodies and the central nervous system on the physiology of reproduction in *Helisoma duryi* (Mollusca: Pulmonata). Ph. D Thesis. York University, Toronto, Ontario.
17. Nieland, M. L., Goudsmit, E. M. (1969) Ultrastructure of galactogen in the albumen gland of *Helix pomatia. J. Ultrastr. Res. 29,* 119–140.
18. Reich, G., Doble, K. E., Price, D. A., Greenberg, M. J. (1997) Effects of cardioactive peptides on myocardial cAMP levels in the snail *Helix aspersa. Peptides, 18,* 335–360.
19. Ruben, R., Lokowiak, K. (1983) Modulation of the *Aplysia* gill withdrawal reflex by dopamine. *J. Neurobiol. 14,* 271–284.
20. Saleuddin, A. S. M., Ashton, M. L., Schollen, L. M., Brekenridge, W. R., Myksys, S. L. (1983) Studies on endocrine control of reproduction in *Helisoma* and *Helix.* In: Lever, J. and Boer, H. H. (eds) *Molluscan Neurobiology.* North-Holland Publishing Co., Amsterdam, pp. 138–141.
21. Seamon, K. B., Daly, J. W. (1983) Forskolin, cyclic AMP, and cellular physiology. *Tr. Biochem. Sci. 4,* 120–123.
22. Sunahara, R. K., Dessauer, C. W., Gilman, A. G. (1996) Complexity and diversity of mammalian adenylyl cyclases. *Ann. Rev. Pharmacol. Toxicol. 36,* 461–480.
23. Tang, W. J., Gilman, A. G. (1992) Adenylyl cyclases. *Cell. 70,* 869–872.
24. Trimble, D. L., Barker, D. L. (1984) Activation by dopamine of patterned motor output from the buccal ganglia of *Helisoma trivolvis. J. Neurobiol. 15,* 37–48.
25. Wekman, T. C., De Vlieger, T. A., Stoof, J. C. (1990) Indications for a hormonal function of dopamine in the central nervous system of *Lymnaea stagnalis. Neuroscience Letters, 108,* 167–172.

Acta Biologica Hungarica 51 (2–4), pp. 255–264 (2000)

CHANGES IN MOLLUSCAN NEUROSECRETORY CELLS DURING REPRODUCTIVE CESSATION: CAUSE OR EFFECT?+

C. JANSE*

Department of Biology, Vrije Universiteit, 1091HV, Amsterdam, The Netherlands

(Received: August 31, 1999; accepted: November 30, 1999)

The pond snail *Lymnaea stagnalis* has a maximum life span of about 22 months. At the age of about 250 days animals start to decrease egg laying activity and at about 500 days most animals ceased egg laying activity. At the age of cessation of egg laying the neurosecretory caudodorsal cells (CDCs) which control egg laying in *Lymnaea* exhibit reduced branching patterns. At this stage the cells still exhibit their physiological properties. CDCs still contain biologically active peptides and in the isolated CNS they still exhibit an afterdischarge upon electrical stimulation. Probably in the intact animal cessation of egg laying occurs because the CDCs are not activated anymore by natural egg laying inducing stimuli. In very old animals CDCs exhibit signs of degeneration indicating that cell death occur. After an extended period of no egg laying of *Lymnaea* physiological changes occur in the CDCs. CDCs from animals after an extended period of no egg laying failed to exhibit an afterdischarge. In such CDCs chemical and electrical coupling among the CDCs are reduced.

Morphologically reduced CDCs predominantly fail to exhibit an afterdischarge. However, there are minimally branched CDCs that still could give an afterdischarge. Probably morphological reduction is not the only factor that defines afterdischarge failure. At present we suggest the following sequence of changes. 1. Morphological reduction of CDC branching patterns. 2. Cessation of egg laying. 3. Physiological changes in the CDCs resulting in afterdischarge failure. 4. Further morphological and physiological deterioration of CDCs.

Keywords: Mollusc – *Lymnaea stagnalis* neurosecretory cells – egg laying – reproductive senescence – morphology – neurophysiology.

INTRODUCTION

In many animal species female reproductive activity ceases at old age. In mammals, during senescence profound changes take place in the endocrine system that controls reproductive activity. These changes either result from oocyte depletion in the ovaries or from changes in brain centres that control reproductive activity [29]. In mammals as yet experimental results are not decisively in favour of one or the other hypothesis. Reproductive cessation also occurs among the lower animals [5]. Mol-

+ Presented at the 9th ISIN Symposium on "Neurobiology of Invertebrate", July 1–5, 1999, Tihany, Hungary.

*E-mail: cjanse@bio.vu.nl

0236-5383/2000/$ 5.00

luscs, especially several gastropod species, provide suitable model systems for studies on neuroendocrine control of reproduction [8]. Among the gastropods *Lymnaea* has a well-known nervous and neuroendocrine system and much is known on the biology and physiology of the animal and on the neuroendocrine control of female reproductive activity. In addition, the nervous and the neuroendocrine system are well accessible for different techniques [8]. This paper describes the role of the neuroendocrine caudodorsal cells (CDCs) in reproductive senescence of *Lymnaea*.

Survival and reproductive activity during the life of Lymnaea

Lymnaea cultured under laboratory conditions, has a median life span of about 12 months and a maximum life span of about 22 months. The age-specific death rate increases with age resulting in a rectangular survival curve (Fig. 1A) which is characteristic for ageing animals [9, 24]. In cultured *Lymnaea*, egg laying starts at an age of about 90 days. Up to an age of about 250 days the number of egg masses produced per snail and the number of eggs per egg mass increases. At about 250 days animals start to decrease egg laying and the first animals cease egg laying [9]. *Lymnaea* exhibits a considerable individual variability in the age at which it enters its post-reproductive state. At about 500 days of age most animals have ceased egg-laying activity and are in their post-reproductive period (Fig. 1B). Only of few molluscan

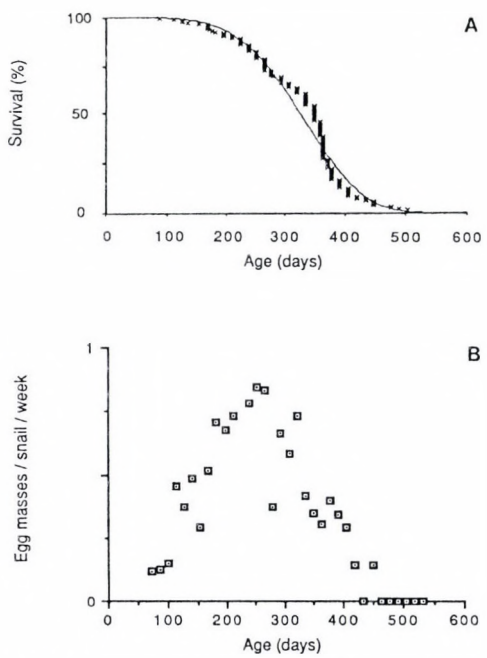

Fig. 1. Survival (A) and egg laying (B) of *Lymnaea* with age

species the fate of the animals after their reproductive period is known. The opisthobranch *Aplysia* [27] and the cephalopod *Octopus* die shortly after cessation of reproductive activity. In *Octopus* this is caused by inhibition of eating behaviour after egg laying is completed [28].

In Lymnaea *the neurosecretory egg laying controlling CDCs are physiologically intact at cessation of egg laying*

In the pond snail *Lymnaea stagnalis* egg laying is under neuroendocrine control. The paired dorsal bodies (DBs), comprising the only real endocrine organ of the animal, control oocyte growth and maturation and secretory activity of the female accessory sex organs [6, 7, 19]. The neurosecretory caudodorsal cells (CDCs) in the brain of *Lymnaea* control egg-laying behaviour. CDCs occur in two groups of about 50 cells, each group is located in one of the paired cerebral ganglia. The CDCs contain a great number of different peptides [7, 22]. Just before the start of ovulation and egg laying the CDCs exhibit massive characteristic electrical discharge activity that lasts about one hour and secrete CDC hormone and multiple other peptides into the haemolymph. This induces a stereotyped pattern of overt and covert behaviours which terminates in the deposition of an egg mass (Fig. 2) [8]. In the isolated central nervous system intracellular stimulation of one CDC induces the characteristic electrical activity (afterdischarge) (Fig. 3B).

Old non-reproductive animals still lay eggs upon injection with artificial hormone and their CDCs still contain active CDC hormone [10, 17]. Obviously, these animals

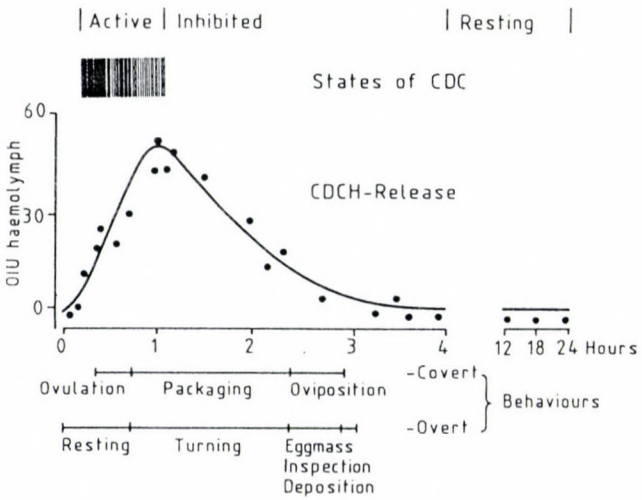

Fig. 2. CDC electrical activity induces an increase in CDC-hormone (CDC-H) level (OIU: ovulation inducing units) and the characteristic covert and overt behaviours of *Lymnaea* during egg laying. For further explanation see text

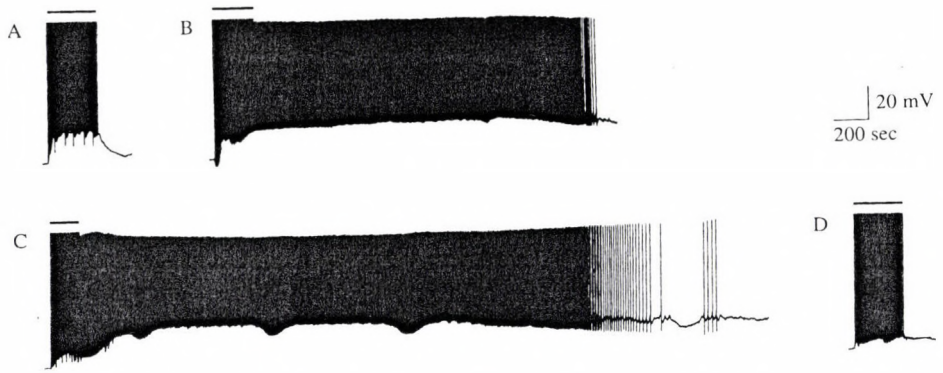

Fig. 3. Repeated electrical stimulation does not induce an afterdischarge in CDCs in the inhibited state from egg-laying animals (A) and in old animals that did not lay eggs for more than 8 weeks (D). An afterdischarge is induced in resting state CDCs from egg-laying animals (B) and in CDCs from animals that did not lay eggs for about 4 weeks (C)

do not release CDC hormone (in sufficient amounts). Old animals that ceased reproduction respond less to CDC-hormone injection than old still reproductive animals of the same age [10]. In *Lymnaea*, sensitivity of female reproductive organs to CDC hormone is controlled by hormone secreted by the DBs [3, 4, 19]. DBs in old animals degenerate [18], thus in old non-laying animals DB-hormone levels in the blood might be decreased. This might explain the decrease in sensitivity of peripheral female reproductive organs to CDC hormone. Implantation of cerebral ganglia of young animals (3 months of age), including the DBs, into old (10 months) animals with reduced egg laying indeed induces an increase of the egg-laying frequency [12].

In *Lymnaea* cessation of female reproductive activity is not primarily due to the CDCs not being able to produce the electrical discharge activity; CDCs in the isolated CNS from animals that ceased egg laying still produce an afterdischarge upon electrical stimulation (Fig. 3C) [10]. CDCs of post-reproductive animals brought into afterdischarge by electrical intracellular stimulation still exhibit morphological characteristics of active secretion [13]. Moreover, CDCs in the isolated CNS from post-reproductive animals, electrically brought into afterdischarge still secrete peptides that activate CDCs in an isolated CNS kept in the same recording basin [Janse, unpublished results). This indicates that CDCs in animals that just ceased egg laying can still release peptides but probably do not do so because they remain electrically silent.

Physiological changes in CDCs do occur but after the animal ceases egg laying

Electrophysiological experiments showed that CDCs of old non-reproducing animals can easily be brought into afterdischarge with electrical stimulation [10]. Such CDCs exhibit a longer lasting afterdischarge than those of both old and young reproductive

animals. However, in animals after 8 weeks of no egg laying, electrical stimulation fails to induce an afterdischarge in the CDCs. This indicates that after a prolonged period of no egg laying, CDCs lose the ability to respond with an afterdischarge upon electrical stimulation (Fig. 3D) [16].

To insure synchronous discharges, CDCs in adult egg-laying animals are chemically and electrically coupled [1, 26]. Each CDC is electrically coupled to the other CDCs (including the contralateral ones) and receives peptidergic input from other CDCs as well as from itself. Electrical coupling has an efficacy of about 5% (postsynaptic response related to the presynaptic voltage change) (Fig. 4). The excitatory peptidergic input is activated by action potentials in the same or in one of the other CDCs and consists of a depolarizing after potential (DAP) (Fig. 4). The amplitude of the DAP provides a measure for the efficacy of peptidergic transmission among CDCs [1]. Efficacy of peptidergic transmission varies during the egg-laying cycle and the concurrent changes in CDC excitability. Resting state CDCs (animals one or more days after egg mass production, electrical stimulation readily induces an afterdischarge (Fig. 3B), [21] exhibit DAPs with a high amplitude and CDCs in the inhibited state (animals immediately after egg laying, electrical stimulation fails to induce an afterdischarge (Fig. 3A), [21] exhibit DAPs with a low amplitude [1].

DAP amplitude and electrical coupling also differ among CDCs from animals which differ in egg-laying history. Table 1 shows results of measurements of DAP amplitudes in CDCs (induced by actionpotentials from a contralateral CDC) and of

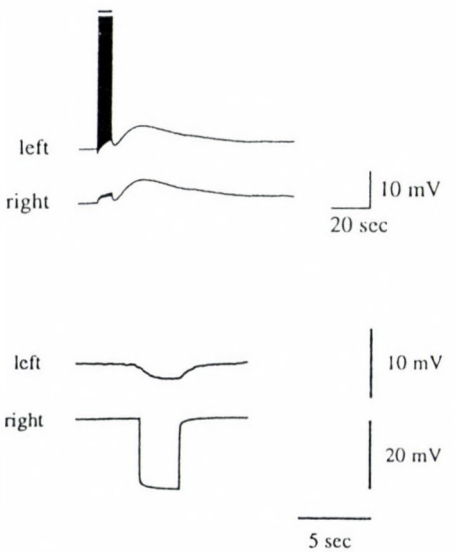

Fig. 4. Simultaneous recordings of pairs of CDCs during chemical (upper panels) and electrical (lower panels) coupling. Depolarizing after potentials (DAP) in two CDCs by stimulation of one CDC in the left cerebral ganglion (upper panel) and postsynaptic potential in a CDC in the left cerebral ganglion during a hyperpolarizing stimulus in a CDC in the right cerebral ganglion (lower panel)

electrical coupling rates between left and right CDCs from different animal groups. The table shows that DAP amplitude and electrical coupling of CDCs from animals after 4 weeks of no egg laying (CEL-4) do not differ from those in resting state (EL-R) CDCs. DAP amplitude and electrical coupling rate are, however, significantly reduced in CDCs from animals after 8 weeks of no egg laying (CEL-8). DAPs in CDCs from these animals are comparable to those of inhibited state CDCs (EL-I) from egg-laying animals. The resting membrane potential of the CDCs does not change with the egg-laying history of the animal (Table 1).

Table 1
Resting membrane potential (RMP), chemical transmission (DAP amplitude) and electrical coupling (%) of CDCs from *Lymnaea* with different egg laying history

Animal group	RMP (mV) Mean ± SEM (n)	DAP amplitude (mV) Mean ± SEM (n)	Electrical coupling (%) Mean ± SEM (n)
EL-R	65 ± 1.10 (10)	8.16 ± 1.29 (9)	5.36 ± 0.81 (10)
EL-I	64 ± 0.94 (14)	2.89 ± 0.68 (9)	3.89 ± 0.85 (9)
CEL-4	65 ± 1.76 (18)	7.14 ± 1.17 (13)	3.35 ± 0.65 (15)
CEL-8	63 ± 1.28 (16)	0.91 ± 0.40 (15)	1.79 ± 0.55 (14)

ANOVA combined with Tukey post hoc tests revealed significant differences ($p < 0.05$) for DAP amplitudes between EL-I and EL-R and between CEL-8 and CEL-4 and EL-R. Electrical coupling of CEL-8 differed significantly from EL-R and EL-I. EL-R and EL-I: CDCs from egg-laying animals in the resting and inhibited state, respectively; CEL-4 and CEL-8: CDCs from animals that did not lay eggs for 4 and 8 weeks, respectively; SEM: standard error of the mean. n: number of animals. For further explanation see text.

Morphological changes of CDCs accompany the decrease and subsequent cessation of egg laying in Lymnaea

Branching patterns of CDCs change with age and with the decrease in egg-laying activity of the animals. This was revealed by injecting the cells with LY. In young animals CDCs have an ipsilateral axon that branches extensively in the cerebral commissure which is the neurohaemal area of the CDCs. Ventral CDCs have in addition an axon that crosses the commissure. In the contralateral cerebral ganglion the axon makes a loop and re-enters the commissure to branch extensively in the neurohaemal area. In the loop area CDCs are electrically coupled to each other. The axon that crosses the cerebral commissure makes a great number of collaterals that run parallel to the axon [2]. In CDCs from old animals axonal branching in the neurohaemal area is dramatically reduced [14, 15]. Atrophy also occurs within the collateral system of the CDCs. The progressive reduction of axonal branching is significantly related to the decrease in egg-laying frequency in *Lymnaea* [16]. Notably, morphological reduction already occurs when the animal still lays eggs and there is no dramatic further morphological reduction after the animal ceases egg laying.

This suggests that reduction of CDC branching precedes cessation of egg-laying activity.

Previously, it has been suggested that sensory input to the CDCs is impaired in old animals that ceased egg laying [10]. In egg-laying *Lymnaea* sensory input projects on the ventral CDCs in a special area of fine axonal branches (spines) near the soma [23, 25]. The chemical contacts on the CDC spines are probably of cholinergic nature. These contacts might comprise the cholinergic tactile sensory input received by the CDCs and the input that activates the CDC-system [8, 25]. Atrophy might include the loss of these spines. A gradual loss of spinal structures may explain the decrease and subsequent cessation of egg laying activity in *Lymnaea*. The observation that old egg-laying animals respond less and old non-laying animals do not respond at all to the natural egg-laying inducing stimulus (exposure to clean aerated water) [10] is in agreement with this idea. EM studies are needed to help resolve this.

As mentioned above, it was shown that CDCs of old non-reproductive animals still contain an ovulation-inducing factor. Moreover, factors secreted by these cells are still able to induce an afterdischarge in other CDCs. Immunocytochemical results indeed showed strong CDC-peptide staining of the neurohaemal area in old animals (including non-layers), and corroborate these findings. Immunocytochemical results also showed axons in the neurohaemal area protruding into the connective tissue layer of the perineurium, which were packed with stained material. This suggests that there is still synthesis and transport of CDC-peptides, but no release. Immunocytochemical staining of the cell somata and of crossing axons is much weaker in old animals than in young animals suggesting that peptide synthesis and transport occur at a reduced rate in old animals [15]. These conclusions are corroborated by mass spectrometric analysis that showed that CDCs from old non-laying *Lymnaea* still contain different peptides some of which however in lower amounts [17].

Are morphological changes in CDCs related to physiological changes?

In a series of experiments electrophysiological properties of CDCs were determined and subsequently the same CDCs were filled with LY [16]. The results in Table 2 show that minimally branched CDCs predominantly fail to produce an afterdischarge upon electrical stimulation. Yet, there are minimally branched CDCs which exhibit an afterdischarge after electrical stimulation whereas, on the other hand relatively intact CDCs occur that fail to do so. Minimally branched CDCs only differ significantly from extensively branched cells in their electrical coupling rate being reduced [16]. Afterdischarge failure in CDCs is not easily explained solely by this difference. Possibly, reduction of CDC branching and afterdischarge failure in CDCs from animals that ceased egg laying originate differently. Reduced branching in CDCs indeed already occurs in egg-laying animals whereas the permanent state of afterdischarge failure in CDCs only occurs in animals that have experienced a long period of no egg laying. Possibly, the failure of afterdischarge induction in CDCs is related to the long

Table 2
Induction of afterdischarges (ADs) in CDCs of different classes of axonal branching

CDC branching class	Age (days) Mean ± SEM	CDCs exhibiting AD	CDCs without AD	Totals
Ext.+ Moderate	363 ± 21.5	15	6	21
Minimal	449 ± 17.1	13	17	30

The distribution of CDCs exhibiting an afterdischarge over the different morphological classes differed significantly (G-test; $P < 0.05$). Ext.: extensively branched CDCs. AD: afterdischarge. See also Table 1 and text.

period of inactivity of the cells. Consistent with this proposal is the observation that relatively extensively branched CDCs in animals that exhibited a prolonged period of no egg laying also show failure of afterdischarge induction.

The finding that degenerated, ventral CDCs occur in old animals and that in old animals granular glial cells occur among the CDCs [15] indicates that neuronal atrophy in ventral CDCs, as observed with LY-fills, is followed by neuronal death. This implies that at some stage of morphological reduction physiological properties also deteriorate. That we did so far not found CDCs in such a stage might be due to the last stages of deterioration proceeding very fastly. Moreover, it can be expected that at a particular stage of morphological reduction CDCs are not easy to record from with intracellular electrodes.

The sequence of changes during reproductive senescence in Lymnaea

During the process of decrease and cessation of egg laying the following sequence of changes probably take place. During the decrease of egg-laying frequency morphological reduction of the branching patterns of CDCs occurs. Then, animals cease egg laying and enter the post-reproductive period. At this time point the extent of morphological reduction of CDCs varies but severely reduced branching patterns prevail. At this stage the CDCs are physiologically still intact. During the extended post-reproductive period physiological changes take place in the CDCs. Electrical and chemical transmission among CDCs become reduced and electrical stimulation of the cells fails to induce an afterdischarge. The LY-fills never showed a total axonal loss. This might suggest that morphological reduction of CDCs does not proceed. Immunocytochemical stainings, however, revealed degeneration among the CDCs. Probably, during the extended period of no egg laying morphological and physiological properties continue to deteriorate and CDCs degenerate.

Thus the present results indicate that the decrease and cessation of egg-laying activity originates from morphological changes in the CDCs resulting in a gradual loss of synaptic input. During the process of reproductive inactivity CDCs undergo a further loss of morphological and physiological properties and finally degenerate.

REFERENCES

1. Brussaard, A. B., Schluter, N. C. M., Ebberink, R. H. M., Kits, K. S., TerMaat, A. (1990) Discharge induction in molluscan peptidergic cells requires a specific set of four autoexcitatory neuropeptides. *Neurosci. 39,* 479–491.
2. De Vlieger, T. A., Kits, K. J., TerMaat, A. M. (1980) Morphology and electrophysiology of the ovulation hormone producing neuroendocrine cells of the freshwater snail *Lymnaea stagnalis* (L.). *J. Exp. Biol. 84,* 259–271.
3. Dogterom, G. E., van Loenhout, H., Geraerts, W. P. M. (1983) Synchronous maturation of the female reproductive system and of the ovulation hormone-producing system in *Lymnaea stagnalis. Gen. Comp. Endocr. 52,* 242–246.
4. Dogterom, G. E., van Loenhout, H., Koomen, W., Roubos, E. W., Geraerts, W. P. M. (1984) Ovulation hormone, nutritive state, and female reproductive activity in *Lymnaea stagnalis. Gen. Comp. Endocr. 55,* 29–35.
5. Finch, C. E. (1990) *Longevity, senescence, and the genome.* University of Chicago Press, Chicago.
6. Geraerts, W. P. M., Joosse, J. (1975) Control of vitellogenesis and of growth of female accessory sex organs by the Dorsal Body Hormone (DBH) in the hermaphrodite freshwater snail *Lymnaea stagnalis. Gen. Comp. Endocrinol. 27,* 450–464.
7. Geraerts, W. P. M., Tensen, C. P., Hogenes, Th. M. (1983) Multiple release of peptides by electrically active neurosecretory caudo dorsal cells of *Lymnaea stagnalis. Neurosci. Lett. 41,* 151–155.
8. Geraerts, W. P. M., TerMaat, A., Vreugdenhil, E. (1988) The peptidergic neuroendocrine control of egg-laying behavior in *Aplysia* and *Lymnaea.* In: H. Laufer and R. G. H. Downer (eds) *Endocrinology of selected invertebrate types, vol. 2,* Alan R. Liss, Inc. New York, pp. 141–231.
9. Janse, C., Slob, W., Popelier, C. M., Vogelaar, J. W. (1988) Survival characteristics of the mollusc *Lymnaea stagnalis* under constant culture conditions: effects of aging and disease. *Mech. Ageing Dev. 42,* 263–274.
10. Janse, C., Ter Maat, A., Pieneman, A. W. (1990) Molluscan ovulation hormone containing neurons and age-related reproductive decline. *Neurobiol. Aging 11,* 457–463.
11. Janse, C., Wildering, W. C., Popelier, C. M. (1989) Age-related changes in female reproductive activity and growth in the mollusc *Lymnaea stagnalis. J. Gerontol. 44, B* 148–155.
12. Janse, C., Wildering, W. C., van der Roest, M. (1991) Neuroendocrine and neural aging in the pond snail *Lymnaea stagnalis.* In: K. S. Kits, H. H. Boer, J. Joosse (eds). *Molluscan Neurobiology.* North Holland Publishing Co., Amsterdam. pp. 179–185.
13. Janse, C., van Minnen, J., van der Roest, M., Roubos, E. W. (1994) Female reproductive aging in the pond snail *Lymnaea stagnalis. Neth. J. Zool. 44,* 385–394.
14. Janse, C., Roest, M. van der, De Jeu, M., Boer, H. H. (1995) Degeneration of CDCs and egg laying in the pond snail *Lymnaea stagnalis. Acta Biol. Hung. 46,* 229–239.
15. Janse, C., Roest, M. van der, Jansen, R. F, Montagne-Wajer, C., Boer, H. H. (1996) Atrophy and degeneration of peptidergic neurons and cessation of egg-laying in the aging pond snail *Lymnaea stagnalis. J. Neurobiol. 29,* 202–212.
16. Janse, C., Peretz, B., Roest, M. van der Dubelaar, E. J. G. (1999) Excitability and branching of neuroendocrine cells during reproductive senescence. *Neurobiol. Aging* 20, 675–693.
17. Jimenez, C. R. (1997) Generation of complex peptide diversity in neuroendocrine cells of *Lymnaea stagnalis* and the rat. Thesis. Vrije Universiteit. Amsterdam. The Netherlands.
18. Joosse, J. (1964) Dorsal bodies and dorsal neurosecretory cells of the cerebral ganglia of *Lymnaea stagnalis. L. Arch. Neerl. Zool. 15,* 1–103.
19. Joosse, J. (1988) The hormones of molluscs. In: Laufer, H., Downer, G. H. (eds) *Endocrinology of selected invertebrate types,* vol. II. Alan R. Liss Inc. New York, pp. 89–140.
20. Joosse, J., Geraerts, W. P. M. (1983) Endocrinology. In: Saleudin, A. S., Wilbur, K. M. (eds). *The Mollusca Part I. Physiology, vol. 4.,* Acad. Press New York, pp. 317–406.
21. Kits, K. S. (1980) States of excitability in ovulation hormone producing neuroendocrine cells of *Lymnaea stagnalis* (Gastropoda) and their relation to the egg-laying cycle. *J. Neurobiol. 11,* 397–410.

22. Li, K. W., Jimenez, C. R., Van Veelen, P. A., Geraerts, W. P. M. (1994) Processing and targeting of a molluscan egg-laying peptide prohormone as revealed by mass spectrometric peptide fingerprinting end peptide sequencing. *Endocrinol. 134,* 1812–1819.
23. Roubos, E. W. (1984) Cytobiology of the ovulation-neurohormone producing caudo-dorsal cells of the snail *Lymnaea stagnalis. Int. Rev. Cytol. 89,* 295–346.
24. Slob, W., Janse, C. (1988) A quantitative method to evaluate the quality of interrupted animal cultures in aging studies. *Mechs Ageing Dev. 42,* 275–290.
25. TerMaat, A., Roubos, E. W., Lodder, J. C., Buma, P. (1983) Integration of synaptic input modulating pacemaker activity of electrotonically coupled neuroendocrine Caudo-Dorsal Cells in the pond snail. *J. Neurophysiol. 49,* 1392–1409.
26. TerMaat, A., Geraerts, W. P. M. Jansen, R. F., Bos, N. P. (1988) Chemically mediated positive feed back generates long-lasting afterdischarge in a molluscan neuroendocrine system. *Brain Research 438,* 77–82.
27. Van Heukelem, W. F. (1979) Aging in lower animals. In: *The Biology of Aging.* Behnke, J. A., Finch, C. E., Moment, G. B. (eds). Plenum Press, New York, pp. 115–130.
28. Wodinsky, J. (1977) Hormonal inhibition of feeding and death of *Octopus:* control by optic gland secretion. *Science 198,* 948–951.
29. Wise, P. M., Krajnak, K. M., Kashon, M. L. (1996) Menopause: The aging of multiple pacemakers. *Science 273,* 67–70.

Acta Biologica Hungarica 51 (2–4), pp. 265–273 (2000)

PRE- AND POSTSYNAPTIC EFFECTS OF EUGENOL AND RELATED COMPOUNDS ON *HELIX POMATIA* L. NEURONS+

J. SZABADICS* and L. ERDÉLYI

Department of Comparative Physiology, József Attila University, Középfasor 52, H-6726 Szeged, Hungary

(Received: August 31, 1999; accepted: November 30, 1999)

We showed how eugenol blocks the synaptic transmission and gave a possible interpretation how it inhibits the excitation-contraction coupling that several authors described previously [3, 9]. Eugenol acts both in the pre- and postsynaptic side of the neurons. It blocks the Ca^{2+}-currents, decreases the membrane potential of the neurons, increases the inward resistance and decreases the GABA, ACh and glutamate evoked excitatory responses in submillimolar concentration.

Keywords: Eugenol – membrane effects – neurotransmitters – identified neurons – *Helix pomatia.*

INTRODUCTION

Eugenol is the major component of the clove oil (80–95%). It is also found in a lot of spice-plants (e.g. *Thymus* spp., *Cinnamomum* spp.) and in some plants widely used by the perfumery industry (*Cistus* spp., *Pelargonium* spp., *Camellia* spp.). Eugenol is known as insect attractant, as analgesic agent against toothache and it is widely used in dental cement preparation, mainly in combination with zinc oxide, which also has a bacteriostatic activity. Eugenol structurally relates to guaiacol and vanillin. Vanillin is used as additive in a number of foods and perfumes. Guaiacol is known as medicament against influenza, catarrh and coughing. Guaiacol occurs naturally in the resin of the beech tree [1, 10].

It was shown in previous studies that eugenol reversibly attenuated the compound action potential (cAP) of the rat vagus and phrenic nerves [2, 3, 4]. It decreased the amplitude of both miniature and evoked end-plate potential (mepp, EPP) recorded in diaphragm muscle preparations [3]. It decreased the systemic blood pressure and myocardial contractile force in rat when it was applied intravenously [13]. Eugenol is toxic for animals, the LD_{50} is 1.93 mg/kg for rats. Death is caused by respiratory

+ Presented at the 9th ISIN Symposium on "Neurobiology of Invertebrates", July 1–5, 1999, Tihany, Hungary.

*Corresponding author, E-mail: 4532.387@stud.u.-szeged.hu

0236-5383/2000/$ 5.00

failure [7]. Okhubo and Kitamura reported an eugenol activated Ca^{2+}-permeable ion channel in neurons of the rat dorsal root ganglion [11].

We studied the actions of eugenol and structurally related compounds on membrane events, Ca-currents, spontaneous and stimulus evoked excitatory postsynaptic potentials in neurons of the snail, *Helix pomatia* L. In this paper we present evidence that the studied vanilloids modulate the pre- and postsynaptic processes on this neuronal preparation.

MATERIAL AND METHODS

The experiments were carried out on isolated suboesophagal ganglia of *Helix pomatia* L. The snails were collected locally, kept in the laboratory and fed by lettuce and chickweed. After removing of ganglia from the animals, we pinned it to a Silastic-covered floor of a 5 ml plexiglass recording chamber. The connective tissue covering the neurons was removed by dissection without enzymatic treatment.

The preparation was perfused (8–12 ml/min) with physiological solution of the following composition (mM): NaCl 130; KCl 4; $CaCl_2$ 7; HEPES 5 (pH = 7.45 ± 0.025). The Ca-current-isolating solution contained the following compounds (mM): TEA-Cl 50; CsCl 10; $CaCl_2$ 10; KCl 1; Tris-Cl 50; 3,4-diAP 2 (pH = 7.45 ± 0.025). At first, the concentrated eugenol (0.05 ml) was dissolved in 0.4–0.5 ml ethanol (70%), this solution was diluted in 800 ml normal physiological solution, such the final concentration of the solution was 0.5 mM. The guaiacol was dissolved in same way.

After preparation, the individual cells were visualized under a binocular microscope and penetrated with a low resistance (~3–3.5 MOhm) glass microelectrode filled with 1 M KCl and K-citrate, except in the Ca-current-isolating experiments, where it was filled with 1 M CsCl. The experiments were made with current-clamp and single electrode voltage-clamp technique at room temperature (22–25 °C). The recording setup was composed of a homemade amplifier connected to a Hitachi VC 6025 digital oscilloscope and a personal computer. The hardware was a Labmaster DMA with TL-1-125 kHz interface (Axon Instruments, Inc.) in connection with a mathematical coprocessor and acquisition software. The values of the stimulus and transmitter evoked responses were expressed by mean and S.D. The neurotransmitters were applied with pressure from a tightened glass capillary, kept about 50 μm near to the cell. The transmitters were diluted in normal physiological solution.

RESULTS

Eugenol and guaiacol decreased the membrane potential (MP) of the studied neurons to more positive potential value but eugenol was more effective than guaiacol (Fig. 1A). Both compounds increased the input resistance (R_{in}) of the neuronal membrane (Fig. 1B). Vanillin and *o*-aminophenol had no or moderate effects on MP and R_{in}

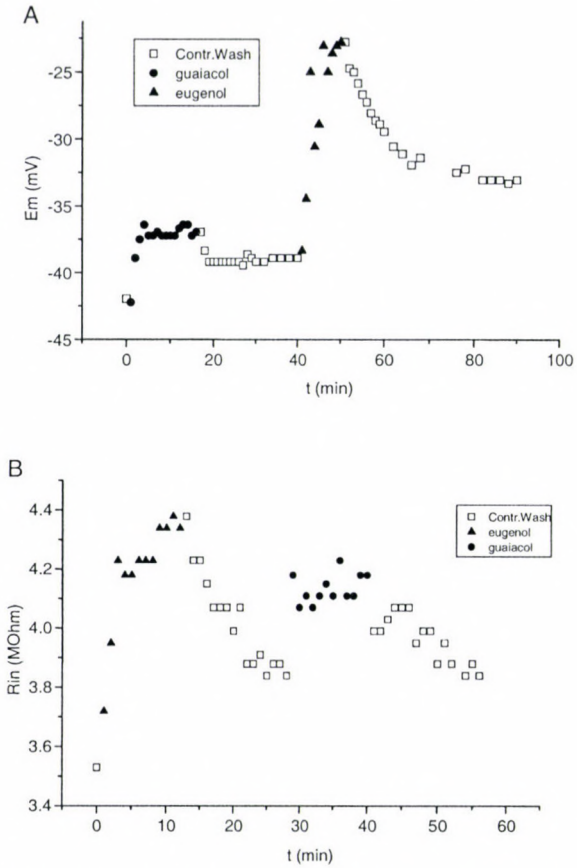

Fig. 1. A. Guaiacol and eugenol (1 mM) reversibly decreased the membrane potential of the neurons. *B.* Eugenol and guaiacol (0.5 mM) increased the input resistance of the cells

when they were applied in equimolar dose. The responses developed within twelve minutes application of the compounds but 30–40 minutes washing time needed for partial recovery, especially in with eugenol. Although eugenol depolarized the neurons, it inhibited the spike generation. Figure 3A shows three consecutive synaptically evoked spikes in control solution (left record). Eugenol blocked the spike potentials (middle record) which recovered after washing (right record).

Ca-currents were isolated and studied in identified V1, LPa3 and RPa3 neurons in Ca^{2+} and Ba^{2+} containing media. Both protocols gave similar results. Eugenol and guaiacol decreased the Ca- or Ba-currents in a dose-dependent, reversible way (Fig. 2. A–C). Figure 2. E shows the dose-response relationship of the compounds on Ca-currents activated in V1 neuron ($IC_{50} = 0.61$ mM, $IC_{50} = 6.79$ mM, for eugenol and guaiacol, respectively). The compounds did not change the voltage dependency of the activation and inactivation of the Ca-currents.

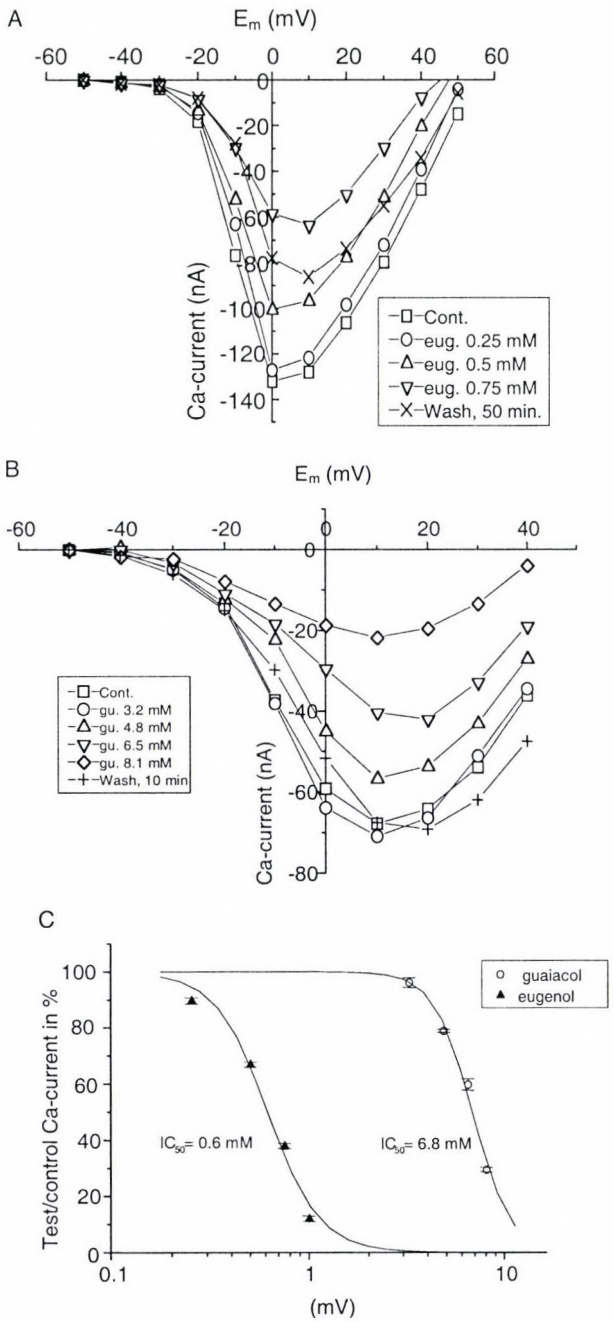

Fig. 2. A. Effects of eugenol on Ca-current in V1 neuron (Vh = –50 mV). *B.* Guaiacol decreased the isolated Ca-current but was less potent than eugenol (V1 neuron, Vh = –50 mV). *C.* Dose-response curves of eugenol and guaiacol on Ca-currents (Vh = –50 mV, Vc = –20 mV, n = 3, mean and SD., V1 cell).

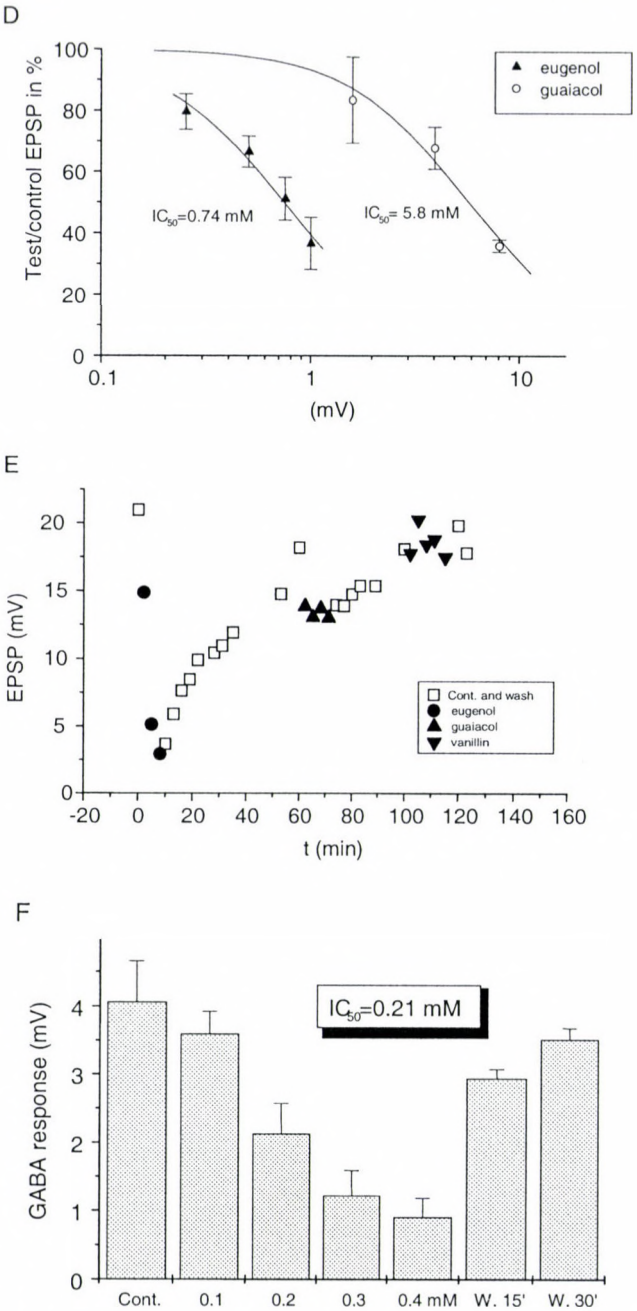

Fig. 2. D. Dose-dependent effects of eugenol and guaiacol on evoked EPSPs (MP = –100 mV, LPa2 and LPa4 cells, n = 5, mean and SD). *E.* Effects of eugenol, guaiacol and vanillin on evoked EPSPs. All compounds were applied in 0.5 mM dose (MP = –120 mV, LPa cell, after right pallial nerve stimulation). *F.* Effects of eugenol on GABA evoked depolarization in V1 neuron (MP = –100 mV, n = 4)

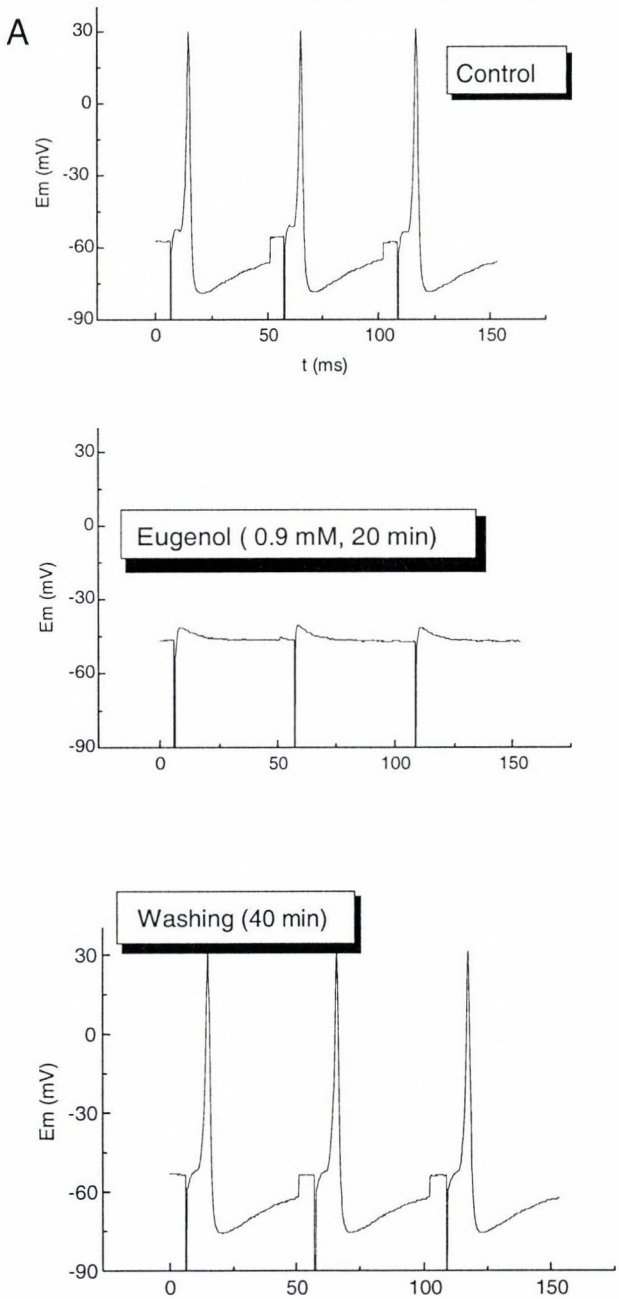

Fig. 3. A. Eugenol reversibly blocks the synaptically evoked spikes (LPa3 cell, stimulation of the anal nerve, 0.9 mM eugenol)

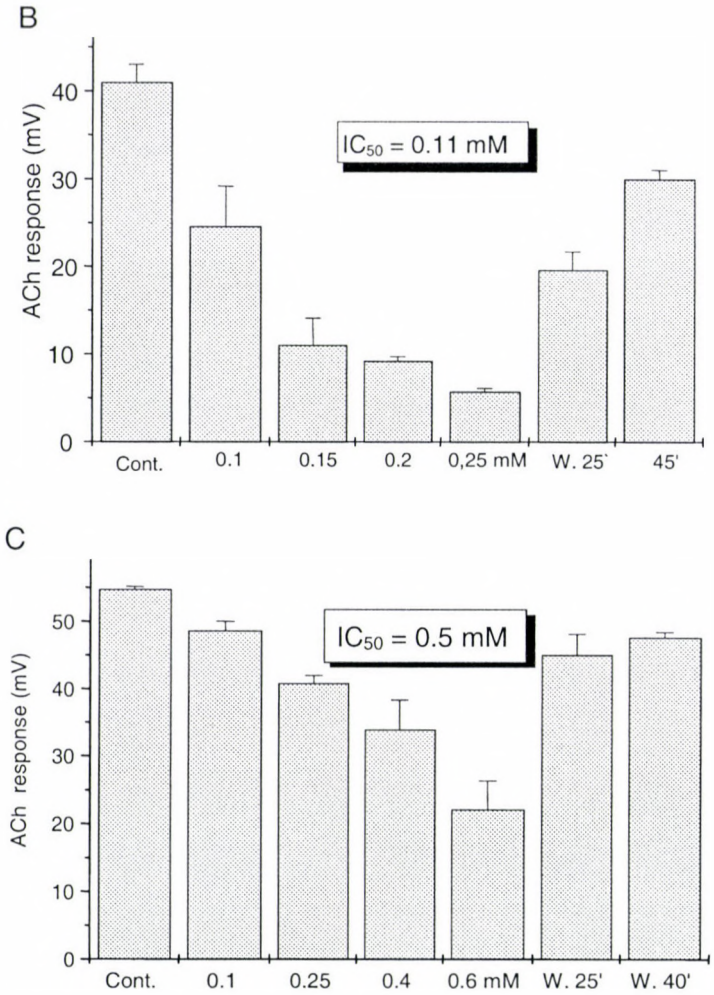

Fig. 3. B. Effects of eugenol on the desensitizing ACh response (RPa3 neuron, MP = –100 mV, n = 3). *C.* Eugenol attenuates the non-desensitizing ACh response (MP = –100 mV, n = 3)

Eugenol and guaiacol decreased the stimulus evoked EPSPs in a dose-dependent way (Fig. 2D) and the actions were reversible. The half-blocking dose (IC_{50}) was 0.77 mM and 6.2 mM for eugenol and guaiacol, respectively. Vanillin and *o*-aminophenol had no effects on evoked EPSPs in equimolar concentration (Fig. 2E). Eugenol decreased the frequency of quantal release and spontaneous EPSPs in a dose-dependent and reversible way without significant modulation of their mean amplitude.

We studied the acetylcholine (ACh) and gamma-aminobutyric acid (GABA) induced depolarizing responses in details as an indicator of changes of the postsy-

naptic membrane receptor sensitivity to eugenol. ACh application caused two types of depolarizing responses on the studied neurons. One of these responses can be characterized as highly desensitizing because after the peak it declined to the base line in 10–20 second after continuous release of ACh from the micropipette. Most of the identified neurons responded this way (LPa2, 3, RPa 2, 3, RPl1, LPl1 and V1). The response can be totally blocked by 250 μM d-tubocurarine. The other type of ACh evoked response did not desensitize. The desensitizing ACh response was more sensitive to eugenol than the non-desensitizing one. As can be seen in Fig. 3B and C, the half-blocking dose was 0.11 and 0.5 mM for the two types of ACh responses studied in different neurons. The actions of eugenol on ACh responses were partially reversible.

The LPa4 and V1 neurons responded with depolarization when GABA added at −100 mV. Eugenol also decreased the GABA induced depolarization by a dose-dependent and reversible manner (Fig. 2. F). The half-blocking dose was 0.21 mM in this case.

DISCUSSION

In contrast to findings in skeletal muscle of vertebrates where eugenol did not affect the membrane potential, we found eugenol induced depolarization in all of neurons studied [3, 9]. However, the spike attenuating character of the compound proved to be common both in vertebrate and invertebrate neuronal systems [3, 4, 8].

It was previously described that eugenol activates a Ca^{2+}-permeable current in rat dorsal root ganglion cells [11] but we found that eugenol increased the inward resistance of the snail neurons. Thus, the conductance decreasing effect of the drug predominates in the snail neuronal preparation.

It was shown that both eugenol and guaiacol decreased the peak amplitude of the Ca- or Ba-current in some identified neurons of the snail in a dose-dependent and reversible manner. Earlier both facilitation and attenuation of the Ca-currents were reported by vanillin in some *Helix* neurons [6]. If we compare the IC_{50} value of eugenol and guaiacol on Ca-current and stimulus evoked EPSPs, this initiates the suggestion that a Ca-mechanism may influence the synaptic efficacy. Indeed, the presynaptic Ca-channels can be one of the target sites for the compounds if they behave similarly as the somatic ones. However, another postsynaptic target site can be the neurotransmitter receptor system. We presented evidence here that the ACh and GABA induced depolarizing responses were also attenuated by eugenol. It was shown earlier that capsaicin, zingeron and vanillin also attenuated the ACh, GABA and 5-HT evoked inward currents with different potencies [5].

It looks like that the structures of the molecules are closely related to the effects. The basic molecule can be the guaiacol which has two substituents on the benzene ring, one hydroxy- and one methoxy-group which is the vanillyl head of the other studied compounds. Methoxy-group sends electrons into the benzene ring and retains the dissociation of the proton from the hydroxy-group. The allyl substituent of the

eugenol in para position emphasis this effect. While the aldehyde-group of vanillin sucks electron from the benzene ring and can help the dissociation of the hydroxy-group's proton. The solubility feature and hydrophobicity of the molecules are also different in character. Thus, we suppose that eugenol acts on the target channel or receptor proteins in the lipid environment of the membrane and both hydroxy- and methoxy-groups are important for the actions.

REFERENCES

1. *Dictionary of Organic Compounds* (fifth edition) (1982) ed.: Buckingham, New York, Chapman and Hall, pp. 3708–3716.
2. Brodin, P., Östravik, D. (1982) Effects of therapeutic and pulp protecting materials on nerve transmission *in vitro*. *Scand. J. Dent. Res. 91,* 46–50.
3. Brodin, P., Roed, A. (1984) Effects of eugenol on rat phrenic nerve and phrenic nerve diaphragm preparation. *Arch. Oral. Biol. 29(8),* 611–615.
4. Brodin, P. (1985) Differential inhibition of A, B and C fibres in the rat vagus nerve by lidocaine, eugenol and fromaldehyde. *Arch. Oral. Biol. 30(6),* 477–480.
5. Erdélyi, L., Such, Gy. (1988) Pre- and postsynaptic effects of capsaicin on snail neurons. In: Symposia Biologica Hungarica 36 (ed. Salánki J.), Akadémiai Kiadó, Budapest, pp. 603–616.
6. Erdélyi, L. (1992) Vanillin modulates the fast outward and calcium currents in *Helix neurons. Acta Biol. Hung. 43,* 15–24.
7. Hume, W. R. (1984) An analysis of the release and the diffusion through dentin of eugenol from zinc oxide-eugenol mixtures. *J. Dent. Res. 63,* 881–884.
8. Kozam, G. (1977) The effects of eugenol on nerve transmission. *Oral. Surg. 44(5),* 799–805.
9. Leal-Cardoso, J. H., Coelho-de-Soza, A. N., Souza, I. T., Figueiredo, I. M. (1994) Effects of eugenol on excitation-contraction coupling in skeletal muscle. *Arch. Int. Pharmacodyn. Ther. 327(1),* 113–124.
10. Neumüller, O.-A.: Römpp Vegyészeti Lexikon (Hungarian translation, ed.: K. Polinszky, Budapest 1981) pp. 335., 881.
11. Ohkubo, T., Kitamura, K. (1997) Eugenol activates Ca^{2+}-permeable currents in rat dorsal root ganglion cells. *J. Dent. Res. 76(11),* 1737–1744.
12. Sticht, F. D., Smith, R. M. (1971) Eugenol: some pharmacologic observations. *J. Dent. Res. 50(6),* 1531–1535.

Acta Biologica Hungarica 51 (2–4), pp. 275–286 (2000)

AMPHETAMINE ELICITED POTENTIAL CHANGES IN VERTEBRATE AND INVERTEBRATE CENTRAL NEURONS[+]

M.-C. TSAI, Y.-H. CHEN and S.-S. HUANG

Department of Pharmacology, College of Medicine, National Taiwan University, No. 1., Sec.1., Jen-Ai Road, Taipei, Taiwan

(Received: August 31, 1999; accepted: November 30, 1999)

The effects of amphetamine on potential changes in both vertebrate and invertebrate central neurons and factors affecting the potential changes were tested. The animals studied included mice, newborn rat and African snail. Seizure was elicited after lethal doses of *d*-amphetamine (75 mg/kg, i.p.) administration in mice. Repetitive firing of the action potentials were elicited after *d*-amphetamine (1–30 μM) administration in thin thalamic brain slices of newborn rat. Bursting firing of action potentials in the giant African central RP4 neuron were also elicited after *d*-amphetamine or *l*-amphetamine (0.27 mM) administration. The amphetamine elicited bursting firing of action potentials was not blocked even after high concentrations of *d*-tubocurarine, atropine, haloperidol, hexamethonium administration. Therefore, the amphetamine elicited potential changes may not be directly related to the activation of the receptors of the neuron. The bursting firing of action potentials elicited by amphetamine occurred 20–30 min after amphetamine administration extracellularly, even after high concentrations of *d*-amphetamine administration (0.27, 1 mM). However, the bursting firing of potentials occurred immediately if amphetamine was administrated intracellularly at lower concentration. Extracellular application of ruthenium red, the calcium antagonist, abolished the amphetamine elicited bursting firing of action potentials. If intracellular injection of EGTA, a calcium ion chelator, or injection with high concentrations of magnesium, the bursting firing of potentials were immediately abolished. These results suggested that the active site of amphetamine may be inside of the neuron and the calcium ion in the neuron played an important role on the bursting of potentials. In two-electrode voltage clamped RP4 neuron, amphetamine, at 0.27 mM, decreased the total inward and steady outward currents of the RP4 neuron. *d*-Amphetamine also decreased the calcium, Ia and the steady-state outward currents of the RP4 neuron. Besides, amphetamine elicited a negative slope resistance (NSR) if membrane potential was in the range of –50 to –10 mV. The NSR was decreased in cobalt substituted calcium free and sodium free solution. The effects of secondary messengers on the amphetamine elicited potential changes were tested. The bursting firing of action potentials elicited by amphetamine in central snail neurons decreased following extracellular application of [1] H8 (N-(2-methyl-amino) ethyl-3-isoquinoline sulphonamide dihydrochloride), a specific protein kinase A inhibitor and [2] anisomycin, a protein synthesis inhibitor. However, the bursting firing of action potentials were not affected after [1] extracellular application of H7 (1,(5-isoquinolinesulphonyl)-2-methylpiperasine dihydrochloride), a specific protein kinase C (PKC) inhibitor, or [2] intracellular application of GDPβS, a G protein inhibitor. The oscillation of membrane potential of the bursting activity was blocked after intracellular injection of 3'-deoxyadenosine, an adenylyl-cyclase inhibitor. These results suggested that the bursting firing of action potentials elicited by *d*-amphetamine in snail neuron may be associated with the cyclic AMP second messenger system; on the other hand, it may not

[+] Presented at the 9th ISIN Symposium on "Neurobiology of Invertebrates", July 1–5, 1999, Tihany, Hungary.

*Corresponding author, E-mail: mctsai@ccms.ntu.edu.tw

0236-5383/2000/$ 5.00

be associated with the G protein and protein kinase C activity. It is concluded that amphetamine elicited potential changes in both vetebrate and invertebrate central neurons. The changes are closely related to the ionic currents and second messengers of the neurons.

Keywords: Amphetamine – membrane potentials – neurons – mice, rat, snail.

INTRODUCTION

It is well known that amphetamine possesses effective central stimultory actions in vertebrates. Large doses of amphetamine can induce a psychotic state resembling paranoid schizophrenia as well as seizure and death [17]. The mode of action of amphetamine was mainly attributed to its facilitatory effects on the dopamine releasing process. However, the dopamine receptor blockers did not protect against seizures but do protect against death [7]. The mechanism of amphetamine elicited seizure remained unclear. We tested the effects of amphetamine on the potential changes in central neurons of vertebrates and invertebrates.

The story of amphetamine started from Chinese Herbs, *ephedra sinica.* The herb was used for the treatment of asthma for five thousand years in China. The Japanese scientist, Nagaii isolated its main component, i.e. ephedrine at 1887 and it was used as effective bronchodilator for the treatment of asthma in western world after Chen published the pharmacological effects of ephedrine in *JPET* in 1926 [1]. The stable and effective properties of ephedrine lead Americans to plant the *ephedra* herb in California, U.S.A. However, the Americans could not extract EPHEDRINE from the American *ephedra,* i.e. *ephedra genetaceae.* Then, American chemists, Miller and Piness, in 1928, tried to synthesize the substitute of ephedrine through organic chemical synthesis [9]. They synthesized a phenyl amino ethanol compound. Amphetamine was first synthesized by American chemists Munch and Hartung at 1931. Amphetamine and methamphetamine can be synthesized through phenylacetone and ephedrine using hydrogenation methods (H2/Pd-C methods). At 1935, Prinzmetal and Bloomberg find that benzedrine, i.e. amphetamine, had a central stimulant activity and it was used for the therapy of insomnia [10]. At 1947, Harris and Searle used it for the tretment of obesity, etc. However, the "honeymoon" period waned after the second World War II as the amphetamine failed to live up to the therapeutic expectations, and, more important, as their potential for serious dependency became apparent in the waves of abuse that occurred first in Japan and then throughout many of the other industrialized nations of the world. The abuse of amphetamine became conspicuously manifest in the United States as the "speed freak" epidemic of the 1960s [6]. The governmental regulation of the amphetamine had become highly restrictive. Amphetamine is classfied as abused drug and it is controlled under the Narcotic acts among nations. The medical use of amphetamine had been confined to the Bureau of Narcotics, Department of Health in our country. There are many illegal amphetamine users in Taiwan. The amphetamine intoxicated patients also show convulsion-like symptoms before fatality. Our previous studies revelaed that *d*-amphetamine elicited convulsion of mice after large dose of injection

(i.p.) and it also elicited bursting firing of action potentials in some particular central neurons of newborn rat and snail. Pentylenetetrazol, a convulsant also elicited bursting firing of potentials in cerebral cortex of cat [12] and snails [13, 14] central neurons. The research goal of the present study is to understand the effects of amphetamine on both vetebrate and invertebrate central neurons and factors which affect the bursting firing of action potentials, the factors included receptors, ions and second messengers, mainly cyclic AMP and GMP antagonists were tested.

RESULTS AND DISCUSSION

The animals we studied included mice, newborn rat and African snail. We used both *in vivo* and *in vitro* techniques. General electrophysiological techniques were followed. In the in vivo study, we repetitively injected d-amphetamine to the mice (10 mg/kg, i.p. up to 75 mg/kg) and the animal showed seizure before death. Pretreatment of haloperidol did not protect the fatality. Bursting firing of action potentials are closely related to the seizure of the animal. We tested whether *d*-amphetamine elicites the bursting firing of potential changes in central neuron of vertebrate. Conventional electrophysiological techniques with single patching electrodes for brain slices from newborn rat were used. Slices were obtained from the thalamus of 5- to 10-day old Wistar rats. Sagital sectional slices of about 200 μm thickness were prepared and transferred to a incubation chamber in aCSF for at least 1 h at room temperature under continuous oxygenation. Conventional patch pipettes were made from standard wall glass capillaries (o.d. 1.5 mm) by a puller (Brown micropipette puller, P-87). Whole potentials or currents were recorded with Axopatch 1-D amplifier. A gigaohm seal (mostly >10 GΩ) was established in the cell attached mode prior to perforation of the patch membrane for whole cell recording. There were two types of neurons in the thalamic slices. One type of neuron showed regular discharge potentials and *d*-amphetamine did not change the firing pattern of action potential of this type of neuron. However, *d*-amphetamine reversibly decreased the resting membrane potential and the amplitude of the action potential of this type of neuron. There were some neurons which were sensitive to *d*-amphetamine. Twenty min after *d*-amphetamine (27 μM) administration, the action potential changed into bursting pattern. The amplitude of action potentials was also decreased after *d*-amphetamine adminstration. If holding the neuron at same membrane potential (i.e. –80 mV) and passing a constant current for 200 msec, action potential was elicited in control neuron. The repetitive firing of the potentials was elicited after *d*-amphetamine (1–30 μM) administration. The results suggested that *d*-amphetamine may facilitate the excitability of vertebrate central neurons.

The effect of *d*-amphetamine on total inward and outward currents of thalamic neurons was also tested. The membrane currents were elicited from a holding potentials of –70 mV to test potentials of –10, 20 and 50 mV. *d*-Amphetamine at concentration from 13.5 to 270 μM decreased the total inward and outward currents of the neuron reversibly.

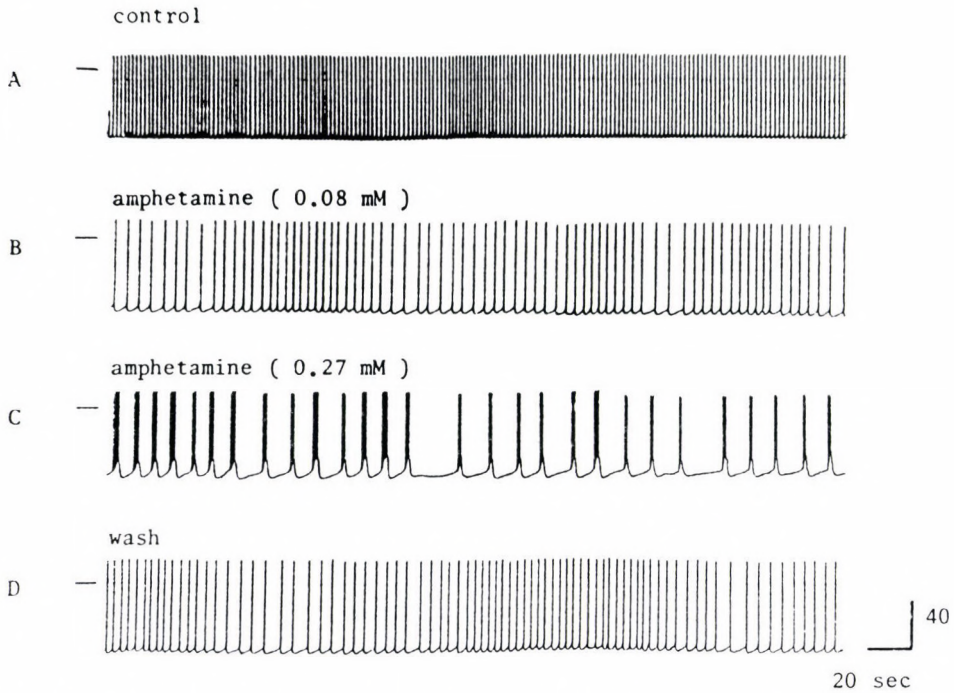

Fig. 1. Effects of *d*-amphetamine on a central RP 4 neuron of snail. Figs A, B, C and D were recorded from the same neuron. A: Control. The neuron shows spontaneous firing of action potentials. B: 40 min after application of *d*-amphetamine (0.08 mM). C: 20 min after application of *d*-amphetamine (0.27 mM). D: 120 min after after washing off *d*-amphetamine (0.27 mM) following recording in C. The horizontal bar on the top left side indicates the membrane potential at 0 mV. Note that *d*-amphetamine at 0.08 mM did not, while at 0.27 mM did elicit bursting of action potentials of RP4 neuron reversibly

The invertebrate animals, such as snail possess a giant neuron. Which is convenient for stable and continuous electrophysiological recording or intracellular injection of chemical compounds. Therefore, we tested the effects of amphetamines on the central neurons of giant African snail (Fig. 1).

The giant African snail was carried from Africa to Taiwan by the Japanese scholar, Shimojoi, who imported it from Singapore 150 years ago [11]. The central nervous system of the neuron was separted into several ganglia. After removing the external sheaths and lightly stained with methylene blue, the neurons were easily identified and numbered for further identification [15, 16]. Conventional two-electrode voltage clamp techniques were followed [15]. The drugs were applied either intracellularly or extracellularly, and the calcium content of the neuron was tested using ratiometric confocal measurements using calcium green and Texas red fluorescent probes [4]. The right parietal 4 neuron, which is similar to PON (periodical oscillation neuron) neuron as described by professor Takeuchi in Gifu university. The

neuron has several receptors, ACh, GABA elicited hyperpolarization responses and dopamine and glutamate elicited depolarization responses and serotonin elicited biphasic responses. *d*-Amphetamine elicited bursting firing of action potentials of the neuron by a concentration dependent manner (Fig. 1). However, *d*-amphetamine did not alter the potential changes in LP5 neuron of the same preparation at the same concentrations tested [16].

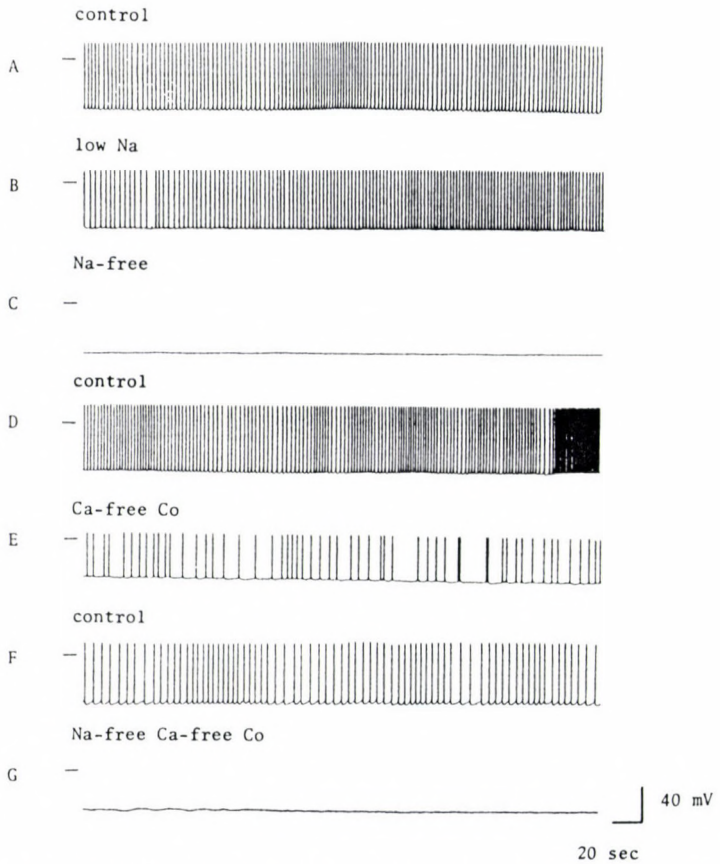

Fig. 2. Effects of Na^+ and Ca^{2+} ions on the spontaneously generated action potentials of RP4 neuron. A: Control. Action potentials from a RP4 neuron. B: 30 min after low Na^+ (20 mM) saline was perfused. C: 30 min after Na^+-free saline was perfused following recording in B. D: Action potentials from another RP4 neuron. E: 30 min after Co^{2+}-substituted Ca^{2+}-free saline was perfused. F: Action potentials from another RP4 neuron. G: 30 min after Na^+-free and Co^{2+}-substituted Ca^{2+}-free saline was perfused. The horizontal bar on the top left side indicates the membrane potential at 0 mV. Note that the action potentials of RP4 neuron disappeared in Na^+-free saline and Na^+-free and Co^{2+}-substituted Ca^{2+}-free saline, while the potentials existed in low Na^+ (20 mM) saline and in Co^{2+}-substituted Ca^{2+}-free saline with a decreased amplitude

d-Amphetamine elicited bursting firing of action potentials in RP4 by a dose dependent manner. The effect was reversible. The potentials return to normal pattern after continuous perfusion for 2 h. Similar results were found after *l*-amphetamine application [8]. It appeared that both *d*-amphetamine and *l*-amphetamine had similar potency eliciting the bursting firing of action potentials in RP4 neuron. However,

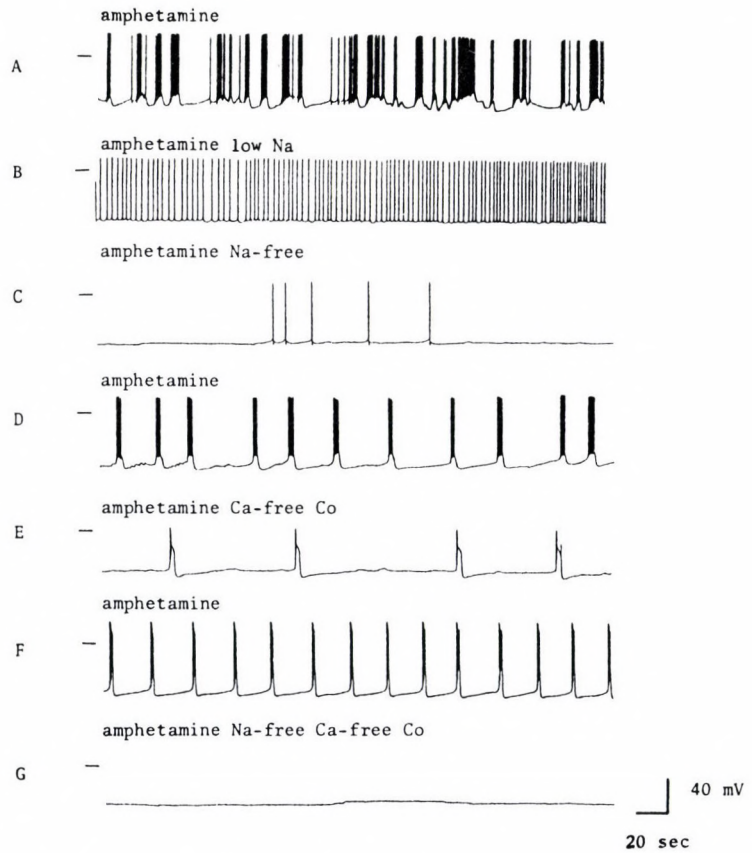

Fig. 3. Effects of Na^+ and Ca^{2+} ions on the *d*-amphetamine-elicited bursting activity of RP4 neuron. A: Bursting activity elicited by *d*-amphetamine from RP4 neuron. B: 30 min after low Na^+ (20 mM) saline was perfused from A. C: 30 min after Na^+-free saline was perfused following recording in B. D: Bursting activity elicited by *d*-amphetamine from another RP4 neuron. E: 30 min after Co^{2+}-substituted Ca^{2+}-free saline was perfused following recording in D. F: Bursting activity elicited by *d*-amphetamine from another RP4 neuron. G: 30 min after Na^+-free and Co^{2+}-substituted Ca^{2+}-free saline was perfused following recording in F. The horizontal bar on the top left side indicated the membrane potential at 0 mV. Note that the *d*-amphetamine-elicited bursting activity of RP4 neuron was changed to a single regular firing pattern in low Na^+ (20 mM) saline, while the bursting activity disappeared in Na^+-free saline. The *d*-amphetamine-elicited bursting activity existed in Co^{2+}-substituted Ca^{2+}-free saline with decreased amplitude. However, it also disappeared in Na^+-free and Co^{2+}-substituted Ca^{2+}-free saline

dopamine, norepinephrine and methamphetamine did not elicit the bursting firing of action potential of the RP4 neuron. Methamphetamine was a potent central stimulant and it did not elicit the bursting firing of potential changes. The results suggested that the bursting firing of potential changes elicited by *d*-amphetamine may not be directly related to the central stimulatory effect of amphetamine [8].

The factors related to the bursting firing of potential changes elicited by amphetamine were also tested. The factors tested included receptors, ionic currents and secondary messengers, etc.

The amphetamine-elicited bursting firing of action potentials was not blocked even after high concentrations of *d*-tubocurarine, atropine, haloperidol, hexamethonium administration. Therefore, the amphetamine elicited potential changes may not directly related to the activation of the receptors of the neuron [16].

The bursting firing of action potentials elicited by amphetamine occurred 20–30 min after amphetamine administration extracellularly, even after high concentration of *d*-amphetamine administration (0.08, 0.27, 1 mM). However, the bursting firing of potentials occurred immediately if amphetamine was administrated intracellularly at lower concentration. Therefore, the results suggested that the active site of amphetamine may be intracellularly in the neuron [2].

The effects of ions, i.e. calcium, sodium as well as potassium ions, on the bursting firing of action potential were tested (Figs 2, 3). If extracelluar calcium ion was removed by perfusion with calcium free solution, the amplitude of bursting firing of potentials elicited by amphetamine decreased, however, the pattern still remained even after 2 h of continuous perfusion with calcium free solution. The results suggested that the extracellular calcium ions may not be the main source contributing to the potentials. However, upon intracellular injection of EGTA, calcium ion chelator or high concentration of magnesium, the bursting firing of potentials was abolished immediately. Besides, ruthenium red, the calcium antagonist, abolished the amphetamine elicited bursting firing of action potentials. These results suggested that the calcium ion in the neuron play an important role of the bursting of potentials [2]. To support this view, we studied if intracellular injection of calcium also elicits bursting firing of action potentials. However, intracellular injection of calcium ion did not further potentiate the bursting firing of potential changes in amphetamine-treated neuron. The calcium ion-content in the neuron appeared to remain at its optimal condition to express the potential changes [2, 4].

The intracellular calcium content was also tested by the ratiometric measurement using a confocal laser microscope. The neuron was injected with calcium green and Texas red. The calcium content in the RP4 neuron was increased after amphetamine administration. These results suggested that intracellular calcium ion played an important role for the potential changes elicited by amphetamine [4].

The effects of sodium ions on the bursting firing of action potential were also tested. If extracelluar sodium was removed by perfusion with sodium free solution, the bursting firing of potentials elicited by amphetamine was initially decreased, then abolished (Figs 2, 3). However, the bursting firing of potentials remained if tetrodotoxin was administered. The results suggested that extracellular sodium plays

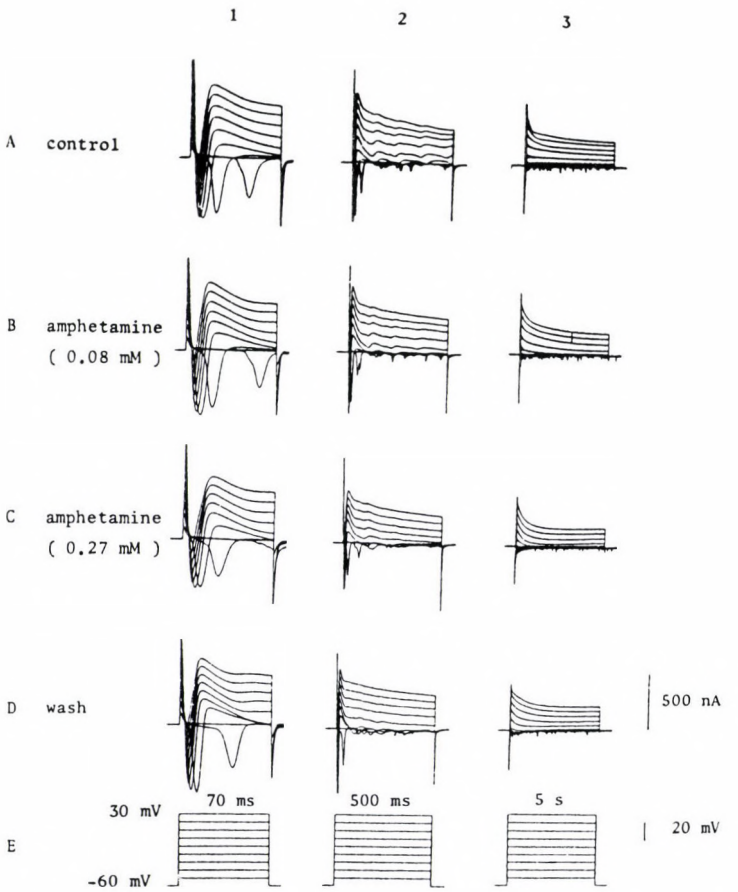

Fig. 4. Effects of *d*-amphetamine on fast inward and outward currents in the RP4 neuron. The membrane currents were elicited from a holding potential of –60 mV to test potentials of –50, –40, –30, –20, –10, 0, 10, 20 and 30 mV for 70 msec. A: Control, total inward and outward currents recorded in normal physiological saline. B: Fast inward and outward currents recorded 40 min after incubation of *d*-amphetamine (80 μM). C: Fast inward and outward currents 40 min after incubation of *d*-amphetamine (0.27 mM) following recording in B. D: Fast inward and outward currents 120 min after washing off *d*-amphetamine (0.27 mM) from C. E: Voltage step commands. Note that *d*-amphetamine at 80 μM did not, while at 0.27 mM did decrease the total inward and outward currents of the neuron reversibly

an important role of the bursting firing of potential changes elicited by amphetamine and the sodium channel was not sensitive to tetrodotoxin, the conventional sodium channel blocker. Ouabain, the sodium pump inhibitor, increased the frequency of the spontaneously generated action potentials and increased the frequency of the action potentials in amphetamine treated preparation [16].

The amphetamine elicited bursting firing of action potentials was also dependent on the temperature of the solution perfused. Amphetamine elicited bursting firing of potentials in room temperature, whereas it did not elicit the bursting firing of potenitals if it was perfused at 4 °C for 2 h. It appears that the effect of amphetamine on the potential changes is closely related to the enzyme kinetics and the sodium ion played an important role of the bursting firing of potential changes [16].

The effects of potassium ion, on the bursting firing of action potentials were tested. The membrane of the neuron were depolarized by increasing the concentration of extracelluar potassium. The frequencies of the spontaneously generated action potentials were also increased [15]. *d*-Amphetamine increased the frequency of the spontaneous contraction of the portal vein of rat [18], it also increased the quantal content of endplate potentials of the neuromuscular transmission [15]. These effects were associated with the potassium ion concentration of the medium.

The roles of the ionic currents on the bursting firing of action potentials in central snail neuron elicited by *d*-amphetamine were tested using two-electrode voltage clamping method. Amphetamine, at 80 μM did not, while at 0.27 mM did decreased the total inward and steady outward currents of the RP4 neuron (Figs 4, 5). *d*-Amphetamine also decreased the calcium, Ia and the steady-state outward currents of the RP4 neuron. Besides, amphetamine elicited a negative slope resistance (NSR) if membrane potential was kept in the range of –50 to –10 mV. The NSR was decreased in cobalt substituted calcium free and sodium free solutions. *d*-Amphetamine decreased the fast calcium current while it did not alter the amplitude of the slow calcium current. It appears that *d*-amphetamine elicited a calcium- and sodium-dependent negative slope resistance change which may contribute in some part to the bursting firing of action potentials [5].

The role of the intracellular second messengers on the bursting firing of action potentials in central snail neuron elicited by *d*-amphetamine was tested [3]. The bursting firing of action potentials was decreased following extracellular application of [1] H8 (N-(2-methyl-amino) ethyl-3-isoquinoline sulphonamide dihydrochloride), a specific protein kinase A inhibitor and [2] anisomycin, a protein synthesis inhibitor. However, the bursting firing of action potentials was not affected after [1] extracellular application of H7 (1,(5-isoquinolinesulphonyl)-2-methylpiperasine dihydrochloride), a specific protein kinase C (PKC) inhibitor, or [2] intracellular application of GDPβS, a G protein inhibitor. The oscillation of membrane potential of the bursting activity was blocked after intracellular injection of 3'-deoxyadenosine, a inhibitor of adenylyl-cyclase. These results suggested that the bursting firing of action potentials elicited by *d*-amphetamine in snail neurons may be associated with the cyclic AMP second messenger system; on the other hand, it may not be associated with the G protein and protein kinase C activity. The relationships between the bursting firing of potential changes elicited by amphetamine and the protein kinase activity in the neuron were closely related. Extracellular application of H8 (N-(2-methyl-amino) ethyl-3-isoquinoline sulphonamide dihydrochloride), a specific protein kinase A inhibitor, decreased not only the bursting firing of potential changed elicited by *d*-amphetamine, it also decreased the NSR elicited by *d*-amphetamine in

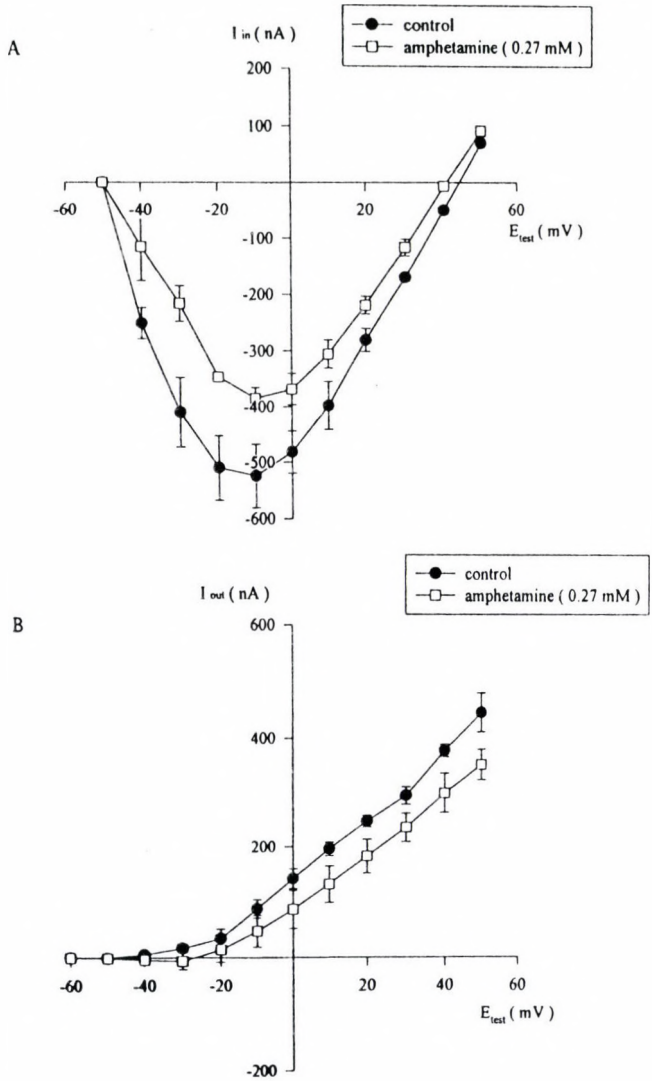

Fig. 5. A: Current-voltage relationships of the peak total inward currents before (●) and after (□) *d*-amphetamine (0.27 mM) application. The currents were elicited by a 70 msec duration of command step from holding potential of –60 mV to test potentials of –50, –40, –30, –20, –10, 0, 10, 20, 30, 40 and 50 mV in normal physiological solution. B: Current-voltage relationships of the steady-state outward currents before (●) and after (□) *d*-amphetamine (0.27 mM) application. The currents were elicited by a 500 msec duration of command step from holding potential of –60 mV to test potentials of –50, –40, –30, –20, –10, 0, 10, 20, 30, 40 and 50 mV in normal physiological solution. The steady-state outward currents were measured 500 msec after holding the potentials. Each points reflects the mean ± SEM of 3 preparations

central snail RP4 neuron. Extracellular application of H7 (1,(5-isoquinolinesulphonyl)-2-methylpiperasine dihydrochloride), a specific protein kinase C (PKC) inhibitor, did not alter the bursting firing of potential change elicited by *d*-amphetamine and it also did not alter the NSR elicited by *d*-amphetamine. It appeared that intracellular calcium ion, second messengers and the ionic currents of the neuron play important factors on the bursting firing of action potentials elicited by amphetamine. The interactions among those factors remained an interesting subject for further studies (Fig. 6).

It is concluded that both *d*- and *l*-amphetamine elicited bursting firing of potential changes in both vetebrate and invertebrate central neurons. The effect is closely related to intracellular second messengers and ionic currents. The bursting firing of action potential elicited by amphetamine in the giant African snail may provide an experimental animal model for testing anticonvulsants.

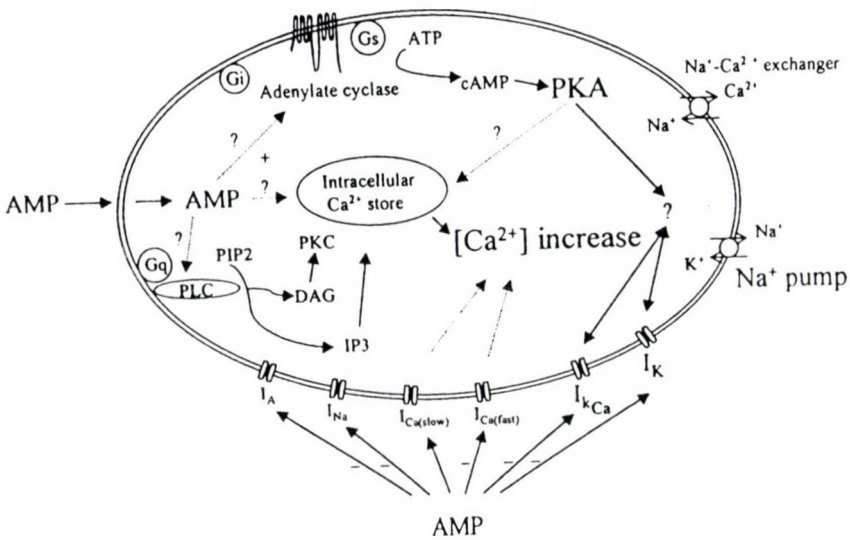

Fig. 6. A model describing the sites related to the bursting firing of action potentials elicited by amphetamine (AMP). Positive (+) and negative (–) signs indicates enhancement and suppression of the effects. Amphetamine acts intracellularly: (1) activating the second messenger system, (2) increasing intracellular free calcium ion concentration, and (3) activating the currents related to the membrane excitability

ACKNOWLEDGEMENT

The work was supported by a grant, NSC-89-2320-B002-009, from National Science Council, Taipei, Taiwan.

REFERENCES

1. Chen, K. K. (1926) The acute toxicity of ephedrine. *J. Pharmacol. exp. Therap. 27,* 61–76.
2. Chen, Y. H., Tsai, M. C. (1996) Bursting firing of action potential in central snail neuron elicited by *d*-amphetamine: role of intracellular calcium ions. *Comp. Physiol. Pharmacol. 115A,* 195–205.
3. Chen, Y. H., Tsai, M. C. (1997) Bursting firing of action potential in central snail neuron elicited by *d*-amphetamine: role of cytoplamic second messengers. *Neuronsci. Res. 27,* 295–304.
4. Chen, Y. H., Tsai, M. C. (1998) Ratiometric confocal Ca^{2+} measurements with visible wavelength indicators in *d*-amphetamine treated central snail neuron. *Gen. Pharmacol. 31,* 783–788.
5. Chen, Y. H., Tsai, M. C. (2000) Action potential bursts in central snail neurons elicited by *d*-amphetmaine: roles of ionic currents. *Neuroscience 96,* 237–248.
6. Chiarello, R. J., Cole, J. O. (1987) The use of psychostimulants in general psychiatry. *Arch. Gen. Psychiatry. 44,* 286–295.
7. Derlet, R. W., Albertson, T. E., Rice, P. (1990) The effect of SCH 23390 against toxic doses of cocaine, *d*-amphetamine and methamphetamine. *Life Sci. 47,* 821–827.
8. Huang, S. S., Chuang, Y. C., Chen, Y. H., Tsai, M. C. (1999) Effects of *l*-amphetamine on the central neurons of the snail. *Gen. Pharmacol. 32,* 381–392.
9. Miller, H., Piness, G. (1928) A synthetic substitute for ephedrine. *J.A.M.A. 91,* 1033–1035.
10. Prinzmetal, M., Bloomberg, W. (1935) The use of bezedrine for the treatment of narcolepsy. *J.A.M.A. 105,* 2051–2054.
11. Rees, W. J. (1950) The giant African snail. *Proc. Zool. Soc. Lond. 120,* 577–599.
12. Sugaya, E., Onozuka, M., Kishi, K. (1982) Intracellular protein changes during pentylenetetrazol induced bursting activity in snail neurons. *Brain Res. 253,* 271–279.
13. Sugaya, E., Goldring, S., O'Leary, J. L. (1964) Intracellular potentials discharge in cat. *Electrocephalogr. Clin. Neurophysiol. 17,* 661–669.
14. Tsai, M. C., Chen, Y. H. (1989) A new method for screening anticonvulsants. 1. effects of anticonvulsants on pentylenetetrazol induced neuronal activity of the giant African snail *Achatina fulica* Ferussac. *Asia Pacific J. Pharmacol. 4,* 203–207.
15. Tsai, M. C., Ho, C. C., Chen, Y. H. (1995) Effects of (+)-amphetamine on motor nerve terminals of mouse skeletal muscle. *Asia Pacific J. Pharmacol. 10,* 53–58.
16. Tsai, M. C., Chen, Y. H. (1995) Bursting firing of action potential in central snail neuron elicited by *d*-amphetamine: role of electrogenic sodium pump. *Comp. Physiol. Pharmacol. 111C,* 131–141.
17. Woolverton, W. L., Kandel, D., Schuster, C. R. (1978) Tolerence and cross-tolerance to cocaine and *d*-amphetamine. *J. Pharmac. exp. Ther. 205,* 525–535.
18. Wu, N. Y., Chen, Y. H., Huang, S. S., Tsai, M. C. (1998) Effects of *d*-amphetamine on the frequency of the spontaneous contraction of the portal vein in rat. *Gen. Pharmacol. 30,* 669–683.

Acta Biologica Hungarica 51 (2–4), pp. 287–307 (2000)

INVERTEBRATES IN NEUROTOXICOLOGY[+]

J. SALÁNKI*

Balaton Limnological Research Institute of the Hungarian Academy of Sciences,
P.O. Box 35, H-8237 Tihany, Hungary

(Received: August 31, 1999; accepted: November 30, 1999)

Due to the relative simplicity of their nervous system, invertebrate animals were widely used in the past decades for studying the processes of excitability at membrane level, as well as the mechanisms of neuronal events and interneuronal communication. Parallel with investigating basic questions of neurobiology, lower animals have also been the object of toxicological studies, because simple invertebrate preparations with well-known physiological, biochemical and pharmacological characteristics proved to be excellent models for testing the action of natural and synthetic compounds important to human pharmaceutical research as well as in searching suitable chemicals for pest control.

In the last ten-fifteen years with the growing interest towards environmental protection, a new field was opened for the application of invertebrates, namely, testing and monitoring the presence and harmful effects of anthropogenic toxic substances. Invertebrates are used today both as passive and as active biomonitors to detect and evaluate the level of pollution in a given ecosystem, and to study the effects and mechanisms of action of pollutants. Invertebrate nervous systems are suitable objects in clarifying the mechanisms of action of toxic chemicals at various levels of the neural regulation.

Toxic influences can be reflected in behavioural alterations, by the modification of the function of different organs as well as the neural regulation, presented by examples on mussels and snails. In case of neurotoxicity, the targets of action are the elements of the nervous system. Alterations can occur in the permeability (ion channels) of the neuronal membrane influencing excitability, potential generation and propagation of nerve impulse, in the transmitter system (synthesis, release, elimination and binding to the receptors), in the interneuronal and neuroeffector connections responsible for co-ordinated and adequate responses to the internal and external challenges.

For the future, it can be predicted that neurotoxicological research with new compounds cannot be effective without using invertebrate preparations, since, due to animal protection and restrictions in animal experimentation, the permission of the use of vertebrates is much more limited in most of the developed countries, and this trend is certainly to be expanded.

Keywords: Neurotoxicology – ionic channels – transmitters – behaviour – heavy metals – mussel – snail.

[+] Presented at the 9th ISIN Symposium on "Neurobiology of Invertebrates", July 1–5, 1999, Tihany, Hungary.

*E-mail: salanki@tres.blki.hu

0236-5383/2000/$ 5.00

INTRODUCTION

Invertebrate animals, being progenitors of vertebrates in the evolution, represent a special group in the animal kingdom. The recognition of similarities in the structural organisation and regulation of life processes in simpler, invertebrate phyla and in higher animals, including men, resulted in a growing interest towards studies with invertebrate animals, a long time ago. It was in 1949, when the paper of Hodgkin and Katz appeared in Journal of Physiology with the title "The effect of sodium ions on the electrical activity of the giant axon of the squid" [4]. Although Hodgkin worked already for several years on crustacean axons studying the propagation of the nerve impulse, it is obvious, that the fundamental achievements published in the following years together with Huxley on a cephalopod mollusc gave the greatest impetus to use invertebrate animals as objects in neuroscience, as we call today this broad field of research. The solving of a long-standing problem, the ionic basis of nerve impulse, generated rapid development in the understanding of a series of elementary neuronal events, like excitation and inhibition, the ionic processes at the postsynaptic membrane during synaptic transmission, the activation of individual neurones and signalling in the nervous system.

In the mid-fifties another invertebrate animal appeared on the scene of neurophysiology, the gastropod mollusc, *Aplysia*, and soon after the terrestrial and aquatic snails, with the great advantage of the occurrence of giant, identifiable neurones in their ganglia. Arvanitaki and Chalazonitis [1, 2] and Tauc [25] were the pioneers of research with gastropod neurones, followed soon by very active groups working all over the developed world, from Japan to the Unites States, extending the studies on giant neurones to a wide scale of problems, from membrane permeability to synaptic transmission, organisation and functioning of neuronal assemblies, behavioural regulation and even the mechanisms of learning. Parallel with these studies, beside molluscs also other invertebrate groups, crustaceans, insects and some worms became favourite objects in neurobiology. As most powerful preparations the crustacean stretch receptor cell and the neuromuscular junction, the stomatogastric ganglion of the lobster, the eye of the horseshoe crab should be mentioned. In insects the sensory system and the neuromuscular synapse, the problem of circadian rhythm and motor pattern regulation called much attention, while among worms the *Hirudo* Retzius cell and nerve elements of *Ascaris* and *Lumbricus* have been investigated in many laboratories.

Invertebrates as models for vertebrates

The wide scale of preparations in different invertebrates gave the chance to discover the variability in the mode of regulation of identical functions. For example, although the central nervous system is involved in each group in heart regulation, the excitatory and inhibitory substances are different in insects, crustaceans, and various groups of molluscs, and neither is identical with the extracardial regulation of the

vertebrate heart [9]. Apart from such negative examples, studies on invertebrate preparations resulted in a large amount of data, proving, that basic structures, principles and mode of action in the neural regulation is similar over the animal kingdom. So, the basic properties of excitable membranes, the ionic channels and intracellular regulation, the processes of impulse transmission and input-output organisation follow the same scheme in all groups of animals, including vertebrates, even, if there are significant differences in particular events or signal substances. These results led to the recognition that studies on invertebrates are important not only for description of neural regulation in lower animals, but they can be models in clarifying the functioning of the vertebrate nervous system, as well.

The great advantage of the relative simplicity and easy handling of isolated brain or complex preparations of lower animals over vertebrates was one of the reasons, why invertebrates became popular in neurobiology. They can often be used for research without special care, they do not require constant temperature or oxygen supply and preparations can survive in good conditions for many hours or even days in the experimental chamber. To access the nervous system and manipulate with it is comparatively simple even if very sophisticated and miniaturised techniques are applied. These circumstances and the large size of neurones allowing visual control of manipulation facilitated the introduction and application of new, not yet fully developed, but promising, advanced techniques in experimentation with invertebrates much earlier, than with vertebrates. The measuring of membrane potential, recording of spikes and synaptic events with microelectrodes not only from gastropods but from crustaceans and insects could be accomplished in many laboratories much earlier, than from vertebrate neurones. The voltage clamp and patch clamp techniques could be performed also easier from invertebrate neurones. Staining techniques for identification and localisation of neurones as well as axonal branching in *in vivo* conditions [5], cell isolation and single cell perfusion techniques [8] were all applied first in invertebrate preparations. Cell mapping and functional characterisation of identified neurones, up to exact description of networks with restricted number of neurones, as well as monitoring of input-output relations of identified nerve cells is possible even today only on invertebrate animals and preparations.

Due to the structural and technical advantages invertebrates played a key role in the progress of our knowledge during the past half century especially in the biophysics of the excitable membranes, in the action of signal molecules, in sensory, central and motor pattern regulation and in neural processes underlying behavioural phenomena.

Beside the basic discoveries of Hodgkin and Huxley on the role of potassium, sodium and chloride permeability in establishing the resting potential, and the role of sodium and potassium currents in action potential generation, studies on invertebrates contributed also to the realisation of calcium permeability and Ca-currents in many neurones. Discovery of a number of biophysical properties of the membrane, and description of subgroups of voltage and ligand gated channels were made first also in invertebrates. The nerveous system of invertebrates contributed to a great deal in recognising specific chemical substances as transmitters, like serotonin, dopamine,

amino acids and others, as well as some neuropeptides, not known earlier in vertebrates [28]. The role of calcium in transmitter release, the co-localisation of transmitters, the excitatory and inhibitory mode of action of transmitters, all important discoveries in neurobiology, were also described or confirmed in invertebrates. A series of new findings were reported first on invertebrates concerning the synthesis, release and elimination of transmitters as well as their specific binding to the postsynaptic membrane. With studying the connection between two or more neurones, and to the receptor or effector organs simple sensory-motor patterns were described and analysed in invertebrates long before appropriate preparations were available in vertebrates. The basic elements of motor pattern regulation were discovered this way, even, if later the command neurone theory failed to stay as a general principle and the multifunctional character of neurones and the overlapping and restructuring network organisation – described also in invertebrates – seems to fit better to experimental findings. In disclosing the neuronal basis of many behavioural phenomena like orientation, avoidance, feeding, egg laying, rhythmic and periodic activities, learning and others, fundamental experiments were conducted and knowledge has accumulated on invertebrate animals bound mainly to the special regulatory system of a given species or phyla, but they may have significance also to the understanding of behaviour of higher animals.

With the successful application of the microelectrode technique and later the introduction and employment of cultured nerve tissue and brain slice techniques in vertebrates allowed to employ higher animals for investigating elementary neural processes, nevertheless, invertebrate animals and preparations do not loose their significance in these studies.

Toxic substances as tools in neurobiology

While investigations and results obtained on invertebrate brains contributed mainly to understanding of physiological processes of the neural regulation, a special approach was present from the beginning: studying the effect of drugs on the nervous system, called neuropharmacology. From another aspect neuropharmacology belongs to a greater discipline, neurotoxicology. Neurotoxicology deals with the biological effects, as well as the mechanisms of the action of poisons and toxic chemicals on the neural regulation.

Toxic substances of biological origin affecting adversely the functioning of other livings and especially of the nervous system are products of plants and animals, like poisons of mushrooms and higher plants, toxins of coelenterates, molluscs and fish, venoms of arthropods, snakes and others, well-known and even used for various purposes, for example as specific channel blockers, enzyme inhibitors, therapeutic drugs, and so on. The other two main groups of toxicants include inorganic substances of geological origin, like heavy metals, and the products of chemical technologies, synthesised for application in industry, agriculture, health-care and generally in everyday life. In the course of utilising these compounds for the purpose they

were produced for, the chemicals or their by-products or brake-down components are dispersing in the environment, causing pollution in nature, able to accumulate and affect all livings, including humans.

Invertebrate nervous system has been used in studying the effects of toxic chemicals since long, although the motive of these studies was very varying. Some of the drugs, like atropine, nicotine, curare, bungarotoxin, TEA, TTX, ouabain and others were applied as a tool in clarifying the mechanisms of impulse generation, propagation and transmission, the synthesis, release and elimination of transmitter substances, the course of intracellular events, etc. The use of toxic substances in invertebrate neuropharmacology was very profitable in the past 50 years. With the involvement of a wide range of animal species into the sphere of studies and application of various natural and synthetic agonists and antagonists, our knowledge became extremely rich about the mechanisms of neural regulation. In the fifties, the neuropharmacological studies at the neuronal level were focused to the cholinergic transmission, what has been expanded, when new putative transmitters were recognised. Microchemical, autoradiographical and histochemical methods were used to confirm the presence and localisation of the bioactive substances and electrophysiological measurements could prove their action, however, the detailed analysis of the effect on membrane receptors required the use of specific chemical compounds. Specific blockers became soon indispensable in receptor identification. This was the tool decades ago in clarifying the molecular basis of the antagonistic, excitatory and inhibitory action of acetylcholine, and became a necessary approach later, in proving the transmitter role of any substance in the brain. The use of toxic, or non-toxic, but competitive chemicals played a role in the recognition of the further classical transmitters, like the catecholamines, serotonin, amino acids and others up to the nitric oxide, as well as the neuropeptides, as it has been reported in hundreds of research papers. Further on, the ionotropic and metabotropic mode of action at the postsynaptic membrane was discriminated by using pharmacons, and also specific receptor structures and slightly different types of transmitter-receptor bindings were clarified this way.

Use of toxic substances in pest control

A second group of toxicological studies concerns the investigation and use of natural and synthetic chemicals as weapons against harmful invertebrates. Among these substances the organophosphates and carbamates should be mentioned, as potent toxic compounds against insects, acting as cholinesterase inhibitors at neuromuscular and interneuronal connections. The chlorinated hydrocarbon DDT and derivatives, as well as the pyrethroid compound deltamethrin, acting on the sodium-channels are also effective neurotoxic insecticides, studied intensively on various invertebrate preparations. Large number of chemicals were synthesised as possible neurotoxic substances for killing not only insects, but other invertebrates, like parasitic worms, molluscs and arthropods, other than insects.

When producing and applying pesticides for a targeted purpose, there is always the question of the specificity and the effects on other organisms living in the surrounding. Although DDT is a very effective and cheap insecticide, it has been banned in most countries, because it is very persistent, accumulates in the food chain and represents danger for a large scale of other animals and possibly also for humans. This question, however, leads to a new area, called environmental toxicology.

Environmental neurotoxicology

The third field of using invertebrates in neurotoxicology is studying and monitoring anthropogenic pollutants, present in the environment, with the aim, to clarify their neurotoxic effects and the mechanisms of action on elementary and complex neural processes. On one side, investigations are focused to the detection of the reaction of neuronal elements and the mechanisms of action to the pollutants, on the other, model animals and suitable preparations are searched for use in biological monitoring of the threat of the pollution to other animals and men.

Toxic substances, belonging to anthropogenic pollutants, are either natural elements, or they are products of chemical technologies, but in both cases human activity is involved in dispersing them throughout the environment.

Of natural elements toxic metals are stable components of the Earth, with low, but measurable background concentration in the soil, in the aquatic environment and in the air. They are, however, mined, purified, concentrated and used for various purposes since the beginning of civilisation resulting occasionally in high pollution above background level. The other group of toxic substances, present in the environment are synthesised for special purposes, to make life more comfortable and easier.

Among metals aluminum, arsenic, cadmium, lead, mercury and tin are most important, causing neurological disorders in animals and men. The number of organic compounds proved or suggested to be toxic in the environment is very large. The main groups found toxic to animals in low concentrations include polyaromatic and chlorinated hydrocarbons, various other types of pesticides, polychlorinated biphenyls, *p*-dioxins, nitrosamines, organic esters, surface active agents, organometallic compounds.

The origin of toxic substances in the environment is rather different. The highest amount originates from the industry. Metal mining and processing, metal industry and recycling are sources of toxic metal contamination of the environment through waste-water, soil and air. The chemical and pharmaceutical industry, while producing thousands of organic substances as end products, or as components of chemical technologies, as well as solvents, stains, detergents, release a wide variety of toxic compounds into the environment. Energy generation also contribute to toxic contamination.

In agriculture high amount of chemicals are used for plant protection, against weeds, pests, insects, but also contamination of fertilisers have an impact on fields, and soon animal husbandry and food industry. Pollution originating from use of

energy, wear and tear of machines, services and solid wastes are also sources of toxicants.

Domestic wastes of settlements contain high amount and great variety of toxic chemicals, used in household and everyday life. Heating with coal and oil, transportation, corrosion of metal elements of buildings and household instruments, solid waste deposits and incineration of wastes are all sources of inorganic and organic toxic compounds, released into the sewage, waste reservoirs, air, and contaminating the soil.

All these toxic substances can be solubilized and get through the food chain into all livings, bacteria, plants and animals. Taken up by the organisms they can have an action on the metabolism, on cell membranes and also on the neural regulation.

Due to the great impact of toxic substances on human health, toxicology developed as a subject concentrating mainly on vertebrates. Nevertheless, for today, invertebrate animals became also popular objects in studying the effects of harmful substances, especially in environmental toxicology, gaining great significance in the past two decades. In the course of our research on invertebrate nervous system, we were involved in these studies, and further on, I want to demonstrate some of our results obtained at this area, as examples of using invertebrates in environmental neurotoxicology.

In evaluating the toxic effects of harmful chemical compounds, as a rule, mortality tests are used. The lethal doses or lethal concentrations express the toxicity of a substance in exact values. As usual, LD_{50} or LC_{50}, the dose or concentration causing 50 per cent mortality within 24, 48 or 72 hours are determined. In environmental toxicology, however, the sublethal and chronic effects of pollutants seem to be even more important than acute toxicity, since environmental pollution rarely causes mass mortality, although it may happen as a result of an incident or in extreme circumstances.

In monitoring the effect of low-level and chronic pollution of animals, and also to elucidate the mechanisms of action of toxic substances on the nervous system, four main approaches are used: observation of the behaviour of the animals, studies of structural alterations, studies on biochemical processes including molecular events, and functional investigations at neuronal level [10]. Behaviour and behavioural patterns are very valuable indicators especially in case the selected function is vital for the animal or the population, like pray capture, feeding, avoidance or reproduction. However, observations and measurements on the behaviour are not providing information about the mechanism of the action. Morphological changes in various regions of the nervous system or of the nerve elements have been observed especially in chronic intoxications of vertebrates and could be indicative also in invertebrates, preferably in combination with the other methods. Biochemical and molecular approaches are very useful, since toxicants as chemical compounds cause lesions primarily at this level. However, this type of studies will only give an answer to consequences in functions, if they are combined with studying the effect of the toxicants at neuronal level. Functional studies of the neural regulation utilise electrophysiological techniques, answering the question, what is the way and mechanism the pollutants influence the excitability of nerve cells, the collection of information, the

transmission of nerve impulse, and finally, by these processes the behaviour and adaptability of the animal. The best way is to combine all these approaches, both for acute and chronic studies.

Action of pollutants on molluscan behaviour

Concerning behavioural studies in environmental neurotoxicology I wish to demonstrate three methods we developed and used during the past years in Tihany. Two of them are the filtering pattern of the bivalve mussel, *Anodonta*, the third one is the locomotory activity of the pulmonate snail, *Lymnaea stagnalis*. The filtering activity of the bivalves consists of two main elements: pumping of the water by the opening and closing of the shell valves, called as ventilation movement, and, passing of the water inside the body, getting in through the inhalant siphon and leaving the animal through the exhalant siphon. The locomotory activity of Lymnaea consists of upward and downward movements, called negative and positive geotaxis, as well as of horizontal movements, which is rather irregular. The effects of pollutants were tested on these behavioural patterns under laboratory conditions.

Ventilation activity of the freshwater mussel in control and under the effect of pollutants

The closing and opening of the shells in bivalves are performed by the contraction and relaxation of the adductor muscles, situated inside, between the two shells. Due to the presence of a phasic and a tonic part of the adductors, both fast, short time contractions, and long-lasting contractions can be present, depending on the stimulus, arriving from the nervous system. The force opening the shells at muscle relaxation is given by the property of the ligament, connecting the two shells at their edges. The method of recording the shell movements is based on the approaching and departing of the valves. The technique can be a simple mechanical one [14], or a more sophisticated instrument with electronic parts [27]. Recently we are registering the activity of 16 animals with the help small sensors attached to the shells and collecting the data on line, in digitalized form on a computer.

In control conditions, the ventilation activity of the mussels is characterised by the periodicity of long lasting, 10–20 hours openings with shorter, 4–6 hours closures. During open time, due to fast adductor contractions and relaxations water pumping takes place, therefore this period is called activity, in contrast to the closed time, called rest period. Ventilation supports food and oxygen uptake and elimination of excretions.

The periodic activity as a behavioural phenomenon proved to be a simple and reliable method for testing the harmful effects of a number of environmental pollutants. We tested mainly the effect of toxic heavy metals, namely of cadmium, copper, mercury, lead, tin, as well as organic pollutants, trymethyl tin, deltamethrin and PCB 118 congener.

As a general rule, toxic substances caused shortening of the active periods, and elongation of the duration of the rest, as demonstrated for the effect of mercury (Fig. 1).

The effect of the toxicants was usually concentration dependent, with more expressed reaction at higher concentrations. At quantitative evaluation, the mean duration of the active and resting periods are calculated, and the effect of the drug is expressed as deviation from the values obtained in control conditions (Fig. 2). As it was expected, there were differences between the effects of various pollutants. The threshold concentrations causing reduction of activity were different, being the most toxic mercury and less toxic lead. Lower concentrations of the metals caused often potentiation of active periods, especially if they were not longer than 10 hours in the control [13].

Of organic compounds the pyrethroid insecticide, also deltamethrin proved to be an inhibitor of the activity of the mussel. At the lowest effective concentration (1 μg/l), as a result of reduction of the resting periods, increase of activity occurred, but at higher concentrations massive reduction of the activity was observable, showing the high sensitivity of the mussel to the drug [6]. Another organic pollutant, a polychlorinated biphenyl congener caused similar effect on the periodic activity. In one-week-long experiment 5 μg/l PCB 118 resulted in nearly 50 per cent reduction of the duration of the active periods, and a more than 50 per cent elongation of the rest periods. This means, that under the effect of the drug the activity of the mussel was reduced to a degree, observable in the presence of 100 μg/l mercury.

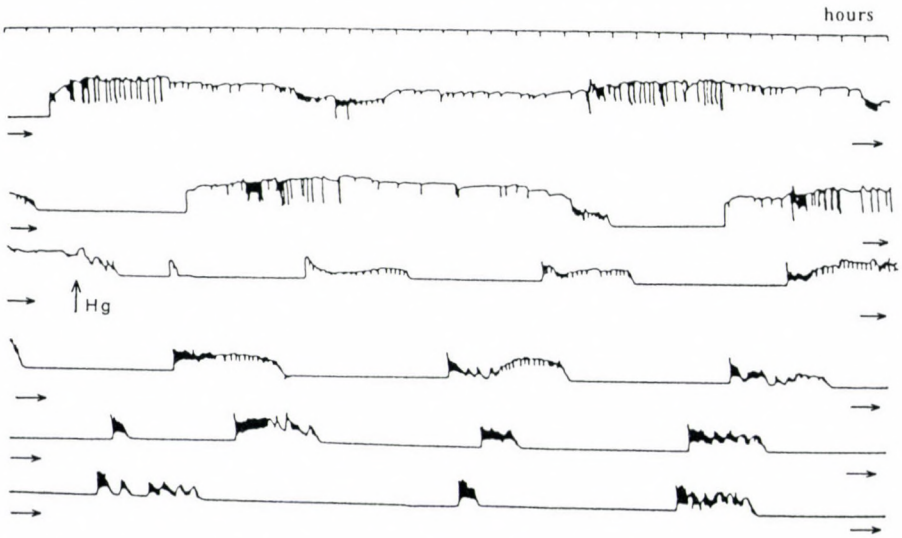

Fig. 1. Effect of mercury (10 μmol/l) on the periodic activity of the freshwater mussel (*Anodonta cygnaea* L.). Continuous registration of the open and closed position of the valves (activity and rest of the animal) for seven days. Active periods shorten and rest periods lengthen after application of mercury chloride (arrow). Time scale in hours

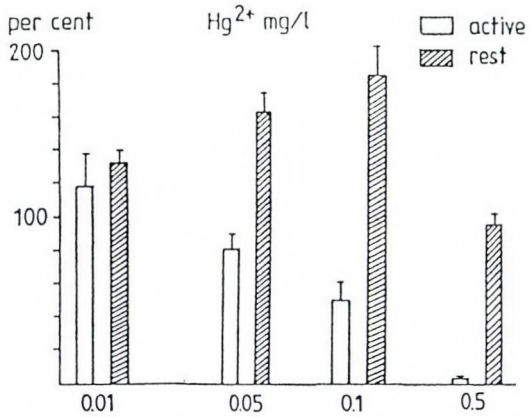

Fig. 2. Concentration dependence of the effect of mercury on the periodic activity of the freshwater mussel (*Anodonta cygnaea* L.). Change of the duration of the active and rest periods is expressed in per cent of the control (100 per cent). With increasing mercury concentration the duration of the active periods shorten

The definite, well measurable response of the mussel's periodicity to harmful substances offers a practical method in invertebrate neurotoxicology. The method can be used not only in laboratory but also at open field as it was shown years ago in our studies [12] and has been utilised in The Netherlands for constructing the Mussel Monitor [7]. There is, however, a disadvantage of this technique in laboratory studies, namely, the long-duration exposure, needed for reliable evaluation of the results. The other method introduced for studying mussel behaviour avoids this inconvenience.

Siphon activity of the freshwater mussel in control and under the effect of pollutants

For the measurement of the siphon reaction to toxicants 30 minutes long exposure is sufficient. It can be performed during activity, at the open period of the valves. The siphon activity is recorded with a mechano-electric transducer, monitoring the force of the water-flow coming out of the exhalant siphon [26]. A small umbrella is placed opposite to the water flow, close to the outflow siphon. In control, the siphon is usually open, and a small fluctuation in the strength of the water outflow can be recorded. After adding toxic substances into the water, time to time closure of the siphon appears (Fig. 3). The effect can be expressed as change of the duration of the open time.

The effect is concentration dependent, but it depends also on the duration of the exposition time. As seen in the Fig. 3., in the presence of 12.5 μg/l $HgCl_2$ about 20–30 second long water flow alternates regularly with similar duration of break, and

with time the amplitude of the umbrella-movement diminishes, referring to the reduction of the strength of the water flow. Copper, lead and zinc evoked similar to the mercury reaction, however, the siphon activity was rather insensitive to another toxic metal, cadmium [18]. Organic toxicants were also tested successfully with this behavioural reaction [6].

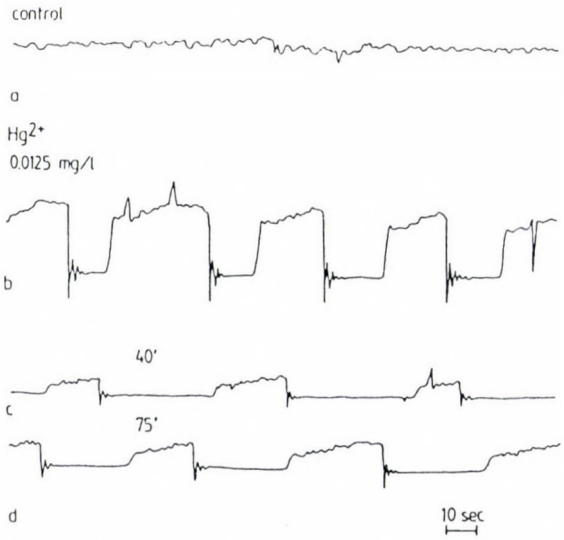

Fig. 3. Effect of mercury on the siphon activity of the freshwater mussel. The water emission through the exhalant siphon was recorded using a mechano-electric transducer system. In control (a) the outflow siphon is open and the water emission is permanent. After application of mercury into the water (b) the siphon closed time to time for short periods and with time (c and d) also the strength of water flow reduced

Snail locomotion in monitoring the effect of pollutants

The third method we introduced as a toxicological test, based on locomotion of aquatic snails. The procedure is suitable for both acute and chronic measurements. Snails are placed separately in a narrow aquarium, allowing upward, downward and horizontal movements. The locomotion is recorded on a video-tape, and evaluated according to distance, time and direction of the movements. In acute testing the measurement is performed for 12 hours, recording the activity for 30 minutes in every hour, while in three-week chronic exposure the measurements take place every third day for 30 minutes. Parallel recordings of untreated animals serve as control. As an example the effect of 20 μg/l mercury is shown (Fig. 4). The locomotion was reduced by 30 per cent, remaining at the same level during the half day long exposition. Measuring the locomotion of the snails for three weeks, differences were found in the

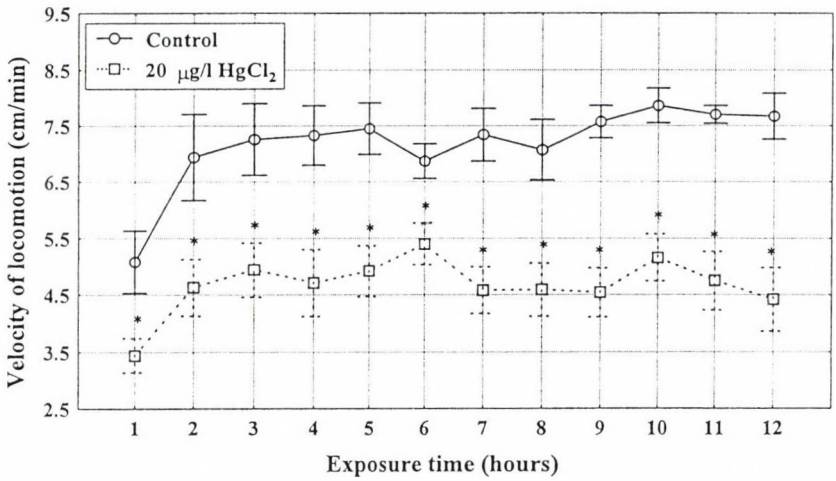

Fig. 4. Effect of mercury on the locomotion of the pond snail *Lymnaea stagnalis* L. Velocity of movement was reduced by about 30 per cent as compared to the control

response to mercury and copper. The depressive effect of mercury increased with time, while the inhibitory effect of copper slightly reduced after two weeks exposure. Nevertheless, the animal's activity did not return to the control level even in a week after placing them into copper-free water.

The positive and negative geotaxis are essential components of the locomotor behavioural in snails, and the changes occurring under the effect of pollutants are indicative to the harmful effects exerted by the drugs on the regulatory mechanisms.

As a short conclusion on behavioural approach it can be stated that toxic heavy metals and some organic pollutants modify specifically the activity pattern of mussels and snails, and these patterns can be used in testing the effect of harmful drugs. The responses are not specific to the drug, nevertheless, they are not monotonous, unspecific reactions, showing, that the central effect of different pollutants can vary depending on their involvement in physiological processes responsible for the regulation of the behaviour.

In the functioning of nervous system underlying behaviour regulation signal molecules play determining role. In mussels serotonin, dopamine and acetylcholine, while in snails also a number of other substances, glutamate, GABA, noradrenaline, various neuropeptides and others have been detected as substances of brain functioning. Toxic drugs influencing behaviour should have an effect on the action of transmitters. For clarification the mechanisms of the effect of harmful substances on behaviour, studies on the functioning of the neuronal membrane is necessary.

Neuronal membranes in monitoring the effect of heavy metals

Neuronal membranes can be a target of toxic substances, which may influence membrane properties in several aspects [10]. The effect of pollutants can be monitored by investigating their action on the response of neuromembranes to neurotransmitters, being a basic event in interneuronal communication, and so, in neuronal regulatory processes. Identified neurones of *Lymnaea stagnalis* L. and *Helix pomatia* L. were used in studying the acute effect of heavy metals on the transmitter activated response and on voltage and ligand gated ionic channels. Cadmium, mercury, lead, tin and copper were tested on Ach, dopamine, GABA, glutamate and serotonin induced membrane effects [12, 20, 23]. Due to the heterogeneity of the neurones the response to the transmitters varied to a great extent (Table 1). Various toxic metals modified differently the transmitter response, and the effects were often concentration- and time-dependent. With increasing the concentration and/or duration of the metal treatment potentiation may turn to depression.

Some characteristic responses and their modification by heavy metals are demonstrated in Figs 5–10. Experiments were performed on neurones of isolated ganglia. Transmitters were applied locally to the neurone under study in a short pulse, while treatment with heavy metals took place in perfusion of the whole ganglion. The activity of a single or more neurones were recorded using conventional microelectrode technique.

ACh sensitive neurones are rather numerous in the snail brain, and some of them are well identifiable. Application of ACh causes either excitation, or inhibition, depending on the ionic channels it opens. Both actions could be modified by low concentration of heavy metals. Figure 5 demonstrates the effect of 10^{-6} mol/l $HgCl_2$ on the ACh-evoked depolarisation (A) and hyperpolarisation (B). The firing of the neurones remained intact, however the effect of ACh was strongly modified: the excita-

Table 1
Heavy metal effects on ligand-gated responses reported so far in invertebrates

Signal molecule	Neurone response	Cd	Hg	Pb	Sn	Cu
ACh	excitation	+, –	+, –	–	–	–
	inhibition	–	–			
DA	excitation					–
	inhibition	–				
GABA	inhibition	–	+	–	+, –	–
Glutamate	excitation		+	+		
	inhibition		+			
5HT	excitation	+, –	–	–		+, –
	inhibition	–		ø		–

+: potentiation. –: depression. ø: no effect.

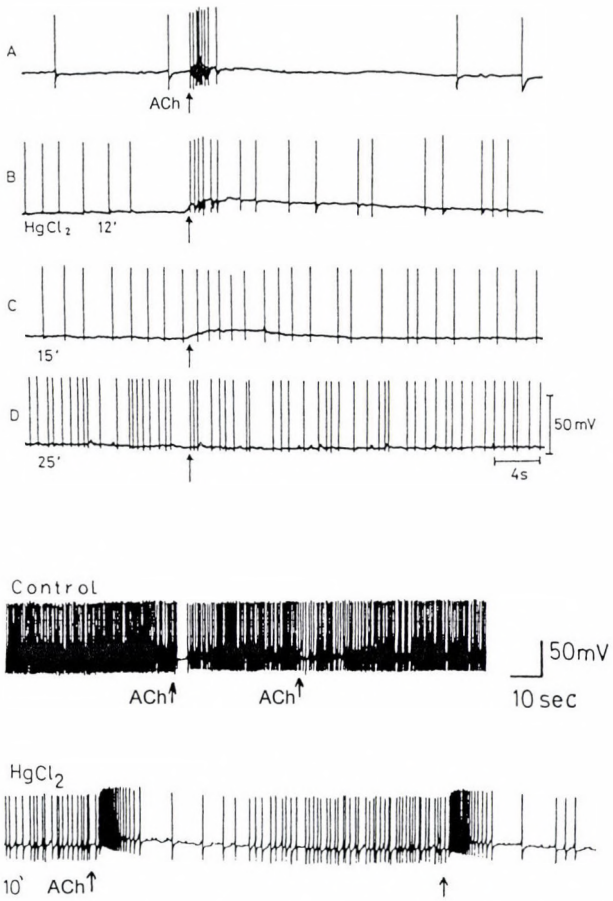

Fig. 5. Upper records: Effect of $HgCl_2$ (10^{-6} mol/l) on the ACh (10^{-4} mol/l) induced depolarisation and excitation of a neurone in the ganglion of *Helix pomatia* L. A – control, B, C, D – ACh application after 12, 15 and 25 min treatment with mercury. Lower records: effect of $HgCl_2$ (10^{-6} mol/l) on the inhibitory effect of ACh (10^{-6} mol/l) on a *Lymnaea stagnalis* L. neuron. Control, and the effect of ACh after 10 min treatment with mercury. Inhibitory effect of ACh turned to excitatory. Spiking of the neurone became also reduced

tory effect on neurone A became abolished, while the inhibitory effect on neurone B turned to excitatory [19, 22]. The ACh-induced depolarisation was abolished also by lead, as shown in Fig. 6. The activity of two neurones is recorded simultaneously, both responding to ACh with depolarisation. Under the effect of 10^{-6} mol/l $PbCl_2$ the responses were strongly reduced within 6 min, and became eliminated after 30 min.

Serotonin application evokes in most cases excitation, as shown on the two neurones studied simultaneously (Fig. 7). The responses were, however, somewhat different: the excitation of the first neurone was of short duration, while that of the second one a longer lasting, with two phases. Lead eliminated the short response of both

neurones within two minutes, but the protracted phase of the 5HT response on the second neurone remained intact, referring to the involvement of two different mechanisms in the 5HT effect.

In some neurones serotonin application results not depolarisation, but hypepolarisation, similarly to dopamine. Cadmium ions cause in most cases elimination of the transmitter evoked responses. As Fig. 8. demonstrates, Cd^{2+} eliminated the inhibitory effect of both 5HT and DA, and DA effect even turned to excitation, referring to a complex mechanism.

Since the action of the transmitters is determined by ionic currents they induce, the effect of the metals should be realised either on the transmitter ligand binding, or on the channel itself. Studies on ligand gated channels showed, that the same metal may have different action on different channels.

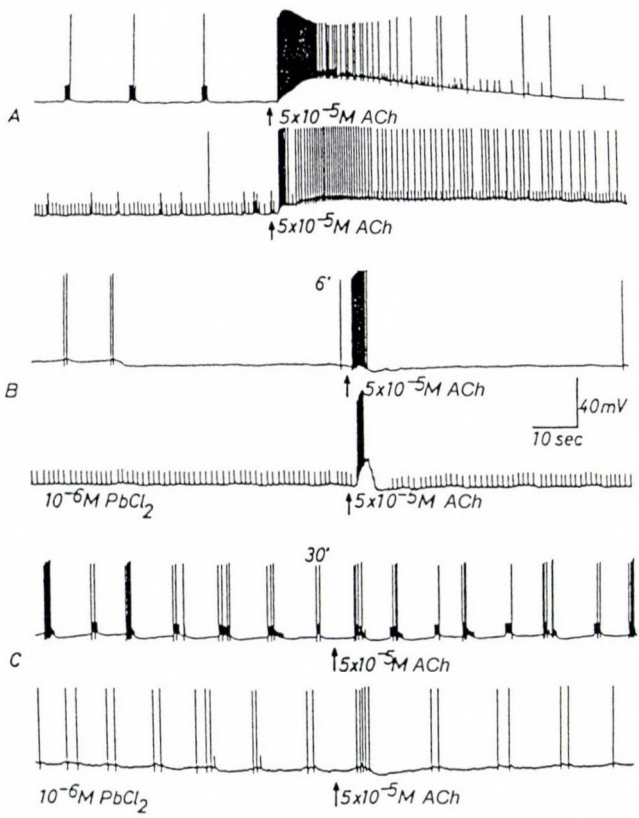

Fig. 6. Effect of lead on the ACh induced excitation of two neurones in the brain of *Lymnaea stagnalis* L. A – parallel recordings of the activity of two neurones and the effect of ACh. B and C – effect of ACh under $PbCl_2$ treatment, after 6 and 30 min. The depolarisation caused by ACh shortened rapidly, however, the fast depolarisation and excitation was rather resistant to lead treatment

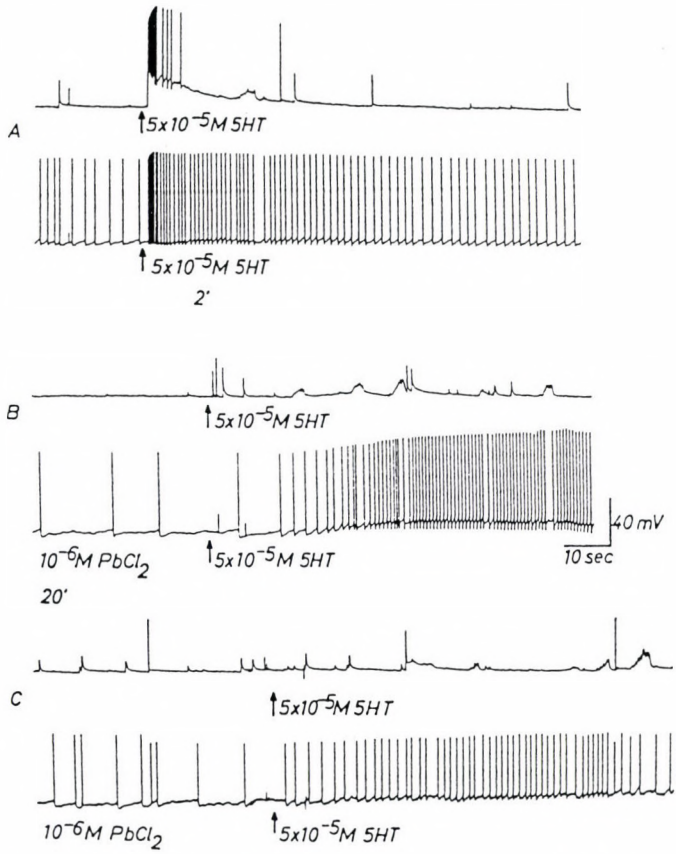

Fig. 7. Effect of lead on the 5-HT induced excitation of two neurones in the brain of *Lymnaea stagnalis* L. A – parallel recordings of the activity of two neurones and the effect of 5-HT. B and C – effect of 5-HT under $PbCl_2$ treatment, after 2 and 20 min. The fast response to 5-HT was inhibited by lead in both neurones, but the slow response in the second neurone remained intact even after 20 min lead treatment

ACh-activated chloride and sodium channels were potentiated, the potassium channel was inhibited by 10 μmol/l mercury ions in *Aplysia* pleural ganglion on medial and anterior neurones, possessing various Ach receptors [3]. Chloride channels activated by glutamate [11] and GABA (Fig. 9) were also potentiated by mercury. The action of mercury on GABA induced Cl-current was concentration dependent. Only low concentrations caused potentiation, higher concentrations resulted in inhibition [11]. These results suggest, that mercury ions act directly on the chloride channel.

Lead had a similar potentiating effect on the glutamate activated chloride channels which was augmented by pretreatment of the preparation with lead [15], however, cadmium ions caused depression on the GABA activated inward current (Fig. 10).

Tin caused depression of the ACh activated inward current in a concentration dependent manner, and the effect depended also on the time of preapplication [16].

The results with ligand gated channels suggest that the metals are involved probably not in transmitter binding, but in modifying the channel properties directly. It was supported by the effect of the metals (cadmium, copper, lead and mercury) on voltage activated K-currents, what could be different on various identified neurones [17, 21].

In nature the toxic substances act for long time on the animal, therefore chronic treatments can be more informative in this respect. After two weeks long exposure to cadmium and lead some interesting results were obtained on the voltage dependent Ca- and K-currents of well-identified *Lymnaea* neurones [24].

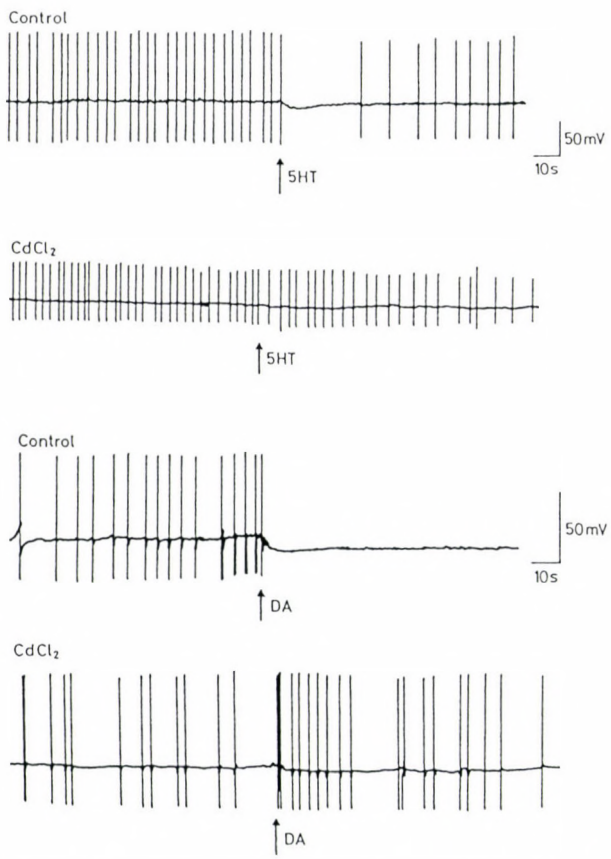

Fig. 8. Effect of cadmium on the serotonin (10^{-6} mol/l) and dopamine (10^{-6} mol/l) induced hyperpolarisation in *Lymnaea* neurones. 5-HT effect was eliminated, while DA effect was reversed after 10 min treatment of the preparation with 10^{-6} mol/l $CdCl_2$

The Ca-current was potentiated significantly, showing probably the increase of the density of the Ca-channels in the membrane. Under chronic cadmium and lead treatment also the early phase of the K-current has changed, depending, whether in control it was present in the given neurone, or not. In the first case it was diminished after two weeks exposition of the animals to the metals, in the other case however, the early potassium current appeared. The significance of these changes can be a subject of speculation, fitting into the frame of accommodation of the animal to the polluted environment.

Summarising the results obtained with toxic metals on ionic channels, it can be concluded, that each metal exerts its own specific effect on the neuronal membrane.

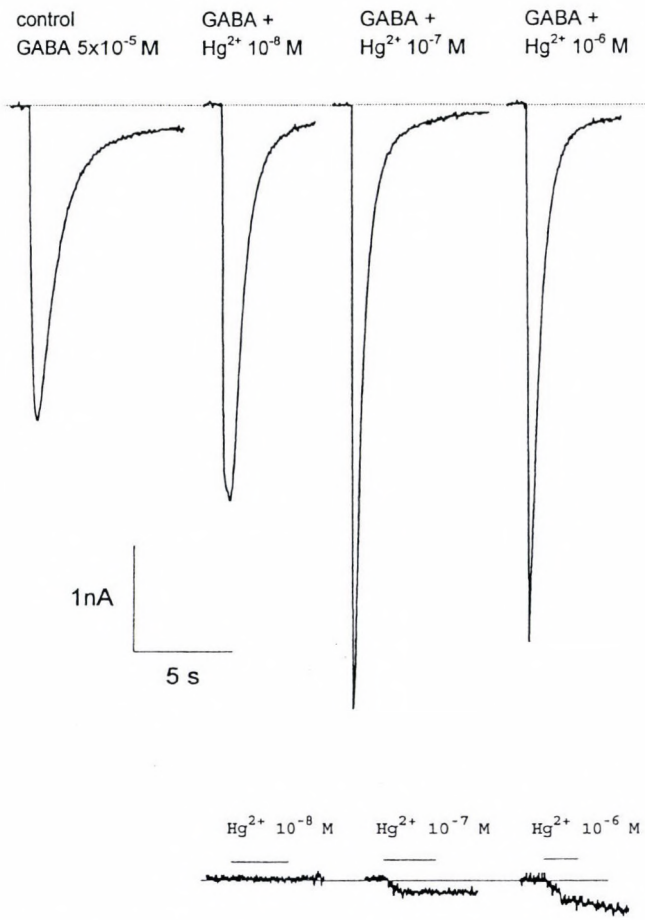

Fig. 9. Effect of mercury on the γ-amino butyric acid (GABA) induced Cl-current in a Lymnaea neurone. $HgCl_2$ in low concentrations significantly potentiated the inward Cl-current, while mercury itself evoked only a very small effect

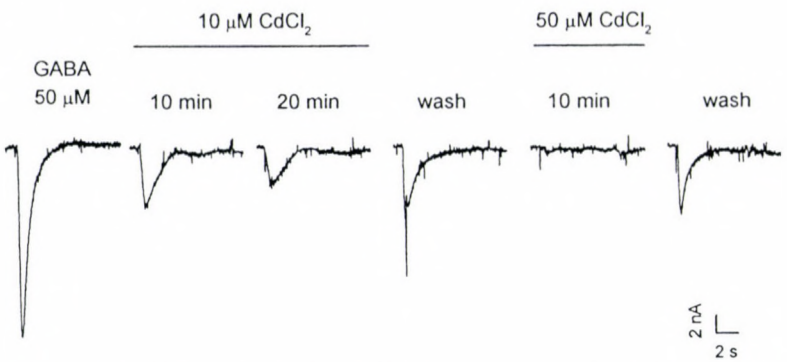

Fig. 10. Effect of cadmium on GABA induced inward Cl-current in a Lymnaea neurone. GABA was applied in a short pulse in 50 μmol/l concentration in control, and under treatment of the preparation with $CdCl_2$. The inhibitory effect of cadmium was concentration and time dependent. Wash out resulted in partial restoration, within 30 min

Even in cases when the effect of different metals seems to be similar, for example on transmitter evoked responses, the mechanism of action may differ from each other. Due to the great variability of the neurones in their receptor and channel structures and their role in brain functioning, these result can give important, but only partial explanation to the question what is the way heavy metals exert their effect on the regulation of life processes and behaviour.

CONCLUSIONS

Returning to the original question, how can we use and what can we learn from invertebrates in neurotoxicology, my reply is:

1. Invertebrates, and among them molluscs, are sensitive to toxic substances and give well-measurable reactions to environmental pollutants, therefore can be applied in toxicological testing.
2. A wide range of behavioural phenomena can be used to test the harmful effect of chemical substances, much cheaper, than with vertebrates.
3. The mechanism of action can be studied on a simple brain – organ systems, supplying data on the general but specific toxicity of substances.
4. Studies can be performed at the cellular level, suitable to clarify the effect of toxicants at membrane receptors, channels and intracellular processes.
5. By combining different techniques and methods on invertebrates, not only practical, neurotoxicological questions can be answered, but by using various toxic substances, our basic neurobiological knowledge will also be expanded and enriched.

For the future it can be predicted that neurotoxicological research cannot be effective without using invertebrate preparations. Due to animal protection and restrictions in animal experimentation the use and sacrifice of vertebrates is less and less

permissible in most of the developed countries and this trend will certainly expand. For this reason, neurobiologists working with invertebrate animals should think about, how to utilise their preparations, knowledge and experiences for application in neurotoxicological research.

ACKNOWLEDGEMENTS

These studies were supported by the US-Hungarian Joint Fund, grant No. 036/91, and by OTKA, grant No. 2757 and 20944.

REFERENCES

1. Arvanitaki, A., Chalazonitis, N. (1955) Potentiels d'activité du soma neuronique géant *(Aplysia). Arch. Sci. physiol. 9,* 115–144.
2. Chalazonitis, N., Arvanitaki, A. (1961) Slow changes during and following repetitive synaptic activation is ganglion nerve cells. *Bull. Inst. Océanogr. Monaco 58,* 1–23.
3. Győri, J., Fejtl, M., Carpenter, D. O., Salánki, J. (1994) Effect of $HgCl_2$ on acetylcholine, carbachol, and glutamate currents of *Aplysia* neurons. *Cell. Mol. Neurobiol. 14,* 653–664.
4. Hodgkin, A. L., Katz, B. (1949) The effect of sodium ions on the electrical activity of the giant axon of the squid. *J. Physiol. 108,* 37–77.
5. Kater, S. B., Nicholson, C. (1973) *Intracellular Staining in Neurobiology.* Springer-Verlag, New York, USA.
6. Kontreczky, Cs., Farkas, A., Nemcsók, J., Salánki, J. (1997) Short- and long-term effects of deltamethrin on filtering activity of freshwater mussel (*Anodonta cygnea* L.). *Ecotoxicology and Environmental Safety 38,* 195–199.
7. Kramer, K. J. M., Jenner, H. A., De Zwart, D. (1898) The valve movement response of mussels: a tool in biological monitoring. *Hydrobiologia 188/189,* 433–443.
8. Krishtal, O. A., Pidoplichko, V. I. (1975) Intracellular perfusion of snail giant neurons. *Neurophysiology 7,* 327–329.
9. Leak, L. D., Walker, J. W. (1980) *Invertebrate Neuropharmacology.* Blackie, Glasgow and London, UK.
10. Narahashi, T. (1996) Effects of metals on ion channels. In: Chang, L. W. (ed.) *Toxicity of Metals.* CRC Press, Inc., Lewis Publishers, New York, pp. 677–698.
11. Rubakhin, S. S., Győri, J., Carpenter, D. O., Salánki, J. (1995) $HgCl_2$ potentiates GABA activated currents in *Lymnaea stagnalis* L. neurones. *Acta Biol. Hung. 46,* 431–444.
12. Salánki, J. (1988) Invertebrates in neuroscience. In: Salánki, J., S.-Rózsa, K. (eds.) *Neurobiology of Invertebrates. Transmitters, Modulators and Receptors.* Akadémiai Kiadó, Budapest, pp. 1–10.
13. Salánki, J. (1995): Biphasic and combined effects of heavy metals on the periodic valve mevements of the freshwater bivalve, *Anodonta cygnea.* In: Munawar, M., Hänninen, O., Roy, S., Munawar, N., Käsenlampi, L., Brown, D. (eds) *Bioindicators of Environmental Health.* SPB Academic Publishing, Amsterdam, pp. 97–104.
14. Salánki, J., Balla, L. (1964) Ink-lever equipment for continuous recording of activity in mussels (mussel actograph). *Annal. Inst. Biol., Tihany 32,* 117–121.
15. Salánki, J., Győri, J., Carpenter, D. O. (1994) Action of lead on glutamate-activated chloride currents in *Helix pomatia* L. neurons. *Cell. Mol. Neurobiol. 14,* 755–768.
16. Salánki, J., Győri, J., Platochin, A., S.-Rózsa, K. (1998) Neurotoxicity of environmental pollutants: effects of tin ($SnCl_2$) on ACh induced currents in snail neurones. *Russ. J. Physiol. 84,* 1061–1073.
17. Salánki, J., Osipenko, O. N., Kiss, T., Győri, J. (1991) Effect of Cu^{2+} and Pb^{2+} on membrane excitability of snail neurons. In: Kits, K. S., Boer, H. H., Joosse, J. (eds.) *Molluscan Neurobiology.* North-Holland, Amsterdam–Oxford–New York, pp. 214–220.

18. Salánki, J., Turpaev, T. M., Nichaeva, M. (1991) Mussel as a test animal for assessing environmental pollution and the sub-lethal effect of pollutants. In: Jeffrey, D. W., Madden, B. (eds) *Bioindicators and Environmental Management.* Academic Press, London, pp. 235–244.
19. S.-Rózsa, K., Salánki, J. (1985) Effects of heavy metals on the chemosensitivity of neural somata of *Lymnaea stagnalis* L. In: Salánki, J. (ed.) *Heavy Metals in Water Organisms.* Akadémiai Kiadó, Budapest, pp. 387–400.
20. S.-Rózsa, K., Salánki, J. (1987) Excitable membranes – object for evaluating the effect of heavy metal pollution. *Acta Biol. Hung. 38,* 31–45.
21. S.-Rózsa, K., Salánki, J. (1990) Heavy metals regulate physiological and behavioral events by modulating ion channels in neuronal membranes of molluscs. *Environ. Monit. Ass. 14,* 363–375.
22. S.-Rózsa, K., Salánki, J. (1991) Ion channels of nerve membrane as targets for environmental pollutants. In: Jeffrey, D. W., Madden, B. (eds) *Bioindicators and Environmental Management.* Academic Press, London, pp. 389–399.
23. S.-Rózsa, K., Salánki, J., Présing, M. (1988) Use of *Lymnaea stagnalis* in monitoring heavy metal pollution. In: Yasuno, M., Whitton, B. A. (eds) *Biological Monitoring of Environmental Pollution.* Tokai Univ. Press, Tokyo, pp. 247–255.
24. Szűcs, A., Salánki, J., S.-Rózsa, K. (1994) Effects of chronic exposure to cadmium- or lead-enriched environments on ionic currents of identified neurons in *Lymnaea stagnalis* L. *Cell. Mol. Neurobiol. 14,* 769–780.
25. Tauc, L. (1958) Processus post-synaptiques d'excitation et d'inhibition dans le soma neuronique de l'*Aplysia* et de l'Escargot. *Arch. Ital. Biol. 96,* 78–110.
26. Turpaev, T. M., Nechaeva, M. V., Salánki, J., Véró, M. (1991) A method for registration of the water flow through the exhalant siphon of lamellibranche molluscs. *J. Gen. Physiol. (Moscow) 52,* 728–730. (in Russian).
27. Véró, M., Salánki, J. (1969) Inductive attenuator for continuous registration of rhythmic and periodic activity of mussels in natural environment. *Med. Biol. Eng. 7,* 235–237.
28. Walker, R. J., Brooks, H. L., Holden-Dye, L. (1996) Evolution and overview of classical transmitter molecules and their receptors. *Parasitology 113,* S3–S33.

Acta Biologica Hungarica 51 (2–4), pp. 309–316 (2000)

BIOACCUMULATION AND TOXICITY OF ALUMINIUM IN THE POND SNAIL AT NEUTRAL pH+

CATHY R. MCCROHAN,[1]* M. M. CAMPBELL,[1] R. JUGDAOHSINGH,[2] S. BALLANCE,[1] J. J. POWELL[2] and K. N. WHITE[1]

[1]School of Biological Sciences, University of Manchester, 1.124 Stopford Building, Oxford Road, Manchester M13 9PT, UK and
[2]The Rayne Institute, St Thomas' Hospital, London SE1 7EH, UK

(Received: August 31, 1999; accepted: November 30, 1999)

The low solubility of aluminium (Al) at neutral pH means that it largely exists as colloidal particulates in aquatic systems. However, the pond snail *Lymnaea stagnalis* accumulates significant amounts of Al following exposure to water containing added Al (up to 500 μgl^{-1}) at pH 7. This is accompanied by depression of behavioural activity (locomotion, feeding) which subsequently recovers, suggesting tolerance to the metal. The presence of silica ameliorates behavioural toxicity of Al, but does not prevent uptake of the metal. *In vitro* studies using the isolated central nervous system demonstrate toxicity at the cellular level. Extracellular application of Al (100 μM) led to membrane depolarisation, bursts of action potentials and action potential broadening.

The chemical form in which Al is applied influences the extent of bioaccumulation and toxicity. Detailed knowledge of its solution chemistry is therefore essential.

Keywords: Aluminium – neurotoxicity – *Lymnaea stagnalis* – behaviour – neutral pH.

INTRODUCTION

Aluminium is ubiquitous in the environment and highly neurotoxic. It has previously been presumed to be relatively unavailable to aquatic organisms under natural conditions. At neutral pH, Al is largely insoluble, forming colloidal polyhydroxides. Furthermore, many organisms possess effective barriers to Al uptake; for example, Al has been shown to bind to mucus in the mammalian gut, preventing absorption [18].

We have used a multidisciplinary approach to examine the bioavailability and toxicity of Al in freshwater macroinvertebrates, particularly the pond snail *Lymnaea stagnalis*. Our laboratory studies show that Al is both accumulated by and toxic to *L. stagnalis* exposed to concentrations commonly found in the environment at neutral pH [6].

+Presented at the 9th ISIN Symposium on "Neurobiology of Invertebrates", July 1–5, 1999, Tihany, Hungary.

*Corresponding author, E-mail: Cathy.McCrohan@man.ac.uk

0236-5383/2000/$ 5.00

The main factor influencing bioavailability of Al at neutral pH is the presence of complexing ligands, which include organic material and silicic acid. The former includes extracellular mucopolysaccharides, which are known to bind Al. Soluble silica is found in high concentrations in natural waters and has been shown to ameliorate the toxic effects of aluminium in a range of organisms [1, 10], presumably owing to formation of aluminosilicate complexes. Our studies, reviewed here, have concentrated on investigations into the role of mucus, different counter ions, and silicic acid in the bioaccumulation and toxicity of Al. We have compared the effects of exposure to Al as the nitrate, chloride or lactate, all of which allow formation of colloidal hydroxy polymers of Al, and maltol, which forms a stable soluble complex with Al. Experiments were carried out both in the presence and in the absence of silicic acid.

Bioaccumulation of aluminium

Snails showed significant accumulation of Al in the soft tissues following continuous (30 days) exposure to water of known composition to which Al (0–500 μgl^{-1} as the nitrate) was added, at pH 7.0 ± 0.5. Snails were sampled every 5 days for tissue analysis by graphite furnace atomic absorption spectroscopy [7]. In addition, the water was sampled daily so that a mean for actual Al concentration in the water column could be calculated for each treatment. After 30 days exposure, sampling continued for a further 20 days in clean water with no added Al.

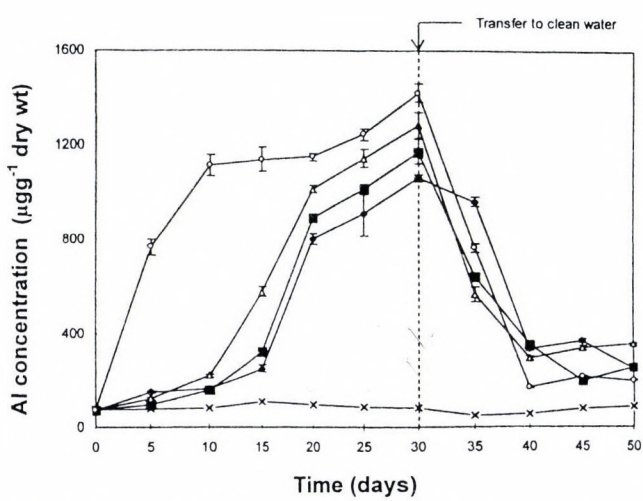

Fig. 1. Aluminium concentration in whole soft tissues of *L. stagnalis* (mean ± s.e.m., n = 5), exposed to an average of 38 (×), 78 (■), 181 (△), 234 (◆) and 285 (○) μgl^{-1} Al for 30 days and uncontaminated water for a further 20 days

Figure 1 shows the concentrations of Al in the whole soft tissues of *L. stagnalis* during 30 days Al exposure and 20 days recovery. Significant accumulation compared to controls occurred by day 10. This led to tissue concentrations of 800–1400 $\mu g g^{-1}$ dry weight by day 30, representing concentration factors up to 1.5×10^4 compared to the water.

Analysis of the partitioning of Al between different organs over the 30 days exposure and 20 days recovery indicated some redistribution of Al after about day 20 (Fig. 2). A greater proportion of the Al was found in the digestive gland after this time. Indeed concentrations of Al in the digestive gland remained significantly elevated even after 20 days in clean water. We have suggested that the digestive gland acts as a 'sink' for Al and that some event may be triggered at day 20 leading to sequestering of Al by the digestive gland [7]. Indeed, recent X-ray microprobe analysis studies in our laboratory have shown the presence of Al-containing granules in digestive and excretory cells of the gland [8].

Accumulation of Al by the snail is influenced by the presence of complexing ligands. Pedal mucus secreted by the snail during locomotion binds Al, significantly reducing Al concentration in the water column [11]. However, this does not reduce accumulation of Al since the snail grazes on the mucus. Ingestion of Al bound to mucus appears to be a major route of Al uptake for this organism. In contrast snails exposed to Al as the maltol complex over a 48 hour period did not significantly accumulate the metal. Maltol forms a stable soluble complex with Al at neutral pH, retaining it in solution and preventing both formation of hydroxy polymers and binding to mucus. Although addition of silicic acid [7770 $\mu g l^{-1}$) increased the rate at which Al precipitated from the water column, it did not prevent or reduce accumulation of Al by snails.

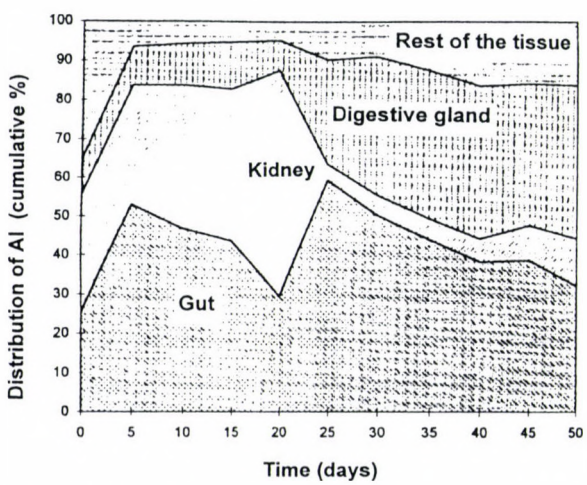

Fig. 2. Distribution of Al (% of total) in different tissues of *L. stagnalis* exposed to an average of 285 $\mu g l^{-1}$ Al for 30 days and uncontaminated water for a further 20 days

In summary, we have shown that Al is bioavailable to snails at neutral pH. Furthermore, its uptake is probably enhanced owing to binding of colloidal Al hydroxide by mucus secreted both by snails and by microorganisms in the substrate biofilm, which they graze.

Behavioural effects of aluminium

Snails exposed to Al (as the nitrate) in the water over the short term (up to about 14 days) showed reduced behavioural activity compared to controls. Locomotory activity (Fig. 3), behavioural state score (a measure of arousal: 16), spontaneous feeding movements and feeding responses to food stimuli all showed similar trends [3, 15]. After this time, the snails appeared to acclimatise to the presence of Al, suggesting tolerance to the metal. Indeed, snails reared for up to a year in the presence of 100 or 500 μgl^{-1} added Al showed no significant behavioural differences from controls [15].

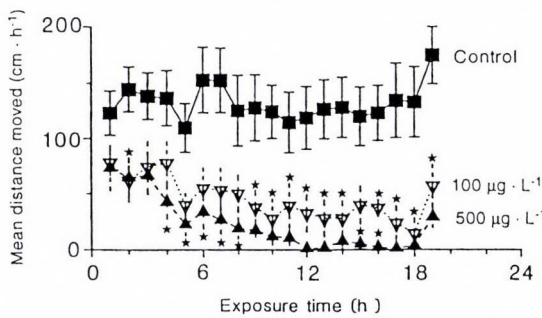

Fig. 3. Effect of exposure to added Al (0, ■; 100, ▽; 500 μgl^{-1} ▲) for 18 hours on locomotory activity (mean ± s.e.m., n = 10). *$p < 0.05$ compared to control

Experiments have been carried out to investigate the effect of different complexing ligands and silica on the behavioural toxicity of Al in *L. stagnalis* [3]. Snails were exposed to Al nitrate, lactate or maltol (500 μgl^{-1}) for 14 days and spontaneous feeding movements monitored on days 0, 2, 7 and 14. Snails exposed to Al as the nitrate or lactate showed significant depression of feeding activity on day 2, compared to controls. Activity subsequently recovered to control levels by day 14. Snails exposed to Al maltol did not show any change in behaviour until day 7, suggesting that Al in this form was less bioavailable. In a further experiment, snails were exposed to Al in the presence or absence of added silica (7770 μgl^{-1}). The feeding response to presentation of a food stimulus (sucrose) was significantly depressed in the presence of Al (added as the nitrate), but this effect was reversed in the presence of silica (Fig. 4).

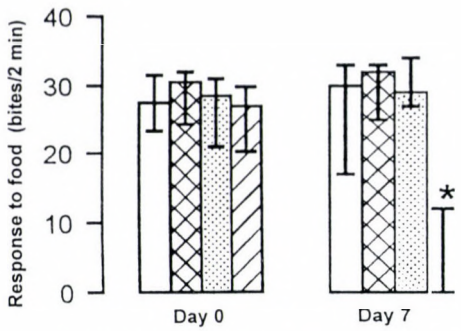

Fig. 4. Silica ameliorates the depression of feeding response seen after 7 days exposure to Al. Open columns – control, no added Al or Si; crosshatched columns – Si alone added (7770 μgl^{-1}); stippled columns – Si plus Al (500 μgl^{-1}) added; hatched columns – Al alone added. Columns show median ± interquartile range (n = 12). *$p < 0.005$ compared to control

These results again suggest that Al is more bioavailable in a form that will readily polymerise as the colloidal hydroxide (i.e. nitrate or lactate rather than maltol). The reduction in activity following exposure to Al may be an active strategy by the snail to reduce uptake and hence toxicity of the metal; uptake of metals is known to be reduced at lower metabolic rates [5]. Furthermore, although silicic acid did not prevent accumulation of Al by the snail, it did ameliorate the behavioural effects of the metal. This suggests a role for silica in facilitating detoxification of accumulated metal.

Behavioural toxicity studies provide an excellent means by which to demonstrate quantifiable and sublethal responses, which have relevance to both the survival of the individual and the structure of the freshwater community. Furthermore, in *L. stagnalis* behavioural responses can be correlated with changes in neural activity in identified neurons and networks [17].

Neurophysiological responses to aluminium

We have exploited the highly accessible central nervous system preparation of the snail to examine the cellular actions of Al *in vitro*. Previous studies of the actions of Al, e.g. on cultured cells, have used a range of Al compounds, concentrations and methods of application. In our studies, all at pH 7.5, we have used Al-containing saline solutions with defined chemistry, which have been analysed in parallel studies for the presence of soluble and labile Al species [4]. Aluminium (100 μM) was added to the saline bathing the CNS as the chloride, lactate or maltol, and electrophysiological responses recorded intracellularly from identified neuron right parietal dorsal 1 (RPD1). When Al was added to the saline as the chloride or the lactate (both prepared as stock solutions at pH 3), analysis showed that it precipitated almost imme-

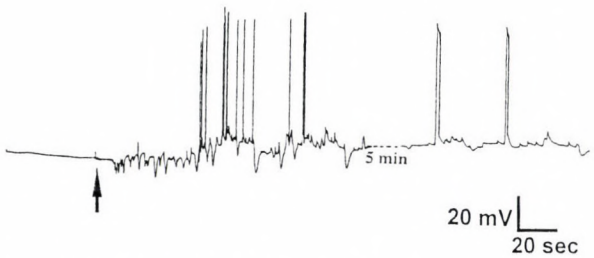

Fig. 5. Effect of superfusion of 100 μM Al lactate on firing activity of neuron RPD1. Arrow – onset of Al application. Aluminium induces membrane depolarisation, firing activity and marked action potential broadening

diately, with only 20–30% remaining in solution over the 60 min experimental period [4]. In contrast, the Al maltol complex was stable to hydrolysis and 100% remained in solution. Electrophysiological responses reflected this difference. Both Al chloride and Al lactate caused significant depolarisation of the membrane, accompanied by bursts of action potentials and action potential broadening (Fig. 5). In addition, spike afterhyperpolarisation was reduced. In contrast, Al maltol had no significant effect on electrophysiological properties of RPD1. Preliminary experiments involving prior addition of silicic acid to the bathing medium showed no amelioration of the toxic actions of Al. This was unexpected considering the amelioration of behavioural responses in the presence of silicic acid.

These *in vitro* experiments support the hypothesis that Al, when present in a weakly bound form that is able to precipitate at neutral pH, may still be toxic. Its mechanism of action is unknown, nor is it known whether it acts intracellularly, extracellularly or both. Our results so far suggest effects on repolarisation mechanisms, which could be accounted for by an inhibition of K^+ conductance, including Ca-dependent K^+ currents. Studies by others using a range of cell preparations point to alterations in Ca^{2+} currents and intracellular Ca^{2+} homeostasis following exposure to Al [e.g. 2, 9, 14]. In one study [12], Al was shown to inhibit Ca^{2+} entry into synaptosomes via voltage-gated Ca^{2+} channels and it was suggested that this was due to competition between Al and Ca^{2+} at binding sites on or within the channel. The 'giant' neurons of the snail provide an ideal experimental subject in which to explore further the cellular mechanism and site of Al toxicity and also the chemical form in which it exerts its actions at physiological pH.

GENERAL DISCUSSION

Our most important finding to date is the accumulation of significant amounts of Al by *L. stagnalis* under neutral conditions when Al is largely insoluble. Although this finding may not extrapolate to vertebrates, which appear to have effective barriers to Al uptake, it could have major implications for freshwater invertebrate populations.

As suggested earlier, the snail probably ingests the majority of Al by grazing on mucus and related compounds in secreted biofilms.

The apparent behavioural acclimatisation of *L. stagnalis* to Al after about 14 days exposure is worth further investigation. Our studies suggest that the digestive gland selectively accumulates Al after approximately 20 days. This may be due to activation of a detoxification mechanism that sequesters Al into granules for storage and subsequent excretion. As a class A (oxygen-seeking: 13) metal, Al is likely to be handled differently by organisms compared to class B (sulphur-seeking) and borderline metals, such as copper, zinc and cadmium. A potential role for silica in detoxification cannot be ruled out; silica ameliorated the behavioural effects of Al in intact animals, but appeared not to do so when applied directly to the isolated CNS.

The isolated CNS clearly provides an excellent model system for investigation of the cellular actions of Al. Numerous studies of the actions of Al on isolated or cultured preparations have already been carried out. However, our experiments show that a detailed knowledge of its chemistry in the applied solution is essential.

ACKNOWLEDGEMENTS

This work was supported by the BBSRC, UK, the Special Trustees of St Thomas' Hospital and the Wellcome Trust.

REFERENCES

1. Birchall, J. D., Exley, C., Chappell, J. S., Phillips, M. J. (1989) Acute toxicity to fish eliminated in silicon rich acid waters. *Nature 338,* 146–148.
2. Busselberg, D., Platt, B., Michael, D., Carpenter, D. O., Haas, H. L. (1994) Mammalian voltage-activated calcium channel currents are blocked by Pb^{2+}, Zn^{2+} and Al^{3+}. *J. Neurophysiol. 71,* 1491–1497.
3. Campbell, M. M., White, K. N., Jugdaohsingh, R., Powell, J. J., McCrohan, C. R. Effect of aluminium and silicic acid on the behaviour of the freshwater snail *Lymnaea stagnalis. Can. J. Fish. Aquat. Sci.* (in press).
4. Campbell, M. M., Jugdaohsingh, R., White, K. N., Powell, J. J., McCrohan, C. R. Aluminium toxicity in a molluscan neuron: effects of counter ions. *J. Toxicol. Environ. Hlth. 59,* 253–270.
5. Denton, G. R. W., Burdon-Jones, C. (1981) Influence of temperature and salinity on the uptake, distribution and depuration of mercury, cadmium and lead by the black lip oyster, *Saccostrea echinata. Mar. Biol. (Berlin) 64,* 317–326.
6. Dixon, E, Gardner, M. (1998) Reactive aluminium in UK surface waters. *Chem. Speciation Bioavailability 10,* 11–17.
7. Elangovan, R., White, K. N., McCrohan, C. R. (1997) Bioaccumulation of aluminium in the freshwater snail *Lymnaea stagnalis* at neutral pH. *Environ. Pollut. 96,* 29–33.
8. Elangovan, R., White, K. N., McCrohan, C. R., Ballance, S., Powell, J. J. (2000) Localization and fate of aluminium in the digestive gland of the freshwater snail *Lymnaea stagnalis. Tissue & Cell 32,* 79–87.
9. Farkas, I., Erdélyi, L. (1994) The effect of aluminium on the calcium currents in *Helix* neurons. *Cell Molec. Neurobiol. 14,* 809–817.
10. Hammond, K. E., Evans, D. E., Hodson, M. J. (1995) Aluminium/silicon interactions in barley (*Hordeum vulgare* L.) seedlings. *Plant and Soil 173,* 89–95.

11. Jugdaohsingh, R., Campbell, M. M., Thompson, R. P. H., McCrohan, C. R., White, K. N., Powell, J. J. (1998) Mucus secretion by the freshwater snail *Lymnaea stagnalis* limits aluminium concentrations of the aqueous environment. *Environ. Sci. Technol. 32,* 2591–2595.
12. Koenig, M. L., Jope, R. S. (1987) Aluminium inhibits the fast phase of voltage dependent calcium influx into synaptosomes. *J. Neurochem. 49,* 316–320.
13. Nieboer, E., Richardson, D. G. S. (1980) The replacement of the nondescript term 'heavy metals' by a biological and chemically significant classification of metal ions. *Environ. Pollut. 1,* 3–26.
14. Petersen, O. H., Wakui, M., Petersen, C. C. H. (1992) Intracellular effects of aluminium on receptor-activated cytoplasmic Ca^{2+} signals in pancreatic acinar cells. In: *Aluminium in Biology and Medicine.* Ciba Foundation Symposium 169, Wiley, Chichester, pp. 237–253.
15. Truscott, R., McCrohan, C. R., Bailey, S. E. R., White, K. N. (1995) Effects of aluminium and lead on activity in the freshwater pond snail *Lymnaea stagnalis. Can. J. Fish. Aquat. Sci. 52,* 1623–1629.
16. Tuersley, M. D., McCrohan, C. R. (1987) Food arousal in the pond snail *Lymnaea stagnalis. Behav. Neural. Biol. 48,* 222–236.
17. Whelan, H. A., McCrohan, C. R. (1996) Food related conditioning and neural correlates in the freshwater snail *Lymnaea stagnalis. J. Mollusc. Stud. 62,* 483–494.
18. Whitehead, M. W., Thompson, R. P. H., Powell, J. J. (1996) Regulation of metal absorption in the gastrointestinal tract. *Gut 39,* 625–628.

Acta Biologica Hungarica 51(2–4), pp. 317–324 (2000)

TIME-DEPENDENT ACTIONS OF ALUMINATES ON MEMBRANE AND ACTION POTENTIALS OF SNAIL NEURONS+

T. Csóti and L. Erdélyi

Department of Comparative Physiology, József Attila University of Sciences, P.O. Box 533, H-6701 Szeged, Hungary

(Received: August 31, 1999; accepted: November 30, 1999)

Aluminum (Al) is one of the elements, which is frequently subjected to experiments, however, the neurological observations with it are rather conflicting. The cause of this controversiality is not known but relates to some human disorders such as Alzheimer's disease and others as well.

We studied the time-dependent actions of $AlCl_3$ base solutions on resting membrane potential (E_m), input resistance (R_{in}) and spike shape in giant neurons of the snail *Helix pomatia* L. at pH 7.7 and room temperature (22–24 °C) by use of intracellular technique.

We reported significant differences in the effectiveness of the various Al solutions depending on the time of storage before use in the experiments (0, 2 and 6 days at room temperature). Freshly prepared and applied Al solutions caused a significant and dose-dependent depolarization with a concomitant decrease of R_{in} and the amplitude of the action potentials, but the 6 days solutions induced a hyperpolarization. Ouabain (0.1 mM) antagonized the hyperpolarization. The pH (7.1 or 7.7) and the time of the storage in combination also modified the direct membrane effects.

Our experiments show that Al can induce differential membrane effects depending on the presence of various aluminum compounds. Namely, the predominate aluminum-monomer at pH 7.7 the $Al(OH)_4^-$ might cause depolarization but the polynuclear aluminum complexes after polymerization of the monomers could hyperpolarize the neuronal membrane. We suppose, that the time-dependent equilibrium of various aluminum complexes plays a role in generating controversies in this field and emphasize again the importance of standardization of the experimental protocol.

Keywords: Helix neurons – aluminum – pH-dependence – membrane properties.

INTRODUCTION

Aluminum (Al) is the most common metal and third most abundant element on the earth crust; still it has no known biological function. This metal is characterized as a toxic element, which causes morphological, physiological and biochemical alterations in the living organisms [4, 12]. In case of animals and man it is well docu-

+ Presented at the 9th ISIN Symposium on "Neurobiology of Invertebrates", July 1–5, 1999, Tihany, Hungary.

*Corresponding author, E-mail: tcsoti@hotmail.com, Phone: (36) 62-454149, Fax: (36) 62-454249

0236-5383/2000/$ 5.00

mented that aluminum-evoked alterations occur in the nervous system [3]. However, the connection between Al and nervous diseases is not generally accepted [10] and the molecular mechanism of the aluminum actions, which may generate the disorders, is not known. Thus, the results are conflicting and the controversiality is the main feature of the experimental literature in this field. This is valid for morphological, biochemical and physiological studies in more or less extent.

As related to the electrophysiological observations both Al-induced hyperpolarization [14] and depolarization [2] were reported in Helix and Lymnaea neurons, but Franceschetti et al. [6] found no significant modulation of E_m and R_{in} in CA1 pyramidal neurons after Al exposure. Blaustein and Goldman [1] reported an attenuation of the AP-amplitude in lobster axon, and Campbell et al. [2] found a prolongation of APs in snail neurons after Al administration but these effects were not confirmed in CA1 pyramidal [6] and mammalian olfactory neurons [11]. This controversiality, which is not typical for other neurotoxic metals [7] might due to the complex chemistry of aluminum in aqueous solution. To investigate this problem we studied the effects of differentially standardized Al-solutions on resting membrane potential (E_m), input resistance (R_{in}) and action potential (AP) shape of *Helix* neurons.

MATERIALS AND METHODS

The experiments were carried out on isolated suboesophagal ganglia of *Helix pomatia* L. The snails were collected locally, kept in the laboratory and fed *ad libitum.* After removing of ganglia from the animals, we pinned it to a Silcastic-covered floor of a 5 ml plexiglass recording chamber. The connective tissue covering the neurons was removed by dissection without enzymatic treatment.

The preparation was superfused (8–12 ml/min) with physiological solution *(Ringer)* of the following composition (mM): NaCl 130; KCl 4; $CaCl_2$ 7; HEPES 5; (pH 7.7 ± 0.025). To examine the effects of aluminum we employed the following solutions. 1. *Stock solution:* $AlCl_3 \cdot 6H_2O$ crystals were dissolved in bidistilled water (100 mM), and stored for at least two weeks at pH 3.8 and room temperature. This solution was diluted by Ringer to the final concentration and adjusted pH 7.7 before experiments called *(Stock-diluted Al-suspension).* 2. *Fresh Al-suspension:* $AlCl_3 \cdot 6H_2O$ crystals were dissolved in Ringer solution to a final concentration of 0.001–1 mM, immediately before experimentation and applied at pH 6.8, 7.3 or 7.7, respectively. 3. *Stored Al-suspension:* $AlCl_3 \cdot 6H_2O$ crystals were dissolved in Ringer solution stored for 24–144 hours (±3 hours) before experiments at room temperature and at pH 7.7 or 7.1, respectively. All Al-suspensions were homogenized by manual shaking before experiments. The pH values were adjusted with 1M NaOH.

After preparation, the individual cells identified according to Sakharov and Salánki [9] were visualized under a binocular microscope and penetrated with a low resistance (~3–3.5 MOhm) glass microelectrode filled with 1 mM KCl and K-citrate. The experiments were made under current-clamp at room temperature (21–23 °C). The recording set-up was composed of a homemade amplifier connected to a Hitachi

VC 6025 digital oscilloscope and a personal computer. The hardware was a Labmaster DMA with TL-1-125 kHz interface (Axon Instruments, Inc.) in connection with a mathematical coprocessor and acquisition software. R_{in} was measured by injection of current pulses into the cell (25 ms, –4, 4, 8, 16 nA). APs were activated by 4 nA current injections into the cell.

Data are expressed as mean ±SD values and n refers to the number of preparations in all cases. Statistical significance was determined by ORIGIN 4.1 16 bit software using paired Student's *t*-tests. Probabilities of less than 5% ($p < 0.05$) were considered significant.

RESULTS

Time-dependent effects of Al-suspensions on resting membrane potential (E_m) and input resistance (R_{in})

As it is shown in the Fig. 1A, fresh Al-suspension or for up to 72 h stored Al-suspensions (0.3 mM) depolarized the LPl1 neuron by 20% as a maximum response, but a 144 hrs-stored Al-suspension caused 17 per cent hyperpolarization of the same neuron in equimolar dose. The hyperpolarizing action of Al ceased in the LPl1 neuron after ouabain (0.1 mM) preincubation (Fig. 1B). Similar changes of the membrane potential were not found after application of fresh or stored Ringer solution without

Table 1

Membrane potential and the input resistance measured at control (I.) and differently prepared 0.3 mM $AlCl_3 \cdot 6H_2O$-containing solutions (II.–IV.)

	Superfused solution (concentration, pH of the test-solution)	Membrane potential (mv)	Input resistance (MOhm)
I.	Ringer solution, pH 7.7 (Control)	–55.72 ± 1.97, $n = 15$	1.75 ± 0.08, $n = 15$
II.	Fresh Al-suspension (0.3 mM, pH 7.7)	–43.89 ± 6.55, $n = 9$ (***, r)	0.71 ± 0.12, $n = 9$ (***, r)
	48 h-stored Al-suspension, stored at pH 7.7 (0.3 mM, pH 7.7)	–47.45 ± 7.44, $n = 6$ (*, r)	1.12 ± 0.17, $n = 6$ (**, r)
	144 h-stored Al-suspension stored at pH 7.7 (0.3 mM, pH 7.7)	–59.81 ± 3.64, $n = 6$ (*, r)	1.56 ± 0.27, $n = 6$
III.	Stock-diluted Al-suspension (0.3 mM, pH 7.7)	–50.88 ± 4.365, $n = 6$	1.45 ± 0.32, $n = 6$
IV.	144 h-stored Al-suspension, stored at pH 7.1 (0.3 mM, pH 7.7)	–52.37 ± 5.65, $n = 6$	1.41 ± 0.56, $n = 6$

Mean ±SD, *n:* number of the independent experiments, *: $p < 0.05$, **: $p < 0.01$, ***: $p < 0.001$; r: reversible actions.

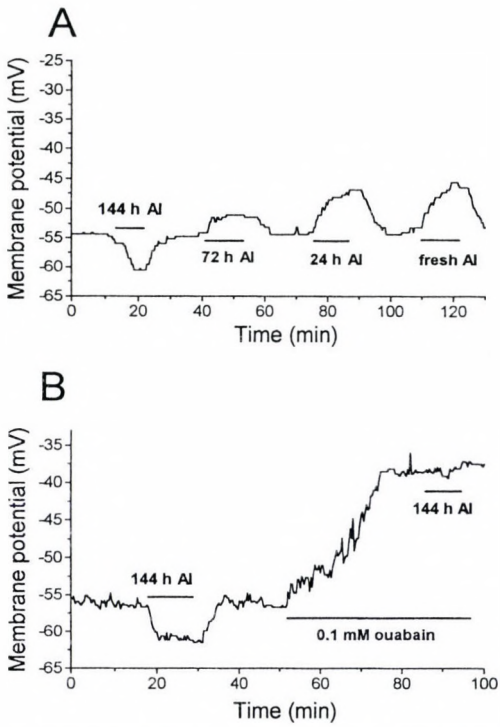

Fig. 1. (A) Time-dependent actions of 0.3 mM Al-suspensions on the membrane potential of the LPl1 neuron at pH 7.7. Fresh or for up to 72 h-stored Al-suspensions (0.3 mM) depolarized the LPl1 neuron, but the 144 h-stored Al-suspension caused hyperpolarization of the same neuron in equimolar dose. *(B)* Ouabain (0.1 mM) antagonized the 144 h-stored Al-suspension evoked hyperpolarization

Al. Both the depolarizing and the hyperpolarizing actions of Al were concentration-dependent (see Fig. 2A). The threshold concentration (CC_{tr}) of fresh Al-suspension was 0.05 mM which sifted to 0.1 mM in the 48 hrs-stored Al-suspension in the LPa3 neuron as marked by stars in Fig. 2A ($P < 0.05$). The K_d value of fresh Al-suspension, was 0.231 mM, which decreased to 0.113 mM in 48 h-stored Al-suspension. Threshold concentration of 144 h-stored Al-solution was 0.3 mM and the K_d value was 0.057 mM. A significant and concentration-dependent decrease of R_{in} of LPa3 neuron appeared after administration of fresh Al-suspension ($CC_{tr} = 0.1$ mM; $K_d = 0.153$ mM, $n = 4$) and 48 h-stored Al-suspension ($CC_{tr} = 0.1$ mM; $K_d = 0.091$ mM, $n = 4$), but R_{in} did not differ significantly from control in 144 h-stored Al-suspension (Fig. 2B). The preparation technique of test-suspensions also influenced the result. Namely, we found a significant depolarization of snail neurons after exposure of 0.3 mM fresh Al-suspensions but did not after application of stock-diluted Al-suspension in equimolar dose (compare II and III rows in Table 1). The pH of storage also influenced the effectiveness of Al-suspensions. While 0.3 mM Al-suspension

stored for 144 h at pH 7.7 caused a hyperpolarization, an equimolar Al-suspension, stored for also 144 h, at pH 7.1 did not significantly affect the E_m and R_{in} (see II and IV rows in Table 1).

Time-dependent effects of Al-suspensions on the action potential shape

As can be seen in Table 2, fresh Al-suspension (0.3 mM) significantly decreased the overshoot (OS) and peak potential (PP) and increased the AP duration at 50% amplitude (APD_{50}) activated by 4 nA current injections into the neuron. These changes were not significant after treatment of 48 or 144 h-stored Al-suspensions in the same dose. A significant increase of fast after-hyperpolarization (FAH) occurred after administration the 144 h-stored Al-suspension (0.3 mM), but did not after treatment with fresh Al-suspension (Fig. 3).

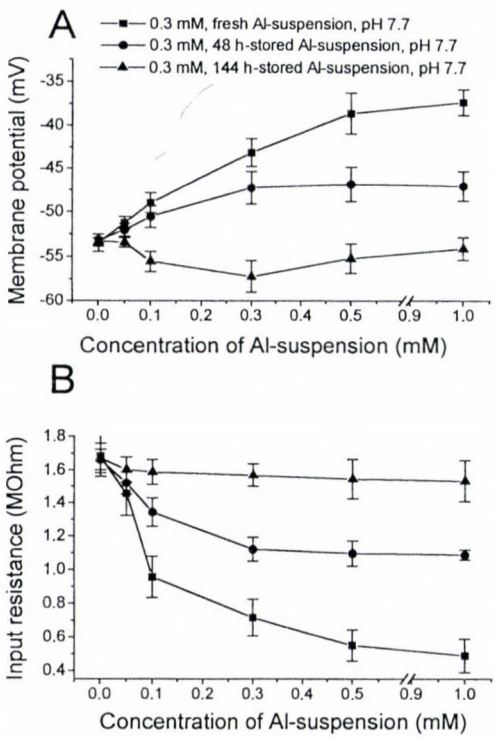

Fig. 2. Concentration-dependent actions of 0.3 mM, 144 (▲), 48 h-stored (●) and freshly prepared and applied Al-suspensions (■) on membrane potential (A) and input resistance (B) at pH 7.7, t = 21 °C. LPa3 neuron (mean ±SD, n = 5)

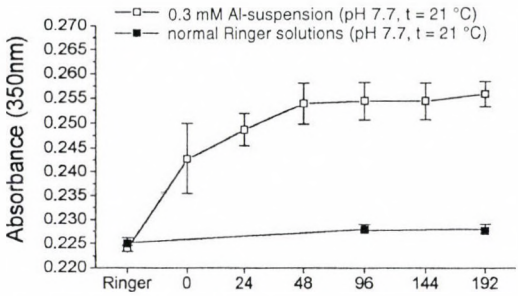

Fig. 3. Time-dependent increase of the absorbance of 0.3 mM, stored Al-suspensions (□) at 350 nm. The absorbance of stored Ringer solutions (■) did not change significantly (mean ±SD, n = 3)

Table 2

Time-dependent actions of 0.3 mM fresh, 24 and 144 h-stored (t = 21 °C, pH 7.7) Al-suspensions on the action potential shape recorded in a V1 neuron

	Control Ringer solution pH 7.7	0.3 mM fresh, Al-suspension, pH 7.7	0.3 mM 48 h-stored, Al-suspension, pH 7.7	0.3 mM 144 h-stored, Al-suspension, pH 7.7
Threshold potential (E_{tr}) (mV)	–28.67 ± 0.87	–25.06 ± 2.95	–23.95 ± 5.14	–29.94 ± 5.48
Overshoot (OS) (mV)	28.4 ± 1.06	14.98 ± 8.8 (***, r)	23.63 ± 16.34	28.70 ± 12.39
Peak potential (PP) (mV)	74.16 ± 2.05	45.55 ± 10.31 (**, r)	62.63 ± 20.64	71.89 ± 26.43
After-hyperpolarization (AHP) (mV)	–8.91 ± 2.81	–7.36 ± 7.58	–8.19 ± 5.35	–18.8 ± 6.18 (*, r)
Action potential duration at 50% amplitude (APD_{50}) (ms)	4.18 ± 1.13	5.11 ± 1.62 (*)	5.09 ± 2.18	5.3 ± 2.16

Mean ±SD, n = 7, *: $p < 0.05$, **: $p < 0.01$, ***: $p < 0.001$; r: reversible. APs were evoked by 4 nA currents injection into the cell.

DISCUSSION

The data reported in this paper demonstrate that changes of the preparation circumstances of the Al-containing test solutions markedly influenced the electrophysiological characteristics of neurons such as E_m, R_{in} and AP. Fresh Al-suspensions caused depolarization and an attenuation of the AP-amplitude which decreased with time, and after 144 h a hyperpolarization predominated and the AP shape was not altered. Also, the time of storage and pH in combination can be an important further modulating factor.

Contrary to previous observations which found Al as depolarizing [2], hyperpolarizing [14] or inactive metal ion [6] on membrane potential, and inhibitory [1] or inactive [11] compound in AP, we observed all of these changes in snail neurons by variation to the time and pH of storage of test-suspensions.

The time-dependence of actions of aluminum could relate to slow oligomerization in the stored suspensions. An olygomerisation of $AlOH^{2+}$ at acidic pH could take place in our 2 weeks-stored stock solution at pH 3.8 [5]. Thus, the composition of aluminates differs from the fresh Al-suspension which were made by direct dissolve of $AlCl_3 \cdot 6H_2O$ crystals immediately before the experiments. Unfortunately, there is no description of the exact chemical transformations of Al-solutions at pH 7.7. We found a time-dependent increase of the absorbance (350 nm) of stored Al-suspensions as it is shown in Fig. 3. An increase of the absorbance refers to an increasing light scattering of the stored Al-suspension, caused by a polymerization-dependent precipitation. One component of this intrinsic chemical process could cause the ouabain-sensitive hyperpolarization. Our results suggest, that the biologically active, depolarizing agent might be the dissolved $Al(OH)_4^-$, which is the predominant aluminate at pH 7.7 [8]. Polymerization of the $Al(OH)_4$ eliminates the depolarization and an unknown, olygomer-aluminate activates the ouabain sensitive Na/K-ATPase as found by Zatta et al. [13].

Our results suggest that the preparation method and time-dependence of the effects can play a role at the controversality of the results in this field and emphasize the importance of the standardization of experiments with aluminum.

REFERENCES

1. Blaustein, M. P., Goldman, D. E. (1968) The action of certain polyvalent cations on the voltage-clamped lobster axon. *J. Gen. Physiol. 51*, 279–291.
2. Campbell, M., McCrohan, C., White, K., Powel, J., Jugdaohsingh, R. (1999) Behavioural and neural toxicity of aluminium in the pond snail at neutral pH. Presented at the *Third Keele Meeting on Aluminium*, United Kingdom.
3. Carpenter, D. O. (1994) The public health significance of metal neurotoxicity. *Cell. Mol. Neurobiol. 14*, 591–596.
4. Dickinson Burrows, W. (1977) Aquatic aluminum: chemistry, toxicology, and environmental prevalence. *CRC Critical Reviews in Environmental Control 7*, 167–215.
5. Flaten, T. P., Garruto, R. M. (1992) Polynuclear ions in aluminum toxicity. *J. Theor. Biol. 156*, 129–132.
6. Franceschetti, S., Bugiani, O., Panzica, F., Tagliavini, F., Avanzini, G. (1990) Changes in excitability of CA1 pyramidal neurons in slices prepared from $AlCl_3$-treated rabbits. *Epilepsy Res. 6*, 34–48.
7. Kiss T., Osipenko, O. N. (1994) Toxic effects of heavy metals on ionic channels. *Pharm. Rev. 46*, 245–267.
8. Lydersen, E. (1990) The solubility and hydrolysis of aqueous aluminium hydroxides in dilute fresh waters at different temperatures. *Nord. Hydrol. 21*, 195–204.
9. Sakharov, D. A., Salánki, J. (1969) Physiological and pharmacological identification of neurons in the CNS of *Helix pomatia*. *Acta Physiol. Acad. Sci. Hung. 35*, 19–30.
10. Traub, R. D., Rains, T. C., Garruto, R. M., Gajdusek, D. C., Gibbs, C. J. Jr. (1981) Brain destruction alone does not elevate brain aluminum. *Neurology 31*, 986–990.

11. Trombley, P. Q. (1998) Selective modulation of $GABA_A$ receptors by aluminum. *J. Neurophysiol. 80,* 755–761.
12. Venugopal, B., Luckey, T. D. (1992) *Metal toxicity in mammals 2.* New York: Plenum Press. pp. 104–112.
13. Zatta, P., Zambenedetti, P., Pizziuti, A., Perazzolo, M. (1995) Different effects of aluminum upon carbonic anhydrases and Na^+/K^+-ATPase. *Neurosci. Lett. 197,* 65–68.
14. Zsíros, V., Rojik, I., Kovács, T., Csóti, T., Erdélyi, L. (1998) Comparative electrophysiological aspects of aluminum action on central neurons and neuronal synapses of invertebrate and vertebrate animals. *Neurotoxicology 19,* 553–556.

Acta Biologica Hungarica 51 (2–4), pp. 325–329 (2000)

HEAVY METALS AND NEUROIMMUNOMODULATION IN *MYTILUS EDULIS*[+]

F. E. NIETO-FERNANDEZ*, KATIA ALCIDE and C. RIALAS

Neuroscience Research Institute, SUNY College at Old Westbury, Old Westbury, New York 11568, USA

(Received: August 31, 1999; accepted: November 30, 1999)

Immunocytes of mussels are the chief immune defense in these organisms. When an immunocyte becomes activated there is a conspicuous change in its morphology (i.e., from round to amoeboid) that can be quantified using image analytical tools. Active immunocytes will typically show larger perimeters and areas and a smaller shape factor. Immunocytes exposed to heavy metals become inactive (Cd, Hg and Pb) thus with smaller perimeters (e.g., $Pb^{2+}{}_{2\ ppm}$: P = 69.72 μ) and areas (e.g., $Pb^{2+}{}_{2\ ppm}$: A = 270 μ^2) and larger shape factors ($Pb^{2+}{}_{2\ ppm}$: SF = 0.65) than the unexposed control cells ($\alpha = 0.05$). Xenobiotics may also interfere with neuroimmunomodulation processes such as nitric oxide (NO) release. The release of NO is catalyzed by a calcium dependent constitutive nitric oxide synthase (cNOS). Presently, we are exploring the effects of heavy metals and other pollutants on cNOS activity, measured as real time NO release, in immunocytes and pedal ganglia from *M. edulis*. Preliminary results suggest that immunocytes exposed to Pb^{2+} (5 ppm) cause NO release and does not seem to inhibit further NO release in the presence of morphine. The possible implications of NO mediated Pb^{2+} neurotoxicity are also explored.

Keywords: Invertebrates – immunocytes – nitric oxide – cNOS – heavy metals.

INTRODUCTION

Heavy metals are ubiquitous in the biosphere, as natural components of the earth, to which humans are constantly being exposed. However industrial uses of metals and other industrial and domestic processes have introduced substantial amounts of potentially toxic heavy metals into the atmosphere and into aquatic and terrestrial environments. The toxicological effects of these heavy metals particularly lead, zinc, arsenic, cadmium and mercury are well known [1, 17]. Lead exposure can have dev-

[+] Presented at the 9th ISIN Symposium on "Neurobiology of Invertebrates", July 1–5, 1999, Tihany, Hungary.

*Corresponding author, E-mail: nietof@oldwestbury.edu

0236-5383/2000/$ 5.00

astating effects on the central and peripheral nervous system, particularly during development [1].

The actual mechanism of toxicity is not that clear. Lead impacts a variety of Ca-dependent processes including nitric oxide (NO) release catalyzed by a constitutive nitric oxide synthase (cNOS). cNOSs comprise the low output path involved in homeostatic processes such as neurotransmission, peristalsis, and moment-to-moment blood pressure regulation. All of the NOSs require NADPH and O_2 as cosubstrates in the reaction.

Herein, preliminary results of the effects of heavy metals on the immunocytes of *M. edulis* using cell conformation state and real time NO release are presented.

MATERIALS AND METHODS

Invertebrate cells

Mytilus edulis specimens were collected from Theodore Roosevelt Memorial Park in Oyster Bay, New York. The mussels were placed in a continuous flow aquarium with artificial seawater (30 ppt) and maintained until used. Hemolymph was removed from the posterior adductor muscle of the mussels by aspiration with a syringe and placed in a pre-cleaned depression slide (40 µl) to evaluate conformational changes.

The cells were exposed to decreasing concentrations of heavy metals (Pb^{2+}, Cd^{2+}, and Hg^{2+}). Ten µl of heavy metal solution prepared with filter-sterilized artificial seawater was added to the slides.

Evaluation of cell conformation

Changes in cellular conformation, which ranged from inactive (round) to active (ameboid), were determined by measurements of cellular area (A), perimeter (P) and shape factor (SF) using an image analysis software package Image-100 [13].

The data was analyzed using an ANOVA with pairwise comparisons ($\alpha = 0.05$).

Direct measurement of nitric oxide (NO) release

NO release from the invertebrate immunocytes was measured directly using an NO-specific amperometric probe (World Precision Instruments, Sarasota, FL) interfaced to a computer via "DUO 18", a computer data acquisition system (WPI). To evaluate NO release, the cells were exposed to morphine 10^{-6} M, a concentration previously demonstrated to induce optimal NO release [8, 12] prior to their exposure to Pb^{2+}.

RESULTS

Cell conformation

As shown in Table 1 cells exposed to the metals had smaller areas and perimeters and larger shape factors than the control cells ($\alpha = 0.05$). These cells are inactive and therefore unable to move and phagocytize foreign particles. Control cells had larger perimeter/area values but their shape factor values were lower indicating a more amoeboid shape. With the exception of Cd^{2+} the magnitude of the effect decreased with concentration. In case of Cd^{2+} at 5 ppm the cells had a SF closer to the control than at 0.5 ppm, a concentration one order of magnitude lower. It is important to emphasize that the three parameters, P, A and SF, must be considered at the same time in order to interpret the results appropriately.

Table 1

Means and standard errors (in parenthesis) for Hg, Cd and Pb. A "*" indicates that the difference with the control is statistically significant (a = 0.05)

		Perimeter (μ)	Area (μ^2)	Shape factor
control		91.49 (1.49)	447.87 (15.22)	0.58 (0.005)
Hg	520 ppm	49.56 (0.68)*	153.14 (3.64)*	0.75 (0.003)*
	52 ppm	48.72 (0.52)*	148.68 (2.76)*	0.77 (0.004)*
	5.2 ppm	54.41 (2.38)*	187.14 (15.65)*	0.78 (0.01)*
	0.5 ppm	73.92 (2.62)*	412.80 (31.17)	0.73 (0.007)*
Cd	500 ppm	59.54 (1.41)*	192.68 (8.50)*	0.67 (0.008)*
	50 ppm	67.75 (2.10)*	257.14 (17.35)*	0.64 (0.01)*
	5 ppm	85.31 (2.59)	368.42 (22.09)*	0.60 (0.01)
	0.5 ppm	87.66 (2.95)	461.74 (31.95)	0.64 (0.01)*
Pb	20 ppm	54.48 (1.24)*	172.78 (7.27)*	0.7 (0.008)*
	2 ppm	69.72 (1.68)*	270.00 (12.80)*	0.65 (0.008)*
	0.2 ppm	81.40 (2.38)*	388.61 (20.53)	0.66 (0.009)*

Nitric oxide

Addition of 5 ppm of Pb^{2+} caused a surge in NO (Fig. 1) well above the scale of detection. The cells were first treated with 10^{-6} morphine which, as previously documented, caused NO release [8, 10, 15]. This type of NO release is catalyzed by a calcium dependent cNOS. Previous work has shown that morphine-induced NO release is preceded by an increase in cytosolic Ca^{2+} concentration. After the exposure to the heavy metal the cells were again treated with morphine which initiated a second burst of NO release (Fig. 1).

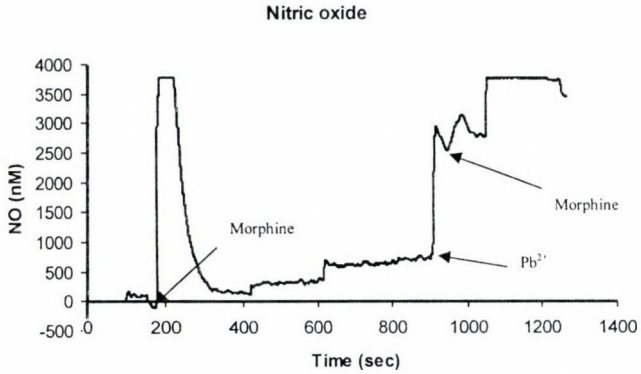

Fig. 1. Nitric oxide release and Pb^{2+} exposure. Morphine (10^{-6} M) was added prior and after the addition of lead

DISCUSSION

In this study the effect of heavy metals on the hemocytes of the blue mussel have been assessed for the first time using cell conformation and image analysis.

This paper further explores the mechanism underlying Pb^{2+} toxicity. It has been documented that Pb^{2+} interferes with Ca^{2+}-dependent cellular processes. cNOS activity is Ca^{2+}-dependent, thus it could be predicted that Pb^{2+} inhibits cNOS. Nevertheless our preliminary results suggest that a possible effect of low levels of Pb^{2+} exposure could be NO production by the immunocytes. In turn, NO release causes the cell to become round [8]. Macrophage production of NO may be the culprit of neuropsychiatric disorders such as AIDS dementia, delirium, schizophrenia, depression and stroke [4].

There is evidence in the literature that supports the involvement of NO in neurotoxicity of Pb^{2+} and other environmental pollutants [5, 6, 14, 16]. These reports used indirect methods to measure NO production that may inaccurately represent the phenomenon. The method utilized in this experiment measures NO release in real time.

Summarizing, exposure to heavy metals causes immunocyte inactivation measured as changes in cell conformation. Cell conformation and image analysis is proposed as an alternative method to assess immunotoxicology. At the same time, lead may effect its toxicity by inducing NO release. Given that, in humans, macrophages can cross the blood/brain barrier, lead neurotoxicity may be related to neuropsychiatric disorders as already postulated in previous studies [2, 3, 4, 7, 9].

ACKNOWLEDGEMENTS

This works was in part supported by the following grants: NIMH COR 17138, NIDA 09010, NIMH 47392 and the Research Foundation and Central Administration of the State University of New York.

REFERENCES

1. Audesirk, G. (1985) Effects of lead exposure on the physiology of neurons. *Prog. Neurobiol. 24,* 199–231.
2. Baker, E. L., Feldman, R. G., White, R. F., Harley, J. P. (1983) The role of occupational lead exposure in the genesis of psychiatric and behavioral disturbances. *Acta Psychiatr. Scand. Suppl. 303,* 38–48.
3. Choi, Y., Raja, S. N., Moore, L. C., Tobin, J. R. (1996) Neuropathic pain in rats is associated with altered nitric oxide synthase activity in neural tissue. *J. Neurol. Sci. 138,* 14–20.
4. Fricchione, G. L., Bilfinger, T. V., Stefano, G. B. (1996) The macrophage and neuropsychiatric disorders. *Neuropsych., Neuropsychol. Behav. Neurol. 9,* 16–29.
5. Gonick, H. C., Ding, Y., Bondy, S. C., Ni, Z., Vaziri, N. D. (1997) Lead-induced hypertension: interplay of nitric oxide and reactive oxygen species. *Hypertension 30,* 1487–1492.
6. Ikeda, M., Komachi, H., Sato, I., Himi, T., Yuasa, T., Murota, S.-I. (1999) Induction of neuronal nitric oxide synthase by methylmercury in the cerebellum. *J. Neurosci. Res. 55,* 352–356.
7. Lane, T. E., Buchmeier, M. J., Watry, D. D., Fox, H. S. (1996) Expression of inflammatory cytokines and inducible nitric oxide synthase in brains of SIV-infected rhesus monkeys: applications to HIV-induced central nervous system disease. *Mol. Med. 2,* 27–37.
8. Liu, Y., Shenouda, D., Bilfinger, T. V., Stefano, M. L., Magazine, H. I., Stefano, G. B. (1996) Morphine stimulates nitric oxide release from invertebrate microglia. *Brain Research. 722,* 123–131.
9. Ma, T., Chen, H. H., Ho, I. K. (1999) Effects of chronic lead (Pb) exposure on neurobehavioral function and dopaminergic neurotransmitter receptors in rats. *Toxicol Lett. 105,* 111–121.
10. Magazine, H. I., Liu, Y., Bilfinger, T. V., Fricchione, G. L., Stefano, G. B. (1996) Morphine-induced conformational changes in human monocytes, granulocytes, and endothelial cells and in invertebrate immunocytes and microglia are mediated by nitric oxide. *J. Immunol. 156,* 4845–4850.
11. Magazine, H. I., Liu, Y., Bilfinger, T. V., Fricchione, G. L., Stefano, G. B. (1996) Morphine-induced conformational changes in human monocytes, granulocytes, and endothelial cells and in invertebrate Immunocytes and microglia are mediated by nitric oxide. *J. Immunol. 156,* 4845–4850.
12. Nieto-Fernandez, F. E., Mattocks, D., Cavani, F., Salzet, M., Stefano, G. B. (1999) Morphine coupling to invertebrate immunocyte nitric oxide release is dependent on intracellular calcium transients. *Comp. Biochem. Phys. Part B.* (in press).
13. Schon, J. C., Torre-Bueno, J., Stefano, G. B. (1991) Microscopic computer-assisted analysis of conformational state: reference to neuroimmunlogy. In: Stefano, G. B., Smith, E. M. (eds) *Advances in Neuroimmnunology.* Manchester University Press, Manchester, pp. 252–259.
14. Selvin-Testa, A., Capani, F., Loidl, C. F., Pecci-Saavedra, J. (1997) The nitric oxide synthase expression of rat cortical and hippocampal neurons changes after early lead exposure. *Neurosci. Lett. 236,* 75–78.
15. Stefano, G. B., Salzet, B., Rialas, C. M., Pope, M., Kustka, A., Neenan, K., Pryor, S., Salzet, M. (1997) Morphine- and anandamide-stimulated nitric oxide production inhibits presynaptic dopamine release. *Brain Res. 763,* 63–68.
16. Tian, L., Lawrence, D. A. (1996) Metal-induced modulation of nitric oxide production in vitro by murine macrophages: lead, nickel, and cobalt utilize different mechanisms. *Toxicol. Appl. Pharmacol. 141,* 540–547.
17. Zelikoff, J. T., Cohen, M. D. (1996) Immunotoxicology of inorganic metal compounds. In: *Experimental Toxicology.* CRC Press. Boca Raton, pp. 198–228.

Acta Biologica Hungarica 51 (2–4), pp. 331–341 (2000)

EVIDENCE OF OPIATES AND OPIOID NEUROPEPTIDES AND THEIR IMMUNE EFFECTS IN PARASITIC INVERTEBRATES REPRESENTING THREE DIFFERENT PHYLA: *SCHISTOSOMA MANSONI, THEROMYZON TESSULATUM, TRICHINELLA SPIRALIS*[+]

S. C. PRYOR* and R. ELIZEE

Neuroscience Research Institute, State University of New York at Old Westbury, P.O. Box 210, Old Westbury, New York 11568-0210, USA

(Received: August 31, 1999; accepted: November 30, 1999)

Studies done in our laboratories have demonstrated that the parasitic trematode, *Schistosoma mansoni* is capable of producing several proopiomelanocortin (POMC) peptides including β-endorphin, adrenocorticotropin (ACTH), melanocyte stimulating hormone (αMSH) and enkephalin [12, 14] as well as morphine [20]. Some of these opioids have been demonstrated to be immunosuppressive and may play an important part in immune evasion by these parasites [13]. The parasitic nematode *Trichinella spiralis* also produces immune suppressive substances *in vitro* as well as causes immune suppression in its encysted stage *in vivo* [8, 9]. We recently have demonstrated the presence of morphine in both infected mice and in the nematode by HPLC and RIA. In a recent study of the leech *Theromyzon tessulatum,* we demonstrated the presence of proopiomelanocortin (POMC) and its derived peptides, ACTH and αMSH, in the immune tissues [28]. The peptide was cloned and extensively purified by HPGPC and reversed-phase HPLC, and then sequenced. The 25.4 kDa protein was purified by gel permeation chromatography, anti-ACTH-affinity column separation followed by reversed-phase HPLC. Its amino acid determination was performed by Edman degradation, enzymatic treatments and electrospray mass spectrometry. The structure of the leech POMC-like precursor and its derived peptides demonstrates considerable amino acid sequence similarity with mammalian POMC. Taken together, these studies demonstrate that opiates and opioid neuropetides are present in invertebrates and their immunoregulatory actions have been conserved during evolution. The role of opiates and opioid peptides in immune and behavior modification of hosts is also discussed.

Keywords: Trichinella spiralis – Theromyzon tessulatum – Schistosoma mansoni – morphine – proopiomelanocortin.

INTRODUCTION

Opiate like substances have been isolated from a number of parasitic invertebrates over the last several years in our laboratories at the Old Westbury Neuroscience Research Institute. The proopiomelanocortin (POMC) peptides β-endorphin, adrenocorticotropin (ACTH), melanocyte stimulating hormone (αMSH) and met-

[+] Presented at the 9th ISIN Symposium on "Neurobiology of Invertebrates", July 1–5, 1999, Tihany, Hungary.

*Corresponding author, E-mail: pryors@oldwestbury.edu

0236-5383/2000/$ 5.00

enkephalin [12, 14] as well as morphine [20] have been found in the parasitic trematode *Schistosoma mansoni.* A morphine-like substance has also been found in the parasitic nematode *Trichinella spiralis* and in the blood plasma of mice infected with *T. spiralis.* Recently, we have demonstrated the presence of proopiomelanocortin (POMC) and its derived peptides including β-endorphin, adrenocorticotropin (ACTH), melanocyte stimulating hormone (αMSH) and met-enkephalin in the parasitic annelidian, *Theromyzon tessulatum* [28]. The presence of opiate-like substances in these three phylogeneticly diverse organisms indicates that opiates play a role in the physiology of a broad range of invertebrates. The trematode and nematode are internal parasites and opiates, which are known to be immune suppressive, may not only function as neurotransmitters internally for these organisms but may also effect the immune system of the parasitized host. There have also been a number of studies that have demonstrated opiate-like behavioral effects in experimental animals parasitized by these and other internal parasites. The leech, *T. tessulatum*, is an ectoparasite and presumably does not use these opiate like substances for immune regulation of the host but we have demonstrated that they interact with other signaling molecules as chemical messengers in the leech.

METHODS AND RESULTS

Schistosoma mansoni

The presence of POMC derived neuropeptides β-endorphin, adrenocorticotropin (ACTH), melanocyte stimulating hormone (aMSH) and met-enkephalin have been demonstrated in all stages of life for *S. mansoni* by HPLC and RIA analysis [12, 14, 20]. Additionally, opioid neuropeptides and morphine have been detected in the incubation medium of these parasites under various conditions using radio immune assay. Table 1 shows the concentration of ACTH and β-endorphin is actually greater in the incubation medium than in the adult worm. This indicates that these substances are probably synthesized *de novo* and released in to the medium. No αMSH was found in the incubation medium but was found in abundance on co-incubation with polymorphonuclear leukocytes while ACTH was absent. It has been demonstrated that neutral endopeptidase on the surface of PMNs convert ACTH to this immune suppressive peptide. This was confirmed by adding the NEP inhibitor phosphoramidon to the incubation medium. Phosphoramidon significantly lowered the level of αMSH and raised the level of ACTH. In contrast, the aminopeptidase inhibitor bestatin did not lower the levels of αMSH or raise the levels of ACTH.

As shown in Fig. 1, morphine and codeine-like molecules are also present in *Schistosoma mansoni* following HPLC separation and RIA analysis [20]. The codeine-like material is found in much smaller concentrations than the morphine-like material, indicating, as in mammals and *Mytilus edulis*, the potential rapid conversion of codeine to morphine. Table 2 demonstrates the effect of various incubation conditions on the concentration of morphine like material in the worms and in the

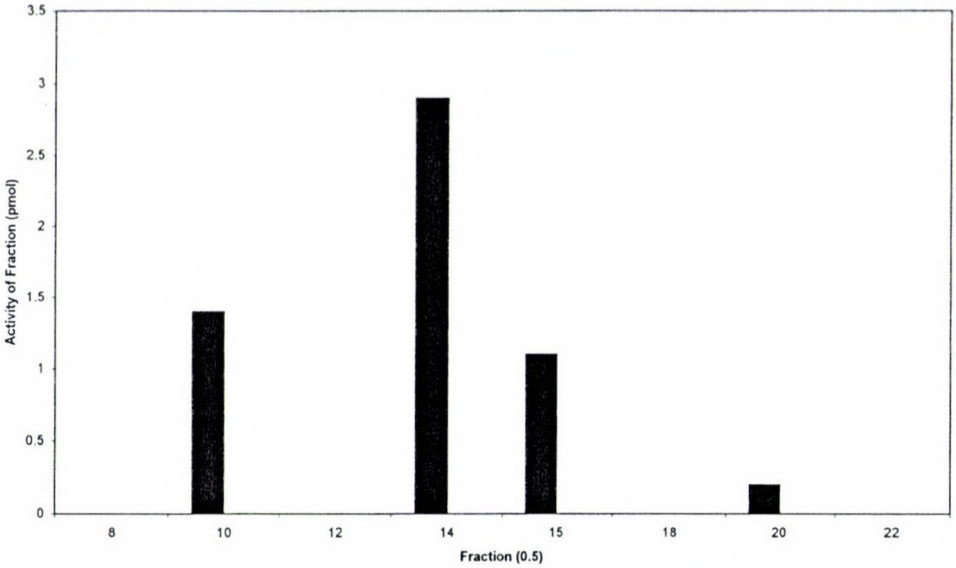

Fig. 1. Opiate RIA activity in HPLC fractions of *S. mansoni* (0.72 g dry wt.) extract. Fraction size was 0.5 ml and fractions 14 (fraction 15 is trailing of 14) and 20 correspond to the positions of authenic morphine and codiene

incubation medium [20]. Co-incubation of *Schistosoma mansoni* with human PMN increases the endogenous levels of morphine in the adult worms and in the incubation medium. This finding suggests that the cells by direct contact, signal factor(s) or both maybe in dynamic communication with the worm. EDTA, a chelator of divalent cations, also has a strong stimulating effect in the synthesis of morphine-like material by the worm. The endogenous material corresponding to morphine mimics authentic morphine in its ability to induce *in vitro* immunocyte rounding and immobility. These effects were reversed by adding 10^{-6} M naloxone.

Table 1
RIA of ACTH, αMSH and β-endorphin in *S. mansoni* adult worms and incubation medium (from Duvaux-Miret et al., 92)

Sample	ACTH	αMSH	β-endorphin
	Experiment A, peptide conc. in pmol/g wet wt.		
Parasites	0.296 ± 0.07	1.840 ± 0.11	0.222 ± 0.12
Medium	1.265 ± 0.32	ND	0.740 ± 0.13
	Experiment B, peptide conc. in fmol/ml		
PMN	ND	29.7 ± 0.0	2.1 ± 0.9
PMN+ phos.	5.0 ± 1.3	22.0 ± 0.0	2.0 ± 0.7
PMN+ bestatin.	4.1 ± 0.1	36.0 ± 5.1	1.3 ± 0.1

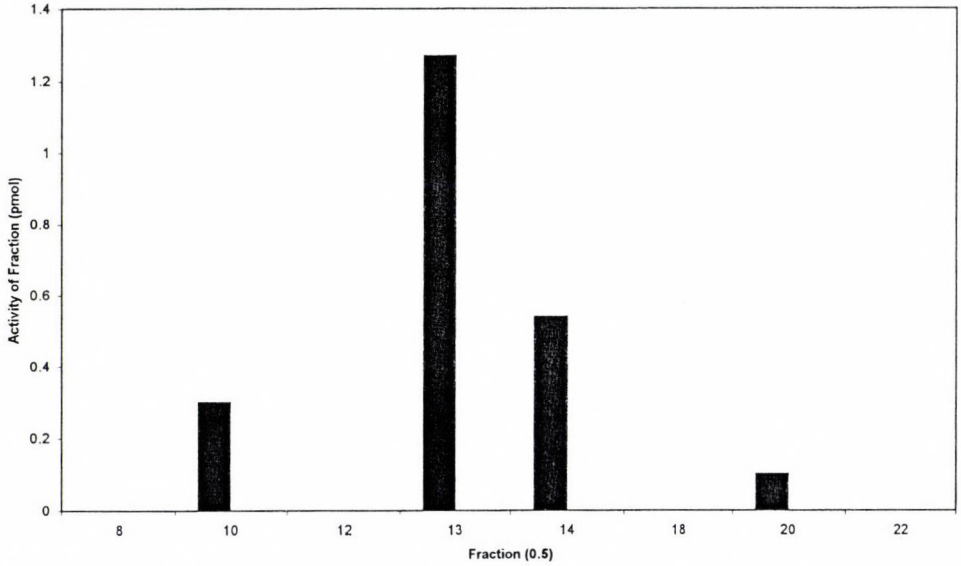

Fig. 2. Opiate RIA activity in HPLC fractions of *T. spiralis* (0.15 g dry wt) extract. Fraction size was 0.5 ml and fractions 13 (fraction 14 is trailing of 13) corresponds to the position of authentic morphine

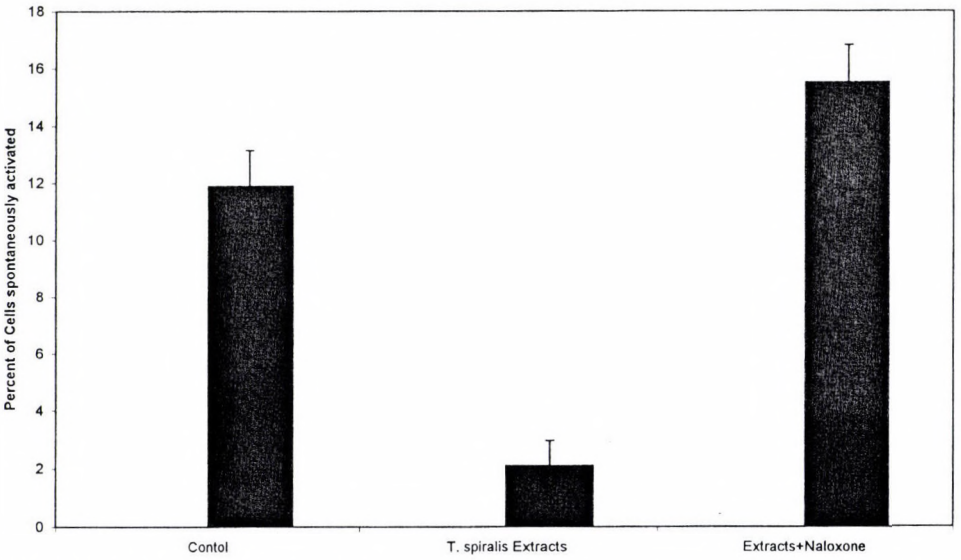

Fig. 3. The effect of EDTA treated *T. spiralis* extracts and *T. spiralis* extracts+Naloxone (10^{-6} M) on the spontaneous activation of mouse granulocytes

Trichinella spiralis

The presence and secretion of an opiate like substance has also been examined in *Trichinella spiralis*. The results of our experiments in *Trichinella spiralis* shown in Fig. 2 demonstrate that morphine and codeine-like molecules are present following HPLC separation and RIA [27]. The endogenous material corresponding to morphine mimics authentic morphine in its ability to induce *in vitro* immunocyte rounding and immobility as shown in Fig. 3. These effects were reversed by adding 10^{-6} M naloxone. These results are very similar to that obtained with *Schistosoma mansoni.*

Theromyzon tessulatum

In a recent study of the leech *Theromyzon tessulatum,* we demonstrated the presence of proopiomelanocortin (POMC) and its derived peptides, adrenocorticotropin (ACTH) and melanocyte stimulating hormone (MSH), in the immune tissues [28]. The peptide was cloned and extensively purified by HPGPC and reversed-phase HPLC, and then sequenced. The 25.4 kDa protein was purified by gel permeation chromatography, anti-ACTH-affinity column separation followed by reversed-phase HPLC. Its amino acid determination was performed by Edman degradation, enzymatic treatments, and electrospray mass spectrometry. As shown in Table 3, the structure of the leech POMC-like precursor demonstrates considerable amino acid sequence similarity with mammalian POMC. The sequence identity of met-enkephalin, α-MSH and ACTH is 100, 84.6 and 70%, respectively, whereas γ-MSH, β-endorphin, and γ-LPH exhibit only a 45, 20 and 10% sequence identity with their vertebrate counterparts. No dibasic amino acid residues were found at the C-terminus of γ- and β-MSH peptides. In contrast, the leech α-MSH is C-terminally flanked by the Gly-Arg-Lys amidation signal. ACTH and CLIP are C-terminally flanked by

Table 2
The presence of morphine-like material in *S. mansoni* and its incubation medium following various treatments

Number of worms	KCl (50 mM)	EDTA (50 mM)	PMN	Morphine-like material in worm (pmol/100)	Morphine-like material in medium (pmol/ml)
0			+	0	0
400				0	0.4
400	+			0	0
400		+		3.3	0
400	+	+		0.2	0
200			+	11.8	0
200	+		+	11.0	0
200		+	+	20.6	0
200	+	+	+	9.6	0.2

dibasic amino acid residues. Using RT-PCR strategy with degenerated oligonucleotide primers based on the biochemical data, the complete coding region of the leech POMC was obtained.

Circulating levels of ACTH and MSH were 10 and 1 fmol/μl hemolymph, respectively. Morphine, in a dose-dependent manner, increased the levels of both peptides threefold and this effect was blocked by naloxone treatment (Table 4). Leech ACTH was processed to MSH by neutral endopeptidase (24.11; NEP) and angiotensin-converting enzyme (ACE); the activity of these enzymes was inhibited by phosphoramidon and captopril, respectively, resulting in significantly diminishing MSH levels (5 fmol/ml hemolymph compared to 15, $P < 0.01$). Leech MSH had the same activity as authentic MSH in two bioasssay systems. Taken together, the study demonstrates that ACTH and MSH are present in invertebrates and their immunoregulatory actions have been conserved during evolution.

Table 3

Percentage of sequence identity of leech POMC-derived peptides with that of selected vertebrates

Leech	Percentage sequence identity		
	Human	Rat	*X. laevis*
POMC	19.8	14.7	35.4
ACTH	75.5	68.9	60
γMSH	46.7	46.7	38.4
αMSH	84.6	64.6	84.6
CLIP	95	95	80
β-endorphin	20	20	25.9
Met-enkephalin	100	100	100

Table 4

Effects of the injection in leeches of opiates with or without inhibitors on the ACTH- and α-MSH like peptide levels

Solution	ACTH-like peptide (fmol/μl hemolymph)	α-MSH-like peptide (fmol/μl hemolymph)
Control	10 ± 2.04	1.14 ± 0.95
Morphine (10^{-6} M)	39 ± 4.6	15 ± 3.33
Morphine (10^{-6} M) + naloxone (10^{-6} M)	5.6 ± 2.89	3 ± 1.15

DISCUSSION

This overview of our work with parasitic invertebrates demonstrates commonalities of diverse phyla in the presence of opiates and opioid neuropeptides and their immune modulation. The presence of POMC and its derived peptides in both *Schistosoma mansoni* and *Theromyzon tessulatum* suggests that it arose early in evolutionary history and was developed for both neurological and immunological functions in invertebrates. Morphine may be an even older mechanism of pain and stress control given that it is present in nematodes which ostensibly lack POMC genes [4].

The function of opiates and opioid neuropeptides as modulators of host immunity and behavior is somewhat more problematic. Parasitic infection has long been known to cause immune suppression but the mechanisms are only now being investigated. The POMC neuropeptides ACTH, αMSH, and β-endorphin found to be released into the incubation media by *S. mansoni* have all been implicated in immune modulation of the host. ACTH can be converted to αMSH by means of neutral endopeptidase (NEP) which is present on the surface of PMN s [29]. αMSH has been shown to counteract the inflamatory action of interleukin 1 and tumor necrosis factor on PMNs. *In vitro* incubation with aMSH caused cell rounding and a decrease in cell area in both PMNs and invertebrate hemocytes. The same *in vitro* inactivation of these cells is also observed when co-incubated with ACTH and NEP.

The direct inhibitory effects of ACTH and αMSH favor the hypothesis that these chemicals mask the adult organisms from the definitve hosts immune system. This is supported by the observation of a decrease in IFNγ and Il-2 levels during schistosomiasis after maturation of the worms and oviposition [16, 23]. This is consistent with *in vitro* observation of a decrease in IFNγ production by T cells co-incubated with ACTH.

The effects of ACTH and aMSH on the immune system of the intermediate host was demonstrated by an elegant experiment by Duvaux-Miret and her colleagues [12]. Hemocytes drawn from the pericardiac area of the infected snail host were found to be inactivated. When these cells were incubated with anti-ACTH and/or anti-MSH antibodies, the inactivation was reversed. Anti-MSH was more effective in a shorter time period and incubation with both anti-sera was synergistic [12]. The presence of αMSH in the host snail is also evidenced by an increase in the number of circulating hemocytes during infection. This same phenomenon in another mollusc, *M. edulis* can be attributed to inactivation by αMSH, which results in an inhibition of margination [34].

There have also been a number of reports over the years of immunomodulatory effects of β-endorphin (BE). Among the reported effects of BE are antibody production inhibition, diminution of T lymphocyte chemotactic factor production by monocytes, and augmentation of granulocyte migration [6, 30, 31]. Some of these effects are reversible by the prototypical opioid antagonist naloxone while others are not. Since the N terminal of the peptide is the opiate ligand, the effects that cannot be blocked by naloxone must be attributed to the G terminal end. The complexity of effects makes it difficult to speculate on BEs role in immune manipulation by the par-

asite. However, the upregulation of the immune response toward the schistosomula as well as some of the immune suppression against the adult may be effected by BE. β-Endorphin has been shown to be more potent than ACTH or αMSH, since it has the potential to iniate activity at 10^{-10} M [33] and to resist degradation better than the other two peptides. These two aspects make it a better candidate for acting at some distance from the site of infection. BE levels have been shown to be elevated in the blood plasma of mice infected with *S. mansoni* [17].

Opiate alkaloids such as morphine have long known to be immunosuppressive [36]. As early as 1898, Cantacuzene noted the inhibitory effect of exogenous morphine on cells of the immune system [2, 11]. More recently, it has been noted that injection of morphine in vertebrate animals results in deficient macrophage function [38] and alteration of T cell activity [39]. Morphine also antagonizes the chemotaxis induced by IL-1a or TNFα in human granulocytes and monocytes [21, 24, 35]. These observations have also been made on Mytilus and Leucophae immunocytes [36]. Morphine may also interact with neuropeptides and other immune regulators. The administration of morphine has been demonstrated to increase the blood plasma levels of ACTH, CRH, AND glucocorticoid [5, 10, 15, 22]. Morphine also up regulates the expression of neutral endopeptidase 24.11 in human granulocytes, thus increasing the conversion of ACTH to the immune suppressive αMSH [37].

Effects of parasitism on analgesia

The apparent opiate effects of several parasitic infections have been explored in experimental animals in recent years including the studies undertaken over the last five years in our laboratory. These studies centered around opiate-mediated effects on analgesia and activity levels of infected animals. The behavioral effects of parasitism resemble in many respects that seen in animals exposed to experimental stress conditions. A basic reaction to aversive or stressful stimuli in mammals is a reduction in pain sensitivity or nociception [1, 19]. This analgesia has been considered an adaptive response since pain might distract the animal from behavior critical to survival in situations of danger [7, 19]. The mechanism of nociception has been attributed to endogenous opioid peptides. These include enkephalins, endorphins and dynorphins. Recently the role of endogenous morphine on nociception has also been examined. Several opioid/opiate receptors including μ, δ and κ are targets of opiates and opioid peptides and play different roles during the duration of the analgesic reaction.

Infection with a range of parasites have been shown to induce alterations in nociceptive behavior. *Schistosoma mansoni* infected male hamsters exhibit a chronic increase in nociceptive thresholds over controls that is blocked by the prototypic opiate antagonist naloxone [18]. Infection with *Trichinella spiralis* produced a similar chronic analgesia in male white mice that was blocked with naloxone [25]. Mice infected with the intestinal nematode, *Nippostrongylus brasiliensis,* showed an analgesia that rose over the course of infection, reaching a peak with maximum egg pro-

duction and then subsiding as the infection was cleared. This analgesia was blocked by naloxone and the δ-receptor blocker naltrindole [26].

An unanswered aspect of host behavior and immune modifications by parasitic infection is the source and nature of the opioids that are involved in the effect. While opiate and opioid blood serum levels are increased by infection with both *S. mansoni* and *T. spiralis*, it is not clear whether these substances are produced endogenously as a reaction to parasitic infection or directly secreted by the parasites. There, in fact, may be a complex interaction of these two sources given the ability of morphine to induce the activation of opioid neuropeptides. These questions are currently under investigation in our laboratories.

REFERENCES

1. Amit, Z. T., Galina, Z. H. (1986) Stress-induced analgesia: adaptive pain suppression. *Physiol. Rev. 66,* 1091–1120.
2. Atchard, C., Bernard, H., Gagneux, C. (1909) Action de la morphine sur les proprietes leucocytaires. I-eucodiagnostic du morphinisnie. *Bull. Soc. Med. Hosp., Paris 28,* 958.
3. Bateman, A., Singh, A., Kral, T., Solomon, S. (1989) The immune-hypothalamic-pituitary-adrenal axis. *Endocrine Rev. 10,* 92–112.
4. Bargmann, C. I. (1998) Neurobiology of the *Caenorhabditis elegans* Genome. *Science 282,* 2028–2033.
5. Bayer, B. M., Flores, C. M. (1990) Effects of morphine on lymphocyte function: Possible mechanisms of interaction. In: Watson, R. R. (ed.), *Drugs of Abuse and Immune Function.* CRC Press, Boca Raton, pp. 151–174.
6. Blalock, J. E. (1989) A molecular basis for bidirectional communication between the immune and neuroendocrine systems. *Physiol. Review 69,* 1–32.
7. Blanchard, R. D., Blanchard, C. D., Rodgers, J., Weiss, S. M. (1990) *Neurosci. Biobehav. Rev. 14,* 463–472.
8. Bruschi, F., Carulli, G., Azzara, A., Marini, A., Ruocco, L., Ambrogi, F. (1989) Modulating effects by *Trichinella spiralis* "senso stricto" excretory/secretory antigens of human neutrophil functions. *Wiadomosci Parazytologiczne 35,* 391–400.
9. Bruschi, F., Pozio, E., Carulli, G., Polidori, R., Azzara, A. (1990) Inhibition of leukocyte function by serum from patients with trichinellosis. *J. Parasitol. 76,* 577–579.
10. Bryant, H. U., Yoburn, B. B., Inturrisi, C. E., Bernton, E. W., Holaday, J. W. (1988) Morphine-induced immunosuppression is not related to serum morphine concentrations. *Eur. J. Pharmacol. 149,* 165.
11. Cantacuzene, J. (1899) Nouvelles recherches sur led mode de destruction des vibrions dans l'organisme. *Ann. Inst. Pasteur 129,* 274–300.
12. Duvaux-Miret, O., Stefano, G. B., Smith, E. M., Capron, A. (1992) Neuroimmunology of host-parasite interactions: proopiomelanocortin derived peptides in the infection by *Schistosoma mansoni. Adv. Neuroimmunol. 2,* 297–311.
13. Duvaux-Miret, O., Stefano, G. B., Smith, E. M., Dissous, C., Capron, A. (1992) Immunosuppression in the definitive hosts of the human parasite, *Schistosoma mansoni* by release of immunoreactive neuropeptides. *Proc. Nat. Acad. Sci. USA 89,* 778–781.
14. Duvaux-Miret, O., Leung, M. K., Capron, A., Stefano, G. B. (1993) *Schistosoma mansoni:* an enkephalinergic system that may participate in internal and host-parasite signaling. *Expl. Parasitol. 76,* 76–84.
15. Eisenberg, R. M. (1985) Plasma corticosterone changes in response to central or peripheral administration of kappa and sigma opiate agonists. *J. Pharmacol. Exp. Therap. 233,* 863–869.

16. Grzych, J. M., Capron, M., Dissous, C., Capron, A. (1984) Blocking activity of rat monoclonal antibodies in experimental schistosomiasis. *J. Immunol. 133,* 998–1004.
17. Isseroff, H., Sylvester, P. W., Bessette, C. L., Jones, P. L., Fisher, W. G., Rynkowski, T. A., Gregor, K. R. (1989) Schistosomiasis: role of endogenous opioids in the suppression of gonadal steriod secretions. *Comp. Biochem. Physiol. 94 A,* 41–45.
18. Kavaliers, M., Podesta, R. B., Hirst, M., Young, B. (1984) Evidence for the activation of the endogenous opiate system in hamsters infected with human blood flukes, *Schistosoma mansoni. Life Sci. 35,* 2365–2373.
19. Kavaliers, M., Podesta, R. B. (1988) Opioid involvement in parasite-induced behavioral modifications: evidence from hamsters infected with *Schistosoma mansoni. Can. J. Zool. 66,* 2653–2657.
20. Leung, M. K., Dissous, C., Capron, A., Woldegaber, H., Duvaux-Miret, O., Pryor, S., Stefano, G. B. (1995) *Schistosoma mansoni:* The presence and potential use of opiate-like substances. *Exp. Parasitol. 81,* 208–215.
21. Makman, M. H., Bilfinger, T. V., Stefano, G. B. (1995) Human granulocytes contain an opiate receptor mediating inhibition of cytokine-induced activation and chemotaxis. *J. Immunol. 154,* 1323–1330.
22. Nikolarakis, K. E., Pfeiffer, A., Stalla, G., Herz, A. (1989) Facilitation of ACTH secretion by morphine is mediated by activation of CRF releasing neurons and sympathetic neuronal pathways. *Brain Res. 498,* 385–388.
23. Pearce, E. J., James, S. L., Hieny, S., Laiiar, D. E., Sher, A. (1988) Induction of protective immunity against *Schistosoma mansoni* by vaccination with schistosome piramyosin (Sm97) a non-surface parasite antigen. *Proc. Natl. Acad. Sci. USA 85,* 5678–5682.
24. Perez-Castrillon, J.-P., Perez-Arellano, J.-P., Garcia-Palomo, J.-D., Jimenez-Lopez, A., De Castro, S. (1992) Opioids depress in vitro human monocyte chemotoxis. *Immunopharmacology 23,* 57–61.
25. Pryor, S. C., Mendez, M., Cherian, E. (1997) Opioid involvement in behavior changes of male mice infected with *Trichinella spiralis. Anim. Biol. 6,* 83–89.
26. Pryor, S. C., Carter, C., Mendes, M., Cherian, C. (1998) Opioid involvement in behavior modifications of mice infected with the parasitic nematode, *Nyppostrongylus brasiliensis. Life Sci. 63,* 1619–1628.
27. Pryor, S. C., Carter, C., Purohit, S. S. (1999) Elevated levels of morphine in mice infected with *Trichinella spiralis.* (in preparation).
28. Salzet, M., Salzet-Raveillon, B., Cocquerelle, C., Verger-Bocquet, M., Pryor, S. C., Rialas, C. M., Laurent, V., Stefano, G. B. (1997) Leech immunocytes contain proopromelanocortin: nitric oxide mediates hemolymph proopromelanocortin processing. *J. Immunol.* 159, 5400–5411.
29. Shipp, M. A., Stefano, G. B., D'Adamio, L., Switzer, S. N., Howard, F. D., Sinisterra, J., Scharrer, B., Reinherz, E. (1990) Downregulation of enkephalin-mediated inflammation responses by CD I O/neutral endopeptidase. *Nature 347,* 394–396.
30. Sibinga, N. E., Goldstein, A. (1988) Opioid peptides and opioid receptors in cells of the immune svstem. *Ann. Rev. Immunol. 6,* 219–249.
31. Smith, E. M., Hughes, T. K., Leung, M. K., Stefano, G. B. (1991) The production and action of ACTH-related peptides in invertebrate hemocytes. *Adv. Neuroimmunol. 7.*
32. Smith, E. M., Hughes, T. K., Hashemi, F., Stefano, G. B. (1992) Immunosuppressive effects of ACTH and opiate-like substances in *S. mansoni* MSH and their possible significance in human immunodeficiency virus infection. *Proc. Nat. Acad. Sci. USA 89,* 782–786.
33. Stefano, G. B. (1989) Role of opioid neuropeptides in immunoregulation. *Prog. Neurobiol. 33,* 149–159.
34. Stefano, G. B., Cadet, P., Scharrer, B. (1989) Stimulatory effects of opioid neuropeptides on locomotory activity and conformational changes in invertebrate and human immunocytes: evidence for a subtype of receptor. *Proc. Natl. Acad. Sci. USA 86,* 6307–6311.
35. Stefano, G. B., Bilfinger, T. V. (1993) Human neutrophil and macrophage chemokinesis induced by cardiopulmonary bypass: Loss of DAME and EL-I chemotaxis. *J. Neuroimmunol. 47,* 189–198.

36. Stefano, G. B., Digenis, A., Spector, S., Leung, M. K., Bilfinger, T. V., Makman, M. H., Scharrer, B., Abumrad, N. N. (1993) Opiate like substances in an invertebrate, a novel opiate receptor on invertebrate and human immunocytes, and a role in immunosuppression. *Proc. Nat. Acad. Sci. USA 1,* 1099–11103.
37. Stefano, G. B., Kushnerik, V., Rodriquez, M., Bilfinger, T. V. (1994) Inhibitory effect of morphine on granulocyte stimulation of tumor necrosis factor and substance *P. Int. J. Immunopharmacol. 16,* 329–334.
38. Tubaro, E., Borelli, G., Croce, C., Cavallo, G., Santiangeli, C. (1983) Effect of morphine on resistance to infection. *J. Infectious Diseases 148,* 656–666.
39. Weber, R. J., Band, L. C., Decosta, B., Pert, A., Rice, K. C. (1991) Neural control of immune function: Opioids, opioid receptors and immunosuppression. *Nat. Inst. Drug Abuse Res. Monograph 1059,* 96–102.

Acta Biologica Hungarica 51 (2–4), pp. 343–348 (2000)

THE FUNCTIONAL ROLE OF OCTOPAMINERGIC NEURONS IN INSECT MOTOR BEHAVIOR+

H.-J. PFLÜGER* and C. DUCH**

Freie Universität, Fachbereich Biologie, Chemie, Pharmazie; Institut für Biologie, Neurobiologie; Königin-Luise-Str. 28-30, D-14195 Berlin, Germany

(Received: August 31, 1999; accepted: November 30, 1999)

The role of efferent, octopaminergic dorsal unpaired median (DUM) neurons in insects is examined by recording from them during motor behaviour. This population of neuromodulatory neurons is divided into sub-populations which are specifically activated or inhibited during ongoing motor behavior. These neurons are always activated in parallel to the respective motor circuits, and in addition to their modulatory effects on synaptic transmission may also cause metabolic changes in their target tissues.

Keywords: Insects – biogenic amines – octopamine – neuromodulation – motor behavior – DUM neurons.

INTRODUCTION

The biogenic amine, octopamine has a variety of effects in the central nervous system of insects: (i) It is involved in processes of sensitization, habituation and memory including olfactory associative learning [2, 6, 23, 49], (ii) if iontophoretically applied to a certain thoracic neuropil, motor patterns such as those shown during walking [48] or flying [50] are released, most likely by influencing membrane properties of some target neurons in the respective networks [43]. More is known about the peripheral modulatory effects of octopamine: (i) It influences the sensitivity of proprioceptors [9, 33, 42, 45], (ii) it presynaptically modulates transmitter release from motor terminals [18], (iii) it reduces basic tension and causes an increase in twitch amplitudes and relaxation rates of skeletal muscles, and inhibits myogenic rhythms of visceral muscle [17, 19, 30, 31, 32, 37, 35, 54, 58]. Interestingly, it also modulates metabolic processes in flight muscles of insects, where it increases the concentration of fructose-2,6-bisphosphate thus stimulating glycolysis [5, 7, 8, 56].

+ Presented at the 9th ISIN Symposium on "Neurobiology of Invertebrates", July 1–5, 1999, Tihany, Hungary.

*Corresponding author, E-mail: pflueger@neurobiologie.fu-berlin.de

**Present address: University of Arizona, 611 Gould Simpson Bldg, Tucson, AZ 85721, USA.

0236-5383/2000/$ 5.00

It also is reported to act as a neurohormone by influencing adipokinetic activity [1, 36], and recent experiments suggest a role in improved oxygen permeability and hence respiratory efficiency [59].

Only in a few cases could these octopaminergic effects be mimicked by stimulating the neurons which contain octopamine. The great majority of octopaminergic neurons belong to the class of unpaired median neurons with either dorsal or ventral somata (DUM or VUM neurons [16, 18, 25, 26, 35, 38, 51, 52, 53, 55]. With the exception of the suboesophageal VUMmx neuron in the honey bee [23], central effects of octopamine could not be mimicked by stimulating individual DUM or VUM neurons. In contrast, many of the previously described peripheral modulatory effects were also observed when stimulating individual DUM or VUM neurons.

DUM neuron activity during motor behavior such as the locust kick

The locust, used here as our model insect, provides very favourable features for investigating when the population of octopaminergic unpaired median neurons is used in behavior. Firstly, the system of its DUM and VUM neurons has been well documented [15, 53, 55], and the different types of DUM neurons have been described according to the nerves which their axons exit [13, 15, 55], or according to their target muscles [25]. Secondly, the networks of many motor behaviors have been studied on a cellular level (see [11]). Previous studies postulated a collective activation of all unpaired median neurons [27, 36]. During cricket walking it was shown that some prothoracic DUM neurons were active, but a correlation to the step period or walking speed was not described [22]. It may be from observations such as these that the notion of the DUM neurons being part of a general arousal system arose [27]. When examining the role of DUM neurons during the locust kick [12], very different results were obtained, namely, that only DUMETi, innervating the extensor tibiae musle, and DUM3, -4, -5 neurons which, among others, innervate the flexor tibiae muscle, were activated during a kick. Others, such as DUM3, -4 neurons, which most likely innervate flight power muscles (see [15, 53]) were inhibited. Their results clearly showed that the DUM neurons involved in this particular behavior were activated in parallel with the motor networks in the corresponding thoracic ganglion. Therefore, whenever the locust started a kick program the respective octopaminergic neurons were activated and others were inhibited.

DUM and VUM neuron activity during fictive motor behavior

Support for this came from a string of other experiments in which patterns were released from whole or parts of isolated nervous systems, and which (by correlating them with motor patterns of intact insects) were called fictive motor patterns [46, 47]. Thus, the muscarinic agonist pilocarpin induces fictive walking patterns, and, in agreement with a specific activation of DUM neurons, only the activity of DUM neu-

rons which supply leg and other thoracic muscles was coupled to the centrally evoked rhythm [4]. In *Manduca* larvae pilocarpin similarly induced fictive crawling rhythms [28], and activated all VUM neurons which innervate body wall muscles [29].

The DUM neuron population is divided into subpopulations

From these experiments it can be concluded, in contrast to previous suggestions, that unpaired median neurons are activated differentially during specific behaviors, and are divided into subpopulations. How exactly are these subpopulations defined? When recordings are made from pairs of DUM/VUM neurons in locusts [40] or *Manduca* larvae [41], it is obvious that some DUM or VUM neurons receive postsynaptic potentials (PSPs) which are common to both neurons. In a detailed survey Baudoux and Burrows [3] and Duch et al. [15] found that such subpopulations are defined by common PSPs from (i) local interneurons, (ii) intersegmental interneurons and (iii) interneurons that are only active during a particular motor program. In the first two cases such common PSPs can be observed whenever recordings from the respective pairs of DUM neurons were made, in the latter case the common PSPs are only apparent when a particular motor behavior is shown. Unfortunately, all attempts to identify some of the presynaptic neurons to DUM or VUM neurons have failed so far. For the intersegmental common inputs evidence from *Manduca* [29] and locusts [15] points to unknown descending neurons in the subesophageal ganglion.

Activity of DUM neurons during locust flight

The finding that during a locust kick the population of DUM3, -4 neurons, which most likely innervates the flight power muscles, is inhibited seems surprising because, provided the kick pattern is similar to that shown during jumps [10, 24, 39], locusts open their wings during jumps. But when recording from DUM neurons in a restrained and dissected locust, but with intact wing bases and partly movable wings, a similar result was obtained: (i) DUM neurons which most likely exclusively innervate flight power muscles are inhibited, and (ii) in contrast, DUM neurons which innervate leg and other thoracic muscles are activated during short bouts of flight activity. This is also true for pharmacologically-induced fictive flight patterns using the octopamine agonist, chlordimeform. These experiments reveal that the respective DUM neurons receive either an inhibitory or an excitatory synaptic drive during periods of motor behavior. Electrical stimulation of the sensory nerve containing the sensory axons of the receptors of the wing tegula clearly demonstrates that they contribute in an important fashion to this inhibition. The fact that inhibition is also shown in isolated and fictively flying nervous systems may also suggest a participation of central inhibitory pathways [14]. These results contradict all previous results

obtained for DUM neurons from similarly restrained flying locusts [36, 42, 44]. Nevertheless, we believe that an inhibition of DUM neurons during flight makes a lot of sense. It has been shown that octopamine stimulates one of the substances that increases the glycolytic activity of muscle, fructose-2,6-bisphosphate [56, 78]. During flight, however, flight muscles rely on lipid metabolism [57], and therefore octopamine concentrations should decrease. Indeed, measurements of octopamine concentrations within a flight power muscle after ten minutes of flight reveal a dramatic decrease [20]. This is an interesting discrepancy to what happens in the hemolymph. There, octopamine concentrations increase significantly during the first ten minutes of flight [20, 21, 34]. Perhaps the octopamine concentration in the hemolymph is too low to affect the octopamine receptors of the muscles, or hemolymph flow within the intact organism is very different from what we believe. In addition, the concentration of fructose-2,6-bisphosphate in the resting insect's flight muscles is very high if compared to a resting vertebrate muscle, for example ([56], and personal communication). This could be explained by the DUM3,4 neurons which in a resting, nonflying animal can be active with frequencies up to 1 Hz. This activity would ensure that the resting muscle relies on glycolytic activity, and that energy for the very first moments of flight activity comes from glycolysis.

ACKNOWLEDGEMENTS

We thank Mary Wurm, Berlin, for help with the English manuscript. H.-J. P. is supported by SFB 515 (DFG), and C. Duch was a member of the graduate college "Signalketten".

REFERENCES

1. Agricola, H., Hertel, W., Penzlin, H. (1988) Octopamine: neurotransmitter, neuromodulator and neurohormon. *Zool. Jb. Physiol. 92,* 1–45.
2. Bacon, J. P., Thompson, K. S. J., Stern, M. (1995) Identified octopaminergic neurons provide an arousal mechanism in the locust brain. *J. Neurophysiol. 74,* 2739–2743.
3. Baudoux, S., Burrows, M. (1998) Synaptic activation of efferent neuromodulatory neurones in the locust *Schistocerca gregaria. J. Exp. Biol. 201,* 3339–3354.
4. Baudoux, S., Duch, C., Morris, O. T. (1998) Coupling of efferent neuromodulatory neurons to rhythmical leg motor activity in the locust. *J. Neurophysiol. 79,* 361–370.
5. Becker, A., Schlöder, P., Steele, J. E., Wegener, G. (1996) The regulation of trehalose metabolism in insects. *Experimentia 52,* 433–439.
6. Bicker, G., Menzel, R. (1989) Chemical codes for the control of behaviour in arthropods. *Nature 337,* 33–39.
7. Blau, C., Wegener, G. (1994) Metabolic integration in locust flight: the effect of octopamine on fructose 2,6-bisphosphate content of flight muscle *in vivo. J. Comp. Physiol. B 164,* 11–15.
8. Blau, C., Wegener, G., Candy, D. J. (1994) The effect of octopamine on the glycolytic activator fructose 2,6-bisphosphate in perfused locust flight muscle. *Insect Biochem. Molec. Biol. 24,* 677–683.
9. Bräunig, P., Eder, M. (1998) Locust dorsal unpaired median (DUM) neurones directly innervate and modulate hindleg proprioceptors. *J. Exp. Biol. 201,* 3333–3338.
10. Burrows, M. (1995) Motor patterns during kicking movements in the locust. *J. Comp. Physiol. 176,* 289–305.
11. Burrows, M. (1996) The neurobiology of an insect brain. Oxford University Press, Oxford.

12. Burrows, M., Pflüger, H. J. (1995) Action of locust neuromodulatory neurons is coupled to specific motor patterns. *J. Neurophysiol. 74,* 347–357.
13. Campbell, H. R., Thompson, K. J., Siegler, M. V. S. (1995) Neurons of the median neuroblast lineage of the grasshopper: A population study of efferent DUM neurons. *J. Comp. Neurol. 358,* 541–551.
14. Duch, C., Pflüger, H.-J. (1999) DUM neuron activity during locust flight: a model system for amine mediated peripheral adjustments to a central motor pattern. *J. Comp. Physiol. A, 184,* 489–499.
15. Duch, C., Mentel, T., Pflüger, H.-J. (1999) Distribution and activation of different types of octopaminergic DUM neurons in the locust. *J. Comp. Neurol. 403,* 119–134.
16. Evans, P. D. (1985) Octopamine. In: Kerkut, G. A., Gilbert, G. (ed.). *Comprehensive Insect Physiology Biochemistry Pharmacology.* Oxford, Pergamon Press, pp. 499–530.
17. Evans, P. D., Siegler, M. V. S. (1982) Octopamine mediated relaxation of maintained and catch tension in locust skeletal muscle. *J. Physiol. 324,* 93–112.
18. Evans, P. D., O'Shea, M. (1977) An octopaminergic neuron modulates neuromuscular transmission in the locust. *Nature 270,* 257–259.
19. Evans, P. D., O'Shea, M. (1978) The identification of an octopaminergic neuron and the modulation of a myogenic rhythm in the locust. *J. Exp. Biol. 73,* 235–260.
20. Goosey, M. W., Candy, D. J. (1980) The D-octopamine content of the haemolymph of the locust, *Schistocerca americana gregaria* and its elevation during flight. *Insect Biochem. 10,* 393–397.
21. Goosey, M. W., Candy, D. J. (1982) The release and removal of octopamine by tissues of the locust *Schistocerca gregaria. Insect Biochem. 12,* 681–685.
22. Gras, H., Hörner, M., Runge, L., Schürmann, F.-W. (1990) Prothoracic DUM neurons of the cricket *Gryllus bimaculatus.* Responses to natural stimuli and activity in walking behavior. *J. Comp. Physiol. A 166,* 901–914.
23. Hammer, M. (1993) An identified neurone mediates the unconditioned stimulus in associative olfactory learning in honeybees. *Nature 366,* 59–63.
24. Heitler, W. J., Burrows, M. (1977) The locust jump. I. The motor programme. *J. Exp. Biol. 76,* 63–84.
25. Hoyle, G. (1978) The dorsal unpaired median neurons of the locust metathoracic ganglion. *J. Neurobiol. 9,* 43–57.
26. Hoyle, G., Dagan, D. (1978) Physiological characteristics and reflex activation of DUM (octopaminergic) neurons of the locust metathoracic ganglion. *J. Neurobiol. 9,* 59–79.
27. Hoyle, G., Dagan, D., Moberly, B., Colquhun, W. (1974) Dorsal unpaired median insect neurons make neurosecretory endings on skeletal muscle. *J. exp. Zool. 187,* 159–165.
28. Johnston, R. M., Levine, R. B. (1996) Crawling motor patterns induced by pilocarpine in isolated larval nerve cords of *Manduca sexta. J. Neurophysiol. 76,* 3178–95.
29. Johnston, R., Consoulas, Chr., Pflüger, H.-J., Levine, R. B. (1999) Patterned activation of unpaired median neurons during fictive crawling in Manduca larvae. *J. Exp. Biol. 202,* 103–113.
30. Kalogianni, E., Pflüger, H. J. (1992) The identification of motor and unpaired median neurons innervating the locust oviduct. *J. Exp. Biol. 168,* 177–198.
31. Kalogianni, E., Theophilidis, K. (1993) Centrally generated rhythmic activity and modulatory function of the oviductal dorsal unpaired median (DUM) neurons in two orthoptheran species *(Calliptamus* sp. and *Decticus albifrons). J. Exp. Biol. 198,* 507–520.
32. Malumud, J. G., Mizisin, A. P., Josephson, R. K. (1988) The effects of octopamine on contraction kinetics and power output of a locust flight muscle. *J. Comp. Physiol. A 162,* 827–835.
33. Matheson, T. (1994) Octopamine enhances the response of thoracic but not phasic neurons of a locust proprioreceptor. *J. Physiol. 480,* 99P.
34. Orchard, I. (1982) Octopamin in insects: neurotransmitter, neurohormone and neuromodulator. *Can. J. Zool. 60,* 659–669.
35. Orchard, I., Lange, A. B. (1985) Evidence for octopaminergic modulation of an insect visceral muscle. *J. Neurobiol. 16,* 171–181.
36. Orchard, I., Ramirez, J. M., Lange, A. B. (1993) A multifunctional role for octopamine in locust flight. *Annu. Rev. Entomol. 38,* 227–249.
37. O'Shea, M., Evans, P. D. (1979) Potentiation of neuromuscular transmission by an octopaminergic neuron in the locust. *J. Exp. Biol. 79,* 169–190.

38. Plotnikova, S. N. (1969) Efferent neurons with several axons in the ventral nerve cord of the asian grasshopper *Locusta migratoria. J. Evol. Biochem. Physiol. 5,* 276–277.
39. Pflüger, H.-J., Burrows, M. (1978) Locusts use the same basic motor pattern in swimming as in jumping and kicking. *J. Exp. Biol. 75,* 81–93.
40. Pflüger, H.-J., Watson, A. H. D. (1988) The structure and distribution of Dorsal Unpaired Median (DUM) neurones in the abdominal nerve cord of male and female locusts. *J. Comp. Neurol. 268,* 329–345.
41. Pflüger, H. J., Witten, J. L., Levine, R. B. (1993) Fate of abdominal ventral unpaired median cells during metamorphosis of the hawkmoth, *Manduca sexta. J. Comp. Neurol. 335,* 508–522.
42. Ramirez, J.-M., Orchard, J. (1990) Octopaminergic modulation of the forewing stretch receptor in the locust *Locusta migratoria. J. Exp. Biol. 149,* 255–279.
43. Ramirez, J.-M., Pearson, K. G. (1991) Octopamine induces bursting and plateau potentials in insect neurons. *Brain Res. 549,* 332–337.
44. Ramirez, J.-M., Pearson, K. G. (1991) Octopaminergic modulation in the flight system of the locust. *J. Neurophysiol. 66,* 1522–37.
45. Ramirez, J.-M., Büschges, A., Kittmann, R. (1993) Octopaminergic modulation of the femoral chordotonal organ in the stick insect. *J. Comp. Physiol. A 173,* 209–219.
46. Ryckebusch, S., Laurent, G. (1993) Rhythmic patterns evoked in locust leg motor neurons by the muscarinic agonist pilocarpine. *J. Neurophysiol. 69,* 1583–95.
47. Ryckebusch, S., Laurent, G. (1994) Interactions between segmental leg central pattern generators during fictive rhythms in the locust. *J. Neurophysiol. 72,* 2771–85.
48. Sombati, S., Hoyle, G. (1984) Generation of specific behaviours in a locust by local release into the neuropile of the natural neuromodulator octopamine. *J. Neurobiol. 15,* 481–506.
49. Sombati, S., Hoyle, G. (1984) Central nervous sensitisation and dishabituation of reflex action in an insect by the neuromodulator octopamine. *J. Neurobiol. 15,* 455–480.
50. Stevenson, P. A., Kutsch, W. (1988) Demonstration of functional connectivity of the flight motor system in all stages of the locust. *J. Comp. Physiol. 162,* 247–259.
51. Stevenson, P. A., Pflüger, H. J., Eckert, M., Rapus, J. (1992) Octopamine immunoreactive cell populations in the locust thoracic-abdominal nervous system. *J. Comp. Neurol. 315,* 382–397.
52. Stevenson, P. A., Pflüger, H.-J., Eckert, M., Rapus, J. (1994) Octopamine-like immunoreactive neurones in locust genital abdominal ganglia. *Cell Tiss. Res. 275,* 299–308.
53. Stevenson, P. A., Spörhase-Eichmann, U. (1995) Localisation of octopaminergic neurones in insects. *Comp. Biochem. Physiol. Biochem. Mol. Biol. 110,* 203–15.
54. Stevenson, P. A., Meuser, S. (1997) Octopaminergic innervation and modulation of a locust flight steering muscle. *J. Exp. Biol. 200,* 633–642.
55. Watson, A. H. D. (1984) The dorsal unpaired median neurons of the locust metathoracic ganglion: neuronal structure and diversity, and synaptic integration. *J. Neurocytol. 13,* 303–327.
56. Wegener, G. (1996) Flying insects: model systems in exercise physiology. *Experimentia 52,* 404–412.
57. Wegener, G., Michel, R., Newsholme, E. A. (1986) Fructose-2,6-bisphosphate as a signal for changing from sugar to lipid oxidation during flight in locusts. FEBS Lett. 201, 129–132.
58. Whim, M. D., Evans, P. D. (1988) Octopaminergic modulation of flight muscles in the locust. *J. Exp. Biol. 134,* 247–266.
59. Zeng, H., Loughton, B. G., Jennings, K. R. (1996) Tissue specific transduction systems for octopamine in the locust *(Locusta migratoria). J. Insect Physiol.* 42, 765–769.

Acta Biologica Hungarica 51 (2–4), pp. 349–354 (2000)

TYRAMINE INJECTIONS REDUCE LOCUST VIABILITY+

H. Torfs, Wendy Van Poyer, J. Poels, Elfriede Swinnen, A. De Loof and J. Vanden Broeck*

Department of Biology, Laboratory for Developmental Physiology and Molecular Biology, K.U. Leuven, Zoological Institute, Naamsestraat 59, B-3000 Leuven, Belgium

(Received: August 31, 1999; accepted: November 30, 1999)

In the locust nervous system, tyramine is the direct precursor for octopamine synthesis and, as an octopamine analogue, it can activate octopamine receptors. Furthermore, the identification of specific tyramine receptors in *Locusta migratoria* and *Drosophila melanogaster* suggests that it is an important transmitter or modulator candidate. In this paper, we report that repeated tyramine injections reduced the viability of last instar larvae of *Locusta* and *Schistocerca.* In addition, a retardation of the last ecdysis was observed as a sublethal effect of the repeated tyramine treatment. Moreover, egg deposition by adult females was also retarded and/or drastically reduced. These effects show similarity to sublethal effects described for certain "insecticidal" octopamine receptor agonists, such as formamidines and phenylimino-imidazolidines. Since certain formamidine compounds were also shown to be agonists for the cloned tyramine receptors, it cannot be excluded that some lethal or sublethal consequences of tyramine administration are the result of an interaction with specific tyramine receptors.

Keywords: Amines – formamidines – octopamine – tyramine – G protein-coupled receptors.

INTRODUCTION

Monophenolic amines such as octopamine and tyramine are present in the insect CNS. Tyramine (TA) is derived from the amino acid tyrosine via the action of a tyrosine decarboxylase enzyme, whereas octopamine (OA) is produced by hydroxylation of TA. Several effects of TA are reported, but, from these studies, it is not entirely clear whether TA acts as an OA-mimic or whether it exerts these activities as a natural, endogenous messenger molecule [5, 14]. Recent studies have indicated that a specific TA-uptake system is present in the locust nervous system [6]. The distribution patterns of OA and of TA show some important differences and there are specific, but distinct, binding sites for [^{3}H]-OA and [^{3}H]-TA [9]. Moreover, α_2-adrenore-

+ Presented at the 9th ISIN Symposium on "Neurobiology of Invertebrates", July 1–5, 1999, Tihany, Hungary.

*Corresponding author, E-mail: Jozef.VandenBroeck@bio.kuleuven.ac.be

0236-5383/2000/$ 5.00

ceptor-like phenolamine receptors which display a much higher affinity for TA than for any other endogenous amine (e.g. OA or dopamine) were cloned from *Drosophila melanogaster* and from *Locusta migratoria* [1, 13, 16, 19]. These receptors are pharmacologically distinct from the OA-receptor subtypes that have been described in insect tissues [7, 18, 20]. The fruitfly TA-receptor, when expressed in cultured mammalian cells, shows high affinities towards the insecticidal formamidine compounds demethyl-chlordimeform and amitraz [8]. Therefore, in addition to OA-receptors, TA-receptors may be target sites for certain formamidines. Yohimbine (Yoh), an α_2 antagonist, possesses a high affinity for the cloned TA-receptors [16, 20]. It is a relatively good antagonist for locust OA_1-mediated effects in the *extensor tibiae* muscle preparation and a very weak antagonist for OA_2-mediated effects [7, 14].

In order to investigate the effects of TA, we performed a number of simple injection experiments and monitored the viability of last instar larvae and adult locusts.

MATERIALS AND METHODS

Insect breeding

Locusts (*Locusta migratoria* and *Schistocerca gregaria*) were kept under stable humidity and temperature (30 °C) conditions. Artificial light sources were used to mimic a constant day/night rhythm with 13 h of daylight. The animals were fed with fresh or frozen grasses and rolled oats. In addition, the desert locusts (*Schistocerca gregaria*) were fed with fresh cabbage leafs. The two species were kept in separate rooms and they did not leave the gregarious phase.

Injection experiments

Control and experimental animals were derived from the same synchronized breed: all locusts (*Locusta* or *Schistocerca*) used in a single experiment had the same age. Each control or experimental group (of at least ten insects) contained equal numbers of males and females and all animals were treated in a very similar way. Experimental animals were injected by using a graded Hamilton syringe with a diluted solution of one of the following substances (purchased from Sigma) dissolved in PBS (phosphate buffered saline) at different concentrations: p-tyramine (TA), (+/–)-octopamine (OA), yohimbine (Yoh), a mixture of p-tyramine and yohimbine (TA/Yoh) or a mixture of (+/–) octopamine and yohimbine (OA/Yoh). Control animals were injected with PBS. All injections were repeated with an interval of one day. The last instar larvae, adults (after the last ecdysis) and dead insects were counted daily in each group of animals. The results were visualized by using the SLIDE or CORRELCHART computer programmes.

RESULTS

The result of several independent injection experiments is displayed in Fig. 1. We can summarize the observed effects as follows:

(1) The control animals injected with PBS did not significantly differ from the non-injected animals in the main cage. The moment at which the last ecdysis took place was identical. In addition, these control animals remained healthy and extremely small numbers of dead animals were obtained even after multiple repeats of the injections.

(2) In some experimental groups, the viability of the animals was severely affected. Repeated injections with 4 µl of TA at concentrations above 10^{-4} M (which is the TA concentration in the injected solution and not the resulting TA-titre in the insect's haemolymph) clearly had an insecticidal effect. This lethal effect was usually not immediate. It occurred after several daily injections. In sublethal conditions, the moment at which the last ecdysis took place was retarded. Although the effect of tyramine injections was stronger, similar effects were also observed when octopamine was injected.

(3) Interestingly, co-injection of yohimbine together with tyramine or octopamine clearly antagonized these lethal or sublethal effects, whereas injection with yohimbine alone had only a slight effect on locust viability. The observation indicates that yohimbine blocked the deleterious effects of (repeated) tyramine and/or octopamine injections.

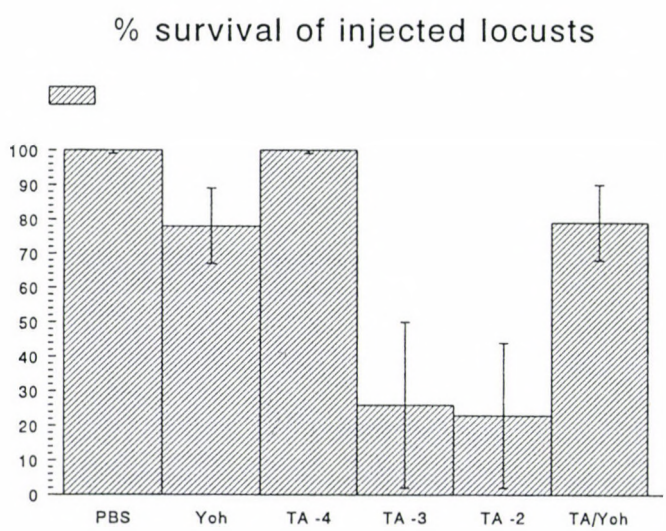

Fig. 1. Histogram showing the percentages of surviving animals *(Schistocerca gregaria)* obtained from injection experiments with *Schistocerca gregaria* last instar larvae. Injected solutions contained 4 µl of PBS (PBS), 4 µl of a 0.1 mM yohimbine solution (Yoh), 4 µl of a 0.1, 1 and 10 mM TA solution (TA-4, TA-3, TA-2) or 6 µl of a TA/Yoh mixture (4 µl 1 mM TA + 2 µl 0.1 mM Yoh)

(4) Repeated injections of adult locusts with tyramine (and to a lesser extent with octopamine) appeared to retard the moment of egg deposition. This was shown by comparing several experimental (injections with TA or OA) and control groups (injections with TA or OA in combination with yohimbine) of adult locusts. In an experiment with *Schistocerca,* the TA-treated animals showed a delay of 2–3 days for egg deposition and for subsequent larval hatching. In a similar experiment with *Locusta,* the TA-injected animals deposited no eggs during the time of the experiment. A delay of about 5 days was observed for the OA-injected group compared to the TA/Yoh or OA/Yoh groups. Again, yohimbine antagonized the effects of TA and of OA.

DISCUSSION

Many physiological effects of OA as well as the pharmacology of OA binding sites have been intensely studied in locusts. Compounds such as formamidines and phenylimino-imidazolidines, which are thought to interact as agonists with OA-receptors, or cocaine, which probably affects the octopaminergic system, possess an insecticidal activity [3, 12]. Sublethal effects of these compounds have been described and include many behavioural effects related to crucial physiological processes of insects: hatching and eclosion, control of locomotion, the "arousal syndrome", egg deposition, phototaxis and learning, growth delay and developmental retardation, etc. [2, 3, 4, 11].

The effects observed after injection of TA (and of OA) appear to be very similar to the ones that are elicited by formamidine insecticides. Since the pharmacodynamics of TA administration into the haemolymph are not fully understood, there are some unknown elements: (1) the true concentration of TA (or OA) present in the haemolymph before and after the injections and the effect of inactivation and/or uptake mechanisms for TA (or OA) [6, 10, 15, 17]; (2) the accessibility of the possible target sites and the role of the existing blood-brain barrier; (3) the effect of repeated injections on octopaminergic and/or tyraminergic systems, on feedback and desensitization mechanisms. Therefore, it is quite difficult to speculate about the physiological mechanisms that are responsible for the observed effects. The repeatedly injected TA (and OA) has probably mimicked the effect of formamidines in a direct or indirect way. Specific receptor targets could have mediated the lethal and sublethal effects of TA (or OA). Alternatively, TA may have induced (additional) changes to the octopaminergic or tyraminergic systems. The idea that specific receptors might be involved, is supported by the observation that the effects of TA appeared to be stronger than these of OA and by the remarkable fact that yohimbine was a very good antagonist for these effects. Cloned TA receptors from fruitfly and locust display a high affinity for yohimbine and have a much higher affinity for TA than for OA. Furthermore, it was reported that TA-receptors indeed represent potential target sites for certain formamidine compounds [8].

Our results form a basis for further studies on the role(s) of phenolamines in insects. The elucidation of the specific functions of OA and of TA will probably depend on the characterization and localization of the pharmacologically distinct receptor subtypes that are involved in mediating the cellular responses to these amines [18]. This will most probably enrich our understanding of the complicated aminergic systems in insects and of the mode of action of certain insecticidal compounds.

ACKNOWLEDGEMENTS

The authors especially thank T. Janssen, Julie Puttemans and Marijke Christiaens for technical assistance and for help with preparation of the figure, Maria Van der Eeken for help with typesetting of the manuscript and Steve Kotanen for English text correction. R. Jonckers is gratefully acknowledged for insect breeding. Research was supported by the E.U. (BIO4-CT96-0699) and by the Belgian "Interuniversity Poles of Attraction Programme" (IUAP/PAI-IV P4/30, Belgian State, Prime Minister's Office – Federal Office for Scientific, Technical and Cultural Affairs). J.Vd.B. is a Senior Research Associate of the FWO-Flanders and W.V.P. and J.P. obtained a PhD. fellowship from the IWT-Flanders.

REFERENCES

1. Arakawa, S., Gocayne, J. D., McCombie, W. R., Urquhart, D. A., Hall, L. M., Fraser, C. M., Venter, J. C. (1990) Cloning, localization, and permanent expression of a *Drosophila* octopamine receptor. *Neuron 2,* 343–354.
2. Cascino, P., Nectoux, M., Guiraud, G., Bounias, M. (1989) The formamidine amitraz as a hyperglycemic alpha-agonist in worker honeybees *(Apis mellifera mellifera* L.) in vivo. *Biomed. Environ. Sci. 2,* 106–114.
3. Coats, J. R. (1982) *Insecticide Mode of Action.* Academic Press, New York, London.
4. Corbet, S. A. (1991) A fresh look at the arousal syndrome of insects. *Adv. Insect Physiol. 23,* 81–116.
5. Downer, R. G. H., Hiripi, L. (1994) Biogenic amines in insects. In: Borkovec, A. B., Loeb, M. J. (eds) *Insect Neurochemistry and Neurophysiology 1993.* CRC Press Inc., Boca Raton, pp. 23–38.
6. Downer, R. G. H., Hiripi, L., Juhos, S. (1993) Characterization of the tyraminergic system in the central nervous system of the locust, *Locusta migratoria migratoides. Neurochem. Res. 18,* 1245–1248.
7. Evans, P. D., Robb, S. (1993) Octopamine receptor subtypes and their modes of action. *Neurochem. Res. 18,* 869–874.
8. Hall, L. M., Hannan, F., Feng, G., Eberl, D. F., Kousky, C. (1994) Cloning and molecular analysis of G-protein coupled receptors in insects. In: Borkovec, A. B., Loeb, M. J. (eds) *Insect Neurochemistry and Neurophysiology 1993.* CRC Press Inc., Boca Raton, pp. 53–71.
9. Hiripi, L., Juhos, S., Downer, R. G. H. (1994) Characterization of tyramine and octopamine receptors in the insect *(Locusta migratoria migratorioides)* brain. *Brain Research 633,* 119–126.
10. Linn, C. E. Jr., Poole, K. R., Roelofs, W. L. (1994) Studies on biogenic amines and metabolites in the nervous tissue and hemolymph of male cabbage looper moths. III. Fate of injected octopamine, 5-hydroxytryptamine and dopamine. *Comp. Biochem. Physiol. 108C,* 99–106.
11. M'Diaye, K., Bounias, M. (1991) Sublethal effects of the formamidine amitraz on honeybee gut lipids, following in vivo injections. *Biomed. Environ. Sci. 4,* 376–383.
12. Nathanson, J. A., Hunnicutt, E. J., Kantham, L., Scavone, C. (1993) Cocaine as a naturally occurring insecticide. *Proc. Nat. Acad. Sci. USA 90,* 9645–9648.
13. Robb, S., Cheek, T. R., Hannan, F. L., Reale, V., Hall, L., Midgley, J. M., Evans, P. D. (1994) Agonist-specific coupling of a cloned *Drosophila* octopamine/tyramine receptor to multiple second messen-

gers. In: Borkovec, A. B., Loeb, M. J. (eds) *Insect Neurochemistry and Neurophysiology 1993.* CRC Press Inc., Boca Raton, pp. 351–354.
14. Roeder, T. (1994) Mini Review. Biogenic amines and their receptors in insects. *Comp. Biochem. Physiol. 107C,* 1–12.
15. Roeder, T., Gewecke, M. (1989) Octopamine uptake systems in thoracic ganglia and leg muscles of *Locusta migratoria. Comp. Biochem. Physiol. 94C,* 143–147.
16. Saudou, F., Amlaiky, N., Plassat, J.-L., Borrelli, E., Hen, R. (1990) Cloning and characterization of a *Drosophila* tyramine receptor. *EMBO Journal 9,* 3611–3617.
17. Shampengtong, L., Wong, K. P., Ho, B. C. (1987) N-acetylation of dopamine and tyramine by mosquito pupae *(Aedes togoi). Insect Biochem. 17,* 111–116.
18. Vanden Broeck, J. (1996) G protein-coupled receptors in insect cells. *Int. Rev. Cytol. 164,* 189–268.
19. Vanden Broeck, J., Verhaert, P., De Loof, A. (1994) Cloning, sequencing and tissue distribution of a putative locust G protein-coupled receptor. In: Borkovec, A. B., Loeb, M. J. (eds) *Insect Neurochemistry and Neurophysiology 1993.* CRC Press Inc., Boca Raton, pp. 367–370.
20. Vanden Broeck, J., Vulsteke, V., Huybrechts, R., De Loof, A. (1995) Characterization of a cloned locust tyramine receptor cDNA by functional expression in permanently transformed *Drosophila* S2 cells. *J. Neurochem. 64,* 2387–2395.

Acta Biologica Hungarica 51 (2–4), pp. 355–362 (2000)

ACETYLCHOLINE, GABA, GLUTAMATE AND NO AS PUTATIVE TRANSMITTERS INDICATED BY IMMUNOCYTOCHEMISTRY IN THE OLFACTORY MUSHROOM BODY SYSTEM OF THE INSECT BRAIN[+]

F.-W. SCHÜRMANN*

Institut für Zoologie und Anthropologie der Georg-August-Universität, Berlinerstr. 28, D-37073 Göttingen, Germany

(Received: August 31, 1999; accepted: November 30, 1999)

The distribution of glutamate, GABA and ChAT and of NADPH-diaphorase was immunocytochemically and histochemically investigated in the mushroom bodies of the cricket *(Gryllus bimaculatus)* and of the fruitfly *(Drosophila melanogaster)*. Glutamate and NO are considered as putative transmitters of mushroom body Kenyon cell types. In the input area (calyces) of the mushroom bodies of *Drosophila*, the majority of olfactory projection neurons is stained with antibodies against ChAT. In addition, small GABA-immunoreactive presynaptic fibres of extrinsic neurons occur intermingled with the ChAT-immunoreactive elements in the calyces, and occupy distinct compartments in the stalk and lobes. Complex synaptic connectivity of putatively cholinergic and GABAergic extrinsic neurons and of Keyon cell dendrites within the calycal glomeruli of mushroom bodies is discussed.

Keywords: Mushroom bodies – immunocytochemistry – GABA – glutamate – ChAT – *Gryllus bimaculatus* – *Drosophila melanogaster*.

INTRODUCTION

The mushroom bodies represent a prominent neuropile in the brain of insects, widely considered as secondary olfactory neuropile. Many recent approaches deal with the contribution of mushroom bodies to odor discrimination, multimodal integration, olfactory memory and to locomotory activities, or with their structural design and development [3, 4, 14] in a number of favorite model species, among them crickets and fruitflies. In crickets and in flies, the mushroom bodies are similarly and relatively simply structured [7, 14].

Immunocytological studies on the distribution of neuroactive compounds considerably contribute to the understanding of the compartmental organization of the mushroom bodies, and, moreover, allow to allocate transmitters and modulators to mushroom body neurons [4]. These morphological techniques are useful tools for

[+] Presented at the 9th ISIN Symposium on "Neurobiology of Invertebrates", July 1–5, 1999, Tihany, Hungary.

*E-mail: fschuer@gwdg.de

0236-5383/2000/$ 5.00

complementing functional models on synaptic interactions. Biogenic amines and neuropeptides have been demonstrated in extrinsic neurons, connecting the mushroom bodies with other neuropiles of the brain. GABA and acetylcholine are abundant transmitters in the insect nervous system, occurring in distinct groups of extrinsic mushroom body neurons as well [1, 4, 15]. On the other hand, the transmitters of the Kenyon cells, the abundant local intrinsic neurons, which determine the form of the mushroom bodies, have poorly been investigated.

The present immunocytochemical and histochemical study describes the distribution of glutamate and NO in intrinsic mushroom body Kenyon cell populations and of GABA and acetylcholine in extrinsic neurons of mushroom bodies, comparing the cricket *Gryllus bimaculatus* and the fruitfly *Drosophila melanogaster*.

MATERIAL AND METHODS

Adults of *Gryllus bimaculatus* and *Drosophila melanogaster* (wildtype, Kanton strain) from the institute's breeding colonies, were fixed and further processed for immunocytology according to different protocols described in detail elsewhere [1, 2, 11, 15]. For Cy-3-immunofluorescence preparations, vibratome-sections were preferentially used. The following primary antibodies were used: antisera against glutamate (No. 607, kindly provided by O. Ottersen, Oslo); against GABA (Incstar, Stillwater, USA), and against *Drosophila* choline acetyltransferase (ChAT) (kindly provided by P. M. Salvaterra, Duarte USA). NADPH-diaphorase histochemistry served for the demonstration of putative NO synthase (NOS) [10]. Immunostainings were viewed by either conventional light microscopy or by confocal microscopy, photographed or stored by a computer.

RESULTS

Labeling of Kenyon cells

The mushroom bodies of crickets contain three separate populations of Kenyon cells (KI–III) with separate clusters of somata and axonal fibres collected in discrete bundles running in parallel through the calyces and stalks and terminating in the α- and β-lobes (Fig. 1) [11]. In *Gryllus*, the three populations of Kenyon cells can be clearly discriminated by their glutamate-like immunoreactivity. Strong glutamate-like immunoreactivity, most prominent in the somata, is found in the KIII-neurons, whereas the KII-cells are less intensely stained (Figs 2, 3). In contrast, central KI-cells appear devoid of glutamate-like immunostaining.

In the fruitfly *Drosophila*, the mushroom bodies show a subcompartmental organization due to clustering of Kenyon cells and axonal fibres [14]. We failed to detect a clear glutamate-like staining of sets of Kenyon cells. A selective glutamate-like staining by use of a ABC-DAB-procedure and a different antiserum for the fruitfly

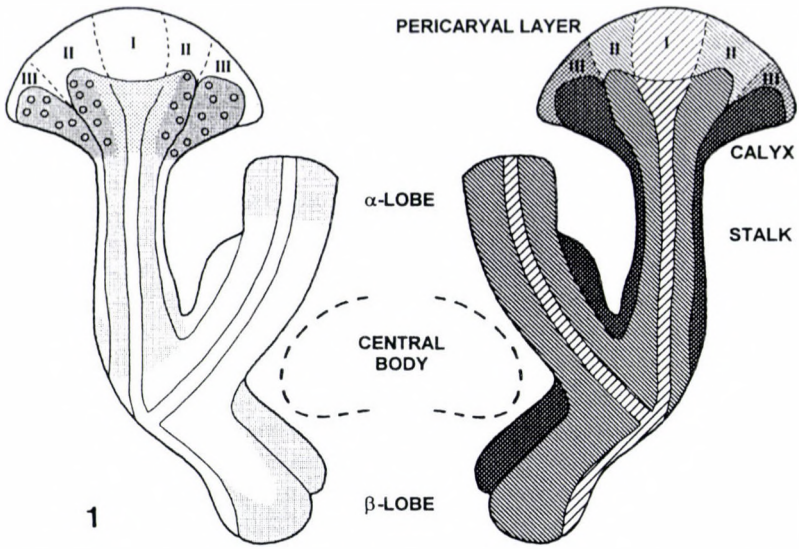

Fig. 1. Scheme of cricket mushroom bodies. Right: Clusters of Kenyon cell type somata (I–III) give rise to fibre bundles, projecting through the calyces, stalks and terminating in the α- and β-lobes. Type III cells show strong, type II cells medium glutamate-like immunoreactivity and type I cells lack staining. Left: The compartments formed by the Kenyon cells receive extrinsic cells in different neuropile portions (stippled labels: immunoreactive putative GABAergic neurons with discrete subdivisions in the stalk and in the lobes and in all parts of the calyx; circles: olfactory fibre projections of putative cholinergic neurons restricted to the calyx)

mushroom bodies has been recently reported [13]. There, pronounced immunoreactivity was demonstrated in the mushroom bodies in comparison to surrounding neuropile, and the glutamate-like immunostaining in the mushroom bodies could not be related to extrinsic elements.

With NADPH-diaporase histochemistry, widely used as indicator for NOS and NO, a selective strong staining of the mushroom bodies of the cricket was obtained, using different modes of fixation (Figs 4, 5, but s. *Drosophila* and other species [6]). In *Gryllus*, the somata of the KIII-neurons appear strongly stained (Fig. 4), whereas a distinct labeling of other Kenyon cell types was not consistently found.

Labeling of extrinsic neurons

GABA-like immunoreactivity in the mushroom bodies of *Gryllus* and *Drosophila* is clearly allocated to extrinsic neurons. In both species, these stained fibres project into all parts of the calyces, forming tiny bouton-like swellings. In the stalk and the lobes, GABA-like immunostaining is distributed in neuropile portions, with various degrees of staining intensity (Figs 1, 6–8). In the cricket, GABA-like immunoreac-

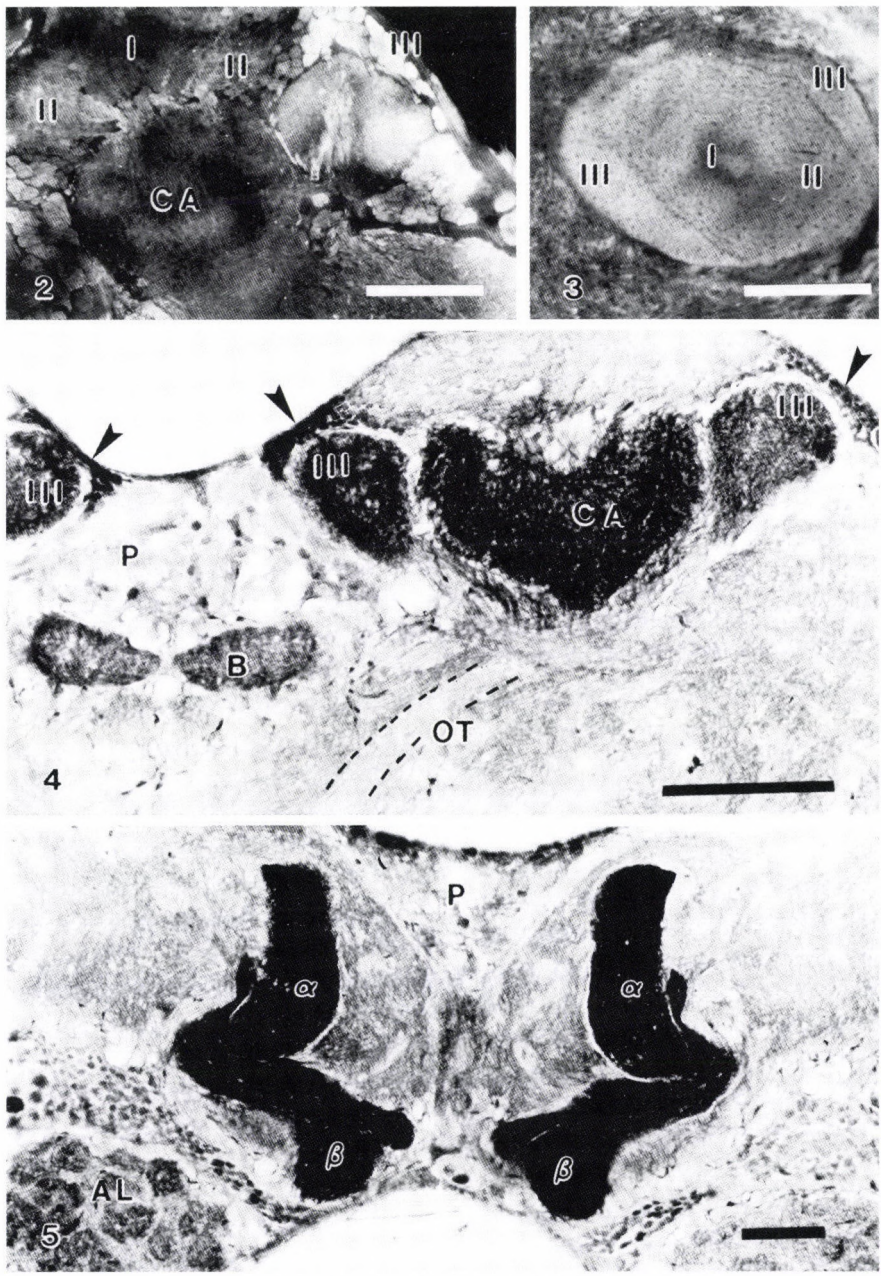

Figs 2–5. Labeling of Kenyon cells in *Gryllus bimaculatus*. 2, 3: Glutamate-like immunofluorescence. Differential staining of Kenyon cell somata (I–III) and of their fibre bundles in the cross-sectioned stalk, CA calyx. 4, 5: Strong NADPH-diaphorase staining of the mushroom body calyces, the α- and β-lobes, and in Kenyon cell type III somata neighbouring the posterior calyx (arrowheads). Note unstained massive tract (OT) of olfactory projection neurons; AL antennal lobe glomeruli, B bridge, P pars intercerebralis. Scale bars (2, 4): 100 μm, (3): 50 μm

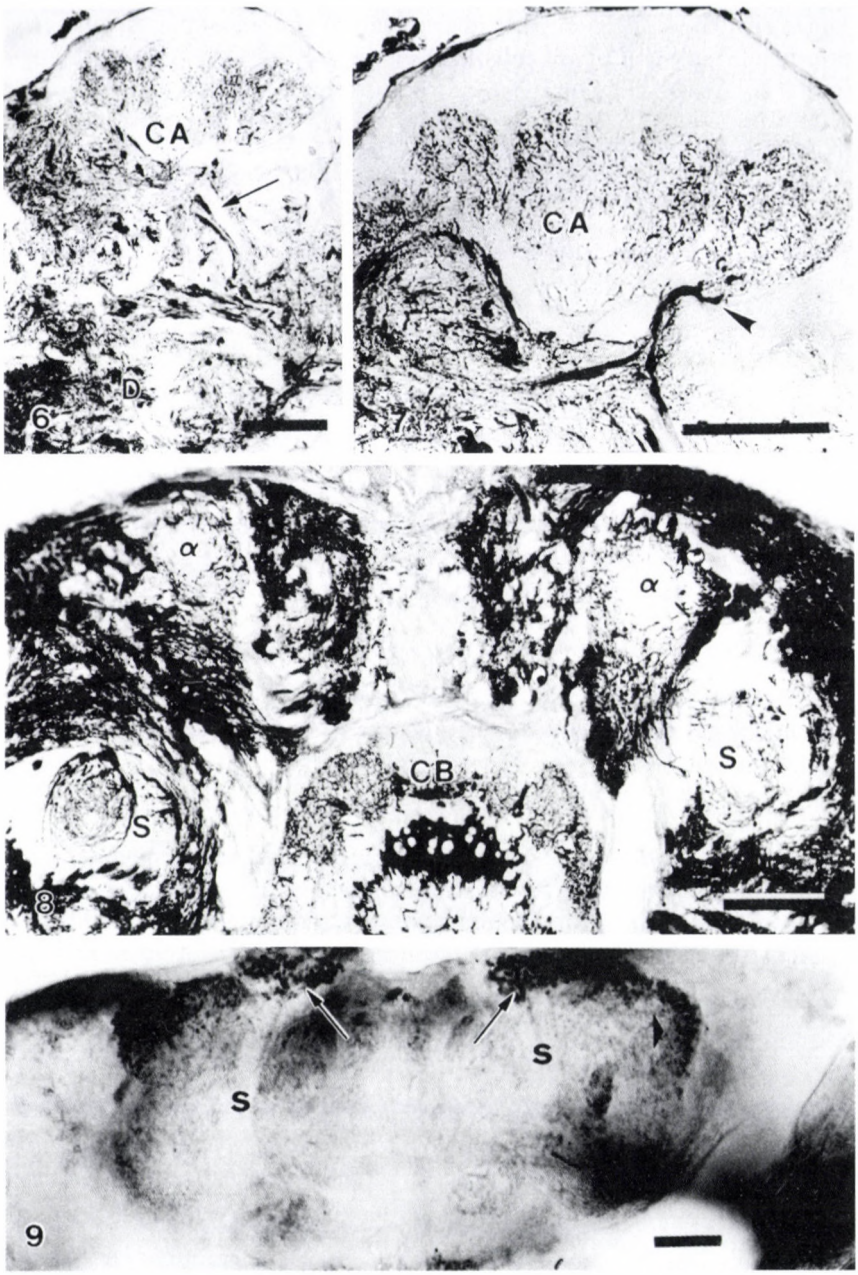

Figs 6–9. Labeling of extrinsic neurons in the mushroom bodies. 6–8: *Gryllus bimaculatus,* GABA-like immunostaining. In the calyces (CA), lobes, and in surrounding neuropile. Note unstained tract of olfactory projection neurons (arrow) connecting to the deutocerebrum (D). The immunoreactive fibre (arrowhead) arborizes in the calyces. The stalks (S) and α-lobes show immunoreactive fibres invading only portions of the neuropile; central body (CB). Scale bars 100 μm. 9: *Drosophila melanogaster;* ChAT-like immunostaining of olfactory projection neurons in the calyces (arrows) and in the lateral protocerebrum (triangles), S stalks. Scale bar 25 μm

tivity is distributed in different parts of the neuropilar compartments constituted by the fibre bundles of the Kenyon cells. The distribution of GABA-like immunoreactivity in the columnar stalk and lobes indicates further functional subdivisions in the Kenyon cell fibre bundles. In *Drosophila*, the GABA-like immunoreactivity in the lobes is also non-randomly distributed.

ChAT-like immunoreactivity taken as an indicator for acetylcholine in *Drosophila* is restricted to the calyces (Fig. 9). Confocal images of immunofluorescent whole mounts and semi-thin sections of peroxidase-antiperoxidase stained preparations show large boutons of the projection neurons of the inner antenno-cerebral tract, connecting the mushroom bodies with the antennal lobes. These projection neurons terminate in a large projection field in the lateral protocerebrum (lateral horn) [12, 15]. Stalk and most parts of the lobes lack substantial immunoreactivity compared to background staining. In the cricket, no ChAT-like immunostaining is detected with the antiserum against *Drosophila* ChAT. Acetylcholine-esterase histochemistry marks large parts of the cricket brain, with strong staining of the calyces, but no staining is present in the stalks and the lobes [5].

DISCUSSION

We address the discussion to (1) the putative transmitters in distinct sets of Kenyon cells and (2) the possible mode of synaptic interaction of intrinsic Kenyon cells and extrinsic, putatively GABAergic and cholinergic neurons, which encounter to close contact in the calyces.

The compartmental organization of the mushroom body neuropile has been seen previously in classical histological investigations [7]. The knowledge on discrete subdivisions of the mushroom bodies is reflected and substantially complemented by mapping the distribution of functional substances (transmitters) used in the synaptic transfer between neurons. From the glutamate-like staining in Kenyon cells, we tentatively suggest glutamate as a transmitter in these intrinsic neurons in both species studied. In the cricket, large portions of the Kenyon cells appear as strongly labeled as antennal motorneurons, which use glutamate as an excitatory transmitter [11]. As in crickets, prominent labeling of serveral brain neuropiles is found in the bee. In the corpora pedunculata of the bee, a subset of Kenyon cells shows faint glutamate-like immunoreactivity [2], not as prominent as in *Gryllus* and in *Drosophila* [11, 13]. Interestingly, Kenyon cells in *Gryllus* might employ NO as a colocalized transmitter. In this species, a population of Kenyon cells shows histochemically stained somata, and there is no evidence for this species that the NADPH diaphorase staining mainly occurs in extrinsic neurons as discussed for several other insect species [6]. The histochemical NADPH diaphorase staining used is a selective, but not a specific marker for NO-synthase distribution, which awaits further unequivocal demonstration by immunocytochemistry.

Chemical heterogeneity of Kenyon cell types has been shown previously [4, 9]. The differential glutamate-like staining of Kenyon cells in the cricket is consistent

with the distribution of the three classes of non-isomorphic Kenyon cells. This finding supports the view of functional differences between the Kenyon cell types, by no means investigated and understood from electrophysiological experiments.

Putative GABAergic extrinsic elements encountered in the calyx and in parts of the stalk and lobes [3, 4, 7] have been interpreted as feedback neurons, connecting the neuropilar compartments of the mushroom bodies [1]. The view of a GABAergic feedback input into the calyces is supported by immuno-electron microscopy [8]. However, the synaptic circuitry is too complex for a simplifying explanation based on light microscopical studies, and physiological investigations are lacking. ChAT-like immunoreactive projection neurons of the main antennal cerebral tract in *Drosophila* [12, 15] and acetylcholinesterase activities in the corresponding tract and neurons of the cricket brain [5] are interpreted as cholinergic neurons, the only elements serving for the direct transfer of olfactory information from the primary antennal lobe neuropile to the mushroom bodies. In crickets and in *Drosophila*, these putatively cholinergic projection neurons meet other (intrinsic and extrinsic) neurons in the calyces, the main site of inputs of different modalities [7]. In *Drosophila,* the frequent large presynaptic ChAT-like immunoreactive boutons in the calyx glomeruli are connected to tiny fibres, interpreted as Kenyon cell dendrites from immuno-electron microscopical studies [12]. GABAergic elements ranging among small presynaptic boutons are expected to be synaptically coupled with the Kenyon cell dendrites as well. Thus, from the present and previous studies a complex synaptic coupling of a single Kenyon cell, receiving both excitatory and inhibitory input, is proposed. This view, based on the distribution of the two classical transmitters acetylcholine and GABA in the calyces, extends the interpretation of synaptic coupling of intrinsic and extrinsic neurons in the main input sites, drawn previously from conventional electron microscopy [7]. However, this model remains incomplete in many details, because the calyces hold a number of extrinsic neurons containing biogenic amimes and neuropeptides [4], but with synaptic circuitry still undescribed.

ACKNOWLEDGEMENTS

Thanks are due to Dr. I. Meinertzhagen, Halifax, for discussion and for kindly providing laboratory support to FWS during a sabbatical visit, and to Mrs. M. Knierim and Mrs. M. Winkler, Göttingen, for excellent technical work. Supported by the DFG-SFB 406.

REFERENCES

1. Bicker, G., Schäfer, S., Kingan, T. G. (1985) Mushroom body feedback interneurons in the honeybee show GABA-like immunoreactivity. *Brain Res. 360,* 394–397.
2. Bicker, G., Schäfer, S., Ottersen, O. P., Storm-Mathisen, J. (1988) Glutamate-like immunoreactivity in identified neuronal populations of insect nervous systems. *J. Neurosci. 8,* 2108–2122.
3. Heisenberg, M. (1998) Special issue: Mushroom bodies. *Learning & Memory 5,* 1–190.
4. Homberg, U. (1994) Distribution of neurotransmitters in the insect brain. In: Rathmeyer W. (ed.) *Progress in Zoology.* Fischer Verlag, Stuttgart, pp. 1–88.

5. Lee, A. N., Metcalf, R. L., Booth, G. M. (1973) House cricket acetylcholine esterase: Histochemical localization and in situ inhibition by O,O-dimethyl S-aryl phosphothioates. *Ann. Entomol. Soc. Am. 66,* 333–343.
6. Müller, U. (1997) The nitric oxide system in insects. *Prog. Neurobiol. 51,* 363–381.
7. Schürmann, F.-W. (1987) The architecture of the mushroom bodies and related neuropiles in the insect brain. In: Gupta A. P. (ed.) *Arthropod Brain: Its Evolution, Development, Structure and Functions.* Wiley, New York, pp. 231–264.
8. Schürmann, F.-W., Elekes, K. (1987) Synaptic connectivity in the mushroom bodies of the honeybee brain: Electron microscopy and immunocytochemistry of neuroactive compounds. In: Menzel, R., Mercer, A. (eds) *Neurobiology and Behaviour in Honeybees.* Springer, Berlin, pp. 225–234.
9. Schürmann, F.-W., Erber, J. (1990) FMRFamid-like immunoreactivity in the brain of the honeybee *(Apis mellifera).* A light and electron microscopic study. *Neuroscience 38,* 797–807.
10. Schürmann, F.-W., Helle, J., Knierim-Grenzebach, M., Pauls, M., Spörhase-Eichmann, U. (1997) Identified neuronal cells and sensory neuropiles in the ventral nerve cord of an insect stained by NADPH-diaphorase histochemistry. *Zoology 100,* 98–109.
11. Schürmann, F.-W., Ottersen, O. P., Honegger, H.-W. (1999) Glutamate-like immunoreactivity marks compartments of the mushroom bodies in the brain of the cricket. *J. Comp. Neurol.* (in press).
12. Schürmann, F.-W., Meinertzhagen, I., Seyan, H., Yasuyama, K. (1999) Putative cholinergic neurons form the link between the mushroom bodies and antennal lobe olfactory neuropile in the *Drosophila* brain. In: Elsner, N., Eysel, U. (eds) *Göttingen Neurobiology Report,* Thieme, Stuttgart, vol. II, p. 620.
13. Sinakevitch-Pean, I., Plotnikova, S. I., Geffard, M., Bockaert, J., Grau, Y. (1998) Glutamate-like immunoreactivity in the adult brain Drosophila melanogaster. *Eur. J. Neurosc. 10,* 285.
14. Strausfeld, N. J., Hansen, L., Li, Y., Gomez, R. S., Ito, K. (1998) Evolution, discovery, and interpretations of arthropod mushroom bodies. *Learning & Memory 5,* 11–37.
15. Yasuyama, K., Kitamoto, T., Salvaterra, P. M. (1995) Immunocytochemical study of choline acetyltransferase in *Drosophila melanogaster:* An analysis of cis-regulatory regions controlling expression in the brain of cDNA-transformed flies. *J. Comp. Neurol. 361,* p. 25–37.

Acta Biologica Hungarica 51 (2–4), pp. 363–367 (2000)

SOCIAL AGGRESSIVENESS OF FEMALE AND SUBORDINATE MALE CRICKETS IS RELEASED BY OPIATE RECEPTOR ANTAGONIST+

VARYA DYAKONOVA[1,2]*, F.-W. SCHÜRMANN[1] and D. A. SAKHAROV[2]

[1]Institut für Zoologie und Anthropologie, Universität Göttingen, Germany and
[2]Institute of Developmental Biology, Russian Academy of Sciences, Moscow, Russia

(Received: August 31, 1999; accepted: November 30, 1999)

1. In the cricket *Gryllus bimaculatus,* effects of opiate receptor antagonist naloxone, 9 or 30 μg per animal, on aggressive behavior were investigated.
2. Naloxone had no significant impact on aggression of isolated and dominant males. In contrast, the drug caused a dramatic release of social aggression in female and subordinate male crickets.
3. The results suggest that activity of the opioid system contributes to suppress aggression in subordinate males, as well as in females, during social contacts.

Keywords: Aggressive behavior – endogenous opioid system – social status – insects – *Gryllus bimaculatus.*

INTRODUCTION

Aggressiveness is known to depend upon animal social status and to differ between sexes. A vast amount of information about neurochemical mechanisms underlying sex- and social rank-related differences in aggression concerns mammals. Little is known of how aggressiveness is regulated in invertebrate animals. Serotonin was found involved in control of aggression in crustaceans [3, 6], and octopamine in a model insect, the cricket [11]. In both instances, studies have been focused on male agonistic behavior. Much of the female aggressiveness and mechanisms of its regulation in invertebrates remains obscure.

In previous experiments on crickets, we found that drugs interfering with opiate receptors influenced social status and rank-related escape responses [4]. These findings indicated that the endogenous opioid system known to control aggressive behavior in vertebrate animals [7–9] might also participate in the regulation of social aggression in insects. The aim of the present work was to examine whether tonic activity of the endogenous opioid system contributes to the control of aggressiveness in crickets. We studied the effects of an opiate receptor antagonist, naloxone, on

+ Presented at the 9th ISIN Symposium on "Neurobiology of Invertebrates", July 1–5, 1999, Tihany, Hungary.

*Corresponding author, E-mail: compar@cityline.ru

0236-5383/2000/$ 5.00

social aggression in both males and females. Additional attention was directed to males differing in their social experience, specifically, to fight winners, fight losers, and specimens taken from isolation.

MATERIALS AND METHODS

Crickets (*Gryllus bimaculatus*) two weeks after imaginal moult were taken from a breeding colony (28 °C, 12 h–12 h light-dark cycle) and isolated for at least 12 hours prior to an experiment. Solution of the drug, naloxone hydrochloride (Sigma), or vehicle (ringer for crickets), 50 μl, was injected into the abdominal cavity. In three hours after injection, control and experimental pairs of matched in size and weight crickets (±20 mg) were placed in a transparent plastic container with movable opaque wall in the middle. After short adaptation (10–15 min), the wall was removed and crickets were allowed to meet.

The cricket fight develops in a stepwise manner. According to [1, 2, 10], the following 6 steps (fight levels) can be distinguished: **0.** no interaction; **1.** pre-established dominance; **2.** bilateral antennal fencing; **3.** unilateral mandible spreading (by one animal in a pair); **4.** bilateral mandible spreading (by the two animals); **5.** mandible engagement; **6.** physical combat. We evaluated (i) the level of fight at which dominant-subordinate relationships were established, (ii) total duration of fight. After the establishment of social rank, we recorded for 1 min the following parameters of the winner (dominant) behavior: (i) rival song duration, (ii) time of chasing, (iii) number of attacks, and (iv) number of mandible spreadings. After 1st interaction, crickets were separated for 15 min and then combined again, and loser behavior (fight or escape) was analyzed.

The aggression of paired females (number, level and duration of fights, if any) was similarly evaluated for 3 min since the beginning of contact.

There were two experimental male groups, one treated with 9 μg naloxone, the another with 30 μg naloxone, and one female group treated with 9 μg naloxone (62 pairs altogether). Each experimental group had a respective control (50 pairs altogether).

For quantitative temporal analysis the ongoing behavior was directly observed or video-taped. Data was analyzed with a use of RTIME software [5]. Significance of differences between experimental groups and their respective controls was tested by Student's *t*-test, or Wilcoxon test, or Fisher's exact test.

RESULTS

First interaction, previously isolated males

No significant difference in the intensity of fight was seen between controls, on the one hand, and experimental pairs treated with 9 or 30 μg naloxone, on the other. The median level of fight was 5 in all groups. Slight insignificant decrease in the per-

centage of contact fights (levels 5 and 6) was seen in crickets received 30 μg naloxone (52% in comparison with 64% in the control). Total duration of fight was significantly shorter in the group treated with 30 μg naloxone (6.127±1.263 sec, compare to 9.0 ± 1.2 sec in the control, $p < 0.05$), while in crickets received 9 μg, it was insignificantly changed (8.1 ± 1.3 sec).

Postfight behavior, winners

No significant difference in parameters characterizing dominant behavior was found between control and naloxone-treated crickets. Duration of rival songs averaged 9.0 ± 3.1 sec at 9 μg naloxone; 13.7 ± 1.3 sec at 30 μg naloxone; 11.0 ± 2.3 sec and 10.7 ± 2.7 sec in related controls. Duration of chasing was 8.8 ± 2.5 sec; 9.8 ± 1.7 sec in the naloxone groups, and 10.3 ± 1.1 sec and 12.2 ± 2.1 sec, in the controls. Similarly, there were no difference in the performance of open mandibles between control and naloxone groups, median number of attacks with mandible spreading was 2 in all groups with lower and upper quartiles 1 and 3, respectively.

Second interaction, losers

In the second interaction test, 41% of losers treated with 9 μg naloxone and 61% with 30 μg naloxone, in contrast to 19% of the control group ($p < 0.05$ and <0.001, respectively), showed the renewed willingness to fight with their respective dominants (Fig. 1A). The median level of the second fight in both naloxone groups reached 4, whereas in controls it was only 1. This difference was statistically significant, $p < 0.01$). In accord with increased intensity of fight, the mean duration of the second fight was higher in naloxone groups: 4.9 ± 0.8 sec and 5.9 ± 1.9 sec versus 1.4 ± 0.6 sec in the control, $p < 0.001$ (Fig. 1B).

Females

Females placed together on a limited territory also tend to determine which animal is dominant and which is subordinate. However, in comparison to males, females use to establish rank at lower levels of fighting [1]. Higher level fights (levels 3 through 6) were seen in ca. 30% female pairs only, whereas in males in ca 90%.

Naloxone increased markedly the number, intensity and duration of female fights. In 93% of naloxone-treated pairs, fight escalated beyond the level 3 (Fig. 1B). Correspondingly, the median level of fight was 3 in the naloxone group, and 1 in control, $p < 0.005$; the respective mean duration of fight averaged 5.2 ± 1.0 sec and 1.7 ± 0.6 sec, $p < 0.01$.

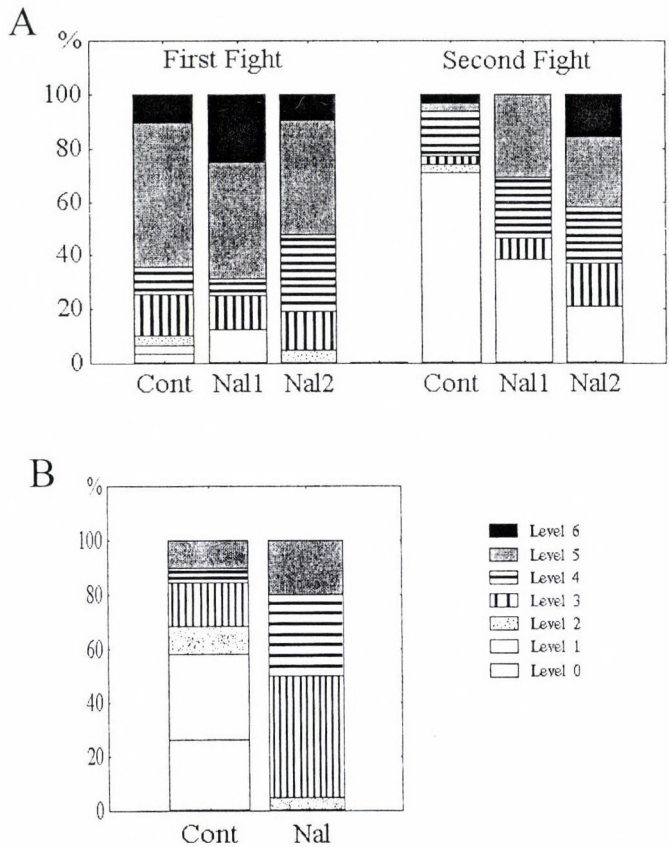

Fig. 1. Effects of naloxone on level of aggression in male (A) and female crickets (B). First Fight, initial fight in pairs of isolated, socially naive, male crickets; Second Fight, fight in the same pairs in 15 min after the 1st interaction. Crickets were injected prior to the initial fight with ringer (Cont), 9 μg naloxone (Nal1) or 30 μg naloxone (Nal_2). Level 0: no interaction; level 1: pre-established dominance; level 2: bilateral antennal fencing; level 3: unilateral mandible spreading; level 4: bilateral mandible spreading; level 5: mandible engagement; level 6: physical combat (level evaluation according to Stevenson et al. [10])

CONCLUSION

Our results provide an evidence for involvement of the endogenous opioid system into the control of aggressive state of male and female crickets. We found that the opiate antagonist naloxone caused a release of social aggression in subordinate male crickets and in females. In contrast, aggressiveness of isolated and dominant males was not potentiated by the drug. We presume that, in females and subordinate males, aggression is maintained at a low level due to activation of the endogenous opioid system. Lack of potentiating action of naloxone on well-expressed aggression of iso-

lated and dominant males may indicate that their opiate targets related to the control of aggression are not occupied by endogenous ligands.

The results thus confirm our previous reports [4] that opioid status defines social rank-related differences between male crickets. These opioid-related differences are now extended to male aggressiveness. Furthermore, the results suggest that a similar mechanism may underlay sex-related differences in social aggression of insects. It may be concluded that a linkage of the opioid system to the aggressive behavior is well represented in invertebrates indicating that it could appear early in animal evolution.

ACKNOWLEDGEMENTS

We thank Dr. H. Gras for offering his computer programs for behavioral experiments and data analysis. We are grateful to Prof. R. Hustert for generously allowing us to use the videoequipment of his department. The work was supported by grants from DAAD-NATO (1998) and IR-97-0798.

REFERENCES

1. Adamo, S. A., Hoy, R. R. (1995) Agonistic behaviour in male and female field crickets, *Gryllus bimaculatus,* and how behavioural context influences its expression. *Animal. Behav. 49,* 1491–1501.
2. Alexander, R. D. (1961) Aggressiveness, territoriality, and sexual behavior in field crickets (Orthoptera: Gryllidae). *Behavior 17,* 130–223.
3. Antonsen, B. L., Paul, D. H. (1997) Serotonin and octopamine elicit stereotypical agonistic behaviors in the squat lobster *Munida quardrispina* (Anomura, Galatheidae). *J. Comp. Physiol. A 181,* 501–510.
4. Dyakonova, V. E., Sakharov, D. A., Schürmann, F.-W. (1999) Effects of serotonergic and opioidergic drugs on escape behavior and social status of male crickets. *Naturwissenschaften 86,* 435–437.
5. Gras, H., Hackenberg, K. (1992) RTIME: a program for time-series measurements and evaluation in electrophysiology with the AT-PC. *Comput. Meth. Prog. Biomed. 37,* 31–39.
6. Huber, R., Delago, A. (1998) Serotonin alters decisions to withdraw in fighting crayfish, *Astacus astacus:* the motivational concept revisited. *J. Comp. Physiol. A 182,* 573–583.
7. Konig, M., Zimmer, A. M., Steiner, H., Holmes, P. V., Crawley, J. N., Brownstein, M. J., Zimmer, A. (1996) Pain responses, anxiety and aggression in mice deficient in pre-proenkephalin. *Nature 383,* 535–538.
8. Lynch, W. C., Libby L., Johnson, H. F. (1983) Naloxone inhibits intermale aggression in isolated mice. *Psychopharmacology-Berlin. 79,* 370–371.
9. Panksepp, J., Herman, B. H., Vilberg, T., Bishop, P., DeEskinazi, F. G. (1980) Endogenous opioids and social behavior. *Neurosci. Biobehav. Rev. 4,* 473–487.
10. Stevenson, P. A., Hofmann, H., Schoch, K., Schildberger, K. (2000) The fight and flight responses of crickets depleted of biogenic amines. *J. Neurobiol.* (in press)
11. Stevenson, P. A., Dyakonova, V., Schildberger, K. (1999) The octopamine agonist chlordimeform and the aggressive behaviour of the cricket. In: Elsner, N., Eysel, U. (eds) Proc. 27th Göttingen Neurobiol. Conf., Georg Thieme Verlag, Stuttgarg, New York, p. 670.

Acta Biologica Hungarica 51 (2–4), pp. 369–377 (2000)

POTENCIES OF NATURALLY-OCCURRING AKH/RPCH PEPTIDES IN *LOCUSTA MIGRATORIA* IN THE ACETATE UPTAKE ASSAY *IN VITRO* AND COMPARISON WITH THEIR POTENCIES IN THE LIPID MOBILISATION ASSAY *IN VIVO*[+]

G. GÄDE[1]*, M. J. LEE[2]**, G. J. GOLDSWORTHY[2] and R. KELLNER[3]

[1]Zoology Department, University of Cape Town, Rondebosch 7701, South Africa
[2]Biology Department, Birkbeck College, London WC1E 7HX, United Kingdom
[3]Merck KGaA, Biomed Fo/GBT, Darmstadt, Germany

(Received: August 31, 1999; accepted: November 30, 1999)

The biological potencies of a number of naturally-occurring octa- and decapeptides of the large AKH/RPCH family of peptides were determined in *Locusta migratoria* using the lipid-mobilising assay *in vivo* and the acetate uptake assay *in vitro*. The most potent of the newly-tested peptides in the *in vitro* assay, Phl-CC, differs from the endogenous major locust peptide, Lom-AKH-I, only by an exchange of serine versus threonine at position 10. However, the most active peptide in the *in vitro* assay remains Lom-AKH-III. At the other extreme is the peptide Mem-CC which contains a tyrosine residue at position 4 rather than the more typical phenylalanine. This peptide is over 20 000 times less potent than Lom-AKH-III in the *in vitro* assay, and also results in an unusual dose-response curve in the *in vivo* assay. Only a few peptides are approximately equipotent in both assays, but mostly the bioanalogues have a higher potency *in vitro*. The majority of them are 2- to 10-fold more potent *in vitro*, but Ani-AKH and Lom-AKH-III are 19- and 48-fold more potent. The results are discussed in relation to either the actions of proteases or of possible preferential binding of different receptors involved in the different assays.

Keywords: Locusta migratoria – acetate uptake assay – lipid mobilisation – AKH/RPCH peptides – receptor interaction.

INTRODUCTION

Peptides of the AKH/RPCH family have been found in all insect or crustacean species which have been investigated. They are pleiotropic with various well-described actions, mostly catabolic, or glucacon-like in nature [6, 9] although they are not thought to have any sequence homology to this mammalian hormone [8]. Their best-known actions in insects include hypertrehalosaemia, hyperlipaemia and hyperprolinaemia [5].

In addition to their ubiquity and pleiotropy, there are also a wide variety of homologous structures (over thirty), which have been found in the arthropod species that have

[+] Presented at the 9th ISIN Symposium on "Neurobiology of Invertebrates", July 1–5, 1999, Tihany, Hungary.

*Corresponding author, E-mail: ggade@botzoo.uct.ac.za
**Present address: Foods Research, Unilever Research, 3133AT Vlaardingen, The Netherlands.

0236-5383/2000/$ 5.00

been investigated over the last twenty-three years. The elucidation of all these different structures has been motivated by an attempt to determine potential evolutionary pathways for these peptides, and suggest a possible candidate for the ancestral adipokinetic hormone [3, 7]. To date, a number of arthropod families have been investigated for members of the AKH/RPCH family, and for unknown reasons, there is more variation in their structure within certain insect orders (such as Caelifera) than others (such as Ensifera and Odonata) and in Crustacea. There are no established reasons why this is so, nor is it known why certain individual species should contain more than one AKH variant. It can only be tentatively suggested that multi-variants exist in order to fulfil different physiological roles within the insect during its development.

In addition to providing information about the possible ancestral variant, investigations into the adipokinetic group of peptides clearly demonstrate which residues are most subject to natural variation. It is clear that positions 1, 4, 5, 8, and in nona- and decapeptides, position 9 are quite highly conserved (see Fig. 1 in [14]), whilst position 2, 3, 6, 7 and 10 are relatively variable [14]. These studies have also demonstrated the necessity for blocked termini, with pyroglutamate at the N-terminus and an amidated C-terminus.

One of the model insect species for investigating the actions of AKHs is *Locusta migratoria*. Using this insect, a vast body of information is available on the classical adipokinetic response as well as on other physiological actions of AKHs, such as activation of glycogen phosphorylase, inhibition of protein synthesis, lipid synthesis and uridine incorporation into RNA [9]. However, information regarding the AKH receptors in insects is very patchy [19]. Some authors, however, have attempted to define receptor requirements of locusts by measuring the two major biological responses, lipid mobilisation *in vivo* and acetate uptake *in vitro* [6, 14]. The present paper examines the potencies of a number of recently discovered bioanalogues of the AKH/RPCH family in the acetate uptake assay *in vitro* and compares the results with those achieved for the lipid mobilisation assay *in vivo* [2, 4]. We then compare the present data on potencies with that for existing ones from previous studies and hypothesize as to why two different biological assays should vary in their sensitivity to the various structures of neuropeptides from the AKH/RPCH family.

MATERIALS AND METHODS

Migratory locusts, *Locusta migratoria*, were reared as outlined elsewhere [15], and adult female locusts between day 2 and 7 after the imaginal moult were used for the acetate uptake assay *in vitro* as described previously [11, 12]. For the *in vivo* lipid mobilisation assay adult male locusts at least 14 days after the imaginal moult were used [2, 4]. In both assays a full dose response curve was obtained for each peptide.

The peptides used in this study were synthesised by standard solid phase chemistry, purified on reversed-phase liquid chromatography, and their identity verified by sequence determination (via Edman degradation technique) and by matrix-assisted laser desorption/ionisation mass spectrometry.

RESULTS

Table 1 lists the name [18] and primary structure of the peptides used in the present study and reports the calculated EC_{50} values of the *in vitro* assay and the ED_{50} values obtained in the *in vivo* assay measuring lipid mobilisation [2, 4]. Moreover, the ratio between the ED_{50} and EC_{50} values is given; since the blood volume of the locusts is assumed as 300 µl, a ratio of 1.0 indicates the same potency of a given peptide in each assay. For comparative reasons (see Results and Discussion), data of previous studies on potencies of bioanalogues are given as well in Table 1.

Some typical concentration-potency curves for a few representative peptides *in vitro* are shown in Fig. 1 and compared with Lom-AKH-I and Lom-AKH-III.

Overall, it is clear from Table 1 that none of the peptides investigated here is more potent in the acetate uptake assay than Lom-AKH-III. The pyrgomorphid decapeptide Phl-CC is structurally very similar to Lom-AKH-I, and unsurprisingly therefore, quite similar in potency. However, the other pyrgomorphid peptide, Phm-AKH, is considerably less active, although it closely resembles Phl-CC and Lom-AKH-I. The other decapeptide tested, Del-CC from blister beetles, is fairly potent, but the cicada peptide Plc-HrTH is not. This latter peptide, however, is also the least potent in the series of decapeptides tested here for its lipid mobilising action. Comparing the ED_{50}/EC_{50} ratios of the decapeptides, only two, Phm-AKH and the blaberid Bld-HrTH are approximately equipotent in both assays; the other decapeptides are mostly between 3- and 10-fold more potent *in vitro*, with the exception of the horse fly's

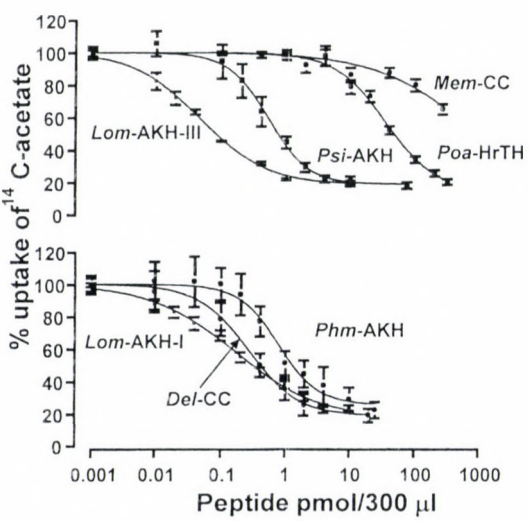

Fig. 1. The potencies of selected naturally-occurring octapeptides (upper panel) and decapeptides (lower panel) of the AKH/RPCH family in the acetate uptake assay *in vitro*

Table 1

Sequences and experimental activities of AKH analogues in the acetate uptake assay *in vitro* and the lipid mobilisation assay *in vivo*. All peptides are blocked at both termini

Name	Sequence	*In vitro* EC_{50} (pmol/300 µl)	*In vivo* ED_{50} (pmol)	Ratio
Decapeptides				
Lom-AKH-I	pQLNFTPNWGT	0.21[a]	0.7[a]	3.3
Phl-CC	pQLTFTPNWGS	0.22*	2.2[b]	10
Taa-HoTH	pQLTFTPGWGY	0.28[a]	24.8[c]	89
Cam-HrTH-II	pQLTFTPNWGT	0.31[a]	2.0[a]	6.5
Rom-CCI	pQVNFTPNWGT	0.38[a]	2.0[a]	5.3
Del-CC	pQLNFSPNWGN	0.78*	6.5[b]	8.3
Phm-AKH	pQLNFTPNWGS	1.41*	1.0[b]	0.71
Bld-HrTH	pQVNFSPGWGT	3.6[d]	3.8[d]	1.1
Hez-HrTH	pQLTFSSGWGN	5.75[a]	60.8[c]	10
Plc-HrTH-II	pQVNFSPSWGN	6.29*	23.5[b]	3.7
Nonapeptide				
Mas-AKH	pQLTFTSSWG	6.80[a]	10.0[a]	1.5
Octapeptides				
Lom-AKH-III	pQLNFTPWW	0.04[a]	1.9[a]	48
Grb-AKH	pQVNFSTGW	0.30[a]	1.0[a]	3.3
Lom-AKH-II	pQLNFSAGW	0.46[a]	6.5[a]	14
Pab-RPCH	pQLNFSPGW	0.48[a]	4.6[a]	9.6
Psi-AKH	pQVNFTPGW	0.49*	1.5[b]	3.1
Scg-AKH-II	pQLNFSTGW	0.76a	2.0[a]	2.6
Ani-AKH	pQVNFSPSW	0.93*	17.5[b]	19
Ers-AKH	pQLNFTPSW	1.05*	6.5[c]	6.2
Pea-CAH-II	pQLTFTPNW	1.06[a]	5.0[a]	4.7
PeaCAH-I	pQVNFSPNW	1.55[a]	5.0[a]	3.2
Lia-AKH	pQVNFTPSW	1.76*	8.6[c]	4.9
Emp-AKH	pQVNFTPNW	2.22*	5.0[c]	2.3
Tem-HrTH	pQLNFSPNW	2.90*	6.8[c]	2.3
Taa-AKH	pQLTFTPGW	–	8.4[b]	–
Miv-CC	pQINFTPNW	7.48*	16.0[b]	2.1
Pht-HrTH	pQLTFSPDW	9.88*	–	–
Asn^7-Pht-HrTH	pQLTFSPNW	15.5*	39.5[c]	2.5
Ona-CC	pQYNFSTGW	16.4*	17.5[b]	1.1
Poa-HrTH	pQITFTPNW	34.9*	162.0[c]	4.6
Asn^7-Mem-CC	pQLNYSPNW	358.0*	203.0[c]	0.6
Mem-CC	pQLNYSPDW	920.0*	atypical	–

Peptides are given in order of length and then in order according to potency in the *in vitro* assay. Data are either from present study* or taken from published data: [11][a] [4][b] [2][c], [10][d] and Gäde, unpublished[e]. The symbol "–" indicates that the potency has not been determined.

Taa-HoTH, which is very much more potent in the *in vitro* assay than in the *in vivo* assay.

There are vast difference in potencies in the *in vitro* assay between the tested octapeptides. Four peptides, originating from odonate species, Psi-AKH, Ani-AKH, Ers-AKH and Lia-AKH (in order of decreasing potency) as well as the mantid and tenebrionid peptides (Emp-AKH and Tem-HrTH), are about 12- to 73-fold less active than the octapeptide Lom-AKH-III. The termite peptide Miv-CC, the blowfly peptide Pht-HrTH and its analogue as well as the beetle peptide Ona-CC and the cockroach peptide Poa-HrTH are intermediately potent (between 100- and 1000-fold less than Lom-AKH-III). The beetle peptide Mem-CC and its analogue exhibit very little activity in this assay and are 23 000- and 9 000-fold less potent than Lom-AKH-III. In general, the peptides from the intermediary and very low potency groups are also the ones with the lowest potencies in the *in vivo* assay. Interestingly, the ED_{50}/EC_{50} ratio for the Mem-CC analogue is below one and it is approximately 1 for Ona-CC. The majority of the remaining octapeptides are 2- to 10-fold more potent *in vitro*, but Ani-AKH and Lom-AKH-III are 19- and 48-fold more potent.

DISCUSSION

First, we look at the *in vitro* data only, and compare the results with previously achieved ones. Second, we take the relative potencies in the two different assays into account and ask why the relative potencies of the different assays vary. Finally, we highlight some of the outstanding and urgently awaited studies concerning the adipokinetic hormones in locusts.

Examination of the *in vitro* data reveals some interesting details in both the decapeptides and octapeptides. These are discussed separately below.

Decapeptides

Four peptides are structurally very similar: Lom-AKH-I, Phl-CC, Phm-AKH and the stick insect peptide Cam-HrTH-II. In fact, Cam-HrTH-II and Lom-AKH-I differ only in an Asn to Thr exchange at position 3, and Phm-AKH and Phl-CC are the respective counterparts containing both Ser at position 10 instead of Thr. One would have expected that the biological potencies *in vitro* are very similar as shown for the *in vivo* response (see Table 1) [2, 4]. This is true for the Asn^3 to Thr^3 exchange [11]. The conservative exchange at position 10 of one neutral amino acid with a hydroxylated side chain, namely Thr, with another one, namely Ser, does also not affect potency when Cam-HrTH-II and Phl-CC are compared. The lower potency of Phm-AKH could be speculatively explained, by default, by some sort of interaction of the Asn residue at position 3 with Ser at position 10. An alternative explanation is a gross experimental error.

Overall, the exchange at position 5, again from Thr to Ser, as in Del-CC and at the same time at position 10 to Asn, does slightly affect potency. Conversely, when another Ser residue was introduced at position 7, potency was quite low as in Plc-HrTH. Other naturally – occurring decapeptides previously [11] had Gly at position 7 (the lepidopteran peptide Hez-HrTH and the blaberid peptide Bld-HrTH) which seemed to be responsible for their low potencies. Since this position 7 is an integral part of the proposed beta-turn [1, 20], the small Gly residue may not constrain the molecule sufficiently.

Octapeptides

The majority of the naturally – occurring octapeptides tested are only up to 100-fold less potent than Lom-AKH-III. Even within this broad range, it is not clear what specific interactions cause changes in potency. However, it becomes more obvious for peptides in the range 100- to 1000-fold less potent than Lom-AKH-III. Specifically, the residues Ile or Tyr at position 2 are not tolerated well by the receptor. This is especially apparent when the following comparisons are made: Miv-CC (Ile^2) is more than 3-times less potent than its counterpart Emp-AKH (Val^2). Similarly , Poa-HrTH (Ile^2) is even 32-times less potent than Pea-CAH-II (Leu^2; 11). The same is true for Ona-CC (Tyr^2) and its partner Scg-AKH-II (Leu^2) which results in a 20-fold loss of potency [11]. The Leu/Val to Ile exchange is rather conservative, and loss in activity *in vivo* has been explained "by the fact that the branched side chain of Ile apparently restricts conformational freedom necessary for good receptor interaction" [4]. The change from Leu^2 to Tyr^2 is more dramatic. Here, a non-aromatic amino acid with hydrophobic side chain is replaced by an aromatic one with a hydrophilic side chain. Another possible trend is that the combination of Thr^3 and Ser^5, as in Asn^7 – Pht-HrTH, is not well tolerated, since the molecule Pea-CAH-II (Thr^3 and Thr^5) is 140-times more potent [11]. A negatively charged form of the former peptide, Pht-HrTH, was actually somewhat more potent than the neutral form. The reverse was true in Mem-CC, but this compound is very difficult to compare due to its exceptionally low potency *in vitro* and peculiar behaviour *in vivo*. It appears that Tyr, which is typically Phe in all other AKH members, interferes in some way with the optimal interaction of the hormone with the locust receptor.

Relative potencies in the two assays

Why should the relative potencies of the different assays vary? The assay *in vitro* is generally more sensitive to the peptides than the assay *in vivo* (9.4 ± 3.3; although the perhaps more representative median value is just 3.7). This value is certainly not constant amongst the different peptides as has been mentioned above; there is a wide range of sensitivity ratios between 0.7 and 89 of the natural peptides tested here. Although this ratio is rarely less than 1.0, it can be much higher; an analogue

described previously was over 700 times more potent in the acetate uptake assay *in vitro* than the lipid mobilisation assay *in vivo* [10].

There are two obvious possible explanations for this difference in potencies. The first is that there are two receptors involved in the two assays that have different preferences for the different peptides. This might be expected as the fat body is most sensitive to the actions of adipokinetic hormones *in vitro* when obtained from adult locusts which are less than about a week old, whereas the AKHs have the greatest lipid mobilisation effects *in vivo* in adults which are 2–3 weeks old. This hypothesis would explain such large variations in peptide potencies between the assays. An alternative one, which does not necessarily conflict with the previous one (i.e. the two are not mutually exclusive) is that the peptides are differentially hydrolysed or absorbed *in vivo*, and this takes place with sufficient rapidity that it affects the measured potency of the peptides. Of the three *Locusta* peptides, Lom-AKH-III is known to be far more susceptible to inactivation *in vivo* [16], or by bovine chymotrypsin *in vitro* [12] than either Lom-AKH-I or -II. A third contributor to the observed variation in potency ratios is experimental error in one or both of the estimations of potency. At this point we do not consider this to be the dominant factor which would explain the variation in peptide potency across the bulk of the peptides investigated, although it cannot be discounted at the level of an individual peptide.

In view of the apparently very different potencies in the two assays, is it possible to come to any general conclusions about the differences for each assay for particular AKH structures? It has been noted previously that the acetate uptake assay has a relatively higher preference for hydrophobic peptides than the *in vivo* lipid mobilisation assay, as indicated by a high ratio [11, 12]. This was readily observable for the AKHs containing two tryptophan residues [13], and for peptides with hydrophobic additions to the hydroxyl moeity of one or both of the threonine residues on the AKHs [15, 17]. The two peptides with the highest ratio in Table 1 are both quite hydrophobic: Lom-AKH-III and Taa-HoTH both have a structure containing an aromatic amino acid residue substitution, and are tolerated better in the acetate uptake assay compared with the lipid mobilisation assay. No straightforward conclusions appear possible with those peptides that are more potent *in vivo* than *in vitro*.

Future studies

The present study has contributed for a somewhat better understanding of potency patterns in the two bioassays. A number of questions have remained outstanding for some time. One of the most pressing of these is information relating to the receptors in *Locusta*. We urgently need to know whether there are specific receptors for each of the three Lom-AKHs and what their primary and tertiary structures and their localisation are. Moreover, do the receptors vary during the development of the locust or are they identical at any one time and only change in the different phases, solitary or gregarious, of the insect? Molecular biological techniques rather than protein chemical ones will need to be utilised to answer these questions during the next decade.

ACKNOWLEDGEMENTS

Work described here was partially financially supported by the Foundation for Research Development (Pretoria, South Africa; GG), University of Cape Town staff award (GG), Volkswagen Foundation (Hannover, Germany; GG and RK), SERC Invertebrate Neuroscience Initiative (GJG) and the BBSRC (GJG).

REFERENCES

1. Cusinato, O., Drake, A. F., Gäde, G., Goldsworthy, G. J. (1998) The molecular conformations of representative arthropod adipokinetic peptides determined by circular dichroism spectroscopy. *Insect Biochem. Molec. Biol. 28,* 43–50.
2. Gäde, G. (1993) Structure-activity-relationships for the lipid-mobilizing action of further bioanalogues of the adipokinetic hormone red pigment-concentrating hormone family of peptides. *J. Insect Physiol. 39,* 375–383.
3. Gäde, G. (1996) The revolution in insect neuropeptides illustrated by the adipokinetic hormone/red pigment-concentrating hormone family of peptides. *Z. Naturforsch. 51c,* 607–617.
4. Gäde, G. (1997) Sequences of recently identified adipokinetic peptides: what do they tell us with respect to their hyperlipaemic activity in migratory locusts? *Invertebr. Neurosci. 3,* 217–222.
5. Gäde, G., Auerswald, L. (1998) Insect neuropeptides regulating substrate mobilisation. *S. Afr. J. Zool. 33,* 65–70.
6. Gäde, G., Hoffmann, K.-H., Spring, J. H. (1997) Hormonal regulation in insects: facts, gaps, and future directions. *Physiol. Rev. 77,* 963–1032.
7. Gäde, G., Reynolds, S. E., Beeching, J. R. (1994) Molecular evolution of peptides of the AKH-RPCH family. In: Davey, K. G., Peter, R. E., Tobe, S. S. (eds), *Perspectives in Comparative Endocrinology.* National Research Council of Canada, Ottawa, pp. 119–128.
8. Goldsworthy, G. J. (1994) The adipokinetic hormones of insects: are they the insect glucagons? In: Davey, K. G., Peter, R. E., Tobe, S. S. (eds). *Perspectives in Comparative Endocrinology.* National Research Council of Canada, Ottawa, pp. 486–492.
9. Goldsworthy, G. J., Lee, M. J., Luswata, R., Drake, A., Hyde, D. (1997) Structures, actions and receptors for locust adipokinetic hormones. *Comp. Biochem. Physiol. 117B,* 483–496.
10. Lee, M. J., Cusinato, O., Luswata, R., Wheeler, C. H., Goldsworthy, G. J. (1997) N-terminal modifications to AKH-I from *Locusta migratoria* and their effects on activity. *Regulatory Peptides 69,* 69–76.
11. Lee, M. J., Goldsworthy, G. J. (1995) Acetate uptake assay; the basis of a rapid method for determining potencies of adipokinetic peptides for structure-activity studies. *J. Insect Physiol. 41,* 163–170.
12. Lee, M. J., Goldsworthy, G. J. (1995) The preparation and use of dispersed cells from fat body of *Locusta migratoria* in a filtration plate assay for adipokinetic peptides. *Anal. Biochem. 228,* 155–161.
13. Lee, M. J., Goldsworthy, G. J. (1996) Modified adipokinetic peptides containing two tryptophan residues and their activities *in vitro* and *in vivo* in *Locusta. J. Comp. Physiol. 166B,* 61–67.
14. Lee, M. J., Goldsworthy, G. J. (1998) New perspectives on the structures, assays and actions of locust adipokinetic hormones. In: Coast, G. M., Webster, S. M. (eds), *Arthropod Endocrinology – Perspectives and Recent Advances.* The Society for Experimental Biology Seminar Series, Cambridge University Press, Cambridge. pp. 149–171.
15. Lee, M. J., Goldsworthy, G. J., Poulos, C., Velentza, A. (1996) Synthesis and biological activity of adipokinetic hormone analogues modified at the C-terminus. *Peptides 17,* 1285–1290.
16. Oudejans, R. C. H. M., Vroemen, S. V., Jansen, R. F. R., van der Horst, D. J. (1996) Locust adipokinetic hormones: carrier-independent transport and differential inactivation at physiological concentrations during rest and flight. *Proc. Natl. Acad. Sci. USA 93,* 8654–8659.

17. Poulos, C., Karagiannis, K., Lee, M., Goldsworthy, G. (1994) Synthesis and biological activity of locust AKH-I and its analogues with modifications at the threonine residues. *Int. J. Peptide Protein Res. 44,* 589–593.
18. Raina, A. K., Gäde, G. (1988) Insect peptide nomenclature. *Insect Biochem. 18,* 785–787.
19. Ziegler, R., Jasensky, R., Morimoto, H. (1995) Characterization of the adipokinetic hormone receptor from the fat body of *Manduca sexta. Regul. Peptides 57,* 329–338.
20. Zubrzycki, I. Z., Gäde, G. (1994) Conformational study on an insect neuropeptide of the AKH/RPCH family by combined ^{1}H-NMR spectroscopy and molecular mechanics. *Biochem. Biophys. Res. Comm. 198,* 228–235.

Acta Biologica Hungarica 51 (2–4), pp. 379–394 (2000)

PHYSIOLOGICAL AND PHARMACOLOGICAL STUDIES ON NEMATODES+

R. J. WALKER,* C. J. FRANKS, D. PEMBERTON, CANDIDA ROGERS and LINDY HOLDEN-DYE

School of Biological Sciences, University of Southampton, Southampton, SO16 7PX, UK

(Received: August 31, 1999; accepted: November 30, 1999)

Classical transmitters and neuroactive peptides act as transmitters or modulators within the central and peripheral nervous systems of nematodes, for example *Ascaris suum* and *Caenorhabditis elegans*. Acetylcholine (ACh) and gamma-aminobutyric acid (GABA) are respectively the excitatory and inhibitory transmitters onto somatic body wall muscle while 5-hydroxytrypamine (5-HT) is the excitatory transmitter onto pharyngeal muscle. 5-HT also reduces ACh-induced contractions of somatic muscle and this action of 5-HT is mediated through activation of adenylate cyclase while that on pharyngeal muscle is mediated through inositol phosphate activation. Glutamate, dopamine and octopamine also have transmitter roles in nematodes. Neuroactive peptides of the RFamide family can excite somatic muscle, for example, AF-1 (KNEFIRFamide), AF-2 (KHEYLRFamide), AF-3 (AVPGVLRFamide) and AF-4 (GDVPGVLRFamide) or inhibit and relax this muscle, for example, PF-1 (SDPNFLRFamide), PF-2 (SADPNFLRFamide) and PF-4 (KPNIRFamide). In addition PF-3 (AF-8) (KSAYMRFamide) has a biphasic action on pharyngeal muscle, excitation followed by inhibition while AF-1 only inhibits this muscle. The peptide effects can be either pre- or postsynaptic or both and are likely to be mediated through second messenger systems. In addition these peptides modulate the action of classical transmitters, particularly ACh.

Keywords: Ascaris suum – acetylcholine – GABA – monoamines – FMRFamide-like peptides.

INTRODUCTION

Nematodes are a highly successful group of animals, certainly as judged by the range of habitats they have colonised. These include free living species, for example, *Caenorhabditis elegans,* parasitic species in plants, such as *Heterodera rostochiensis,* and parasitic species in animals, such as *Ascaris suum.* Although there are only around 15,000 recorded species it is likely that there could be up to one million yet to be identified worldwide [1]. There is considerable literature on the structure, life cycles and distribution of nematode species but relatively little on their physiology

+ Presented at the 9th ISIN Symposium on "Neurobiology of Invertebrates", July 1–5, 1999, Tihany, Hungary.

*Corresponding author, Department of Physiology and Pharmacology, School of Biological Sciences, University of Southampton, Southampton, SO16 7PX, UK.

0236-5383/2000/$ 5.00

and pharmacology. This is surprising since many parasitic species are of considerable economic importance and attempts have been made over the past 50 years or so to find selective and potent anthelmintics. A number of compounds are available but as with other pesticides, resistance has developed to these compounds. If an attempt is to be made to design new target specific anthelmintics then it is important to have a full understanding of the physiology and pharmacology of the target organs, such as, the nervous and muscle systems. It is also necessary to determine their physiology and pharmacology if full use of the *C. elegans* genome project is to be realised. This is now complete and provides key data in our search for future target sites for anthelmintics [13]. The aim of this report is to present data from our laboratory illustrating progress on our understanding of the physiology and pharmacology of nematodes, taking *A. suum, Ascaridia galli* and *C. elegans* as our model animals.

MATERIALS AND METHODS

A. suum were obtained from a local abattoir and maintained for up to a week in artificial perienteric fluid (APF) of the following composition in mM: NaCl 67, Na acetate 67, $CaCl_2$ 3, $MgCl_2$ 15.7, KCl 3, glucose 3, Tris 5, pH 7.6, with glacial acetic acid. The temperature was maintained at 37 °C. *A. galli* were obtained from experimentally infected fowl *(Gallus gallus)* or commercially from Central Veterinary Labs., Weybridge, UK. They were maintained in Earle's balanced salts (EBSS) of the following composition in mM: NaCl 116, $CaCl_2$ 1.8, $MgSO_4$ 0.8, KCl 5.4, NaH_2PO_4 1, glucose 3, phenol red-Na 0.003, pH 7.6 with NaOH. *A. galli* could be kept for 3–4 days in the EBSS at 42 °C. *C. elegans,* wild type (Bristol strain), were routinely cultured in the laboratory and dissected in Dent's solution with the following composition in mM: NaCl 140, $CaCl_2$ 3, $MgCl_2$ 1, KCl 6, Hepes 10, pH 7.4. In some experiments a modified Dent's solution was used where a high magnesium to calcium ratio was used with the following composition in mM: NaCl 140, KCl 6, $CaCl_2$ 1, $MgCl_2$ 10, Hepes 5, pH 7.4.

For the muscle strip pharmacology studies and electrophysiological recordings, conventional techniques were employed [26]. The IC-50 value is the concentration of antagonist required to reduce the response to an agonist by 50%. The EC-50 value is the concentration of agonist required to produce 50% of the response. The pA_2 value is the log of the reciprocal of the concentration of an antagonist that necessitates doubling the concentration of agonist to produce the same response.

The peptides used in this study were either obtained commercially or synthesised within the School of Biological Sciences, University of Southampton.

RESULTS

The results will be divided into two sections, those describing classical transmitter studies and those describing studies using neuroactive peptides.

Classical transmitters

Nematodes employ the same transmitter chemicals as other animal groups and there is good evidence for acetylcholine (ACh), gamma-aminobutyric acid (GABA), 5-hydroxytryptamine (5-HT, serotonin), glutamic acid and dopamine as transmitters in nematodes. A summary of their distribution and actions on somatic and pharyngeal muscle in *A. suum* is shown in Table 1.

Table 1
Summary of the distribution and physiological actions of classical transmitters on nematode nervous, somatic and pharyngeal muscle

Transmitter	Distribution	Physiological actions		
		somatic muscle	nervous system	pharyngeal muscle
Acetylcholine (ACh)	Excitatory motor neurons; Sensory neurones; e.g. amphids	excitatory	excitatory	inhibitory
Gamma-aminobutyric acid (GABA)	Inhibitory motorneurons and interneurons	inhibitory	inhibitory	inhibitory
Glutamate	Interneurons; M3 motorneurons (pharynx)	modulatory	excitatory	inhibitory
Serotonin (5-HT)	ENS-pharyngeal; Neurons in male tail and female reproductive system	modulates	inhibitory	stimulatory/ excitatory
Dopamine	Sensory neurones in female reproductive system	modulatory	inhibitory	inhibitory
Octopamine		modulatory	inhibitory	

Acetylcholine (ACh)

ACh is the excitatory transmitter onto body wall somatic muscle in nematodes and the pharmacological profile has been determined [6]. Using a range of cholinergic agonists, antagonists and toxins, it was found that the receptor on somatic muscle resembles the mammalian neuronal nicotinic receptor. Dimethylphenylpiperazinium (DMPP) was a potent agonist while mecamylamine and benzoquinonium were potent antagonists. Interestingly hexamethonium was a very weak antagonist while dihydro-beta-erythroidine was inactive. By comparison with vertebrate studies, the subunit composition whose pharmacology most resembled *A. suum* somatic muscle ACh receptor was $\alpha_3\beta_2$. This was based on the observation that both neuronal bungarotoxin, 100 nM blocked 5 μM ACh by 82%, and neosuragatoxin, IC-50 117 nM, were active as ACh antagonists on *A. suum* muscle. In contrast alpha-bungarotoxin

was a very weak antagonist with a pA_2 of 5.85 μM [7]. Cytisine was a very weak agonist while crude Conus toxin was inactive. Two analogues of the wasp venom philanthotoxin were also tested on this ACh receptor. Philanthotoxin 433 was a potent antagonist at the *A. suum* receptor with an IC-50 value of 0.25 μM, (Fig. 1). The antagonism was largely reversible with 75% recovery after 10 minutes wash. Philanthotoxin 343 was less potent with an IC-50 value of 1.55 μM and the block reversed more quickly with 100% recovery following a 10 minute wash.

ACH, threshold 500 nM, depolarises and excites pharyngeal muscle of *C. elegans* and this action is mimicked by pilocarpine.

A putative levamisole binding subunit, asar-1, has been obtained from *A. suum*. The cDNA encodes for a nicotinic ACh receptor alpha subunit, as defined by the presence of two vicinal cysteines in the N-terminal region. This subunit has a 78.9% predicted amino acid identity with the putative nicotinic ACh receptor subunit UNC38 from *C. elegans*. asar-1 is the first subunit for a ligand-gated ion channel cloned from *A. suum*.

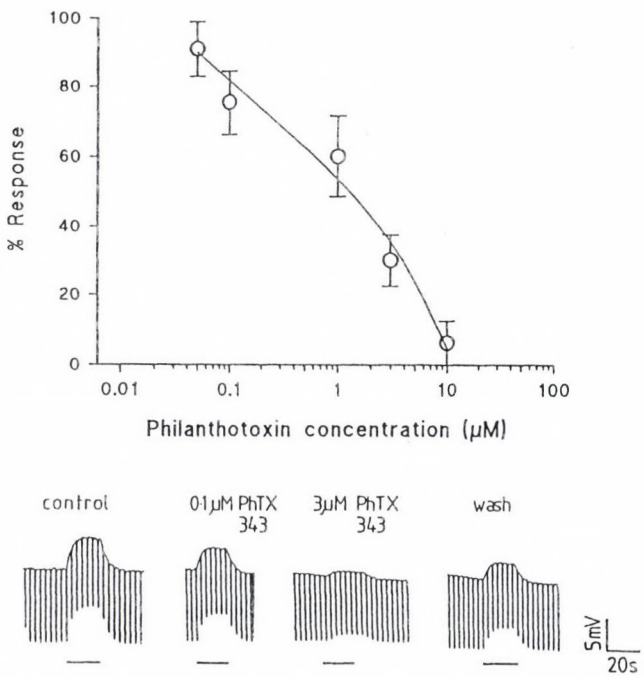

Fig. 1. Effect of philanthotoxin 343 on the ACh response in *A. suum*. The graph shows the percentage response (conductance change) against increasing concentrations of toxin. The trace shows control responses to 5 μM ACh, as indicated by bar, and the reduction of the response with 0.1 μM and 3.0 μM toxin. There is partial recovery on washing

Gamma-aminobutyric acid (GABA)

GABA is the inhibitory postsynaptic transmitter onto *A. suum* body wall muscle. The pharmacological profile of this receptor has been investigated and in terms of agonist profile it resembles the vertebrate GABA-A receptor with dihydro-muscimol being a potent agonist. In contrast the vertebrate GABA-A antagonist bicuculline is inactive while picrotoxin has a very low potency as an antagonist, that is, high μM towards 1 mM. This is of interest since GABA inhibition onto *A. suum* muscle is mediated through an increase in conductance to chloride [14]. However bicuculline was found to block the *A. suum* somatic muscle ACh receptor in the high μM range. The vertebrate GABA-A receptor is modulated by a number of compounds, including benzodiazepines and barbiturates but neither flurazepam nor pentobarbitone altered this GABA response. In this respect the *A. suum* GABA receptor resembles the vertebrate GABA-C receptor [27]. However two groups of compounds were identified which did antagonise the *A. suum* GABA receptor, that is, avermectins and a series of azole derivatives. Avermectin and its derivatives irreversibly antagonise the action of GABA but are required in the μM range [15]. The azole compounds of which SN 606078, 2-(2,6-dichloro-4-trifluromethylphenyl)-4-(4,5-dicyano-1H-imidazol-2-yl)-2H-1,2,3-triazole, is the lead compound, can block the GABA inhibition in the low μM range, with SN 610272 having an IC-50 value of 1.3 μM [2]. This block is reversible and it is likely that further derivatives can be synthesised with higher potencies.

GABA also has an inhibitory action on the pharyngeal muscle of *A. suum,* with a threshold of around 1 μM and an EC-50 of 23 μM [4]. This action of GABA can be potentiated by ivermectin, for example, 1 pM ivermectin can increase the threshold inhibition induced by GABA by a factor of ten. In addition ivermectin, 1–1000 nM, can directly inhibit pharyngeal muscle pumping. However around 20% of preparations failed to respond to 500 nM ivermectin. Very high concentrations of picrotoxin, around 1 mM, can also block the GABA inhibition on this muscle, for example, the inhibition induced by 10 μM GABA.

GABA, threshold low μM, induces a rapid depolarization of *C. elegans* pharyngeal muscle which is mediated through an increase in chloride conductance. In this muscle the chloride equilibrium potential is more positive than the muscle cell membrane potential, resulting in a rapid depolarization. This action of GABA is potentiated by the GABA uptake blocker nipecotic acid, indicating the presence of an uptake system for GABA inactivation in this preparation.

Glutamic acid

Glutamic acid does not have a direct effect on *A. suum* body wall muscle but does have a presynaptic action to reduce muscle activity. Glutamate can inhibit somatic muscle spontaneous muscle action potentials and also reduce excitatory junction potentials (ejps) recorded intracellularly from the muscle. This effect of glutamate is

mimicked by kainate. Glutamate also inhibits pharyngeal muscle pumping activity in *A. suum* with a threshold concentration of around 10 μM and an EC-50 value of 491 μM [4]. As with GABA, the response to glutamate can be potentiated by 1 pM ivermectin. In the presence of this concentration of ivermectin, the threshold response to glutamate decreased tenfold, that is, to 1 μM.

Glutamate also inhibits pharyngeal pumping in *C. elegans* but here the response is not potentiated by ivermectin. This glutamate inhibition appears as a depolarization since as already mentioned, the chloride equilibrium potential is more positive than the cell membrane potential. The actions of barbiturates have been investigated on glutamate gated chloride channels from *C. elegans,* GluClα and GluClβ following expression in *Xenopus* oocytes. GluClα is activated by ivermectin while GluClβ is activated by glutamate [10]. Interestingly barbiturates decreased the glutamate-induced response of these co-expressed channels in a concentration-dependent manner.

5-Hydroxytryptamine (5-HT, serotonin)

5-HT does not have a direct effect on *A. suum* body wall muscle but does attenuate ACh-induced contractions of the muscle though concentrations up to 1 mM are required. 5-HT also reduced ejps recorded from the muscle with a threshold of around 1 μM. 5-HT stimulates cAMP production in somatic muscle. 5-HT has a much clearer role in the physiology of the pharyngeal muscle system. On this preparation 5-HT induces and maintains pumping when the isolated preparation is perfused in the high μM range, for example, 100 to 200 μM [3]. This effect is concentration-dependent, threshold 10 μM and an EC-50 value of 44.4 μM. 5-HT has no effect on cAMP production in pharynx muscle but does activate IP_3 levels. 5-HT can directly stimulate action potentials in pharynx muscle of *C. elegans* in a concentration dependent manner, threshold 50 nM. There is relatively little effect on muscle membrane potential, the effect being an increase in action potential frequency.

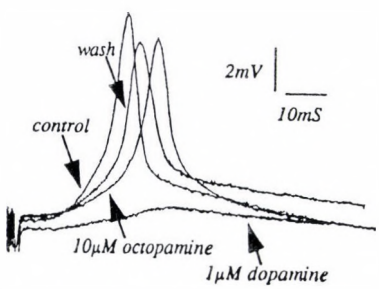

Fig. 2. Effect of dopamine, 1 μM, and octopamine, 10 μM, on excitatory junction potentials (ejps) recorded from a somatic muscle cell of *A. suum.* Both amines reduced the amplitude of the ejps and these effects reversed following washing. In case of dopamine, the ejp was virtually abolished

Dopamine

Dopamine does not have a direct effect on *A. suum* body wall muscle but does attenuate ejps recorded from this muscle. The threshold for this inhibitory effect is around 1 μM and a similar effect is observed with octopamine (Fig. 2). Both compounds also inhibit pharyngeal pumping in *A. suum.* Both dopamine and octopamine inhibit pharyngeal muscle action potentials in *C. elegans,* with threshold in the high nM range.

Neuroactive peptides

In addition to classical transmitters, a number of peptide families have been identified in nematodes, including the FMRFamide family, first described in molluscs. For example, in *C. elegans* FMRFamide peptides are encoded by at least 18 different genes and so far 53 peptides have been identified in *C. elegans* and around 20 in *A. suum* [24]. The main members of this family, isolated from *A. suum* and *Panagrellus redivivus,* and which will be discussed here are listed in Table 2. The actions of these peptides have been investigated on both somatic body wall muscle of *A. suum, A. galli* and *C. elegans.* Since these peptides are widespread in nematodes they are likely to play a key role in the physiology of a number of systems including locomotion, feeding and egg-laying. For example, injection of RFamides into whole *A. suum* can induce heightened motor activity for up to two hours followed by paralysis, for example, AF-2, while injection of PF-1 induces flaccidity. Results from using these peptides will now be described.

Table 2
Name, sequence and action of a number of RFamide peptides on somatic and pharyngeal muscle of *A. suum*

Peptide	Sequence	Action on *A. suum*	
		somatic muscle	pharyngeal muscle
A. suum			
AF-1	KNEFIRFamide	excitatory	inhibitory
AF-2	KHEYLRFamide	biphasic	
AF-3	AVPGLRFamide	excitatory	no effect
AF-4	GDVPGVLRFamide	excitatory	no effect
AF-8/PF-3	KSAYMRFamide	excitatory	biphasic
P. redivirus			
PF-1	SDPNFLRFamide	inhibitory	no effect
PF-2	SADPNFLRPamide	inhibitory	no effect
PF-4	KPNFIRFamide	inhibitory	no effect

Note: A – alanine; D – aspartic acid; E – glutamic acid; F – phenylalanine; G – glycine; H – histidine; I – isoleucine; K – lysine; L – leucine; M – methionine; N – asparagine; P – proline; R – arginine; S – serine; T – threonine; V – valine; Y – tyrosine.

AF-1 (KNEFIRFamide) and AF-2 (KHEYLRFamide)

These two peptides were the first peptides to be isolated in a nematode, that is in *A. suum* [8, 9]. Both have rather complex actions on *A. suum* somatic muscle strips, and an example for AF-1, 1 μM, is shown in Fig. 3. AF-1 can elicit an increase in muscle tension (Fig. 3a), accompanied by a series of phasic contractions and relaxations. Alternatively AF-1 can elicit a simple increase in muscle tension (Fig. 3b). A comparison of the excitatory actions of ACh, 3 μM, and AF-1, 1 μM, are shown in Fig. 3c. In this case AF-1 elicited an increase in phasic activity without an increase in muscle tone. These actions of AF-1 can be long lasting, for example, over two hours. AF-2 can also increase frequency and amplitude of spontaneous muscle contractions which can last for over one hour. The threshold for these AF-2 induced responses is around 10 nM. AF-2, 100 nM, can potentiate the increase in muscle tension induced by ACh [26]. In electrophysiological recordings from the muscle, AF-2 100 nM, can also potentiate ejps recorded from somatic muscle cells. Interestingly AF-2 failed to

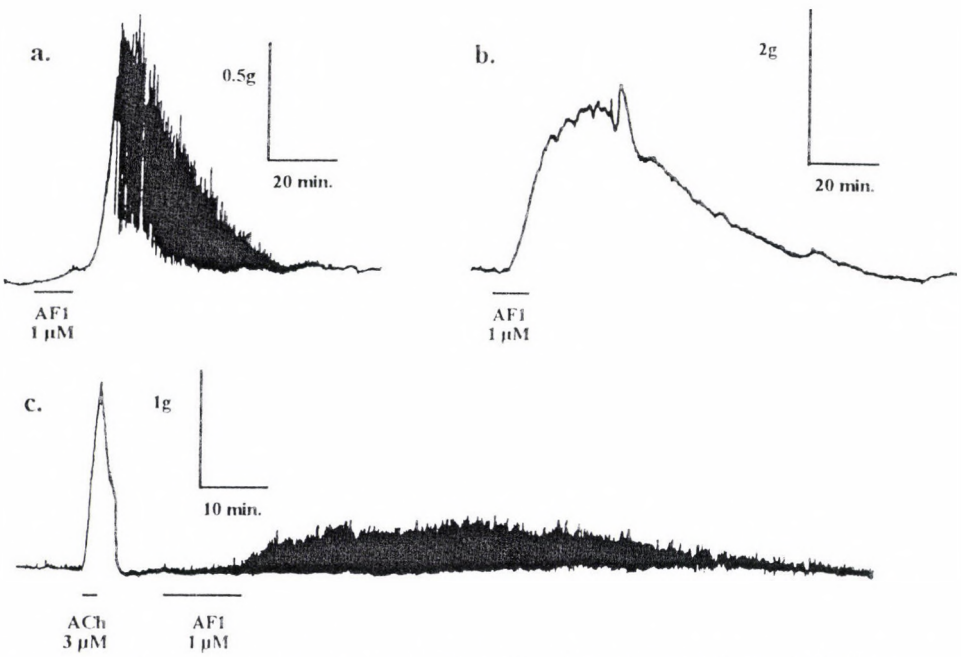

Fig. 3. The effect of AF-1 on the *A. suum* dorsal muscle strip. Each trace is from a similar but separate preparation. The tissue was perfused with artificial perienteric fluid containing AF-1, 1 μM (a) AF-1, 1 μM, elicited an increase in muscle tension, but also an increase in phasic contractions and relaxations. (b) AF-1, 1 μM, elicited an increase in muscle tension, but did not elicit phasic activity to any extent. (c) ACh, 3 μM, elicited an increase in muscle tension of approximately 1.5 g, in the same dorsal muscle strip, AF-1, 1 μM, elicited an increase in phasic contractions and relaxations, but not an increase in basal muscle tone

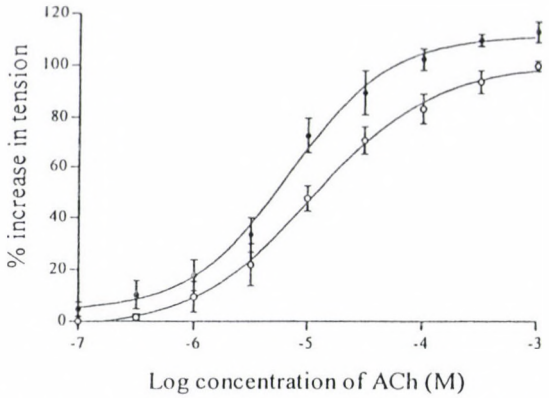

Fig. 4. Concentration-response curve for ACh on a dorsal muscle strip of *A. suum* in the absence and presence of 1 μM AF-2. ACh was added to the dorsal muscle strip in increasing concentrations for 10 sec, washed for 30 sec and re-equilibrated for 2 min. Following a 3 min exposure of the tissue to the peptide, the concentration-response curve was repeated. The curve with open circles represents the concentration-response curve in the absence of AF-2 and the closed circles represents the concentration-response curve in the presence of peptide

potentiate depolarization of muscle cells induced by ACh. This indicates that AF-2 can act presynaptically on excitatory motoneurones to enhance ACh release and in turn ejp amplitude. In contrast to its excitatory action on somatic muscle, AF-1 is inhibitory on *A. suum* pharyngeal muscle. However both AF-1 and AF-2 are excitatory on *C. elegans* pharyngeal muscle, threshold around 50 nM.

AF-2 can elicit a biphasic effect, relaxation of *A. suum* somatic muscle strip preceding the sustained contraction, threshold 10 nM. In the presence of 1 μM AF-2, a concentration-response curve for ACh is potentiated (Fig. 4). For example, 1 μM AF-2 potentiated the effect of 10 μM ACh by 140 ± 22% compared to control response ($P < 0.001$). Interestingly 1 μM AF-2 increased the maximum response to ACh. This concentration of AF-2 also increased the rate of relaxation of the contraction elicited by ACh, 10 μM. For example, in the absence of AF-2, the relaxation rate of the ACh contraction was 0.19 ± 0.04 $gsec^{-1}$. In the presence of AF-2, the relaxation rate increased to 0.45 ± 0.14 $gsec^{-1}$, giving a relative relaxation rate of 2.3 compared to control ($P = 0.01$) [21]. These effects of AF-2 are long-lasting and a three minute application can take over 90 minutes to reverse. If the muscle is incubated with AF-2 for longer, for example, five minutes, then the peptide effect on ACh response appears to be irreversible. The possible involvement of a second messenger system in the potentiation of ACh response by AF-2 was investigated and the results summarised in Table 3. The phosphodiesterase inhibitor, IBMX 500 μM, blocked the AF-2 induced potentiation of the ACh contraction, i.e. AF-2 enhanced the ACh response from an initial value of 100% to 157 ± 30% but in the presence of 500 μM IBMX, AF-2 only increased the ACh response from 100% to 102 ± 25%. Theophylline, 100 μM, also inhibited this AF-2 induced potentiation of the ACh response, Table 3.

However caffeine failed to have an inhibitory effect on the peptide response. Both forskolin, an adenylate cyclase activator, and dibutyryl cAMP, a membrane permeable analogue of cAMP, also reduced the AF-2 effect on the ACh response, Table 3. However 8-Br-cGMP, a membrane permeable analogue of cGMP, had no effect. The protein kinase C activator, phorbol 12-myristate 13 acetate (PMA), 10 ng ml^{-1}, had a direct effect on the muscle strip, initial relaxation followed by a slow steady contraction over a 4–5-hour period. PMA depletes levels of protein kinase C by irreversibly activating the protein kinase C system. PMA had no effect on the ACh contraction but did reduce the potentiation of the ACh response by AF-2 and this reduction was significant ($P = 0.05$).

Table 3

The effect of methylxanthines and second messengers on the AF-2 induced potentiation of the ACh contraction

Compound	Concentration	Control	Experimental	% Difference
IBMX	500 μM	157 ± 30%	102 ± 25%	–55% (n = 7; p < 0.001)
Theophylline	100 μM	158 ± 25%	117 ± 32%	–41% (n = 6; p < 0.001)
Caffeine	5 μM	145 ± 23%	133 ± 14%	–12% (n = 6; N.S.)
Forskolin	10 μM	130 ± 5%	102 ± 10%	–28% (n = 5; p < 0.01)
Dibutyryl cAMP	100 μM	159 ± 35%	119 ± 11%	–40% (n = 5; p < 0.001)
8-Br-cGMP	100 μM	142 ± 19%	140 ± 22%	–2% (n = 3; N.S.)

The control value is in the presence of AF-2 but without the test compound. N.S. = not significant. IBMX, isobutylmethylxanthine

AF-1 is inhibitory on *A. suum* pharyngeal muscle [5] and this effect is concentration dependent with a threshold of 1 nM. However unlike PF-3, AF-1 exhibits no clear excitatory component. Interestingly AF-2 has no effect on pharyngeal muscle pumping.

AF-3 (AVPGVLRFamide) and AF-4 (GDVPGVLRFamide)

Both AF-3 and AF-4 are excitatory on *A. suum* and *A. galli* somatic muscle and this action has been investigated using muscle strip pharmacology, intracellular recording from muscle cells and second messenger level measurements [27, 28]. As with AF-1 and AF-2, both AF-3 and AF-4 also potentiate ACh contractions. Both peptides are considerably more potent than ACh in exciting body wall muscle. For example, on *A. suum* body wall muscle strip, the EC-50 values for ACh, AF-3 and AF-4 are 13 ± 1 μM, 24 ± 6 nM and 37 ± 2 nM, respectively. Using intracellular recordings and measuring depolarization, the EC-50 values for AF-3 and AF-4 were considerably higher, i.e. 681 ± 329 nM and 901 ± 229 nM, respectively. However in each case AF-4 was slightly less potent than AF-3. The depolarization elicited by AF-3 and

AF-4 were not blocked by ACh antagonists, such as, benzoquinonium, and so it is unlikely that these peptides act through the release of ACh. *A. galli* muscle was also excited by AF-3 and AF-4 though this muscle was less sensitive, EC-50 values for contraction of the muscle strips were 721 ± 236 nM and 371 ± 177 nM for AF-3 and AF-4 respectively. Though AF-4 was slightly more potent than AF-3 on *A. galli* somatic muscle, this difference was not significant. The effects of AF-3 on both *A. suum* and *A. galli* muscle have been further investigated. Both forskolin, 10 μM, and IBMX, 500 μM, inhibit AF-3 induced contractions of *A. suum* muscle strip by 22% and 27% respectively. AF-3, 1 μM, also decreased basal levels of cAMP in *A. suum* somatic muscle from 1721 ± 134 pmol mg^{-1} to 1148 ± 133 pmol mg^{-1} (P 0.05; n = 5). Foskolin, 10 μM, potentiated the basal level and this presentation was reduced by AF-3.

AF-3 and AF-4 have no apparent effect on pharyngeal muscle pumping (Table 2).

PF-1 (SDPNFLRFamide) and PF-2 (SADPNFLRFamide)

Although PF-1 and PF-2 were first identified in *P. redivivus* [12] they both have potent inhibitory and relaxing actions on somatic muscle of *A. suum* and *A. galli.* For example, 1 μM PF-1, elicits a relaxation of the *A. suum* muscle strip which lasts for 3–4 hours and almost completely blocks the increase in muscle tone elicited by ACh. Threshold relaxation can be obtained with PF-1 at around 1nM and this peptide inhibits ACh induced contractions in a concentration dependent manner (Fig. 5). In this experiment, a standard contraction was obtained to 10 μM ACh and then this concentration was applied in the presence of ever increasing concentrations of PF-1. On washing there was partial recovery. Intracellular recording from somatic muscle cells confirmed that PF-1 hyperpolarized the membrane potential, for example,

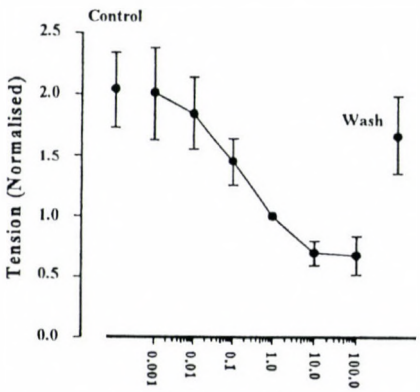

Fig. 5. Concentration-response relationship for the inhibition of ACh contractions by PF-1. Increases in isometric tension, elicited by consecutive concentrations of ACh (10 μM •), were incrementally reduced by increasing concentrations of PF-1 (0.001–100 μM). The effect of PF-1 was reversed after a period of washing. Each point is the mean of four determinations, indicated by error bars

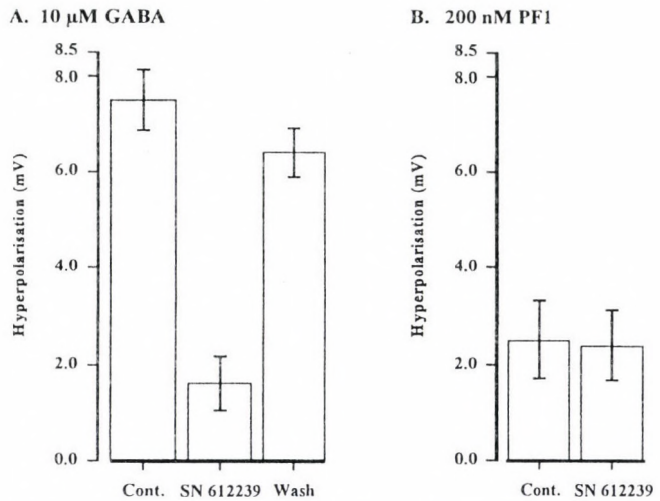

Fig. 6. Histograms to show that the response to PF-1 is not antagonised by SN 612239. A. Histogram shows the mean response to GABA, 10 μM, in normal APF and in the presence of SN 612239, 10 μM. Hyperpolarizations elicited by 10 μM GABA, in the presence of SN 612239, were significantly reduced compared to the control, $n = 5$, $P < 0.005$. Following 20 min wash in APF, the block was reversed. B. Hyperpolarizations elicited by PF-1, 200 nM, in the presence of SN 612239, 10 μM, were not significantly different from control values, $n = 4$, $P > 0.3$

200 nM hyperpolarized the membrane potential by 1.9 ± 0.3 mV (n = 11). Compared to GABA hyperpolarization, the PF-1 effect was slow in onset and the duration very variable, ranging from 5 to 60 minutes. The EC-50 for PF-1 was 349 ± 87 nM compared to 26.3 ± 3.5 μM for GABA. In contrast to the position with GABA, PF-1 inhibition failed to induce a consistent change in input conductance. PF-1 inhibited spontaneous muscle action potentials but often without clear hyperpolarization of the membrane potential. The GABA antagonist, SN 612239 10 μM, failed to block the PF-1 (200 nM) hyperpolarization while it consistently reduced GABA (10 μM) hyperpolarization (Fig. 6). The ionic events associated with PF-1 hyperpolarization were investigated and compared with those to GABA, the latter being a chloride event. No evidence was found for a role for chloride in the PF-1 hyperpolarization. Low potassium, 0.1 mM, saline resulted in an increased hyperpolarization, but this response was not consistent. However in four cells 100 nM PF-1 elicited a mean hyperpolarization of 4 ± 0.7 mV in normal APF while in low potassium APF, the hyperpolarization increased to 5.81 ± 1.0 mV, $P < 0.05$. The presence of a mixture of tetraethylammonium (TEA), 5 mM, and 4-aminopyridine (4-AP), 250 μM, blocked PF-1 hyperpolarization reversibly. All this provides evidence for a potassium component in the PF-1 response. Experiments using *A. galli* somatic muscle confirmed the work described for *A. suum* and work on *A. suum* using PF-2 showed that it had a similar effect to PF-1. Neither PF-1 nor PF-2 have any apparent effect on pharyngeal muscle pumping (Table 2).

PF-4 (KPNFIRFamide)

PF-4 is another peptide first identified in *P. redivivus* but which has potent relaxing and inhibitory effects on *A. suum* somatic muscle [16]. The action of this peptide is particularly interesting because it is fast and the effect is mediated primarily through an increase in permeability to chloride. Both events which are shared with the GABA response on somatic muscle. However PF-4 is considerably more potent that GABA, with an EC-50 value of 98 nM, compared with GABAs EC-50 value in this study of 59 μM. Unlike the hyperpolarization seen with GABA, that to PF-4 can be described in two phases, an initial fast phase which occurs within one minute of application. This hyperpolarization then declines to a steady plateau after a minute, the membrane potential then slowly returns to control value. While the action of GABA, 30 μM, is blocked by ivermectin, 10 μM, that to PF-4, 1 μM, is unaltered. This strongly suggests that the PF-4 hyperpolarization is through a receptor which is distinct from the GABA receptor on somatic muscle.

PF-3 (AF-8) (KSAYMRFamide)

PF-3 or AF-8 has been identified in both *A. suum* and *P. redivivus* and is excitatory on somatic muscle [22] and biphasic on *A. suum* pharyngeal muscle [3]. PF-3 causes an initial increase in amplitude and frequency of pumping with a threshold of around 0.1 nM. This enhanced activity is then followed by an inhibitory phase with reduced amplitude of contraction and reduction in frequency. Higher concentrations of peptide induce increasing degrees of inhibition, for example, 1 nM, completely stops pharyngeal pumping. As the concentration of PF-3 increases, the initial excitatory phase decreases as the period of inhibition increases.

DISCUSSION

It is clear that both classical transmitters and RFamide neuropeptides have key roles in the normal physiology of nematodes. The evidence for ACh as the somatic muscle excitatory transmitter and for GABA as the inhibitory transmitter onto somatic muscle is good. The initial experiments were conducted using *A. suum* as the model preparation [18, 19]. Motoneurones are present which contain either ACh or GABA. The GABA receptor resembles mammalian GABA-A receptors, being linked to fast chloride-mediated event, activated by muscimol but this agonist binding site does not recognise bicuculline and has a very low affinity for picrotoxin. This suggests a possible similarity with the proposed GABA-C receptor [20]. Although ACh is also the excitatory neuromuscular transmitter in vertebrates, there are differences as might be expected between the nematode somatic muscle ACh receptor and the vertebrate ACh nicotinic receptor on striated muscle. On balance the nematode ACh receptor more closely resembles the vertebrate neuronal nicotinic ACh receptor but further

work is required to clarify the position. There are interesting differences, particularly in terms of the antagonist profiles of the two receptors. In addition to its role as a neuromuscular transmitter in nematodes there is evidence for the occurrence of ACh-containing sensory neurones, for example, in the amphids.

Biogenic amines, including 5-HT, dopamine and octopamine are also involved in the regulation of physiological processes in nematodes. 5-HT has a key role in pharyngeal muscle activity and probably also has a role in somatic muscle excitability, both events acting through second messenger systems. 5-HT also has a role in egg-laying [29]. Recently two 5-HT receptors have been cloned in *A. suum* [17] and one of these has 77% homology to the *C. elegans* 5-HT receptor [25] and around 65% homology to mammalian 5-HT-2 receptors. It is therefore possible that one of the receptors in *A. suum* has 5-HT-2 properties. This is a possible area which could be exploited in developing novel anthelmintics. Dopamine is likely to have a role in the regulation of the reproductive system and possibly also as a sensory transmitter. Glutamate is present in motoneurones regulating the pharynx, for example, M-3 in *C. elegans,* and probably plays a key role in modulating pharyngeal activity. It is likely that this glutamate receptor may be one of the sites for ivermectin action in *A. suum.* Glutamate also has an indirect role in regulating somatic muscle. The pharmacology of this glutamate receptor which is located on DE-2 motoneurones of *A. suum* has been studied in detail [11] where glutamate is excitatory and kainic acid is a potent agonist.

From immunocytochemical and molecular biological studies it is clear that peptides and in particular RFamides play an important role in the normal physiology of nematodes. Probably more than half of the neurones contain immunoreactive material to RFamides and so are likely to release it following activation. These peptides can inhibit or excite or have biphasic actions on muscle systems in nematodes, either directly or indirectly through the nervous system. The total number of RFamide peptides so far identified in nematodes is astounding and it will be of great interest to analyse all their actions both in the peripheral and in the central nervous system. For example, AF-2 clearly has an important modulatory role in the excitation of somatic body wall muscle of *A. suum.* It is likely that this effect is, at least partly, mediated through a second messenger system. The induction of phasic contractions by AF-2 would suggest it can modify the contraction-relaxation cycle. In *C. elegans* there is a twitching gene and animals with mutations in the twitching gene, unc 22, possess constant twitching in their somatic musculature [23]. It is possible that AF-2 modifies this protein, resulting in the phasic activity. The potentiating effect of AF-2 on ACh contraction would appear to be associated with a decrease in cAMP levels since raising cAMP reduces this potentiation. In addition depletion of protein kinase C system also reduces AF-2 potentiation of ACh contractions. cAMP can inhibit protein kinase C and so it is possible that AF-2 acts to potentiate the ACh response either indirectly by inhibition of cAMP production or directly to increase protein kinase C levels [21]. In addition to a postsynaptic action, AF-2 acts presynaptically to release ACh since AF-2 potentiates ejps but not ACh-induced depolarizations of the muscle cell membrane potential. However it is possible that AF-2 could inhibit the inhibito-

ry motoneurones which indirectly would enhance excitatory events. Experiments using AF-3 and AF-4 provide further evidence that these excitatory peptides activate nematode somatic muscle through inhibition of cAMP.

It is also likely that other neuroactive peptides including AF-3, AF-4, PF-1, PF-2 and PF-4 have important regulatory roles in muscle function in nematodes. Peptides such as PF-1 and PF-4 have very potent inhibitory or relaxing actions on nematode muscle and clearly have key modulatory roles in the action of ACh and GABA on somatic muscle. Although many of these actions are relatively slow and long-lasting, the action of PF-4 on *A. suum* somatic muscle is fast and in this respect mimics the action of GABA on this muscle. In future experiments it will be of interest to explore the interactions between PF-4 and GABA in normal physiology of this muscle.

In this paper the actions of neuroactive peptides and chemical transmitters have been reviewed in nematodes. It is likely that the receptors for neuropeptides, amines and glutamate will provide potential target sites for new anthelmintics. However it is clear that studies on the physiology and pharmacology is still in its infancy, particularly concerning receptors located on neurones and hopefully the next few years should provide exciting developments following on the genomic information gained from research on *C. elegans*.

ACKNOWLEDGEMENTS

Grateful thanks to BBSRC, Wessex Medical Trust, Hoechst Roussel Vet and the Royal Society for financial support.

REFERENCES

1. Barnes, R. S. K., Calow, P., Olive, P. J. W. (1988) *The Invertebrates: A New Synthesis.* Blackwell Scientific Publications, Oxford, pp. 582.
2. Bascal, Z., Holden-Dye, L., Willis, R. J., Smith, S. W. G., Walker, R. J. (1996) Novel azole derivatives are antagonists at the inhibitory GABA receptor on the somatic muscle cells of the parasitic nematode, *Ascaris suum. Parasitology 112,* 253–259.
3. Brownlee, D. J. A., Holden-Dye, L., Fairweather, I., Walker, R. J. (1995) The action of serotonin and the nematode peptide KSAYMRFamide on the pharyngeal muscle of the parasitic nematode, *Ascaris suum. Parasitology 111,* 379–384.
4. Brownlee, D. J. A., Holden-Dye, L., Walker, R. J. (1997) Actions of the anthelmintic ivermectin on the pharyngeal muscle of the parasitic nematode, *Ascaris suum. Parasitology 115,* 553–561.
5. Brownlee, D. J. A., Holden-Dye, L., Walker, R. J. (1999) Actions of nematode FMRFamide-related peptides (FaRPs) on the pharyngeal muscle of the parasitic nematode, *Ascaris suum. Annals N.Y. Acad. Sci. 897,* 228–238.
6. Colquhoun, L., Holden-Dye, L., Walker, R. J. (1991) The pharmacology of cholinoceptors on the somatic muscle cells of the parasitic nematode, *Ascaris suum. J. exp. Biol. 158,* 509–530.
7. Colquhoun, L. M., Holden-Dye, L., Walker, R. J. (1993) The actions of nicotinic receptor specific toxins on the somatic muscle cells of the parasitic nematode, *Ascaris suum. Mol. Neuropharmac. 3,* 11–16.
8. Cowden, C., Stretton, A. O. W., Davis, R. E. (1989) AF-1, a sequenced bioactive neuropeptide isolated from the nematode *Ascaris suum. Neuron 2,* 1465–1473.

9. Cowden, C., Stretton, A. O. W. (1993) AF-2, an *Ascaris* neuropeptide: isolation, sequence and bioactivity. *Peptides 14,* 423–430.
10. Cully, D. F., Vassilatis, D. K., Liu, K. K., Paress, P. S., Van der Ploeg, L. H. T., Schaeffer, J. M., Arena, J. P. (1994) Cloning of an avermectin-sensitive glutamate-gated chloride channel from *Caenorhabditis elegans. Nature 371,* 707–711.
11. Davis, R. E. (1998) Neurophysiology of glutamatergic signalling and anthelmintic action in *Ascaris suum:* pharmacological evidence for a kainate receptor. *Parasitology 116,* 471–486.
12. Gary, T. G., Price, D. A., Bowman, J. W., Winterowd, C. A., Mackenzie, C. D., Garrison, R. D., Williams, J. F., Freiedman, A. R. (1992) Two FMRFamide-like peptides from the free-living nematode *Panagrellus redivivus. Peptides 13,* 209–214.
13. Hodgkin, J., Horvitz, H. B., Jasny, B. R., Kimble, J. (1998) *C. elegans:* Sequence to Biology. *Science 282,* 2011.
14. Holden-Dye, L., Krogsgaard-Larsen, P., Nielsen, L., Walker, R. J. (1989) GABA receptors on the somatic muscle cells of the parasitic nematode, *Ascaris suum:* Stereoselectivity indicates similarity to a GABA-A type agonist recognition site. *Br. J. Pharmacol. 98,* 841–851.
15. Holden-Dye, L., Walker, R. J. (1990) Avermectin and avermectin derivatives are antagonists at the 4-aminobutyric acid (GABA) receptor on the somatic muscle cells of *Ascaris:* is this the site of anthelmintic action? *Parasitology 101,* 265–271.
16. Holden-Dye, L., Brownlee, D. J. A., Walker, R. J. (1997) The effects of the peptide KPNFIRFamide (PF-4) on the somatic muscle cells of the parasitic nematode *Ascaris suum. Br. J. Pharmac. 120,* 379–386.
17. Huang, X., Diaz, F., Duran, E., Hinman, C., Komuniecki, R. W. (1997) Characterization of serotonin receptors in the pharynx of parasitic nematode *Ascaris suum. Amer. Soc. Neurosci. Absts. 23,* 1217.
18. Johnson, C. D., Stretton, A. O. W. (1985) Localization of choline acetyltransferase within identified motoneurones of the nematode, *Ascaris. J. Neurosci. 5,* 1984–1992.
19. Johnson, C. D., Stretton, A. O. W. (1987) GABA immunoreactivity in inhibitory motoneurones of the nematode, *Ascaris. J. Neuroscience. 7,* 223–235.
20. Johnston, G. A. R. (1986) Multiplicity of GABA receptors. In: Olsen, R. W., Venter, J. C. (ed.) *Benzodiazepine/GABA Receptors and Chloride Channels: Structural and Functional Properties.* Alan R. Liss Inc., New York, pp. 57–71.
21. Keating, C. D. I. (1996) The identification of, and studies on, a FMRFamide-related peptide from the nematode *Haemonchus contortus.* PhD Theses, University of Southampton.
22. Maule, A. G., Shaw, C., Bowman, J. C., Halton, D. W., Thompson, D. P., Geary, T. G., Thim, L. (1994) KSAYMRFamide: A novel FMRFamide-related heptapeptide from the free-living nematode, *Panagrellus redivivus,* which is myoactive in the parasitic nematode, *Ascaris suum. Biochem. Biophys. Res. Commun. 200,* 973–980.
23. Moerman, D. G., Benian, G. M., Barstead, R. J., Schriefer, L. A., Waterson, R. H. (1988) Identification and intracellular localisation of the unc-22 gene product of *C. elegans. Genes Dev. 95,* 93–105.
24. Nelson, L. S., Kim, K. Y., Memmott, R. E., Li, C. (1998) FMRFamide-related gene family in the nematode, *Caenorhabditis elegans. Science 281,* 1696–1690.
25. Olde, B., McCombie, W. R. (1997) Molecular cloning and functional expression of a serotonin receptor from *Caenorhabditis elegans. J. Mol. Neurosci. 8,* 53–62.
26. Pang, F.-Y., Mason, J., Holden-Dye, L., Franks, C. J., Williams, R. G., Walker, R. J. (1995) The effects of the nematode peptide, KHEYLRFamide (AF-2), on the somatic musculature of the parasitic nematode *Ascaris suum. Parasitology 110,* 353–362.
27. Qian, H., Dowling, J. E. (1993) Novel GABA responses from rod-driven retinal horizontal cells. *Nature 361,* 162–164.
28. Trim, N., Brooman, J. E., Holden-Dye, L., Walker, R. J. (1998) The role of cAMP in the actions of the peptide AF-3 in the parasitic nematodes *Ascaris suum* and *Ascaridia galli. Mol. Biochem. Parasitol. 93,* 263–271.
29. Weishenker, D., Garriga, G., Thomas, J. H. (1995) Genetic and pharmacological analysis of neurotransmitters controlling egg laying in *Caenorhabditis elegans. J. Neurosci. 15,* 6975–6985.

Acta Biologica Hungarica 51 (2–4), pp. 395–408 (2000)

DISTRIBUTION OF *EISENIA* TETRADECAPEPTIDE IMMUNOREACTIVE NEURONS IN THE NERVOUS SYSTEM OF EARTHWORMS+

MÁRIA CSOKNYA[1]*, O. MATSUSHIMA[3], J. BARNA[1], J. HÁMORI[1] and K. ELEKES[2]

[1]Department of General Zoology and Neurobiology, Janus Pannonius University, Ifjúság u. 6, H-7624 Pécs, Hungary
[2]Department of Experimental Zoology, Balaton Limnological Research Institute of Hungarian Academy of Sciences, Tihany, Hungary
[3]Department of Biological Science, Hiroshima University, Higashi-Hiroshima, Japan

(Received: August 31, 1999; accepted: November 30, 1999)

A detailed mapping of *Eisenia*-tetradecapeptide-immunoreactive neurons in the central and peripheral nervous system combined with quantitative morphological measurements was performed in *Eisenia fetida* and *Lumbricus terrestris.*

In *Eisenia,* most labelled neurons were observed in the ganglia of the ventral cord (20.38% of the total cell number of the ganglion) and 15.67% immunoreactive cells occurred in the brain, while 6% of the neurons could be shown in the subesophageal ganglion. In the case of *Lumbricus,* most immunoreactive cells were found in the subesophageal ganglion (16.17%) and in the ventral ganglia (12.54%). The brain contained 122 ETP-immunoreactive cells (5.6%). The size of the immunoreactive cells varied between 35–75 μm. A small number of *Eisenia*-tetradecapeptide immunoreactive fibres were seen to leave the ventral ganglia via segmental nerves, and labelled processes could also be observed in the stomatogastric system and the body wall. Labelled axon branches originating from the segmental nerves formed an immunoreactive plexus both between the circular and longitudinal muscle layer and on the inner surface of the longitudinal muscle layer. This inner plexus was especially rich in the setal sac. Among the superficial epithelial cells the body wall contained a significant number of immunoreactive cells.

Only a few *Eisenia*-tetradecapeptide immunoreactive neurons and fibres occurred in the stomatogastric ganglia. In the enteric plexus the number of immunoreactive neurons and fibres decreased along the cranio-caudal axis of the alimentary tract. *Eisenia*-tetradecapeptide immunoreactive cells were also present among the epithelial cells in the alimentary canal. Some of these cells resembled sensory neurons in the foregut, while others showed typical secretory cell morphology in the midgut and hindgut.

Keywords: *Eisenia*-tetradecapeptide – nervous system – immunocytochemistry – *Eisenia fetida* – *Lumbricus terrestris* – Annelida.

INTRODUCTION

The central nervous system (CNS) of earthworms contains only a small number (<10 000) of neurons. These neurons, however, present a wide variety of chemical character. More than 50% of them are neurosecretory (peptidergic) cells playing a role in regeneration, reproduction, osmoregulation and metabolic processes [8, 14].

+ Presented at the 9th ISIN Symposium on "Neurobiology of Invertebrates", July 1–5, 1999, Tihany, Hungary.

*Corresponding author, E-mail: 5-HT@ttk.jpte.hu

0236-5383/2000/$ 5.00

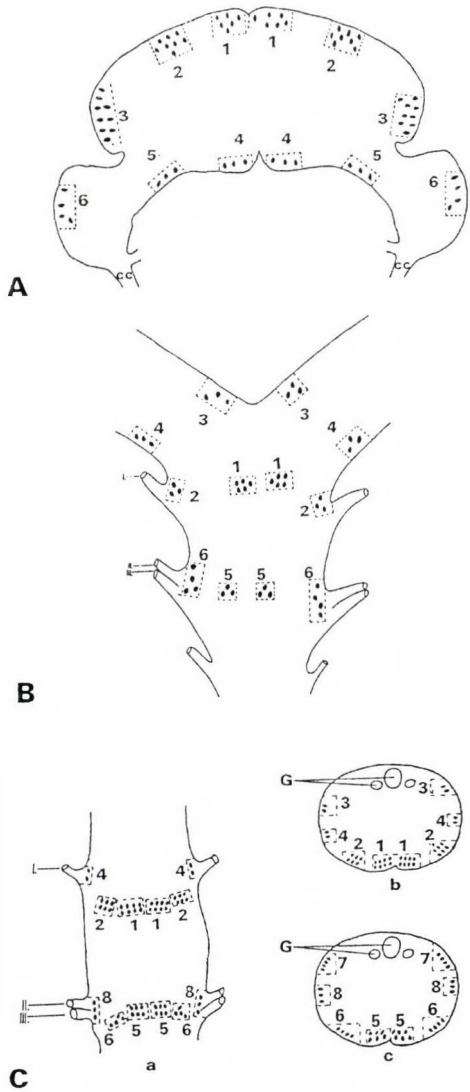

Fig. 1. Schematic representation of the distribution of ETP-IR neurons in the central nervous system of *Eisenia fetida.* A: ETP-IR neuron groups in the brain (frontal view). cc: circumpharyngeal connectives. 1: Dorsomedial, 2: Dorsolateral, 3: Lateral, 4: Ventromedial, 5: Ventrolateral, 6: Posterolateral cell groups. B: ETP-IR cell groups in the subesophageal ganglion (frontal view). 1: Ventromedial cell groups, 2: Cells at the origin of the 1st segmental nerves, 3: Medial, 4: Lateral groups at the origin of circumpharyngeal connectives, 5: Ventromedial cell groups, 6: Cells at the origin of 2nd, 3rd segmental nerves. C: ETP-IR neurons in the ventral cord ganglion. a: horizontal section of the whole ganglion, b: frontal view of the rostral part of the ganglion, c: frontal view of the caudal part of the ganglion, G: giant fibres. 1: Ventromedial, 2: Ventrolateral, 3: Dorsolateral cell groups, 4: Cells at the origin of 1st segmental nerves, 5: Ventromedial, 6: Ventrolateral, 7: Dorso-lateral cell groups, 8: Cells at the origin of 2nd, 3rd segmental nerves

The neurosecretory cells contain some of the peptides that are known to occur in the nervous system of vertebrates, whereas others contain neuropeptides characteristic of invertebrates only [1, 22].

Recently, Ukena et al. [20] isolated a tetradecapeptide (GFKDGAADRISHGF-amid) from the crop and gizzard of *Eisenia fetida*, and called it *Eisenia*-tetradecapeptide (ETP). This peptide was similar to the tetradecapeptide of *Pheretima* [19, 20] and the myoactive tetradecapeptide of molluscs [10, 13]. Physiological assays proved that ETP stimulated the contraction of the isolated gut [20, 21] suggesting that this peptide plays a role in the regulation of gut motility. The presence of ETP-immunoreactive (IR) neurons in the CNS and the alimentary canal of *Eisenia fetida* was already demonstrated [21].

The aim of our study was to map and quantify the distribution of ETP-IR neurons in the CNS and to study the patten of ETP-IR innervation in the periphery, the stomatogastric nervous system (SNS) and the body wall of two annelid species: *Eisenia fetida* and *Lumbricus terrestris*.

MATERIALS AND METHODS

Investigations were carried out on adult earthworms (*Eisenia fetida* and *Lumbricus terrestris*, Oligochaeta, Annelida). The anterior (10–20th segments), middle (30–35th segments) and posterior (last 10 segments) parts of the body were dissected, and fixed either in Zamboni-fixative [23] or 4% paraformaldehyde. Following fixation, the segments were dehydrated and embedded in Paraplast.

Immunostaining with anti-ETP antiserum (20; diluted 1 : 500) was performed on 7 μm thick serial sections. For the visualisation of the immunoreaction an ExtrAvidin peroxidase kit (diluted 1 : 20; Sigma) was used. The quantitative analysis of the ETP-IR neurons was performed by a Macintosh NIH-image 1.52 programme.

RESULTS

Distribution of ETP-IR neurons in the CNS of Eisenia fetida

Brain

The cerebral ganglion contains 160 ETP-IR neurons representing 15.6% of the total number of neurons in the brain. These ETP-IR neurons are localised in six groups (Table 1, Fig. 1A) situated on the dorsal (no. 1, dorsomedial, no. 2, dorsolateral cell groups), lateral (no. 3, lateral, no. 6, posterolateral cell groups) and ventral (no. 4, ventromedial, no. 5, ventrolateral cell groups) sides of the brain (Figs 1A, 3).

The largest neurons in the cerebral ganglion belong to the dorsomedial cell group. Their average diameter is 66.2 ± 4.1 μm. The diameter of the neurons in the other groups is 46–65 μm. A thin primary neurite originates from the perikaryon, giving off a few branches which enter the neuropil. The majority of the branches crosses the

Table 1

Distribution, number and diameter of ETP-IR neurons in the central nervous system of *Eisenia fetida*

Ganglion	Cell groups		Number of cells	Average diameter (μm) n = 30
	signs	localization		
Cerebral ganglion	1.	Dorsomedial	30	66.2 ± 4.1
	2.	Dorsolateral	38	61.1 ± 6.3
	3.	Lateral	44	64.9 ± 4.3
	4.	Ventromedial	14	56.7 ± 4.1
	5.	Ventrolateral	16	65 ± 3.6
	6.	Posterolateral	18	46.9 ± 5.7
	Number of ETP-IR neurons		160	
	Number of total neurons in the cerebral ganglion		1021	
	% of ETP-IR neurons		15.67	
Subesophageal ganglion	1.	Ventromedial	26	69.6 ± 2.1
Rostral part	2.	At the origin of I. segmental nerve	16	35.6 ± 4.4
	3.	Medial group, at the origin of circumpharyngeal connective	14	46.2 ± 4.3
	4.	Lateral group at the origin of circumpharyngeal connective	16	68.1 ± 5.4
Caudal part	5.	Ventromedial	16	75.5 ± 5.9
	6.	At the origin of 2nd, 3rd segmental nerves	14	61.4 ± 6.39
	Number of ETP-IR neurons		102	
	Number of total neurons in the subesophageal ganglion		1675	
	% of ETP-IR neurons		6	
Ventral cord ganglion	1.	Ventromedial	42	44.3 ± 4.7
Rostral part	2.	Ventrolateral	32	52.5 ± 6.1
	3.	Dorsolateral	10	48.2 ± 8
	4.	At the origin of I. segmental nerve	12	40.6 ± 3.2
Caudal part	5.	Ventromedial	32	60 ± 6.4
	6.	Ventrolateral	18	69.8 ± 6.3
	7.	Dorsolateral	18	67.3 ± 5.2
	8.	At the origin of 2nd, 3rd segmental nerves	16	46 ± 4
	Number of ETP-IR neurons		178	
	Number of total neurons in the ventral ganglion		873	
	% of ETP-IR neurons		20.38	

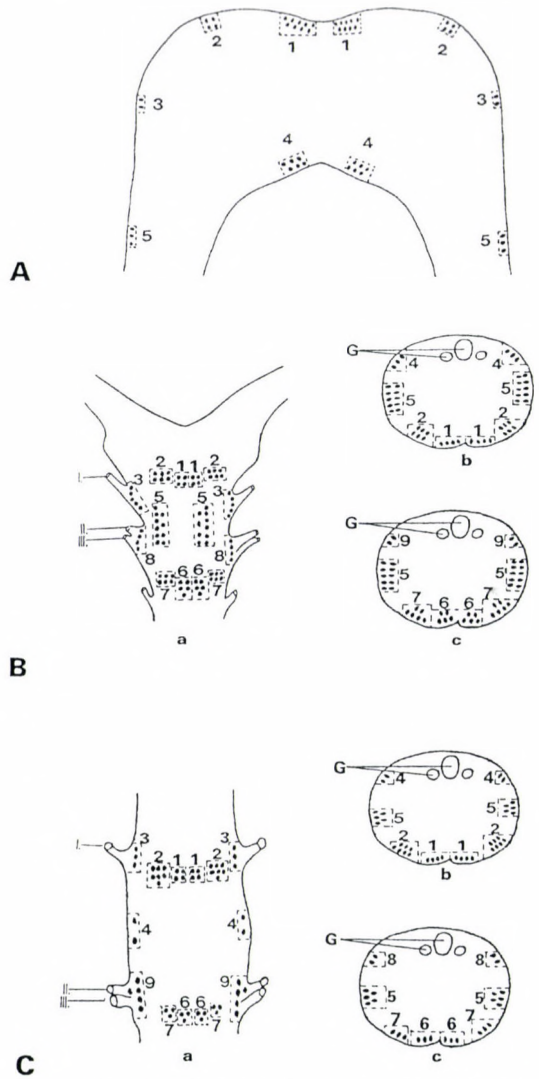

Fig. 2. Schematic representation of the distribution of ETP-IR neurons in the central nervous system of *Lumbricus terrestris*. A: ETP-IR neurons in the brain (frontal view). cc: circumpharyngeal connectives. 1: Dorsomedial, 2: Dorsolateral, 3: Lateral, 4: Ventromedial cell groups, 5: Cells at the origin of the circumpharyngeal connectives. B: ETP-IR neurons in the subesophageal ganglion. a: section of the whole ganglion. b: frontal view of the rostral part of the ganglion. c: the caudal part of the ganglion. G: giant fibres. 1: Ventromedial, 2: Ventrolateral cell groups, 3: Cells at the origin of the 1st segmental nerves, 4: Dorsolateral, 5: Lateral, 6: Ventromedial, 7: Ventrolateral cell groups, 8: Cells at the origin of 2nd, 3rd segmental nerves, 9: Dorsolateral cell groups. C: ETP-IR neurons in the ventral cord ganglion. a: horizontal section of the whole ganglion. b: frontal view of the rostral part of the ganglion, c: frontal view of the caudal part of the ganglion. G: giant fibres. 1: Ventromedial, 2: Ventrolateral cell groups, 3: Cells at the origin of 1st segmental nerve, 4: Dorsolateral, 5: Lateral, 6: Ventromedial, 7: Ventrolateral cell groups, 8: Dorsolateral cell groups, 9: Cells at the origin of 2nd, 3rd segmental nerves

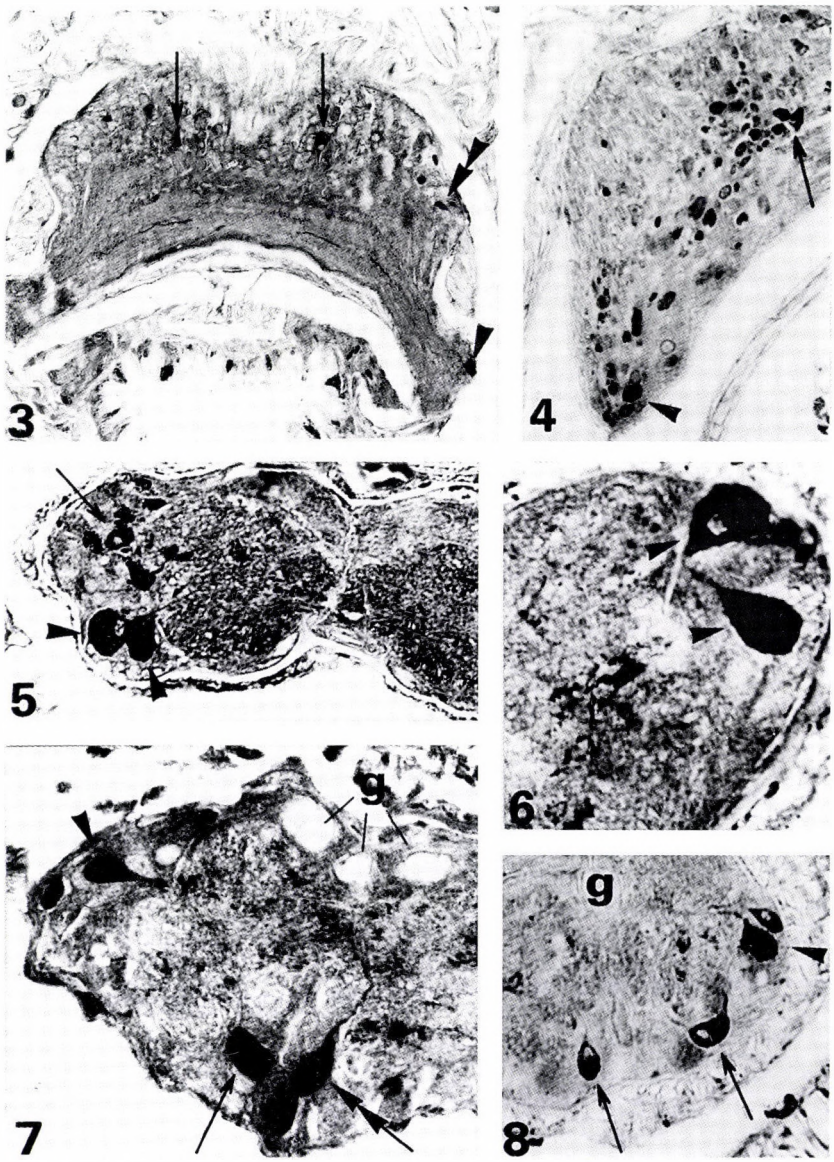

Fig. 3. ETP-IR neurons in the cerebral ganglion of *Eisenia fetida.* Dorsomedial (arrows), lateral (double arrowhead), posterolateral (arrowhead) cells. ×110. *Fig. 4.* ETP-IR neurons in the cerebral ganglion of *Lumbricus terrestris.* Dorsomedial cells (arrow) and cells at the origin of the circumpharyngeal connective (arrowhead). ×110. *Fig. 5.* ETP-IR neurons (arrowheads) at the origin of the 1st segmental nerve in the subesophageal ganglion of *Eisenia fetida* and the lateral cells (arrow). ×210. *Fig. 6.* High magnification of the neurons (arrowheads) situated at the origin of the 1st segmental nerve. ×430. *Fig. 7.* ETP-IR neurons in the ventral ganglion of *Eisenia fetida.* Ventromedial (arrow) and dorsolateral (arrowhead) cells in the rostral part of the ganglion. A heterolateral cell (double arrow) from the ventro-medial cell group. g: giant fibres. ×210 *Fig. 8.* ETP-IR neurons in the ventral ganglion of *Eisenia fetida.* Ventromedial (arrows), ventrolateral (arrowhead) cells. g: giant fibre. ×210

midline of the brain and join the ventral commissure. A few neurons belonging to the lateral and ventrolateral cell groups send their axons to the circumpharyngeal connectives via the ventral commissure.

Subesophageal ganglion

In the subesophageal ganglion 102 ETP-IR cells can be found. They are distributed in six pairs of symmetrically arranged groups. ETP-IR neurons represent 6% of the total population of nerve cells in this ganglion (Table 1). In the rostral part there are four groups. These are the ventromedial (no. 1) cell group and those situated both at the origin of the 1st segmental nerve (no. 2) and at the circumpharyngeal connective (nos 3, 4; Figs 1B, 5, 6). In the caudal part of the ganglion two groups can be distinguished. These are the ventromedial group (no. 5) and a cell group at the origin of the 2nd and 3rd segmental nerves (no. 6). Both the rostral and caudal ventromedial cells (nos 1, 5) and the lateral (no. 4) neurons are large cells (68–75 μm), whereas the diameter of the others varied between 35 and 60 μm.

A few axons belonging to the nerve cells of the 3rd and 4th groups project through the circumpharyngeal connectives and enter the neuropil of the brain. Their neurites can be followed both ipsi- and contralaterally. The ETP-IR cells localised at the origin of the segmental nerves (nos 2, 6) partly project to the periphery via segmental nerves, partly arborise near their perikaryon or enter through the connectives of the ganglion into the longitudinal tracts.

Ventral ganglion

In each ventral cord ganglion there are 178 ETP-IR cells amounting to 20.4% of the total number of the nerve cells. The main ETP-IR cell groups in both the rostral and caudal part of this ganglion are the ventromedial (nos 1, 5), ventrolateral (nos 2, 6) and dorsolateral (nos 3, 7; Fig. 6). Cell groups can also be observed at the origin of the 1st, 2nd and 3rd segmental nerves (nos 4, 8; Table 1, Figs 1C, 7, 8).

The primary neurites of the ETP-IR cells (nos 1, 2, 3, 5, 6) enter the neuropil and project both contra- and ipsilaterally (Fig. 7). A few neurites belonging to the cells situated in the lateral side of the ganglion (nos 4, 8), innervate peripheral organs (body wall, sexual organs, alimentary tract) via the segmental nerves.

Distribution of ETP-IR neurons in the CNS of Lumbricus terrestris

Brain

The brain contains 122 labelled neurons (Table 2) representing 5.6% of the total number. These cells are arranged in five groups localised on the dorsal (nos 1, 2), lateral (no. 3) and ventral (nos 4, 5) side of this ganglion (Figs 2A, 4). The diameter of the neurons is 49–67 μm.

Table 2
Distribution, number and diameter of ETP-IR neurons in the central nervous system of *Lumbricus terrestris*

Ganglion	Cell groups		Cell number	Average diameter (μm) n = 30
	mark	localization		
Cerebral ganglion	1.	Dorsomedial	46	49 ± 8.9
	2.	Dorsolateral	20	59.14 ± 12.79
	3.	Lateral	12	67.13 ± 11.6
	4.	Ventromedial	30	67.1 ± 10.3
	5.	At the origin of the circumpharyngeal connectives	14	61.9 ± 10
	Number of ETP-IR neurons		122	
	Number of total neurons in the cerebral ganglion		2173	
	% of ETP-IR neurons		5.6	
Subesophageal ganglion	1.	Ventromedial	20	63.14 ± 10.7
Rostral part	2.	Ventrolateral	30	61 ± 11.4
	3.	At the origin of 1st segmental nerve	26	42.6 ± 5.7
	4.	Dorsolateral	16	61.3 ± 11
	5.	Lateral	50	52.5 ± 8.8
Caudal part	6.	Ventromedial	24	61.9 ± 7.7
	7.	Ventrolateral	28	52.8 ± 6.8
	8.	At the origin of 2nd, 3rd segmental nerves	22	46.7 ± 4
	9.	Dorsolateral	12	51.9 ± 6.3
	Number of ETP-IR neurons		228	
	Number of total neurons in the subesophageal ganglion		1410	
	% of ETP-IR neurons		16.17	
Ventral cord ganglia	1.	Ventromedial	20	65.6 ± 12
Rostral part	2.	Ventrolateral	36	62.4 ± 7.2
	3.	At the origin of 1st segmental nerve	14	50 ± 3
	4.	Dorsolateral	12	56.85 ± 4.3
	5.	Lateral	24	76.7 ± 12
Caudal part	6.	Ventromedial	14	58.3 ± 9.7
	7.	Ventrolateral	14	61.2 ± 10
	8.	Dorsolateral	12	61.7 ± 4.1
	9.	At the origin of 2nd, 3rd segmental nerves	24	49.2 ± 3.2
	Number of ETP-IR neurons		170	
	Number of total neurons in the ventral ganglion		1355	
	% of ETP-IR neurons		12.54	

The primary neurites of the dorsomedial (no. 1) and ventromedial (no. 4) neurons enter the neuropil and project contra- or ipsilaterally. The dorsolateral (no. 2) and lateral (no. 3) neurons and those which situate at the origin of the circumpharyngeal connective (no. 5) project partly to the neuropil, and partly leave the brain through the circumpharyngeal connectives.

The distribution of the ETP-IR fibres in the neuropil is unequal. Its dorsal and ventral parts contain much more IR fibres than the other parts. Similarly the ventral commissure is rich in ETP-IR fibres because many branches of these neurites enter this commissure.

Subesophageal ganglion

The subesophageal ganglion contains much more ETP-IR cells than that of *Eisenia*. The 228 ETP-IR neurons (16.2% of the total neurons) can be found in nine cell groups (Table 2, Fig. 2B). The pattern of ETP-IR cells in the rostral and caudal parts of the subesophageal ganglion is similar. In both parts of the ganglion there are ventromedial (nos 1, 6), ventrolateral (nos 2, 7) and dorsolateral (nos 4, 9) groups. Also some neurons are located at the origin of the segmental nerves (nos 3, 8). The diameter of ETP-IR neurons in the different cell groups of this ganglion varies between 42 and 63 μm (Table 2).

The primary neurites of the neurons of both ventromedial cell groups (nos 1, 6) arborise near the perikarya, while the neurites of the labelled neurons in the ventrolateral cell groups (nos 2, 7) branch far from their cell bodies in the neuropil [3]. Some axonal branches leave the ganglion through the connectives. The arborisation of the neurites of the ETP-IR neurons in both dorsolateral cell groups (nos 4, 9) is rich and can be found under the giant fibres. The majority of the axons of those neurons belonging to the 3rd and 8th cell groups run to peripheral organs (the body wall and the gut) via the segmental nerves.

Ventral ganglia

In each ventral cord ganglion of *Lumbricus* there are 170 ETP-IR neurons (12.5% of the total neuron number) which belong to nine cell groups (Table 2, Fig. 2C). These are the ventromedial (nos 1, 6), ventrolateral (nos 2, 7) and dorsolateral (nos. 4, 9) cell groups, and the cells that are situated at the origin of the segmental nerves (nos 3, 9). The diameter of the lateral cells is the largest (76.7 ± 12 μm) while the diameter of the other labelled neurons is smaller (49–65 μm).

The primary neurites of the ventromedial (nos 1, 6), ventrolateral (nos 2, 7) and dorsolateral (nos 4, 8) neurons take part in the formation of the neuropil. The majority of the neurites of the lateral neurons (no. 5) similarly to the above-mentioned neurites enter the neuropil, branch and run further in the longitudinal tracts of the ventral ganglia. Neurons situated near the origin of the segmental nerves (nos 3, 9) send their neurites into these nerves.

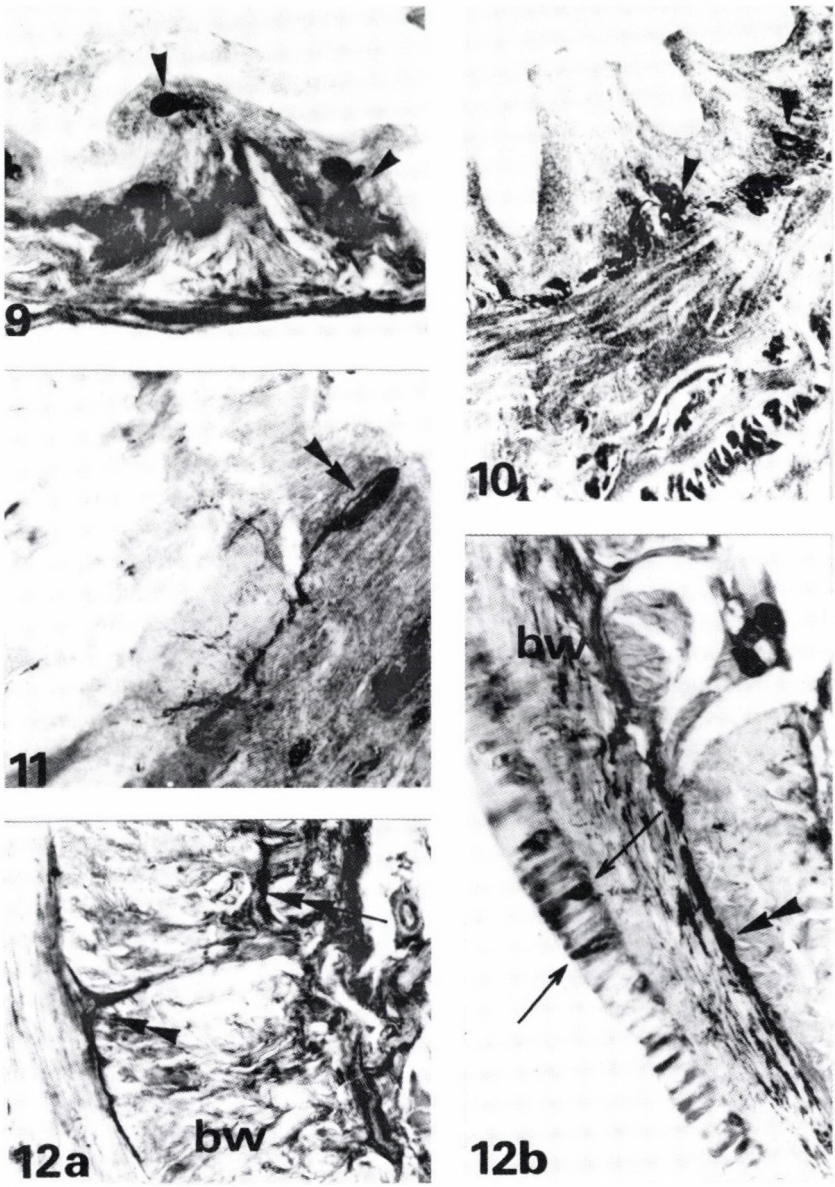

Fig. 9. ETP-IR neurons (arrowheads) in the pharyngeal plexus of *Eisenia fetida.* ×430. *Fig. 10.* ETP-IR neurons (arrowheads) in the enteric plexus of the hindgut of *Eisenia fetida.* ×210. *Fig. 11.* ETP-IR sensory cells among the epithelial cells are (double arrowheads) in the calciferous gland of the *Eisenia fetida.* ×430. *Fig. 12a, b* ETP-IR fibres between the circular and longitudinal muscle layers (double arrowheads) and on the surface of the longitudinal muscle layer (double arrow) of the body wall (bw) in *Eisenia fetida.* There are ETP-IR cells (arrows) among the epithelial cells. a, b ×210

Distribution of ETP-IR neurons in the stomatogastric nervous system

ETP-IR neurons and fibres can be observed in both the stomatogastric ganglia (STG) and enteric plexus. In each STG three ETP-IR neurons and some labelled fibres can be found. Their processes arborise near the perikarya. The IR fibres belong to either the neurons of STG or originate from the CNS via circumpharyngeal connectives. In the enteric plexus the frequency of the neurons decreases along the cranio-caudal axis of the gut (Fig. 9). The plexus of the hindgut contains only a few ETP-IR cells and fibres (Fig. 10). The neurons of the enteric plexus have a few processes but some multipolar neurons also occur. We observed IR cells among the superficial epithelial cells of the alimentary tract. These cells have a central process which run toward the enteric plexus (Fig. 11) but their perikarya are among the epithelial cells of the foregut.

ETP-IR elements in the body wall

The body wall is richly innervated by ETP-IR fibres in both species. The segmental nerves ramify into smaller branches and sometimes IR neurons can be seen in them. The nerve branches further arborise and run either to the inner surface of the longitudinal muscle or spread between the circular and longitudinal muscle layers where they form a plexus (Figs 12a, b). The ETP-IR plexus is particularly dense in the setal sac. There are numerous elongated IR cells in the superficial epithelial layer (Fig. 12b).

DISCUSSION

The present study provides evidence that ETP-IR neurons are present in all parts of the CNS and peripheral nervous system including the SNS of earthworms *Eisenia fetida* and *Lumbricus terrestris*.

There is no substantial difference in the number of ETP-IR cells in these species. The ratio between ETP-immunopositive and ETP-negative neurons in the various ganglia is different. The ratio is higher in the ventral ganglia than in the brain. It suggests that ETP-mediated actions have a more prominent role in these ganglia than in the higher centres.

The IR neurons represent a small but well-defined population in different ganglia of the CNS (i.e. cerebral, subesophageal and ventral cord ganglion). Their distribution can be compared to the location of neurons immunoreactive to other signal molecules.

In the brain the dorsomedial, dorsolateral and lateral ETP-IR neurons (near the circumpharyngeal connectives) seem to overlap partly with serotonin-, octopamine- and GABA-IR cells [3, 16, 17, 18]. In the subesophageal and ventral cord ganglia the main ETP-IR cell groups (except the medial group) show similarities with the cell

groups that contain the above-mentioned signal molecules. In case of proctolin the dorsomedial cells in the brain and lateral cells in the ventral cord ganglia [11] have similar localisation to those of ETP-immunopositive neurons. There is only a minor overlap between the FMRFamide- [7, 15] and ETP-IR cells groups at the dorsomedial region of the brain and ventromedial region of the ventral cord ganglia. Both octopamine and ETP are present in ventromedial and ventrolateral cells [3] of the ventral cord ganglia. These similarities suggest a possible colocalisation of ETP with several neuroactive substances. To clarify this issue experiments are in progress in our laboratory.

Two cell types can be distinguished on the basis of the axonal arborisation and projection patterns of ETP-IR neurons of the CNS. The majority of ETP-immunopositive neurons are interneurons (nos 3, 4 in subesophageal ganglion and 1, 5 in the ventral cord ganglia in *Eisenia*; nos 1, 6 in the subesophageal ganglion and nos 1, 2, 6, 7 in the ventral cord ganglia in *Lumbricus*). The other cell groups in both species contain at least a few projection neurons. The neurites of these cells enter a neighbouring ganglion through the connectives but before leaving it may also arborise in the neuropil of the parent ganglion. These cells may be homo- or heterolateral cells [9].

Some ETP-IR nerves project to the periphery. These efferent neurons belong to the lateral cell groups in both subesophageal- (nos 2, 6 in *Eisenia*; nos 3, 8 in *Lumbricus*) and ventral ganglia (nos 4, 8 in *Eisenia*; nos 3, 9 in *Lumbricus*). Millott [12] described the branches of the segmental nerves in the earthworm. Accordingly the body wall and the gut are innervated by those fibres originating from these nerves.

According to Ukena et al. [21], with the exception of the pharynx, the submucous plexus of the alimentary tract contains ETP immunoreactive elements. Our results prove that ETP-IR cells and fibres occur in all the regions of the alimentary tract. The pharynx has an abundant ETP innervation. Similarly to other signalling systems like 5-HT [2], octopamine [3, 4], GABA [18] and FMRFamide [15], the earthworm pharynx is supplied by ETP innervation, which is partly intrinsic (pharyngeal plexus) and partly extrinsic (from the CNS). The presence of several signalling systems suggests that the pharynx is a reflex centre.

Some ETP-IR cells located in the gut epithelium appear to be sensory neurons on the basis of their morphology. Earlier some monoamine (5-HT, OA), peptide (FMRFamide) and GABA containing sensory neurons have been demonstrated in the gut epithelium of the earthworms [4, 6].

Among the gut epithelial cells of the mid- and hindgut an other ETP-IR cell type can be seen. These cells appear to be glandular cells with similarity to the gastrointestinal peptide secreting cells in vertebrates [5]. In this case ETP may act as a local hormone.

Our results suggest that ETP may play a versatile role (modulatory neurohormone) in both central and peripheral regulatory processes of annelids, including feeding and locomotion of the animals.

ACKNOWLEDGEMENTS

The authors are grateful to Edit Kiss for technical assistance. The imagine-analysis system used in this study was kindly provided by Prof. Gyula Lázár, Department of Anatomy, Pécs University Medical School. This work was supported by National Scientific Research Programs (OTKA) Grant 030959 to M. Cs., and MTA-JPTE Adaptation Biological Research Group, Pécs.

REFERENCES

1. Al-Yousuf, S. A. H. (1992) Neuropeptides and immunocytochemistry in annelids. *Int. Rev. Cytol. 133,* 231–308.
2. Csoknya, M., Lengvári, I., Hiripi, L., Elekes, K.,Vincze, J., Szelier, M., Hámori, J. (1993) Serotonin content during the regeneration of nervous system in earthworm (*Lumbricus terresris* L., Oligohaeta). *Acta Biol. Szeged 39,* 39–49.
3. Csoknya, M., Lengvári, I., Hiripi, L., Eckert, M., Rapus, J., Elekes, K. (1996) Octopamine in the central nervous system of Oligochaeta: an immunocytochemical and biochemical study. *Cell Tissue Res. 285,* 27–37.
4. Csoknya, M., Barna, J., Bánvölgyi, T., Hiripi, L., Eckert, M., Hámori, J., Elekes, K. (1997) Octopamine-containing neurons in the alimentary tract of the earthworm. *Brain Res. 778,* 414–417.
5. Eckert, R., Randall, D., Augustine, G. (1988) *Animal physiology, mechanism and adaptations.* Freeman, New York.
6. Ehinger, B., Myhrberg, H. E. (1971) Neuronal localization of dopamine, noradrenaline and 5-HT in the central and peripheral nervous system of *Lumbricus terrestris* (L.). *Histochemistry 28,* 265–275.
7. Fujii, K., Ohta, N., Sasaki, T., Sekizawa, Y., Yamada, C., Kobayashi, H. (1989) Immunoreactive FMRFamide in the nervous system of the earthworm, *Eisenia fetida. Zool. Sci. 6,* 951–961.
8. Golding, D. W., Whittle, A. C. (1977) Neurosecretion and related phenomena in annelids. In: Bourne, G. H., Danielli, J. F., Jeon, K. W. (eds). *International Review of Cytology* (Suppl. 5). *Aspects of Cell Control Mechanisms.* Academic Press. Inc. New York, pp. 189–302.
9. Günther, J. (1971) Mikroanatomie des Bauchmarks von *Lumbricus terrestris* L. (Annelida, Oligochaeta). *Z. Morphol. Tiere 70,* 141–182.
10. Harada, A., Yoshida, M., Minakata, H., Nomoto, K., Muneoka, Y., Kobayashi, M. (1993) Structure and function of the molluscan myoactive tetradecapeptides. *Zool. Sci. 10,* 257–265.
11. Lengvári, I., Csoknya, M., Lubics, A., Szelier, M., Hámori, J. (1994) Proctolin immunoreactive elements in the nervous system of earthworm *(Lumbricus terrestris). Acta Biol. Hung. 45,* 337–345.
12. Millott, N. (1943) The visceral nervous system of the earthworm: I. Nerves controlling the tone of the alimentary canal. *Proc. Roy. Soc. Lond. B. 131,* 271–295.
13. Ohta, N., Kanda, T., Kuroki, Y., Kubota, I., Muneoka, Y., Kobayashi, M. (1990) Three novel tetradecapeptides isolated from the ganglia of the molluscs, *Achatina fulica* and *Fusinus ferrugineus.* In: Yanaihara, N. (ed.) *Peptide Chemistry,* Protein Research Foundation, Osaka: pp. 57–62.
14. Olive, P. J. W. (1979) Endocrine adaptation in Annelida. In: Barrington, E. J. W. (ed.) *Hormones and evolution.* Vol. 1. Academic Press, Inc., New York, pp. 73–118.
15. Reglődi, D., Slezák, S., Lubics, A., Szelier, M., Elekes, K., Lengvári, I. (1997) Distribution of FMRFamide-like immunoreactivity in the nervous system of *Lumbricus terrestris. Cell Tissue Res. 288,* 575–82.
16. Spörhase-Eichmann, U., Gras, H., Schürmann, F. W. (1987) Patterns of serotonin-immunoreactive neurons in the central nervous system of the earthworm *Lumbricus terrestris* L. I. Ganglia of the ventral nerve cord. *Cell Tissue Res. 249,* 604–614.
17. Spörhase-Eichmann, U., Gras, H., Schürmann, F. W. (1987) Patterns of serotonin-immunoreactive neurons in the central nervous system of the earthworm *Lumbricus terrestris* L. II. Rostral and caudal ganglia. *Cell Tissue Res. 249,* 625–632.

18. Telkes, I., Csoknya, M., Buzás, P., Gábriel, R., Hámori, J., Elekes, K. (1996) GABA-immunoreactive neurons in the central and peripheral nervous system of the earthworm, *Lumbricus terrestris* (Oligochaeta, Annelida). *Cell Tissue Res. 285,* 463–475.
19. Takahashi, T., Furukawa, Y., Moneoka, Y., Matsushima, O., Ikeda, T., Fujita, T., Minakata, H., Nomoto, K. (1995) Isolation and characterization of four novel bioactive peptides from a polychaete annelid, *Perinereis vancaurica. Comp. Biochem. Physiol. 110C,* 297–304.
20. Ukena, K., Oumi, T., Matsushima, O., Ikeda, T., Fujita, T., Minakata, H., Nomoto, K. (1995) A novel gut tetradecapeptide isolated from the earthworm *Eisenia fetida. Peptides 16,* 995–999.
21. Ukena, K., Oumi, T., Morishita, F., Furukawa, Y., Matsushima, O., Takahama, H., Miyata, S., Ikeda, T., Minakata, H., Nomoto, K. (1997) Immunochemical demonstration of *Eisenia* tetradecapeptide, a bioactive peptide isolated from the gut of the earthworm *Eisenia fetida,* in tissues of earthworm. *Cell Tissue Res. 288,* 567–573.
22. Watson, W. H., Groome, J. R., Chronwall, B. M., Bishop, J., O'Donohue, T. L. (1984) Presence and distribution of immunoreactive and bioactive FMRFamide-like peptides in the nervous system of the horseshoe crab, *Limulus polyphemus. Peptides 5,* 585–592.
23. Zamboni, L., De Martino, L. (1967) Buffered picric acid-formaldehyde: A new rapid fixative for electron microscopy. *J. Cell Biol. 35,* 148B.

Acta Biologica Hungarica 51(2–4), pp. 409–416 (2000)

REORGANIZATION OF PEPTIDERGIC SYSTEMS DURING BRAIN REGENERATION IN *EISENIA FETIDA* (OLIGOCHAETA, ANNELIDA)+

T. BÁNVÖLGYI[1]*, J. BARNA[1], MÁRIA CSOKNYA[1], J. HÁMORI[1] and K. ELEKES[2]

[1]Department of General Zoology and Neurobiology, Janus Pannonius University, Ifjúság u. 6, H-7624 Pécs, Hungary
[2]Department of Experimental Zoology, Balaton Limnological Research Institute of the Hungarian Academy of Sciences, Tihany, Hungary

(Received: August 31, 1999; accepted: November 30, 1999)

After the extirpation of the brain reorganization of the peptidergic (FMRFamide, neuropeptide Y, proctolin) systems was studied in the newly forming cerebral ganglion of the annelid *Eisenia fetida*. During regeneration, all immunoreactive fibres appear on the 1st–2nd postoperative day. At the beginning of regeneration, immunoreactive neurons and fibres form a mixed structure in the wound tissue. On the 3rd postoperative day, FMRFamide positive and neuropeptide Y-immunoreactive, while on the 7th postoperative day proctolin-immunoreactive neurons appear in the loose wound tissue. From the 25th postoperative day a capsule gradually develops around it. The neurons of the preganglion move to the surface of the newly appearing preganglion. The number of these cells gradually increase, and by the 72th–80th postoperative days the localization and number of peptide-immunoreactive neurons is similar to that in the intact one.

The neurons of all examined peptidergic systems may originate from the neuroblasts, situated on the inner and outer surface of the intact ganglia (e.g. suboesophageal and ventral cord ganglia). In addition FMRFamide and proctolin immunoreactive neurons may take their derive by mitotic proliferation from the pharyngeal neurons, too.

Keywords: Brain regeneration – peptidergic neurons – FMRFamide – proctolin – Neuropeptide Y – earthworm – *Eisenia*.

INTRODUCTION

The central nervous system (CNS) of oligochaetes possess a good regenerative capability. The regeneration is controlled by several external (e.g. food, temperature) and internal (e.g. signal molecules) factors, and this is also true for the neuroregeneration. It has been known that serotonin, dopamine and octopamine play a role in the activation of the cell adhesion molecules and influence the proliferation and migration of the neurons [9, 13, 14, 19].

+ Presented at the 9th ISIN Symposium on "Neurobiology of Invertebrates", July 1–5, 1999, Tihany, Hungary.

*Corresponding author, E-mail: vakapad@ttk.jpte.hu

0236-5383/2000/$ 5.00

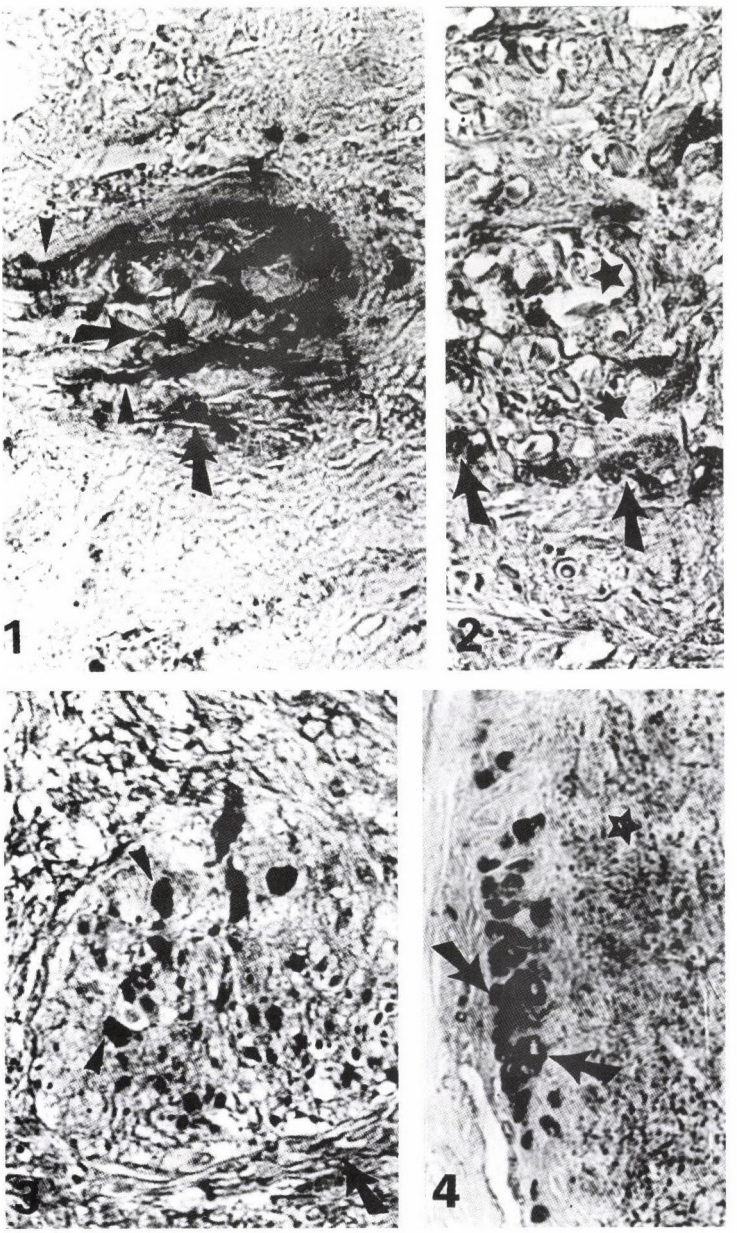

Fig. 1. The frontal section of the forming preganglion on the 12th postoperative day. FMRFamide-IR cells (arrows) and IR fibres (arrowheads) can be seen. ×200. *Fig. 2.* On the 7th postoperative day proctolin-IR cells (arrows) are present in the wound tissue (asterisks). ×200. *Fig. 3.* A capsule (arrow) is gradually built a round the preganglion from the 28th postoperative day. Proctolin-IR neurons (arrowheads). ×200. *Fig. 4.* On the 56th postoperative day, all cells of the dorsomedial (arrows) NPY-IR neuron group can be observed. Note the many NPY-IR fibres (asterisk) in the neuropil. ×200

FMRFamide and proctolin, both typical invertebrate neuropeptides, have been suggested to play a hormon-like role in the ontogenesis and regeneration of invertebrates [16, 17, 18]. Despite the well-known regenerative capacity of some lower invertebrates the mechanism of regeneration and the effects of the signal molecules influencing this process have not yet been investigated in detail, neither have been the origin appearence and organisation of neurons containing these signal molecules during brain regeneration. Therefore the aim of the present study was to investigate the reorganization of the brain, with special attention to some neuropeptide-containing components.

MATERIAL AND METHODS

Our investigations were carried out on adult specimens of *Eisenia fetida* (Oligochaeta, Annelida). Before operation the animals were anasthetised in carbonated water. The dorsal side of the body wall in 4th–8th segments were cut and the brain was removed by cutting the circumpharyngeal connectives. After brain extirpation the animals isolated from each other, were kept, in soil in a climate box at 10 °C temperature and 60% humidity.

At different postoperative time points (5th, 10th, 24th hours 3rd, 5th, 7th, 10th, 12th, 28th, 35th, 42nd, 48th, 56th, 63rd, 72nd, 76th, 80th days) the first eight segments were cut and fixed. The sample tissues were fixed in Zamboni-solution [20] for FMRFamide-, in 4% PFA in phosphate-buffered saline for NPY-, and in GPA solution (15 ml saturated picric acid, 5 ml 25% glutaraldehyde, 0.2 ml glacial acetic acid, 5) for proctolin immunocytochemistry. After fixation the tissue samples were dehydrated and embedded in Paraplast and immunochemistry was carried out on 7 μm serial sections.

For immunostaining the following antisera were used: anti-FMRFamide (1 : 1000; Chemicon) and anti-Neuropeptide Y (1 : 2000; Sigma), anti-proctolin (1 : 500; 10). The visualization of the immunoreaction was performed with ExtrAvidin kit (1 : 20; Sigma) and the diaminobenzidine reaction.

RESULTS AND DISCUSSION

The regeneration of the brain can be divided into two main periods, from which the first period is not related directly to neuroregeneration. In this period the wound caused by the brain extirpation is partly closed by muscular contractions, and partly by the epithelial cells spreading actively over it. The new epithelial cells originate from the basal cells with gradual differentation [6]. The newly formed epithelial layer is unpigmented. Later the muscle layers also regenerate and on the 2nd and 3rd postoperative days the reorganization of the body wall is finished. At the place of the removed brain a loose wound tissue is built from the coelomocytes [12]. The wound tissue is organized as a loose structure which gradually becomes separated into two

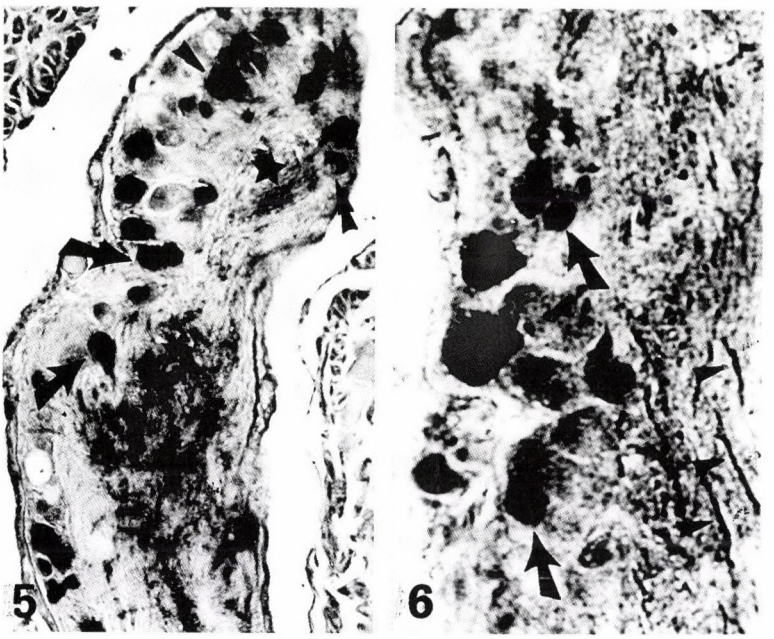

Fig. 5. The main FMRFamide cell groups on the 80th postoperative day. Dorsomedial (arrows), dorsolateral (arrowhead), lateral cell group (double arrowhead). IR fibres (asterisks) in the neuropil. ×180.
Fig. 6. High magnification picture of the dorsomedial FMRFamide-IR neurons (arrows). IR fibres (arrow-heads) in the neuropil. ×350

parts, forming the hemispheres of the new brain. The preganglion, where fibres and neuronal somata form a loose mixed structure, becomes more compact with increasing number of the nervous elements in it.

The second period is the neural regeneration: at the beginning of this process (from the 2nd and 3rd postoperative day) peptidergic fibres appear in the loose wound tissue. Some of these fibres are regenerated axons of neurons located in the subesophageal ganglion, projecting either ipsi- or contralaterally in the brain. These axons can be detected earlier than those belonging to the newly appearing neurons in the regenerating brain itself.

Beside the immunoreactive (IR) fibres, and perikarya can be found on the 3rd postoperative day. The order of appearance of the IR neurons is the following: on the 3rd postoperative day 13 FMRFamide-IR cells and 15 NPY-IR cells, and by the 7th postoperative day 13 proctolin-positive cells can already be found (Figs 1, 2). From the 25th–35th postoperative days a connective tissue capsule is formed around the preganglion (Fig. 3). The capsule is completely closed by the end of the gangliogenesis. At the same time most IR cells move to the surface of preganglion (dorsal, lateral and ventro-lateral), meanwhile some move to the ventral side. The number of these IR neurons increases substantially later on until the 56th postoperative day. From the 7th to the 35th postoperative day the proctolin-IR cell numbers increase

faster, however, from the 35th to the 65th postoperative day the increase is smaller than before.

On the 56th postoperative day (Fig. 4), the dorsomedial, dorsolateral, lateral, posterolateral and central-IR cell groups can be found in the new brain but the number of the IR cells in the different groups is lower than in the intact earthworm (Fig. 7). By the 80th postoperative day the last (ventromedial) cell group also appears and the number of the peptidergic neurons is similar to that of the intact worm (Figs 5, 6, 8).

It has been known that the regeneration capacity depends on enviromental conditions [15] and the phylogenetic position of the species [11]. The centralization especially the cephalization of the nervous system gradually decreases the capability for regeneration.

The brain regeneration of *Eisenia fetida* can be divided into two main periods, namely the organization of the wound tissue and the gangliogenesis. The wound tissue serves as the sceleton for the immigrating neurons.

On the basis of the appearance and migration of the nervous elements the gangliogenesis of the brain can be divided into four stages; (i)–(ii) appearance of the different peptidergic-IR elements (fibres and neurons); (iii) capsule develops and the ganglion begins to be formed; (iv) IR cells occupy their final positions. These stages are similar to those described recently in the case of the reorganization of GABA-ergic elements [2, 3, 4]. The time-scale of the reappearance of the peptidergic neurons is different. FMRFamide- and NPY-IR cells from the 3rd, proctolin IR neurons from the 7th postoperative day can be seen.

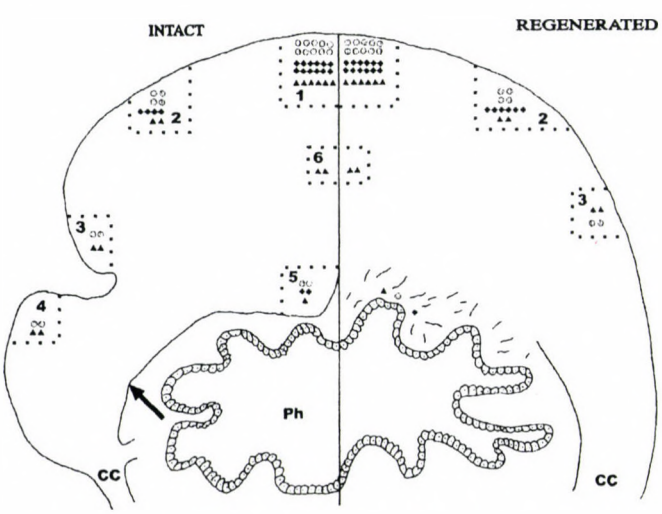

Fig. 7. Schematic drawing of the intact and regenerating brain (56th postoperative day). 1: dorsomedial, 2: dorsolateral, 3: lateral, 4: posterolateral, 5: ventromedial, 6: central cell groups. cc: circumpharyngeal connectives, Ph: pharynx, ▲: NPY-IR cells, ●: proctolin-IR cells, ♦: FMRFamide-IR cells, →: capsule

The first FMRFamide and NPY-IR neurons appear and can be seen together with some monoaminergic [7] and GABA-IR neurons [2]. Our observations contradict those of Reuther et al. [18] who stressed that the serotoninergic nervous elements appear earlier in development than the peptidergic ones.

Some monoamines [12] and also peptides or amino acids (GABA, 1) seem to accelerate the process of regeneration. Serotonin and GABA have a stimulatory effect on the neuronal regeneration [2]. These peptides might act as hormones, stimulating the migration and/or proliferation of neuroblasts.

One major unsolved question is the origin of the new neurons. The missing neurons would presumably be replaced by those deriving from the neuroblasts or the

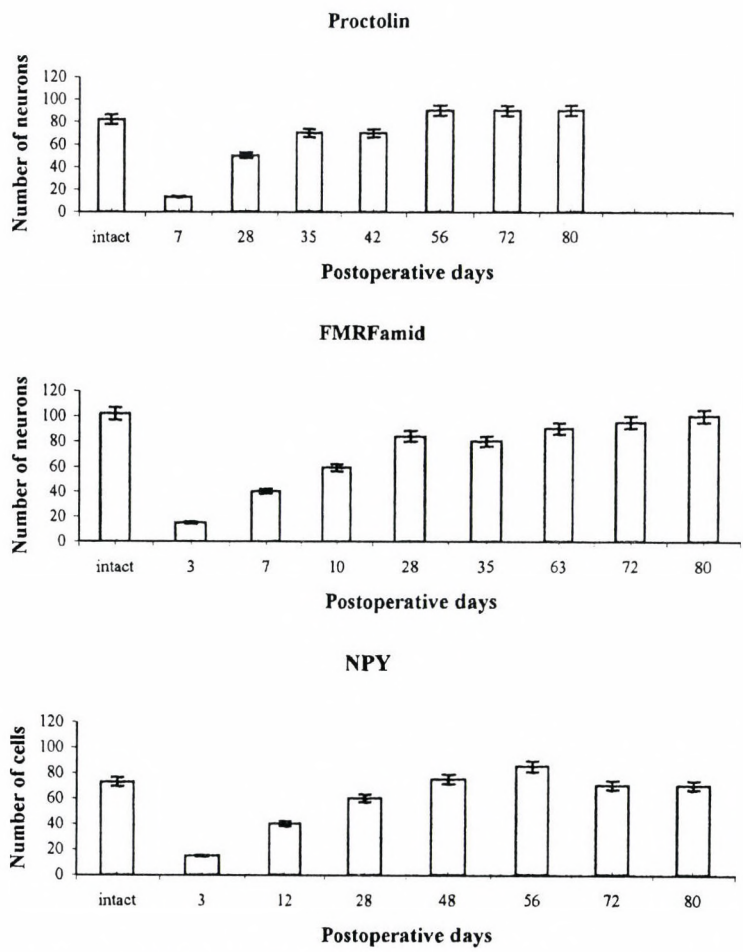

Fig. 8. The number of peptidergic (proctolin-, FMRFamide-, NPY-) IR cells during brain regeneration in *Eisenia fetida*

proliferation of the mature neurons. In adult earthworms neuroblasts can be found in the inner and outer surface of the intact ganglia and the peritoneum. Our earlier results indicate that such cells can be labelled after the GABA-, 5HT immunocytochemistry [2, 3, 4, 8].

At the same time, some FMRFamide- and proctolin-IR neurons may derive from the neurons of dorsal pharyngeal plexus by mitotic proliferation.

ACKNOWLEDGEMENTS

Authors are grateful to Edit Kiss for technical assistance. This work was supported by National Scientific Research Programs (OTKA) Grant 030959 to M. Cs., and MTA-JPTE Adaptation Biological Research Group, Pécs, and the Founds for Research and Development in Higher Education (No. 0816/6409005)

REFERENCES

1. Antonopoulos, J., Pappas, J. S., Pamavelas, J. G. (1997) Activation of the GABAA receptor inhibits the proliferative effects of bFGF in cortical progenitor cells. *Eur. J. Neurosci. 9,* 291–298.
2. Bánvölgyi, T., Barna, J., Telkes, I., Csoknya, M., Elekes, K., Hámori, J. (1997) Effect of GABA-treatment on the regeneration of the brain of *Eisenia fetida* (Oligochaeta, Annelida). In: Elsner, N., Wässle, H. (eds) Proc. 25th Göttingen Neurobiology Conference, G. Thieme Verlag, Stuttgart–New York, p. 951.
3. Bánvölgyi, T., Barna, J., Csoknya, M., Hámori, J., Elekes, K. (1998) Peptidergic and aminergic neurons in the regenerating brain of the *Eisenia* (Oligochaeta). *Eur. J. Neurosci. 10, Suppl. 10,* 202.72.
4. Bánvölgyi, T., Barna, J., Csoknya, M., Hámori, J., Elekes, K. (1998) Regeneration of FMRFamide-immunoreactive and proctolin-immunorective neurons in the brain of *Eisenia fetida. Neurobiology 6,* 165.
5. Boer, H. H., Schot, L. P. C., Roubos, E. W., Maat, A., Lodder, J. C., Reicheld, D. (1979) ACTH-like immunoreactivity in two electronically coupled giant neurons in the spond snail *Lymnea stagnalis. Cell Tissue Res. 202,* 231–240.
6. Chapron, C. (1970) Structure et évolution des cellules de régénération mésodermiques dans les jeunes régénérats du lombricien *Eisenia foetida* (Saw). *J. Microsc. 9,* 347–354.
7. Csoknya, M., Hiripi, L., Juhos, Sz., Elekes, K., Szelier, M., Lengvári, I., Hámori, J. (1994) Monoamine content of the normal and regenerating nervous system in annelids. *Eur. J. Neurosci. 6, Suppl. 6,* 27.01.
8. Csoknya, M., Barna, J., Bánvölgyi, T., Kiss, E., Telkes, I., Hámori, J., Elekes, K. (1997) The chemical and neuroanatomical characterization of the brain regeneration in earthworms *(Eisenia fetida). Neurobiology 5,* 1115.
9. Curry, W. J., Fairweather, I., Johnston, C. F., Halton, D. W., Buchanan, K. D. (1989) Immunocytochemical demonstration of vertebrate neuropeptides in the earthworm *Lumbricus terrestris* (Annelida, Oligochaeta). *Cell Tissue Res. 257,* 577–586.
10. Eckert, M., Ude, I. (1983) Immunocytochemical techniques for the identification of peptidergic neurons. In: Strausfeld, N. J. (ed.) *Functional Neuroanatomy.* Springer, Heidelberg, Berlin, New York, pp. 000–000.
11. Hibbard, E. (1963) Regeneration in the severed spinal cord of the Cordate larvae of the *Petromyzon marinus. Exp. Neurol. 7,* 175–185.
12. Jamieson, B. G. M. (1981) *The ultrastructure of the Oligochaeta.* Academic Press, London, New York, Toronto, Sidney, San Francisco.
13. Koritsánszky, S., Hartwig, H. G. (1974) The regeneration of the monoaminergic system in the cerebral gangion of the earthworm, *Allolobophora caliginosa. Cell Tissue Res. 151,* 171–186.

14. Martelly, I., Franquinet, R., LeMoigne, A. (1981) Relationship between variations of cAMP, neuromodulators and the stimulation of nuclei acid synthesys during planarian *(Polycelis tenuis)* regeneration. *Hydrobiologia 84,* 195–201.
15. Needham, A. E. (1952) *Regeneration and Wound Healing.* Wiley, New York.
16. O'Shea, M., Schaffer, M. (1985) Neuropeptide function: the invertebrate contribution. *Ann. Rev. Neurosci. 8,* 171–98.
17. Palmberg, I., Reuter, M. (1990) Neural subsets in regenerating *Microstomum lineare.* Immunocytochemistry of FMRF/RF-amide and 5-HT. In: Gustafsson, M. K. S., Reuter, M. (eds), *The Early Brain,* Acta Academy Press, Åbo (Turku), pp. 147–160.
18. Reuter, M., Gustafsson, M. (1996) Neuronal signal substances in asexual multiplication and development in flatworms. *Cell. Mol. Neurobiol. 16,* 591–616.
19. Stefano, G. B., Scharrer, B. (1981) High affinity binding of an enkephalin analog in the cerebral ganglion of the insect *Leucophaea maderae* (Blattaria). *Brain Res. 225,* 107–114.
20. Zamboni, L., De Martino, L. (1967) Buffered picric acid-formaldehyde: new rapid fixative for electron microscopy. *J. Cell Biol. 35,* 148A.

Acta Biologica Hungarica 51 (2–4), pp. 417–431 (2000)

THE CENTRAL NERVOUS SYSTEM, ITS CELLULAR ORGANISATION AND DEVELOPMENT, IN THE TADPOLE LARVA OF THE ASCIDIAN *CIONA INTESTINALIS*+

I. A. MEINERTZHAGEN[1]*, A. G. COLE[2] and S. STANLEY[2]

[1]Neuroscience Institute, Life Sciences Centre, Dalhousie University, Halifax, Nova Scotia, Canada B3H 4J1
[2]Department of Biology, Life Sciences Centre, Dalhousie University, Halifax, Nova Scotia, Canada B3H 4J1

(Received: August 31, 1999; accepted: November 30, 1999)

From its numerical composition, the central nervous system (CNS) of the ascidian larva is one of the simplest known nervous systems having a chordate plan. Fewer than 350 cells together constitute a caudal nerve cord, an interposed visceral ganglion containing motor circuits for swimming and, rostrally, an expanded sensory vesicle containing major sensory and interneuron regions of the CNS. Some cells are ependymal, with ciliated surfaces lining the neural canal, while others are clearly either sensory receptors or motoneurons, but most are distinguishable only on cytological grounds. Although reassignments between categories are still being made, there is evidence for determinacy of total cell number. We have made three-dimensional cell maps either from serial semithin sections, or from confocal image stacks of whole-mounted embryos and larvae stained with nuclear markers. Comparisons between the maps of neural tubes in embryos of successive ages, that is, between cells in one map and their progeny in older maps, enable us to follow the line of mitotic descent through successive maps, at least for the caudal neural tube. Details are clear for the lateral cell rows in the neural tube, at least until the latter contains ~320 cells, and somewhat for the dorsal cell row, but the ventral row is more complex. In the hatched larva, serial-EM reconstructions of the visceral ganglion reveal two ventrolateral fibre bundles at the caudalmost end, each of 10–12 axons. These tracts include at least five pairs of presumed motor axons running into the caudal nerve cord. Two pairs of axons decussate. Complementing this vertebrate feature in the CNS of the larval form of *Ciona,* we confirm that synapses form upon the somata and dendrites of its neurons, and that its motor tracts are ventral.

Keywords: Confocal microscopy – serial EM – decussation – ependymal cells – visceral ganglion – neural tube – neurulation – blastomere.

INTRODUCTION

Ascidians have come under close scrutiny from zoologists ever since the structure of the larval form of their life-cycle and its embryonic development were first clearly reported, and correctly inferred [20] to support their taxonomic position close to the ancestral stock of all chordates [2, 4, 16], including vertebrates. This position derives

+ Presented at the 9th ISIN Symposium on "Neurobiology of Invertebrates", July 1–5, 1999, Tihany, Hungary.

*Corresponding author, E-mail: IAM@IS.DAL.CA

0236-5383/2000/$ 5.00

from the chordate body form of the tadpole larva [19], which is among the simplest of any group of animals with chordate characters. In ascidians, as in other urochordates [6], these characters include the anatomical characteristics of the dorsal tubular central nervous system (CNS) [6, 7, 19], and its derivation from a neural plate [9, 26, 27] by the process of neurulation [23]. Recent, more powerful molecular evidence joins with what is already morphologically intuitive to confirm the homology of urochordate and vertebrate CNS plans. The expression of dorsoventral patterning genes in the vertebrate neural tube is, for example, conserved in the ascidian embryo [10, 32]. Thus from a number of different perspectives we can view the CNS of the ascidian larva as not only numerically accessible but also prototypically chordate.

In the ascidian larva, these chordate credentials are all to be found in a CNS which both is numerically simple, in the larva of *Ciona intestinalis* about 340 cells [25], and arises in an experimentally well characterised embryo [31]. The latter undergoes rapid cleavage to form a free-swimming dispersive larva, before metamorphosing to an adult [8]. Although the attribution of the CNS cells to such simple categories as those that manifest either a neuronal or an ependymal phenotype has so far only been possible on rather insecure cytological grounds (see, however, [36], it is clear that the number of neurons is few, estimated to be about 100 in the case of *Ciona* [25].

During development, the ascidian embryo undergoes a pattern of radial cleavages [9, 31] which, unlike the embryos of vertebrates, are both invariant and synchronised and which partition the egg's cytoplasm into blastomeres, the progeny of which assume particular fates in the differentiated larva. Because cleavage is thought to be both invariant and synchronised, the pattern of mitotic descent, or cell-lineage, previously described for the neural plate of the *Ciona* embryo up to between the 9th and 11th cleavages [23], is normally an important and perhaps wholly fixed prognosis of normal embryonic cell fate. Thus at any time in development each cell of the neural plate, or its progeny, is proposed to have not only a fate, but also a position and, thereby, a set of neighbours, that are all totally predictable. The relationship between the eventual fate of the cell in the CNS of the larva, for example whether it will be neuronal or glial, and if neuronal whether it will be sensory or motor, or whether it will secrete a particular transmitter, and the preceding cell-lineage in the embryo which gives rise to the cell is still not clear, however. This awaits the development of usable cell maps for the CNS in the final larva as well as in its preceding embryonic stages. Our report communicates recent progress towards those ends.

MATERIALS AND METHODS

Animals

Adult *Ciona intestinalis* (Fig. 1A) were obtained either from the Department of Marine Resources, Marine Biological Laboratory, Woods Hole, MA, or from a population off the coast of Tasmania, Australia (courtesy of Dr. D. Nicol). These were used to produce larvae (Fig. 1B) by cross-fertilization [11, 24]. For light and electron

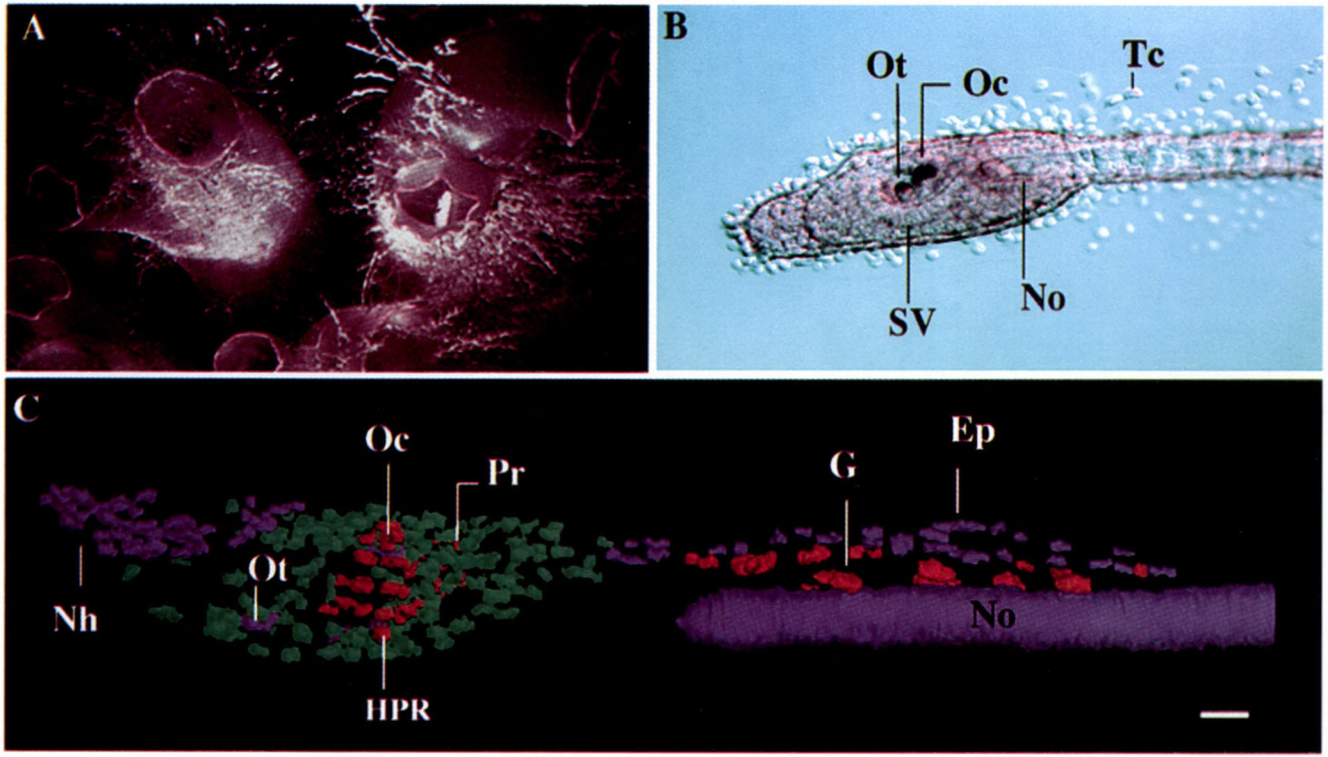

Fig. 1. The CNS in the tadpole larva of *Ciona intestinalis*. A: Adult *Ciona intestinalis*. Note large atrial and branchial siphon of each zooid. B: Trunk and rostral tail of larva, Nomarski optics. Internal organisation reveals the outline of the sensory vesicle (SV), containing the pigmented ocellus (*Oc*) and otolith (*Ot*), in relation to the rostral end of the notochord (*No*). The transparent tunic is revealed by the presence of numerous test cells (*Tc*). C: Computer 3-D reconstruction of the CNS revealed from the locations of nuclei relative to the outline of the notochord, *No* (cf B), and the rostral neurohypophysis (*Nh*). Nuclei of the following receptor systems include: pigment cells of the otolith (*Ot*) and ocellus (*Oc*); photoreceptors (*Pr*); and hydrostatic pressure receptors (*HPR*). In the elongate visceral ganglion lie nuclei of ganglion cells (*G*) and ependymal cells (*Ep*). Scale bar 10 μm

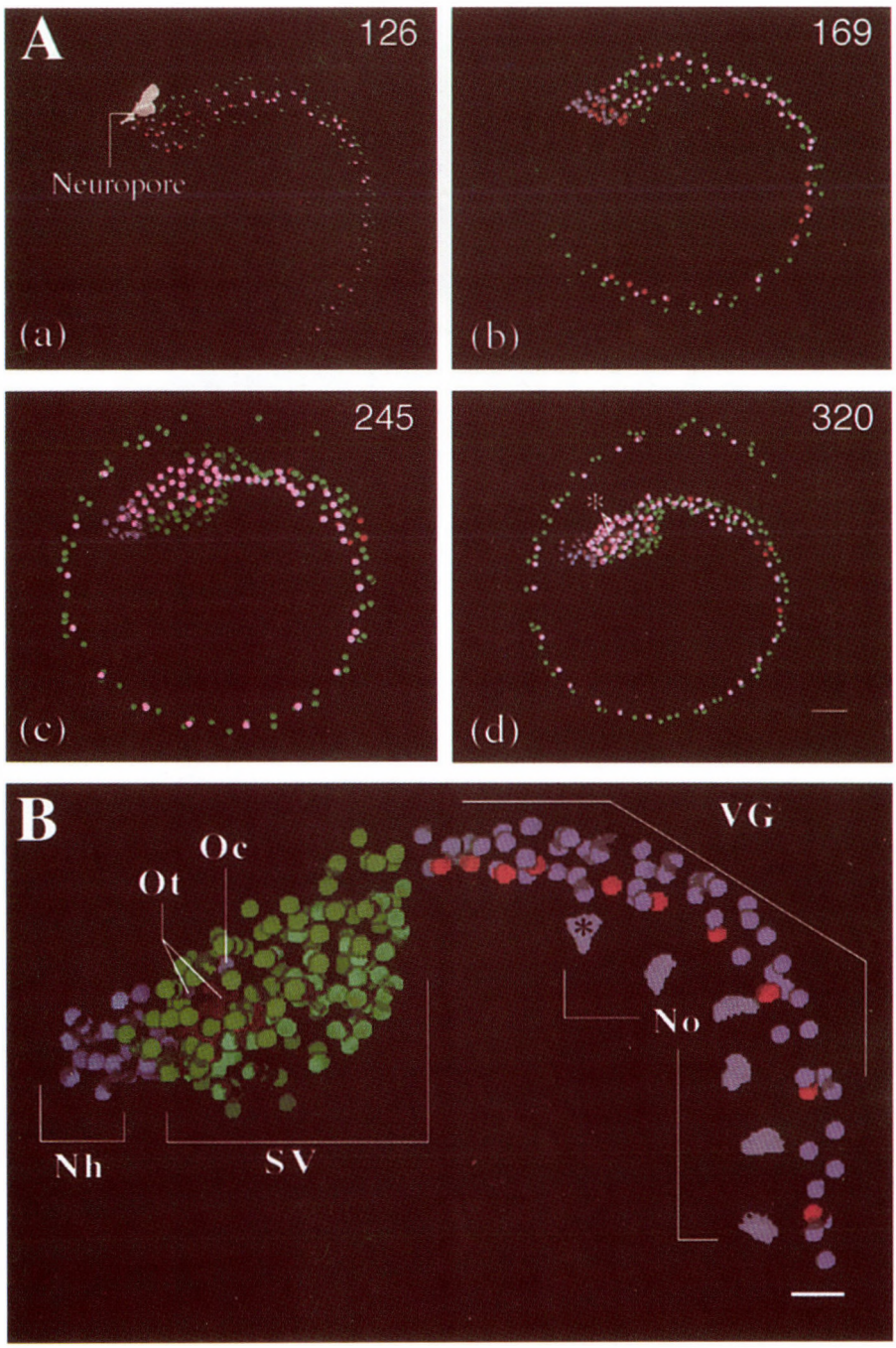
A
126
Neuropore
(a)
169
(b)
245
(c)
320
(d)
B
Oc
Ot
VG
No
Nh
SV

microscopy, Tasmanian larvae were fixed and embedded as previously reported [25]. For confocal microscopy, Woods Hole larvae were fixed in 4% paraformaldehyde in sea water.

Cell maps from 3-D reconstructions

To gain an understanding of the three-dimensional distribution of cells within the larval CNS, we have created a virtual 3-D reconstruction from a transversely sectioned larva (Fig. 1C), using a series of semithin sections 1 μm thick stained with toluidine blue. The 500 or so sections from one entire larva were photographed using a Zeiss Axiophot microscope equipped with both brightfield optics for a 63×/1.4 objective (for the outline of the entire larva) and phase contrast microscopy for a 100×/1.3 objective (for the cells of the CNS). The images of consecutive negatives, every fourth for the 63× series and every second for the 100× series, were aligned, captured with a CCD camera, and brought into 3-D reconstruction software (ICAR: ISG Technologies Inc.), from which the digitised outlines of profiles were then reconstructed, all as previously reported [22]. Cell identity was made from the cytological appearance of the perikaryon and the size of its nucleus. Cells were also identified from their position with respect to the neural canal, which is lined by ependymal cells [25].

Confocal microscopy

To follow the final one or two divisions that produce the cells of the larval CNS, we labelled nuclei in fixed wholemount preparations of *Ciona intestinalis* embryos using a 1 : 200 solution of the fluorescent nuclear probe BOBO-3 (Molecular Probes Inc., Eugene, OR) in PBS containing 4% Triton-X100. Image stacks of wholemount preparations were then collected by confocal microscopy (Zeiss LSM410). Software (NIH Image, v. 1.41S) was then used to mark artificially the nuclei of the CNS with-

←

Fig. 2. The CNS of the ascidian larva reconstructed from confocal image stacks of nuclei stained with BOBO-3. Reconstructions are of nuclei that were first selected and highlighted in pseudo-colour using software (NIH Image). A: Larvae at four successive stages of increasing age, when the CNS contains the following numbers of cells: (a) 126 cells, the neuropore, reconstructed from the surface of the embryo, is almost completely closed over; (b) 169 cells; (c) 245 cells; (d) 320 cells. The nucleus of the otolith and its corresponding pigment granules is marked with an asterisk (*). Also labelled are cells which constitute the left lateral row, and descendants of these cells (highlighted in yellow); cells that are visibly mitotically active (red); and cells located rostrally, which are presumed to be the cells of the neurohypophysis but have a final position in the larva which is currently not known (green). Scale bar: 20 μm. B: Rostral end of CNS enlarged from (d), above, when the CNS has in total 320 cells, close to the final number in the hatched larva. Reconstructed profiles are colour coded to match the corresponding regions of cells in figure 1c. Profiles of notochord nuclei (*), from one optical section, are reconstructed to indicate the position of the notochord. Nh: neurohypophosis; SV: sensory vesicle; VG: visceral ganglion; Ot: otolith nucleus and corresponding pigment granules; Oc: ocellus nuclei; No: notochord. Scale bar: 10 μm

in these three-dimensional stacks. The labels, coloured discs superimposed on the nuclear centres, were then reconstructed to convey detailed cell maps of the relative nuclear positions within the embryonic CNS (Fig. 2A, B). We used the number and relative positions of cell nuclei, and their cytological appearance, to identify the nuclei of the same cells in different larvae, then by linking cells in one map to their progeny in older maps from the locations of dividing nuclei (Fig. 2A [a–d]), we followed cells through consecutive maps, thereby recording the lineage of mitotic ancestry.

Serial-EM reconstructions

To trace the pathways and connections of identified cells within the larval CNS, we examined two series of ultrathin sections, both 70 nm thick, one of about 2,000 sections on which most analysis was undertaken. This was cut from the rostralmost portion of the nerve cord through to the level of the otolith in the sensory vesicle. We viewed sections from this series on a Philips 201C EM and photographed every third section at ×2.250 on 35 mm film, making montages of ≤6 frames per section to cover the largest area of the visceral ganglion. Images were scanned into digital format, and printed on paper to provide working micrographs. The presence of neurites and synapses was used either to confirm or identify neurons and then to trace their connections through consecutive prints. Because the cells of the visceral ganglion could not immediately be identified from cell maps previously depicted using manual methods [25], the neurons traced in our EM series have so far been given arbitrary numbers, commencing in the neck region. Profiles of axon pathways were traced in the descending tracts that passed through the visceral ganglion, either from the sensory vesicle or into the nerve cord.

RESULTS AND DISCUSSION

The arrangement of cells within the CNS

Of the approximately 340 CNS cells, about 65 constitute the caudal nerve cord of the tail [25], with four cells in a cross-section each lining the neural canal [23, 25] (Fig. 3). These are mostly ependymal cells, non-neuronal cells with ciliated surfaces lining the neural canal [14]. Rostral to these lies the visceral ganglion, within which some cells innervate the lateral muscle bands of the tail. The positions of these cells have now been reconstructed from the locations of their nuclei in three dimensions (Fig. 1C). Although total cell number confirms that reported previously by Nicol and Meinertzhagen [25], with 266 ± 3 cells in the trunk region of the CNS (the sensory vesicle plus the visceral ganglion), there are some reassignments between the categories of cells. In their original communication, Nicol and Meinertzhagen [25] reported at least 45 cells in the visceral ganglion, but the exact border between visceral ganglion and nerve cord is difficult to establish by light microscopic appearance

of the cells alone. By one criterion, the border of the visceral ganglion could be assigned to the place at which the neuropile split into two ventrolateral bundles (see below). At this level the cross-section of the ganglion contains only four cell bodies, and is thus like the nerve cord. The final determination of cell type will have to await the development of sufficient molecular markers that can distinguish different cell types (see Conclusions and Prospects, below). Six cells (arranged in three pairs) previously identified as neck cells between the visceral ganglion and sensory vesicle [25] also belong to the visceral ganglion. The caudalmost pair of the three appears to be motoneurons. Together, the six cells augment the number of visceral ganglion cells to approximately 51, arranged as dorsal ("capstone"), ventral ("keel") and double lateral rows (Fig. 3). Further anteriorly, approximately 215 cells lie in the rostralmost sensory vesicle, with many cells in cross-section (Fig. 3). Despite the small variation in total cell complement, and residual uncertainty in assigning cells to individual types, the census of cells supports the idea that cell number is determinate. The total cell numbers do differ somewhat between specimens, however, and do not include the approximately 40 cells of the neurohypophysis, about which still little is known and which will give rise to the adult CNS (Figs 1C, 2B).

Of the cells in the sensory vesicle, some populations are readily recognisable (Fig. 1C). For example, Nicol and Meinertzhagen [25] enumerate 17 photoreceptors, their

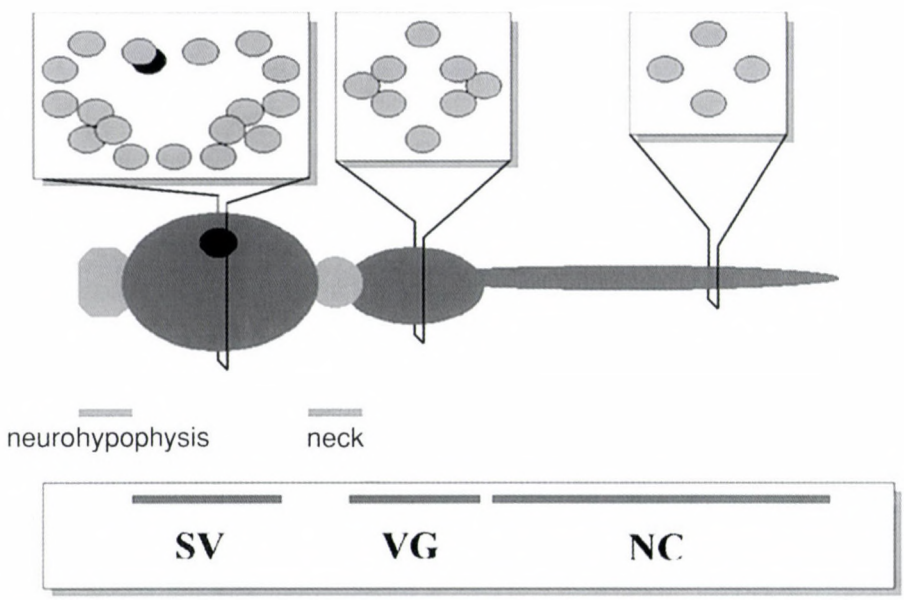

Fig. 3. Cross-sectional composition of the developing CNS at different stations along the axial length of the neural tube. In the region of the caudal nerve cord the cross-section comprises four rows of cells (dorsal, ventral, and two lateral), in the visceral ganglion region there are two to three lateral rows, while in the expanded rostral region of the neural tube that will give rise to the sensory vesicle the organisation of cells into rows is hard to discern

three lens cells, and one pigment-cup cell, a single otolith cell, and 17–21 other receptors, referred to as presumed hydrostatic pressure receptors. These are all distinguishable from their cytological appearance and relative position, and have been identified in other ultrastructural ways (reviewed in [39]). The remaining cells cannot yet be identified individually by these criteria alone. Because nuclear position itself appears too variable between larvae, it seems unlikely that such identification will even be possible *post hoc*, at least from position alone. The possibility of such identification seems unlikely even by reference to distinct expression markers, unless these were to involve only small subsets of cells. We have reconstructed too few specimens to be certain on this point, however, and so far do not have appropriate markers for cells that could directly test this point. On the other hand, from the example of the photoreceptor nuclei, which can be reliably identified as members of a small group, we think it should ultimately be possible to identify cells as members of a number of such small groups. In the future, this process of identification will likely make use of confocal image stacks (Fig. 2B).

Patterns of mitotic division

The early cleavage of the *Ciona* embryo has been widely studied ([9, 21, 24, 27; reviewed in [31]). Previous descriptive reports based on embryonic cell maps in *Ciona* have revealed the pattern of later cell divisions in the neural plate [23]. The mapping methods used in that study were not fully representational, however, and introduced distortions. These originated in an attempt to map the cells of the neural tube as a planar projection, as if the tube were unrolled, compatible with the arrangement of cells within the original neural plate. This strategem was adopted because computer methods to manipulate the images were not then routinely available. As a result the maps of Nicol and Meinertzhagen [23] cannot be superimposed directly upon an actual larva. More recent imaging methods using confocal microscopy do not suffer from these limitations and are therefore better suited to tracing the later development of the CNS from the neural plate. Using confocal image stacks of wholemount preparations we derived complete reconstructions of the entire embryo, in which the non-specific labelling of nuclei was used to select and highlight those within specific tissues. It was thereby possible to reconstruct the positions of the nuclei of the CNS (Fig. 2A). The outlines of the CNS were clear in such confocal image stacks, with an obvious border created by differences between the size and appearances of cells in the CNS and in the surrounding tissues, the notochord and muscle in the tail, and the endoderm in the trunk. Only in the neck region was there the possibility to confuse nuclei in the CNS with nuclei in the surrounding mesenchyme. In this region, we sometimes used reconstructions of the nuclear positions to arbitrate the identity of cells, depending on whether the nucleus fell within or beyond the smooth contour of the CNS.

We concentrated on the CNS at stages after closure of the neuropore. This has previously been reported to occur at about 60% of development [23], when the CNS has

approximately 130 cells (Fig. 2A[a]). The neural tube arises posteriorly from left and right blastomeres A4.1 and anteriorly from left and right blastomeres a4.2 [9, 23, 31], and begins as a double row of dorsal and a double row of ventral cells, and single rows of bilaterally symmetrical lateral cells. Eventually the caudal neural tube contains only four rows in cross-section (Fig. 3), which are produced when the original dorsal and ventral rows shear their positions longitudinally, so that their original double rows finally converge upon two single rows [24]. This shearing was visible in confocal reconstructions from the patterns of nuclear pairing, which were originally bilateral, but eventually shifted, so that one nucleus moved anterior to the other. The process is invariant for the fewer cells of the dorsal rows, whereas the ventral rows exhibited variation in which pairs of nuclei sheared at which time. Possibly this difference in precision between the dorsal and ventral rows is associated with the requirement for the dorsal cells of the neural plate, as it undergoes neurulation, to meet their contralateral counterparts at the edges of the curling plate and seal along the dorsal surface of the neural tube. The ventral cells, by contrast, already abut their contralateral partners within the neural plate.

In addition to shearing their positions, the dorsal and ventral cells also multiplied, dividing longitudinally to elongate their row. Posteriorly, the lateral cells likewise divided longitudinally in the region of the tail and presumptive visceral ganglion, contributing to the elongation of the neural tube (Fig. 4). Anteriorly, cells which gave rise to the caudal portion of the lateral cell walls of the sensory vesicle divided dorsoventrally, creating two rows of anterior lateral cells by a stage at which the neur-

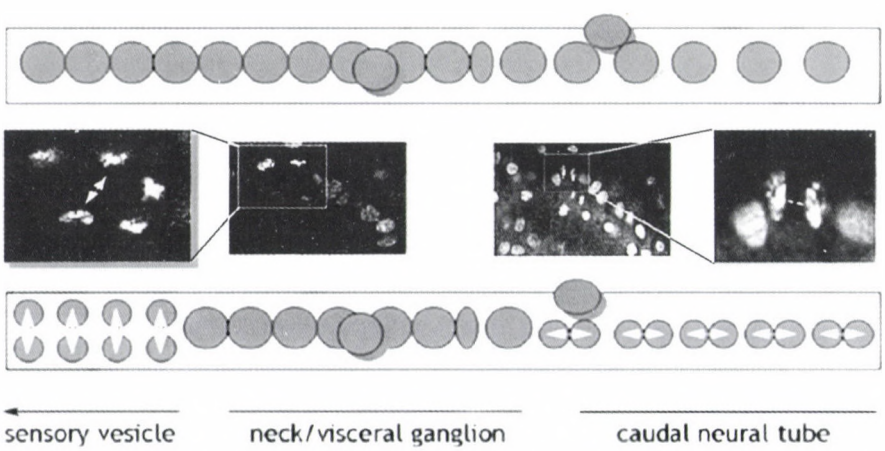

Fig. 4. The transformation of lateral rows of cells in the neural tube, by mitoses directed rostocaudally in the caudal neural tube, which elongate the tube, and dorsoventrally in the presumptive sensory vesicle region, which enlarge the diameter of the rostral portion of the neural tube. Top panel: the original row, prior to closure of the neuropore. Bottom panel: orientations of mitoses within the row. Middle panels: mitotic figures, shown from both low magnification and enlarged insets from confocal image stacks of the corresponding regions

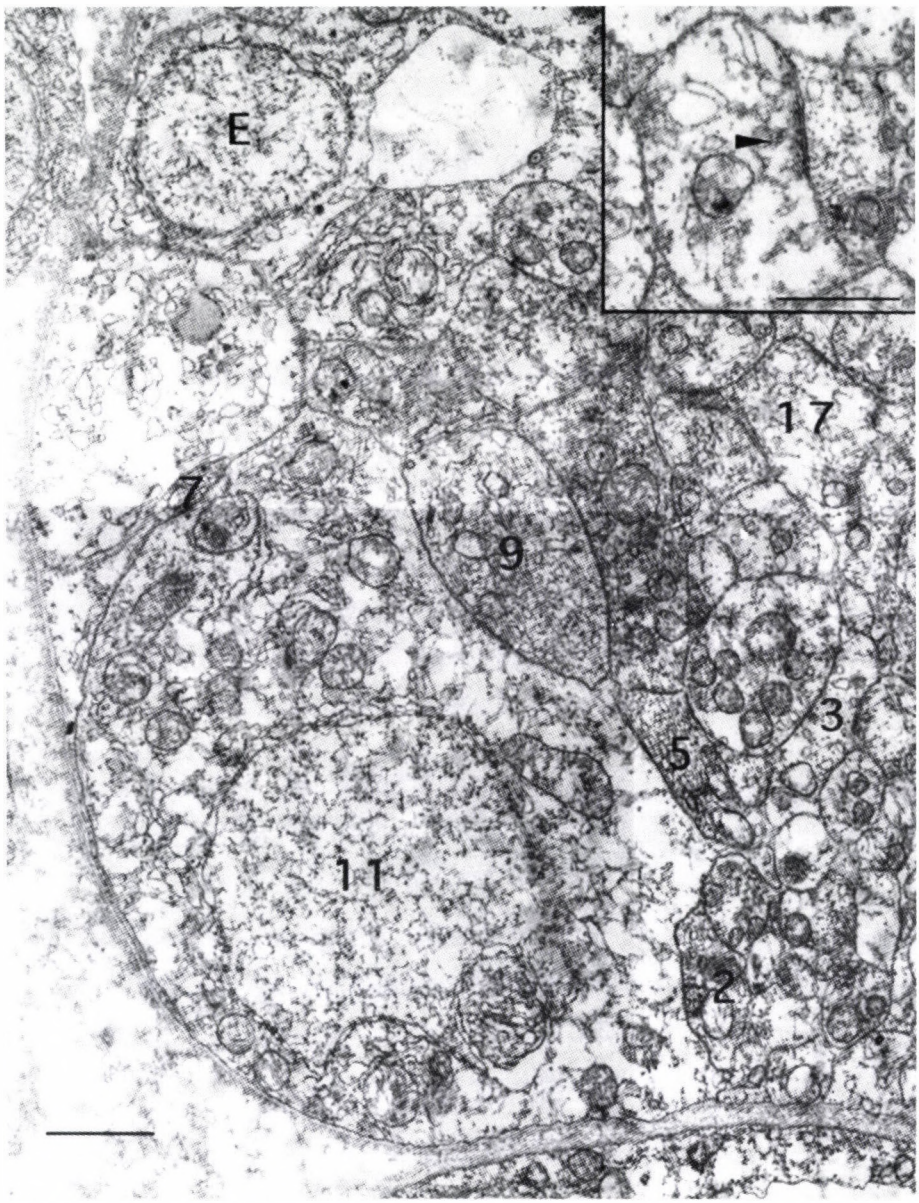

Fig. 5. Electon micrograph of the neural tube in the region of the presumptive visceral ganglion, with one cell body (11), several axon profiles (3, 5, 7, 9, 17) and an ependymal cell (E) labelled. Inset: Synaptic contact at which a single presynaptic site (arrowhead). Scale bar: 2 μm (inset 1 μm)

al tube comprised approximately 110 cells (Figs 2A [a], 4), before neuropore closure. At the time of pigmentation, when the neural tube is already composed of approximately 250 cells, only a few cells within the presumptive visceral ganglion and sensory vesicle regions were still mitotically active (Fig. 2A). As a result, the overall increase in cell number within the neural tube, which since about 20% of development increased non-linearly, began to level off. Whether any further increases that occurred through later mitoses [3] were sufficient to increase cell number above that in the final larva is still not resolved, as is the possibility of the intervention of apoptoses [30] to cut back the final number of cells. The role of the latter, if it exists, must be rather small, however.

The visceral ganglion

In order to gain some functional insight to the organisation of neurons into circuits that mediate swimming and to compare these with vertebrate counterparts [17], we have traced the connections of 29 neurons in the visceral ganglion of the larval CNS (Fig. 5). About 80 axon profiles constituted the centrally located neuropile in the neck region between sensory vesicle and visceral ganglion, some descending from sensory receptors and interneurons in the sensory vesicle. This number approximates the number of 100 neurons previously estimated in the entire CNS [25], suggesting that most neurons of the sensory vesicle may have descending pathways. Caudally, the number of profiles was smaller and the neuropile eventually separated into two ventrolateral bundles each of 10–12 fibres that ran into the caudal nerve cord. Output pathways from the visceral ganglion arose from 5 pairs of presumed motoneurons, so identified because their axons entered the central neuropile region of the visceral ganglion, descended in the ventrolateral tracts and were then traced out to their neuromuscular junctions. Four such pairs have also been tentatively identified from larval preparations immunostained with antibody UA301 [36]. Motor pathways in the tail have been distinguished physiologically into those innervating the rostral regions of the ventral muscle band, which drive symmetrical swimming movements, and those innervating the length of the dorsal muscle bands, which produce asymmetrical tail flicks [4]. Two pairs of fibres decussated, but the remaining fibre pairs did not, descending in the ipsilateral tracts. No other fibre tracts passed between cell bodies in the interior of the visceral ganglion, and the nerve cord. The ventrolateral bundles contained motor pathways that innervated the dorsal and middle muscle bands, forming neuromuscular junctions.

Axon tracts also arose from the peripheral nervous system, a system of slender axon bundles joining the visceral ganglion from dorsocaudal and ventrocaudal epidermal neurons alongside the nerve cord [36], previously identified using tubulin antibodies [12]. Likewise, peripheral nerves running from a rostral direction joined the sensory vesicle. They arose from papillary neurons and from rostral-trunk epidermal neurons, which stain for both acetylcholinesterase [18] and antibody UA301 [36].

The synaptic organisation appears to be rather simple. Synaptic contacts of visceral ganglion neurons had a single postsynaptic element (Fig. 6). As previously reported in the larvae of *Amaroucium* [1] and *Diplosoma* [37], many arose from axon terminals contacting the soma. Only one morphological class of clear, round 50 nm synaptic vesicle was apparent. Although the presence of clear, round vesicles suggested the presence of fast classical neurotransmitters in at least some vesicles, a search for such transmitters in the larva of the related *Molgula* failed to reveal immunoreactivity against many tested transmitters [40]. There may be different classes of synaptic vesicle, however, based on the inclusion of synaptic vesicles up to 70 nm in diameter, and on the observation of occasional dense-core vesicles. The latter were not seen at sites of synaptic contact, however, but rather seemed to be typical of the paracrine release of neuromodulators [15].

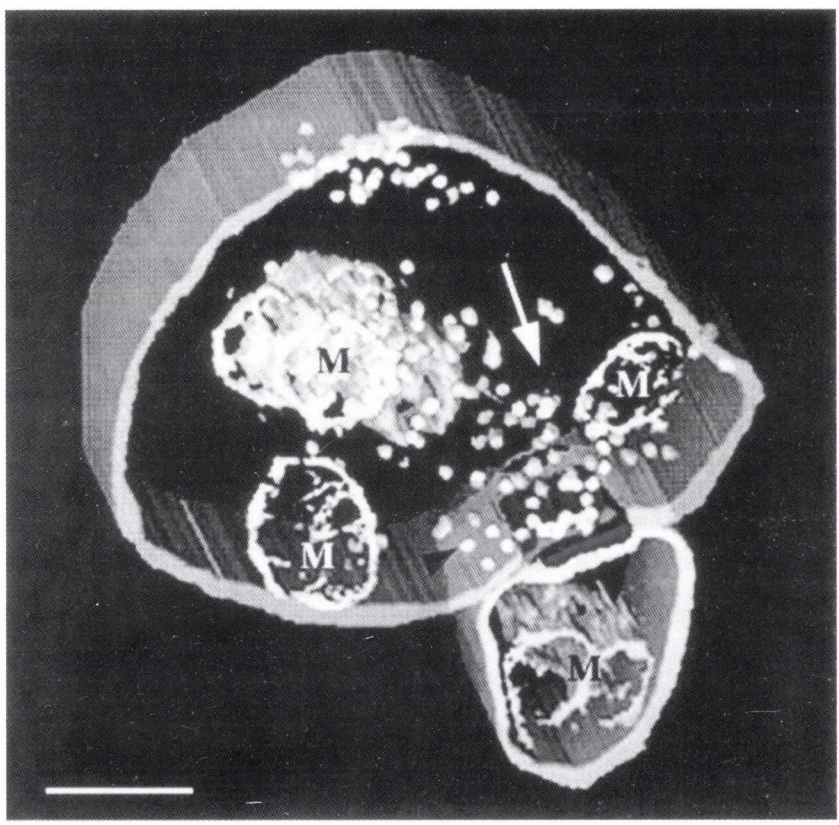

Fig. 6. Reconstruction of a single synaptic contact (arrow) reveals the features typical of a vertebrate synapse: synaptic vesicles (arrowhead), mitochondria (M), presynaptic (dark region with halo of vesicles) and postsynaptic membranes. Scale bar: 0.5 μm

Conclusions and prospects

Ready comparison can be made between work on the ascidian larva and similar but more advanced studies on the nematode *Caenorhabditis elegans*. The nervous systems of these two organisms are of comparable numerical complexity [25, 41], and the cell-lineage is well described for both animal groups, ascidian [23, 31] and nematode [34, 35], that for *C. elegans* being now complete. Recent analyses of *C. elegans* [34, 35] exposes hitherto unsuspected variations in cell-lineage, highlighting a problem which may also apply for future work on *Ciona*. Our previous work on cell-lineage in *Ciona* was derived by mapping the neural plate and its progeny in detail from a single embryo for each developmental stage examined [23]. Examination of confocal image stacks now allows us to analyse a small population of embryos for each stage, exposing for the first time small variations in cell position among different animals of the same age. In both cases, embryos have been fixed and examined as individuals within a series. A preferred approach would be to examine cell-lineage in real time, as in the initial analysis in *C. elegans* derived by following the mitotic patterns of individual cells, one at a time [35], and in a subsequent four-dimensional analysis of development simultaneously for all cells in a single embryo [34]. Conklin's [9] analysis of embryonic development was undertaken partially from observations on living embryos, but only for early cleavages; real-time analysis of later divisions has not so far been possible. Only from the latter will it be possible to assess the full extent of temporal synchronisation in embryonic cleavages, and the geometrical reproducibility of their plane and, from these, whether fate in the larval CNS arises from a fixed lineage in the embryo.

The possibility to derive the cell-lineage for all cells, by use of confocal maps of nuclear positions within the CNS, promises to facilitate the further analysis of ascidian embryogenesis, particularly with respect to the localization of identified gene products to particular cells in the larval CNS. Currently, a not unreasonable expectation is that each cell type in the larval CNS will eventually have a specific expression marker, and for each blastomere to express a specific sequence of such markers in the embryo. This at least was the hope that impelled a search for immunoreactivity to different transmitter antibodies among the larval neurons of *Molgula*; but for unknown reasons that quest proved unsuccessful [40]. A growing number of alternative markers has now been reported in recent years. They include: antibody UA301, which recognises the entire CNS of *Ciona* and may be neuron-specific [36]; and *in situ* probes for a sodium channel gene [29], and for the calmodulin gene [13]. The latter stain the entire CNS, while an *in situ* probe for *Hox*-related genes labels, along with non-neural cells, ependymal cells in the nerve cord. In a different approach, green fluorescent protein expression under the control of a neuron-specific promoter of the gene for the synaptic protein synaptotagmin has been used to label motor neurons in *Halocynthia roretzi* [28]. The possibility that alternative promoters can be used to drive expression of marker proteins in different classes of neurons offers the eventual prospect that cell-specific neuronal markers may eventually become available.

A current uncertainty that exists in the literature on the ascidian larval CNS is the full extent of differences between species. These are obviously considerable, clear not only for the receptor systems of the sensory vesicle [40] but also for the motor neurons, which from current evidence number three in *Halocynthia* [28], compared with at least five pairs in *Ciona*. Such differences suggest the value, but also the limitations, of concentrating initially upon a single species, and remind us that only approaches applicable to a wide variety of species will ultimately yield valid conclusions about the relationship between the ascidian embryo and the larval CNS to which it gives rise.

ACKNOWLEDGEMENTS

Supported by grants to I.A.M. from NSERC (OPG 0000065), and the Killam Trust of Dalhousie University, and by Dalhousie Graduate Scholarship (to A.G.C.).

REFERENCES

1. Barnes, S. N. (1971) Fine structure of the photoreceptor and cerebral ganglion of the tadpole larva of *Amaroucium constellatum* (Verrill) (Subphylum: Urochordata; Class: Ascidiacea). *Z. Zellforsch. 117,* 1–16.
2. Berrill, N. J. (1955) *The Origin of Vertebrates.* Clarendon Press, Oxford.
3. Bollner, T., Meinertzhagen, I. A. (1993) The patterns of bromodeoxyuridine incorporation in the nervous system of a larval ascidian, *Ciona intestinalis. Biol. Bull. 184,* 277–285.
4. Bone, Q. (1972) *The Origin of Chordates.* Oxford University Press, London.
5. Bone, Q. (1992) On the locomotion of ascidian tadpole larvae. *J. Mar. Biol. Assoc. U.K. 72,* 161–186.
6. Bone, Q., Mackie, G. O. (1982) Urochordata. In: Shelton, G. A. B. (ed.) *Electrical Conduction and Behaviour in "Simple" Invertebrates.* Clarendon Press, Oxford, pp. 473–535.
7. Burighel, P., Cloney, R. A. (1997) Urochordata: Ascidiacea. In: Harrison, F. W., Ruppert, E. E. (eds). *Microscopic Anatomy of Invertebrates, Volume 15: Hemichordata, Chaetognatha, and the Invertebrate Chordates.* Wiley-Liss Inc., New York, pp. 221–347.
8. Cloney, R. A. (1978) Ascidian metamorphosis: review and analysis. In: Chia, F.-S., Rice, M. E. (eds) *Settlement and Metamorphosis of Marine Invertebrate Larvae.* Elsevier, New York, pp. 255–282.
9. Conklin, E. G. (1905) Organization and cell-lineage of the ascidian egg. *J. Acad. natl. Sci. Philadelphia 13,* 1–119.
10. Corbo, J. C., Erives, A., Di Gregorio, A., Chang, A., Levine, M. (1997) Dorsoventral patterning of the vertebrate neural tube is conserved in a protochordate. *Development 124,* 2335–2344.
11. Costello, D. P., Henley, C. (1971) *Methods for Obtaining and Handling Marine Eggs and Embryos,* 2nd Edn. Marine Biological Laboratory, Woods Hole, MA.
12. Crowther, R. J., Whittaker, J. R. (1994) Serial repetition of cilia pairs along the tail surface of an ascidian larva. *J. exp. Zool. 268,* 9–16.
13. Di Gregorio, A., Villani, M. G., Locascio, A., Ristoratore, F., Aniello, F., Branno, M. (1998) Developmental regulation and tissue-specific localization of calmodulin mRNA in the protochordate *Ciona intestinalis. Develop. Growth Different. 40,* 387–394.
14. Dilly, P. N. (1964) Studies on the receptors in the cerebral vesicle of the ascidian tadpole. 2. The ocellus. *Quart. J. microsc. Sci. 105,* 13–20.
15. Fuxe, K., Agnati, L. F. (1991). Two principle modes of electrochemical communication in the brain: volume versus wiring transmission. In: Fuxe, K., Agnati, L. F. (eds) *Volume Transmission in the Brain: Novel Mechanisms.* Raven Press, New York, pp. 1–9.
16. Garstang, W. (1928) The morphology of the Tunicata, and its bearings on the phylogeny of the Chordata. *Quart. J. microsc. Sci. 72,* 51–187.

17. Grillner, S., Ekeberg, O., El Manira, A., Lansner, A., Parker, D., Tegner, J., Wallen, P. (1998) Intrinsic function of a neuronal network – a vertebrate central pattern generator. *Brain Res. Rev. 26,* 184–197.
18. Jia, W.-G., Meinertzhagen, I. A. (1987) Development of the ascidian larval nervous system: the specific staining of neurons. *Soc. Neurosci. Abstr. 13,* 1142.
19. Katz, M. J. (1983) Comparative anatomy of the tunicate tadpole, *Ciona intestinalis. Biol. Bull. 164,* 1–27.
20. Kowalewski, A. O. (1867) Entwicklungsgeschichte der einfachen Ascidien. *Mém. Acad. Sci. St. Petersbourg, Sér 7 (10),* 1–19.
21. Meedel, T. H., Whittaker, J. R. (1984) Lineage segregation and developmental autonomy in expression of functional muscle acetylcholinesterase mRNA in the ascidian embryo. *Dev. Biol. 105,* 479–87.
22. Meinertzhagen, I. A., Hu, X. (1996) Evidence for site selection during synaptogenesis: The surface distribution of synaptic sites in photoreceptor terminals of the flies *Musca* and *Drosophila. Cell molec. Neurobiol. 16,* 677–698.
23. Nicol, D., Meinertzhagen, I. A. (1988) Development of the central nervous system of the larva of the ascidian, *Ciona intestinalis* L. II. Neural plate morphogenesis and cell lineages during neurulation. *Dev. Biol. 130,* 737–766.
24. Nicol, D., Meinertzhagen, I. A. (1988) Development of the central nervous system of the larva of the ascidian, *Ciona intestinalis* L. I. The early lineages of the neural plate. *Dev. Biol. 130,* 721–736.
25. Nicol, D., Meinertzhagen, I. A. (1991) Cell counts and maps in the larval central nervous system of the ascidian *Ciona intestinalis* (L.). *J. comp. Neurol. 309,* 415–429.
26. Nishida, H. (1987) Cell lineage analysis in ascidian embryos by intracellular injection of a tracer enzyme. III. Up to the tissue restricted stage. *Dev. Biol. 121,* 526–541.
27. Nishida, H., Satoh, N. (1985) Cell lineage analysis in ascidian embryos by intracellular injection of a tracer enzyme. II. The 16- and 32-cell stages. *Dev. Biol. 110,* 440–454.
28. Okada, T., Katsuyama, Y., Ono, F., Okamua, Y. (1999) Identification of three motor neurons in the ascidian tadpole larva with neuronal expression of a green fluorescent protein (in preparation).
29. Okamura, Y., Ono, F., Okagaki, R., Chong, J. A., Mandel, G. (1994) Neural expression of a sodium channel gene requires cell-specific interactions. *Neuron 13,* 937–948.
30. Oppenheim, R. W. (1991) Cell death during development of the nervous system. *Ann. Rev. Neurosci. 14,* 453–501.
31. Satoh, N. (1994) *Developmental Biology of Ascidians* (Developmental and Cell Biology Series, Vol. 29). University Press, Cambridge.
32. Satoh, N., Jeffrey, W. R. (1995) Changing tails in ascidians: developmental insights into the origin and evolution of chordates. *Trends Genet. 11,* 354–359.
33. Schnabel, R. (1997) Why does a nematode have an invariant cell lineage? *Semin. Cell & Dev. Biol. 8,* 341–349.
34. Schnabel, R., Hutter, H., Moerman, D., Schnabel, H. (1997) Assessing normal embryogenesis in *Caenorhabditis elegans* using a 4D microscope: Variability of development and regional specification. *Dev. Biol. 184,* 234–265.
35. Sulston, J. E., Schierenberg, E., White, J. G., Thomson, J. N. (1983) The embryonic cell lineage of the nematode *Caenorhabditis elegans. Dev. Biol. 100,* 64–119.
36. Takamura, K. (1998) Nervous network in larvae of the ascidian *Ciona intestinalis. Dev. Genes Evol. 208,* 1–8.
37. Torrence, S. A. (1983) *Ascidian larval nervous system: Anatomy, ultrastructure and metamorphosis.* Ph. D. Thesis, University of Washington, Seattle.
38. Torrence, S. A. (1986) Sensory endings of the ascidian static organ (Chordata, Ascidiacea). *Zoomorphol. 106,* 61–66.
39. Torrence, S. A., Cloney, R. A. (1988) Larval sensory organs of ascidians. In: Thompson, M. F., Sarojini, R., Nagabhushanam, R. (eds) *Marine Biodeterioration.* Oxford University Press and IBH, New Delhi, pp. 151–164.
40. Vorontsova, M. N., Nezlin, L. P., Meinertzhagen, I. A. (1997) Nervous system of the larva of the ascidian *Molgula citrina* (Alder and Hancock, 1848). *Acta Zool. (Stockh.) 78,* 177–185.
41. White, J. G., Southgate, E., Thomson, J. N., Brenner, S. (1986). The structure of the nervous system of the nematode *Caenorhabditis elegans. Phil. Trans. Roy. Soc. Lond. Ser. B. 314,* 1–340.

Acta Biologica Hungarica 51 (2–4), pp. 433–437 (2000)

SENSORY ORGANS OF ADULT *AMPHILINA FOLIACEA* (AMPHILINIDA)[+]

VASILINA A. DUDICHEVA and NATALIA M. BISEROVA*

Institute for Biology of Inland Waters RAS, 152742 Borok, Russia

(Received: August 31, 1999; accepted: November 30, 1999)

The distribution and morphological diversity of the sensory structures on the body surface, proboscis and caudal cavity of adult *Amphilina foliacea* have been investigated. Fifteen different types of receptors are described. Along with nonciliated and uniciated receptors bi- and multiciliated receptors have been found for the first time. The zonal distribution of the sensory structures and their coincidence within the same areas of the body surface have been revealed. The concentration of sensory structures at the posterior end may indirectly confirm a hypothesis of the unavailability of developed attachment disk in ancestors of amphilinids.

Keywords: Amphilina foliacea – sensory organs – ultrastructure.

INTRODUCTION

Amphilina foliacea is a parasite of sturgeon fish. It is located in the body cavity and inner tissue of the host. Amphilinidea is not a well-known group. The life cycle, ultrastructure various organs of *A. foliacea* and several types of sense receptors of larval *Austramphilina elongata* have been described [4, 10]. In the present work the distribution and morphological diversity of the sensory organs of adult *A. foliacea* are described.

MATERIAL AND METHODS

Adult *A. foliacea* were removed from the body cavity of *Acipenser ruthenus* caught in the lower Volga River. Worms were fixed in 2.5% glutaraldehyde in 0.1 M phosphate buffer, postfixed in a solution of 1% OsO_4, dehydrated in a series of ethanol.

[+] Presented at the 9th ISIN Symposium on "Neurobiology of Invertebrates", July 1–5, 1999, Tihany, Hungary.

*Corresponding author, E-mail: biserova@ibiw.jaroslavl.ru

0236-5383/2000/$ 5.00

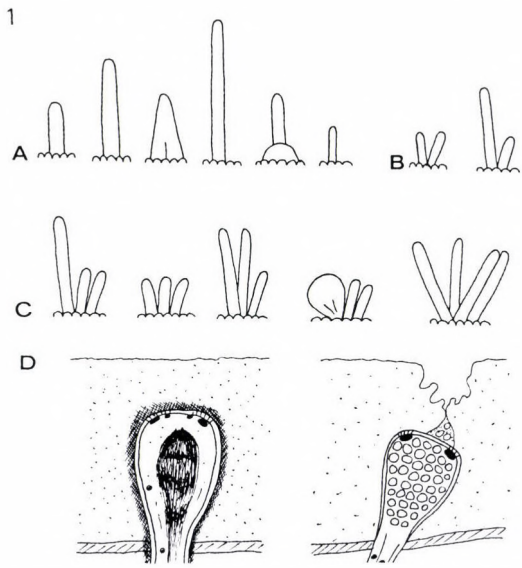

Fig. 1. Scheme of receptors of adult *Amphilina foliacea*. A – uniciliate, B – biciliate, C – multiciliate, D – nonciliate

For SEM the specimen were dried at a critical point, mounted on stubs and examined with SEM-25S. For TEM the material was embedded in Artaldit. Ultrathin sections were stained with uranylacetate, lead citrate and examined with JEM 100C.

RESULTS

The distribution of the sense cilia is different in worms specimens of various sizes. The cilia of small worms (1 sm.) concentrate mainly in areas along the lateral margins and body ends. The sense cilia of large worms (3 sm.) occur seldom on the cell crests and are evenly located. Six types of uniciliate receptors have been distinguished (Figs 1, 2): 1. short cilia (length 200–420 nm, width 170–180 nm); 2. long cilia (l. = 600–1000 nm, w. = 150 nm); 3. conical cilia (l. = 370–700 nm, w. = 180–280 nm); 4. very long cilia (l. = 1000–1200 nm, w. = 150 nm); 5. short cilia on a spherical base (l. = 650–715 nm, w. = 100–150 nm, base ~300 nm); 6. short, thin cilia (l. = 120–300 nm, w. = 60–80 nm).The receptor types have different distribution on the body surface: type 1 occurs all over the body surface; 3 coincides with body ends; 5 coincides with dorsal and ventral body surface; 4 was found near the spermduct pore at the posterior end.

Biciliate receptors are found mainly at the lateral margins. They have 2 modifications: with cilia equal or diverse long (Figs 1, 2). Multicilliate receptors coincide mainly with latero-ventral surface of the posterior end. They can have 3 or 4 cilia

(Fig. 1). The receptors with 3 cilia are the most diverse. The receptors with 4 cilia are distributed mainly at ventral surface (Fig. 2).

The sensory neurones are found in the tissue of the posterior end. Their processes extend to the subtegument (Fig. 3). The processes and neurones contain dense-cored vesicles in the cytoplasm.

The 2 types of nonciliate receptors are found (Fig. 1). The receptors of type one occur in the proboscis walls and caudal cavity walls. They do not reach the body surface. The fibrous sheath of intercellular matrix extends along the receptor (Fig. 4). There are 2 electron-dense collars, septate desmosome, neurotubules, electron-dense vesicles (50–80 nm) and a rootlet, which exhibits a periodical striation. The second type occurs only in the proboscis walls (Fig. 1). It also does not reach the body surface. There is an electron-dense collar and septate desmosome, neurotubules and light vesicles (62–156 nm), that fill all receptors. A rootlet is absent. A separation of light vesicles from distal part of the receptor occurs under basal membrane of tegument. Around the proboscis, on the periphery of nervous bundle the sensory neurones are found. The cytoplasm contains ribosomes and electron-dense vesicles, which are similar to vesicles in the receptors. Their processes extend to the proboscis walls.

DISCUSSION

There are many data on the ultrastructure of the receptors of sensory structures of mature cestodes, monogeneans and trematodes [1, 2, 5, 6, 7, 10, 11].

Nonciliate receptors of type one of adult *A. foliacea* were described earlier [3]. The ultrastructure of nonciliate receptors of larval *A. elongata* [9] has similar (thin fibrous sheath) and different indications (a periodical striation is absent). The receptors of Gyrocotylida have not a fibrous sheath, but a periodical striation is present [10]. The nonciliate receptor of type 2 is similar to that of cestodes. The ultrastructure of nonciliate receptors of adult *A. foliacea* is similar to that of other parasitic Plathelminthes [8, 11].

Multiciliate structures are typical features for many groups of flatworms, except for cestodes. Multiciliate receptors of adult amphilinids have been found for the first time. A larval *A. elongata* have quadruciliate papillae at the anterior end [9]. A peculiar feature of multiciliate papillae of adult *A. foliacea* is their position mainly at the posterior end. The free-living turbellaria, adult and larval monogeneans, trematodes, aspidogastreans also have the multiciliate structures,which probably are chemosensory [6, 10, 11]. It is possible, that multiciliate structures of adult *A. foliacea* serve as a polyfunctional complex for several receptors. *A. elongata* also has clusters of quadry- and uniciliate receptors [9]. Dendrites of fourth multiciliate receptors of macrostomids can extend together through the epidermal cells [8]. The form of sensory complex of different receptors is typical for cercaria *Echinostoma revolutum* [11]. However, cilia of receptors from the complex have never a close association as cilia of *A. foliacea*. The zonal distribution of the receptors was described for turbellaria and cestodes. The receptors of turbellaria concentrate in sensory areas at the

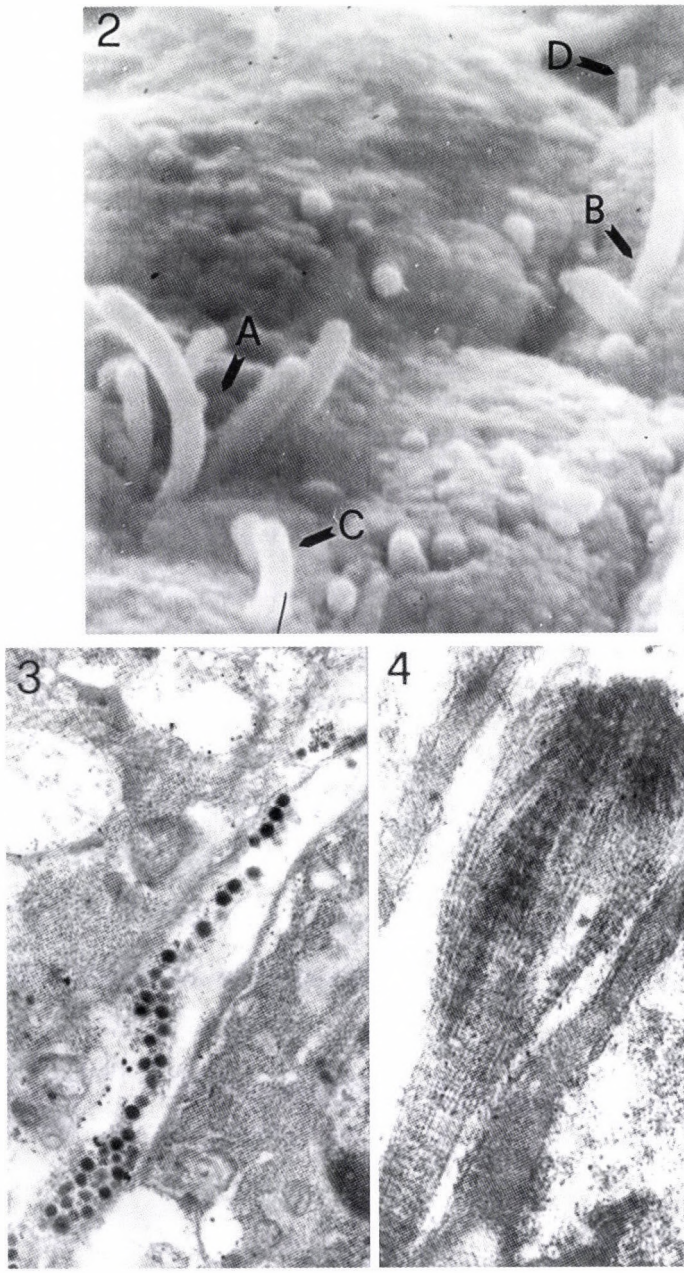

Fig. 2. The ciliate receptors on ventral body surface. A – multiciliate, B – biciliate, C – uniciliate of type one, D – uniciliate of type six. ×20 000. *Fig. 3.* The processes of sensory neurons in subtegument at posterior end. ×15 000. *Fig. 4.* The nonciliate receptor of type one in the proboscis wall. ×30 000

anterior end, along the lateral margins [8]. The receptors of cestodes coincide with margin surface of attachment organ [1]. The distribution of receptors of *A. foliacea* is similar to that in some turbellaria. The quantity of sensory organs at the posterior end of *A. foliacea* exceeds that of turbellaria. As the mature *A. foliacea* preserves the caudal cavity and larval hooks [6]. The concentration of sense structure at the posterior end can indirectly confirm a hypothesis on availability of developed attachment disk in ancestors of amphilinids.

ACKNOWLEDGEMENT

Supported by RFBR, grant 98-04-48432 and INTAS 96-1365.

REFERENCES

1. Biserova, N. M. (1991) The distribution of receptor structure and peculiarities of ultrastructure of nervous system of cestodes of three lower order. *J. gen. biol. 52,* 551–563 (in Russian).
2. Biserova, N. M., Korneva, J. V. (1999) The sensory apparatus and peculiarities of form of nervous system *Triaenophorus nodulosus* (Cestoda) in ontogenesis. *Parasitology 33,* 39–48.
3. Davydov, V. G., Kuperman, B. I. (1993) The ultrastructure of the tegument and the peculiarities of the biology of *Amphilina foliacea* adult (Plathelminthes, Amphilinidea). *Folia Parasitol. 40,* 13–22.
4. Dubinina, M. N. (1982) Parasitic worms of the class Amphilinida (Plathelminthes). Trudy Zool. Inst. Acad. Nauk USSR, Nauka, Leningrad, 100. (in Russian).
5. Gustafsson, M. K. S. (1990) The cell of cestode. *Diphyllobotrium dendriticum* as a model in cell biology. In: Gustafsson, M. K. S., Reubar, Maria (eds) *The Early Brain.* ABO Academy Press, pp. 13–45.
6. Halton, D. W., Maule, A. G., Shaw, C. (1997) Trematode neurobiology. In: Fried, B., Graczyk, T. K. (eds) *Advances in Trematode Biology.* New York, CRC Press, pp. 353–354.
7. Lyons, K. M. (1972) *Sense Organs of Monogeneans.* Academic Press, London.
8. Harrison, F. W., Boditsh, B. J. (eds) (1991) *Microscopic anatomy of Invertebrates. Vol. 2. Plathelminthes and Nemertinea.* pp. 7–140.
9. Rohde, K., Watson, N., Garlik, P. R. (1986) Ultrastructure of three types of sense receptors of larval *Auatramphilina elongata* (Amphilinidea). *Int. J. Parasitol. 16,* 3, 245–251.
10. Xylander, W. E. R. (1987) Ultrastructure of the lycophora larva of *Gyrocotyle urna* (Cestoda, Gyrocotylidea) – II. Receptors and nervous system. *Zool. Anz. 219,* 239–255.
11. Zdárská, Z. (1992) Transmission electron microscopy of sensory receptors of *Echinostoma revolutum* (Froelich 1802) cercaria (Digenea: Echinostomatidae). *Parasitol. Res. 78,* 598–606.

Acta Biologica Hungarica 51(2–4), pp. 439–442 (2000)

THE ULTRASTRUCTURE OF GLIA-LIKE CELLS IN LATERAL NERVE CORDS OF ADULT *AMPHILINA FOLIACEA* (AMPHILINIDA)[+]

NATALIA M. BISEROVA

Institute for Biology of Inland Waters RAS, 152742 Borok, Russia

(Received: August 31, 1999; accepted: November 30, 1999)

The ultrastructure of main lateral nerve cords (MCs) of adult *A. foliacea* was studied. By examination of the serial sections it has been found that some glia-like cells are located on a periphery of MC. The processes of glia-like cells surround MCs and penetrate into the cord and surround the group of adjacent axons and pairs of neurones. There is a fine extracellular matrix between processes of glia-like cells. The numerous tight junctions occur between processes. The difference between the perykaryon's cytoplasm of glia-like cells in anterior, posterior and central part of MCs was found.

Keywords: Ultrastructure – nervous system – Amphilinida – glia-like cells.

INTRODUCTION

Amphilina foliacea Rudolphi 1819 is a typical representative of Amphilinida, which comprises a few species. Adult *A. foliacea* occurs predominantly in the body cavity of the European species, but also in internal organs, such as liver [8]. Different species of Gammaridae serve as intermediate hosts for *A. foliacea*. The systematic position and the phylogenetic relationship of Amphilinida have been discussed for a long time. The morphology has been described by Dubinina [6]. The ultrastructure of the surface tegument, as well as the glands and the net-like excretory system have been investigated earlier [5]. As to the nervous system, only scattered data on the general structure [6], chemical composition [10] and fine structure [3] are available.

I present here the results of the first detailed investigation of the glia-like cells in the nervous system of *A. foliacea*.

[+] Presented at the 9th ISIN Symposium on "Neurobiology of Invertebrates", July 1–5, 1999, Tihany, Hungary.

*E-mail: biserova@ibiw.jaroslavl.ru

0236-5383/2000/$ 5.00

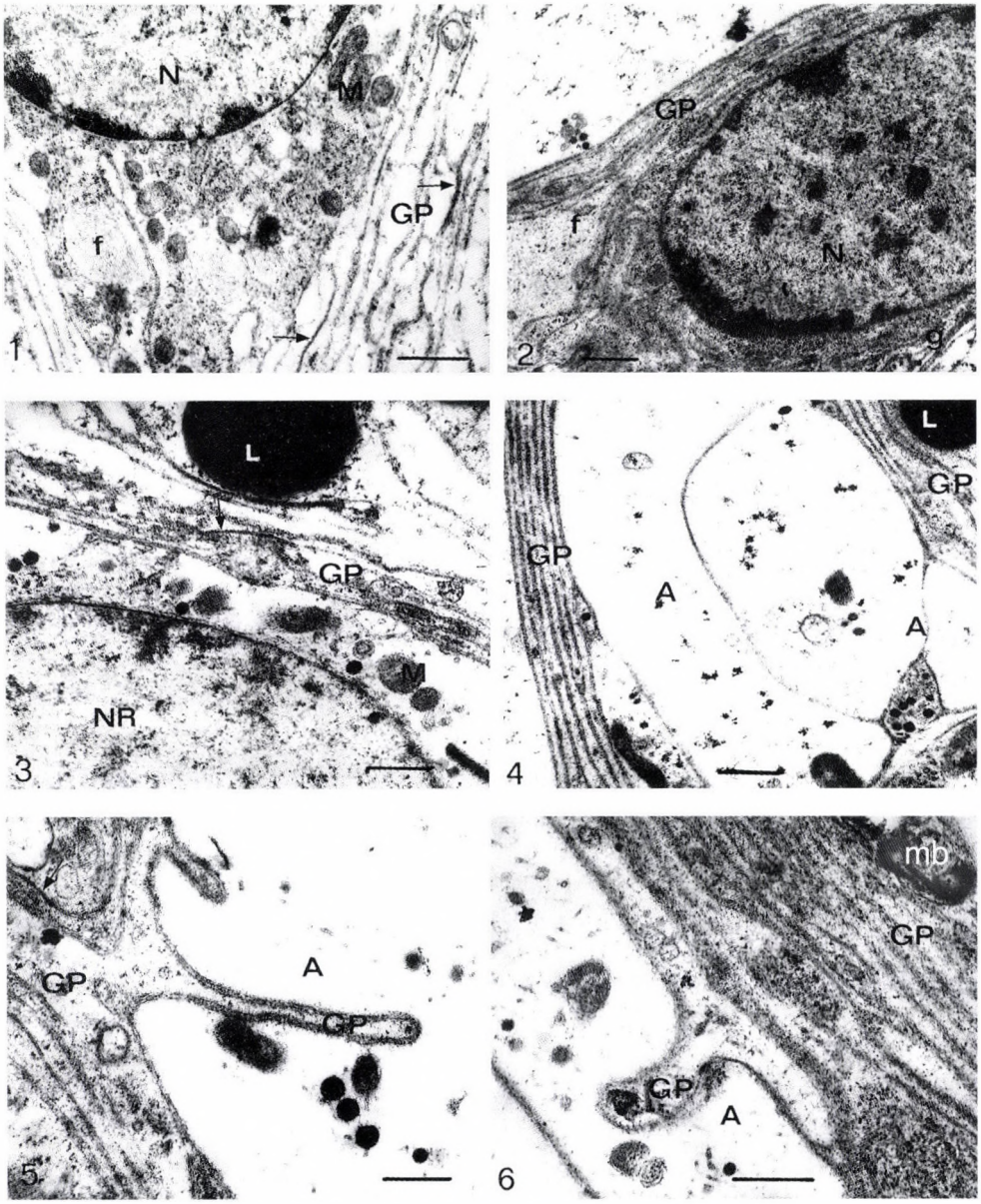

Fig. 1. Glia-like cell closes cerebral ganglion. Magnification of negative. *Fig. 2.* Glia-like cell in posterior part of MCs. *Fig. 3.* Neurone on periphery of MCs with 2–3 layers of envelope. *Fig. 4.* Group of adjacent axons and surrounding multilayer envelope. *Figs 5, 6.* Relationship between axons and glia-like processes. A – axons; f – fibrillar matrix into glia-like cell; g – glycogen; GP– glial processes; m – mitochondrion; n – nucleus; r – ribosome; → – thigh junction between glial processes. Bars = 1 μm

MATERIAL AND METHODS

Adult specimens of *Amphilina foliacea* were obtained from the body cavity of *Acipenser ruthenus* and *Acipenser gueldenstaedti* from the Volga river in the vicinity of Volgograd and Astrakhan (Russia). The worms were fixed in 2% glutaraldehyde in 0.05 M sodium cacodylate buffer (pH 7.2). Postfixation was performed in 1% osmium tetroxide in the same buffer, dehydration was through a series of ethanol and acetone and embedment was in Araldite. Sections were examined with a JEM 100C microscope.

RESULTS

The ultrastructure of the main lateral nerve cords (MCs) of adult *A. foliacea* was studied. They pass along the whole length of body and are represented by compact blends of processes and cells forming lateral ganglia at certain distances one from another. The study of transversal sections has shown that the boundary or peripheral zone of MCs always has thin light processes enveloping the cord (Fig. 1). The boundary processes often penetrate into the cord and surround the groups of neurites. By examination of the serial sections it has been found that some glial-like cells are located on a periphery of MCs (Figs 1, 2). The nucleus has round or oval shape and contains a dense round nucleolus and blocks of chromatin near a nuclear membrane. The glia-like cells are located often in pairs. The perykaryon's cytoplasm is poor in organelles and contains rarely microtubules, fibrillar matrix, a few glycogen granules, lipid droplets, ribosomes and smooth ER elements. Synaptic vesicles can not be found. The cell bodies sends off numerous thin processes. The cytoplasm of the processes is "clear". The processes of glia-like cells surrounding MCs penetrate into the cord and surround the group of adjacent axons and pairs of neurones. The multilayered envelope of MCs includes 8–10 layers; of axon clusters – 4–6 layers; of neurones – 2–3 layers (Figs 3–6). Synaptic contacts formed by processes of glia-like cells have not been observed. There is a fine extracellular matrix between the processes of glia-like cells. Numerous tight junctions occurr between processes (Figs 1, 3). In the central part of the body, the parenchymal cells containing a great quantity of glycogen are adjacent to the processes of glia-like cells. This glycogen-containing processes form long gap-junctions with boundary processes of the glia-like cells. There are differences between the perykaryonal cytoplasm of glia-like cells in the anterior, posterior and central part of MCs. Namely, near the cerebral ganglion glia-like cells contain more mitochondra and ribosomes (Fig. 1), while in the central part of MCs they are poor in organelles; and the posterior end glia-like cells contain an electron deuse cytoplasm, free ribosomes, more glycogen granules and lipid droplets and a thin fibrillar matrix (Fig. 2).

DISCUSSION

Data presented here, show that (1) there are glia-like cells which surround MCs in Amphilinida; (2) the ultrastructure of the cells differs across different parts of CNS.

Multilayered cells have been observed around neurones and nerve fibres in a wide range of free-living flatworms. Putative glia cells were found in the CNS of endemic *Geocentrophora* (Prorhynchida, Platyhelmintes) from Lake Baikal [4]. The fusiform cells with a long and narrow nucleus were found in *Strongilostoma simplex* [1]; their cytoplasm has thin processes, which penetrate into between the nerve cells. A typical marker of vertebrate glia cells (S-100) could be demonstrated in nervous system of *Crenobia alpina* [7]. In most of the parasitic flatworms a glia-like cell type have not been observed, with the exceptions of *Multicotyle purvisi* and *Fasciola hepatica* [7]. In Cestoda, it has been shown that for similar function can used the cells of excretory system [2]. Their processes surround cerebral ganglion and penetrate into the neuropile.

The systematic position and the phylogenetic relationships of Amphilinida have been discussed for a long time. The glia-like cells described here were formerly known in free-living primitive flatworms only. The new data on the presence of the similar glia-like cells in the evolutionary old endoparasitic Amphilinida are interesting for the comparative neurobiology of flatworms.

ACKNOWLEDGEMENT

Supported by RFBR, grant 98-04-48432 and INTAS 96-1365.

REFERENCES

1. Bedini, C., Lanfranchi, A. (1998) Ultrastructural study of the brain of a Typhloplanid flatworm. *Acta Zoologica* (Stockholm) *79,* 3, 243–249.
2. Biserova, N. M. (1997) Structure of a scolex nervous system of the *Triaenophorus nodulosus* (Cestoda: Pseudophyllidea). *Parazitologia, 31,* 3, 249–259. (In Russian)
3. Biserova, N. M., Frolova, V. A. (1997) First study of ultrastructure of the central nervous system in adult *Amphilina foliacea* (Amphilinida). In: *Simpler Nervous Systems.* Abst. 5th east European conference ISIN, Moscow, p. 8.
4. Bockerman, I., Reuter, M., Timoshkin, O. (1994) Ultrastructural study of the central nervous system of endemic Geocentrophora (Prorhynchida, Platyhelmintes) from Lake Baikal. *Acta Zoologica* (Stockholm), 75, 1, 47–55.
5. Davydov, V. G., Kuperman, B. I. (1993) The ultrastructure of the tegument and peculiarities of the biology of *Amphilina foliacea* adult (Plathelminthes: Amphilinidea). *Folia parasitologia* 40, 13–22.
6. Dubinina, M. N. (1982) *Parasitic worms of the class Amphilinida (Plathelminthes).* Trudy Zool. Inst. Acad. Nauk USSR. Nauka. Leningrad (In Russian.)
7. Halton, D. W., Gustafsson, M. K. S. (1996) Functional morphology of the platyhelminth nervous system. *Parasitology 113,* 47–72.
8. Popova, L. B., Davydov, V. G. (1988) Studies of localization of *Amphilina foliacea* (Amphilinidae Dubinina, 1974) in definitive hosts. *Helmintologia 25,* 129–138.
9. Shishov, B. A. (1991) Aminergic and cholinergic elements in the nervous system of helminths. In: *Morphological Principles of Platyhelmints Phylogenetics.* Proceed. Zool. Inst. RAS. *241,* 112–137 (In Russian).

Acta Biologica Hungarica 51 (2–4), pp. 443–445 (2000)

OBITUARY

LADISLAV TAUC (1926–1999)

AN APPRECIATION FROM JACQUES STINNAKRE

I spoke with Ladislav Tauc a few weeks before he died. As usual he was amusing and friendly. With characteristic humour he said he was very sorry not to be able to attend our triannual meeting in Hungary, since for him it was a "kind of pilgrimage", because "I have been subjected to the vivisectionist's knife". Professor Jacques Stinnakre, Ladislav Tauc's first student and long time collaborator, was good enough to let me have details of his funeral eulogy to Ladya, some of which I have reproduced below.

"Ladya was born in the Czech Republic in the small town of Pardubice, in Bohemia. As a student at the Masaryk University of Brno, he started research in the Laboratory of Plant Physiology, where his passion for biophysics and electronics had led him to become interested in the phenomenon of bioelectricity and it was there that he investigated the effect of light on plant growth. However, in Czechoslovakia at that time, methods in electrophysiology were not practical and it was in France, in the laboratory of biophysics at 'L'Ecole Normale Superieure', rue d'Ulm, that Ladislav Tauc came to complete his training – thanks to a grant obtained from the French Government. There he met Alfred Fessard with whom he would collaborate in the future. His work progressed rapidly and soon he found that the electrical responses he observed on the cell membrane in young pea plants under the influence of light, resulted from photochemical processes taking place in peripheral neighbouring cells. These results channelled his interests towards processes that occur at the cellular level and in particular the membrane potential.

To record the membrane potential he would have to access the cytoplasm of the cell, a task more difficult to perform than attaching a metal wire to the end of a squid axon: one must go through the membrane with an isolated electrode without short-circuiting it. Thanks to contact with De Fonbrune, who built micro-tools from glass, Ladislav Tauc thought about the glass tubes pulled by embryologists to manipulate cell nuclei and became one of the first people in the world, and certainly the first in France, to use intracellular microelectrodes. The cellulose cell wall of plants caused him great problems but by 1953 he was able to make recordings. Thus he became a pioneer in plant electrophysiology.

Akadémiai Kiadó, Budapest

Surrounded by neurophysiologists and encouraged by Alfred Fessard, Ladya turned towards the nervous system, and more specifically towards the nerve cells as he postulated that to understand how the nervous system functions, one must first understand the details of the elementary mechanisms occurring at a cellular level. He explored many preparations (the striated muscle fiber, the electric organ of squids and giant neurones in snails) before settling on the giant neurones of the sea hare, *Aplysia.* It is to Tauc that several generations of neuroscientists owe gratitude for exploring this exceptional model nervous system. In 1954, following very long expeditions to Arcachon where, during the summer, *Aplysia* are in abundance, and further experiments done on *Aplysia* at l'Institute Marey, he described the properties of neurones: evoked and spontaneous action potentials, local potentials, and inhibitory and excitatory synaptic potentials.

We must underline, I think, the importance of his discovery that synaptic transmission resulted directly from (pre-)synaptic activity and is maintained regardless of whether the cell soma (nucleus) of the neurone is inactive or even absent. His results confirmed the hypothesis of Sir John Eccles, that the action potential is initiated at the excitable axon hillock. Thus neurones are differentiated, and act as integrators, not merely as relays: the membrane properties and cytoplasmic contents vary from one region of the cell to the next. This work, published essentially on his own, made Ladislav Tauc so well known that in 1960 he started some lengthy and fruitful periods of collaboration with some well known, and soon to be well known, scientists from Argentina, the United States of America, England, Spain, Poland, Japan, Italy and, of course, France.

The direction followed by Ladislav Tauc enriched new ideas about synaptic transmission, reminding us that a single transmitter substance can provoke excitatory or inhibitory responses depending on the nature of the receptors present on the target cells. Variable synaptic responses are now known under the name of synaptic plasticity, which manifests itself as habituation, desensitisation, facilitation, potentiation, etc. Another important step was the discovery of a group of neurones in the buccal ganglion of *Aplysia,* which permitted simultaneous monitoring and control of the activity in the presynaptic and postsynaptic neurones. Combined with the introduction of intracellular injections, this discovery was the starting point for many other investigations, which are still being pursued today with the analysis of the properties of synapses using toxins, antibodies, peptides and nucleic acids.

After his retirement, Ladislav Tauc did not lose his interest in experiments to measure certain membrane parameters, notably by optical means. Throughout his career, Ladislav Tauc was always the originator of new concepts concerning the physiology of neurones and was involved in the use of important new technology wherever appropriate. His intelligence, sharply focused mind and commitment permitted the transformation of the Department of Cellular Neurophysiology at CNRS, directed by Alfred Fessard, to the Laboratory of Cellular Neurobiology and then later to the Laboratory of Cellular and Molecular Neurobiology, which still exists under the direction of Maurice Israel. After 35 years of continuing contributions in Neuro-

biology, with all its difficulties, we owe him, and all those who have accompanied him along the way, a debt of gratitude: thank you Ladislav Tauc.

Ladislauv Tauc was a member of the Biological Society, the Society for Neuroscience, the International Society or Invertebrate Neuroscience and many more. He was on many editorial committees for international reviews. He received a prize at The German Science Academy in 1964 and a silver medal at the C.N.R.S. in 1966. To honour his memory, a decision has recently been taken to re-introduce the 'Conference en Neurobiologie de Gif sur-Yvette' which he initiated and maintained with the help from his colleagues at the laboratory for almost 20 years. The new conferences will be called 'Conferences Ladislav Tauc en Neurobiologie'."

Translated by Mino C D Belle, Bill Winlow, Department of Biological Sciences University of Central Lancashire, Preston PR12HE, UK
and Craigie Chapas, Editorial Assistant, The Physiological Society, P.O. Box 11319, London, WC1E 7JF, UK.

ACTA BIOLOGICA HUNGARICA

Volume 51, 2000

INDEX

Number 1

Numbers 2–4

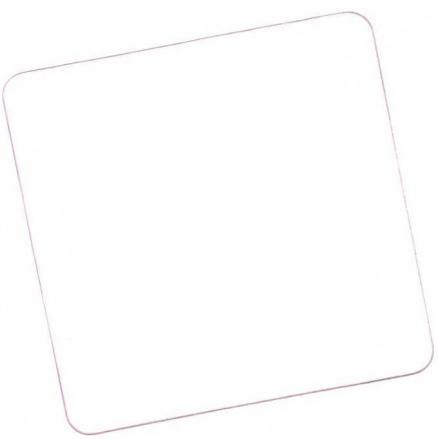

DIRECTIONS TO CONTRIBUTORS

ACTA BIOLOGICA HUNGARICA publishes original works in the field of experimental biology.

Manuscripts should be addressed to Dr. János Salánki, Editor-in-Chief or Dr. Károly Elekes, Editor, *Acta Biologica Hungarica,* H-8237 Tihany, Hungary.

Only original papers will be published and a copy of the Publishing Agreement will be sent to the authors of papers accepted for publication. Manuscripts will be processed only after receiving the signed copy of the agreement.

The manuscripts should not exceed 16 typed pages in general. The manuscripts should be typed double-spaced, on one side of the paper. In order to assure rapid publication, contributors are requested to submit two copies of the manuscript including an abstract (max. 200 words), tables and figures. An electronic version of the manuscript (including the figures) should also be submitted on a 3.5" diskette, using Word for Windows 7.0, 6.0 or 2.0 wordprocessor package in Microsoft Windows '95 or Windows 3.1 system. Each table should be typed on a separate sheet, numbered and provided with a title. All figures, either photographs or drawings or graphs, should be numbered consecutively. Figure legends should be typed in sequence on a separate sheet. Color plates (micrographs and drawings) will be charged to the authors.

Papers should be headed with the title of the paper, the names of the authors (male authors use initials, female authors use one given name in full), department, institute and town where the work was performed. A running title, not to exceed 50 letter spaces, should be included on a separate sheet and immediately following the summary 5 keywords must be supplied.

The *full paper* should be divided into the following parts in the order indicated:

1. *Abstracts*
2. *Introduction*
3. *Materials and Methods*
4. *Results*
5. *Discussion*
6. *References.* Papers – the essential ones only – cited in the manuscript should be listed on a separate sheet in alphabetical order according to the first author's surname. The references should be numbered so that each may be referred to in the text by its number only.

Examples:

1. Boas, N. F. (1953) Method for determination of hexosamine in tissue. *J. Biol. Chem. 204,* 553–563.

2. De Duve, C. (1959) Lysosomes, a new group of cytoplasmic particles. In: Hayashi T. (ed.) *Subcellular Particles.* Ronald Press, New York, pp. 1–72.

3. Umbreit, W. E., Burris, R. H., Stauffer, I. F. (1957) *Manometric Techniques.* Burgess Publishing Co., Minneapolis.

Short communication. Manuscripts, in English, should not exceed 1000 words (4 types pages) including references. The text of manuscripts containing tables and/or figures must be correspondingly shorter. Accepted short communications will be published within six months after submission of manuscripts. In order to speed up publication, no proof will be sent to authors.

Authors will be furnished, free of charge, with 25 reprints. Additional reprints may be obtained at cost.